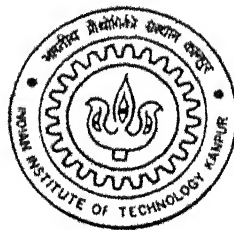


PROBABILISTIC RESPONSE OF LAMINATED COMPOSITE PANELS WITH RANDOM MATERIAL PROPERTIES

By

BHRIGU NATH SINGH

TH
AE/2001/D
Si 64P



DEPARTMENT OF AEROSPACE ENGINEERING
Indian Institute of Technology Kanpur
AUGUST, 2001

**PROBABILISTIC RESPONSE OF LAMINATED
COMPOSITE PANELS WITH RANDOM MATERIAL
PROPERTIES**

A Thesis Submitted

in Partial Fulfillment of the Requirements

for the Degree of

DOCTOR OF PHILOSOPHY

by

Bhritu Nath Singh

to the

DEPARTMENT OF AEROSPACE ENGINEERING

INDIAN INSTITUTE OF TECHNOLOGY KANPUR, INDIA

August, 2001

24 JUN 2007

पुरुषोत्तम - विज्ञान केन्द्र पुस्तकालय
भारतीय प्रौद्योगिकी संस्थान कानपुर
अवधि क्र० A . 139685



A139685



CERTIFICATE

It is certified that the work contained in the thesis entitled **PROBABILISTIC RESPONSE OF LAMINATED COMPOSITE PANELS WITH RANDOM MATERIAL PROPERTIES**, by **Bhrigu Nath Singh**, has been carried out under our supervision and that this work has not been submitted elsewhere for a degree.

Dayanand Yadav

Dr. Dayanand Yadav

Professor

Dept. of Aerospace Engineering

I. I. T. Kanpur 208 016, India

N.G.R. Iyengar

Dr. N. G. R. Iyengar

Professor

Dept. of Aerospace Engineering

I. I. T. Kanpur 208 016, India

August, 2001

SYNOPSIS

Fiber reinforced plastics (FRPs) consisting of strong and continuous fibers embedded in a polymer matrix have been in use over the last 3 decades. FRPs permit tailoring of the properties to have outstanding mechanical behavior such as high strength and stiffness to weight ratios, excellent corrosion resistance and very good fatigue characteristics. These have found use in a variety of applications like aerospace, mechanical, civil, chemical, and other industries. Because of the ability to tailor its properties, these materials are being increasingly used in many new sensitive applications that open new challenges and invite new mathematical complexities for the analyst/designer.

The basic building block for the laminate is the lamina. The lamina is orthotropic. The thickness of the lamina is approximately 0.1 mm to 0.15 mm, and hence cannot be used by itself for carrying load. The laminae are stacked together to arrive at a laminate of required thickness. The laminate in general turns out to be anisotropic.

The parameters characterizing the behavior of a composite laminate are many. Some of these may be enumerated as: - lay up sequence, fiber orientation, individual lamina thickness, inter- laminar material, fiber volume fraction, voids, curing process etc. Any variations in these parameters during manufacturing and fabrication result in variation in the behavior characteristics of the laminate.

The effectiveness of quality control during manufacturing and fabrication of a component depends on the strictness of the control and the number and types of parameters

required to be controlled. Due to economic reasons complete quality control is not practical for any material. The lack of complete control is reflected as random variation in the component characteristics like geometrical and material properties. It can be seen that these variations in composite laminates are more pronounced than in components made from conventional metallic materials as these have fewer parameters involved in fabrication/manufacturing. Dispersions in composite material properties are further enhanced by variations in the material properties of the constituent components. On the whole, the material property variations for metallic materials are with small standard deviation (SD) while composite laminates may have large SD.

In resin-matrix composites, the properties of matrix materials are strongly dependent on processing condition. The influence of processing conditions has been brought out well in literature. Fiber-matrix interface properties change with the processing procedure of fibers and curing cycle of the laminate. The strength of the fiber matrix interface plays an important role in determining the properties of the composites. Thus, owing to the inherent uncertainties involved in manufacturing/processing techniques of composites, the end product can have significant variations in the mechanical properties about the desired values. Experimental data from various sources also endorse these observations. It is important to note that the data from different divisions of the same company show dispersion in system properties. Non-standard testing methods could also be one of the reasons for such uncertainties. The variability in characteristics of the basic building blocks of laminates- the fibers and the matrix materials may add to the dispersion in the properties of the end product. It can, therefore, be concluded that variability in properties at the micro level is finally reflected at the macro-level in form of lamina properties.

Normally, in structural analysis, the system is modeled by assuming the various parameters involved like mechanical characteristics, boundary conditions etc., to be

deterministic. The concept of factor of safety is introduced at different stages to account for the uncertainties that cannot be quantified. In real situation, the system parameters are seldom deterministic. Most of the parameters can be accurately expressed in a probabilistic sense only. When the system parameters are uncertain, the derived response parameters like deflection, natural frequencies, buckling loads, dynamic response etc. are also random, being function of these basic system parameters. Depending on the sensitivity of the response parameter to the input random variables and their characteristics, the statistics of the response parameters can vary. In certain structures this can cause mode localization. A probabilistic approach yields a more accurate prediction of the system behavior and will result in a better design. The risk of failure of the structures and its performance can be evaluated accurately by adopting a probabilistic approach. Use of factor of safety approach may work with metallic materials as these have small SD of material properties and the actual allowable stress may be very close to the mean values. However, in the case of composites, inspite of effective quality control in manufacturing/fabrication processes, as we normally do in sensitive applications like aerospace etc., the design stresses will have to be much less than respective mean values to account for the widely scattered data. Finally, all these would negate the basic idea of weight optimization, which is one of the important parts of design consideration particularly in aerospace projects.

Computer simulations of some of the proposed configurations of aeronautical and large outer-space installations often show closely packed/overlapping natural frequencies of some of the components. In such cases, even the slightest shift in characteristics of the components can have pronounced effect on the response of the structures.

Considerable information exists in open literature on the distribution of ultimate tensile strength of FRPs. Similar information on dispersion of the elastic moduli, shear moduli, Poisson's ratio etc. is limited. As mentioned earlier, uncertainties in several

parameters like the fiber volume fraction, fiber orientation, void volume, fiber matrix interface properties etc. have significant effects on the response of fiber-reinforced composites. The uncertainties in the factors mentioned above are in turn reflected on the characteristics of the lamina stiffness parameters like the longitudinal modulus, transverse modulus, in-plane and out-of-plane shear moduli, Poisson's ratio etc. These can be treated as primary variables, since these are the basic parameters at the macro-level of the laminate that are usually considered for formulation of any structural analysis problem. At this stage it is relevant to mention that point-to-point variations of these properties over the structure particularly in composite made of prepegs, which is normally the case in large scale manufacturing of primary composite structures, are very small. These facts have been verified experimentally in literature. The above considerations indicate the need for more accurate probabilistic approach in the analyses of these sensitive composite structures.

Apart from randomness in material properties, there could be randomness in loading, geometry and boundary conditions. The external loading in engineering problems is influenced by many parameters that, in general are not under control and, is, therefore, random in nature. Some examples are, acoustic loading on aircraft fuselage, rocket and spacecraft panels, due to jet and rocket exhaust noise, track induced loads on aircraft during ground runs, water pressure on ship and submarine hulls during high-speed operations and under water explosion.

For reliability of design, especially for sensitive engineering applications, accurate prediction of system behavior of the structures made up of composites in presence of randomness in system properties as well as excitation favors a probabilistic analysis approach by modeling their mechanical properties and excitation as random.

From the methodological point of view, stochastic analysis can be classified into two approaches. The first one is statistical approach, including the Monte Carlo simulation

(MCS); the second is non-statistical approach such as perturbation method, second moment analysis, and the local integral method. The expansion method like Neumann is another MCS technique, where the handling of the system matrix is improved by introducing Cholesky's decomposition scheme, thus reducing the computation time required in the MCS. Usually real life structures are so complex that it is not always possible to analyze them with classical methods. Deterministic finite element method is combined with statistical approaches and /or non-statistical methods so that the complex structure with uncertain parameters subjected to random loading can be analyzed. This is also referred to as stochastic finite element method. In the study first order perturbation technique has been combined with classical approach and finite element method for evaluation of probabilistic response. Monte Carlo simulation has been used for validation of the results.

The perturbation approach as applied to problems of random media is an extension of the method used in nonlinear analysis. Given certain smoothness conditions, the functions and operators involved can be expanded in a Taylor series about their respective mean values. This kind of expansion is applicable when the randomness is small in comparison to the mean values. This condition is satisfied in most of the engineering problems particularly in aerospace applications and hence, the approach can generally be adopted for almost all practical situations. The expanded forms of the terms are introduced in the system equations. The different order of solution can be obtained from this expanded form. These solutions can be combined to get the total solution of the problem as the characteristics of the response. The consideration of number of terms in the expanded form depends on level of fluctuation in the random quantity. More number of terms should be included in the equations depending on the magnitude of the random fluctuations. This task is considerably complicated, thus greatly limiting the applicability of the method. Further, secular terms appear in higher order expansions. These are terms for which the magnitude increases with increasing

approximation orders, thus causing the expansion to diverge. For small fluctuation as is generally the case in composites, first two terms would be sufficient. This fact has been brought out clearly in the present study as well.

The Monte Carlo method is a versatile mathematical tool capable of handling situations where all other methods fail to succeed. The method has been known and used extensively in various fields such as health care, agriculture, econometrics, science and engineering. However, in engineering mechanics it is rapidly gaining serious attention only following the recent widespread availability of inexpensive computational systems. The usefulness of the MCS is based on the fact that the next best situation to having the probability distribution function of a certain quantity is to have a corresponding large population. The implementation of the method consists of numerically simulating a population corresponding to the random quantities in the physical problem, solving the deterministic problem associated with each realization of that population, and obtaining a population corresponding to the random response quantities. This population can then be used to obtain statistics of the response variables. In the present investigation this technique is used for validation of results obtained with the perturbation technique.

The analysis of structures with deterministic characteristics to random external excitations is well established and has been studied for large class of problems. However, the structural response of panels with random material parameters to deterministic as well as random excitation is quite complicated and still not fully understood. This is particularly true for buckling, free and forced vibration of composite panels. An exhaustive survey of the literature indicates that a large number of publications have appeared on the subject for isotropic beams and plates with uncertain system parameters. However, the response of laminated composite panels is not fully addressed. Further, the limitation of classical laminate theory (CLT), first order shear deformation theory (FSDT) and higher order shear

deformation theory (HSDT) have been well understood for the deterministic analysis. The efficacies of these theories for the second moments of structural response in probabilistic approach are at a nascent stage and still not fully developed. The literature review presented also reveals that these aspects have not received adequate attention of the researchers. Some concrete effort in this direction is still needed. As matter of fact, these issues, which are in the heart of the problem, have provided the motivation for the present study.

In the present work a comprehensive study has been conducted to obtain the second-order statistics of buckling loads, natural frequencies and dynamic response of laminated composite shallow panels of rectangular planform which can take into account the complete effects of shear deformations and rotatory inertia with random material properties subjected to deterministic as well as random excitation. Higher order shear deformation theory has been used to model the system behavior. The efficacies of various theories have been examined particularly with respect to variances of the structural response. The classical approach and the finite element method in conjunction with first order perturbation technique have been proposed for the random response analysis. The assumptions made in the present study may be enumerated as below:

- The deformations of the panel are very small in comparison to thickness of the panel.
- The thickness –curvature ratio (h/R) is taken to be very small, $h/R \ll 1$. The limit of this parameter is taken to be $h/R=0.2$. The curvature parameters a/R_1 and b/R_2 are varied from 0 to 0.5 for two types of curved shallow panels, i.e., spherical and cylindrical.
- The transverse shear stresses are assumed to vary parabolically through the thickness and to vanish at the top and bottom surfaces of the panel, satisfying the traction free surface conditions.

- The lateral displacement 'w' of any lamina is given by the displacement of the laminate mid-plane.
- The lamina material properties have been modeled as random variables (RVs) as is the case in most practical applications.
- Excitation is modeled as a random process in time.
- Excitation and material properties are assumed to be independent.

The investigations reported in this thesis have been divided into seven chapters, in each of which attention has been focused on a particular aspect of the aforementioned problem.

In *Chapter I*, an overview of the problem has been presented. The available techniques in literature for addressing the problems with stochasticity are reviewed. The perturbation technique appears to be quite common for analyses of structures with parameter uncertainties, while this is not a common method in the presence of external excitations, which are random. In general, Monte Carlo simulation seems to be the ideal choice for checking the validity of the proposed techniques. At the end of this chapter, motivation and scope for the present study are presented.

Chapter II includes a review of the pertinent literature available along with observations and objective for the present study. Literature is classified based on investigations related with isotropic materials and composite materials with parameter uncertainties subjected to deterministic as well as random loading.

In *Chapter III*, a general formulation for curved panels based on higher order shear deformation theory (HSDT) is presented. In addition to stochastic classical approach (SCA), (deterministic classical method + probabilistic analysis), the stochastic finite element method (SFEM) (deterministic FEM + probabilistic analysis) has also been used for obtaining solutions in this study. For deterministic finite element analysis with the displacement field based on HSDT, it is necessary to employ an element with C^1 continuity. Realizing the

computational difficulties associated with C^1 continuity element, the derivatives of the out of plane displacement are themselves considered as separate degrees of freedoms (DOFs). Thus, 5 DOFs per node with C^1 continuity element is transformed into a C^0 continuity element with 7 DOFs per node. To make it suitable for C^0 continuity, the displacement field equation for curved panels has been modified for composite plates.

From curved panel formulation, the displacement field models, equilibrium equations, strain-displacement relation and constitutive equations for plates, spherical and cylindrical panels are obtained.

Chapter IV presents specific formulation along with SCA and SFEM for initial buckling analysis of composite plates, cylindrical and spherical panels with random material properties. As mentioned earlier, the basic formulation is based on HSDT. The randomness in material properties is handled using first order perturbation technique. The efficacies of various theories with respect to variance of buckling loads are investigated. Second-order statistics of buckling loads with different combinations of geometrical parameters and boundary conditions are obtained. The sensitivity of random material properties towards buckling response statistics is examined. The results are validated with that of MCS. It has been observed that the two results are in good agreement. From this study it can be concluded that FOPT is capable of capturing the almost complete response behavior statistics. It can also be concluded from the validation that normalized response SD varies linearly with normalized SD of the basic input variables.

In *Chapter V*, some studies related to free vibration of composite laminates, spherical and cylindrical panels with randomness in material properties are attempted. Specific formulation based on HSDT along with SCA and SFEM are outlined. The validation of the results obtained using SCA and SFEM is done by MCS. The second order statistics of random natural frequencies are obtained for composite plates, cylindrical and spherical

panels. Here again, CLT, FSDT and HSDT results are compared with each other. The sensitivity of random material properties is examined with various combinations of geometrical parameters and boundary conditions.

In *Chapter VI*, general formulations of the dynamic problem along with description of the probabilistic solution methodology based on state-space approach are presented. Standard deviation (SD) of transverse displacement of composite plates, cylindrical and spherical panels subjected to deterministic excitation as a function of time for various standard deviations of material properties have been obtained. Sensitivity of response to random material properties has been examined. The response statistics for composite laminated panels with deterministic material properties subjected to random excitation are also presented. Comparisons for mean response as well as response dispersion of plate, cylindrical and spherical panels with time are carried out.

Finally in *Chapter VII*, concluding remarks and a broad perspective for future studies are presented. The classical approach and the finite element method in conjunction with first order perturbation technique have been presented to obtain the second order statistics of initial buckling loads, natural frequencies and dynamic response of composite laminated plates, cylindrical panels and spherical panels with random material properties to deterministic as well as random excitation. The results from the present approach are validated with that of MCS. It has been observed that the variances of the response obtained using the present approach and MCS vary linearly with SD of the material property. It can be concluded that the first order perturbation technique is capable of capturing the complete behavior of the response behavior in the range for the basic input variables considered. This is important as terms up to first order only has been considered in Taylor 's series expansion making the response dispersion a linear function of SD of material property. However, no such restriction regarding linearity was put in case of the MCS approach. Validation of the

present approximation with the results obtained from Monte Carlo simulation shows that for the range of SD of input RVs considered the accuracy is excellent. The nature and magnitude of influence of each one of random variables is different. The behavior of different theories with respect to SD of response is always not on the same lines as with respect to mean response. The stacking sequences, aspect ratios, curvature to side ratios, boundary conditions and thickness ratios also play important role in dispersion of response characteristics.

ACKNOWLEDGEMENTS

I take this opportunity to express my sincere gratitude to all those persons, who have made my most cherished dream-Ph.D., come true.

First of all I express my recondite sense of gratitude and profound appreciation to my thesis supervisors Prof. N.G. R. Iyengar and Prof. Dayanand Yadav, for their inspiration and valuable suggestions in carrying out this work. I find myself fortunate to have worked under them for the freedom and constant encouragement they gave throughout this work. I am highly indebted to them for all those fruitful discussion and for having introduced me to the fascinating world of Composite Materials and Random Vibration. Further, I wish to acknowledge their ever-ready helping attitude. I sincerely admit that I owe them a lot and am ever indebted to them for all that they have done to me.

I am highly indebted to Prof. C. S. Upadhyay for introducing me the Aircraft Structures and useful discussion during entire course of this work. I really appreciate his ever-ready discussion attitude.

I am very much thankful to Prof. C. Venkatesan, Prof. S. Kamle and Prof. Prashant Kumar for all their support and encouragement during entire course of stay.

I sincerely thank Prof. N. N. Kishore, Dept. of Mechanical Engineering, for introducing me the Finite Element Method.

I am thankful to the college authorities of my parent institute, Motilal Nehru Regional Engineering College Allahabad for sponsoring me to pursue Ph.D. degree under Quality

Improvement Program. I am also thankful to the faculty of my parent department, Applied Mechanics for sharing my teaching loads and providing moral supports.

My heartfelt thanks to Mrs. Leela Iyengar, Mrs. Revati Yadav and Mrs. Sangeeta Upadhyay for their hospitality and support.

Sincere thanks are due to my friends Nazirji for his excellent library support and Lalmoni, Mohite, Rohin, and Marimuthu for providing all kind of supports during stay at IITK.

Sincere thanks are due to my other friends Satvatji, Vinodji, Rameshji, Andallibji, Mukulji, dhirendraji, Jhaji, Muthuji and Jaiswalji for their useful discussion in the connection with work and providing moral supports.

I cannot forget Vinayji who always ready for any kind of help during stay at IITK.

My thanks also goes to the staffs like Ahmadji, Bade Tiwariji, Trivediji, Chhote Tiwariji, Guptaji, Ganguliji, Anil, Atul, Mr. Udaibhan, Mr. Raza, Mr. Bhagwandin and Mr. Mukesh for their ever ready helping attitude.

My thanks also goes to QIP, DOSA and DOAA staffs for their encouragement and support.

I do not have adequate words to express my indebtedness to my family members and relations for all their pains and suffering. I express my thanks to all of them for their patience, cooperation and understanding during course of this work.

Finally, I appreciate my wife Sudha for her sincere cooperation and lovely son Aniket and daughter Ichchhita for providing me entertainment.

August, 2001

Bhrigu Nath Singh

Dedicated to
My Late Parents

RESEARCH PUBLICATIONS

The following publications have resulted so far from this work.

Journals

- 1) Singh, B. N., Yadav D. and Iyengar, N. G. R., "Initial buckling of composite cylindrical panels with random material properties", **J. of Composite Structures**, 53 (1), 55-64, 2001.
- 2) Singh, Bhriugu N., Iyengar, N. G. R. and Yadav, Dayanand, "Effects of Random Material Properties on Buckling of Composite Plates", **ASCE J. of Engineering Mechanics**, 127(9), 2001.
- 3) Singh, B.N., Yadav, D. and Iyengar, N.G.R., "Free Vibration of laminated Spherical panels with random material properties", **J. of Sound and Vibration**, 244(2), 321-338, 2001.
- 4) Singh, B.N., Yadav, D. and Iyengar, N. G. R., "Stability analysis of laminated cylindrical panels with uncertain material properties", **J. of Composite Structures**, 54(1), 17-26, 2001.
- 5) Singh, B.N., Yadav, D. and Iyengar, N.G.R., "Natural Frequencies of Composite Plates with Random Material Properties Using Higher Order shear deformation theory", **Int. J. of Mechanical Sciences**, 43(10), 2193-2214, 2001.
- 6) Singh, B. N., Yadav, D. and Iyengar, N. G. R., "Free Vibration Analysis of Laminated Cross-Ply Cylindrical Panels with Random Material Properties", **The Scientific Journal of the Vibration Institute of India**, 2001 (in Press).

International Conference Proceedings

- 1) Singh, B. N., Iyengar, N. G. R. and Yadav, D., "Natural Frequencies of Laminated Cross-Ply Spherical Panels with Random Material Properties", **The Seventh Annual International Conference on Composite Engineering**, Denver, Colorado, USA, pp. 371-372, July 2-8, 2000

- 2) Singh, B. N., Yadav, D. and Iyengar, N. G. R., "Free Vibration Analysis of Laminated Cross-Ply Cylindrical Panels with Random Material Properties", **The First International Conference on VETOMAC-I**, IISc, Bangalore, India, Oct 25-27, 2000 (CD-ROM proceedings).
- 3) Singh B. N., Yadav D. and Iyengar N. G. R., "Buckling analysis of composite plates with uncertainties in material properties using first order shear deformation theory: A statistical approach", Proc. Int. Conf. on Recent Trends in Mathematical Sciences, Dept. of Mathematics, IIT Kharagpur, pp. 235-242, Dec. 20-22, 2000.
- 4) Singh B. N., Iyengar N. G. R. and Yadav D., "Stability analysis of laminated cross-ply thin plates with random material properties using Monte-Carlo simulation", **International Conf. on Mathematical Modeling**, Dept of Mathematics, University of Roorkee, Roorkee, India, Jan. 29-31, 2001.
- 5) Singh B. N., Yadav D. and Iyengar N. G. R., "Effects of uncertainties in material properties on buckling of laminated cross-ply cylindrical panels using Monte-Carlo simulation", **The Eighth Int. Conf. on Structural Safety and Reliability-ICOSSAR '01**, California, USA, June 17-22, 2001 (CD-ROM Proceedings).
- 6) Singh B. N., Iyengar, N.G.R. and Yadav, D., "Dynamic response of composite spherical panels with random material properties under random excitations", **The Eight Annual International Conf. on Composite Engineering**, Spain, August 5-7, 2001.
- 7) Singh, B. N., Iyengar, N.G.R. and Yadav D., "Probabilistic characteristics of buckling response of laminated cross-ply spherical panels with uncertain material properties", **The Second International Conference ICTACEM-2001**, IIT Kharagpur, Dec. 27-30, 2001(accepted for presentation and publication).
- 8) Singh B. N., Yadav, D. and Iyengar, N. G. R., "A C^0 element for free vibration of composite plates with uncertain material properties", **The Eleventh International Conference on Composite Structures (ICCS/11)**, Monash University, Clayton, Australia, Nov. 19-22, 2001(accepted for presentation and publication).

Papers under Consideration for Publication

- 1) Singh, B.N., Iyengar, N.G.R. and Yadav, D., "Free Vibrations of laminated Composite Cylindrical panels with random material properties", **J. of Computers and Structures** (communicated)
- 2) Singh, B. N., Iyengar, N. G. R. and Yadav, D., "Buckling of composite spherical panels with random material properties using shear deformation theories", **ASME J. of Applied Mechanics** (communicated).

- 3) Singh, B. N., Iyengar, N. G. R. and Yadav, D., “ Stability of curved composite panels with random material properties”, **ASCE J. of Aerospace Engineering** (communicated).
- 4) Singh, B. N., Yadav, D. and Iyengar, N. G. R., “ A Probabilistic finite element for free vibration of composite cylindrical panels with random material properties”, **J. Composite Structures** (communicated).
- 5) Singh, B. N., Iyengar, N. G. R. and Yadav, D., “A C^0 finite element investigation for buckling analysis of composite plates with random material properties”, **Structural Engineering and Mechanics, An International Journal** (communicated).

LIST OF CONTENTS

LIST OF TABLES	xxiii
LIST OF FIGURES	xxvi
LIST OF SYMBOLS	xliv
1 INTRODUCTION	
1.1 Overview	1
1.2 Available Techniques	8
1.3 Motivation for the Present Study	11
1.4 Scope of the Present Investigation	11
1.5 Outline	13
2 LITERATURE REVIEW	
2.1 Introduction	14
2.2 Isotropic Materials	15
2.3 Fiber Reinforced Composite Materials	31
2.4 Observations	34
2.5 Objective	35
3 GENERAL FORMULATION	
3.1 Introduction	37
3.2 Shear Deformable Curved Composite Panels	38
3.2.1 Displacement Field Model	39

3.2.2	Strain-Displacement Relations	42
3.2.3	Stress-Strain Relations	43
3.2.4	Equations of Motion	44
3.2.5	The Laminate Constitutive Equations	45
3.3	Spherical Panels	46
3.3.1	Equilibrium Equations	46
3.3.2	Strain-Displacement Relations	48
3.3.3	Constitutive Equations	48
3.4	Cylindrical Panels	49
3.4.1	Equilibrium Equations	49
3.4.2	Strain-Displacement Relations	50
3.4.3	Constitutive Equations	51
3.5	Rectangular Plates	51
3.5.1	The Equilibrium Equations	51
3.5.2	Strain-Displacement Relations	52
3.5.3	Constitutive Equations	53
3.6	Strain Energy of the Laminate	55
3.7	Work done by External Loads	55
3.8	The Kinetic Energy: Vibration	56
3.9	Finite Element Model	57
3.9.1	Mechanical Strain Energy	58
3.10	Summary	59
4	BUCKLING OF COMPOSITE PANELS	
4.1	Introduction	61
4.2	Stochastic Classical Approach (SCA)	62

4.2.1	Formulation	63
4.2.2	Second-order Statistics of Critical Buckling Loads- A Perturbation Approach	64
4.2.3	Results and Discussion	66
4.2.3.1	Buckling Load: Composite Plates	68
4.2.3.2	Buckling Load: Composite Cylindrical Panels	71
4.2.3.3	Buckling Load: Composite Spherical Panels	75
4.3	Stochastic Finite Element Method (SFEM)	82
4.3.1	Formulation	82
4.3.1.1	Prebuckling analysis	82
4.3.1.2	Buckling analysis	83
4.3.1.3	Governing equations	86
4.3.2	Solution- A Perturbation Approach	88
4.3.3	Results and Discussion	90
4.3.3.1	Buckling load: Composite Plates	92
4.3.3.2	Buckling Load: Composite Cylindrical Panels	98
4.3.3.3	Buckling Load: Composite Spherical Panels	101
4.4	Summary	105
5	FREE VIBRATION OF COMPOSITE PANELS	
5.1	Introduction	163
5.2	Stochastic Classical Approach (SCA)	164
5.2.1	Formulation	164
5.2.1.1	Navier Type Solution	165
5.2.1.2	Levy Type Solution	166
5.2.2	Probabilistic Analysis: A Perturbation Technique	168

5.2.3	Results and Discussion	171
5.2.3.1	Composite Plates	172
5.2.3.2	Composite Cylindrical Panels	176
5.2.3.3	Composite Spherical Panels	180
5.3	Stochastic Finite Element Method (SFEM)	184
5.3.1	System Equations Formulation	184
5.3.1.1	Strain Energy	185
5.3.1.2	Kinetic Energy	185
5.3.1.3	Governing Equations	187
5.3.2	Method of Solution	188
5.3.3	Results and Discussion	190
5.3.3.1	Composite Plates	191
5.3.3.2	Composite Cylindrical Panels	194
5.3.3.3	Composite Spherical Panels	197
5.4	Summary	200
6	FORCED VIBRATION RESPONSE OF COMPOSITE PANELS	
6.1	Introduction	254
6.2	Stochastic Classical Approach (SCA)	256
6.2.1	Formulation: State Space Approach	256
6.2.2	Method of Solution	259
6.3	Stochastic Finite Element Method (SFEM)	261
6.3.1	Formulation	262
6.3.1.1	Strain Energy	262
6.3.1.2	Potential Energy	263
6.3.1.3	Kinetic Energy	264

6.3.1.4	Governing Equation	264
6.3.2	Method of Solution: Perturbation Technique	266
6.4	Results and Discussion	267
6.4.1	Validation	268
6.4.2	Composite Plates: Second order statistics	269
6.4.3	Composite Cylindrical Panels: Second order statistics	271
6.4.4	Composite Spherical Panels: Second order statistics	273
6.4.5	Conclusions	274
6.5	Summary	274
7	CONCLUDING REMARKS AND SUGGESTIONS FOR FUTURE STUDIES	
7.1	Introduction	298
7.2	Concluding Remarks	298
7.3	Suggestions for Future Studies	300
	REFERENCES	302
APPENDIX A	DIFFERENTIAL OPERATORS	311
APPENDIX B	STRAIN-DISPLACEMENT MATRIX	314
APPENDIX C	DETAILS OF EQUATIONS (4.11) AND (4.12)	316

LIST OF TABLES

1.1	Variation of reported unidirectional properties for a widely used Graphite/Epoxy system, from five sources (Sources: Major Airframe Company Reports) [1]	5
4.1	Mean Buckling Load, $N_{cr} = \bar{N}_{cr} b^2 / (\bar{E}_{22} h^3)$, $\bar{N}_{cr} = \bar{N}_2$, $\bar{N}_1 = \bar{N}_6 = 0$, for all edges simply supported laminated composite plates	106
4.2	Comparison of nondimensionalised mean buckling loads, $N_{cr} = \bar{N}_{cr} b^2 / (E_{22} h^3)$, $\bar{N}_{cr} = \bar{N}$, for all edges simply supported composite cylindrical panels with $R/b=1$, $R/h=10$ and $b/a=1$	107
4.3	Nondimensionalised mean buckling loads, $N_{cr} = \bar{N}_{cr} b^2 / (E_{22} h^3)$, $\bar{N}_{cr} = \bar{N}$, for all edges simply supported composite cylindrical panels with $R/b=5$ and $b/a=1$	107
4.4	Mean buckling loads, $N_{cr} = \bar{N}_{cr} b^2 / (\bar{E}_{22} h^3)$, $\bar{N}_{cr} = \bar{N}$, for all edges simply supported composite spherical panels with $R/b=5$	108
4.5	Comparison of nondimensionalised mean buckling load, \bar{N}_{cr} of a simply supported anti symmetric square laminates ($N_2 = N_{12} = 0$, $a/h = 10$)	108
4.6	Nondimensionalised mean buckling load, \bar{N}_{cr} laminated composite plates with different support conditions ($N_1 = N_{12} = 0$, $b/a = 1$)	109

- 4.7 Comparison of nondimensionalised mean buckling load, \bar{N}_{cr} for a simply supported laminated composite cylindrical square panel
($N_{x_1} = N_{x_1 x_2} = 0$, $R/b = 5$). 109
- 4.8 Nondimensionalised mean buckling load, \bar{N}_{cr} of a $[0^0/45^0/-45^0/90^0]$ composite cylindrical square panel with different edge conditions
($N_{x_1} = N_{x_1 x_2} = 0$, $R/b = 5$). 110
- 4.9 Nondimensionalised mean buckling load parameter, \bar{N}_{cr} of a $[45^0/-45^0/]$ composite spherical square panel with different edge conditions
($N_{x_1} = N_{x_1 x_2} = 0$, $R/b = 5$). 110
- 5.1 Mean natural frequencies, $\bar{\omega} = (\bar{\omega}^* a^2 \sqrt{\rho/\bar{E}_{22}})/h$, for all edges simply supported composite square plates. 201
- 5.2 Nondimensionalised mean natural frequencies of laminated cylindrical panels with $a/b=1$, $\bar{\omega} = (\bar{\omega}^* a^2 \sqrt{\rho/\bar{E}_{22}})/h$. 202
- 5.3 Nondimensionalised mean natural frequencies of laminated spherical panels with $R_1=R_2=R$, $a/b=1$ and $R/a=5$, $\bar{\omega} = (\bar{\omega}^* a^2 \sqrt{\rho/\bar{E}_{22}})/h$: stacking sequence: $[0^0/90^0]$ for all edges simply supported (SSSS). 203
- 5.4 Nondimensionalised mean fundamental frequency of $[0^0/90^0]$ spherical panels with $R_1=R_2=R$ and $R/a=5$, $a/b=1$, $a/h=10$, $\bar{\omega} = (\bar{\omega}^* a^2 \sqrt{\rho/\bar{E}_{22}})/h$ with Levy type boundary conditions. 203
- 5.5 Comparisons of the nondimensionalised mean fundamental frequency for a square plate, $\bar{\omega} = (\bar{\omega}^* a^2 \sqrt{\rho/\bar{E}_{22}})/h$, for all edges simply supported (SSSS). 204

- 5.6 Nondimensionalised mean fundamental frequency, $\bar{\omega} = (\bar{\omega}^* a^2 \sqrt{\rho/\bar{E}_{22}})/h$,
for a $[0^0/45^0/-45^0/90^0]$ square plate with different boundary conditions. 204
- 5.7 Non-dimensional mean fundamental frequency, $\bar{\omega} = (\bar{\omega}^* a^2 \sqrt{\rho/\bar{E}_{22}})/h$ of a
 $[0^0/45^0/-45^0/90^0]$ composite cylindrical panel with different panel edge
conditions ($a/b = 1$, $R/a = 5$). 205
- 5.8 Comparisons of the nondimensionalised mean fundamental frequency for a
square $[0^0/90^0]$ laminated spherical panel, $\bar{\omega} = (\bar{\omega}^* a^2 \sqrt{\rho/\bar{E}_{22}})/h$, for all
edges simply supported (SSSS). 205
- 5.9 Nondimensionalised mean fundamental frequency, $\bar{\omega} = (\bar{\omega}^* a^2 \sqrt{\rho/\bar{E}_{22}})/h$,
for a $[45^0/-45^0/45^0/-45^0]$ laminate with different boundary conditions. 206

LIST OF FIGURES

1.1	Influence of molding lot series on four mechanical characteristics of a CFRP laminate.	4
3.1	Geometry of curved panel element with stress resultants.	39
3.2	Geometry of spherical panel element.	47
3.3	Geometry of cylindrical panel element.	50
3.4	Geometry of plate element.	52
4.1	Comparison of SD of plate buckling load from Monte Carlo simulation with the present approach, $[0^0/90^0]$ laminate, with $b/a=1$ and $b/h=10$. Key: — HSDT, FSDT, ----- CLT.	111
4.2	Variation of SD of plate buckling loads with SD of basic material properties, $[0^0/90^0]$ laminate with all basic material properties changing simultaneously. Key: As in Figure 4.1.	112
4.3	Variation of SD of plate buckling loads with SD of basic material properties, $[0^0/90^0]$ laminate using HSDT. (a) only E_{11} varying; (b) only E_{22} varying; (c) only G_{12} varying; (d) only G_{13} varying; (e) only G_{23} varying; (f) only ν_{12} varying. Key:- $b/a = 1$: \diamond , $b/a = 2$: $+$, $b/a = 3$: $.$	113
4.4	Comparison of SD of cylindrical panel buckling load from Monte Carlo simulation with the present approach, $[0^0/90^0]$ laminate, with $b/a=1$ and $b/h=10$. Key: — CLT, FSDT, ----- HSDT.	114

- 4.5 Sensitivity of SD of cylindrical panel buckling loads with SD of basic material properties, $[0^0/90^0]$ laminate and $b/a=1$, with all basic material properties changing simultaneously. (a) $b/h=10$; (b) $b/h=100$. Key: As in figure 4.4. 115
- 4.6 Sensitivity of SD of cylindrical panel buckling loads with SD of basic material properties, $[0^0/90^0]$ laminate, with $b/a=1$ and $b/h=10$.
 (a) only E_{11} varying; (b) only E_{22} varying; (c) only G_{12} varying;
 (d) only ν_{12} varying; (e) only G_{13} varying; (f) only G_{23} varying.
 Key: As in Figure 4.4. 116
- 4.7 Sensitivity of SD of cylindrical panel buckling loads with SD of basic material properties, $[0^0/90^0]$ laminate, with $b/a=1$ and $b/h=100$.
 (a) only E_{11} varying; (b) only E_{22} varying; (c) only G_{12} varying;
 (d) only ν_{12} varying; (e) only G_{13} varying; (f) only G_{23} varying.
 Key: As in Figure 4.4. 117
- 4.8 Sensitivity of SD of cylindrical panel buckling loads with SD of basic material properties, $[0^0/90^0/90^0/0^0]$ laminate and $b/a=1$, with all basic material properties changing simultaneously; (a) $b/h=10$; (a) $b/h=100$.
 Key: As in Figure 4.4. 118
- 4.9 Sensitivity of SD of cylindrical panel buckling loads with SD of basic material properties, $[0^0/90^0/90^0/0^0]$ laminate, with $b/a=1$ and $b/h=10$.
 (a) only E_{11} varying; (b) only E_{22} varying; (c) only G_{12} varying;
 (d) only ν_{12} varying; (e) only G_{13} varying; (f) only G_{23} varying.
 Key: As in Figure 4.4. 119
- 4.10 Variation of SD of cylindrical panel buckling loads with SD of basic material properties, $[0^0/90^0/90^0/0^0]$ laminate, with $b/a=1$ and $b/h=100$.
 (a) only E_{11} varying; (b) only E_{22} varying; (c) only G_{12} varying;
 (d) only ν_{12} varying; (e) only G_{13} varying; (f) only G_{23} varying.
 Key: As in Figure 4.4. 120

- 4.11 Comparison of spherical panel buckling load from Monte Carlo simulation with the present approach, $[0^0/90^0]$ laminate, with $R/b=5$, $b/a=1$ and $b/h=10$.
Key:- PT: FSDT —; HSDT
MCS: FSDT ∇ ; HSDT ...+.... 121
- 4.12 Sensitivity of SD of spherical panel buckling loads with SD of basic material properties with all basic material properties changing simultaneously, $b/h=10$ and $R/b=5$. Key: — FSDT, HSDT. 122
- 4.13 Sensitivity of SD of spherical panel buckling loads with SD of basic material properties with all basic material properties changing simultaneously, $b/h=100$ and $R/b=5$. Key: As in Figure 4.12. 123
- 4.14 Sensitivity of SD of spherical panel buckling loads with SD of basic material property, E_{11} for $b/h=10$ and $R/b=5$. Key: As in Figure 4.12. 124
- 4.15 Sensitivity of SD of spherical panel buckling loads with SD of basic material property, E_{11} for $b/h=100$ and $R/b=5$. Key: As in Figure 4.12. 125
- 4.16 Sensitivity of SD of spherical panel buckling loads with SD of basic material property, E_{22} for $b/h=10$ and $R/b=5$; Key: As in Figure 4.12. 126
- 4.17 Sensitivity of SD of spherical panel buckling loads with SD of basic material property, E_{22} for $b/h=100$ and $R/b=5$. Key: As in Figure 4.12. 127
- 4.18 Sensitivity of SD of spherical panel buckling loads with SD of basic material property, G_{12} for $b/h=10$ and $R/b=5$. Key: As in Figure 4.12. 128
- 4.19 Sensitivity of SD of spherical panel buckling loads with SD of basic material property, G_{12} for $b/h=100$ and $R/b=5$. Key: As in Figure 4.12. 129
- 4.20 Sensitivity of SD of spherical panel buckling loads with SD of basic material property, G_{13} for $b/h=10$ and $R/b=5$. Key: As in Figure 4.12. 130

- 4.21 Sensitivity of SD of spherical panel buckling loads with SD of basic material property, G_{13} for $b/h=100$ and $R/b=5$. Key: As in Figure 4.12. 131
- 4.22 Sensitivity of SD of spherical panel buckling loads with SD of basic material property, G_{23} for $b/h=10$ and $R/b=5$. Key: As in Figure 4.12. 132
- 4.23 Sensitivity of SD of spherical panel buckling loads with SD of basic material property, G_{23} for $b/h=100$ and $R/b=5$. Key: As in Figure 4.12. 133
- 4.24 Sensitivity of SD of spherical panel buckling loads with SD of basic material property, ν_{12} for $b/h=10$ and $R/b=5$. Key: Same as in Figure 4.12. 134
- 4.25 Sensitivity of SD of spherical panel buckling loads with SD of basic material property, ν_{12} for $b/h=100$ and $R/b=5$. Key: As in Figure 4.12. 135
- 4.26 Validation of buckling load for a square plate by the present approach, with Monte Carlo simulation, $[0^\circ/90^\circ]$ laminate, with $b/h=5$.
Key- \diamond : Present approach, $+$: MCS. 136
- 4.27 Variation of SD/mean of the nondimensionalised buckling loads with SD of basic material properties, square laminate with all basic material properties changing simultaneously.
(a) $b/h=5$ and $[60^\circ/-60^\circ/60^\circ/-60^\circ]$; (b) $b/h=10$ and $[60^\circ/-60^\circ/60^\circ/-60^\circ]$;
(c) $b/h=5$ and $[30^\circ/-30^\circ/30^\circ/-30^\circ]$; (d) $b/h=10$ and $[30^\circ/-30^\circ/30^\circ/-30^\circ]$;
(e) $b/h=5$ and $[45^\circ/-45^\circ/45^\circ/-45^\circ]$; (f) $b/h=10$ and $[45^\circ/-45^\circ/45^\circ/-45^\circ]$.
Key: — CCCC, CFCE, ----- SSSS. 137
- 4.28 Variation of SD/mean of the nondimensionalised buckling loads with SD of basic material properties, $[60^\circ/-60^\circ/60^\circ/-60^\circ]$ square plate, with $b/h=5$.
(a) only E_{11} varying; (b) only E_{22} varying; (c) only G_{12} varying;
(d) only G_{13} varying; (e) only G_{23} varying; (f) only ν_{12} varying.
Key: As in Figure 4.27. 138
- 4.29 Variation of SD/mean of the nondimensionalised buckling loads with SD of basic material properties, $[60^\circ/-60^\circ/60^\circ/-60^\circ]$ square plate, with $b/h=10$.

- (a) only E_{11} varying; (b) only E_{22} varying; (c) only G_{12} varying;
 (d) only G_{13} varying; (e) only G_{23} varying; (f) only ν_{12} varying.
 Key: As in Figure 4.27. 139
- 4.30 Variation of SD/mean of the nondimensionalised buckling loads with SD
 of basic material properties, $[30^0/-30^0/30^0/-30^0]$ square plate, with $b/h=5$
 (a) only E_{11} varying; (b) only E_{22} varying; (c) only G_{12} varying;
 (d) only G_{13} varying; (e) only G_{23} varying; (f) only ν_{12} varying.
 Key: As in Figure 4.27. 140
- 4.31 Variation of SD/mean of the nondimensionalised buckling loads with SD
 of basic material properties, $[30^0/-30^0/30^0/-30^0]$ square plate, with $b/h=10$.
 (a) only E_{11} varying; (b) only E_{22} varying; (c) only G_{12} varying;
 (d) only G_{13} varying; (e) only G_{23} varying; (f) only ν_{12} varying.
 Key: As in Figure 4.27. 141
- 4.32 Variation of SD/mean of the nondimensionalised buckling loads with SD
 of basic material properties, $[45^0/-45^0/45^0/-45^0]$ square plate, with $b/h=5$.
 (a) only E_{11} varying; (b) only E_{22} varying; (c) only G_{12} varying;
 (d) only G_{13} varying; (e) only G_{23} varying; (f) only ν_{12} varying.
 Key: As in Figure 4.27. 142
- 4.33 Variation of SD/mean of the nondimensionalised buckling loads with SD
 of basic material properties, $[45^0/-45^0/45^0/-45^0]$ square plate, with $b/h=10$
 (a) only E_{11} varying; (b) only E_{22} varying; (c) only G_{12} varying;
 (d) only G_{13} varying; (e) only G_{23} varying; (f) only ν_{12} varying.
 Key: As in Figure 4.27. 143
- 4.34 Validation of results by the present SFEM approach with Monte Carlo
 simulation and available results for $[0^0/90^0]$ square cylindrical laminate,
 with $R/b=5$ and $b/h=10$. Key:- \diamond : Present approach, $+$: SCA, $:$
 MCS 144
- 4.35 Variation of SD/mean of the nondimensionalised buckling loads with SD
 of basic material properties, $[0^0/45^0/-45^0/90^0]$ square cylindrical laminate

and $R/b=5$, with all basic material properties changing simultaneously.

(a) $b/h=2$; (b) $b/h=5$.

Key:- \diamond : CCCC, $+$: CCCF, $:$: CCCS, \times : CFCF, Δ : SSSS.

145

- 4.36 Variation of SD/mean of the nondimensionalised buckling loads with SD of basic material properties, $[0^0/45^0/-45^0/90^0]$ square cylindrical laminate, with $R/b=5$ and $b/h=2$.

(a) only E_{11} varying; (b) only E_{22} varying; (c) only G_{12} varying;

(d) only G_{13} varying; (e) only G_{23} varying; (f) only ν_{12} varying.

Key: As in Figure 4.35.

146

- 4.37 Sensitivity of SD/mean of the nondimensionalised buckling loads with SD of basic material properties, $[0^0/45^0/-45^0/90^0]$ square cylindrical laminate, with $R/b=5$ and $b/h=5$.

(a) only E_{11} varying; (b) only E_{22} varying; (c) only G_{12} varying;

(d) only G_{13} varying; (e) only G_{23} varying; (f) only ν_{12} varying.

Key: As in Figure 4.35.

147

- 4.38 Validation of results for a $[0^0/90^0]$ spherical panel variance of nondimensionalised buckling load.

148

- 4.39 Variation of standard deviation (SD) of the nondimensionalised-buckling load of a $[45^0/-45^0/45^0/-45^0]$ laminated spherical square panel with all basic material properties changing Simultaneously. Key: — CCCC, CFCF, ----- SSSS.

149

- 4.40 Variation of SD/mean of the nondimensionalised buckling load of a $[45^0/-45^0/45^0/-45^0]$ square spherical laminate with SD of E_{11} . Key: As in Figure 4.39.

150

- 4.41 Variation of SD/mean of the nondimensionalised buckling load of a $[45^0/-45^0/45^0/-45^0]$ square spherical laminate with SD of E_{22} . Key: As in Figure 4.39.

151

- 4.42 Variation of SD/mean of the nondimensionalised buckling load of a $[45^0/-45^0/45^0/-45^0]$ square spherical laminate, with SD of G_{12} . Key: As in Figure 4.39. 152
- 4.43 Variation of SD/mean of the nondimensionalised buckling load of a $[45^0/-45^0/45^0/-45^0]$ square spherical Laminate with SD of G_{13} . Key: As in Figure 4.39. 153
- 4.44 Variation of SD/mean of the nondimensionalised buckling load of a $[45^0/-45^0/45^0/-45^0]$ square spherical laminate, with SD of G_{23} . Key: As in Figure 4.39. 154
- 4.45 Variation of SD/mean of the nondimensionalised buckling load of a $[45^0/-45^0/45^0/-45^0]$ square spherical laminate, with SD of ν_{12} . Key: As in Figure 4.39. 155
- 4.46 Comparison of a $[0^0/45^0/-45^0/90^0]$ spherical laminated panel buckling load scattering with a $[0^0/45^0/-45^0/90^0]$ cylindrical laminated panel with all basic material properties changing simultaneously. Key: — Spherical Panel; Cylindrical Panel. 156
- 4.47 Comparison of a $[0^0/45^0/-45^0/90^0]$ spherical laminated panel buckling load scattering with a $[0^0/45^0/-45^0/90^0]$ cylindrical laminated panel with SD of E_{11} . Key: As in Figure 4.46. 157
- 4.48 Comparison of a $[0^0/45^0/-45^0/90^0]$ spherical laminated panel buckling load scattering with a $[0^0/45^0/-45^0/90^0]$ cylindrical laminated panel with SD of E_{22} . Key: As in Figure 4.46. 158
- 4.49 Comparison of a $[0^0/45^0/-45^0/90^0]$ spherical laminated panel buckling load scattering with a $[0^0/45^0/-45^0/90^0]$ cylindrical laminated panel with SD of

	G_{12} . Key: As in Figure 4.46.	159
4.50	Comparison of a $[0^0/45^0/-45^0/90^0]$ spherical laminated panel buckling load scattering with a $[0^0/45^0/-45^0/90^0]$ cylindrical laminated panel with SD of G_{13} . Key: As in Figure 4.46.	160
4.51	Comparison of a $[0^0/45^0/-45^0/90^0]$ spherical laminated panel buckling load scattering with a $[0^0/45^0/-45^0/90^0]$ cylindrical laminated panel with SD of G_{23} . Key: As in Figure 4.46.	161
4.52	Comparison of a $[0^0/45^0/-45^0/90^0]$ spherical laminated panel buckling load scattering with a $[0^0/45^0/-45^0/90^0]$ cylindrical laminated panel with SD of ν_{12} . Key: As in Figure 4.46.	162
5.1	Comparison of results from MCS with the present approach, $[0^0/90^0/90^0/0^0]$ plate, with $a/b=1$, Material -1 and $a/h=10$. Key:- \diamond : first mode, $+$: second mode, $:$: third mode, \times : fourth mode, Δ : fifth mode.	207
5.2	Influence of SD of basic material properties on SD of square of the first five natural frequencies, $[0^0/90^0]$ plate, $a/b=1$, with all basic material properties changing at a time. (a) $a/h=10$ and Material -1; (b) $a/h=10$ and Material -2; (c) $a/h=100$ and Material -1; (d) $a/h=100$ and Material -2. Key: As in Figure 5.1.	208
5.3	Influence of SD of basic material properties on SD of square of the first five natural frequencies, $[0^0/90^0]$ plate, with $a/b=1$, Material -2 and $a/h=10$. (a) only E_{11} varying; (b) only E_{22} varying; (c) only G_{12} varying; (d) only G_{13} varying; (e) only G_{23} varying; (f) only ν_{12} varying. Key: As in Figure 5.1.	209
5.4	Influence of SD of basic material properties on SD of square of the first five natural frequencies, $[0^0/90^0]$ plate, with $a/b=1$, Material -1 and $a/h=10$. (a) only E_{11} varying; (b) only E_{22} varying; (c) only G_{12} varying;	

	(d) only G_{13} varying; (e) only G_{23} varying; (f) only ν_{12} varying. Key: As in Figure 5.1.	210
5.5	Influence of SD of basic material properties on SD of square of the first five natural frequencies, $[0^0/90^0]$ plate, with $a/b=1$, Material -1 and $a/h=100$.	
	(a) only E_{11} varying; (b) only E_{22} varying; (c) only G_{12} varying; (d) only G_{13} varying; (e) only G_{23} varying; (f) only ν_{12} varying. Key: As in Figure 5.1.	211
5.6	Influence of SD of basic material properties on SD of square of the first five natural frequencies, $[0^0/90^0]$ plate, with $a/b=1$, Material -2 and $a/h=100$.	
	(a) only E_{11} varying; (b) only E_{22} varying; (c) only G_{12} varying; (d) only G_{13} varying; (e) only G_{23} varying; (f) only ν_{12} varying. Key: As in Figure 5.1.	212
5.7	Influence of SD of basic material properties on SD of square of the first five natural frequencies, $[0^0/90^0/90^0/0^0]$ plate, $a/b=1$, with all basic material properties changing at a time.	
	(a) $a/h=10$ and Material -1; (b) $a/h=10$ and Material -2; (c) $a/h=100$ and Material -1; (d) $a/h=100$ and Material -2. Key: As in Figure 5.1.	213
5.8	Influence of SD of basic material properties on SD of square of the first five natural frequencies, $[0^0/90^0/90^0/0^0]$ plate, with $a/b=1$, Material -1 and $a/h=10$.	
	(a) Only E_{11} varying; (b) only E_{22} varying; (c) only G_{12} varying; (d) only G_{13} varying; (e) only G_{23} varying; (f) only ν_{12} varying. Key: As in Figure 5.1.	214
5.9	Influence of SD of basic material properties on SD of square of the first five natural frequencies, $[0^0/90^0/90^0/0^0]$ plate, with $a/b=1$, Material -2 and $a/h=10$.	
	(a) only E_{11} varying; (b) only E_{22} varying; (c) only G_{12} varying;	

- (d) only G_{13} varying; (e) only G_{23} varying; (f) only ν_{12} varying.
Key: As in Figure 5.1. 215
- 5.10 Influence of SD of basic material properties on SD of square of the first five natural frequencies, $[0^0/90^0/90^0/0^0]$ plate, with $a/b=1$, Material -1 and $a/h=100$.

(a) only E_{11} varying; (b) only E_{22} varying; (c) only G_{12} varying;
(d) only G_{13} varying; (e) only G_{23} varying; (f) only ν_{12} varying.
Key: As in Figure 5.1. 216
- 5.11 Influence of SD of basic material properties on SD of square of the first five natural frequencies, $[0^0/90^0/90^0/0^0]$ plate, with $a/b=1$, Material -2 and $a/h=100$.

(a) only E_{11} varying; (b) only E_{22} varying; (c) only G_{12} varying;
(d) only G_{13} varying; (e) only G_{23} varying; (f) only ν_{12} varying.
Key: As in Figure 5.1. 217
- 5.12 Influence of SD of basic material properties on SD of square of the fundamental frequency, $[0^0/90^0/90^0/0^0]$ plate, $a/b=1$, Material -1 and $a/h=10$, with all basic material properties changing at a time.

Key: — HSDT, FSDT, ----- CLT. 218
- 5.13 Comparison of influence of SD of basic material properties on SD of square of the fundamental frequency by three theories, $[0^0/90^0/90^0/0^0]$ plate, with $a/b=1$, Material -1 and $a/h=10$.

(a) only E_{11} varying; (b) only E_{22} varying; (c) only G_{12} varying;
(d) only G_{13} varying; (e) only G_{23} varying; (f) only ν_{12} varying.
Key: As in Figure 5.12. 219
- 5.14 Comparison of the present approach results to Monte Carlo simulation, $[0^0/90^0/90^0/0^0]$ cylindrical panel, with $R/a=5$, $a/b=1$ and $a/h=10$.

Key:- \diamond : first mode, $+$: second mode, \in third mode, \times : fourth mode, Δ : fifth mode. 220
- 5.15 Sensitivity of SD of square of the first five natural frequencies with SD of

basic material properties, $[0^0/90^0]$ cylindrical panel, $a/b=1$, with all basic material properties changing simultaneously.

(a) $R/a=5$ and $a/h=10$; (b) $R/a=5$ and $a/h=100$; (c) $R/a=10$ and $a/h=10$; (d) $R/a=10$ and $a/h=100$. Key: As in Figure 5.14. 221

5.16 Sensitivity of SD of square of the first five natural frequencies with SD of basic material properties, $[0^0/90^0]$ cylindrical panel, with $R/a=5$, $a/b=1$ and $a/h=10$.

(a) only E_{11} varying; (b) only E_{22} varying; (c) only G_{12} varying;
(d) only G_{13} varying; (e) only G_{23} varying; (f) only ν_{12} varying.
Key: As in Figure 5.14. 222

5.17 Sensitivity of SD of square of the first five natural frequencies with SD of basic material properties, $[0^0/90^0]$ cylindrical panel, with $R/a=5$, $a/b=1$ and $a/h=100$.

(a) only E_{11} varying; (b) only E_{22} varying; (c) only G_{12} varying;
(d) only G_{13} varying; (e) only G_{23} varying; (f) only ν_{12} varying.
Key: As in Figure 5.14. 223

5.18 Sensitivity of SD of square of the first five natural frequencies with SD of basic material properties, $[0^0/90^0]$ cylindrical panel, with $R/a=10$, $a/b=1$ and $a/h=10$.

(a) only E_{11} varying; (b) only E_{22} varying; (c) only G_{12} varying;
(d) only G_{13} varying; (e) only G_{23} varying; (f) only ν_{12} varying.
Key: As in Figure 5.14. 224

5.19 Sensitivity of SD of square of the first five natural frequencies with SD of basic material properties, $[0^0/90^0]$ cylindrical panel, with $R/a=10$, $a/b=1$ and $a/h=100$.

(a) only E_{11} varying; (b) only E_{22} varying; (c) only G_{12} varying;
(d) only G_{13} varying; (e) only G_{23} varying; (f) only ν_{12} varying.
Key: As in Figure 5.14. 225

5.20 Sensitivity of SD of square of the first five natural frequencies with SD of

- basic material properties, $[0^0/90^0/90^0/0^0]$ cylindrical panel, $a/b=1$, with all basic material properties changing simultaneously. 226
- (a) $R/a=5$ and $a/h=10$; (b) $R/a=5$ and $a/h=100$; (c) $R/a=10$ and $a/h=10$; (d) $R/a=10$ and $a/h=100$. Key: As in Figure 5.14. 226
- 5.21 Sensitivity of SD of square of the first five natural frequencies with SD of basic material properties, $[0^0/90^0/90^0/0^0]$ cylindrical panel, with $R/a=5$, $a/b=1$ and $a/h=10$. 227
- (a) only E_{11} varying; (b) only E_{22} varying; (c) only G_{12} varying;
 (d) only G_{13} varying; (e) only G_{23} varying; (f) only ν_{12} varying.
 Key: As in Figure 5.14. 227
- 5.22 Sensitivity of SD of square of the first five natural frequencies with SD of basic material properties, $[0^0/90^0/90^0/0^0]$ cylindrical panel, with $R/a=10$, $a/b=1$ and $a/h=100$. 228
- (a) only E_{11} varying; (b) only E_{22} varying; (c) only G_{12} varying;
 (d) only G_{13} varying; (e) only G_{23} varying; (f) only ν_{12} varying.
 Key: As in Figure 5.14. 228
- 5.23 Sensitivity of SD of square of the first five natural frequencies with SD of basic material properties, $[0^0/90^0/90^0/0^0]$ cylindrical panel, with $R/a=10$, $a/b=1$ and $a/h=10$. 229
- (a) only E_{11} varying; (b) only E_{22} varying; (c) only G_{12} varying;
 (d) only G_{13} varying; (e) only G_{23} varying; (f) only ν_{12} varying.
 Key: As in Figure 5.14. 229
- 5.24 Sensitivity of SD of square of the first five natural frequencies with SD of basic material properties, $[0^0/90^0/90^0/0^0]$ cylindrical panel, with $R/a=10$, $a/b=1$ and $a/h=100$. 230
- (a) only E_{11} varying; (b) only E_{22} varying; (c) only G_{12} varying;
 (d) only G_{13} varying; (e) only G_{23} varying; (f) only ν_{12} varying.
 Key: As in Figure 5.14. 230

- 5.25 Comparison of results from Monte Carlo simulation with the present approach, $[0^0/90^0/90^0/0^0]$ spherical panel, with $R/a=5$, $a/b=1$ and $a/h=10$ for SSSS.
Key:- \diamond : first mode, $+$: second mode, \square : third mode, \times : fourth mode, Δ : fifth mode. 231
- 5.26 Variation of SD of square of the first five natural frequencies with SD of basic material properties, $[0^0/90^0]$ spherical panel, $R/a=5$, $a/h=10$ and $a/b=1$, with all basic material properties changing simultaneously for SSSS. Key: As in Figure 5.25. 232
- 5.27 Variation of SD of square of the first five natural frequencies with SD of basic material properties, $[0^0/90^0]$ spherical panel, with $R/a=5$, $a/b=1$ and $a/h=10$ for SSSS.
(a) only E_{11} varying; (b) only E_{22} varying; (c) only G_{12} varying;
(d) only G_{13} varying; (e) only G_{23} varying; (f) only ν_{12} varying.
Key: As in Figure 5.25. 233
- 5.28 Variation of SD of square of the fundamental frequency with SD of basic material properties, $[0^0/90^0]$ spherical panel, $R/a=5$, $a/h=10$ and $a/b=1$, with all basic material properties changing simultaneously.
Key:- \diamond : SSSS $+$: SCSC, \square : SFSC, \times : SFSS, Δ : SSSC. 234
- 5.29 Variation of SD of square of the first five natural frequencies with SD of basic material properties, $[0^0/90^0]$ spherical panel, with $R/a=5$, $a/b=1$ and $a/h=10$.
(a) only E_{11} varying; (b) only E_{22} varying; (c) only G_{12} varying;
(d) only G_{13} varying; (e) only G_{23} varying; (f) only ν_{12} varying.
Key: As in Figure 5.28. 235
- 5.30 Comparison of the probabilistic finite element results with MCS and SCA for $[0^0/90^0/90^0/0^0]$ laminated SSSS square plate, with $a/h=10$. 236

- 5.31 Variation of square of the fundamental frequency of a $[0^0/45^0/-45^0/90^0]$ laminated composite square plate with SD of material properties varying simultaneously. Key:- — SSSS, CFCF, ----- CCCC. 237
- 5.32 Variation of normalized SD of square of the fundamental frequency of a $[0^0/45^0/-45^0/90^0]$ laminated square plate with SD of material properties changing at a time for $a/h=5$. Key: As in Figure 5.31. 238
- 5.33 Variation of normalized SD of square of the fundamental frequency of a $[0^0/45^0/-45^0/90^0]$ laminated square plate with SD of material properties changing at a time for $a/h=10$. Key: As in Figure 5.31. 239
- 5.34 Comparison of the probabilistic finite element results with MCS for a $[0^0/90^0/0^0]$ cylindrical square panel. 240
- 5.35 Variation of SD of square of the fundamental frequency of a $[0^0/45^0/-45^0/90^0]$ cylindrical square panel with SD of basic material properties changing simultaneously. Key: — CCCC, CFCF, ---- SSSS. 241
- 5.36 Variation of SD of square of the fundamental frequency a $[0^0/45^0/-45^0/90^0]$ cylindrical square panel with SD of longitudinal elastic modulus E_{11} . Key: As in Figure 5.35. 242
- 5.37 Variation of SD of square of the fundamental frequency of a $[0^0/45^0/-45^0/90^0]$ cylindrical square panel with SD of transverse elastic modulus E_{22} . Key: As in Figure 5.35. 243
- 5.38 Variation of SD of square of the fundamental frequency of a $[0^0/45^0/-45^0/90^0]$ cylindrical square panel with SD of in plane shear modulus G_{12} . Key: As in Figure 5.35. 244
- 5.39 Variation of SD of square of the fundamental frequency a $[0^0/45^0/-45^0/90^0]$

- cylindrical square panel with SD of out-of-plane shear modulus G_{13} . Key:
As in Figure 5.35. 245
- 5.40 Variation of SD of square of the fundamental frequency a $[0^0/45^0/-45^0/90^0]$
cylindrical square panel with SD of out-of-plane shear modulus G_{23} . Key:
As in Figure 5.35. 246
- 5.41 Variation of SD of square of the fundamental frequency a $[0^0/45^0/-45^0/90^0]$
cylindrical square panel with SD of Poisson's ratio ν_{12} . Key: As in Figure
5.35. 247
- 5.42 Comparison of probabilistic finite element results with MCS and SCA for
a $[0^0/90^0/90^0/0^0]$ spherical laminate with $a/b=1$. 248
- 5.43 Variation of dispersion of square of the fundamental frequency of a $[45^0/-$
 $45^0/45^0/-45^0]$ spherical square panel against simultaneous variation of
material properties. Key: As in Figure 5.35. 249
- 5.44 Sensitivity of the square of the fundamental frequency of a $[45^0/-45^0/45^0/-$
 $45^0]$ spherical square panel against individual variation of material
property SD for $a/h=5$. Key: As in Figure 5.35. 250
- 5.45 Sensitivity of the square of the fundamental frequency of a $[45^0/-45^0/45^0/-$
 $45^0]$ spherical square panel against individual variation of material
property SD for $a/h=10$. Key: As in Figure 5.35. 251
- 5.46 Comparison of the scatter of square of the fundamental frequency in $[0^0/-$
 $45^0/45^0/90^0]$ plate, cylindrical and spherical panels against simultaneous
change in material properties.
Key: — Spherical; Cylindrical; ----- Plate. 252
- 5.47 Comparison of the scatter of square of the fundamental frequency of a $[0^0/-$

	45 ⁰ /45 ⁰ /90 ⁰] spherical square panel with plate, cylindrical panel against individual change in material property. Key: As in Figure 5.46.	253
6.1	Validation of mean transverse mid-point displacement of a [0 ⁰ /90 ⁰ /90 ⁰ /0 ⁰] SSSS spherical panel obtained by the present SFEM and SCA approaches with MCS. Key:- — : SCA, : SFEM, ----- : MCS.	276
6.2	Validation of SD of the transverse mid-point displacement for a [0 ⁰ /90 ⁰ /90 ⁰ /0 ⁰] SSSS spherical panel obtained from the present SCA and SFEM approaches with MCS. Key: As in Figure 6.1.	277
6.3	Variation of mean value of the transverse mid-point displacement of a [0 ⁰ /90 ⁰ /90 ⁰ /0 ⁰] SSSS laminate by SCA.	278
6.4	Variation of mean value of the transverse mid-point displacement of a [0 ⁰ /90 ⁰] SSSS laminate by SCA.	279
6.5	Variation of SD of the transverse mid-point displacement of a [0 ⁰ /90 ⁰ /90 ⁰ /0 ⁰] SSSS laminate by SCA with individual material properties as random.	280
6.6	Variation of SD of the transverse mid-point displacement of a [0 ⁰ /90 ⁰] SSSS laminate by SCA.	281
6.7	Variation of SD of the transverse mid-point displacement by SCA of a [0 ⁰ /90 ⁰] SSSS laminate with SD of material property G ₁₂ at t=0.002s and 0.004s.	282
6.8	Variation of SD of the transverse mid-point displacement of a [0 ⁰ /90 ⁰ /90 ⁰ /0 ⁰] SSSS laminate with deterministic material properties and random excitation by SCA.	283
6.9	Mean Transverse mid-point displacement of a [0 ⁰ /45 ⁰ /-45 ⁰ /90 ⁰] CCCC	

	laminate by SFEM.	284
6.10	Variation of SD of transverse mid-point displacement of a $[0^0/45^0/-45^0/90^0]$ CCCC laminate by SFEM.	285
6.11	Variation of the mean transverse mid-point displacement of (a) $[0^0/90^0/90^0/0^0]$ and (b) $[0^0/90^0]$ SSSS cylindrical panels by SCA.	286
6.12	Variation of SD of the transverse mid-point displacement for a $[0^0/90^0/90^0/0^0]$ SSSS cylindrical panel by SCA.	287
6.13	Variation of SD of the transverse mid-point displacement for a $[0^0/90^0]$ SSSS cylindrical panel by SCA. Key: As in Figure 6.6.	288
6.14	Variation of normalized SD of the transverse mid-point displacement of a $[0^0/90^0]$ SSSS cylindrical panel with SD of material property E_{11} at $t=0.002s$ and $0.004s$ by SCA.	289
6.15	Variation of SD of the transverse mid-point displacement of a $[0^0/90^0/90^0/0^0]$ SSSS cylindrical panel with deterministic material properties and random excitation by SCA.	290
6.16	Mean Transverse mid-point displacement of a $[0^0/45^0/-45^0/90^0]$ CCCC cylindrical panel by SFEM.	291
6.17	Variation of SD of transverse mid-point displacement of a $[0^0/45^0/-45^0/90^0]$ CCCC cylindrical panel by SFEM.	292
6.18	Mean transverse mid-point displacement of a $[0^0/90^0/90^0/0^0]$ SSSS spherical panel by SCA.	293
6.19	Sensitivity of transverse mid-point displacement of a $[0^0/90^0/90^0/0^0]$ SSSS spherical panel by SCA.	294
6.20	Sensitivity of transverse mid-point displacement of a $[0^0/90^0/90^0/0^0]$ SSSS	

	spherical panel with deterministic material properties and random loading by SCA.	295
6.21	Mean response of transverse mid-point displacement for a $[0^0/45^0/-45^0/90^0]$ CCCC spherical panel by SFEM.	296
6.22	Sensitivity of the transverse mid point displacement for a $[0^0/45^0/-45^0/90^0]$ CCCC spherical panel by SFEM.	297

LIST OF SYMBOLS

A_{ij}, B_{ij}, etc	Laminate stiffness
a, b	Panel length along x_1 and x_2 respectively
B	Strain displacement matrix
C'_{ij}	Small random coefficients
$Cov(., .)$	Covariance
d_j, b_j	Basic random material property
$E[.]$	Expectation of
E_{ij}	Elastic modulus
G_{ij}	Shear modulus
h	Thickness of the laminate
\bar{I}'_i, I_i	Inertias
J	Jacobian
K	Bending stiffness matrix
L, \mathcal{L}	Differential operators
M	Mass matrix
N, NL	Number of layers
N_{cr}	Buckling load, Nondimensionalised buckling load
NE	Number of elements
$N_{x_1}, N_{x_2}, N_{x_1x_2}$	In-plane loads
N_i, M_i, K_i, Q_i	Stress resultants
psd	Power spectral density
Q_{ij}	Stiffness coefficients
\bar{Q}_{ij}	Material constants in laminate coordinate system
Q_{mn}	Coefficients in double Fourier expansion
q, q^*, Δ	Excitation, eigenvectors
R_1 and R_2	Principal radii of curvatures of the mid-surface
\mathbf{r}	Random variable
\mathbf{r}	Zero-mean random variable
t	Time
U	Strain energy
u, v, w	Displacements of a point on the middle surface
$\bar{u}, \bar{v}, \bar{w}$	Displacements of a point
V	Potential energy

$\text{Var} (.)$	Variance
W	Work done
x_1, x_2, ζ	Cartesian coordinates
\mathbf{Z}	State vector
α, β	Wavelength parameters
α_1 and α_2	Surface metrics
δ_{ij}	Kronecker delta
ε	Strain, small parameter
κ	Curvature
θ_1 and θ_2	Coefficients, slopes
Λ	Vector of unknown displacements
λ	Eigen value
ν_{12}	Poisson's ratio
μ	Mean
ξ_1, ξ_2 and ζ	Curvilinear coordinates or shell coordinates
ρ	Mass density
σ	SD
σ_i	Stresses
ϕ_1 and ϕ_2	Rotations of normal to the mid-surface with respect to ξ_1 and ξ_2
φ_i	Coefficients, shape function for i th node
ω	Nondimensionalised natural frequency
ω^*	Natural frequency
\mathfrak{R}	Matrix of differential operators

CHAPTER I

INTRODUCTION

1.1 Overview

Fiber reinforced plastics (FRPs), a group of advanced composite materials consisting of strong and continuous fibers embedded in a polymer matrix, have been developed over the last 3 decades and used for a great variety of engineering applications in aerospace, mechanical, civil, chemical, and other industries. FRPs have outstanding mechanical properties, such as high strength and stiffness to weight ratios, excellent corrosion resistance, and very good fatigue characteristics, and are being increasingly used in aerospace structures. Because of the above properties, these materials open up new challenges for applications, which however, invite new mathematical complexities for the analyst/designer.

Structural materials can be divided into four basic categories: metals, polymers, ceramics, and composites. Composites, which consist of two or more distinct materials combined in a macroscopic structural unit, are made from various combinations of the materials. Although many man made materials have two or more constituents, they are generally not referred as composites if the structural unit is formed at the microscopic level rather than at the macroscopic level. Thus, metallic alloys and polymer blends are usually not classified as composites.

Composites are generally used as load carrying members because they have desirable properties that cannot be achieved by either of the constituent materials acting alone. The most common example is FRPs consisting of reinforcing fibers embedded in a binder or matrix material. Fibrous reinforcement is effective because materials are much stronger and stiffer in fiber form than in bulk form. There can be no doubt that fibers allow us to obtain the maximum tensile strength and stiffness of a material, but there are obvious disadvantages of using a material in fiber form. Fibers alone cannot support longitudinal compressive loads and their transverse mechanical properties are generally not so good as the corresponding longitudinal tensile properties. Thus, fibers alone are generally not effective as structural materials unless they are held together in a structural unit with a binder or matrix material.

The reinforcing fibers in current use are E-glass, carbon, graphite, aramid and boron. E-glass fiber composites are widely used and their processing technologies are highly developed because of the low cost. They are being used in many structures like hulls of speedboats, antennas, sport goods etc. where the stresses encountered are not high. Carbon/graphite fibers have superior stiffness, better fatigue strength, low thermal expansion coefficient, and good heat resistance. Their performance is good under compression as well as tensile loads. Carbon fibers are being widely introduced into aerospace industry for primary structures because of these advantages. Kevlar (aramid) fibers have very high tensile strength combined with low density, high toughness, and high tensile modulus. However, they have low compressive strength. In view of the above, they are not suitable where compressive strength properties are important. Composites with boron fiber, have excellent compressive as well as tensile characteristics, and are used primarily in aerospace applications where high temperatures are encountered. In certain situations hybrid composites are employed to take advantage of the superior properties of different type of fibers. In many

cases use of hybrid composites result in weight and cost saving when compared to structures made up with a single type of fibers only.

The need for fiber placement in different directions according to the particular application has led to various types of composite, namely continuous fiber, woven fiber, chopped fiber, random fiber and hybrid composites. In the continuous fiber composite laminate, which is being widely used, the individual continuous fiber/matrix laminae are oriented in the required directions and bonded together.

The building block for a structure is a lamina. However, lamina being very thin, cannot be employed for withstanding external transverse loads. In addition to this the desired properties of a structure are also needed. For these reasons, laminae are stacked together in preferred sequence to make a laminate.

A large number of parameters are involved in manufacturing and fabrication of composite components when compared with manufacturing of metallic components. Normally, manufacturing of a continuous fiber reinforced composite structures like a panel, involve the various stages listed below:

- Laminate lay up sequence design
- Actual laying up with design fiber orientation and the individual lamina thickness
- Curing.

Having complete control at each stage of manufacturing is very difficult. This leads to dispersion in the system properties. The main sources introducing variability of properties in composites can be listed as follows [1]:

- Inherent and production related fiber and matrix property dispersion;
- Variations in intermediate materials e.g., prepegs, sheet molding compounds;
- Variation in fabrication process;
- Local and overall variations in fiber volume fraction;

- Variations in fiber orientation resulting from various sources such as resin flow and poor initial placement;
- Voids.

In resin-matrix composites, the properties of matrix materials are strongly dependent on the processing condition [1]. The influence of processing conditions has been clearly brought by Maekawa et al. [2]. The differences in various properties of laminates processed under similar conditions are shown in Fig. 1.1 [2]. Fiber-matrix interface properties are strongly dependent on the processing of the fibers and curing cycle of the composite. Strength of the fiber matrix interface plays an important role in determining the properties of the composites. Thus, owing to the inherent uncertainties involved in manufacturing/processing techniques of composites, the end product can have significant variations in the properties about the desired values.

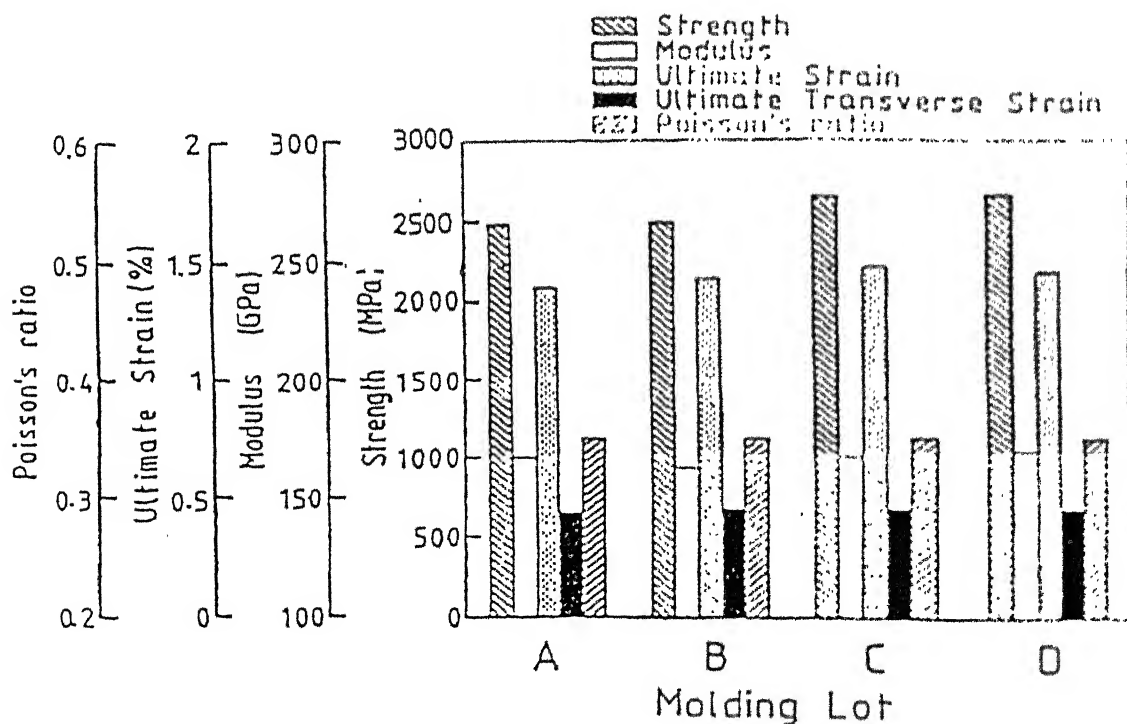


Figure 1.1: Influence of molding lot series on four mechanical characteristics of a CFRP laminate [2].

Experimental data from various sources [1] also endorse these observations (Table 1.1). It is important to note that the data from different divisions of the same company show the dispersion in properties. Non-standard testing method could also be one of the reasons for such uncertainties. The variability in characteristics of the basic building blocks of laminates—the fibers and the matrix materials may add to the dispersion in the properties of the end product. It can, therefore, be concluded that variability in properties at the micro level is finally reflected at the macro-level in form of lamina properties.

Table 1.1: Variation of reported unidirectional properties for a widely used Graphite/Epoxy system, from five sources (Sources: Major Airframe Company Reports) [1]

Property	1	2*	3*	4	5	Max. Diff. %
Elastic Constant ($\times 10^6$ psi)						
• Long. Tensile modulus	20.8	18.1	21	20.6	18.5	16
• Long. Compr. Modulus	18.6	14.5	21	19.8	18.5	45
• Trans. Tensile modulus	1.9	1.8	1.7	1.3	1.6	46
• In-plane shear modulus	0.85	-	0.65	0.8	0.65	31
• Poisson's ratio	0.30	-	-	0.32	0.25	28
Strength Properties ($\times 10^3$ psi)						
Long. Tension	274	190	180	164	169	67
Long. Compression	280	126	180	126	162	122
Trans. Tension	9.5	5.2	8	5.4	6.0	83
Trans. Compression	39	-	30	21	25	86
In-plane shear	17.3	-	12	8.4	-	106
Inter-laminar shear	-	13.5	13	-	7.1	90

* Divisions of the same company

Normally, in the classical method of structural analysis, the system is modeled by assuming the various parameters involved like system characteristics, boundary conditions etc., to be deterministic. Usually during the initial modeling of the structure, the concept of

factor of safety is introduced at different stages. It is expected that uncertainties that cannot be quantified are accounted for through the use of factor of safety.

In real situation, the system parameters are seldom deterministic. Most of the parameters can be accurately expressed in a probabilistic sense only. Thus, we can have different class of problems in which the parameters involved in the analysis are either deterministic or probabilistic or a combination of the two. When the system parameters are uncertain, the derived response parameters like deflection, natural frequencies, buckling loads, dynamic response etc. are also random being function of these basic system parameters. Depending on the sensitivity of the response parameter to the input random variables and the statistics of the input random variables, the statistics of the response parameters can vary. In certain structures this can cause mode localization [3]. The actual stress and deflection may be beyond acceptable limits. A probabilistic approach yields a more accurate prediction of the system behavior and will result in a superior design. The risk of failure of the structures and its performance statistics can be evaluated accurately by adopting a probabilistic approach. As brought out earlier, all these observations are more pertinent to composites in comparison to metallic materials. It may be further argued that a simple factor of safety term introduced during the design process cannot take into account all the effects of property variability found in composites. The allowable stresses for conventional structural materials can be expected to be very close to their respective mean values. This is because of the scatter in these properties is confined to a very narrow domain about the mean value resulting in a small standard deviation (SD), owing to the effective control of the manufacturing/fabrication processes which have fewer parameters, as compared to composites. However, in the case of composite, inspite of effective quality control in manufacturing/fabrication processes, as we normally do in sensitive applications like aerospace, etc., the design stresses will normally have to be much less than respective mean

values, due to widely scattered data [1]. A behavior similar to this can be expected in the case of composite material basic characteristics like elastic moduli, Poisson's ratio, etc. Finally, all these would negate the basic idea of weight optimization, which is one of the important part of design consideration particularly in aerospace projects.

Composite materials are going to be used extensively in primary and secondary structures in aeronautical and space projects, like advanced aircrafts, helicopters, space stations etc. Computer simulations of some of the proposed configurations of such aeronautical and outer space installations often show closely packed/overlapping natural frequencies in some of the components. In such cases, even the slightest shift in characteristics of the components can have pronounced effect on the response of the structures.

Considerable results exist in literature on the distribution of ultimate tensile strength of FRPs [4,5,6]. Similar results on dispersion of the elastic modulus, Poisson's ratio, shear moduli, etc. is limited. Maekawa et al. [2] have presented some experimental results on the distribution of various composite laminate properties like Poisson's ratio, strength, modulus, etc. The detailed study brings out the effect of curing, processing etc. on the material parameters of composite and their reliability. As mentioned earlier, uncertainties in several factors like the fiber volume fraction, fiber orientation, void volume, fiber matrix interface parameters etc. have significant effects on the response of fiber-reinforced composites. The uncertainties in the factors mentioned above are in turn reflected on the characteristics of the lamina stiffness parameters like the longitudinal modulus, transverse modulus, in-plane and out-of-plane shear moduli, Poisson's ratio etc. These can be treated as primary variables, since these are the basic parameters of the laminate that are usually considered for formulation of any structural analysis problem. At this stage it is relevant to mention that point-to-point variations of these properties over the structure particularly in composite made

of prepegs, which is normally the case in large scale manufacturing of composite structures, are very small. These facts have been verified experimentally [7]. These considerations indicate the need for a more accurate probabilistic approach in the analyses of these sensitive composite structures.

Apart from randomness in material properties, there could be randomness in loading, geometry and boundary conditions. The external loading in engineering problems is influenced by many parameters that, in general are not under control and, is, therefore, random in nature. Some examples are, acoustic loading on aircraft, rocket and spacecraft panels, runway roughness, jet and rocket exhaust noise, water pressure on ship and submarine hulls during high-speed operations and under water explosion.

For reliability of design, specially for sensitive engineering applications, accurate prediction of system behavior of the structures made up of composites in presence of randomness in system properties as well as excitations favors a probabilistic analysis approach for composites by modeling their mechanical properties as random variables (RVs) and the excitation as a random process. Laminated composite panels are being widely used in construction of automobile, mechanical, space, and marine structures in recent years. The accurate analysis of these structures is an important field of current area of research.

1.2 Available Techniques

A limited literature is available on the analysis of composite structures with uncertain parameters subjected to random loading. From the methodological point of view, stochastic analysis can be classified into two groups of approaches. The first group is statistical approach, including the Monte Carlo simulation (MCS); the second group is non-statistical approach such as perturbation method, second moment analysis, and the local integral method. The expansion method like Neumann is another MCS technique, where the handling

of the system matrix is improved by introducing Cholesky's decomposition scheme, thus reducing the computation time required in the MCS. Usually real life structures are so complex that it is not possible to analyse them with classical methods. Deterministic finite element method is combined with statistical approaches and/or non-statistical methods so that the complex structures with uncertain parameters subjected to random loading can be analysed. This is referred to as stochastic finite element method. In this the randomness in material parameters are considered at the element level itself, if material parameters are modeled as random field. If the material parameters are modeled as random variable, every element has same statistics of random variable to describe the system behavior. Similarly the case of loading randomness - particularly spatial variation, can be discussed.

The usefulness of the MCS is based on the fact that the next best situation to having the probability distribution function of a certain quantity is to have a corresponding large population. The implementation of the method consists of numerically simulating a population corresponding to the random quantities in the physical problem, solving the deterministic problem associated with each number of that population, and obtaining a population corresponding to the random response quantities. This population can then be used to obtain statistics of the response variables.

The Monte Carlo method is quite a versatile mathematical tool capable of handling situations where all other methods fail to succeed. The method has been known and used extensively in various fields such as health care, agriculture, and econometrics. However, in engineering mechanics it has attracted intense attention only recently following the widespread availability of inexpensive computational systems. Shinozuka and Jan [8] have played a pioneering role in introducing the method to the field of engineering mechanics. They have suggested simulating a random process as the superposition of a large number of sinusoids having a uniformly distributed random phase angle. Later, Shinozuka [9] used fast

Fourier transform (FFT) algorithm in conjunction with the MCS to achieve a more efficient implementation of the simulation procedure.

The perturbation approach as applied to problems of random media is extension of the method used in nonlinear analysis [10,11]. Given certain smoothness conditions, the functions and operators involved can be expanded in a Taylor series about their respective mean values. This kind of expansion is valid only when the randomness is very small as compared to the mean values. This condition, however, is satisfied in most of the engineering problems particularly in aerospace applications and hence, the approach can generally be adopted for almost all practical situations. The expanded forms of the terms are introduced in the system equations. The different order of solution can be separated from this expanded form. These solutions can be combined to get the complete solution of the problem as the characteristics of the response. The consideration of number of terms in the expanded form depends on the level of fluctuation in the random quantity. More number of terms should be included in the equations depending on the magnitude of the random fluctuations. This task is considerably complicated, thus greatly limiting the applicability of the method. Further, secular terms appear in higher order expansions. These are terms for which the magnitude increase with increasing approximation orders, thus causing the expansion to diverge. For small fluctuation as is generally the case in composites, first two terms would be sufficient. This fact has been brought clearly in the present study as well.

The method has been applied extensively in recent years to problem involving random media, particularly, structures made of isotropic materials. Nakagiri and Hisada [12], Hisada and Nakagiri [13], and Liu et al. [14,15,16] have applied the method to linear and nonlinear problems of statics and dynamics.

1.3 Motivation For The Present Study

The analysis of structures with deterministic characteristics to random external excitations is well established and has been studied for large class of problem [17]. However, the structural response of curved and flat panels with random material parameters to deterministic as well as random excitation is quite complicated and still not fully understood. This is particularly true for free and forced vibration and buckling of composite curved panels and plates. An exhaustive survey of the literature indicates that a large number of publications have appeared on the subject for isotropic beams and plates. However, the response of laminated composite curved panels and plates are not fully addressed. Further, the limitations of classical laminate theory (CLT), first order shear deformation theory (FSDT) and higher order shear deformation theory (HSDT) have been well understood for the deterministic analysis. However, the efficacies of these theories for second moments of structural response are at a nascent stage and still not developed at all. Based on deterministic analysis, it is generally believed that for thick laminates, the shear deformation theory is most appropriate, while for thin laminates CLT is suitable. The literature review presented here also reveals that these aspects have not received attention of the researchers. Some concrete effort in this direction is still needed. As a matter of fact, these issues, which are at the heart of the problem, provided the motivation for the present study.

1.4 Scope Of The Present Investigation

In the present work a comprehensive study has been conducted to obtain the second – order statistics of buckling loads, natural frequencies and dynamic response of laminated composite curved and flat panels with random material properties subjected to deterministic as well as random excitations. Higher order shear deformation theory has been used to model

the system behavior. The efficacies of various theories have been examined particularly towards variances in the structural response. The exact mean analysis (classical approach) and finite element method in conjunction with first order perturbation technique have been proposed for the response analysis. The assumptions made in the present study may be enumerated as below.

- The deformations of the panel are very small in comparison to dimensions of the sides. The curved panels are shallow and projected in rectangular plan form. Hence the linear strain-displacement relations are applicable.
- Transverse normal stress is negligible.
- The transverse shear stresses are assumed to vary parabolically through the thickness and to vanish at the panel top and bottom surfaces, satisfying the traction free surface conditions. However, the first order shear deformation theory (FSDT) model assumes the transverse shear stresses to be uniform through the thickness of the laminate and hence a correction factor of 5/6 has been employed while utilizing the FSDT model.
- The lateral displacement 'w' of any lamina is given by the displacement of the mid-plane.
- A C^0 finite element formulation by assuming the slopes as a separate degree of freedom proposed in reference [18] for plate analysis has been extended for curved panel analysis. Though this increases the nodal degree of freedom, the choice of the element is made simpler.
- The material parameter has been assumed to be constant with respect to space and time. This assumption is based on the experimental observation [7] and also found to be the case in most practical applications. The lamina material parameters are modeled as basic random variables (RVs) and are assumed to be uncorrelated for generation of the results.

- Random excitation is in general a function of spatial coordinates and time. The excitation is assumed to vary deterministically in spatial coordinates and assumed to be random in time.

1.5 Thesis Outline

The investigation reported in this thesis has been divided into seven chapters, in each of which attention has been focused on a particular aspect of the afore-mentioned problem.

In *Chapter I*, an overview of the problem has been presented. The available techniques in literature for addressing problems with stochasticity are reviewed. Motivation and scope for the present study are also presented.

Chapter II includes a review of the pertinent literature available in this area.

In *Chapter III*, a general formulation of the problem has been presented that is common to all the problems studied in the thesis.

Chapter IV presents specific formulations along with description of the methodology and numerical examples related to second order statistics of buckling response of composite flat and curved panels with random material parameters.

In *Chapter V*, formulations and probabilistic analysis along with examples related to free vibration of composite flat and curved panels with uncertain material parameter is presented.

Deterministic as well as random vibration studied in *Chapter VI*. The formulations of the problem and detailed probabilistic analysis are presented with example cases.

Finally in *Chapter VII*, concluding remarks and suggestions for future studies are presented.

CHAPTER II

LITERATURE REVIEW

2.1 Introduction

Chapter I present the discussion about the nature and the complexity involved in dealing with the composites. To some extent, the problems that have been studied in the thesis were also discussed. Further, it was concluded that the literature is scanty with regard to dealing with uncertainties in material, loading etc. In this chapter, a critical look is taken at the investigations carried out by researchers in this area. From engineering mechanics perspective, the most common stochastic system problems involve a linear differential equation with random coefficients. These coefficients represent the properties of the system under investigation. They can be treated as random variables or, more accurately and with increasing level of complexities, as random processes with a specified probability structures. Mathematically, the problem can be stated as

$$\mathcal{L} x = f \quad (2.1)$$

where, \mathcal{L} is a stochastic differential operator, x is the random response vector, and f is the random excitation vector. Equation (2.1) with deterministic differential operator and a random excitation has been investigated extensively [17,19-22]. The case where the operator is stochastic is considerably more difficult and only approximate solutions to the problems

have been reported in literature. The pertinent literature may broadly be put into two main groups, which can be further classified into sub groups:

1. Investigation dealing with isotropic materials with system parameters uncertainties
 - a. Eigenvalue analysis
 - i. Buckling
 - ii. Free vibration
 - b. Forced vibration response
 - i. Deterministic excitation
 - ii. Random excitation
2. Investigation dealing with fiber reinforced composite materials with system parameters uncertainties
 - a. Eigenvalue analysis
 - i. Buckling
 - ii. Free vibration
 - b. Forced vibration response
 - i. Deterministic excitation
 - ii. Random excitation

2.2 Isotropic Materials

The detailed treatment of probability theory and its application to theory of structures made of conventional isotropic materials with system parameters uncertainties for static and dynamic analyses can be found in Ref. [23].

Ibrahim [3] has reviewed the work published in the area of vibrations of structures with parameter uncertainties. These include direct problems such as random eigen values and random responses of discrete and continuous systems. The impact of these problem on

related areas of interest such as sensitivity of structural performance to parameter variations, design optimization, and reliability analysis has also been addressed. The reviews also include results of experimental investigations, the phenomenon of normal modes localization, and the effect of mistuning of turbomachinery blades on their flutter and forced response characteristics.

Manohar and Ibrahim [24] have reviewed number of topics on various formulations and solution techniques for structural dynamic problems with parameter uncertainties beyond the work reported in Ibrahim [3]. Different types of uncertainty modeling have been described in terms of material and geometrical properties. These models are based on the probability distribution being either Gaussian or non-Gaussian. It has been found that computational stochastic algorithms including SFEM and MCS are the currently popular approaches in the studies reported. Analytical developments of the random eigenvalue problems are reviewed with reference to typical structural elements. These developments include implementation of statistical energy analysis (SEA), stochastic boundary element method, and interval algebra. Other topic includes forced vibration of single and multi-degree of freedom systems including non-linear systems, localization in disordered periodic structures, and experimental results. Computational stochastic mechanics has been found to have several industrial applications including aerospace, automotive and composite structures elements.

Vaicaitis [25] has presented the analysis for free vibration of clamped-clamped beams with non-uniform and random flexural rigidity (EI) and random mass (ρA), along the axis of the beam. Two-variable perturbation expansion method has been used for the analysis. The spatial random variables have been simulated on a digital computer using the MCS. The results of first three modes for random variations in EI and ρA (case 1) and random variation in EI (case 2) have been obtained along with the results of homogeneous uniform beam. The

accuracy of the method increases with higher frequencies. It is observed that for the particular choice of ρA and the degree of random fluctuations used for numerical computations, frequencies and modes deviate significantly from that for a beam with uniform characteristics. The considerable difference in the results for case 2 is due to the fact that gradual change in the beam stiffness is permitted for this case.

Manohar and Iyengar [26] have discussed a procedure to obtain probability distribution function (PDF) of eigenvalues of simple structural systems like bars, strings, shafts etc. associated with the one dimensional stochastic wave equation which takes into account randomness in specifying mass and stiffness as well as the boundary conditions. They have employed the stochastic averaging method for obtaining the solutions. Expressions for moments of the eigenfunctions and also for joint PDF between two distinct eigenvalues have been obtained. In the numerical example a string which is fixed at the two ends and whose mass varies randomly along the length has been considered to illustrate the working of the approach. Here, the simulation results corresponding to two different mass processes having the same mean and power spectral density (PSD) functions but different PDF have been compared with the theoretical solutions. Since both the processes have the same mean and covariance they lead to the same theoretical solutions. It is observed that the theoretical solution do not compare well with the simulation results when the randomness is non-Gaussian. On the other hand, the comparison is quite good for a Gaussian random process.

Shinozuka and Astill [27] have reported free vibration studies of beam-columns with elastically restrained supports. They have considered random variation of spring constant, axial force, and distributions of material and geometric properties. Second order statistics of eigenvalues have been obtained using a perturbation technique. The computed results have been compared with MCS. It has been shown that perturbation approximation is acceptable for cases where the properties vary randomly within a small range.

Astill et al. [28] examined the problem of impact loading of structures with random geometric and material properties. Their approach is a combination of finite element method and Monte Carlo simulation. For the case of anti-symmetric concrete cylinder they have assumed spatial distributions of Young's modulus and density for each realization of the test sample. Each test cylinder was subjected to same axial impact loading. The algorithm, for a sample size of 100, gives the maximum stress intensities from which the sample mean and standard deviation were computed. For a certain intermediate location of the test cylinder it was found that the axial stress is always different from the corresponding stress in a uniform cylinder.

Elishakoff et al. [29] have developed deterministic governing equations and boundary conditions for mean and covariance functions of displacement for statically determinate beam with stochastically varying stiffness but with deterministic loading. The variational principles have been adopted with Galerkin's and Rayleigh-Ritz methods to find the probabilistic characteristics of the response. Several problems with stochastic stiffness have been exemplified. They have suggested that the displacement corresponding to an associated deterministic beam, which possesses same geometry and load as the original beam but has a deterministic stiffness, be adopted as the trial functions in Galerkin or Rayleigh-Ritz formulation. The numerical examples have clearly illustrated that the proposed method is not based on perturbation, and correctly matches the exact solutions. Most importantly, this method does not have the disadvantage of conventional analysis like SFEM, etc. The method is valid for any level of variation of the stochastic parameters.

Ren et al. [30] have proposed a new kind of finite element for bending of statically determinate beams (Euler-Bernoulli type) with spatially varying random stiffness under deterministic loading. They have obtained mean and variance of displacements at the middle and along the axis of SS beams subjected to uniform loading. The results have been

compared with that of first order perturbation technique (FOPT). For small values of coefficient of variation of stiffness the two results are quite in agreement.

Hien and Kleiber [31] have formulated a stochastic Hamilton variational principle (SHVP) for dynamic problems of linear continuum. The SHVP allows incorporation of probabilistic distributions in the finite element analysis. The combinations of the second moment analysis and the fold mode superposition have been used for stochastic analysis. These have been simplified by transformation of correlated RVs to a set of uncorrelated RVs through standard eigenproblem. A procedure based on Fourier analysis and synthesis has been used to eliminate secular terms from perturbation approach. Second order statistics of the response has been obtained for the following cases (i) cantilever beams subjected to axial load with spatially varying random modulus of elasticity, (ii) plates with all edges simply supported or clamped with random thickness subjected to concentrated center load and (iii) two degree of freedom spring –mass system with random spring constants subjected to sinusoidal forcing functions. The results have also been compared with MCS and are found to be quite satisfactory up to 20 percent variation of the random parameter.

Singh and Lee [32] have employed direct product technique to obtain statistical properties of frequencies for spring-mass damper system with randomness in damping subjected to random excitation amplitude with deterministic frequency. The results have been compared with MCS and FOPT results.

Lee and Singh [33] have further employed the same technique for estimation of second order statistics of eigensolutions for different degrees of freedom of damped/undamped spring –mass system with stiffness and mass as random parameters. The results have been compared with MCS. It has been found that up to 20 percent of coefficient of variation (COV) of mass, the results are in close agreement with MCS. However with first order perturbation, it is in agreement with MCS only up to 10 percent COV.

In another paper, Lee and Singh [34] have also obtained the dynamic response of a linear time invariant, proportionally damped vibrating system of N dimensions with uncertain parameter matrices M , C and K . Each matrix is assumed to be symmetric and positive definite. They have also assumed that the amplitude of excitation is randomly distributed, but the time history, represented by, impulse and sinusoidal functions is deterministic and arbitrary. The first example studied by them is an undamped single degree of freedom system subjected to unit impulse excitation with uniformly distributed random stiffness. Standard deviations of the impulsive response are found to be in reasonably good agreement with MCS except that the oscillations in simulation response die out slowly. The second example considered is a damped single degree of freedom system with random stiffness. The results obtained with proposed technique are very close to MCS results as compared to FOPT. They have observed that small fluctuations in damping ratio do not affect the impulsive response significantly.

A general approach for solving the statistics of the eigenvalues has been presented by Collins and Thomson [35]. This method can take into account correlation between matrix elements and provides statistics of eigenvalues and eigenvectors. Linear equations for dynamic system have been formulated for finding the statistics of eigenvalues and eigenvectors. The approach has been validated by an independent MCS.

Caravani and Thomson [36] have brought out the influence of damping uncertainty on the frequency response of a multi degree-of-freedom system. A statistical linear model has been presented to obtain second order statistics of the response. A hypothesis regarding the statistical correlation of damping coefficients has also been presented. Validation of the presented model has been done by MCS. The technique is applicable to different forms of damping and other system parameters.

Chen and Soroka [37] have studied the response of a multi-degree of freedom dynamic system with statistical properties to deterministic excitation. The perturbation technique has been used for the formulation. Response statistics has been obtained. To show the effect of stiffness variations, the results have been compared with the response of the system without stiffness variations. It is observed that the probabilistic excitation always provides larger response values than the deterministic excitation. In yet another paper [38] they have looked into the case of impulse response of an analogous system employing a similar technique. Statistical moments of the impulse response function have been obtained.

Mok and Murray [39] have investigated the free vibration of a slender bar with slightly different characteristics from those of a uniform bar. A simple, approximate solution obtained by ignoring the higher order terms and their products with varying system parameters like area of cross section, elastic modulus, density etc. has been presented. Experimental results, obtained for free-free flexural vibrations, have been found to agree well with the theoretical predictions.

Grigoriu [40] has detailed a method for calculating probabilistic characteristics of the eigenvalues of stochastic symmetric matrices. Perturbation technique has been used for obtaining approximate expressions for eigensolutions. Several examples from dynamics and elasticity have been solved. The results have been compared with exact solutions.

The exact expression of the stochastic stiffness matrix of the structure is obtained by Deodatis [41] in terms of integrals of the stochastic field describing the random material properties multiplied by a deterministic shape function. These integrals are RVs and are called as weighted integrals. Two approaches, one based on principle of stationary potential energy and the other based on principle of virtual work, have been used. The above approaches in conjunction with FEM have been used to evaluate the response. The response variability and safety index of stochastic framed structures have been obtained by Deodatis

and Shinozuka [42] using the approach presented in [41]. They have employed the first order Taylor series expansion for the response variability and FOSM for safety index.

Bucher and Brenner [43] have described a method for analyses of structural systems with random properties subjected to dynamic loading. They have used the weighted integral technique. Mass and stiffness terms have been expanded in terms of weighted integrals. MCS and response surface method have been used to determine the threshold exceedence probabilities of the response.

A methodology for analyzing structures with random stress-strain behavior has been presented by Millwater et al. [44]. This methodology characterizes the uniaxial engineering stress-strain curve by five engineering parameters. The parameters are elastic modulus (E), engineering stress at initial yield (σ_y), initial plastic hardening slope (h_y), engineering stress at the point of ultimate load (σ_u) and engineering strain at the point of ultimate load (ϵ_u). Letting these parameters to be random will simulate uncertainties in the stress-strain behavior of a structure. This methodology has been integrated into the NESSUS (Numerical Evaluation of Stochastic Structures Under Stress) probabilistic structural analysis system. With this system, probabilistic finite element analysis of structures with random stress-strain behavior can be analyzed in an automated fashion. Thus, reliability of complex structures with non-linear stochastic material behavior can be computed. As an example, problem of a thick cylinder under internal pressure has been taken. The internal pressure and stress-strain curve is random. The stress-strain parameters have been modeled as lognormal distribution with correlation. The response quantity is the cumulative distribution function of the equivalent plastic strain at the inner radius. They have also computed the probabilistic sensitivity or relative importance of the random variables.

Chen and Zhang [45] have described a method to determine the response sensitivity for complex stochastic structures subjected to arbitrary deterministic excitation. The

probabilistic problem has been converted into a deterministic one using a perturbation technique (PT). The response sensitivity has been calculated with respect to parameters like beam cross-sectional area, plate thickness etc.

A technique for computing the instantaneous transient response statistics of undamped linear multi-degree of freedom system subjected to arbitrary deterministic excitation, when random uncertainties are introduced into the stiffness matrix, has been described by Prasthofer and Beadle [46]. The PT has been used to model the uncertainties. The response uncertainty has been presented as a function of the model uncertainty for an impulsive excitation function.

A method has been presented by Bliven and Soong [47] for analysis of natural frequencies of elastic beams having randomly varying characteristics. The method is based on a lumped parameter model. The uncertainties may be due to material inhomogeneities or geometrical imperfections. Statistics of natural frequencies of a SS beam have been obtained for stiffness varying randomly with position along the beam.

Zhang and Chen [48] have presented a method to estimate the standard deviations of eigenvalue and eigenvector of random multiple degree of freedom (MDOF) systems. The method can be applied not only to the MDOF systems with distinct eigenvalues, but also to multi degree of freedom systems with uncertainties in mass and stiffness matrix elements. They have used both the sensitivity and the perturbation technique to develop the methodology. Example of free vibration analysis with mass modeled as random variable have been presented for obtaining the mean and standard deviations of the first six eigenvalues and two eigenvectors for a beam problem and the first three eigenvalues and two eigenvectors for a truss problem.

Low [49] has analyzed beams with arbitrary boundary conditions. A straightforward root- searching algorithm has been presented for the eigenproblem of the beam system. The

ends of the beam are generally attached to prescribe mechanical components. The system frequency equations have been obtained by incorporating the boundary conditions. Given the beam model, the implicit form of the frequency equation can be solved symbolically for the exact roots, which then have been used for evaluating the natural frequencies followed by the associated mode shapes. They have found that the analytical results are in close agreement with experimental results. This is due to the fact that the exact boundary conditions were incorporated into the system frequency equation.

Vanmarke and Grigoriu [50] have presented results on the study of beams with rigidity varying randomly along the axis. Static analysis of a cantilever beam with uniformly distributed and a concentrated load on the tip has been performed using FEM. Random elastic characteristics of each element have been represented by the local spatial average over the element, with the correlation function represented by a parameter called scale of fluctuation. Second order statistics of deflection have been evaluated using the approach.

A general procedure for formulating problems involving random fields, using probabilistic FEM has been described by Liu et al. [51]. The random field has been discretized into a mean vector and a co-variance matrix. To reduce computational efforts, the above correlated vector has been transformed into an uncorrelated vector using an eigenvalue orthogonalisation. The method has been applied to several problems, including a two-dimensional plane-stress beam-bending problem. An independent MCS technique has been employed to check the results. In another paper Liu et al. [15] have described a finite element method applicable to truss structures for determination of the probabilistic distribution of the dynamic response of trusses due to material and geometric variations.

A solution for free vibration response of thin plates supported on non-uniform lateral elastic edge supports has been obtained by Gorman [52]. Method of superposition has been used. The stiffness of elastic supports can have any distribution along the edges including

discontinuities and local concentrations. Results have been presented for square and rectangular plates.

Iwan and Jenson [53] have developed a general methodology for solving a partial differential equation with random coefficients. They have introduced random shape functions to approximate the solution in spatial domain and in random space. A system of linear ordinary differential equations are derived using weighted residual method, by means of the spectral decomposition of the covariance matrix. The random field is described in terms of uncorrelated RVs. A FEM has been used in conjunction with the proposed method to obtain the full solution of several problems. The second order statistics of the dynamic response has been evaluated. In another paper Jenson and Iwan [54] have analyzed MDOF linear system with uncertain parameters to stochastic excitations. The excitation has been modeled as modulated Gaussian white noise process and the uncertain parameters modeled as RVs. A method based on an expansion of the response in terms of a series of orthogonal polynomials that depends on the coefficient of the spectral decompositions of the uncertain parameters have been developed. Modified Euler method has been used for obtaining the solutions. Second order statistics for dynamic response has been obtained for primary-secondary system. It has been found that uncertainties in stiffness parameter may have a strong influence on the response of secondary system.

Chen et al. [55] have presented a probabilistic method to evaluate the effect of uncertainties in geometrical and material properties of structures on the random vibration response. The FOPT has been used to deal with randomness in system parameters. They have also conducted the sensitivity analysis. Truss and beam problems have been considered to illustrate the working of the approach. They have obtained mean and SD of the response for the two problems investigated. The method proposed is more accurate compared to other

methods, but needs a great deal of computational efforts, and hence it is often used for comparison purposes rather than as a practical engineering tool.

Zhang and Ellingwood [56] have studied the elastic stability of structural members and frames with uncertain material properties. The uncertain properties are modeled as continuous random field by a series expansion involving orthogonal functions. The SFEM with FOPT/and or second order PT has been used for obtaining the results. The effects of the correlation length of the random field and the coefficient of variations of rigidity on the mean and scatter of the buckling response have been obtained. The results have been compared with MCS results.

Shinozuka [57] has obtained the response variability of statically determinate structures arising from homogeneous one-dimensional uni-variate material property fields. Utilizing Green's function formulation that uses the first order second moment method (FOSM), the upper and lower bounds of the static response variability have been obtained for bar and beam problems.

Bucher and Shinozuka [58] have extended the earlier work of Shinozuka [57]. In this, the response variability of linear structures due to spatial variation of elastic properties subjected to deterministic and random loading have been investigated. They have considered statically determinate/indeterminate beams and 2-D structures as examples for their study. Green's function formulation along with FOSM has been used in this work. The second order statistics of static response have been obtained and validated with that of MCS.

Kardara et al. [59] have further extended the work of Bucher and Shinozuka [58]. They have considered the same approach for evaluation of response variability of a beam with a higher degree of indeterminacy and multi-bay multi-story frames due to spatial variation of geometry or material properties. The coefficient of variation of structural response has been obtained and compared with MCS.

Deodatis and Shinozuka [60] have developed a methodology to analytically and numerically evaluate the spectral distribution free upper bounds of the response variability of stochastic systems. The structural systems examined consist of linearly, elastic, statically determinate and indeterminate beams subjected to static loads. They have used variability response function approach for analytical evaluation of these bounds and fast Monte Carlo simulations for numerical evaluation.

Wall and Deodatis [61] have extended weighted integral method [41] and the concept of response variability function [60]. They have obtained the response variability in terms of response quantities and the reliability in terms of safety index of two dimensional plane stress-strain stochastic problems. As an example a square plate subjected to in plane loading with random elastic modulus has been considered to illustrate the working of the approach. Elastic modulus has been modeled as a homogeneous stochastic field.

Lawrence [62] has applied Galerkin's method to random operator equations. Appropriate Hilbert spaces are defined for random functions and solutions are projected into these spaces, allowing the first and second moment properties of the solution to be calculated. An equivalent energy based approach similar to Raleigh-Ritz method is developed from which a SFEM is derived. Several one and two dimensional example problems are solved and the results discussed.

Yamazaki et al. [63] have obtained the structural response variability resulting from the spatial variability of material properties of structures subjected to static deterministic loads. The spatial variability is modeled as two-dimensional stochastic fields. They have used three approaches namely FEM with direct MCS, FEM with Neumann expansion in conjunction with MCS and FEM with perturbation technique for mean and SD of response of the framed structures. For the analysis of frame, they have assumed elastic modulus to be Gaussian and loading to be deterministic. It has been found that a second order PT can

improve the results of FOPT only a little, however an enormous CPU time is required as compared to direct MCS. A FOPT results may be quite useful depending on the type of stochastic fields to which the material property in question subscribe. However, the results should be verified by MCS techniques.

Ghanem and Spanos [64] have presented a new method for treating problems involving random media. A complete basis in Hilbert space of random functions is identified. This basis consists of the polynomial chaos, which is an orthogonal polynomial in white noise. The response is expressed as a convergent series along this basis. The method provides a natural extension for deterministic FEM to problems exhibiting random system behavior. The proposed method has been applied to a plate problem involving random variation in the material properties and to a problem of a beam on a random elastic foundation subjected to a random dynamic loading. Good agreement between the results obtained by the proposed method and pertinent MCS results over a wide range of random fluctuations level has been observed.

Spanos and Ghanem [65] have proposed a new method for the solution of problems involving material variability modeled as a stochastic field. The method makes use of the Karhunen-Loève expansion to represent the random material property. The expansion is a representation of the field in terms of a finite set of uncorrelated RVs. The resulting formulation is compatible with FEM. A Neumann expansion is subsequently employed to obtain a convergent expansion of the response process. The usefulness of the proposed approach, in terms of efficiency and accuracy, is exemplified by considering a cantilever beam with random rigidity. The derived results pertaining to the second order statistics of the response are found in good agreement with those obtained by a MCS solution of the problem.

Li et al. [66] have identified and discussed the uncertainties associated with structural parameters and dynamic loading. The structural parameter uncertainties have been treated as

random variables and dynamic wind load has been simulated as a random process. Dynamic wind-induced response of structures with parameter uncertainties is investigated by using SFEM. They have also derived a formula for structural dynamic reliability analysis considering the randomness of structural resistance and loading. Two examples of high-rise structure have also been discussed to illustrate the approach. The calculated results demonstrate that the variation in structural parameters indeed influences the dynamic response and the first passage probability evaluation of structures.

Gupta and Joshi [67] have developed a response spectrum based on stochastic approach for analyzing the earthquake response of structures with uncertain parameters. For this purpose, they have derived the expression for the variances of the root mean-square values of various response quantities at different levels for a multi-degree-of-freedom structure in terms of the covariance of the modal parameters of the structure. They have established the validity of the proposed method by computing a large number of results and comparing them with the corresponding exact results obtained by MCS.

Graham and Siragy [68] have studied the variability of the random buckling loads of beams and plates with stochastically varying material and geometric properties using concept of the variability response function. The elastic modulus, moment of inertia and thickness are assumed to be described by homogeneous stochastic fields. They have obtained expressions for the buckling load and spectral-distribution free upper bounds of the buckling load variability. Examples of beams, unstiffened and stiffened plates have been used to illustrate the technique.

Handa and Anderson [69] have presented a FEM, which estimates the mean values, standard deviations and correlation coefficients of structural displacements, and stresses by taking into account variations in applied loads, dimensions and material properties. A cantilever beam made of steel and wooden roof truss have been considered for the numerical

study. They have found that the degrees of correlation in the primary random variables (applied loads, Young's modulus etc.) can considerably influence the failure risk.

Zhu et al. [70] have presented a formula for statistics of the local averages of random vector fields. The SFEM based on the local averages of random vector fields have been formulated for static, eigenvalue, and stress intensity factor problems. Numerical examples showed that the SFEM based on local averages of random fields generally provides more rapid convergence with increasing number of elements than the SFEM based on mid-point discretization. The convergence of the results depends on the geometry of the element mesh. As in deterministic FEM, the convergence also depends on the order of the interpolation functions used for defining the elements.

Chakraborty and Dey [71] have characterized the real life structural systems by the inherent uncertainty in the definition of their parameters in the context of both space and time. They have proposed a SFEM in the frequency domain. The harmonic forces as well as earthquake-induced ground motion are treated as random process. The uncertain structural parameters are modeled as homogeneous Gaussian stochastic field and discretized by the local average method. The discretized field is simulated by the Cholesky decomposition of respective covariance matrix. Neumann expansion method is introduced in the finite element procedure within framework of MCS. Numerical examples are presented to elucidate the accuracy and efficiency of the proposed method with the direct MCS.

Lei and Qui [72] have presented a method for the dynamic analysis of structures with stochastic parameters to random excitation. They have also presented a procedure to derive the statistical characterization of the dynamic response for structures using dynamic Neumann stochastic FEM. Random equation of motion for structures is transformed into quasi-static equilibrium equation for the solution of displacement in time domain. Neumann expansion method has been used to derive the statistical solution of such a random system,

within framework of MCS. The results are compared with the first order and second order stochastic finite element method and the direct MCS. Numerical examples are examined to show that the approach proposed has a very high accuracy and efficiency in the analysis of compound random vibration.

From the foregoing literature survey, it is observed that almost all the work in this area is related to isotropic materials. In the next section we present a survey of the literature with regard to fiber reinforced composite materials.

2.3 Fiber Reinforced Composite Materials

Very little information is available in open literature for response of structures made of fiber reinforced composite materials, with uncertain system parameters subjected to deterministic or random loading.

Nakagiri et al. [73] have presented a methodology of SFEM applied to uncertain eigenvalue problem of linear vibration, which arises from the fluctuation of the overall stiffness due to uncertain variation of the stacking sequence. The problem has been formulated in the frame of linear elasticity and Kirchhoff-Love's theory of small deflection. The uncertain stacking sequence has been modeled as a random variable, while all the material constants are taken as deterministic. Mean centered perturbation technique has been employed to handle the random behavior. Numerical analyses have been carried out for simply supported graphite-epoxy plates. Second order statistics of the eigen frequency has been obtained.

Engelstad and Reddy [74] have described a probabilistic micro-mechanics approach based on non-linear analysis procedure to predict the variability in the properties of metal matrix composites. MCS, with assumed probabilistic distribution of properties-like fiber,

matrix and inter phase properties, volume and void ratio, strengths, fiber misalignment etc. – have been used to predict the statistics of resultant lamina properties.

Martin and Leissa [75] and Leissa and Martin [76] have studied the problem of plane elasticity, static, buckling and dynamic analysis of composite lamina with variable fiber spacing. The volume fraction has been assumed to vary according to some known functions. This results in variation of elements of stiffness matrix across the width of the lamina. The plane stress problem of such a lamina is governed by a partial differential equation with variable coefficients. Energy method has been used for formulating the problem. Several free vibrations and buckling problems have also been solved. The non-uniform distribution of fibers is found to increase the buckling load by as much as 38 percent and the fundamental frequency by about 21 percent.

Adali et al. [77] have discussed the problem of maximization of critical buckling load of an angle-ply laminated plate, when the properties of the plate are known to be scattered about some mean value. Convex analysis approach has been employed to determine the material properties giving the minimum-buckling load. The results have been presented for uni-axial and biaxial loadings for various aspect ratios.

Vinckenroy and Wilde [78] have used MCS in combination with the FEM to determine the stochastic distribution of the structural response on the basis of the stochastic description of the input (materials, geometry, loads, ...). They have investigated simple as well as complex structures, including a perforated composite plate. The analysis allows establishing variations in the input. The advantage of this method is that it does not require access to the finite element source code and can be used, with some adaptations, with any program code.

Salim et al. [79-81] have employed FOPT for analysis of composite laminates with random material properties. The problem is formulated using classical laminate theory and

energy approach. The material properties have been modeled as RVs. Rayleigh-Ritz technique has been used for the solution. Specially orthotropic composite laminates with all edges simply supported have been analysed with deterministic loading to obtain the SD of deflections [79]. The SD of initial buckling load has been obtained for all edges SS cross-ply plates subjected to compressive force [80]. In another paper [81], they have obtained the second order statistics of natural frequencies of the laminate. The results have been compared with that of MCS.

Raj et al. [82] have obtained the static response of graphite-epoxy composite laminates with randomness in material properties subjected to deterministic loading. The material properties have been modeled as independent random variables. They have used a higher order shear deformation theory to model the plate behavior. The FEM in conjunction with MCS has been used for obtaining the second order statistics of static response. The sensitivity of variation of the SD of the response towards the uncertainties in material properties has been examined for composite plates with different support conditions.

Yadav and Verma [83,84] have investigated free vibration for cylindrical shells with random material properties. In their first paper, they have presented the theoretical formulation and in the second paper they have presented applications of the proposed approach. The behavior of composite shell has been modeled based on classical laminate theory. The material properties are modeled as random variables. The exact mean solution approach for simply supported cylindrical shell has been used. The FOPT has been employed to handle the randomness. Numerical results for mean and SD of first three natural frequencies have been obtained for specially orthotropic, asymmetric and six layer anti-symmetric laminates for simply supported ends in axis-symmetric vibration. In another paper Yadav and Verma [85] have studied the initial buckling of composite cylindrical shells. The mean and SD of initial buckling load for specially orthotropic shells subjected to axial

compression have been obtained. They have used the same formulation and mathematical simplicity as given in [83].

Jagdish [86] has studied the static response of graphite/epoxy and glass/epoxy composite plates with random material properties to random loading. They have formulated the problem using classical laminate theory. The solution of the equations obtained from energy methods have been attempted by Rayleigh-Ritz technique. They have employed FOPT to handle randomness in material properties and loading. The effects of input material properties and loading have been studied on deflection of composite laminates with different boundary conditions, aspect ratios, ply orientations etc.

Raju [87] has studied the initial buckling of composite plates with and without cutouts. The problem has been formulated based on the classical laminate theory. NASTRON based FEM in conjunction with MCS has been used for evaluation of the second order statistics of the buckling loads of rectangular composite laminates with random material properties. The material properties have been modeled as random variables (RVs). It has been found that the plate with cutout is more sensitive compared to plate without cutout. Further, for plates with cutout, as the aspect ratio increases the critical load decreases.

2.4 Observations

A detailed review of the available literature dealing with various aspects of response of isotropic and laminated composite structures with uncertain system parameters subjected to deterministic as well as random external excitations has been presented in the previous sections of this chapter. The review reveals that though quite a bit of information is available on response analysis of structures involving isotropic materials with random system parameters subjected to deterministic as well as random excitations, limited literature is available on analyses of composite structures with random material properties to

deterministic as well as random excitations. From methodological point of view, the non-statistical methods in particular, perturbation technique appears to be quite common for analyses of structures with parameter uncertainties, while this is not a common method in the presence of external excitations which are random. In general, Monte Carlo simulation seems to be the ideal choice for checking the validity of the proposed techniques. Some prefer local integration, direct product, etc. In some cases, where numerical technique is essential due to complexities of the problems, the above approaches have been used in conjunction with finite element methods. At this stage it is important to mention that in most of the cases the solutions have been attempted using first order approximations. The reasons are two fold. Firstly, up to certain level of randomness in the system parameters which is compatible with most engineering applications, the first order approximations gives sufficiently accurate solution when compared with MCS. Secondly, the complexities of the resulting higher order equations create computational problems in obtaining solutions. Introduction of uncertainties in system parameters has been found to result in significant dispersion of the response from the mean values. Similar observations have been found in case of random excitations.

2.5 Objective

Judging from literature review presented in Sections 2.1 to 2.3 and observations in Section 2.4, it is evident that there exist several gaps in analysis of isotropic material structures and composite structures with uncertainties in system parameters. Considerable work has been done on the buckling, free and random vibrations analysis of isotropic structures with parameter uncertainties. However, similar studies related to composite panels/plates are still underdeveloped and hence there is need for such studies to be carried out systematically. With these in view, the objective of the present study is:

- To employ a higher order shear deformation theory (HSDT) displacement model to accurately predict the transverse shear and rotary inertia effects in laminated composite panels with random material properties.
- To develop a suitable probabilistic solution approach using first-order perturbation technique in combination with classical approach and finite element method for the analysis of laminated composite panels with uncertain system parameters to deterministic as well as random excitations.
- To examine the efficacies of CLT and FSDT with HSDT towards probabilistic behavior of the buckling, natural frequency and dynamic response of the laminated composite panels/plates with random material properties.
- To study the probabilistic system response behavior with uncertainties in material properties subjected to in-plane loads and deterministic as well as transverse random excitations. The sensitivity of material properties is also to be examined.

CHAPTER III

GENERAL FORMULATION

3.1 Introduction

In *Chapter II*, on the basis of exhaustive literature survey, it was observed that the information on the response of composite laminates with random material properties is limited. There is need for an in-depth study to find the dispersion in natural frequencies, buckling loads and dynamic response for a composite panel with random material properties. It is also worthwhile from the design point of view to examine the effect of various geometric parameters on the response. Further, for proper quality control during manufacturing of the composite it is good to investigate the sensitivity of the response to the variation in random material properties.

It is well known that even in the case of thin composite laminates the neglect of transverse shear stresses makes the laminate stiffer. Since shear modulus is an independent material property in the composite, it would also affect the design. The classical laminate theory (CLT) developed by Smith [88], Reissner and Stavsky [89], and Lekhnitskii [90] were all based on Kirchhoff's assumptions. The deflections predicted using CLT model were lower, while buckling loads and frequencies were higher as compared to experimental observations. This was mainly due to the fact that the transverse shear stresses and rotatory inertia effects

were neglected in the CLT model. Later many studies were carried out to include these effects, which led to the development of various shear deformation theories [91-94]. The higher order shear deformation theory (HSDT) model developed by Reddy and Liu [95] and Reddy [96] for elastic shells and plates respectively has been employed for the present study. The first order shear deformation theory (FSDT) based on uniform shear stress concept could be obtained from HSDT model. At this stage, it is relevant to mention that the behavior of various theories in deterministic analysis is well known. However, their behavior in probabilistic environment is not yet fully understood. The present study is based on the so-called parabolic shear deformable theory but, for comparison purposes, the results for CLT and FSDT have also been computed.

The system dynamic equations for the composite curved panel with higher order shear deformation theory can be derived by using variational approach [95, 97] or vectorial approach [98, 99]. In the present study variational approach has been employed. The form of the system equations does not change in the random environment and look similar to the deterministic case.

3.2 Shear Deformable Curved Composite Panels

Figure 3.1 shows the geometry of the shell element with stress resultants. Let (ξ_1, ξ_2, ζ) denote the orthogonal curvilinear coordinates (or shell coordinates) such that the ξ_1 and ξ_2 curves are lines of curvature on the mid-surface $\zeta = 0$, and ζ curves are straight lines perpendicular to the mid-surface. R_1 and R_2 denote the values of the principal radii of curvatures of the mid-surface. The lines of principal curvature coincide with the coordinate lines.

The shell under consideration is composed of a finite number of N orthotropic layers of uniform thickness. ζ_k and ζ_{k-1} be the top and bottom ζ -coordinates of the k th lamina.

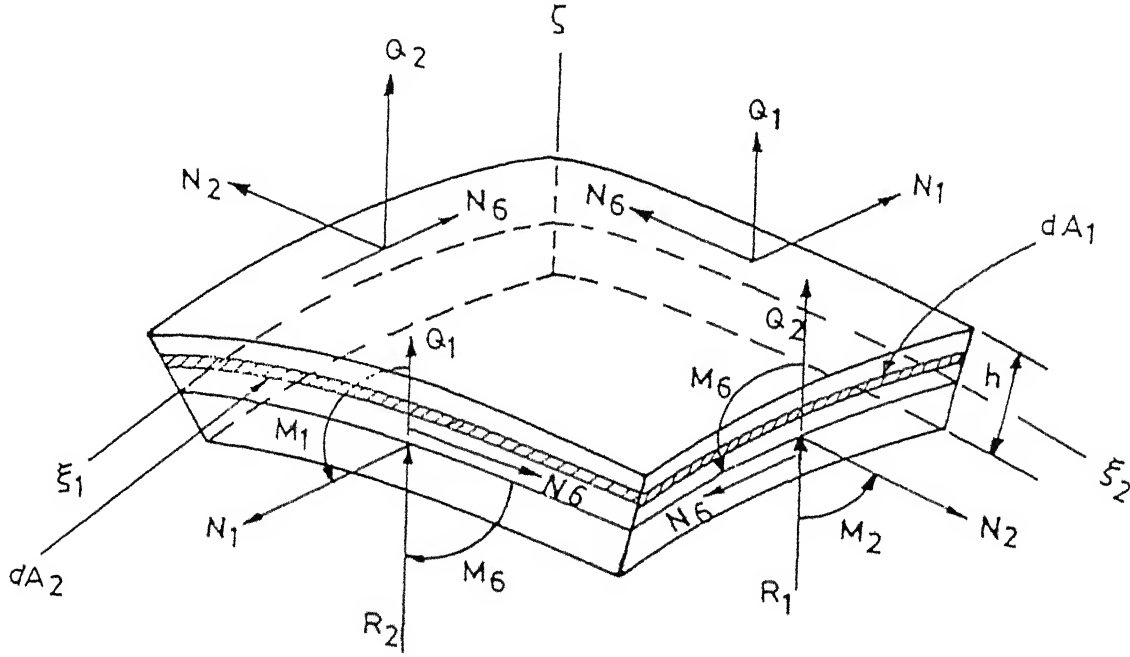


Figure 3.1: Geometry of shell element with stress resultants

3.2.1 Displacement Field Model

The displacement field relations for composite curved panels under consideration are [95]:

$$\begin{aligned}\bar{u}(\xi_1, \xi_2, \zeta, t) &= (1 + \zeta/R_1)u + \zeta\phi_1 + \zeta^2\varphi_1 + \zeta^3\theta_1; \\ \bar{v}(\xi_1, \xi_2, \zeta, t) &= (1 + \zeta/R_2)v + \zeta\phi_2 + \zeta^2\varphi_2 + \zeta^3\theta_2; \quad \bar{w}(\xi_1, \xi_2, \zeta, t) = w,\end{aligned}\tag{3.1}$$

where t is time, \bar{u} , \bar{v} , and \bar{w} are displacements along the ξ_1 , ξ_2 and ζ coordinates, respectively, u , v and w are the displacements of a point on the middle surface and ϕ_1 and ϕ_2 are the rotations at $\zeta = 0$ of normal to the mid-surface with respect to the ξ_2 and ξ_1 axes, respectively. Coefficients φ_1 , φ_2 , θ_1 and θ_2 have system dependent values. The particular choice of the displacement field in Equation (3.1) is dictated by the desire to represent the

transverse shear strains by quadratic functions of the thickness coordinate ζ and by the requirement that the transverse normal strains be zero.

With the above conditions the following relations are obtained [95]:

$$\begin{aligned}\phi_1 &= \phi_2 = 0; & \theta_1 &= -(4/3h^2) (\phi_1 + 1/\alpha_1 (\partial w / \partial \xi_1)) ; \\ \theta_2 &= -(4/3h^2) (\phi_2 + 1/\alpha_2 (\partial w / \partial \xi_2)) ,\end{aligned}\tag{3.2}$$

where α_1 and α_2 are the surface metrics [95] and h is the thickness of the laminate.

Substituting Equation (3.2) into Equation (3.1), we obtain

$$\begin{aligned}\bar{u} &= (1 + \zeta / R_1) u + \zeta \phi_1 + \gamma \zeta^3 (4/3h^2) [-\phi_1 - 1/\alpha_1 (\partial w / \partial \xi_1)] \\ \bar{v} &= (1 + \zeta / R_2) v + \zeta \phi_2 + \gamma \zeta^3 (4/3h^2) [-\phi_2 - 1/\alpha_2 (\partial w / \partial \xi_2)]; \\ \bar{w} &= w.\end{aligned}\tag{3.3}$$

This displacement field, given by Equation (3.3), is used to compute the strains and stresses at any point within the laminate. Note that the displacement field for the first-order shear deformation theory (FSDT) can be deduced from Equation (3.3) by setting $\gamma = 0$. The displacement field for classical laminate theory (CLT) can be obtained from that of the first-order theory by setting $\phi_1 = -1/\alpha_1 (\partial w / \partial \xi_1)$ and $\phi_2 = -1/\alpha_2 (\partial w / \partial \xi_2)$.

In addition to classical approach in conjunction with probabilistic analysis, i.e., stochastic classical approach (SCA), the stochastic FEM (deterministic FEM+ probabilistic analysis) is also used for obtaining the response statistics. For deterministic finite element analysis with the displacement field mentioned above, it is necessary to employ an element with C^1 continuity. Realizing the computational difficulties associated with C^1 continuity element, the derivatives of the out of plane displacement are themselves considered as separate independent degrees of freedoms (DOFs). Thus, 5 DOFs per node with C^1 continuity element is transformed into a C^0 continuity element with 7 DOFs per node.

To make it suitable for C^0 continuity, the displacement field Equation (3.3) needs to be modified. Following the development by Shankara and Iyengar [18] for composite plates, a procedure is being outlined here for curved panels. The displacement field may be expressed using functions as coefficients

$$\begin{aligned}\bar{u} &= (1 + \zeta / R_1)u + f_1(\zeta)\phi_1 + f_2(\zeta)(\partial w / \partial x_1); \\ \bar{v} &= (1 + \zeta / R_2)v + f_1(\zeta)\phi_2 + f_2(\zeta)(\partial w / \partial x_2); \\ \bar{w} &= w.\end{aligned}\tag{3.4}$$

Here x_1 , x_2 and ζ are the Cartesian coordinates ($dx_i = \alpha_i d\xi_i$, $i = 1, 2$). The displacement functions $f_1(\zeta)$ and $f_2(\zeta)$ are represented as

$$f_1(\zeta) = C_1\zeta - C_2\zeta^3 \text{ and } f_2(\zeta) = -C_4\zeta^3;\tag{3.5}$$

where C_1 , C_2 and C_4 are constants with values

$$\begin{aligned}C_1 &= 1; C_2 = C_4 = 4/3h^2; \text{ for HSDT,} \\ C_1 &= 1; C_2 = C_4 = 0; \text{ for FSDT.}\end{aligned}\tag{3.6}$$

The displacement model represented by Equation (3.4) can be rewritten as:

$$\begin{aligned}\bar{u} &= (1 + \zeta / R_1)u + f_1(\zeta)\phi_1 + f_2(\zeta)\theta_1; \\ \bar{v} &= (1 + \zeta / R_2)v + f_1(\zeta)\phi_2 + f_2(\zeta)\theta_2; \\ \bar{w} &= w;\end{aligned}\tag{3.7}$$

where, $\theta_1 = \frac{\partial w}{\partial x_1}$ and $\theta_2 = \frac{\partial w}{\partial x_2}$.

The displacement vector for the model is,

$$\Lambda = (u \ v \ w \ \theta_2 \ \theta_1 \ \phi_2 \ \phi_1)^T\tag{3.8}$$

3.2.2 Strain-Displacement Relations

The strain- displacement relations using Equation (3.3) referred to Cartesian coordinate system are:

$$\begin{aligned}\varepsilon_1 &= \varepsilon_1^0 + \zeta(\kappa_1^0 + \zeta^2 \kappa_1^2); & \varepsilon_2 &= \varepsilon_2^0 + \zeta(\kappa_2^0 + \zeta^2 \kappa_2^2); \\ \varepsilon_4 &= \varepsilon_4^0 + \zeta^2 \kappa_4^1; & \varepsilon_5 &= \varepsilon_5^0 + \zeta^2 \kappa_5^1; & \varepsilon_6 &= \varepsilon_6^0 + \zeta(\kappa_6^0 + \zeta^2 \kappa_6^2),\end{aligned}\quad (3.9)$$

where

$$\begin{aligned}\varepsilon_1^0 &= \partial u / \partial x_1 + w / R_1; & \kappa_1^0 &= \partial \phi_1 / \partial x_1; & \kappa_1^2 &= -(4/3h^2)(\partial \phi_1 / \partial x_1 + \partial^2 w / \partial x_1^2); \\ \varepsilon_2^0 &= \partial v / \partial x_2 + w / R_2; & \kappa_2^0 &= \partial \phi_2 / \partial x_2; & \kappa_2^2 &= -(4/3h^2)(\partial \phi_2 / \partial x_2 + \partial^2 w / \partial x_2^2); \\ \varepsilon_4^0 &= \phi_2 + \partial w / \partial x_2; & \kappa_4^1 &= -(4/h^2)(\phi_2 + \partial w / \partial x_2); & \varepsilon_5^0 &= \phi_1 + \partial w / \partial x_1; \\ \kappa_5^1 &= -(4/h^2)(\phi_1 + \partial w / \partial x_1); & \varepsilon_6^0 &= \partial u / \partial x_2 + \partial v / \partial x_1; & \kappa_6^0 &= \partial \phi_2 / \partial x_1 + \partial \phi_1 / \partial x_2; \\ \kappa_6^2 &= -(4/3h^2)(\partial \phi_2 / \partial x_1 + \partial \phi_1 / \partial x_2 + 2\partial^2 w / \partial x_1 \partial x_2).\end{aligned}\quad (3.10)$$

Equation (3.9) gives the strain-displacement relations corresponding to the displacement field

Equation (3.7) with the mid-plane strains and curvatures expressed as

$$\begin{aligned}\varepsilon_1^0 &= \partial u / \partial x_1 + w / R_1; & \varepsilon_2^0 &= \partial v / \partial x_2 + w / R_2; & \varepsilon_4^0 &= C_1 \phi_2 + \partial w / \partial x_2; \\ \varepsilon_5^0 &= C_1 \phi_1 + \partial w / \partial x_1; & \varepsilon_6^0 &= \partial u / \partial x_2 + \partial v / \partial x_1; \\ \kappa_1^0 &= C_1 (\partial \phi_1 / \partial x_1); & \kappa_2^0 &= C_1 (\partial \phi_2 / \partial x_2); & \kappa_6^0 &= C_1 (\partial \phi_2 / \partial x_1 + \partial \phi_1 / \partial x_2); \\ \kappa_4^1 &= -3C_2 \phi_2 - 3C_4 \theta_2; & \kappa_5^1 &= -3C_2 \phi_1 - 3C_4 \theta_1; \\ \kappa_1^2 &= -C_2 (\partial \phi_1 / \partial x_1) - C_4 (\partial \theta_1 / \partial x_1); & \kappa_2^2 &= -C_2 (\partial \phi_2 / \partial x_2) - C_4 (\partial \theta_2 / \partial x_2); \\ \kappa_6^2 &= -C_2 (\partial \phi_2 / \partial x_1 + \partial \phi_1 / \partial x_2) - C_4 (\partial \theta_1 / \partial x_2 + \partial \theta_2 / \partial x_1).\end{aligned}\quad (3.11)$$

3.2.3 Stress-Strain Relations

The stress-strain relations for k th lamina in the material coordinate axis, whose fibers are oriented with reference to the x_1 is given as [100]

$$\begin{Bmatrix} \sigma_l \\ \sigma_t \\ \sigma_{lt} \\ \sigma_{l\zeta} \\ \sigma_{t\zeta} \end{Bmatrix}_{(k)} = \begin{bmatrix} Q_{11}^{(k)} & Q_{12}^{(k)} & 0 & 0 \\ & Q_{22}^{(k)} & 0 & 0 \\ & & 0 & 0 \\ sym. & & Q_{44}^{(k)} & 0 \\ & & & Q_{55}^{(k)} \end{bmatrix} \begin{Bmatrix} \varepsilon_l \\ \varepsilon_t \\ \varepsilon_{lt} \\ \varepsilon_{l\zeta} \\ \varepsilon_{t\zeta} \end{Bmatrix}_{(k)} ; \quad (3.12)$$

where 'l' and 't' indicate the longitudinal and transverse directions for the lamina. σ_l , σ_t , ε_l and ε_t are stresses and strains in the direction parallel and perpendicular to the fiber direction. σ_{lt} , $\sigma_{t\zeta}$, $\sigma_{l\zeta}$, ε_{lt} , $\varepsilon_{t\zeta}$ and $\varepsilon_{l\zeta}$ are shear stresses and shear strains in the respective planes. The stiffness coefficients are defined in terms of material properties as

$$\begin{aligned} Q_{11} &= E_{11} / (1 - \nu_{12} \nu_{21}); \\ Q_{22} &= \nu_{21} E_{11} / (1 - \nu_{12} \nu_{21}); \\ Q_{21} &= Q_{12}; \quad Q_{66} = G_{12}; \quad Q_{44} = G_{13}; \quad Q_{55} = G_{23}; \quad \nu_{21} = \nu_{12}; \end{aligned} \quad (3.13)$$

where E_{11} and E_{22} are longitudinal and transverse elastic moduli, G_{12} is in-plane shear modulus, G_{13} and G_{23} are the out-of-plane shear moduli and ν_{ij} 's are the Poisson ratios.

The transformed stress-strain relations for the k th lamina with respect to the laminate coordinate system are:

$$\begin{Bmatrix} \sigma_1 \\ \sigma_2 \\ \sigma_6 \\ \sigma_4 \\ \sigma_5 \end{Bmatrix} = \begin{bmatrix} \bar{Q}_{11}^{(k)} & \bar{Q}_{12}^{(k)} & \bar{Q}_{16}^{(k)} & 0 & 0 \\ & \bar{Q}_{22}^{(k)} & \bar{Q}_{26}^{(k)} & 0 & 0 \\ & & \bar{Q}_{66}^{(k)} & 0 & 0 \\ sym. & & & \bar{Q}_{44}^{(k)} & \bar{Q}_{45}^{(k)} \\ & & & & \bar{Q}_{55}^{(k)} \end{bmatrix} \begin{Bmatrix} \varepsilon_1 \\ \varepsilon_2 \\ \varepsilon_6 \\ \varepsilon_4 \\ \varepsilon_5 \end{Bmatrix}_{(k)} \quad (3.14)$$

where $\bar{Q}_y^{(k)}$ are the material constants of the k th lamina in the laminate coordinate system [100, 101].

3.2.4 Equations of Motion

The equations of motion for curved panels subjected to in-plane loads, N_{x_1} , N_{x_2} , and $N_{x_1x_2}$ and distributed transverse dynamic loading q including effects of transverse shear and rotatory inertia may be written using the principal of virtual work [97]. For the present case this yields [95]:

$$\begin{aligned} \partial N_1 / \partial x_1 + \partial N_6 / \partial x_2 &= \bar{I}_1 \ddot{u} + \bar{I}_2 \ddot{\phi}_1 - \gamma \bar{I}_3 \partial \ddot{w} / \partial x_1; \\ \partial N_6 / \partial x_1 + \partial N_2 / \partial x_2 &= \bar{I}'_1 \ddot{v} + \bar{I}'_2 \ddot{\phi}_2 - \gamma \bar{I}'_3 \partial \ddot{w} / \partial x_2; \\ \partial Q_1 / \partial x_1 + \partial Q_2 / \partial x_2 - \gamma (4/h^2)(\partial K_1 / \partial x_1 + \partial K_2 / \partial x_2) \\ &+ \gamma (4/3h^2)(\partial^2 P_1 / \partial x_1^2 + \partial^2 P_2 / \partial x_2^2 + 2\partial^2 P_6 / \partial x_1 \partial x_2) - N_1 / R_1 - N_2 / R_2 \\ &+ N_{x_1} \partial^2 w / \partial x_1^2 + N_{x_2} \partial^2 w / \partial x_2^2 + N_{x_1x_2} \partial^2 w / \partial x_1 \partial x_2 = \\ &\gamma \bar{I}_3 \partial \ddot{u} / \partial x_1 + \gamma \bar{I}_5 \partial \ddot{\phi}_1 / \partial x_1 + \gamma \bar{I}'_3 \partial \ddot{v} / \partial x_2 + \gamma \bar{I}'_5 \partial \ddot{\phi}_2 / \partial x_2 + I_1 \ddot{w} \\ &- \gamma (16I_7/9h^2)(\partial^2 \ddot{w} / \partial x_1^2 + \partial^2 \ddot{w} / \partial x_2^2) - q; \end{aligned} \quad (3.15)$$

$$\partial M_1 / \partial x_1 + \partial M_6 / \partial x_2 - Q_1 + \gamma (4/h^2)K_1 - \gamma (4/3h^2)(\partial P_1 / \partial x_1 + \partial P_6 / \partial x_2) = \bar{I}_2 \ddot{u} + \bar{I}_4 \ddot{\phi}_1 - \gamma \bar{I}_5 \partial \ddot{w} / \partial x_1;$$

$$\partial M_6 / \partial x_1 + \partial M_2 / \partial x_2 - Q_2 + \gamma (4/h^2)K_2 - \gamma (4/3h^2)(\partial P_6 / \partial x_1 + \partial P_2 / \partial x_2) = \bar{I}'_2 \ddot{v} + \bar{I}'_4 \ddot{\phi}_2 - \gamma \bar{I}'_5 \partial \ddot{w} / \partial x_2,$$

where $q(x_1, x_2, t)$ is the distributed transverse load. N_i , M_i , etc. are the stress resultants. The

inertias \bar{I}'_i and \bar{I}_i , $i = 1, 2, 3, 4, 5$ are defined by [95]

$$\bar{I}_1 = I_1 + \gamma 2I_2 / R_1; \quad \bar{I}'_1 = I_2 + \gamma 2I_2 / R_2;$$

$$\bar{I}_2 = I_2 + I_3 / R_1 - \gamma 4I_4 / 3h^2 - \gamma 4I_5 / 3h^2 R_1$$

$$\bar{I}'_2 = I_2 + I_3 / R_2 - \gamma 4I_4 / 3h^2 - \gamma 4I_5 / 3h^2 R_2; \quad \bar{I}_3 = 4I_4 / 3h^2 + 4I_5 / 3h^2 R_1;$$

$$\bar{I}'_3 = 4I_4 / 3h^2 + 4I_5 / 3h^2 R_2;$$

$$\bar{I}_4 = I_3 - \gamma 8I_5/3h^2 + \gamma 16I_7/9h^4; \quad \bar{I}'_4 = I_3 - \gamma 8I_5/3h^2 + \gamma 16I_7/9h^4; \quad (3.16)$$

$$\bar{I}_5 = 4I_5/3h^2 - 16I_7/9h^4; \quad \bar{I}'_5 = 4I_5/3h^2 - 16I_7/9h^4;$$

$$(I_1, I_2, I_3, I_4, I_5, I_7) = \sum_{k=1}^N \int_{\zeta_{k-1}}^{\zeta_k} \rho^{(k)}(1, \zeta, \zeta^2, \zeta^3, \zeta^4, \zeta^6) d\zeta;$$

where $\rho^{(k)}$ is the mass per unit volume of the k th lamina.

3.2.5 The Laminate Constitutive Equations

It can be clearly seen from Equation (3.14) that the stresses in a composite laminate vary from layer to layer and hence a statically equivalent force and moment system is required for analysis. These stress resultants are expressed as [95]

$$(N_i, M_i, P_i) = \sum_{k=1}^N \int_{\zeta_{k-1}}^{\zeta_k} \sigma_i^{(k)}(1, \zeta, \zeta^3) d\zeta, \quad i = 1, 2, 6; \\ (Q_1, K_1) = \sum_{k=1}^N \int_{\zeta_{k-1}}^{\zeta_k} \sigma_5^{(k)}(1, \zeta^2) d\zeta; \quad (3.17)$$

$$(Q_2, K_2) = \sum_{k=1}^N \int_{\zeta_{k-1}}^{\zeta_k} \sigma_4^{(k)}(1, \zeta^2) d\zeta \\ N_i = A_{ij}\varepsilon_j^0 + B_{ij}\kappa_j^0 + \gamma E_{ij}\kappa_j^2; \quad M_i = B_{ij}\varepsilon_j^0 + D_{ij}\kappa_j^0 + \gamma F_{ij}\kappa_j^2; \quad (3.18) \\ P_i = E_{ij}\varepsilon_j^0 + F_{ij}\kappa_j^0 + H_{ij}\kappa_j^2, \quad i, j = 1, 2, 6,$$

$$Q_2 = A_{4j}\varepsilon_j^0 + \gamma D_{4j}\kappa_j^1; \quad Q_1 = A_{5j}\varepsilon_j^0 + \gamma D_{5j}\kappa_j^1; \quad (3.19) \\ K_2 = D_{4j}\varepsilon_j^0 + F_{4j}\kappa_j^1; \quad K_1 = D_{5j}\varepsilon_j^0 + F_{5j}\kappa_j^1, \quad j = 4, 5$$

where A_{ij} , B_{ij} , D_{ij} , E_{ij} , F_{ij} and H_{ij} are the laminate stiffnesses expressed as

$$(A_{ij}, B_{ij}, D_{ij}, E_{ij}, F_{ij}, H_{ij}) = \sum_{k=1}^N \int_{\zeta_{k-1}}^{\zeta_k} \bar{Q}_{ij}^{(k)}(1, \zeta, \zeta^2, \zeta^3, \zeta^4, \zeta^6) d\zeta, \quad i, j = 1, 2, \dots, 6 \quad (3.20)$$

The equations for FSDT can be obtained by setting $\gamma = 0$. With help of FSDT, the CLT equations can be obtained as discussed earlier.

Substitution of the above equations for curved panels into the constitutive equations and then into Equations (3.15), we obtain the equilibrium equation in terms of displacements. The equations of motion may now be written as

$$\mathbf{L} \mathbf{\Lambda} = \mathbf{F} \quad (3.21)$$

where $\mathbf{\Lambda} = (u \ v \ w \ \phi_2 \ \phi_1)^T$ and $\mathbf{F} = (0 \ 0 \ q \ 0 \ 0)^T$ for HSDT & FSDT,

$\mathbf{\Lambda} = (u \ v \ w)^T$ and $\mathbf{F} = (0 \ 0 \ q)^T$ for CLT and \mathbf{L} is a matrix of differential operators.

The above equations are valid for laminated composite curved panels. In the next section, we develop: (1) equilibrium equations, (2) strain-displacement relations, and (3) constitutive equations, for spherical panels, cylindrical panels and rectangular plates.

3.3 Spherical Panels

3.3.1 Equilibrium Equations

Substituting the geometry definitions for spherical panels (Figure 3.2) into Equations (3.15), we get

$$\begin{aligned} \partial N_1 / \partial x_1 + \partial N_6 / \partial x_2 &= \bar{I}_1 \ddot{u} + \bar{I}_2 \ddot{\phi}_1 - \bar{I}_3 \partial \ddot{w} / \partial x_1; \\ \partial N_6 / \partial x_1 + \partial N_2 / \partial x_2 &= \bar{I}'_1 \ddot{v} + \bar{I}'_2 \ddot{\phi}_2 - \bar{I}'_3 \partial \ddot{w} / \partial x_2; \\ \partial Q_1 / \partial x_1 + \partial Q_2 / \partial x_2 - (4/h^2)(\partial K_1 / \partial x_1 + \partial K_2 / \partial x_2) \\ &+ (4/3h^2)(\partial^2 P_1 / \partial x_1^2 + \partial^2 P_2 / \partial x_2^2 + 2\partial^2 P_6 / \partial x_1 \partial x_2) - (N_1 + N_2)/R \\ &+ N_{x_1} \partial^2 w / \partial x_1^2 + N_{x_2} \partial^2 w / \partial x_2^2 + N_{x_1 x_2} \partial^2 w / \partial x_1 \partial x_2 = \\ \bar{I}_3 \partial \ddot{u} / \partial x_1 + \bar{I}_5 \partial \ddot{\phi}_1 / \partial x_1 + \bar{I}_3 \partial \ddot{v} / \partial x_2 + \bar{I}_5 \partial \ddot{\phi}_2 / \partial x_2 + I_1 \ddot{w} - (16I_7/9h^2)(\partial^2 \ddot{w} / \partial x_1^2 + \partial^2 \ddot{w} / \partial x_2^2) - q; \\ \partial M_1 / \partial x_1 + \partial M_6 / \partial x_2 - Q_1 + (4/h^2)K_1 - (4/3h^2)(\partial P_1 / \partial x_1 + \partial P_6 / \partial x_2) &= \bar{I}_2 \ddot{u} + \bar{I}_4 \ddot{\phi}_1 - \bar{I}_5 \partial \ddot{w} / \partial x_1; \end{aligned} \quad (3.22)$$

$$\partial M_6 / \partial x_1 + \partial M_2 / \partial x_2 - Q_1 + (4/h^2)K_2 - (4/3h^2)(\partial P_6 / \partial x_1 + \partial P_2 / \partial x_2) = \bar{I}'_2 \ddot{v} + \bar{I}'_4 \ddot{\phi}_2 - \bar{I}'_5 \partial \ddot{w} / \partial x_2,$$

where the modified inertias \bar{I}'_i and \bar{I}_i , $i = 1, 2, 3, 4, 5, 7$ (Figure 3.2) are given as:

$$\bar{I}_1 = I_1 + \gamma 2I_2 / R; \quad \bar{I}'_1 = I_2 + \gamma 2I_2 / R;$$

$$\bar{I}_2 = I_2 + I_3 / R - \gamma 4I_4 / 3h^2 - \gamma 4I_5 / 3h^2 R$$

$$\bar{I}'_2 = I_2 + I_3 / R - \gamma 4I_4 / 3h^2 - \gamma 4I_5 / 3h^2 R; \quad \bar{I}_3 = 4I_4 / 3h^2 + 4I_5 / 3h^2 R;$$

$$\bar{I}'_3 = 4I_4 / 3h^2 + 4I_5 / 3h^2 R;$$

$$\bar{I}_4 = I_3 - \gamma 8I_5 / 3h^2 + \gamma 16I_7 / 9h^4; \quad \bar{I}'_4 = I_3 - \gamma 8I_5 / 3h^2 + \gamma 16I_7 / 9h^4; \quad (3.23)$$

$$\bar{I}_5 = 4I_5 / 3h^2 - 16I_7 / 9h^4; \quad \bar{I}'_5 = 4I_5 / 3h^2 - 16I_7 / 9h^4;$$

$$(I_1, I_2, I_3, I_4, I_5, I_7) = \sum_{k=1}^N \int_{\zeta_{k-1}}^{\zeta_k} \rho^{(k)}(1, \zeta, \zeta^2, \zeta^3, \zeta^4, \zeta^6) d\zeta;$$

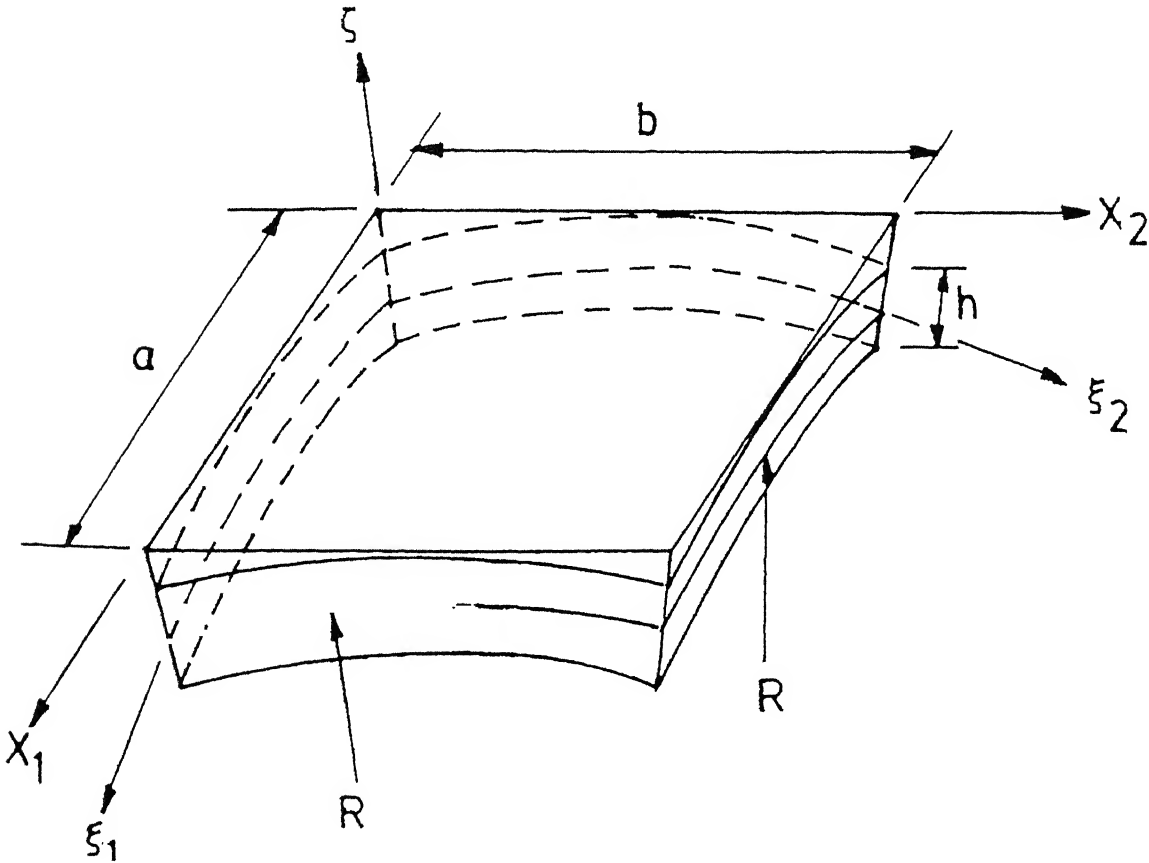


Figure 3.2: Geometry of spherical element

3.3.2 Strain-Displacement Relations

There is no change in Equation (3.9). Using geometrical parameter given in Figure (3.2), Equations (3.10) and (3.11) can be redefined. The modified equations are given by:

$$\begin{aligned}
 \varepsilon_1^0 &= \partial u / \partial x_1 + w / R; \quad \kappa_1^0 = \partial \phi_1 / \partial x_1; \quad \kappa_1^2 = -(4/3h^2)(\partial \phi_1 / \partial x_1 + \partial^2 w / \partial x_1^2); \\
 \varepsilon_2^0 &= \partial v / \partial x_2 + w / R; \quad \kappa_2^0 = \partial \phi_2 / \partial x_2; \quad \kappa_2^2 = -(4/3h^2)(\partial \phi_2 / \partial x_2 + \partial^2 w / \partial x_2^2); \\
 \varepsilon_4^0 &= \phi_2 + \partial w / \partial x_2; \quad \kappa_4^1 = -(4/h^2)(\phi_2 + \partial w / \partial x_2); \quad \varepsilon_5^0 = \phi_1 + \partial w / \partial x_1; \quad (3.24) \\
 \kappa_5^1 &= -(4/h^2)(\phi_1 + \partial w / \partial x_1); \quad \varepsilon_6^0 = \partial u / \partial x_2 + \partial v / \partial x_1; \quad \kappa_6^0 = \partial \phi_2 / \partial x_1 + \partial \phi_1 / \partial x_2; \\
 \kappa_6^2 &= -(4/3h^2)(\partial \phi_2 / \partial x_1 + \partial \phi_1 / \partial x_2 + 2\partial^2 w / \partial x_1 \partial x_2).
 \end{aligned}$$

$$\begin{aligned}
 \varepsilon_1^0 &= \partial u / \partial x_1 + w / R; \quad \varepsilon_2^0 = \partial v / \partial x_2 + w / R; \quad \varepsilon_4^0 = C_1 \phi_2 + \partial w / \partial x_2; \\
 \varepsilon_5^0 &= C_1 \phi_1 + \partial w / \partial x_1; \quad \varepsilon_6^0 = \partial u / \partial x_2 + \partial v / \partial x_1; \\
 \kappa_1^0 &= C_1 (\partial \phi_1 / \partial x_1); \quad \kappa_2^0 = C_1 (\partial \phi_2 / \partial x_2); \quad \kappa_6^0 = C_1 (\partial \phi_2 / \partial x_1 + \partial \phi_1 / \partial x_2); \quad (3.25) \\
 \kappa_4^1 &= -3C_2 \phi_2 - 3C_4 \theta_2; \quad \kappa_5^1 = -3C_2 \phi_1 - 3C_4 \theta_1; \\
 \kappa_1^2 &= -C_2 (\partial \phi_1 / \partial x_1) - C_4 (\partial \theta_1 / \partial x_1); \quad \kappa_2^2 = -C_2 (\partial \phi_2 / \partial x_2) - C_4 (\partial \theta_2 / \partial x_2); \\
 \kappa_6^2 &= -C_2 (\partial \phi_2 / \partial x_1 + \partial \phi_1 / \partial x_2) - C_4 (\partial \theta_1 / \partial x_2 + \partial \theta_2 / \partial x_1).
 \end{aligned}$$

3.3.3 Constitutive Equations

Equations (3.18) and (3.19) represent the constitutive relation. However, the modified definition of strain-displacement relations must be as shown in sub section 3.3.2.

3.4 Cylindrical Panels

3.4.1 Equilibrium Equations

Using the geometrical definitions of cylindrical panels given in Figure 3.3, Equations (3.15) become

$$\begin{aligned}
 \partial N_1 / \partial x_1 + \partial N_6 / \partial x_2 &= \bar{I}_1 \ddot{u} + \bar{I}_2 \ddot{\phi}_1 - \bar{I}_3 \partial \ddot{w} / \partial x_1; \\
 \partial N_6 / \partial x_1 + \partial N_2 / \partial x_2 &= \bar{I}'_1 \ddot{v} + \bar{I}'_2 \ddot{\phi}_2 - \bar{I}'_3 \partial \ddot{w} / \partial x_2; \\
 \partial Q_1 / \partial x_1 + \partial Q_2 / \partial x_2 - (4/h^2)(\partial K_1 / \partial x_1 + \partial K_2 / \partial x_2) \\
 + (4/3h^2)(\partial^2 P_1 / \partial x_1^2 + \partial^2 P_2 / \partial x_2^2 + 2\partial^2 P_6 / \partial x_1 \partial x_2) - N_2 / R \\
 + N_{x_1} \partial^2 w / \partial x_1^2 + N_{x_2} \partial^2 w / \partial x_2^2 + N_{x_1 x_2} \partial^2 w / \partial x_1 \partial x_2 \\
 = \bar{I}_3 \partial \ddot{u} / \partial x_1 + \bar{I}_5 \partial \ddot{\phi}_1 / \partial x_1 + \bar{I}'_3 \partial \ddot{v} / \partial x_2 + \bar{I}'_5 \partial \ddot{\phi}_2 / \partial x_2 + I_1 \ddot{w} - (16I_7/9h^2)(\partial^2 \ddot{w} / \partial x_1^2 + \partial^2 \ddot{w} / \partial x_2^2) - q; \\
 \partial M_1 / \partial x_1 + \partial M_6 / \partial x_2 - Q_1 + (4/h^2)K_1 - (4/3h^2)(\partial P_1 / \partial x_1 + \partial P_6 / \partial x_2) &= \bar{I}_2 \ddot{u} + \bar{I}_4 \ddot{\phi}_1 - \bar{I}_5 \partial \ddot{w} / \partial x_1; \\
 \partial M_6 / \partial x_1 + \partial M_2 / \partial x_2 - Q_2 + (4/h^2)K_2 - (4/3h^2)(\partial P_6 / \partial x_1 + \partial P_2 / \partial x_2) &= \bar{I}'_2 \ddot{v} + \bar{I}'_4 \ddot{\phi}_2 - \bar{I}'_5 \partial \ddot{w} / \partial x_2,
 \end{aligned} \tag{3.26}$$

where the modified inertias \bar{I}'_i and \bar{I}_i (Figure 3.3) are given as:

$$\begin{aligned}
 \bar{I}_1 &= I_1; \quad \bar{I}'_1 = I_2 + \gamma 2I_2/R; \quad \bar{I}_2 = I_2 - \gamma 4I_4/3h^2; \\
 \bar{I}'_2 &= I_2 + I_3/R - \gamma 4I_4/3h^2 - \gamma 4I_5/3h^2R; \quad \bar{I}_3 = 4I_4/3h^2; \\
 \bar{I}'_3 &= 4I_4/3h^2 + 4I_5/3h^2R; \\
 \bar{I}_4 &= I_3 - \gamma 8I_5/3h^2 + \gamma 16I_7/9h^4; \quad \bar{I}'_4 = I_3 - \gamma 8I_5/3h^2 + \gamma 16I_7/9h^4; \\
 \bar{I}_5 &= 4I_5/3h^2 - 16I_7/9h^4; \quad \bar{I}'_5 = 4I_5/3h^2 - 16I_7/9h^4;
 \end{aligned} \tag{3.27}$$

$$(I_1, I_2, I_3, I_4, I_5, I_7) = \sum_{k=1}^N \int_{\zeta_{k-1}}^{\zeta_k} \rho^{(k)}(1, \zeta, \zeta^2, \zeta^3, \zeta^4, \zeta^6) d\zeta;$$

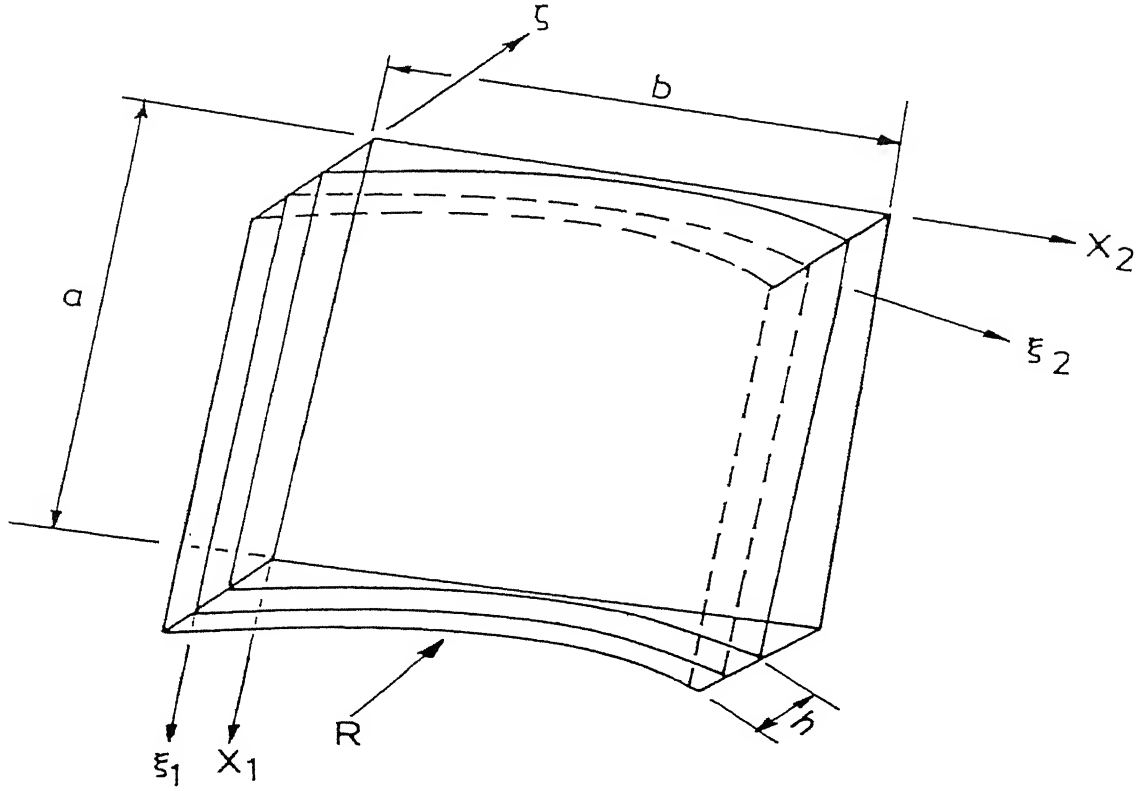


Figure 3.3: Geometry of cylindrical panel element

3.4.2 Strain-Displacement Relations

The strain-displacement relations are obtained by using Equations (3.10) and (3.11) and cylindrical panel geometry definitions (Figure 3.3):

$$\begin{aligned}
 \varepsilon_1^0 &= \partial u / \partial x_1; \quad \kappa_1^0 = \partial \phi_1 / \partial x_1; \quad \kappa_1^2 = -(4/3h^2)(\partial \phi_1 / \partial x_1 + \partial^2 w / \partial x_1^2); \\
 \varepsilon_2^0 &= \partial v / \partial x_2 + w / R; \quad \kappa_2^0 = \partial \phi_2 / \partial x_2; \quad \kappa_2^2 = -(4/3h^2)(\partial \phi_2 / \partial x_2 + \partial^2 w / \partial x_2^2); \\
 \varepsilon_4^0 &= \phi_2 + \partial w / \partial x_2; \quad \kappa_4^1 = -(4/h^2)(\phi_2 + \partial w / \partial x_2); \quad \varepsilon_5^0 = \phi_1 + \partial w / \partial x_1; \quad (3.28) \\
 \kappa_5^1 &= -(4/h^2)(\phi_1 + \partial w / \partial x_1); \quad \varepsilon_6^0 = \partial u / \partial x_2 + \partial v / \partial x_1; \quad \kappa_6^0 = \partial \phi_2 / \partial x_1 + \partial \phi_1 / \partial x_2; \\
 \kappa_6^2 &= -(4/3h^2)(\partial \phi_2 / \partial x_1 + \partial \phi_1 / \partial x_2 + 2\partial^2 w / \partial x_1 \partial x_2).
 \end{aligned}$$

$$\varepsilon_1^0 = \partial u / \partial x_1; \quad \varepsilon_2^0 = \partial v / \partial x_2 + w / R; \quad \varepsilon_4^0 = C_1 \phi_2 + \partial w / \partial x_2;$$

$$\begin{aligned}
\varepsilon_3^0 &= C_1 \phi_1 + \partial w / \partial x_1; \quad \varepsilon_6^0 = \partial u / \partial x_2 + \partial v / \partial x_1; \\
\kappa_1^0 &= C_1 (\partial \phi_1 / \partial x_1); \quad \kappa_2^0 = C_1 (\partial \phi_2 / \partial x_2); \quad \kappa_6^0 = C_1 (\partial \phi_2 / \partial x_1 + \partial \phi_1 / \partial x_2); \\
\kappa_4^1 &= -3C_2 \phi_2 - 3C_4 \theta_2; \quad \kappa_5^1 = -3C_2 \phi_1 - 3C_4 \theta_1; \\
\kappa_1^2 &= -C_2 (\partial \phi_1 / \partial x_1) - C_4 (\partial \theta_1 / \partial x_1); \quad \kappa_2^2 = -C_2 (\partial \phi_2 / \partial x_2) - C_4 (\partial \theta_2 / \partial x_2); \\
\kappa_6^2 &= -C_2 (\partial \phi_2 / \partial x_1 + \partial \phi_1 / \partial x_2) - C_4 (\partial \theta_1 / \partial x_2 + \partial \theta_2 / \partial x_1).
\end{aligned} \tag{3.29}$$

3.4.3 Constitutive Equations

Equations (3.18) and (3.19) can be used by including the parameter definitions given in Figure 3.3. The nature of the equations would be the same.

3.5 Rectangular Plates

3.5.1 The Equilibrium Equations

Adopting the geometrical definitions of cylindrical panels given in Figure 3.4, Equations (3.15) become

$$\begin{aligned}
\partial N_1 / \partial x_1 + \partial N_6 / \partial x_2 &= \bar{I}_1 \ddot{u} + \bar{I}_2 \ddot{\phi}_1 - \bar{I}_3 \partial \ddot{w} / \partial x_1; \\
\partial N_6 / \partial x_1 + \partial N_2 / \partial x_2 &= \bar{I}'_1 \ddot{v} + \bar{I}'_2 \ddot{\phi}_2 - \bar{I}'_3 \partial \ddot{w} / \partial x_2; \\
\partial Q_1 / \partial x_1 + \partial Q_2 / \partial x_2 - (4/h^2)(\partial K_1 / \partial x_1 + \partial K_2 / \partial x_2) + (4/3h^2)(\partial^2 P_1 / \partial x_1^2 + \partial^2 P_2 / \partial x_2^2 \\
+ 2\partial^2 P_6 / \partial x_1 \partial x_2) + N_{x_1} \partial^2 w / \partial x_1^2 + N_{x_2} \partial^2 w / \partial x_2^2 + N_{x_1 x_2} \partial^2 w / \partial x_1 \partial x_2 &= \bar{I}_3 \partial \ddot{u} / \partial x_1 \\
+ \bar{I}_5 \partial \ddot{\phi}_1 / \partial x_1 + \bar{I}_3 \partial \ddot{v} / \partial x_2 + \bar{I}_5 \partial \ddot{\phi}_2 / \partial x_2 + I_1 \ddot{w} - (16I_7/9h^2)(\partial^2 \ddot{w} / \partial x_1^2 + \partial^2 \ddot{w} / \partial x_2^2) - q; \\
\partial M_1 / \partial x_1 + \partial M_6 / \partial x_2 - Q_1 + (4/h^2)K_1 - (4/3h^2)(\partial P_1 / \partial x_1 + \partial P_6 / \partial x_2) &= \bar{I}_2 \ddot{u} + \bar{I}_4 \ddot{\phi}_1 - \bar{I}_5 \partial \ddot{w} / \partial x_1; \\
\partial M_6 / \partial x_1 + \partial M_2 / \partial x_2 - Q_2 + (4/h^2)K_2 - (4/3h^2)(\partial P_6 / \partial x_1 + \partial P_2 / \partial x_2) &= \bar{I}'_2 \ddot{v} + \bar{I}'_4 \ddot{\phi}_2 - \bar{I}'_5 \partial \ddot{w} / \partial x_2,
\end{aligned} \tag{3.30}$$

where the modified inertias \bar{I}'_i and \bar{I}_i , (Figure 3.4) are given below:

पुरुषोत्तम काशीनाथ केलकर पुस्तकालय
 भारतीय प्रौद्योगिकी संस्थान कानपुर
 अवाप्ति क्र० A ..139685.....

$$\begin{aligned}
\bar{I}_1 &= I_1; & \bar{I}'_1 &= I_2; & \bar{I}_2 &= I_2 - \gamma 4I_4/3h^2; & \bar{I}'_2 &= \bar{I}_2; \\
\bar{I}_3 &= 4I_4/3h^2; & \bar{I}'_3 &= \bar{I}_3; \\
\bar{I}_4 &= I_3 - \gamma 8I_5/3h^2 + \gamma 16I_7/9h^4; & \bar{I}'_4 &= \bar{I}_4; \\
\bar{I}_5 &= 4I_5/3h^2 - 16I_7/9h^4; & \bar{I}'_5 &= \bar{I}_5; \\
(I_1, I_2, I_3, I_4, I_5, I_7) &= \sum_{k=1}^N \int_{\zeta_{k-1}}^{\zeta_k} \rho^{(k)}(1, \zeta, \zeta^2, \zeta^3, \zeta^4, \zeta^6) d\zeta;
\end{aligned} \tag{3.31}$$

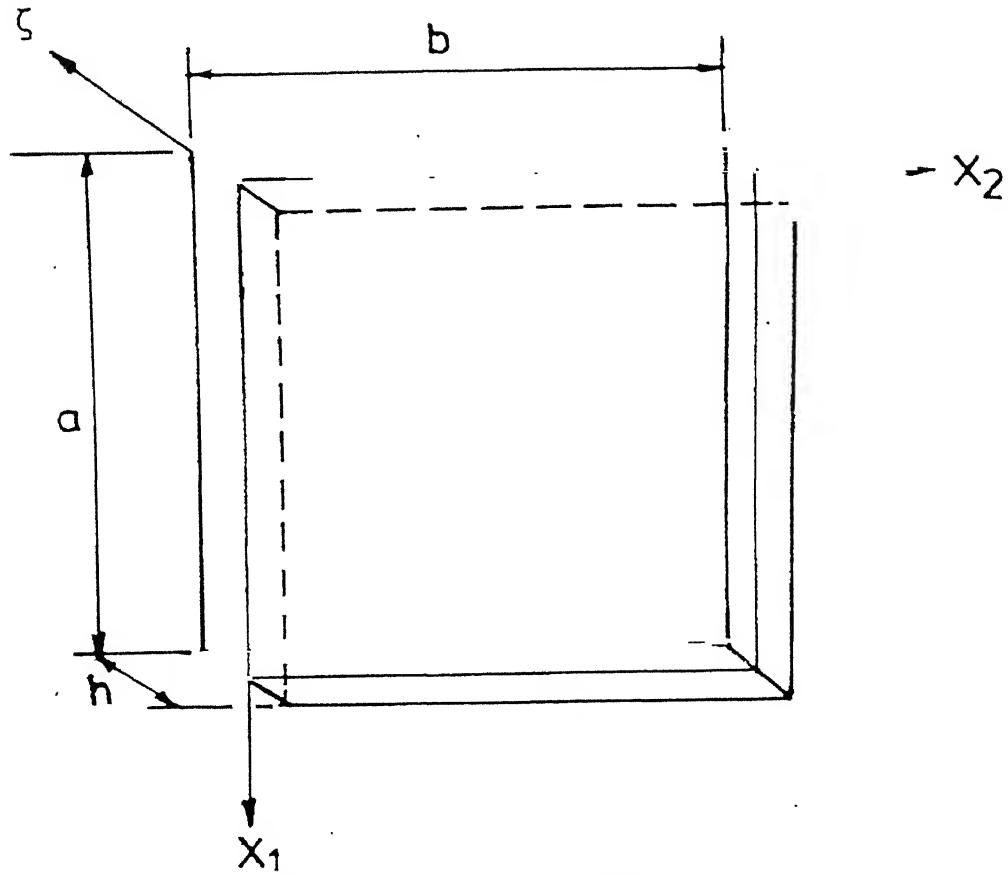


Figure 3.4: Geometry of Plate element

3.5.2 Strain-Displacement Relations

The strain-displacement relations are obtained by using Equations (3.10) and (3.11) and the geometrical relations as defined in Figure 3.4 for plates:

$$\varepsilon_1^0 = \partial u / \partial x_1; \quad \kappa_1^0 = \partial \phi_1 / \partial x_1; \quad \kappa_1^2 = -(4/3h^2)(\partial \phi_1 / \partial x_1 + \partial^2 w / \partial x_1^2);$$

$$\begin{aligned}
\varepsilon_2^0 &= \partial v / \partial x_2; \quad \kappa_2^0 = \partial \phi_2 / \partial x_2; \quad \kappa_2^2 = -(4/3h^2)(\partial \phi_2 / \partial x_2 + \partial^2 w / \partial x_2^2); \\
\varepsilon_4^0 &= \phi_2 + \partial w / \partial x_2; \quad \kappa_4^1 = -(4/h^2)(\phi_2 + \partial w / \partial x_2); \quad \varepsilon_5^0 = \phi_1 + \partial w / \partial x_1; \\
\kappa_5^1 &= -(4/h^2)(\phi_1 + \partial w / \partial x_1); \quad \varepsilon_6^0 = \partial u / \partial x_2 + \partial v / \partial x_1; \quad \kappa_6^0 = \partial \phi_2 / \partial x_1 + \partial \phi_1 / \partial x_2; \\
\kappa_6^2 &= -(4/3h^2)(\partial \phi_2 / \partial x_1 + \partial \phi_1 / \partial x_2 + 2\partial^2 w / \partial x_1 \partial x_2).
\end{aligned} \tag{3.32}$$

$$\begin{aligned}
\varepsilon_1^0 &= \partial u / \partial x_1; \quad \varepsilon_2^0 = \partial v / \partial x_2; \quad \varepsilon_4^0 = C_1 \phi_2 + \partial w / \partial x_2; \\
\varepsilon_5^0 &= C_1 \phi_1 + \partial w / \partial x_1; \quad \varepsilon_6^0 = \partial u / \partial x_2 + \partial v / \partial x_1; \\
\kappa_1^0 &= C_1 (\partial \phi_1 / \partial x_1); \quad \kappa_2^0 = C_1 (\partial \phi_2 / \partial x_2); \quad \kappa_6^0 = C_1 (\partial \phi_2 / \partial x_1 + \partial \phi_1 / \partial x_2); \\
\kappa_4^1 &= -3C_2 \phi_2 - 3C_4 \theta_2; \quad \kappa_5^1 = -3C_2 \phi_1 - 3C_4 \theta_1; \\
\kappa_1^2 &= -C_2 (\partial \phi_1 / \partial x_1) - C_4 (\partial \theta_1 / \partial x_1); \quad \kappa_2^2 = -C_2 (\partial \phi_2 / \partial x_2) - C_4 \partial \theta_2 / \partial x_2; \\
\kappa_6^2 &= -C_2 (\partial \phi_2 / \partial x_1 + \partial \phi_1 / \partial x_2) - C_4 (\partial \theta_1 / \partial x_2 + \partial \theta_2 / \partial x_1).
\end{aligned} \tag{3.33}$$

3.5.3 Constitutive Equations

Equations (3.17), (3.18) and (3.19) can be used by including the parameter definitions given in Figure 3.4 for plates. The nature of the equations would be the same.

Substitution of the respective equations for spherical panels, cylindrical panels and rectangular plates into the constitutive equations and then into Equations (3.22), (3.26) and (3.30), respectively, we obtain the equilibrium equation in terms of displacements for each case corresponding to Equation (3.21) for curved panels. These can also be written symbolically as

$$\mathbf{L} \mathbf{A} = \mathbf{F}; \quad (3.34)$$

where, the elements of the differential operators \mathbf{L} for rectangular plate, cylindrical and spherical panels are given separately in Appendix A.

The present study is concerned with the modeling of system parameters as random variables. This implies that the system parameters do not vary spatially and are also independent of time. The external excitations have been modeled as a random process in time. The solution technique for the deterministic analysis changes with stacking sequence and the edge support conditions of the laminated panel. When two opposite edges are simply supported and with other two side edges having a combination of free, fixed and simple support, a Levy type closed form solution is possible in conjunction with state space approach [102, 103] for cross-ply laminates, where the following laminate stiffness coefficients, $A_{i6}, B_{i6}, D_{i6}, E_{i6}, F_{i6}, H_{i6} = 0, i = 1, 2$; A_{45}, D_{45}, F_{45} are identically equal to zero. The Navier type solution is also possible for cross-ply laminate with all edges simply supported. The two above-mentioned techniques can be used to obtain inhomogeneous ordinary differential equations in time with random coefficients and random input. For combinations of edge supports and stacking sequences that are not amenable to exact solution approach, the inhomogeneous ordinary differential equations with random coefficients and random input can be obtained by employing series type solutions, approximate energy and variational methods, finite element method (FEM) and other numerical techniques. In this study the FEM has been adopted. Further solution of differential equations obtained either using classical approach or FEM for buckling, free vibration, and forced vibration problems is not straight forward as in deterministic analysis.

3.6 Strain Energy Of The Laminate

The elastic strain energy of a laminated composite panel undergoing deformation under the action of external loads is,

$$U = \frac{1}{2} \int_A \bar{\epsilon}^T \mathbf{D} \bar{\epsilon} dA ; \quad (3.35)$$

where

$$\bar{\epsilon} = \left\{ \epsilon_1^0 \quad \epsilon_2^0 \quad \epsilon_6^0 \quad \kappa_1^0 \quad \kappa_2^0 \quad \kappa_6^0 \quad \kappa_1^2 \quad \kappa_2^2 \quad \kappa_6^2 \quad \epsilon_4^0 \quad \epsilon_5^0 \quad \kappa_4^1 \quad \kappa_5^1 \right\}^T ; \quad (3.36)$$

$$\mathbf{D} = \begin{bmatrix} \mathbf{A1} & \mathbf{B1} & \mathbf{E} & \mathbf{0} & \mathbf{0} \\ \mathbf{B1} & \mathbf{D1} & \mathbf{F1} & \mathbf{0} & \mathbf{0} \\ \mathbf{E} & \mathbf{F1} & \mathbf{H} & \mathbf{0} & \mathbf{0} \\ \mathbf{0} & \mathbf{0} & \mathbf{0} & \mathbf{A2} & \mathbf{D2} \\ \mathbf{0} & \mathbf{0} & \mathbf{0} & \mathbf{D2} & \mathbf{F2} \end{bmatrix} ; \quad (3.37)$$

with

$$(\mathbf{A1}_{ij}, \mathbf{B1}_{ij}, \mathbf{D1}_{ij}, \mathbf{E}_{ij}, \mathbf{F1}_{ij}, \mathbf{H}_{ij}) = \sum_{k=1}^N \int_{\zeta_{k-1}}^{\zeta_k} Q_{ij}^{(k)} (1, \zeta, \zeta^2, \zeta^3, \zeta^4, \zeta^6) d\zeta, \quad i, j = 1, 2, 6; \quad (3.38)$$

$$(\mathbf{A2}_{ij}, \mathbf{D2}_{ij}, \mathbf{F2}_{ij}) = \sum_{k=1}^N \int_{\zeta_{k-1}}^{\zeta_k} Q_{ij}^{(k)} (1, \zeta^2, \zeta^4) d\zeta, \quad i, j = 4, 5. \quad (3.39)$$

3.7 Work Done By External Loads

The work done by the applied in-plane forces and transverse external loading in producing out of plane displacement 'w' in the domain of small displacement is,

$$\begin{aligned} W &= \frac{1}{2} \int_A \left[N_{x_1} \left(\frac{\partial w}{\partial x_1} \right)^2 + N_{x_2} \left(\frac{\partial w}{\partial x_2} \right)^2 + 2 N_{x_1 x_2} \left(\frac{\partial w}{\partial x_1} \right) \left(\frac{\partial w}{\partial x_2} \right) + q w \right] dA ; \\ &= \frac{1}{2} \int_A \left\{ \begin{bmatrix} w_{,x_1} \\ w_{,x_2} \end{bmatrix} \right\}^T \begin{bmatrix} N_{x_1} & N_{x_1 x_2} \\ N_{x_1 x_2} & N_{x_2} \end{bmatrix} \left\{ \begin{bmatrix} w_{,x_1} \\ w_{,x_2} \end{bmatrix} \right\} dA + \frac{1}{2} \int_A q w dA . \end{aligned} \quad (3.40)$$

3.8 The Kinetic Energy: Vibration

The kinetic energy of a vibrating panel in bending within domain of small displacement is

$$T = \frac{1}{2} \int_A \left(\sum_{k=1}^{NL} \int_{\zeta_{k-1}}^{\zeta_k} \rho^{(k)} \dot{\mathbf{u}}^T \dot{\mathbf{u}} \right) d\zeta dA; \quad (3.41)$$

where \mathbf{u} is the global displacement vector given by

$$\mathbf{u} = \{\bar{u} \ \bar{v} \ \bar{w}\}. \quad (3.42)$$

Using Equation (3.7), the above equation can be written as

$$\mathbf{u} = \bar{\mathbf{N}} \boldsymbol{\Lambda}; \quad (3.43)$$

where

$$\begin{aligned} \bar{\mathbf{N}} &= \begin{bmatrix} (1 + \zeta/R) & 0 & 0 & 0 & f_2(\zeta) & 0 & f_1(\zeta) \\ 0 & (1 + \zeta/R) & 0 & f_2(\zeta) & 0 & f_1(\zeta) & 0 \\ 0 & 0 & 1 & 0 & 0 & 0 & 0 \end{bmatrix}; \quad \text{for spherical panel} \\ \bar{\mathbf{N}} &= \begin{bmatrix} 1 & 0 & 0 & 0 & f_2(\zeta) & 0 & f_1(\zeta) \\ 0 & (1 + \zeta/R) & 0 & f_2(\zeta) & 0 & f_1(\zeta) & 0 \\ 0 & 0 & 1 & 0 & 0 & 0 & 0 \end{bmatrix}; \quad \text{for cylindrical panel} \\ \bar{\mathbf{N}} &= \begin{bmatrix} 1 & 0 & 0 & 0 & f_2(\zeta) & 0 & f_1(\zeta) \\ 0 & 1 & 0 & f_2(\zeta) & 0 & f_1(\zeta) & 0 \\ 0 & 0 & 1 & 0 & 0 & 0 & 0 \end{bmatrix}. \quad \text{for plate} \end{aligned} \quad (3.44)$$

Using Equation (3.43), the Equation (3.41) can be rewritten as

$$T = \frac{1}{2} \int_A \left(\sum_{k=1}^{NL} \int_{\zeta_{k-1}}^{\zeta_k} \rho^{(k)} \dot{\boldsymbol{\Lambda}}^T \bar{\mathbf{N}}^T \bar{\mathbf{N}} \dot{\boldsymbol{\Lambda}} \right) d\zeta dA = \frac{1}{2} \int_A \dot{\boldsymbol{\Lambda}}^T \mathbf{m} \dot{\boldsymbol{\Lambda}} dA; \quad (3.45)$$

where \mathbf{m} is the inertia matrix, and is given as

$$\mathbf{m} = \sum_{k=1}^{NL} \int_{\zeta_{k-1}}^{\zeta_k} \rho^{(k)} \bar{\mathbf{N}}^T \bar{\mathbf{N}} d\zeta. \quad (3.46)$$

3.9 Finite Element Model

Whenever possible, exact solutions are sought by the analyst. However, such exact closedform or series type solutions, which employ traditional variational methods, become complex and are very difficult/impossible to obtain for structures with complex geometries, arbitrary discontinuous loads, or discontinuous material properties/ or boundary conditions. With the advent of computers, the FEM has been found to be a very versatile tool for solving such complex, real life problems. It utilizes the traditional philosophy of variational methods to obtain the algebraic equations. The domain is divided by surfaces into a number of sub-domain that are commonly known as finite elements and the coordinate functions are developed over each of these elements employing the interpolation theory. The elements are assumed to be connected to one another at a number of discrete points, known as nodes. The interpolation functions that represent geometry and the function are known as shape functions. Depending on the order of shape functions that are used to represent the functions and geometries, various types of elements, such as isoparametric, sub-parametric and super parametric elements can be obtained [104]. The formulation of isoparametric elements is based on nondimensionalized local curvilinear triangular or tetrahedral coordinates so that the numerical integration can be easily performed. Because of accuracy and efficiency in terms of minimum number of integration points, Gaussian quadrature has found extensive application for numerical integrations. In the present thesis, nine noded isoparametric Lagrangian elements have been employed for plate, spherical and cylindrical shallow panels projected in rectangular plan form.

In the finite element method, the domain is discretized into a set of finite elements. Over each of these elements, the displacement vector Λ is represented as,

$$\Lambda = \sum_{i=1}^{NN} \varphi_i \Lambda_i ; \quad (3.47)$$

where φ_i is the interpolation (shape) function for the i th node [104,105], Λ_i is the vector of unknown displacements for the i th node and NN is the number of nodes per element.

The element geometry is also represented by same interpolation functions.

$$\begin{aligned} x_1 &= \sum_{i=1}^{NN} \varphi_i x_{1i} \\ x_2 &= \sum_{i=1}^{NN} \varphi_i x_{2i} \end{aligned} \quad (3.48)$$

The strain vector given in Equations (3.11) and (3.36) may be written as

$$\bar{\varepsilon} = \mathfrak{R} \Lambda \quad (3.49)$$

where, \mathfrak{R} is a matrix of differential operators.

3.9.1 Mechanical Strain Energy

The functional is computed for each element and then summed over all the elements in the domain to get the total functional for the domain. Following this, Equation (3.35) can be written as

$$\begin{aligned} U &= \sum_{e=1}^{NE} U^{(e)} \\ &= \sum_{e=1}^{NE} \frac{1}{2} \int_{A^{(e)}} \bar{\varepsilon}^T \mathbf{D} \bar{\varepsilon} dA \end{aligned} \quad (3.50)$$

where, NE is the number of elements.

From Equations (3.49) and (3.50), we get

$$U^{(e)} = \frac{1}{2} \int_{A^{(e)}} \Lambda^T \mathfrak{R}^T \mathbf{D} \mathfrak{R} \Lambda dA. \quad (3.51)$$

Further, substituting Equation (3.47) in the above equation,

$$U^{(e)} = \frac{1}{2} \int_{A^{(e)}} \Lambda^{T(e)} \mathbf{B}^T \mathbf{D} \mathbf{B} \Lambda^{(e)} dA; \quad (3.52)$$

$$= \Lambda^{T(e)} \mathbf{K}^{(e)} \Lambda^{(e)}. \quad (3.53)$$

Here \mathbf{B} is the strain displacement matrix and $\mathbf{\Lambda}^{(e)}$ is the elemental vector displacement obtained by assembling nodal displacement vectors and

$$\mathbf{B} = [\mathbf{B}_1 \ \mathbf{B}_2 \ \dots \mathbf{B}_n] \text{ with} \quad (3.54)$$

$$\mathbf{B}_i = \mathfrak{R} \ \varphi_i; \quad (3.55)$$

where \mathbf{B}_i is strain displacement matrix for the i^{th} node (Appendix B) and $\mathbf{K}^{(e)}$ is the element bending stiffness matrix given as

$$\mathbf{K}^{(e)} = \frac{1}{2} \int_{A^{(e)}} \mathbf{B}^T \mathbf{D} \mathbf{B} \ dA. \quad (3.56)$$

Transforming from existing coordinate system to natural coordinate system ξ, η , the element stiffness in Equation (3.56) can be represented as

$$\mathbf{K}_{ij}^{(e)} = \int_{-1}^1 \int_{-1}^1 \mathbf{B}_i^T \mathbf{D} \mathbf{B}_j \det \mathbf{J} \ d\xi \ d\eta. \quad (3.57)$$

Here

$$\mathbf{J} = \begin{bmatrix} \frac{\partial x_1}{\partial \xi} & \frac{\partial x_2}{\partial \xi} \\ \frac{\partial x_1}{\partial \eta} & \frac{\partial x_2}{\partial \eta} \end{bmatrix}. \quad (3.57)$$

When numerical integration is adopted, the element stiffness matrix given in Equation (3.57) becomes,

$$\mathbf{K}_{ij}^{(e)} = \frac{1}{2} \sum_{p=1}^N \sum_{q=1}^N W_p W_q \mathbf{B}_i^T \mathbf{D} \mathbf{B}_j \det \mathbf{J}; \quad (3.58)$$

where, W_p, W_q are weights used in Gaussian quadrature [104].

3.10 Summary

General equations for multi-layered laminated composite curved panels based on higher order deformable displacement field suggested by Reddy and Liu [95] have been presented. A procedure has been suggested to convert these equations to CLT and FSDT

form if needed. Further, the displacement field model has been recasted which enables us to employ a C^0 continuous element for the finite element analysis. The equilibrium equations, strain displacement relations and constitutive equations for spherical panel, cylindrical panel and plates are obtained from the curved panel equations.

In *Chapter IV*, the specific formulation along with probabilistic analysis procedure using first order perturbation stochastic classical approach (SCA) and stochastic finite element method (SFEM) are presented for composite panels with random material properties. The second order statistics of buckling loads are obtained for composite laminated laminates, cylindrical and spherical shallow panels.

In *Chapter V*, the specific formulation with random analysis procedure for free vibration problem with random material properties using SCA and SFEM are presented. The second moments of natural frequencies are obtained for composite laminates, cylindrical and spherical panels.

In *Chapter VI*, a similar study for forced vibration problem with random material properties to random loading is presented using SCA and SFEM. The second order statistic of displacement are obtained for composite laminates, cylindrical and spherical panels.

CHAPTER IV

BUCKLING OF COMPOSITE PANELS

4.1 Introduction

The increasing use of high strength and stiffness materials in recent times for structural component design and the need to produce light weight and optimized structures have lead to widespread adoption of thin walled components in aerospace structures. Buckling in any form either precipitates or hastens the collapse of such structures. The aerospace structures, in general, experience complex loading during service life. Buckling may occur in these structures in a variety of forms such as global or local and avoiding buckling failure is an essential requirement in the design of optimized structural components.

As pointed out in *Chapter II*, some literature is available on the analysis of metallic structures with random material properties while very limited literature is available on the study of composite structures with random material properties. Further, to the best of authors' knowledge, not much information is available on buckling analysis of composite beams, plates and shells, with parameter uncertainties. It is also seen that no attempt has been made to study the buckling problem in the presence of uncertainties by taking transverse shear into account. A large volume of information is available on the deterministic buckling analysis of beams, plates and shells using various shear deformation theories [96, 106-110]. In this

chapter an attempt is made to study the buckling response of composite laminated plates, cylindrical and spherical panels with random material properties, taking into account transverse shear effects. As mentioned in *Chapter III*, the lamina material properties are modeled as the basic random variables. The FOPT has been adopted to handle the random scatter. Efficacies of the three theories - classical laminate theory, first-order shear deformation theory and higher order shear deformation theory on dispersion in the buckling load has been examined. Though the comparison of the performances of these theories is well understood for deterministic case, that is, the mean buckling load, their performance with the buckling load dispersion has not been reported.

This Chapter outlines a probabilistic methodology for application of classical approach in conjunction with first order perturbation technique (SCA) to solution of random characteristic equation of buckling evolved from random variation of lamina material properties. This Chapter also outlines finite element method with first order perturbation technique (SFEM) to the uncertain standard eigen value problem of buckling arising from uncertain variation of lamina material properties

4.2 Stochastic Classical Approach (SCA)

For cross-ply laminates with all edges simply supported, exact Navier type solution is possible. When exact solution is combined with probabilistic method, it is possible to analyze the random characteristics equation arising from buckling of composite laminates. In this section, a detailed study is presented to obtain the second order statistics of the buckling loads for composite plates, cylindrical and spherical panels using stochastic classical approach.

4.2.1 Formulation

The boundary condition for all edges simply supported plates and cylindrical and spherical panels can be stated as:

$$u = w = N_2 = M_2 = \phi_1 = 0; \text{ at } x_2 = 0, b,$$

$$v = w = N_1 = M_1 = \phi_2 = 0; \text{ at } x_1 = 0, a.$$

The coordinate systems used are as specified in *Chapter III*.

The displacements satisfying all the boundary conditions can be expressed in the following form for panels with all edges simply supported:

$$u = \sum_{m,n=1}^{\infty} U_{mn} f_1(x_1, x_2); \quad v = \sum_{m,n=1}^{\infty} V_{mn} f_2(x_1, x_2); \quad w = \sum_{m,n=1}^{\infty} W_{mn} f_3(x_1, x_2);$$

$$\phi_1 = \sum_{m,n=1}^{\infty} \phi_{mn}^{(1)} f_1(x_1, x_2); \quad \phi_2 = \sum_{m,n=1}^{\infty} \phi_{mn}^{(2)} f_2(x_1, x_2),$$
(4.1)

where

$$f_1(x_1, x_2) = \cos(\alpha x_1) \sin(\beta x_2); \quad f_2(x_1, x_2) = \sin(\alpha x_1) \cos(\beta x_2);$$

$$f_3(x_1, x_2) = \sin(\alpha x_1) \sin(\beta x_2); \quad \alpha = m\pi/a; \quad \beta = n\pi/b.$$
(4.2)

Substitution of Equation (4.1) into Equation (3.34) results in a homogeneous system of equations

$$\sum_{j=1}^n M_{ij} k_j = 0 \quad (4.3)$$

where \mathbf{k} is a constant column vector and $i, j=1, 2, \dots, 5$ for HSDT and FSDT, and $i, j=1, 2, 3$ for CLT. For a nontrivial solution of \mathbf{k} in Equation (4.3), the determinant of coefficients should be zero:

$$|M_{ij}| = 0 \quad (4.4)$$

Equation (4.4) can be written in expanded form as

$$\begin{vmatrix} a_{11} & a_{12} & a_{13} & a_{14} & a_{15} \\ a_{21} & a_{22} & a_{23} & a_{24} & a_{25} \\ a_{31} & a_{32} & a_{33} - N_{cr} & a_{34} & a_{35} \\ a_{41} & a_{42} & a_{43} & a_{44} & a_{45} \\ a_{51} & a_{52} & a_{53} & a_{54} & a_{55} \end{vmatrix} = 0, \quad \text{for HSDT and FSDT,} \quad (4.5)$$

$$\begin{vmatrix} a_{11} & a_{12} & a_{13} \\ a_{21} & a_{22} & a_{23} \\ a_{31} & a_{32} & a_{33} - N_{cr} \end{vmatrix} = 0, \quad \text{for CLT} \quad (4.6)$$

where the expression for critical buckling load is given as

$$N_{cr} = N_{x_1} + N_{x_2} \beta^2 / \alpha^2 + N_{x_1 x_2} \alpha \beta / \alpha^2 \quad (4.7)$$

In Equations (4.5) and (4.6), a_{ij}^s are functions of system stiffness and wavelength parameters α and β .

Expanding the above determinant (Equations 4.5 and 4.6) gives the expression for N_{cr} in terms of a_{ij}^s .

$$N_{cr} = F(a_{ij}) \quad (4.8)$$

The stiffness elements a_{ij} are random in nature, being dependent on the system material properties, consequently, the buckling loads are also random.

4.2.2 Second- Order Statistics of Critical Buckling Loads– A Perturbation Approach

Consider a class of problems where the random variation of the material properties is very small compared to the mean value. Most engineering structures, including composites fall under this class. Further, it is quite logical to assume that the dispersion in derived quantities like a_{ij}^R and N_{cr}^R are also small as compared to their mean values.

A random variable may be split up as the sum of its mean and the zero mean random part as.

$$N_{cr}^R = \bar{N}_{cr} + N_{cr}^r; \quad a_{ij}^R = \bar{a}_{ij} + a_{ij}^r; \quad (4.9)$$

where, over bar denotes mean value, superscript 'R' denotes random variable and superscript 'r' denotes zero mean random parts.

Substitution of Equation (4.9) in Equations (4.5) and (4.6) results in

$$\begin{vmatrix} \bar{a}_{11} + a_{11}^r & \bar{a}_{12} + a_{12}^r & \bar{a}_{13} + a_{13}^r & \bar{a}_{14} + a_{14}^r & \bar{a}_{15} + a_{15}^r \\ \bar{a}_{21} + a_{21}^r & \bar{a}_{22} + a_{22}^r & \bar{a}_{23} + a_{23}^r & \bar{a}_{24} + a_{24}^r & \bar{a}_{25} + a_{25}^r \\ \bar{a}_{31} + a_{31}^r & \bar{a}_{32} + a_{32}^r & \bar{a}_{33} + a_{33}^r - \bar{N}_{cr} - N_{cr}^r & \bar{a}_{34} + a_{34}^r & \bar{a}_{35} + a_{35}^r \\ \bar{a}_{41} + a_{41}^r & \bar{a}_{42} + a_{42}^r & \bar{a}_{43} + a_{43}^r & \bar{a}_{44} + a_{44}^r & \bar{a}_{45} + a_{45}^r \\ \bar{a}_{51} + a_{51}^r & \bar{a}_{52} + a_{52}^r & \bar{a}_{53} + a_{53}^r & \bar{a}_{54} + a_{54}^r & \bar{a}_{55} + a_{55}^r \end{vmatrix} = 0, \text{ for HSDT and FSDT,}$$

$$\text{and} \quad (4.10)$$

$$\begin{vmatrix} \bar{a}_{11} + a_{11}^r & \bar{a}_{12} + a_{12}^r & \bar{a}_{13} + a_{13}^r \\ \bar{a}_{21} + a_{21}^r & \bar{a}_{22} + a_{22}^r & \bar{a}_{23} + a_{23}^r \\ \bar{a}_{31} + a_{31}^r & \bar{a}_{32} + a_{32}^r & \bar{a}_{33} + a_{33}^r - \bar{N}_{cr} - N_{cr}^r \end{vmatrix} = 0, \quad \text{for CLT.}$$

Expanding Equation (4.10) and collecting same order of magnitude terms and retaining terms only up to first order, we obtain the following relations, which in a symbolic form are

$$\text{Zeroth order: } \bar{N}_{cr} = F(\bar{a}_{ij}) \quad (4.11)$$

$$\text{First order: } N_{cr}^r = F(\bar{a}_{ij}, a_{ij}^r, \bar{N}_{cr}) \quad (4.12)$$

The detailed equations are placed at Appendix C.

Equation (4.11) is a deterministic equation relating only the mean quantities. The mean value of buckling loads can therefore be obtained by any of the standard solution procedure [102].

For the present case a_{ij}^R and N_{cr}^R are random because the material properties are random. Let

$d_1^R, d_2^R, \dots, d_m^R$ denote the random material properties. Following Equation (4.9) the d_j^R can

also be expressed as

$$d_j^R = \bar{d}_j + d_j^r \quad (4.13)$$

According to Taylor's rule when d_j^r is small compared with its mean value, we can expand a_{ij}^R and N_{cr}^R about \bar{d}_j , $j=1, 2, \dots, m$. Keeping only the first order terms, we obtain

$$N_{cr}^r = \sum_{j=1}^n \bar{N}_{cr,j} d_j^r; \quad a_{ik}^r = \sum_{j=1}^n \bar{a}_{ik,j} d_j^r, \quad (4.14)$$

where $,j$ denotes the partial differentiation with respect to d_j^R and the derivatives are evaluated at \bar{d}_j . The terms $\bar{N}_{cr,j}$ are still to be evaluated. Inserting Equation (4.14) in Equation (4.12) and comparing coefficients of random variables gives a set of simultaneous equations in these unknowns. Solution of this set yields the expression for $\bar{N}_{cr,j}$ in the symbolic form

$$\bar{N}_{cr,j} = F(\bar{a}_{ik}, \bar{a}_{ik,j}, \bar{N}_{cr}) \quad (4.15)$$

Use of Equation (4.15) in the first of Equation (4.14) yields the expression of N_{cr}^r in known terms. Using the basic definition of the variance [19, 111], the expression for the variance for the critical buckling load is obtained from Equation (4.14) as

$$\begin{aligned} Var(N_{cr}) &= E \left[\sum_{j=1}^m \bar{N}_{cr,j} d_j^r \sum_{k=1}^m \bar{N}_{cr,k} d_k^r \right] \\ &= \sum_{j=1}^m \sum_{k=1}^m \bar{N}_{cr,j} \bar{N}_{cr,k} E[d_j^r d_k^r] \\ &= \sum_{j=1}^m \sum_{k=1}^m \bar{N}_{cr,j} \bar{N}_{cr,k} Cov(d_j^r, d_k^r) \end{aligned} \quad (4.16)$$

where $E[\]$ stands for expectation and $Cov(d_j^r, d_k^r)$ is the cross covariance between d_j^r and d_k^r .

4.2.3 Results and Discussion

The procedure developed in the previous section is employed to evaluate the second order statistics of critical buckling loads of anti-symmetric and symmetric, cross-ply,

rectangular laminates, cylindrical and spherical panels with all edges simply supported. The following mean values of material properties of graphite/epoxy composite are employed for the computation: $\bar{E}_{11} = 40\bar{E}_{22}$, $\bar{G}_{12} = \bar{G}_{13} = 0.6\bar{E}_{22}$, $\bar{G}_{23} = 0.5\bar{E}_{22}$, $\bar{\nu}_{12} = 0.25$ [112], where \bar{E}_{11} and \bar{E}_{22} denote the longitudinal and transverse elastic moduli, respectively; \bar{G}_{12} is the in plane shear modulus; \bar{G}_{13} and \bar{G}_{23} are the two out of plane shear moduli; and $\bar{\nu}_{12}$ denotes the Poisson ratio. All plies are assumed to have the same thickness and orthotropic material properties along the material axes. The shear correction factors required for FSDT are taken to be 5/6 [112].

The elastic properties of the composite lamina are modeled as the basic variables. These RVs d_j^R are sequenced here as $d_1^R = E_{11}^R$, $d_2^R = E_{22}^R$, $d_3^R = G_{12}^R$, $d_4^R = G_{13}^R$, $d_5^R = G_{23}^R$ and $d_6^R = \nu_{12}^R$, for HSDT and FSDT, and $d_1^R = E_{11}^R$, $d_2^R = E_{22}^R$, $d_3^R = G_{12}^R$ and $d_4^R = \nu_{12}^R$, for CLT.

The mean critical buckling loads have been nondimensionalised as $N_{cr} = \bar{N}_{cr} b^2 / (\bar{E}_{22} h^3)$. The variances of the nondimensionalised buckling loads have been normalized with the corresponding mean values. The effects of the dispersion in the material properties on the nondimensionalised buckling load have been obtained for cross-ply panels by taking the ratio of the SD to mean varying from 0% to 20% [51]. Results have been computed with all the basic properties simultaneously considered as random. Results have also been computed by taking only one property to be random at a time while all others to be deterministic to study the sensitivity of the response to individual material property dispersions. Panels with two stacking sequences $[0^0/90^0]$ and $[0^0/90^0/90^0/0^0]$ have been used for this study to bring out the effect of anti symmetry and symmetry in the stacking sequence.

4.2.3.1 Buckling Load: Composite Plates

Validation study

Figure 4.1 shows the comparison of the results obtained from the present approach with Monte Carlo simulation for $[0^0/90^0]$ laminated plate using the three plate theories. Results have been compared for a square laminate of thickness ratio, $b/h=10$ with only E_{11} assumed to be random. The comparison will serve to validate the applicability of the present FOPT approach. For the MCS technique, the material property samples are obtained by generating a set of random numbers to fit the desired mean and standard deviation (SD). NAG library subroutine G05FDF has been employed assuming the material properties to follow Gaussian distribution. However, the perturbation approach used in the study does not put any limitation on the distribution of material properties as only the second order statistics is utilized. Based on convergence, the number of samples used for the study is 10000. These values are used in Equation (4.8), which is solved repeatedly to generate a sample of the buckling load. This sample is then processed to obtain the mean and the variance. The comparison has been presented for MCS and FOPT results with the three plate theories – CLT, FSDT and HSDT. It is observed that the FOPT results are in close agreement with the MCS.

Second order statistics

Results have been computed for a plate having aspect ratios $b/a=1, 2$ and 3 and thickness ratios $b/h=10$ and 100 with the two stacking sequences.

Tables 4.1(a) and 4.1(b) list non-dimensionalised mean buckling loads with $\bar{N}_{cr} = \bar{N}_{x_2}$ and $\bar{N}_{x_1} = \bar{N}_{x_1x_2} = 0$. Using the three plate theories results are presented for $b/a = 1, 2$ and 3 and $b/h = 10$ and 100 for the two stacking sequences $[0^0/90^0]$ and $[0^0/90^0/90^0/0^0]$.

The higher value of buckling loads, as expected, is observed for symmetric as compared to anti-symmetric cross-ply plates. It is also observed that the classical laminate theory over predicts the buckling loads as compared to FSDT and HSDT for both $b/h=10$ and 100 . It is further observed that these over predictions are large for $b/h=10$ and small for $b/h=100$. Examination of the results reveals that the buckling load increases as the aspect ratio (b/a) increases. It may be noted that the FSDT under predicts the buckling loads for anti-symmetric cross-ply laminates and over predicts for symmetric cross-ply laminates as compared to HSDT for the aspect ratios studied.

Figures 4.2(a)-4.2(f) show the response of CLT, FSDT and HSDT on the dispersion in the buckling loads for anti-symmetric cross-ply laminate, with all the material properties changing simultaneously. Results for three aspect ratios (b/a): 1, 2 and 3 with two thickness ratios (b/h): 10 and 100 have been presented. The buckling load dispersion is over predicted by CLT for $b/h=10$. However, for the thickness ratio (b/h) 100, it is not always so. HSDT predicts largest dispersion for $b/a=1$, CLT for $b/a=2$ and FSDT for $b/a=3$. For the two shear deformation theories, predicted level changes with aspect ratio and thickness ratio, but no pattern is observed.

For a symmetric $[0^0/90^0/90^0/0^0]$ laminate the general trend for the corresponding behavior is found to be similar. Hence, to economize space, the figures have not been presented. A more consistent pattern with CLT predicting the larger dispersion has been observed for the three aspect ratios and the two thickness ratios studied.

The buckling load sensitivity for $[0^0/90^0]$ laminate with $b/a=1, 2, 3$ and $b/h=10$ using HSDT is presented in Figs. 4.3(a) – 4.3(f) with only one basic variable changing at a time. The effects of the individual variations of E_{11}, E_{22}, G_{12} and ν_{12} on the buckling load dispersion decreases as b/a ratio increases. However, the influence of the individual variations of G_{13} and G_{23} increases as b/a ratio increases. SD of E_{11} has dominant effect on

the scattering of the buckling loads for $b/a=1$ and 2. However, for $b/a=3$, G_{13} is the dominant material property. The buckling loads are least affected by changes in ν_{12} . It is observed that the effect of G_{23} is comparable to G_{13} .

The general behavior of the buckling loads with SD/Mean of basic material properties changing only one at a time for symmetric laminate with $b/a=1, 2, 3$ and $b/h=10$ using HSDT has similar trends to anti-symmetric laminate. Hence, the figures have not been presented. For $b/a=1$, the effect of E_{11} is dominant, however for $b/a=2$ and 3, the effect of G_{13} is the most dominant.

Conclusions

The second order statistics of the non-dimensionalised initial buckling loads have been obtained for two stacking sequences of cross-ply graphite – epoxy laminates with all edges simply supported. The following main conclusions can be drawn from this study:

- In mean buckling load analysis, CLT always over predicts the buckling load as compared to shear deformation theories. For scatter in buckling loads, CLT over predicts the dispersions for thick plates as compared to FSDT and HSDT while it does not always over predict dispersions for thin plates.
- For mean analysis, FSDT under predicts the mean buckling load as compared to HSDT for cross-ply anti symmetric laminates and over predicts for symmetric laminates. However, for buckling load dispersion analysis, FSDT does not show a consistent prediction pattern compared to HSDT for cross-ply anti symmetric and symmetric laminates. The relative magnitude depends on laminate construction, aspect ratio and thickness ratio.

- The dispersion in buckling loads always decreases as aspect ratio increases for thick symmetric and anti-symmetric laminates considered for the study against individual variation of longitudinal elastic modulus, transverse elastic modulus, in plane shear modulus and Poisson ratio while it shows a reverse trend with out of plane shear modulus.
- The longitudinal elastic modulus (E_{11}) is the dominant material property in case of symmetric square laminates and anti- symmetric laminates of $b/a=1$ and 2, while, the out of plane shear modulus (G_{13}) is dominant for the plates with aspect ratio =3.

4.2.3.2 Buckling Loads: Composite Cylindrical Panels

Validation

Validation of the present approach for buckling of laminated composite cylindrical panels has been carried out on the lines of the plate. Figure 4.4 illustrates the comparison of the results obtained by the present approach and with Monte Carlo simulation for $[0^0/90^0]$ laminated cylindrical panels with $R/b=5$, $b/a=1$ and $b/h=10$, using the three theories with only one material property E_{11} to be random. Here also the number of sample size selected, based on convergence, is 10000. These values are used in Equation (4.8), which is solved repeatedly to generate a sample of the buckling load. This sample is processed to obtain the mean and the variance of the buckling load. It is observed that the results are in good agreement with the MCS.

Second Order Statistics

The panel parameters used for the two stacking sequences studied are, aspect ratio $b/a=1$, curvature to side ratio $R/b=5$, and side to thickness ratios $b/h=10$ and 100. The material properties are kept the same.

Mean Buckling Loads

Table 4.2 presents the nondimensionalised mean buckling loads with $R/b=1$, $R/h=10$ and $b/a=1$ for stacking sequence of $[0^0/90^0]$ along with the results by Khdeir et al. [113]. The reference uses an exact state space technique for the solution. The present approach is also exact as far as the mean analysis is concerned. A reasonably good agreement between the two is observed.

Table 4.3 lists the nondimensionalised mean buckling loads for cylindrical panel with $R/b=5$, $b/a = 1$ and $b/h = 10$ and 100 for the two stacking sequences using CLT, FSDT and HSDT. Higher values of buckling loads, as expected, are observed for symmetric as compared to anti-symmetric cross-ply panels. The classical laminate theory over predicts the buckling loads as compared to FSDT and HSDT for $b/h=10$ and 100 . These over predictions are large for the thicker panel and small for the thinner panel. It may be noted that the HSDT slightly over predicts the buckling loads for anti-symmetric cross-ply and under predicts for symmetric cross-ply laminates as compared to FSDT results for the cases considered.

Variance of Buckling Loads

$[0^0/90^0]$ Square, cross-ply, anti-symmetric laminate

The variation of nondimensionalized buckling loads with SD of all the basic RVs changing simultaneously for $[0^0/90^0]$, square, anti-symmetric laminate with $R/b=5$ and thickness ratios $b/h=10$ and 100 are presented in Figures 4.5(a) and 4.5(b), respectively. It is seen that the change in buckling loads for $b/h=10$ is smaller than for $b/h=100$. Classical laminate theory shows larger changes in buckling loads for $b/h=10$ and smaller changes for $b/h=100$ as compared to shear deformation theories. The difference in the variation of

buckling loads by FSDT and HSDT is not significant for $b/h=10$ while it is significant for $b/h=100$.

Figures 4.6(a) – 4.6(f) show the sensitivity of buckling loads to dispersion by considering only one basic variable at a time for $b/h=10$. The variations of buckling loads are strongly influenced by dispersion in E_{11} . In general, the CLT over predicts the variation in buckling loads as compared to FSDT and HSDT, while the variation in buckling loads using HSDT and FSDT are of the same order of magnitude for the individual variation of E_{11}, E_{22}, G_{12} and ν_{12} . However, the difference between the results predicted by FSDT and HSDT is considerable for dispersion in G_{13} and G_{23} with FSDT over predicting the variation. It is observed that the buckling loads are least affected with dispersion in ν_{12} .

Figures 4.7(a) – 4.7(f) present the variation in buckling loads due to dispersion in one basic material property for $R/b=5$ and $b/h=100$. The variation of buckling load is maximum for dispersion in E_{11} and least for dispersion in ν_{12} . The FSDT and CLT under predict the variation as compared to HSDT. It may be noted that in spite of over and under predictions in buckling loads, the variance in the buckling loads given by the three theories are of comparable order of magnitude for variations in E_{22}, G_{12} and ν_{12} . However, the difference in variations in buckling loads is observed to be large between HSDT and FSDT for changes in G_{13} and G_{23} .

$[0^0/90^0/90^0/0^0]$ Square, cross-ply, symmetric laminate

Figures 4.8(a) and 4.8(b) show the sensitivity of buckling loads with SD/Mean of basic material properties changing simultaneously for $[0^0/90^0/90^0/0^0]$ square, symmetric laminate with $R/b=5$ and $b/h=10$ and 100 , respectively. The CLT results are more sensitive to

changes in SD/mean of material property as compared to the shear deformation theories for $b/h=10$ while, the FSDT results are more sensitive for $b/h=100$.

Figures 4.9(a) – 4.9(f) show the sensitivity of buckling loads for SD/Mean of basic material properties by changing only one property at a time for $R/b=5$ and $b/h=10$ and 100 . The CLT over predicts the variation in the buckling loads, while FSDT under predicts against changes in the material property SD except for E_{11} and G_{23} . The buckling loads obtained using CLT, FSDT and HSDT are most sensitive to SD/mean of E_{11} and are least sensitive to SD/mean of ν_{12} .

Figures 4.10(a) – 4.10(f) show the influence on buckling loads with SD/Mean of basic material properties changing only one at a time for $R/b=5$ and $b/h=10$ and 100 . The buckling loads are most sensitive to changes in SD/mean of E_{11} for all the three theories considered. The buckling loads obtained by HSDT are least affected by changes in G_{23} and the CLT and FSDT result by ν_{12} . The three theories predict close dispersion in buckling load for variations in E_{22} , G_{12} and ν_{12} with FSDT slightly over predicting the values. The HSDT significantly over predicts the buckling load scatter as compared to FSDT for variation in G_{13} and G_{23} .

Conclusions

The mean and standard deviation of the buckling loads have been computed for two stacking sequences for cross-ply laminated cylindrical panels. On the basis of this study, the following conclusions can be drawn for graphite/epoxy laminates with all edges simply supported:

- There is a significant effect on the mean buckling loads with changes in thickness ratio b/h .

- The buckling loads are sensitive to the variation of SD of material properties. The dominant material property is found to be E_{11} for all the three theories considered.
- The panel buckling loads for anti-symmetric cross-ply laminates show larger variation with changes in thickness ratio as compared to symmetric laminates.
- In general, the CLT over predicts the variation in buckling loads with $b/h=10$ for the two laminates studied. However, the HSDT over predicts the loads for anti-symmetric laminates while FSDT over predicts for symmetric laminates.

4.2.3.3 Buckling Load: Composite Spherical Panels

Validation Study

Validation of the present technique for studying buckling of laminated composite spherical panels has been carried out on the same lines as for the plate. Figure 4.11 shows the results obtained by adopting FOPT and MCS approaches for $[0^0/90^0]$ laminated spherical panels with $R/b=5$, $b/a=1$ and $b/h=10$, using two theories FSDT and HSDT with only E_{11} taken to be random while other input basic variables are kept constant. The sample size selected for MCS, based on convergence, is 10000. The sample values for the material properties have been generated assuming random variables to be distributed normally. It is observed that the results obtained from FOPT are in good agreement with MCS.

Second Order Statistics

The panel geometry employed for the study are: $b/a=1$ and 2, curvature to side ratio, $R/b=5$, and side to thickness ratios, $b/h=10$ and 100, and two stacking sequences $[0^0/90^0]$ and $[0^0/90^0/90^0/0^0]$.

Mean buckling loads

In Table 4.4 the nondimensionalised mean buckling loads with $R/b=5$, $b/a=1$ and 2 and $b/h=10$ and 100 for the two stacking sequences using the two shear deformation theories are presented. It is observed that the mean buckling load increases with increase in b/a and b/h ratios. Further, HSDT gives slightly higher buckling loads as compared to FSDT for anti symmetric laminates and slightly lower values for symmetric laminates for $R/b=5$ and for both the value of b/h . These differences in the predictions are small for thin panels. The higher value of buckling loads, as expected, is observed for symmetric laminates as compared to anti-symmetric laminates. It is also observed that the mean buckling loads increases as aspect ratio increases.

Variance of buckling loads

For $R/b=5$ and $b/h=10$, Figures 4.12(a) and 4.12(b) illustrate the variation of buckling loads for $[0^0/90^0]$ laminate while Figures 4.12(c) and 4.12(d) show the variation of buckling loads for $[0^0/90^0/90^0/0^0]$ laminate, for $b/a=1$ and 2 with SD of all the basic RVs changing simultaneously. It is seen that the dispersions in buckling loads with FSDT and HSDT models are of comparable order of magnitude. However, the HSDT over predicts the variation for anti symmetric laminate, under predicts for symmetric with $b/a=1$. It also over predicts for symmetric laminate with $b/a=2$. It is also observed that there is slight change in buckling loads as the b/a ratio increases for both the stacking sequences.

For $R/b=5$ and $b/h=100$, Figures 4.13(a) and 4.13(b) illustrate the variation of buckling loads for $[0^0/90^0]$ laminate while Figures 4.13(c) and 4.13(d) show variation of buckling loads for $[0^0/90^0/90^0/0^0]$ laminate, for $b/a=1$ and 2 with SD of all the basic RVs changing simultaneously. It is observed that there is some increase in scattering of buckling loads as b/a ratio increases for both the theories considered. The dispersions due to FSDT and

HSDT are of the same order of magnitude for a symmetric square laminate while these are comparable order of magnitude for the remaining cases. It is also observed that FSDT under predicts the dispersions in buckling loads for anti- symmetric square laminate while it over predicts for the remaining cases as compared to HSDT.

Figures 4.14(a)–4.14(d) present the sensitivity of buckling loads to changes in only E_{11} while other properties are kept constant for $[0^0/90^0]$ and $[0^0/90^0/90^0/0^0]$ laminates with $R/b=5$, $b/a=1$ and 2 and $b/h=10$. The buckling load variation obtained using FSDT with changes in E_{11} is highest for symmetric laminates with $b/a=1$ while, it is lowest for symmetric laminates for $b/a=2$. However, the HSDT predicts the highest values for anti-symmetric square laminate and smallest values for symmetric laminates for $b/a=2$. There is significant change in buckling load as b/a ratio changes. The difference between changes in buckling loads due to FSDT and HSDT for the two stacking sequences considered are seen for $b/a=2$ is more compared to $b/a=1$.

Figures 4.15(a)–4.15(d) represent variation in buckling loads due to change in only E_{11} for the two stacking sequences with $R/b=5$, $b/a=1$ and 2 and $b/h=100$. The changes in buckling load due FSDT and HSDT are more sensitive for symmetric laminate with $b/a=2$. The FSDT gives smallest buckling loads dispersions for anti-symmetric square laminate while HSDT predicts almost equal dispersion for symmetric and anti-symmetric square laminates. Higher changes are predicted by the two theories for $b/a=2$ as compared to $b/a=1$ for both stacking sequences. The symmetric laminate with $b/a=2$ is very sensitive to changes in the basic RV.

Figures 4.16(a) – 4.16(d) show the sensitivity of buckling loads with SD/Mean of only E_{22} changing with other material properties constant for the two stacking sequences with $R/b=5$, $b/a=1$ and 2 and $b/h=10$. The FSDT and HSDT results show equal sensitivities to changes in SD/mean of the material property for anti- symmetric laminates with $b/a=1$. The

two theories predict smallest dispersion in buckling loads for symmetric laminate with $b/a=2$.

In general, the scattering in buckling loads decreases as b/a ratio increases.

Figures 4.17(a) – 4.17(d) bring out the sensitivity of buckling loads with SD/Mean of only E_{22} changing while others are kept constant for both the stacking sequences with $R/b=5$, $b/a=1$ and 2 and $b/h=100$. The dispersion in buckling loads predicted by the two shear deformation theories is of the same order of magnitude for the laminate geometries and stacking sequences investigated. It is observed that the dispersion in buckling loads increases as b/a ratio increases. The buckling loads are very sensitive for anti-symmetric laminates as compared to symmetric laminates. It is further observed that the changes in buckling loads for anti-symmetric laminates are most sensitive to changes in basic RVs with aspect ratio $b/a=2$ while least sensitive for symmetric laminates with aspect ratio $b/a=1$.

Figures 4.18(a) – 4.18(d) show the influence of buckling loads with SD/Mean of only G_{12} changing at a time for the two stacking sequences with $R/b=5$, $b/a=1$ and 2 and $b/h=10$. The buckling loads are very sensitive with the changes in SD/mean of G_{12} for anti-symmetric square laminate for the two theories considered. The variation in buckling load is minimum for symmetric laminates with $b/a=2$. In general, the dispersion in buckling loads is seen to be more for anti-symmetric laminates as compared to symmetric laminates. The effect decreases as b/a ratio increases.

Figures 4.19(a) – 4.19(d) show the influence on buckling loads with SD/Mean of only G_{12} changing at a time for the two stacking sequences with $R/b=5$, $b/a=1$ and 2 and $b/h=100$. There is a considerable change in the dispersion of the buckling loads with changes in b/a for symmetric laminates. Further, significant change is seen between symmetric and anti-symmetric laminates for $b/a=2$ while it is of the same order of magnitude for $b/a=1$. The FSDT and HSDT are equally sensitive for the panel geometries and stacking sequences

considered for the study. The FSDT and HSDT predicts highest variation for anti-symmetric square laminate and lowest for symmetric laminate with $b/a=2$.

Figures 4.20(a) – 4.20(d) present the influence on buckling loads with SD/Mean of basic material property with only G_{13} changing at a time for the two stacking sequences with $R/b=5$, $b/a=1$ and 2 and $b/h=10$. It is observed that the HSDT shows least dispersion in buckling loads for anti-symmetric cross-ply laminates and more dispersion for symmetric cross-ply laminates as compared to FSDT. The variation in buckling loads increases as b/a ratio increases for both the stacking sequences. The symmetric cross-ply laminate with $b/a=2$ is more sensitive to variation of buckling loads as compared to the other panel geometries and stacking sequences combination considered for the present study. The anti-symmetric square laminates are least sensitive. In general, the symmetric laminates are more sensitive as compared to anti-symmetric laminates.

Figures 4.21(a) – 4.21(d) represent the influence on buckling loads with SD/Mean of basic material property with only G_{13} changing at a time for the two stacking sequences with $R/b=5$, $b/a=1$ and 2 and $b/h=100$. The FSDT under predicts the scattering in buckling loads for $b/a=1$ and over predicts for $b/a=2$ as compared to HSDT for the stacking sequences considered. The scattering increases as b/a ratio increases. The anti-symmetric laminates are seen to be more sensitive as compared to symmetric laminates.

Figures 4.22(a) – 4.22(d) present the dispersion of buckling loads with SD/Mean of basic material property with only G_{23} changing at a time for the two stacking sequences with $R/b=5$, $b/a=1$ and 2 and $b/h=10$. The scattering in buckling loads increases as b/a ratio increases for stacking sequences considered. The symmetric laminates are more sensitive as compared to anti –symmetric laminates for the panel geometries and stacking sequences considered. It is important to note that the FSDT always over predicts the scattering in buckling loads as compared to HSDT for the geometrical parameters and stacking sequences

considered. The FSDT and HSDT are most sensitive for symmetric laminates of $b/a=2$ and less sensitive for anti-symmetric square laminate.

Figures 4.23(a) – 4.23(d) show the variation of buckling loads with SD/Mean of basic material property with only G_{23} changing for the two stacking sequences with $R/b=5$, $b/a=1$ and 2 and $b/h=100$. The FSDT under predicts the dispersion for symmetric and anti-symmetric square laminates, over predicts for anti-symmetric laminate with $b/a=2$, while it is of the same order of magnitude for symmetric laminate with $b/a=2$. The symmetric laminates are less sensitive as compared to anti-symmetric laminates.

Figures 4.24(a) – 4.24(d) show the sensitivity of buckling loads with SD/Mean of basic material property with only ν_{12} changing at a time for the two stacking sequences with $R/b=5$, $b/a=1$ and 2 and $b/h=10$. The sensitivity of symmetric laminates and anti-symmetric laminates is of the same order of magnitude for $b/a=1$, while for $b/a=2$, the anti-symmetric laminate shows higher sensitivity. The HSDT always over predicts the scattering in buckling loads as compared to FSDT. However, these over predictions have the characteristics very small for both stacking sequences with aspect ratio $b/a=1$, small for symmetric laminate with $b/a=2$ and large for anti-symmetric laminate with $b/a=2$.

Figures 4.25(a) – 4.25(d) plot the influence of buckling loads with SD/Mean of basic material property with only ν_{12} changing at a time for the two stacking sequences with $R/b=5$, $b/a=1$ and 2 and $b/h=100$. The FSDT over predicts the dispersion in buckling loads for anti-symmetric square laminate while it is of the same order of magnitude for other combination of the geometrical parameters and stacking sequence as compared to HSDT. The symmetric laminates are more sensitive as compared to anti-symmetric laminates. There is a significant increase in buckling load scattering as b/a ratio increases. The symmetric laminate with $b/a=2$ shows the largest deviation in buckling loads while, anti symmetric square laminate shows smallest dispersion in the buckling loads.

Conclusions

From the examination of the results for study done on graphite-epoxy laminates with all edges simply supported, the following conclusions can be drawn:

- There is a significant change in mean buckling loads with change in thickness ratio b/h and aspect ratio b/a .
- The higher values of mean buckling loads obtained using HSDT are observed for anti-symmetric laminates with different b/h ratios as compared to FSDT. This trend is reversed for symmetric laminates. It is also observed that these over predictions and under predictions are small for thin spherical panels.
- The buckling loads show different sensitivity to the influence of SD of the six material properties considered. The sensitivity depends on laminate sequencing, shear deformation theories, aspect ratio (b/a) and thickness ratio (b/h). The dominant material property is found to be E_{11} for thick, spherical, square panels and thin panels with aspect ratio $b/a=2$ for the two theories considered. However, the effects of G_{12} for thin square panels and G_{13} for thick symmetric panel with aspect ratio $b/a=2$ are dominant. The effect of G_{23} on scattering of buckling loads is also significant for thick panels with $b/a=2$.
- The panel buckling loads for symmetric and anti-symmetric cross-ply laminates show almost equal changes in scatter with SD/mean of all the basic RVs changing simultaneously for the two theories considered.
- In general, the FSDT predictions of the variation in the buckling loads are of comparable order of magnitude to HSDT.

4.3 Stochastic Finite Element Method (SFEM)

In this section, a stochastic finite element method is proposed to analyze the effects of uncertain material properties on elastic buckling of composite plates, cylindrical and spherical panels. The uncertain material properties are modeled as random variables. The random variables are incorporated into finite element formulation, which results in a random eigenvalue problem. A mean centered first order perturbation technique is then used to find the probabilistic characteristics of the buckling loads. Mean as well as Standard Deviation of the buckling loads of composite panels have been evaluated for various combinations of geometrical parameters, stacking sequences and boundary conditions

4.3.1 Formulation

Buckling analysis requires the development of geometric stiffness matrix. A prebuckling analysis is carried out to compute the displacement and hence the stresses and stress resultants due to unit loading. The panel is assumed to be acted upon by these stress resultants, and the geometric stiffness matrix is computed. In view of the uncertainty in material properties the formulation results in standard random eigenvalue problem. The standard random eigenvalue problem is then solved to obtain the second order statistics of the buckling loads when the panel is subjected to external loading.

4.3.1.1 Prebuckling analysis

In *Chapter III*, it was shown that strain energy due to bending of a composite panel subjected to given loading is given by (refer Equation 3.35)

$$U = \frac{1}{2} \int_A \bar{\epsilon}^T \mathbf{D} \bar{\epsilon} dA; \quad (4.17)$$

Utilizing finite element modeling, it was shown that these equations become (Section 3.9 refer Equations 3.50, 3.52 and 3.53)

$$U = \sum_{e=1}^{NE} U^{(e)} \quad (4.18)$$

$$= \sum_{e=1}^{NE} \frac{1}{2} \int_{A^{(e)}} \bar{\epsilon}^T D \bar{\epsilon} dA$$

$$U^{(e)} = \frac{1}{2} \int_{A^{(e)}} \Lambda^{T(e)} \mathbf{B}^T \mathbf{D} \mathbf{B} \Lambda^{(e)} dA ; \quad (4.19)$$

$$= \Lambda^{T(e)} \mathbf{K}^{(e)} \Lambda^{(e)} , \quad (4.20)$$

where $\Lambda^{(e)}$ and $\mathbf{K}^{(e)}$ are the element displacement vector and stiffness matrices respectively.

4.3.1.2 Buckling analysis

The work done by the applied in-plane forces by taking transverse external loading is zero in producing out of plane displacement 'w' in the domain of small displacement is (Section 3.7 refer Equation 3.40),

$$W = \frac{1}{2} \int_A [N_{x_1} \left(\frac{\partial w}{\partial x_1} \right)^2 + N_{x_2} \left(\frac{\partial w}{\partial x_2} \right)^2 + 2 N_{x_1 x_2} \left(\frac{\partial w}{\partial x_1} \right) \left(\frac{\partial w}{\partial x_2} \right)] dA ;$$

$$= \frac{1}{2} \int_A \begin{Bmatrix} w_{,x_1} \\ w_{,x_2} \end{Bmatrix}^T \begin{bmatrix} N_{x_1} & N_{x_1 x_2} \\ N_{x_1 x_2} & N_{x_2} \end{bmatrix} \begin{Bmatrix} w_{,x_1} \\ w_{,x_2} \end{Bmatrix} dA . \quad (4.21)$$

Using finite element notation, the above equation may be rewritten as,

$$W = \sum_{e=1}^{NE} W^{(e)}$$

$$= \sum_{e=1}^{NE} \frac{1}{2} \int_{A^{(e)}} \begin{Bmatrix} w_{,x_1} \\ w_{,x_2} \end{Bmatrix}^T \begin{bmatrix} N_{x_1} & N_{x_1 x_2} \\ N_{x_1 x_2} & N_{x_2} \end{bmatrix} \begin{Bmatrix} w_{,x_1} \\ w_{,x_2} \end{Bmatrix} dA . \quad (4.22)$$

We have,

$$\begin{Bmatrix} w_{,x_1} \\ w_{,x_2} \end{Bmatrix} = \mathfrak{N}_g \Lambda ; \quad (4.23)$$

where,

$$\mathfrak{R}_g = \begin{bmatrix} 0 & 0 & \frac{\partial}{\partial x_1} & 0 & 0 & 0 & 0 \\ 0 & 0 & \frac{\partial}{\partial x_2} & 0 & 0 & 0 & 0 \end{bmatrix} \text{ and}$$

$$\Lambda = \sum_{i=1}^{NN} \varphi_i \Lambda_i ;$$

with

$$\Lambda_i = (u_i \quad v_i \quad w_i \quad \theta_{2i} \quad \theta_{1i} \quad \phi_{2i} \quad \phi_{1i}) \quad (4.24)$$

Equation (4.23) may be rewritten as,

$$\begin{aligned} \begin{Bmatrix} w_{,x_1} \\ w_{,x_2} \end{Bmatrix} &= \mathfrak{R}_g \sum_{i=1}^{NN} \varphi_i \Lambda_i ; \\ &= \mathbf{B}_g \Lambda^{(e)} ; \end{aligned} \quad (4.25)$$

where $\Lambda^{(e)}$ is the elemental vector displacement obtained by assembling nodal displacement vectors and

$$\mathbf{B}_g = [\mathbf{B}_1 \quad \mathbf{B}_2 \quad \dots \mathbf{B}_n] \text{ with} \quad (4.26)$$

$$\mathbf{B}_i = \mathfrak{R} \varphi_i ; \quad (4.27)$$

Substituting Equation (4.25) into Equation (4.22),

$$\begin{aligned} W^{(e)} &= -\frac{1}{2} \int_{A^{(e)}} \Lambda^{(e)T} \mathbf{B}_g^T \lambda^* \begin{bmatrix} \overline{N'}_{x_1} & \overline{N'}_{x_1 x_2} \\ \overline{N'}_{x_1 x_2} & \overline{N'}_{x_2} \end{bmatrix} \mathbf{B}_g \Lambda^{(e)} dA . \\ &= \Lambda^{T(e)} \lambda^* \mathbf{K}_g^{(e)} \Lambda^{(e)} \end{aligned} \quad (4.28)$$

Here,

$N_{x_1} = \lambda^* \overline{N}_{x_1}$; $N_{x_2} = \lambda^* \overline{N}_{x_2}$; $N_{x_1 x_2} = \lambda^* \overline{N}_{x_1 x_2}$; λ^* denotes the load factor which on multiplication to the applied reference loads \overline{N} , assumed as deterministic in this study, gives the buckling load. The elemental geometric stiffness matrix $\mathbf{K}_g^{(e)}$ is given by,

$$\mathbf{K}_g^{(e)} = \frac{1}{2} \int_{A^{(e)}} \mathbf{B}_g^T \begin{bmatrix} \bar{N}_{x_1} & \bar{N}_{x_2} \\ \bar{N}_{x_2} & \bar{N}_{x_1 x_2} \end{bmatrix} \mathbf{B}_g dA. \quad (4.29)$$

The nodal geometric stiffness sub matrix $\mathbf{K}_{g\ ij}^{(e)}$ for nodes i and j of the e^{th} element in natural coordinates may be written as,

$$\mathbf{K}_{g\ ij} = \int_{-1}^{+1} \int_{-1}^{+1} \mathbf{B}_{gi}^T \begin{bmatrix} \bar{N}_{x_1} & \bar{N}_{x_2} \\ \bar{N}_{x_2} & \bar{N}_{x_1 x_2} \end{bmatrix} \mathbf{B}_{gj} \det \mathbf{J} d\xi d\eta; \quad (4.30)$$

where

$$\mathbf{B}_{gi} = \begin{bmatrix} 0 & 0 & \varphi_{i,x_1} & 0 & 0 & 0 & 0 \\ 0 & 0 & \varphi_{i,x_2} & 0 & 0 & 0 & 0 \end{bmatrix}$$

and

$$\mathbf{B}_{gj} = \begin{bmatrix} 0 & 0 & \varphi_{j,x_1} & 0 & 0 & 0 & 0 \\ 0 & 0 & \varphi_{j,x_2} & 0 & 0 & 0 & 0 \end{bmatrix} \quad (4.31)$$

\mathbf{J} is the Jacobian matrix and is as defined in Equation (3.57).

When numerical integration is adopted, the geometric stiffness matrix given in Equation (4.30) becomes,

$$\mathbf{K}_{g\ ij}^{(e)} = \frac{1}{2} \sum_{p=1}^N \sum_{q=1}^N W_p W_q \det \mathbf{J} \begin{bmatrix} K_{g11} & K_{g12} & K_{g13} & K_{g14} & K_{g15} & K_{g16} & K_{g17} \\ & K_{g22} & K_{g23} & K_{g24} & K_{g25} & K_{g26} & K_{g27} \\ & & K_{g33} & K_{g34} & K_{g35} & K_{g36} & K_{g37} \\ & & & K_{g44} & K_{g45} & K_{g46} & K_{g47} \\ & \text{Sym.} & & & K_{g55} & K_{g56} & K_{g57} \\ & & & & & K_{g66} & K_{g67} \\ & & & & & & K_{g77} \end{bmatrix}; \quad (4.32)$$

In this geometric stiffness sub matrix all elements except K_{g23} are zero. K_{g23} is given by,

$$K_{g23}^{(e)} = \frac{1}{2} \sum_{p=1}^N \sum_{q=1}^N W_p W_q \det \mathbf{J} (\bar{N}_{x_1} \varphi_{i,x_1} \varphi_{j,x_1} + \bar{N}_{x_1 x_2} (\varphi_{i,x_2} \varphi_{j,x_2} + \varphi_{i,x_1} \varphi_{j,x_1}) + \bar{N}_{x_2} \varphi_{i,x_2} \varphi_{j,x_2}) \quad (4.33)$$

4.3.1.3 Governing equations

The governing equations for elastic buckling can be derived by using the principle of Total Potential Energy (TPE). This results in

$$\delta(\Pi_p) = 0 ; \quad (4.34)$$

$$\delta(U + V) = 0 . \quad (4.35)$$

The external work done by the loads relates to the change in external potential energy

$$\delta V = -\delta W \quad (4.36)$$

Substituting Equations (4.20), (4.28) and (4.36) in Equation (4.35)

$$\delta(\mathbf{q}^{*T} \mathbf{K} \mathbf{q}^* - \mathbf{q}^{*T} \lambda^* \mathbf{K}_g \mathbf{q}^*) = 0 ; \quad (4.37)$$

where

$$\mathbf{q}^* = \sum_{e=1}^{NE} \Lambda^{(e)} - \text{Global displacement vector}$$

$$\mathbf{K} = \sum_{e=1}^{NE} \mathbf{K}^{(e)} - \text{Global stiffness matrix}$$

$$\mathbf{K}_g = \sum_{e=1}^{NE} \mathbf{K}_g^{(e)} - \text{Global geometric stiffness matrix}$$

Equation (4.37) leads to the generalized eigen value problem

$$(\mathbf{K} - \lambda^* \mathbf{K}_g) \mathbf{q}^* = 0 . \quad (4.38)$$

Equation (4.38) can be rewritten as

$$(\mathbf{K}_g - \lambda \mathbf{K}) \mathbf{q}^* = 0 ; \quad (4.39)$$

where,

$$\lambda = \frac{1}{\lambda^*} . \quad (4.40)$$

The elastic stiffness matrix \mathbf{K} is decomposed as

$$\mathbf{K} = \mathbf{U}^T \mathbf{U} ; \quad (4.41)$$

with \mathbf{U} being a nonsingular matrix.

Substituting Equation (4.41) into Equation (4.39) and pre-multiplying both sides of the resulting equation by \mathbf{U}^T the standard eigenproblem is obtained as [102, 114]

$$(\mathbf{A} - \lambda \mathbf{I}) \mathbf{q} = 0; \quad (4.42)$$

where,

$$\mathbf{A} = \mathbf{U}^{-T} \mathbf{K}_g \mathbf{U}^{-1}; \quad (4.43)$$

$$\mathbf{q} = \mathbf{U} \mathbf{q}^*.$$

We note that in contrast to the eigenvalue problem given in Equation (4.38), wherein the smallest buckling load is associated with the smallest eigenvalue, by using the equivalent formulation given in Equations (4.39) and (4.42) the largest eigenvalue defines the critical buckling load.

The governing equation for buckling response of laminated composite shallow panels is given by Equation (4.42). In deterministic environment, the buckling load is obtained by solving Equation (4.42) using a standard solution procedure [102]. However, in random environment the elements of matrix \mathbf{A} , being dependent on system material properties, are random in nature and therefore the eigen values λ and eigen vectors \mathbf{q} are also random. It is, therefore, not possible to directly obtain the statistics of buckling load from Equation (4.42). To achieve this, further analysis is required and a probabilistic approach with first order perturbation technique in conjunction with Taylor series. This is presented in the next section.

4.3.2 Solution- A Perturbation Approach

Consider the class of problems where the random variation of material properties is very small as compared to their mean value. Properties of most engineering materials, including composites belong to this class. Further, it is quite logical to assume that the dispersion in derived quantities like A , λ and q will also be small as compared to their mean values.

A random variable may be broken up as the sum of its mean and zero mean random part as [111]

$$A = \bar{A} + A^r; \quad \lambda = \bar{\lambda} + \lambda^r; \quad q = \bar{q} + q^r; \quad (4.44)$$

where, over bar denotes the mean value and superscript 'r' denotes the zero mean random part.

Substitution of Equation (4.44) in Equation (4.42) yields

$$(\bar{A} + A^r) (\bar{q}_j + q_j^r) = (\bar{\lambda}_j + \lambda_j^r) (\bar{q}_j + q_j^r). \quad (4.45)$$

If the components of the matrix A^r are very small, as discussed earlier, Equation (4.45) becomes, to the first order,

$$\bar{A} \bar{q}_j + \bar{A} q_j^r + A^r \bar{q}_j = \bar{\lambda}_j \bar{q}_j + \lambda_j^r \bar{q}_j + \bar{\lambda}_j q_j^r. \quad (4.46)$$

Equation (4.46) can be further broken up as

$$\text{Zeroth order: } \bar{A} \bar{q}_j = \bar{\lambda}_j \bar{q}_j; \quad (4.47)$$

$$\text{First order: } \bar{A} q_j^r + A^r \bar{q}_j = \lambda_j^r \bar{q}_j + \bar{\lambda}_j q_j^r. \quad (4.48)$$

Equation (4.47) involving the mean quantities is a deterministic equation. The mean eigen values and the corresponding mean eigen vectors can be determined by conventional eigen solution procedures. It is assumed that the eigen values are all distinct and the eigen vectors are properly normalized so that the orthogonality conditions are satisfied [102, 114]. The eigen vectors would form a complete orthonormal set and any vector in the space may be

expressed as a linear combination of the eigen vectors. Hence, the j^{th} first order components of the eigen vector can be written as [102]

$$\mathbf{q}_j^r = \sum_{k=1}^n (C_{jk}^r) \bar{\mathbf{q}}_k \quad \text{with } (C_{kk}^r = 0); \quad (4.49)$$

where C_{jk}^r are small random coefficients that are to be determined.

Let $\bar{\mathbf{q}}_1, \dots, \bar{\mathbf{q}}_n$ be eigen vectors corresponding to the eigen values $\bar{\lambda}_1, \dots, \bar{\lambda}_n$ of an $n \times n$ matrix \mathbf{A} . Assume $\bar{\lambda}_i \neq \bar{\lambda}_j$, $i \neq j$. Let $\bar{\mathbf{v}}_1, \dots, \bar{\mathbf{v}}_n$ be eigen vectors corresponding to the eigen values $\bar{\lambda}'_1, \dots, \bar{\lambda}'_n$ of \mathbf{A}^T then

$$(\bar{\mathbf{q}}_i, \bar{\mathbf{v}}_i) \neq 0; \quad (\bar{\mathbf{q}}_i, \bar{\mathbf{v}}_j) = 0, \quad i \neq j \quad (4.50)$$

Using Equations (4.48), (4.49) and (4.50), the expressions for λ_j^r and \mathbf{q}_j^r can be obtained as [102]

$$\lambda_j^r = ((\mathbf{A}^T) \bar{\mathbf{q}}_j, \bar{\mathbf{v}}_j) / (\bar{\mathbf{q}}_j, \bar{\mathbf{v}}_j), \quad j=1, \dots, n. \quad (4.51)$$

$$\mathbf{q}_j^r = \sum_{\substack{k=1 \\ k \neq j}}^n \left(\frac{((\mathbf{A}^T) \bar{\mathbf{q}}_j, \bar{\mathbf{v}}_k)}{(\bar{\lambda}_j - \bar{\lambda}_k) (\bar{\mathbf{q}}_k, \bar{\mathbf{v}}_k)} \right) \bar{\mathbf{q}}^k.$$

As discussed earlier, for the present case \mathbf{A} , λ and \mathbf{q} are random because the material properties are random. Let b_1, b_2, \dots, b_n denote the random material properties. Following Equation (4.44) the b_i can be written as

$$b_i = \bar{b}_i + b_i^r. \quad (4.52)$$

The stochastic finite element method based on the perturbation technique has shown to be accurate and efficient [50, 115]. The random variables, \mathbf{A} , λ and \mathbf{q} can be expressed by the Taylor's series expansion centered at mean value of b_i [114]. Keeping only terms up to the first order, we have

$$\lambda_j^r = \sum_{i=1}^m \bar{\lambda}_{j,i} b_i^r; \quad \mathbf{q}_j^r = \sum_{i=1}^m \bar{\mathbf{q}}_{j,i} b_i^r; \quad \mathbf{A}^r = \sum_{i=1}^m \bar{\mathbf{A}}_{,i} b_i^r; \quad (4.53)$$

where $,i$ denotes partial differentiation with respect to b_i .

Use of Equations (4.51) and (4.53) for the eigen value systems gives

$$\bar{\lambda}_{j,i} = ((\bar{\mathbf{A}}_{,i}) \bar{\mathbf{q}}_j, \bar{\mathbf{v}}_j) / (\bar{\mathbf{q}}_j, \bar{\mathbf{v}}_j);$$

$$j = 1, \dots, n \quad (4.54)$$

$$\bar{\mathbf{q}}_{j,i} = \sum_{\substack{k=1 \\ k \neq j}}^n \left(\frac{((\bar{\mathbf{A}}_{,i}) \bar{\mathbf{q}}_j, \bar{\mathbf{v}}_k)}{(\bar{\lambda}_j - \bar{\lambda}_k) (\bar{\mathbf{q}}_k, \bar{\mathbf{v}}_k)} \right) \bar{\mathbf{q}}^k.$$

From Equation (4.53) the eigen value and mode shape covariance are obtained as [102]

$$Var(\lambda_j) = \sum_{i=1}^m \sum_{k=1}^m \bar{\lambda}_{j,i} \bar{\lambda}_{j,k} Cov(b_i, b_k); \quad Var(\mathbf{q}_j \mathbf{q}_j^{*T}) = \sum_{i=1}^m \sum_{k=1}^m \bar{\mathbf{q}}_{j,i} \bar{\mathbf{q}}_{j,k} Cov(b_i, b_k) \quad (4.55)$$

where $Cov(b_i, b_k)$ is the covariance between b_i and b_k . The variances of λ and \mathbf{q} can be evaluated from Equation (4.55) with the help of Equation (4.54).

4.3.3 Results and Discussion

The method outlined has been used to obtain the second order statistics of the buckling load of laminated composite panels with random material properties. The plies are assumed to be of the same thickness and made up of the same material. The results have been compared with Monte Carlo Simulation. A nine noded Langaragian isoparametric element, which result in 63 DOFs for the HSDT model, is used for discretizing the laminate. The element is found to be quite stable and full and reduced integration rules did have significant effect on the results for panels. All the results obtained in this study have been obtained by employing the full (3×3) integration rule for thick panels and reduced (2×2) integration rule for thin panels. Based on convergence with respect to mean as well as variance of the buckling loads, a (4×4) mesh has been chosen for computation. The following non-dimensional buckling loads have been used for the study:

$$N_{cr} = \bar{N}_{cr} b^2 / (\bar{E}_{22} h^3)$$

The lamina material properties E_{11} , E_{22} , G_{12} , ν_{12} , G_{13} and G_{23} are modeled as random variables. Here E_{11} and E_{22} are longitudinal and transverse elastic moduli, respectively. G_{12} is inplane shear modulus, G_{13} and G_{23} are out of plane shear moduli and ν_{12} is the Poisson ratio. These RVs are selected as

$$b_1 = E_{11}, \quad b_2 = E_{22}, \quad b_3 = G_{12}, \quad b_4 = G_{13}, \quad b_5 = G_{23}, \quad \text{and} \quad b_6 = \nu_{12}.$$

The following dimensionless mean orthotropic material properties have been used [116-118]:

$$\bar{E}_{11} = 40 \bar{E}_{22}, \quad \bar{G}_{12} = 0.6 \bar{E}_{22}, \quad \bar{G}_{23} = 0.5 \bar{E}_{22} \quad \text{and} \quad \bar{\nu}_{12} = 0.25. \quad \text{It is assumed that } \bar{G}_{13} = \bar{G}_{12} \quad \text{and} \quad \bar{\nu}_{13} = \bar{\nu}_{12} \quad \text{for the above material [117].}$$

In the present study various combinations of edge support conditions of clamped (C), free (F) and simple-support (S) have been used for the buckling analysis. For example, CSCF implies clamped edges at $x_1=0$ and a , simply supported at $x_2=0$ and free edge at $x_2=b$. The boundary conditions for the panel are:

Clamped edge (C):

$$u = v = w = \phi_1 = \phi_2 = \theta_1 = \theta_2 = 0;$$

Free edge (F):

$$u \neq v \neq w \neq \phi_1 \neq \phi_2 \neq \theta_1 \neq \theta_2 \neq 0;$$

Simply supported edge (S)

$$v = w = \theta_2 = \phi_2 = 0 \quad \text{or} \quad u = w = \theta_1 = \phi_1 = 0.$$

Second order statistics of non-dimensionalised buckling loads for laminated composite panels are presented for the ratio of the SD to mean of material properties varying

from 0 percent to 20 percent [51]. The sensitivity of simultaneous and individual variation of material properties is investigated in detail for different support conditions.

4.3.3.1 Buckling Load: Composite Plates

Validation study

Mean buckling load

A comparison of the results with those available in the literature validates the effectiveness of the proposed finite element model. The nondimensionalised mean buckling load for an anti-symmetric cross-ply square plate with all edges simply supported and subjected to axial compressive load has been obtained with length to thickness ratio $a/h=10$ by using higher order shear deformation theory for the three stacking sequences $[0^0/90^0]$, $[0^0/90^0/0^0/90^0]$ and $[0^0/90^0/0^0/90^0/0^0/90^0]$. The results are presented in Table 4.5 along with those obtained with other techniques [116-118]. It is seen that the present method yields excellent results.

Standard deviation of buckling load

Figure 4.26 shows the comparison of the results by the present approach with Monte Carlo simulation for $[0^0/90^0]$ laminated, square composite plates with all edges simply supported with $b/h=5$ and with only one material property E_{11} treated to be random. For MCS approach, the samples are generated using NAG subroutine to fit the desired mean and standard deviation (SD) of the material property. These samples are used in Equation (4.42), which is solved repeatedly adopting conventional eigen value solution procedure to generate a sample of the buckling load. This sample is processed to obtain the mean and SD. Overall good agreement is seen between the two results. It can be concluded from the results that the

first order perturbation technique is quite accurate for the range of SD to mean values considered in the study.

Second Order Statistics

Composite plates with three stacking sequences, $[30^0/-30^0/30^0/-30^0]$, $[45^0/-45^0/45^0/-45^0]$ and $[60^0/-60^0/60^0/-60^0]$ with CCCC, CFCF and SSSS boundary conditions for $b/h=5$ and 10 subjected to in-plane compressive load along y-direction have been taken for evaluation of mean and variance of the buckling loads.

Mean buckling load

Table 4.6 presents the nondimensionalised mean buckling loads with $b/h=5$ and 10 for stacking sequences of $[30^0/-30^0/30^0/-30^0]$, $[45^0/-45^0/45^0/-45^0]$ and $[60^0/-60^0/60^0/-60^0]$ graphite-epoxy square plates with CCCC, CFCF and SSSS boundary conditions using HSDT subjected to inplane compressive load. For both b/h ratios, it is observed that the nondimensionalised-buckling load increases as the lamination angle increases. The mean buckling load is higher in the case of plates with all edges clamped for a fixed b/h ratio and lamination angle, while the plate CFCF boundary condition buckles at a lesser load as compared to the rest of the boundary conditions investigated. There is a significant change in non-dimensionalised buckling loads as the b/h ratio changes for all combinations of edge conditions considered.

Standard deviation of buckling load

The SD/mean of the buckling load show a linear variation with changes in the material properties. The amount of scatter depends on the thickness ratio, edge condition and the material property. The behavior also shows sensitivity to the fibre orientation.

Simultaneous variation in material properties

In actual situation all material properties show scatter. Hence from practical considerations, it is appropriate to consider the cases when all the properties vary simultaneously. Figures 4.27(a) and 4.27(b) present the normalized SD of the nondimensionalized buckling load with SD of all the material properties varying simultaneously each assuming the same value for the ratio of its SD to mean for $[60^\circ/60^\circ/60^\circ/60^\circ]$ square laminate with $b/h=5$ and 10 , respectively. Figures 4.27(c) and 4.27(d) represent corresponding behavior for $[30^\circ/30^\circ/30^\circ/30^\circ]$ and Figures 4.27(e) and 4.27(f) for $[45^\circ/45^\circ/45^\circ/45^\circ]$ square laminates.

For lamination angle 60° , it is observed that the buckling load for the plate with all edges clamped is more sensitive while, CFCF plate is less sensitive for $b/h=5$. For $b/h=10$, it is interesting to note that the buckling load of SSSS plate is more sensitive and CFCF plate is less sensitive. It is also observed that the effect of input RVs on scatter in nondimensionalized buckling load is most dominant for CCCC plate with $b/h=5$, while its effect is least on CFCF plate with same thickness ratio.

For lamination angle 30° , with the CCCC edges the buckling load is more sensitive for $b/h=5$, while, it is less sensitive for CFCF plate. It is seen that for $b/h=10$, the SSSS plate is more sensitive and CCCC plate is less sensitive as compared to other boundary conditions.

For lamination angle 45° , the CCCC and SSSS plates show sensitivity of same order of magnitude but more as compared to CFCF plate for $b/h=5$, while, all three types of plates show almost same order of sensitivity for $b/h=10$.

Individual variation of material properties(i) **$[60^0/-60^0/60^0/-60^0]$ anti-symmetric square laminate:**

Figures 4.28(a) - 4.28(f) and 4.29(a) – 4.29(f) show the variation of SD/mean of the nondimensionalized buckling loads for laminate with changes in only one material property at a time, keeping others as constant for $b/h=5$ and 10, respectively.

For $b/h=5$, the effect of individual variation of E_{11} , E_{22} , G_{12} and ν_{12} on variation in the buckling load is strongest for plate with CFCF while it is lowest for CCCC. The effect of G_{13} is largest for CCCC plate and lowest for CFCF plate. The influence of G_{23} is largest for CFCF but of same order of magnitude for SSSS plate while, CCCC plate is least affected. In general, the scattering in buckling load is most affected with changes in G_{13} and least affected with ν_{12} for all the support conditions. As a general behavior, the CCCC plate exhibits the maximum variation in buckling load with changes in G_{13} as compared to any other support conditions.

For $b/h=10$, SSSS plates exhibits a major change with individual changes in E_{11} and ν_{12} , while CCCC plate is least affected. The effect of E_{22} is maximum for CFCF and lowest for CCCC plate. The effects of G_{12} and G_{13} are largest for CFCF and CCCC respectively and lowest for SSSS and CFCF respectively. The CCCC and CFCF plates are more sensitive to changes in G_{23} compared to SSSS plate. In over all sense, the SSSS and CFCF plates are most affected with E_{11} , CCCC plate is most affected with changes in G_{13} and all types of plates are least affected with changes in ν_{12} .

(ii) **$[30^0/-30^0/30^0/-30^0]$ anti-symmetric square laminate:**

Figures 4.30(a)-4.30(f) and 4.31(a)-4.31(f) show the variation of nondimensionalized buckling loads for a $[30^0/-30^0/30^0/-30^0]$ laminate with only one property to be random at a time for $b/h=5$ and 10, respectively.

For $b/h=5$, the effect of G_{13} and G_{23} on dispersion of buckling load is more for plate with SSSS and CCCC, respectively, while dispersion is less for CFCF plate. The influence of E_{22} and ν_{12} for SSSS plate is maximum and minimum for CCCC and CFCF, respectively. The impact of E_{11} and G_{12} on dispersion of buckling load is strongest for CFCF plate, while lowest for SSSS and CCCC plates, respectively. The dispersion in buckling load for CFCF plate is most affected with changes in E_{11} , while for CCCC and SSSS plates, G_{23} variation is most effective. The dispersion in buckling loads for all boundary conditions due to changes in ν_{12} is least.

For $b/h=10$, with individual variation of E_{11} , E_{22} , G_{12} and ν_{12} , the CFCF plate is most sensitive, while CCCC plate is least sensitive. The CCCC plate is more sensitive with changes in G_{13} and G_{23} , while, CFCF plate has lowest sensitivity for these. In general, plates are most affected with changes in G_{13} and least affected with ν_{12} .

(iii) **$[45^\circ/-45^\circ/45^\circ/-45^\circ]$ anti-symmetric square laminate:**

Figures 4.32(a)-4.32(f) and 4.33(a)-4.33(f) present the sensitivity of nondimensionalized buckling loads of $[45^\circ/-45^\circ/45^\circ/-45^\circ]$ laminate with random changes in only one material property at a time for $b/h=5$ and 10, respectively.

For $b/h=5$, the changes in E_{11} , E_{22} , G_{12} and ν_{12} have largest impact on CFCF plate buckling load scattering and least impact on CCCC plate. The effect of G_{13} and G_{23} is strongest for all edges clamped plates, while lowest for CFCF plates. In general, the plate with different boundary conditions are most affected with changes in G_{13} , while, it is least affected with ν_{12} .

For $b/h=10$, with changes in E_{11} , E_{22} and G_{12} the CFCF plate has largest sensitivity while lowest sensitivity is shown by CCCC plate for changes in E_{11} and E_{22} and SSSS plate for G_{12} . The effect of G_{13} , G_{23} and ν_{12} is strongest for CCCC plates, while it is lowest for CFCF

plates. In general the CFCF and SSSS plates are most affected with E_{11} . The CCCC plate is most affected with SD of G_{13} . The least dispersion in buckling load is seen with change in SD of ν_{12} for all plate types considered.

Conclusions

The following main conclusions can be drawn from the study:

- The dispersion in nondimensionalized buckling load decreases as b/h ratio changes from 5 to 10 against simultaneous changes in material properties for CCCC plate, while it slightly increases for SSSS plate.
- For a fixed b/h ratio, the scatter in nondimensionalized buckling load increases as lamination angle increases.
- The CCCC plate with lamination angle 60° and $b/h=5$ is most affected, while the CCCC plate with lamination angle 30° and $b/h=10$ is least affected with SD of one material property changing at a time.
- For fixed lamination angle, the effect of individual variation of E_{11} , E_{22} and G_{12} on scatter in buckling load increases as b/h ratio increase, while the effect of G_{13} and G_{23} decreases. The behavior due to changes in ν_{12} does not show a pattern.
- The sensitivity of buckling load dispersion to variations in individual material properties is different for different edge support conditions. For lamination angle 60° , the CCCC plate with $b/h=5$ is most sensitive to G_{13} , the SSSS plate with $b/h=5$ and 10 is equally most sensitive to G_{13} and E_{11} , respectively and the CFCF plate with $b/h=10$ is most sensitive to E_{11} .
- Among all, the sensitivity of CCCC plate with $b/h=5$ and lamination angle 60° is highest.

- The effect of ν_{12} is least dominant on scatter in non-dimensionalised buckling load.

4.3.3.2 Buckling Load: Composite Cylindrical Panels

Validation study

The validation of the present technique for the study of buckling of laminated composite cylindrical panels has been carried out on the lines of the plate. Figure 4.34 presents the comparison of the buckling load by the present approach employing MCS with those obtained using SCA for $[0^0/90^0]$ laminated cylindrical panels with all edges simply supported. The panel parameters are $R/b=5$, $b/a=1$ and $b/h=10$. Only one material property E_{11} has been modeled as random. An overall good agreement is observed. From this validation study, it can be concluded that the first order perturbation technique along with FEM is acceptable for the range of SD to mean values considered.

Second order statistics

The second order statistics of non –dimensionalised buckling loads of $[0^0/45^0/-45^0/90^0]$ graphite-epoxy cylindrical panels with CCCC, CCCF, CCCS, CFCF and SSSS boundary conditions have been presented.

The panel parameters used are aspect ratio $b/a=1$, curvature-to-side ratio $R/b=5$, side-to-thickness ratios $b/h=2$ and 5.

Mean buckling load

Table 4.7 compares the nondimensionalized buckling load parameter with $R/b=5$, $b/a=1$ and $b/h=10$ for stacking sequences of $[0^0/90^0]$ and $[0^0/90^0/90^0/0^0]$ for laminated

cylindrical panels with all edges simply supported using HSDT along with results obtained with SCA. The SCA results have been obtained by employing an exact approach for the mean analysis. For $b/h=10$, a (4×4) mesh with (3×3) full integration for both bending and shear terms in energy has been used. However, for $b/h=100$, reduced (2×2) integration for shear terms has been used. A good agreement is seen between the two results.

Table 4.8 presents nondimensionalized mean buckling loads with $R/b=5$, $b/a=1$ and $b/h=2$ and 5 for stacking sequence of $[0^0/45^0/-45^0/90^0]$ cylindrical panels with CCCC, CCCF, CCCS, CFCF and SSSS boundary conditions. For $b/h=2$, the difference in mean buckling loads are not significant for CCCC, CCCS and SSSS. However, for $b/h=5$ the non-dimensionalised buckling load shows appreciable change for all combinations of edge conditions considered. It is observed that the buckling load changes significantly with b/h ratio. The buckling load for CCCC boundary condition is the largest as compared to any other support conditions, while it is the smallest for CFCF for both the b/h ratios considered. It is observed that with increase in the thickness of the panel, the rotations of the edge for the simply supported case become progressively smaller, tending in behavior towards the clamped edge.

Standard deviation of buckling loads

Figures 4.35(a) and 4.35(b) show the plot of SD/mean of nondimensionalized loads with SD/mean of all the basic RVs changing at a time for $[0^0/45^0/-45^0/90^0]$ square laminate, $R/b=5$, with edges CCCC, CCCF, CCCS, CFCF and SSSS for thickness ratios $b/h=2$ and 5, respectively. All the input RVs are assumed to have the same SD to mean ratio. For $b/h=2$, it is observed that the scatter in the nondimensionalized buckling loads is of equal order of magnitude for CCCC, CCCS and SSSS boundary conditions. Edge conditions CCCF and CFCF have close values, slightly lower than the previous group. The scatter in the buckling

load is strongest in case of panel with CCCC and CCCS, while it is lowest for CFCF. For $b/h=5$, the sensitivity of nondimensionalized buckling load is most for CCCS edge condition and least for SSSS as compared to any other boundary conditions. The scattering in buckling load decreases as b/h ratio increases. However, the changes are small being minimum for CCCS and maximum for SSSS.

Figures 4.36(a)-4.36(f) show the variation of SD/mean of the nondimensionalized buckling loads with random changes in only one material property at a time, keeping the others as deterministic for $b/h=2$. The effect of E_{11} on scatter in buckling load is lowest for CCCS, while it is largest for panel with CCCF. The effect of E_{22} is strongest for CCCF and CFCF and lowest for CCCS. The effect of G_{12} is strongest for CFCF and lowest for CCCS. The effects of G_{13} and G_{23} are strongest for CCCC and CCCS and lowest for CFCF. The effect of ν_{12} is strongest for CCCF and lowest for CCCS. In general, the scattering in nondimensionalised buckling load is most sensitive to changes in G_{13} and is least affected with ν_{12} .

Variation of nondimensionalized buckling loads with random changes in only one material property at a time for $b/h=5$ are shown in Figures 4.37(a)-4.37(f). The effect of E_{11} on dispersion of buckling load is more for panel with CCCF and less for CCCS compared to any other boundary conditions. The influence of E_{22} , G_{12} and ν_{12} for SSSS panel and G_{13} and G_{23} for CCCS panel is highest and lowest for CCCS and SSSS, respectively. The buckling load in panel with CCCC, CCCS and CFCF are most sensitive to G_{13} , while CCCF and SSSS panels are most affected with changes in E_{11} .

Conclusions

The following conclusions can be drawn from this study:

- The sensitivity of buckling load dispersion due to variation in material properties is dependent on the thickness ratio and boundary conditions of the laminate.

- The dispersion in nondimensionalized buckling load decreases as b/h ratio increases against simultaneous changes in material properties.
- The effects of E_{11} , E_{22} , G_{12} and ν_{12} on scatter in nondimensionalized buckling load increases as b/h ratio increases, while it decreases with changes in G_{13} and G_{23} for all the support conditions considered. However, for CFCF the effect of G_{12} and ν_{12} on dispersion also decreases as b/h ratio increases.
- The dispersion in transverse shear modulus G_{13} affects the buckling response to a large extent. However, for panel with $b/h=5$ and CCCF and SSSS edges conditions the E_{11} is dominant.
- The buckling load is least affected with changes in ν_{12} .

4.3.3.3 Buckling Load: Composite Spherical Panels

Numerical Validation

Validation of the present approach for buckling of laminated composite spherical panels has been carried out on the lines of the plate. A comparison study of the nondimensionalised buckling load obtained by the Finite element technique has been made with Monte Carlo simulation (MCS) for $[0^\circ/90^\circ]$ laminated spherical panels with all edges simply supported using HSDT. The panel parameters considered are $R/b=5$, $b/a=1$ and $b/h=10$. Only one material property E_{11} has been treated as random.

Figure 4.38 shows the comparison of the variances of buckling loads obtained by the two techniques. Both approaches indicate a linear variation between the SD/mean of N_{cr} and E_{11} . It is noted that the difference between the two results is a very small in slope of the two lines.

From this validation study, it can be concluded that the first order perturbation technique along with FEM is acceptable for the range of variations in material properties.

Second Order Statistics: CCCC, CFCF and SSSS Boundary Conditions

Second order statistics of nondimensionalized mean buckling loads for graphite-epoxy composite spherical panels with $R/b=5$, $b/a=1$ and $b/h=5$ and 10 for stacking sequence of $[45^0/-45^0]_s$ with CCCC, CFCF and SSSS boundary conditions are presented. A comparative study for the standard deviation of buckling loads of spherical and cylindrical panel is also presented.

Mean buckling load

Table 4.9 presents nondimensionalized mean buckling loads with $R/b=5$, $b/a=1$ and $b/h=5$ and 10 for stacking sequence of $[45^0/-45^0]_s$ graphite-epoxy spherical panels with CCCC, CFCF and SSSS boundary conditions. It is observed that the buckling load changes significantly with b/h ratio. As expected, the buckling load for CCCC boundary condition is the largest as compared to any other support conditions, while it is the smallest for CFCF for both the b/h ratios considered.

Standard deviation of buckling load

(i) **Effect of all material properties changing simultaneously**

Figures 4.39(a) and 4.39(b) present the sensitivity of the non-dimensionalised buckling load for the above mentioned panels with SD/mean of all the basic RVs changing at a time for $b/h=5$ and 10, respectively. All the input RVs are assumed to have the same SD to mean ratio. The SD of the buckling load increases linearly with the SD of the material properties in all cases. The boundary conditions exhibit some differences in sensitivity for b/h

= 5. However, for the thinner panels the three boundary conditions give very close values. For $b/h=5$, the scatter in the buckling load is largest for CCCC panel, while it is smallest for CFCF. The sensitivity of buckling load increases in case of CCCC and SSSS panels as b/h ratio decreases. However, the trend for CFCF is reverse.

(ii) Effect of individual variation of material properties

Figures 4.40 to 4.45 show the variation of SD/mean of the non-dimensionalised buckling loads, $[45^0/-45^0]_s$ laminate, $R/a=5$ and $b/a=1$, with random changes in only one material property at a time, keeping the others as deterministic for $b/h=5$ and 10.

Longitudinal elastic modulus E_{11} :

The effect of E_{11} on scatter in buckling load is lowest for CCCC, while it is largest for panel with CFCF. The scatter in buckling load increases as b/h ratio increases.

Transverse elastic modulus E_{22} :

The scatter in buckling load is highest for SSSS and is lowest for CFCF. The changes in buckling load are not significant as b/h ratio changes.

In-plane shear modulus G_{12} :

The effect of G_{12} is strongest for CFCF and lowest for CCCC. Increase in the thickness ratio indicates a marginal increase in the buckling load scatter.

Out-of-plane shear modulus G_{13} and G_{23} :

The dispersion in buckling load is more in the case of panel with CCCC edge condition for both b/h ratios considered. The scatter in buckling load with the changes in G_{13} decreases as b/h ratio increases. However, the buckling load shows low sensitivity to change in panel thickness with variation in G_{23} .

Poisson's ratio ν_{12} :

There is insignificant change in buckling load for all support conditions considered in the study. SSSS panels are more sensitive as compared to other support conditions.

Comparison with Cylindrical Panels

The standard deviations computed for spherical panels with geometric parameters $R/b=5$, $b/a=1$ and $b/h=5$ and cylindrical panels with $R/b=5$, $b/a=1$ and $b/h=5$ for $[0^0/45^0/-45^0/90^0]$ laminate are presented in Figures 4.46-4.52 for CFCF support condition.

It is observed that the cylindrical panel is more sensitive as compared to spherical panels with regards to simultaneous change of material properties. Similar trends are seen with individual variation of G_{13} and G_{23} . The spherical panel is more sensitive as compared to cylindrical panels with individual variation of E_{11} , E_{22} , G_{12} and ν_{12} . The spherical panel is most affected with the changes in E_{11} , while cylindrical panel with G_{13} . Both the panels are least affected with changes in ν_{12} .

Conclusions

The following conclusions can be drawn from this study:

- The sensitivity of CCCC and SSSS spherical panels decreases as b/h ratio increases. The trend for CFCF panels is reverse.
- For spherical panels the dominance of G_{13} does not change in case of CCCC and SSSS panels as thickness ratio changes, while it does change from G_{13} for $a/h=5$ to E_{11} for $a/h=10$ in case of CFCF panel.
- Cylindrical panel is more sensitive compared to spherical panel against simultaneous change of material properties.
- Spherical panel is more sensitive to individual variation of in-plane modulus as compared to cylindrical panel, while the trend is reverse for out-of-plane modulus.

4.4 Summary

The classical approach and the finite element method in conjunction with first order perturbation technique are applied to study the buckling response of laminated composite plates, cylindrical and spherical panels with random material properties. Comparing the results obtained from Monte Carlo simulation technique provides the validation of the technique for the present sets of problems. Probabilistic characteristics for initial buckling for various laminate configurations depending on limitations of the proposed methods with change in stacking sequence, aspect ratio and boundary conditions are presented. Efficacies of various theories are also examined.

Table 4.1: Mean buckling load, $N_{cr} = \bar{N}_{cr} b^2 / (\bar{E}_{22} h^3)$, $\bar{N}_{cr} = \bar{N}_2$, $\bar{N}_1 = \bar{N}_6 = 0$, for all edges simply supported laminated composite plates

(a) Stacking sequence: $[0^0/90^0]$

Aspect Ratio (b/a) (1)	Thickness Ratio (b/h=10)			Thickness Ratio (b/h=100)		
	HSDT (2)	FSDT (3)	CLT (4)	HSDT (5)	FSDT (6)	CLT (7)
1	11.563	11.353	12.957	12.941	12.939	12.957
2	35.078	32.820	51.829	51.581	51.538	51.829
3	52.526	44.888	116.612	115.355	115.147	116.612

(b) Stacking sequence: $[0^0/90^0/90^0/0^0]$

1	18.034	19.035	28.978	28.801	28.825	28.978
2	34.235	37.945	104.539	102.399	102.523	104.539
3	40.171	45.617	236.201	225.401	226.293	236.201

Table 4.2: Comparison of nondimensionalised mean buckling loads, $N_{cr} = \bar{N}_{cr} b^2 / (E_{22} h^3)$, $\bar{N}_{cr} = \bar{N}$, for all edges simply supported composite cylindrical panels with $R/b=1$, $R/h=10$ and $b/a=1$

Theories (1)	Anti-symmetric laminate: $[0^0/90^0]$	
	Present approach (2)	Existing results [113] (3)
HSDT	17.23	16.87
FSDT	17.03	16.60
CLT	18.70	18.17

Table 4.3: Nondimensionalised mean buckling loads, $N_{cr} = \bar{N}_{cr} b^2 / (E_{22} h^3)$, $\bar{N}_{cr} = \bar{N}$, for all edges simply supported composite cylindrical panels with $R/b=5$ and $b/a=1$

Theories (1)	Anti-symmetric laminate: $[0^0/90^0]$		Symmetric laminate: $[0^0/90^0/90^0/0^0]$	
	b/h=10 (2)	b/h=100 (3)	b/h=10 (4)	b/h=100 (5)
CLT	13.18726	26.46009	28.99127	30.33047
FSDT	11.57979	26.33854	19.04862	30.17756
HSDT	11.7894	26.35685	18.0414	30.15411

Table 4.4: Mean buckling loads, $N_r = \bar{N}_{cr} b^2 / (\bar{E}_{22} h^3)$, $\bar{N}_{cr} = \bar{N}$, for all edges simply supported composite spherical panels with $R/b=5$

Aspect ratio b/a (1)	Shear deformation theories (2)	[0 ⁰ /90 ⁰]		[0 ⁰ /90 ⁰ /90 ⁰ /0 ⁰]	
		b/h=10 (3)	b/h=100 (4)	b/h=10 (5)	b/h=100 (6)
1	FSDT	12.26125	58.54944	19.37329	62.67375
	HSDT	12.47010	58.56807	18.37209	62.64046
2	FSDT	32.8204	74.51379	38.02923	114.28870
	HSDT	35.29845	74.55733	34.31965	114.163979

Table 4.5: Comparison of nondimensionalised mean buckling loads, \bar{N}_{cr} of a simply supported anti symmetric square laminates ($N_2 = N_{12} = 0$, $a/h = 10$)

Source (1)	\bar{N}_{cr}		
	[0 ⁰ /90 ⁰] (2)	[0 ⁰ /90 ⁰ /0 ⁰ /90 ⁰] (3)	[0 ⁰ /90 ⁰ /0 ⁰ /90 ⁰ /0 ⁰ /90 ⁰] (4)
Noor [116] ^a	10.817	21.280	23.669
HSDT [117] ^b	11.569	22.582	24.462
HSDT [117] ^c	11.563	22.579	24.460
HSDT [118] ^d	11.563	22.579	24.460
HSDT ^e	11.569	22.618	24.506

^a Results obtained by applying a finite difference scheme to the equation of the 3-D elasticity theory. ^b Results obtained using the FEM solution. ^c Results using Navier solution. ^d Results obtained using exact method. ^e Results obtained with C⁰ finite element presented in this study.

Table 4.6: Nondimensionalised mean buckling loads, \bar{N}_{cr} laminated composite plates with different support conditions ($N_1 = N_{12} = 0$, $b/a = 1$)

Support conditions (1)	[60°/-60°/60°/-60°]		[30°/-30°/30°/-30°]		[45°/-45°/45°/-45°]	
	b/h=5 (2)	b/h=10 (3)	b/h=5 (4)	b/h=10 (5)	b/h=5 (6)	b/h=10 (7)
CCCC	13.2984	40.7803	9.9566	25.4798	12.0520	35.433
CFCF	8.3345	17.1185	5.8923	12.0925	7.5939	30.925
SSSS	12.9733	33.0347	9.2449	22.5867	11.6835	16.474

Table 4.7: Comparison of nondimensionalised mean buckling loads, \bar{N}_{cr} for a simply supported laminated composite cylindrical square panel ($N_{x_1} = N_{x_1 x_2} = 0$, $R/b = 5$).

Solution approach (1)	[0°/90°] Anti-symmetric laminate		[0°/90°/90°/0°] Symmetric laminate	
	b/h=10 (2)	b/h=100 (3)	b/h=10 (4)	b/h=100 (5)
SCA	11.7894	26.3568	18.0414	30.1541
SFEM	11.8006	26.3657	18.0116	30.1214

Table 4.8: Nondimensionalised mean buckling loads, \overline{N}_{cr} of a $[0^0/45^0/-45^0/90^0]$ composite cylindrical square panel with different edge conditions ($N_{x_1} = N_{x_1x_2} = 0$, $R/b = 5$).

Support conditions	b/h=2	b/h=5
(1)	(2)	(3)
CCCC	2.2247	11.8064
CCCF	1.8481	6.7919
CCCS	2.2247	11.0044
CFCF	1.5958	6.4451
SSSS	2.2231	8.2298

Table 4.9: Nondimensionalised mean buckling load parameter, \overline{N}_{cr} of a $[45^0/-45^0]_s$ composite spherical square panel with different edge conditions ($N_{x_1} = N_{x_1x_2} = 0$, $R/b = 5$).

Support conditions	Mean buckling loads	
	b/h=5	b/h=10
(1)	(2)	(3)
CCCC	10.6900	31.1272
CFCF	6.8316	14.9970
SSSS	10.3504	27.0607

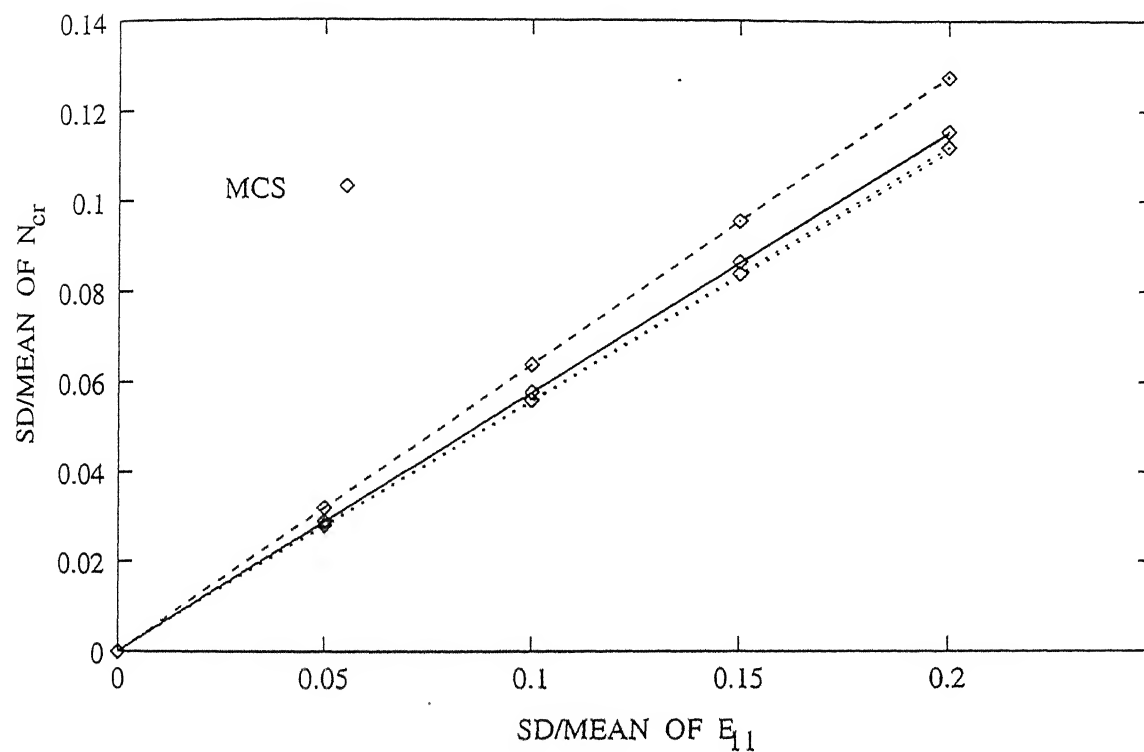


Figure 4.1: Comparison of SD of plate buckling load from Monte Carlo simulation with the present approach, $[0^\circ/90^\circ]$ laminate, with $b/a=1$ and $b/h=10$.

Key: — HSDT, FSDT, - - - CLT.

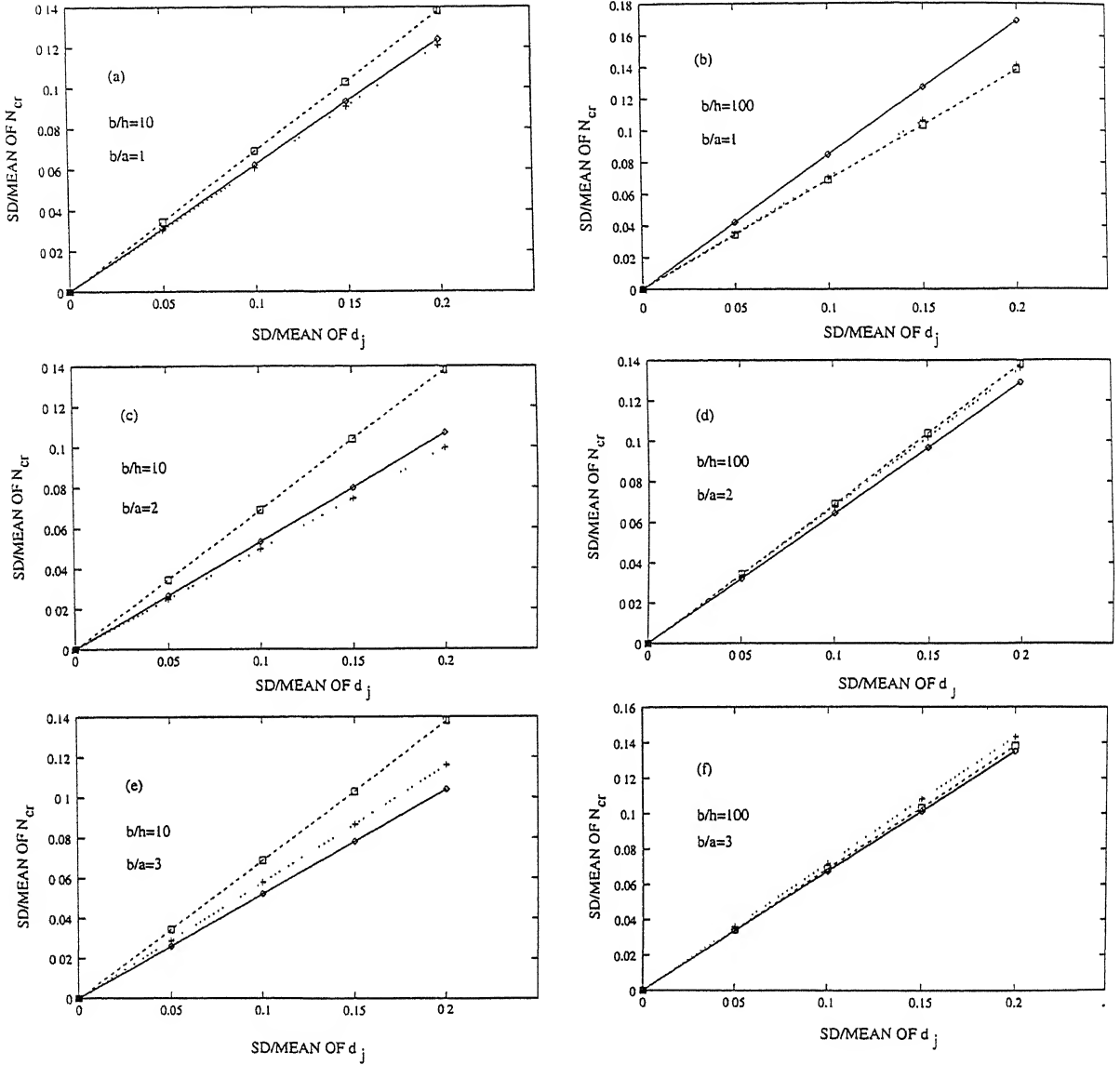


Figure 4.2: Variation of SD of plate buckling loads with SD of basic material properties, $[0^\circ/90^\circ]$ laminate with all basic material properties changing simultaneously.

Key: As in Figure 4.1.

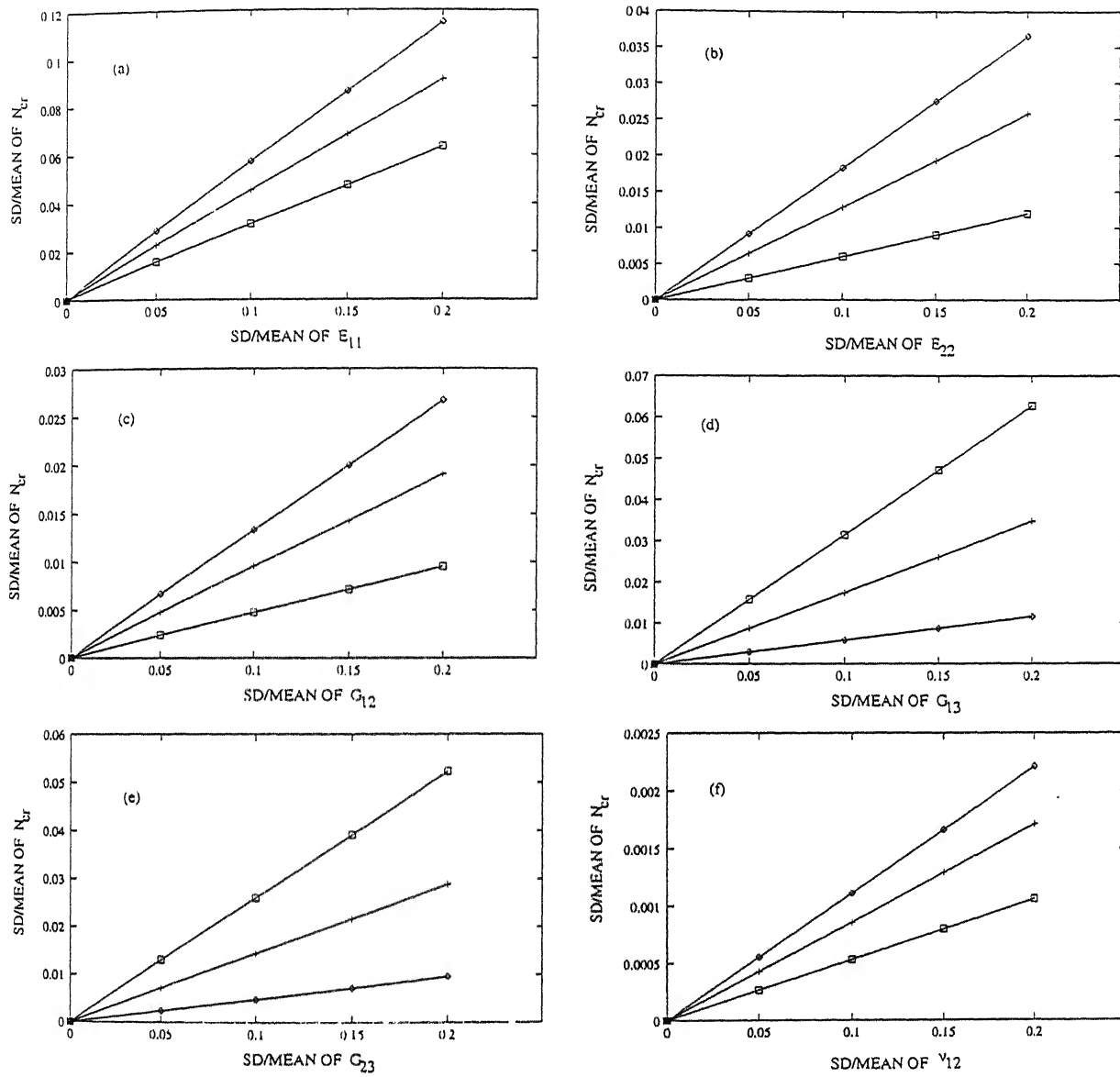


Figure 4.3: Variation of SD of plate buckling loads with SD of basic material properties, $[0^\circ/90^\circ]$ laminate using HSDT.

(a) only E_{11} varying; (b) only E_{22} varying; (c) only G_{12} varying;

(d) only G_{13} varying; (e) only G_{23} varying; (f) only ν_{12} varying.

Key:- $b/a=1$: \diamond , $b/a=2$: $+$, $b/a=3$: \square .

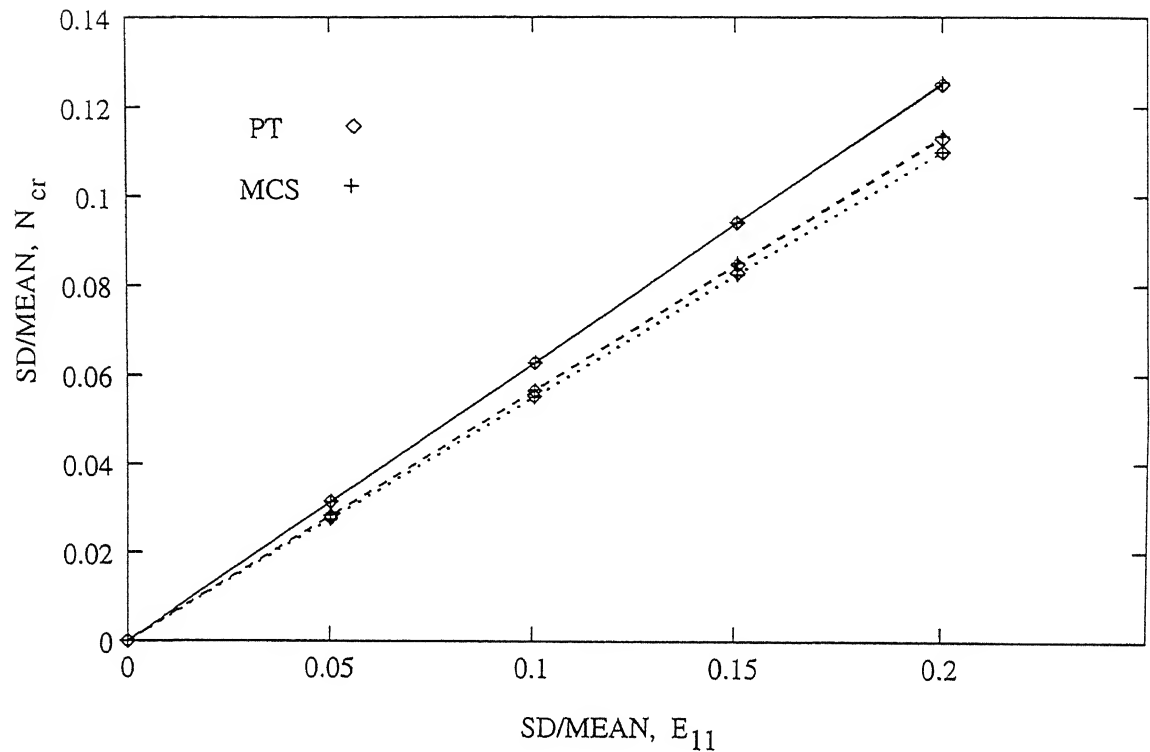


Figure 4.4: Comparison of SD of cylindrical panel buckling load from Monte Carlo simulation with the present approach, $[0^\circ/90^\circ]$ laminate, with $b/a=1$ and $b/h=10$.
Key: — CLT, FSDT, - - - HSDT.

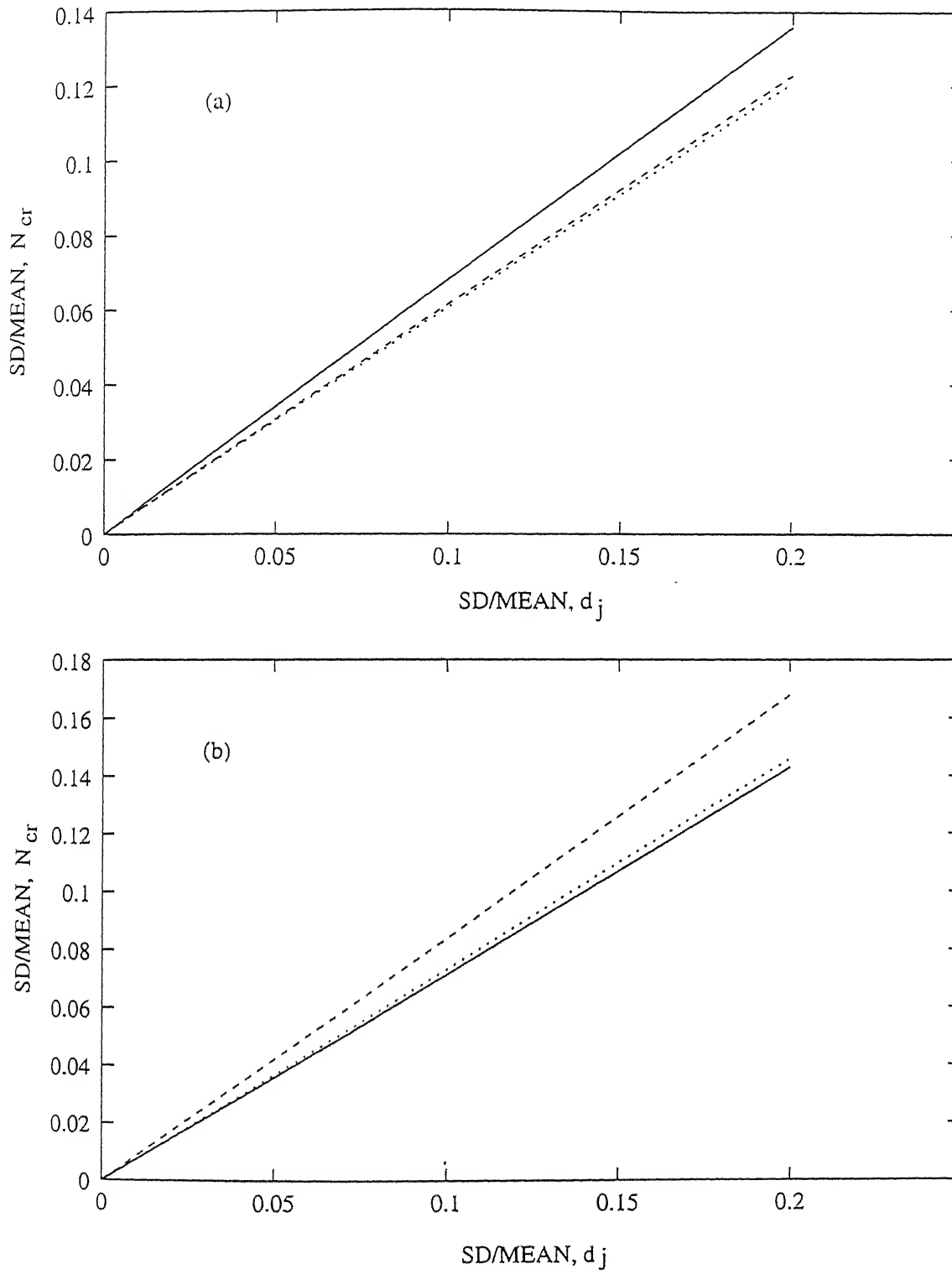


Figure 4.5: Sensitivity of SD of cylindrical panel buckling loads with SD of basic material properties, $[0^\circ/90^\circ]$ laminate and $b/a=1$, with all basic material properties changing simultaneously.

(a) $b/h=10$; (b) $b/h=100$.

Key: As in figure 4.4.

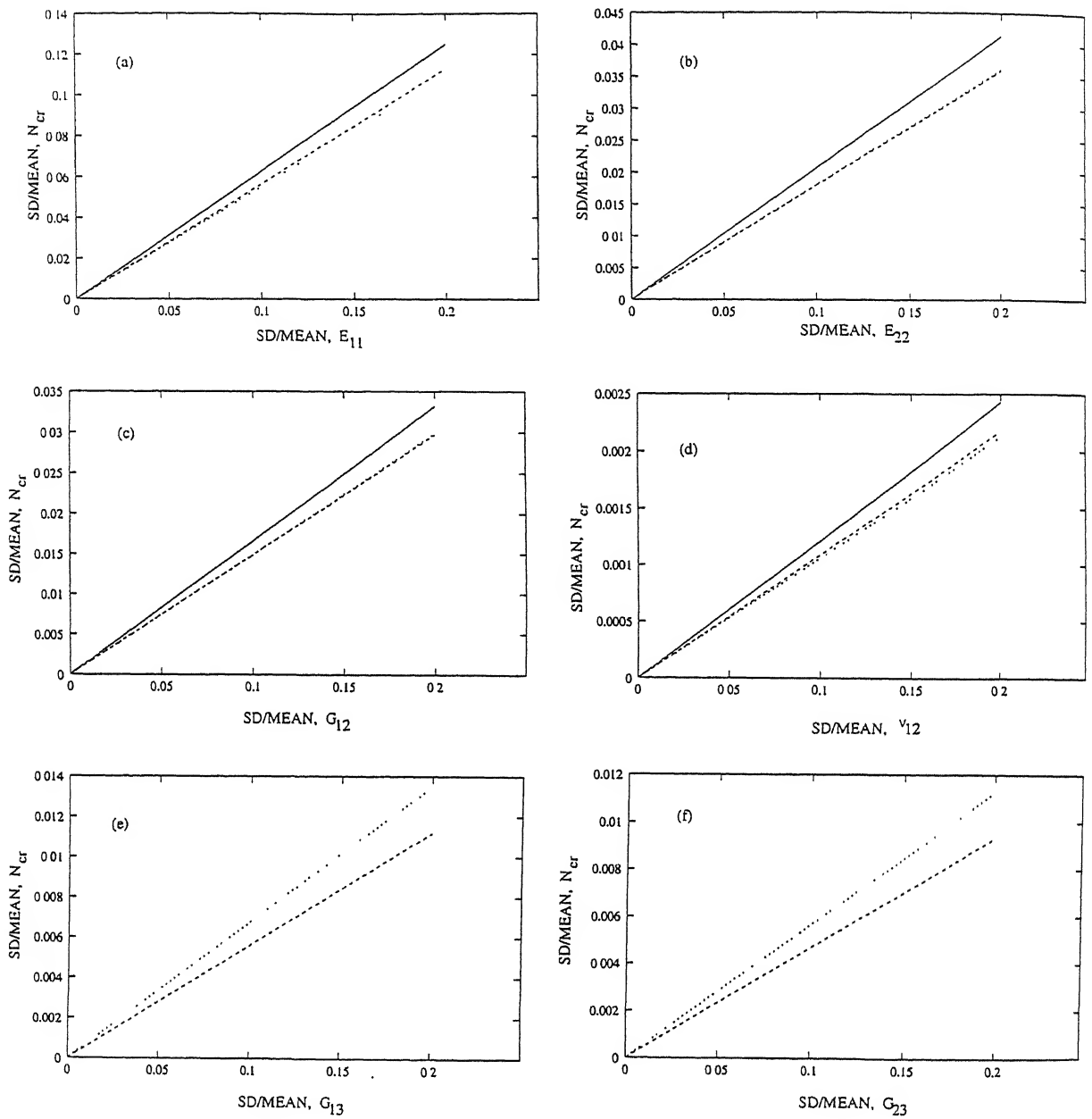


Figure 4.6: Sensitivity of SD of cylindrical panel buckling loads with SD of basic material properties, $[0^\circ/90^\circ]$ laminate, with $b/a=1$ and $b/h=10$.

(a) only E_{11} varying; (b) only E_{22} varying; (c) only G_{12} varying;
 (d) only ν_{12} varying; (e) only G_{13} varying; (f) only G_{23} varying.

Key: As in figure 4.4.

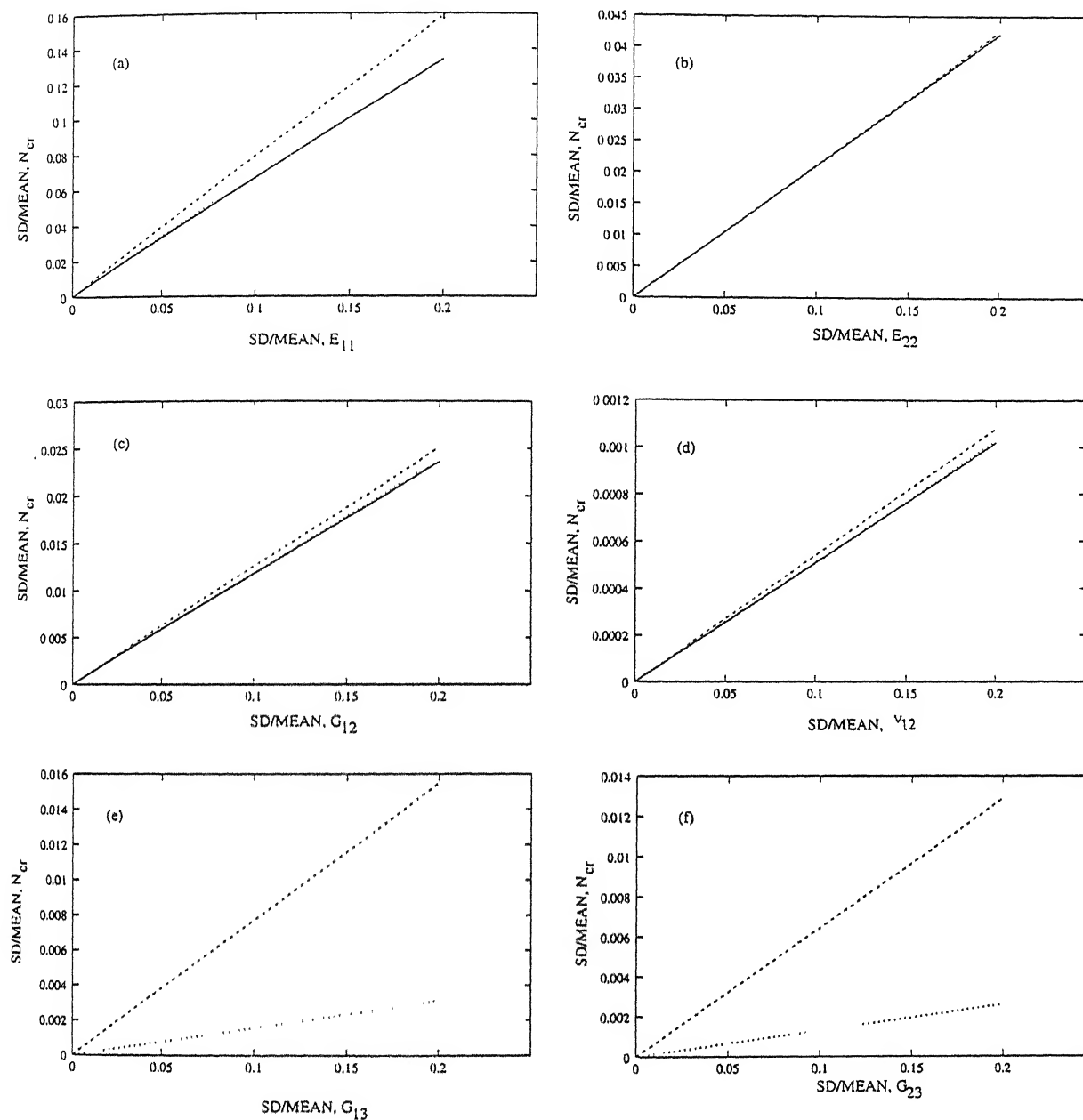


Figure 4.7: Sensitivity of SD of cylindrical panel buckling loads with SD of basic material properties $[0^\circ/90^\circ]$ laminate, with $b/a=1$ and $b/h=100$.

(a) only E_{11} varying; (b) only E_{22} varying; (c) only G_{12} varying;
 (d) only ν_{12} varying; (e) only G_{13} varying; (f) only G_{23} varying.

Key: As in figure 4.4.

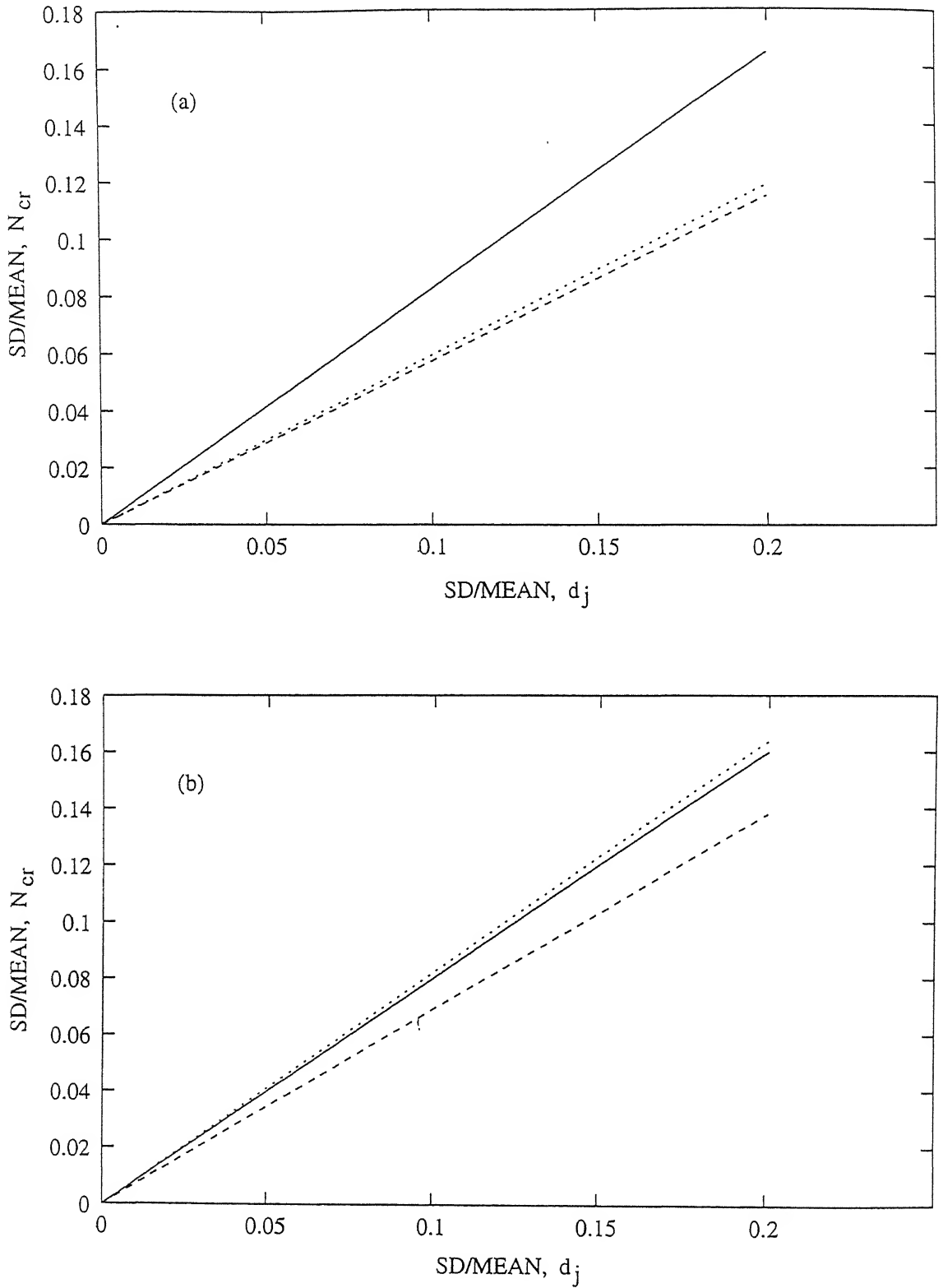


Figure 4.8: Sensitivity of SD of cylindrical panel buckling loads with SD of basic material properties, $[0^\circ/90^\circ/90^\circ/0^\circ]$ laminate and $b/a=1$, with all basic material properties changing simultaneously.

(a) $b/h=10$; (b) $b/h=100$.

Key: As in figure 4.4.

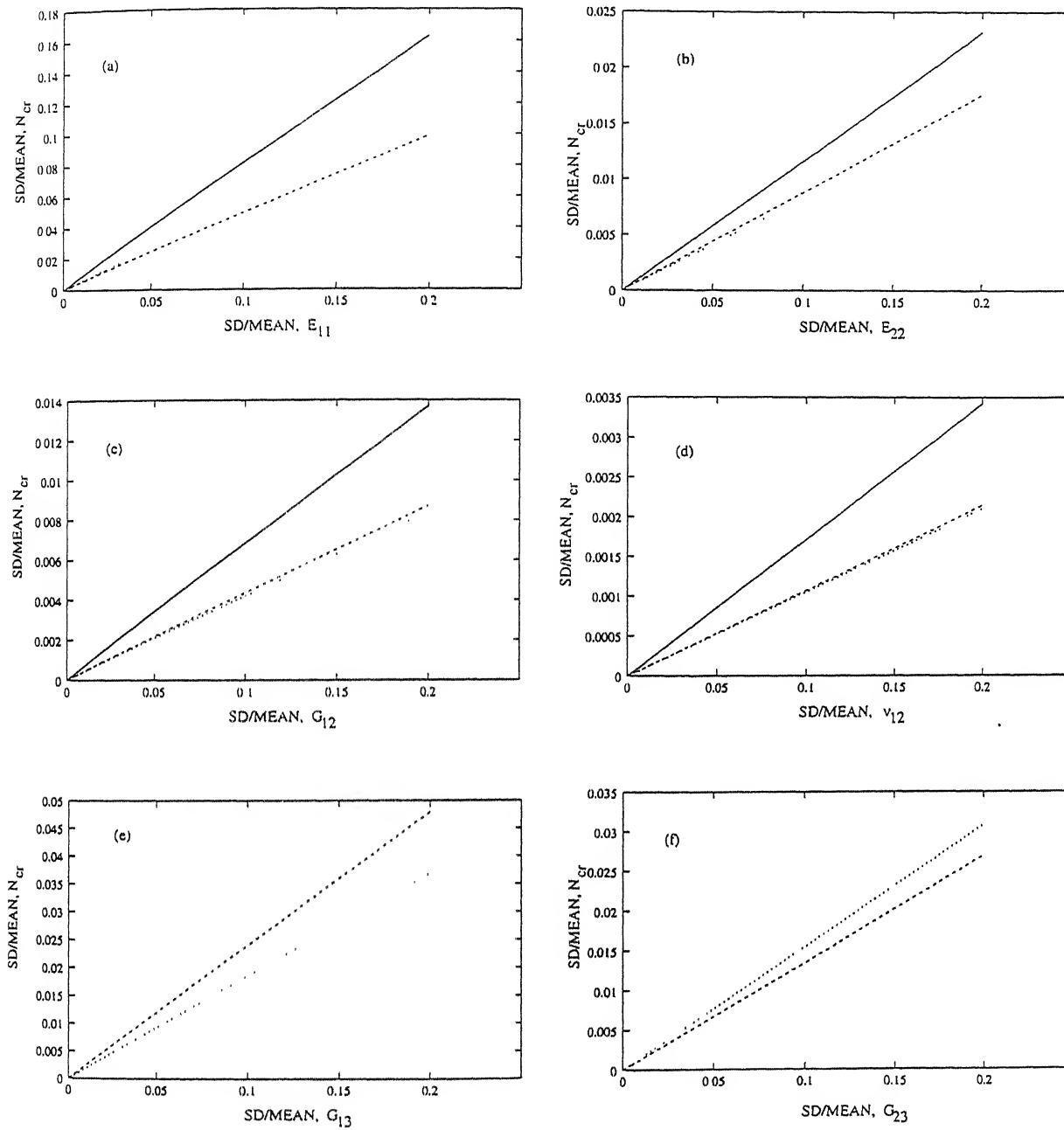


Figure 4.9: Sensitivity of SD of cylindrical panel buckling loads with SD of basic material properties, $[0^\circ/90^\circ/90^\circ/0^\circ]$ laminate, with $b/a=1$ and $b/h=10$.

(a) only E_{11} varying; (b) only E_{22} varying; (c) only G_{12} varying;
 (d) only ν_{12} varying; (e) only G_{13} varying; (f) only G_{23} varying.

Key: As in figure 4.4.

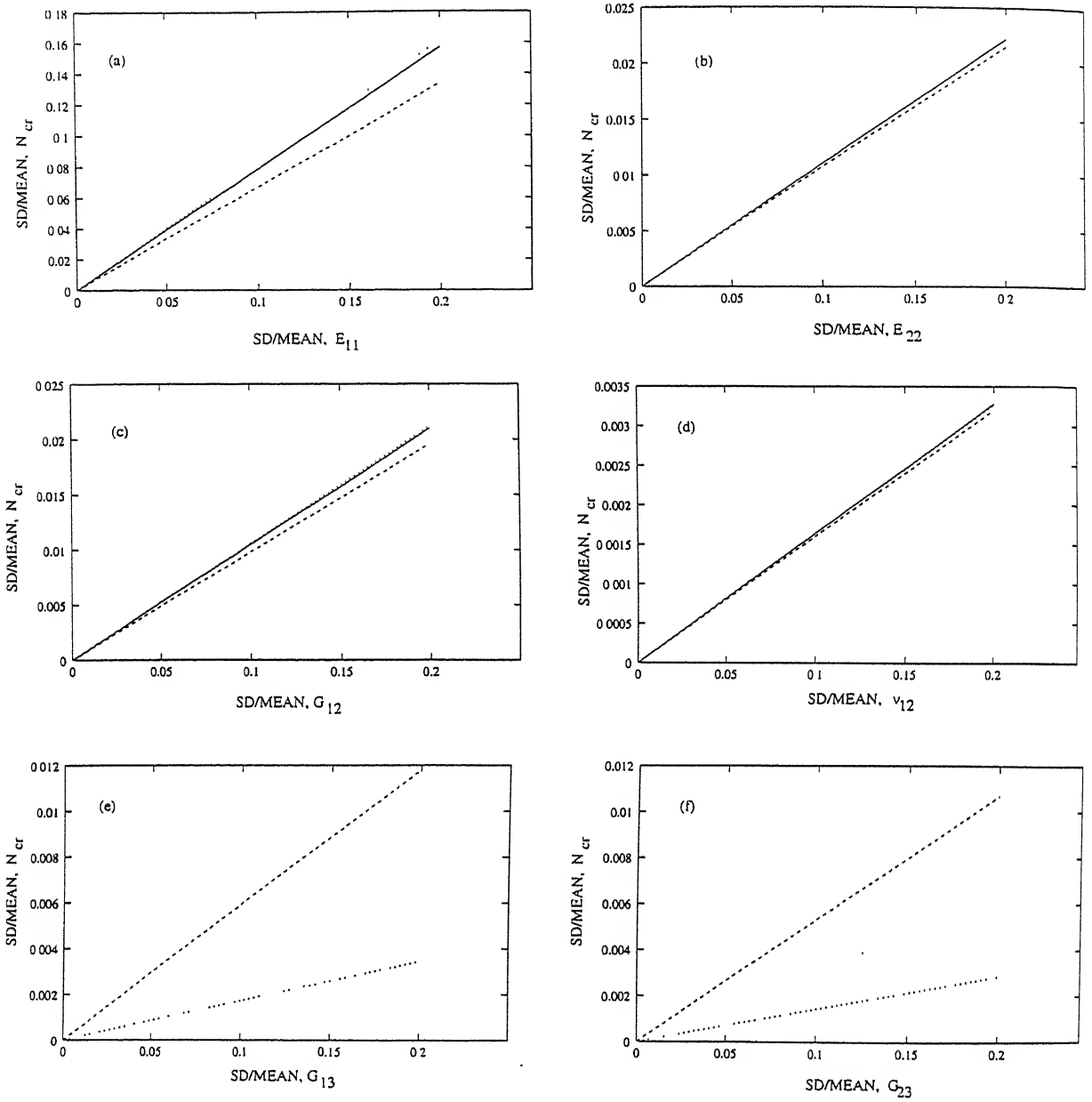


Figure 4.10: Variation of SD of cylindrical panel bucklong loads with SD of basic material properties, $[0^\circ/90^\circ/90^\circ/0^\circ]$ laminate, with $b/1=1$ and $b/h=100$.

(a) only E_{11} varying; (b) only E_{22} varying; (c) only G_{12} varying;
 (d) only ν_{12} varying; (e) only G_{13} varying; (f) only G_{23} varying.

Key: As in figure 4.4.

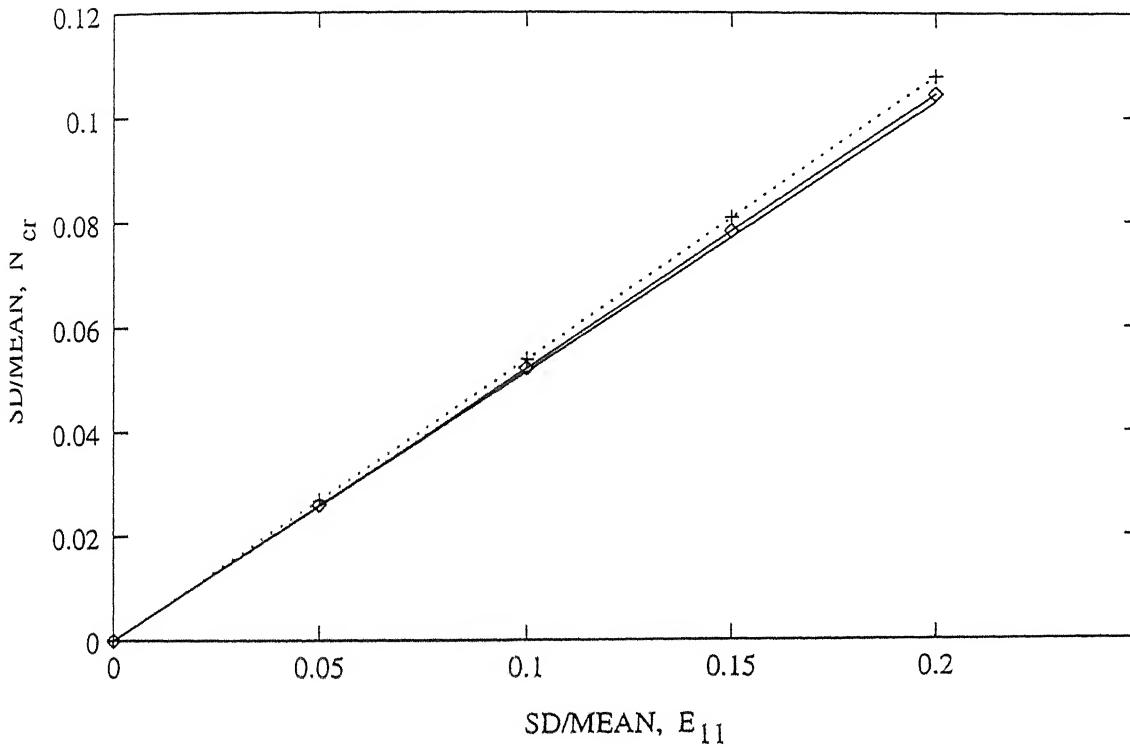


Figure 4.11: Comparison of spherical panel buckling load from Monte Carlo simulation with the present approach, $[0^\circ/90^\circ]$ laminate, with $R/b=5$, $b/a=1$ and $b/h=10$.

Key:- PT: FSDT — ; HSDT

MCS: FSDT —◇—; HSDT ...+...

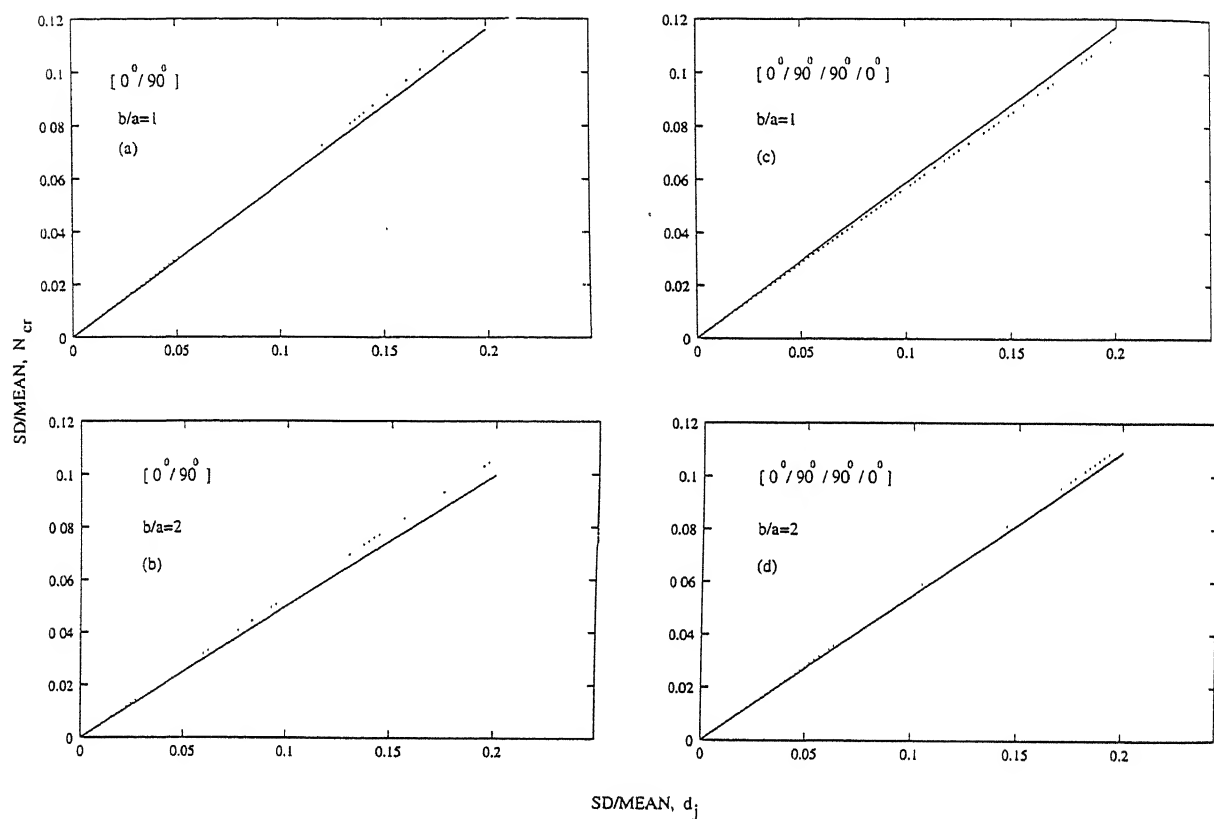


Figure 4.12: Sensitivity of SD of spherical-panel buckling loads with SD of basic material properties with all basic material properties changing simultaneously, $b/h=10$ and $R/b=5$.
Key: — FSDT, HSDT.

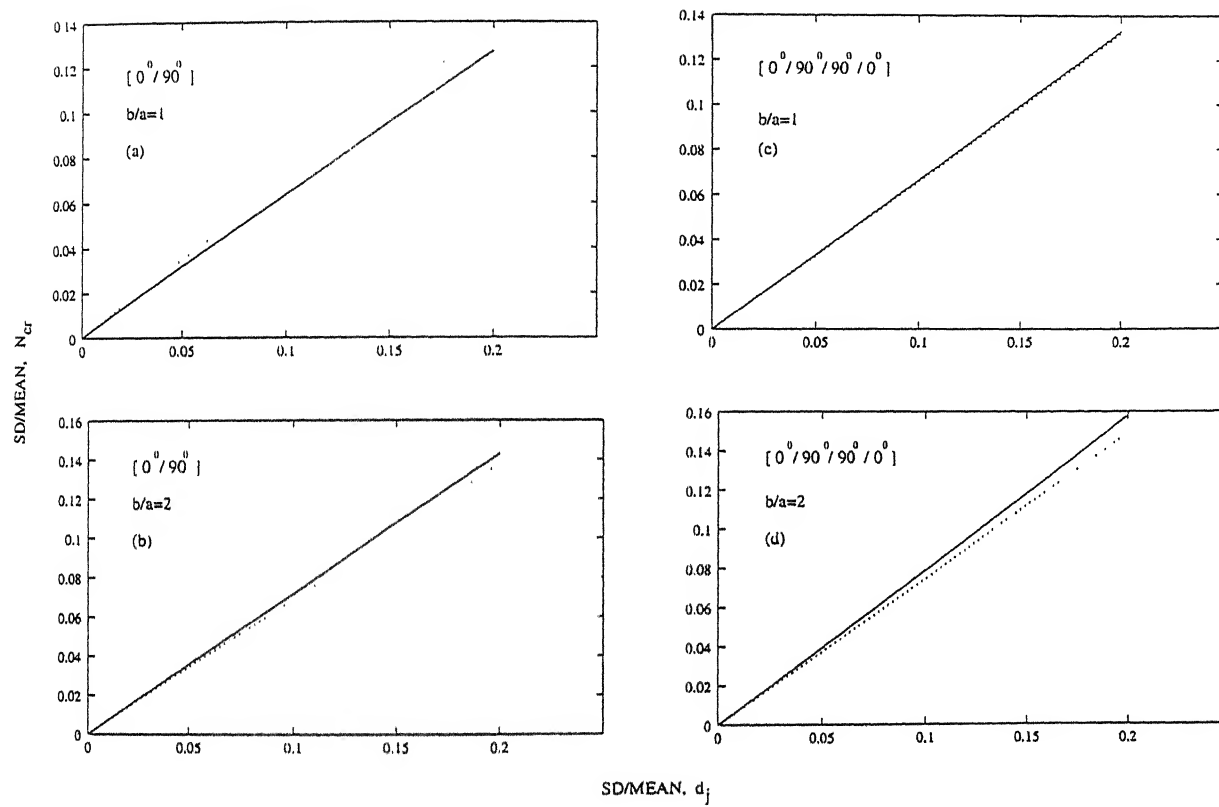


Figure 4.13: Sensitivity of SD of spherical panel buckling loads with SD of basic material properties with all basic material properties changing simultaneously, $b/h=100$ and $R/b=5$.

Key: As in Figure 4.12.

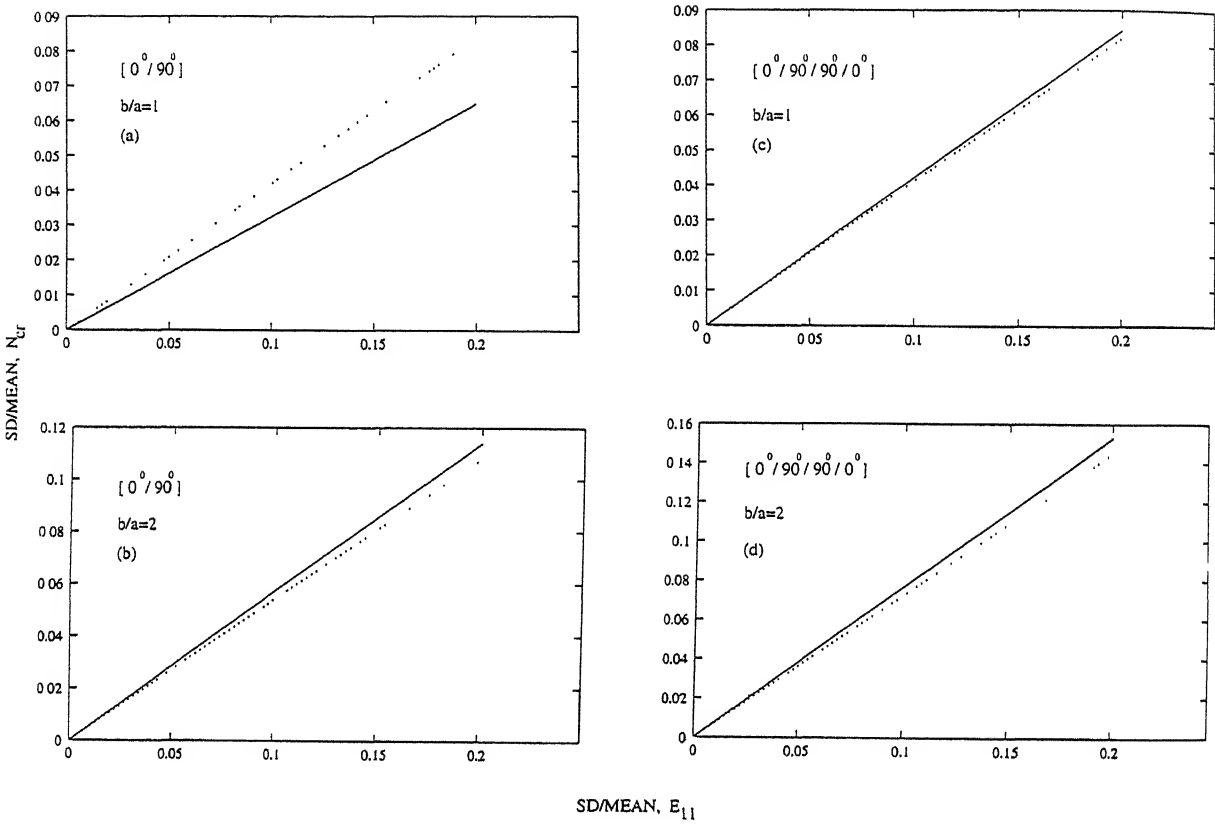


Figure 4.14: Sensitivity of SD of spherical panel buckling loads with SD of basic material property, E_{11} for $b/h=10$ and $R/b=5$.
Key: As in Figure 4.12.

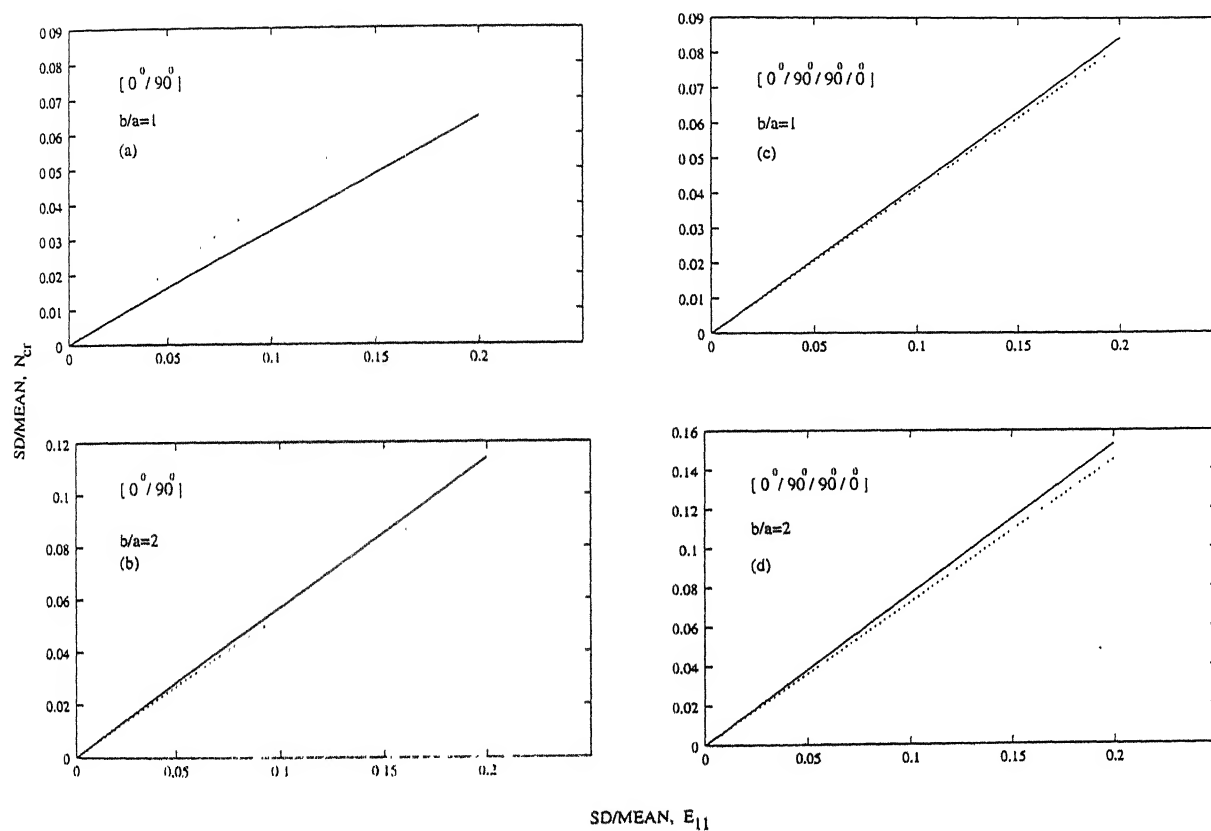


Figure 4.15: Sensitivity of SD of spherical panel buckling loads with SD of basic material property, E_{11} for $b/h=100$ and $R/b=5$.

Key: As in Figure 4.12.

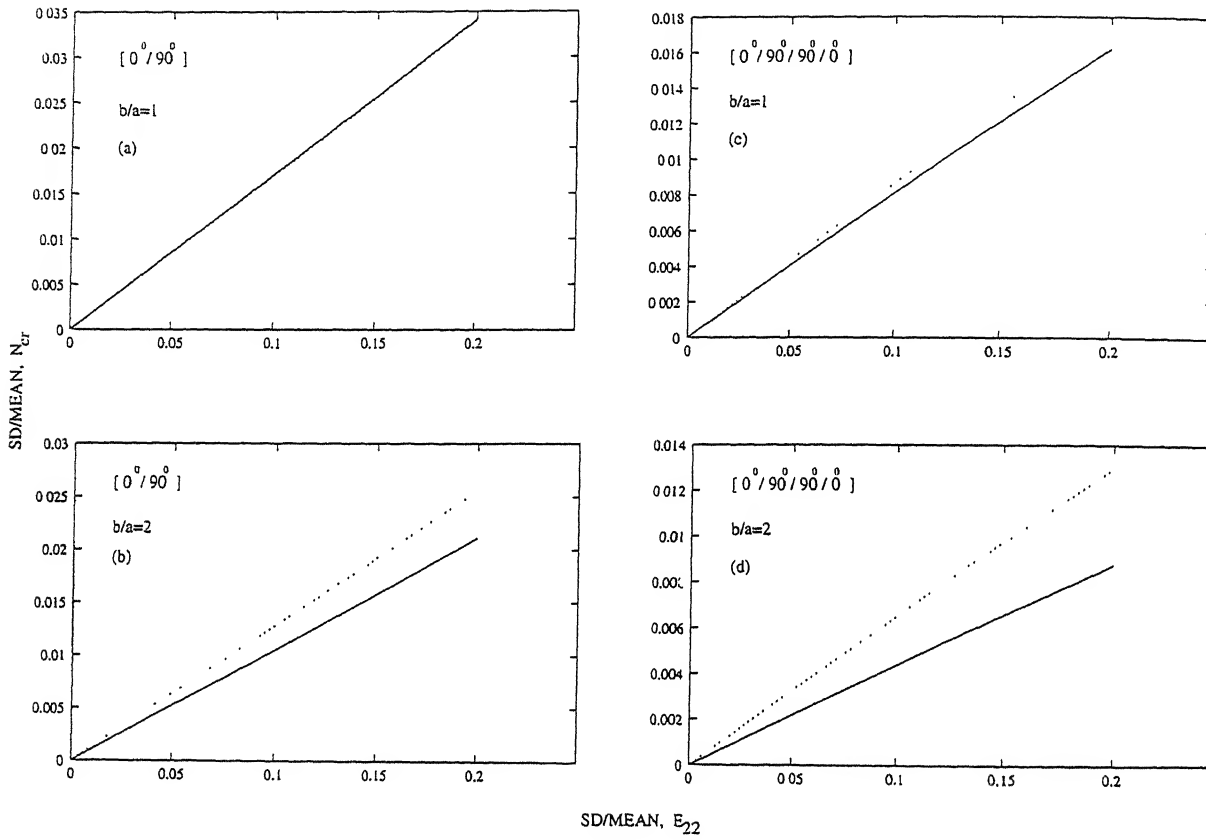


Figure 4.16: Sensitivity of SD of spherical panel buckling loads with SD of basic material property, E_{22} for $b/h=10$ and $R/b=5$.

Key: As in Figure 4.12.

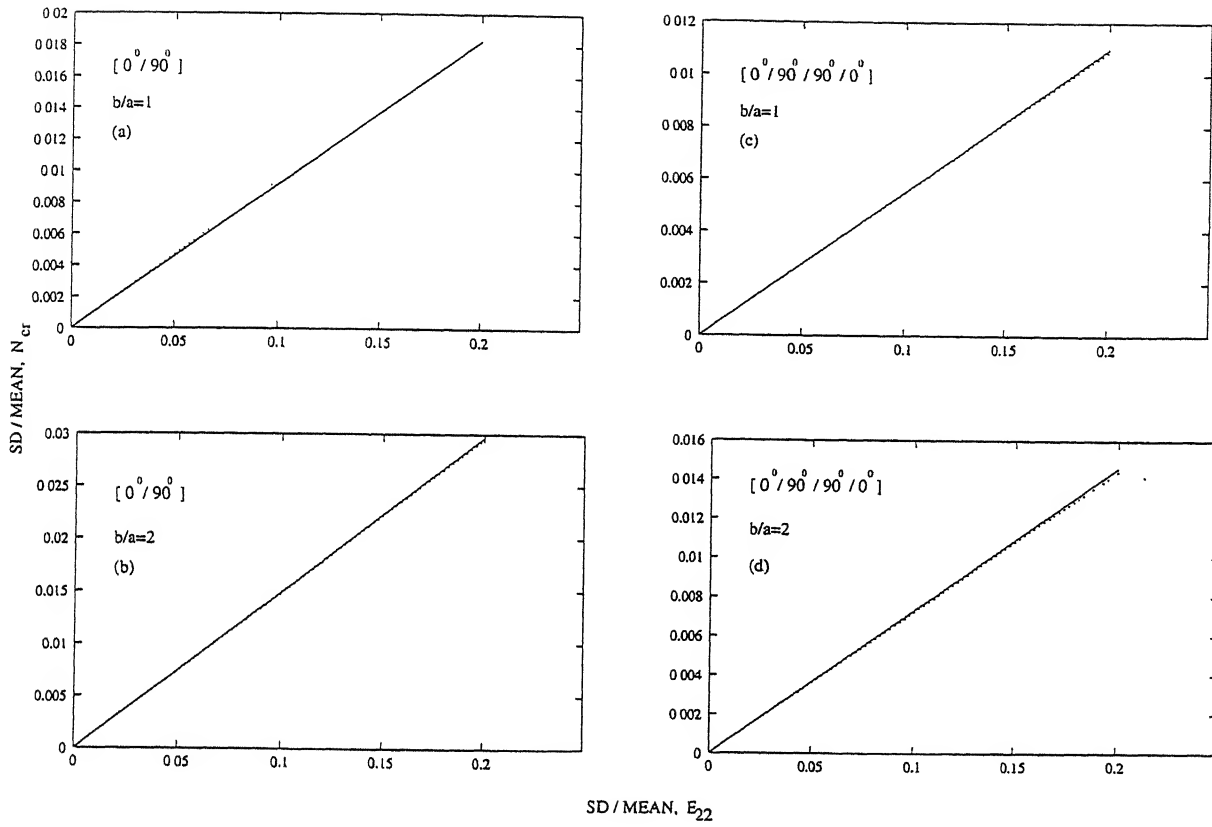


Figure 4.17: Sensitivity of SD of spherical panel buckling loads with SD of basic material property, E_{22} for $b/h=100$ and $R/b=5$.

Key: As in Figure 4.12.

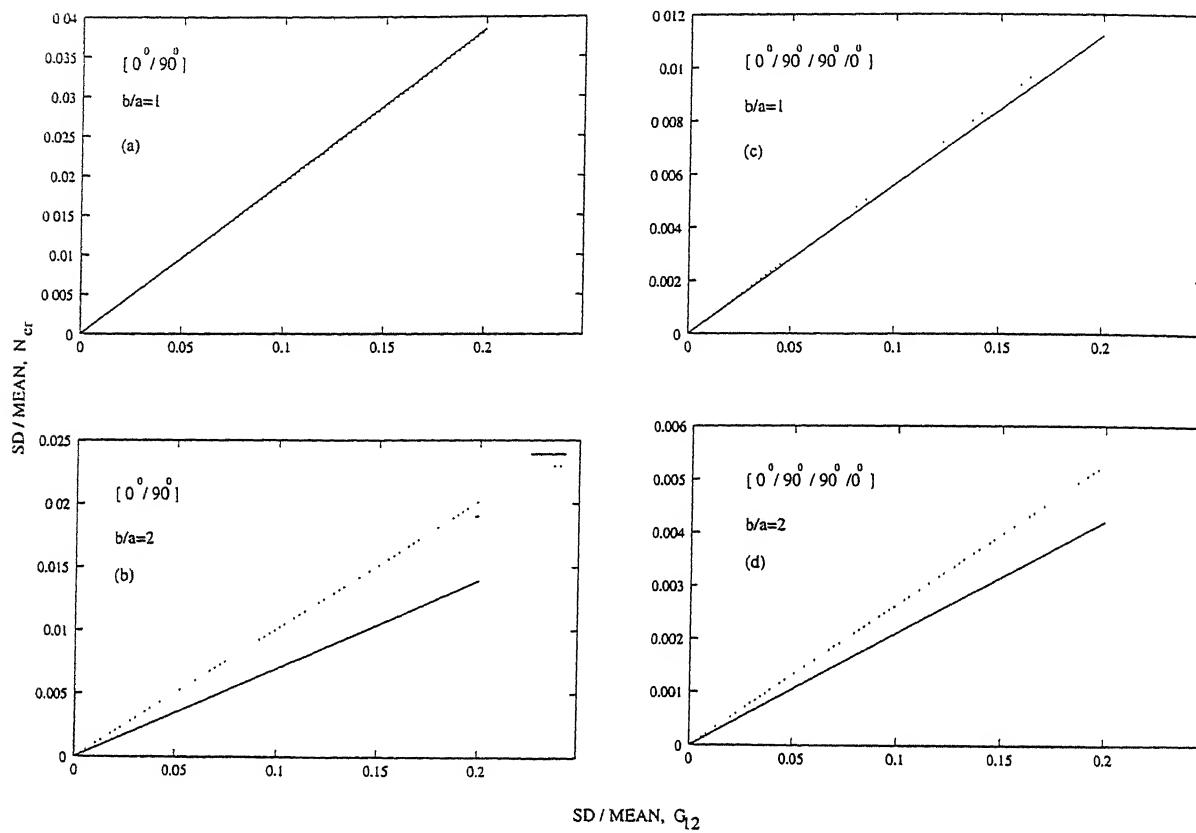


Figure 4.18: Sensitivity of SD of spherical panel buckling loads with SD of basic material property, G_{12} for $b/h=10$ and $R/b=5$.

Key: As in Figure 4.12.

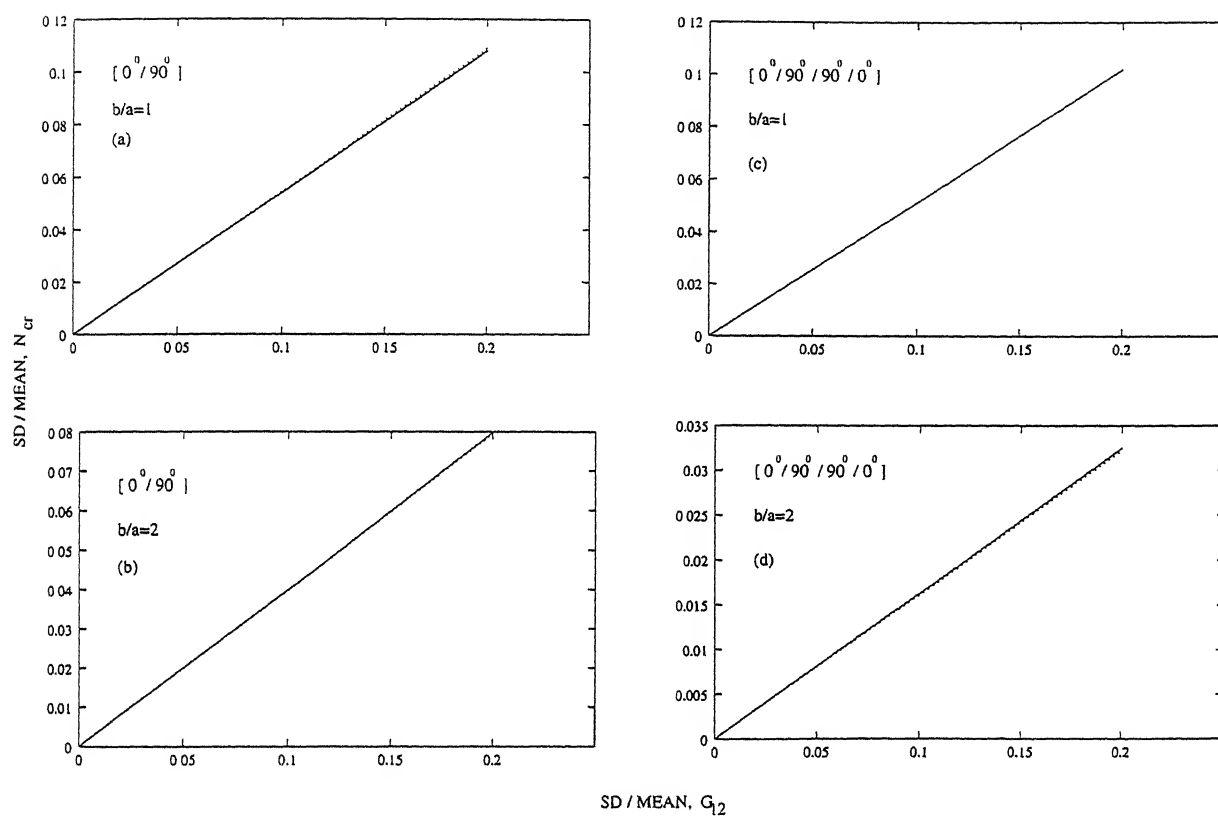


Figure 4.19: Sensitivity of SD of spherical panel buckling loads with SD of basic material property, G_{12} for $b/h=100$ and $R/b=5$.

Key: As in Figure 4.12.

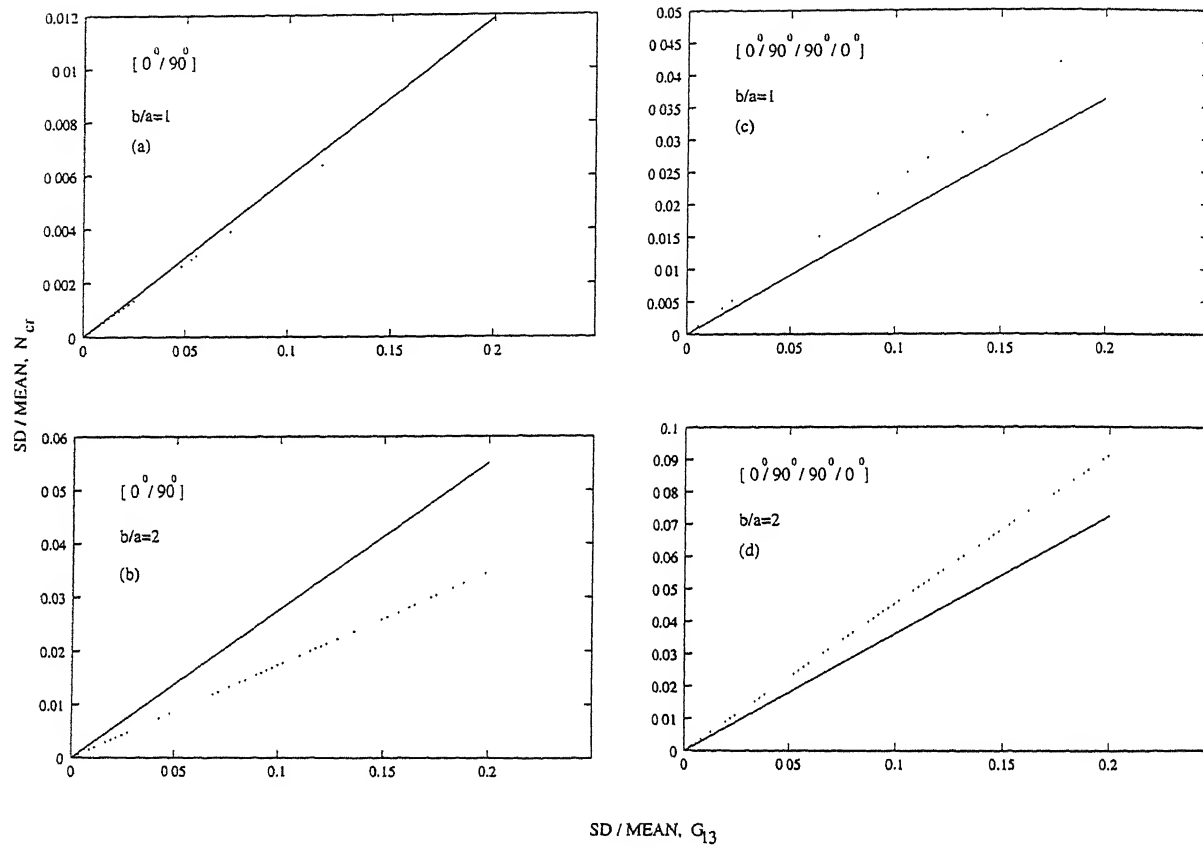


Figure 4.20: Sensitivity of SD of spherical panel buckling loads with SD of basic material property, G_{13} for $b/h=10$ and $R/b=5$.

Key: As in Figure 4.12.

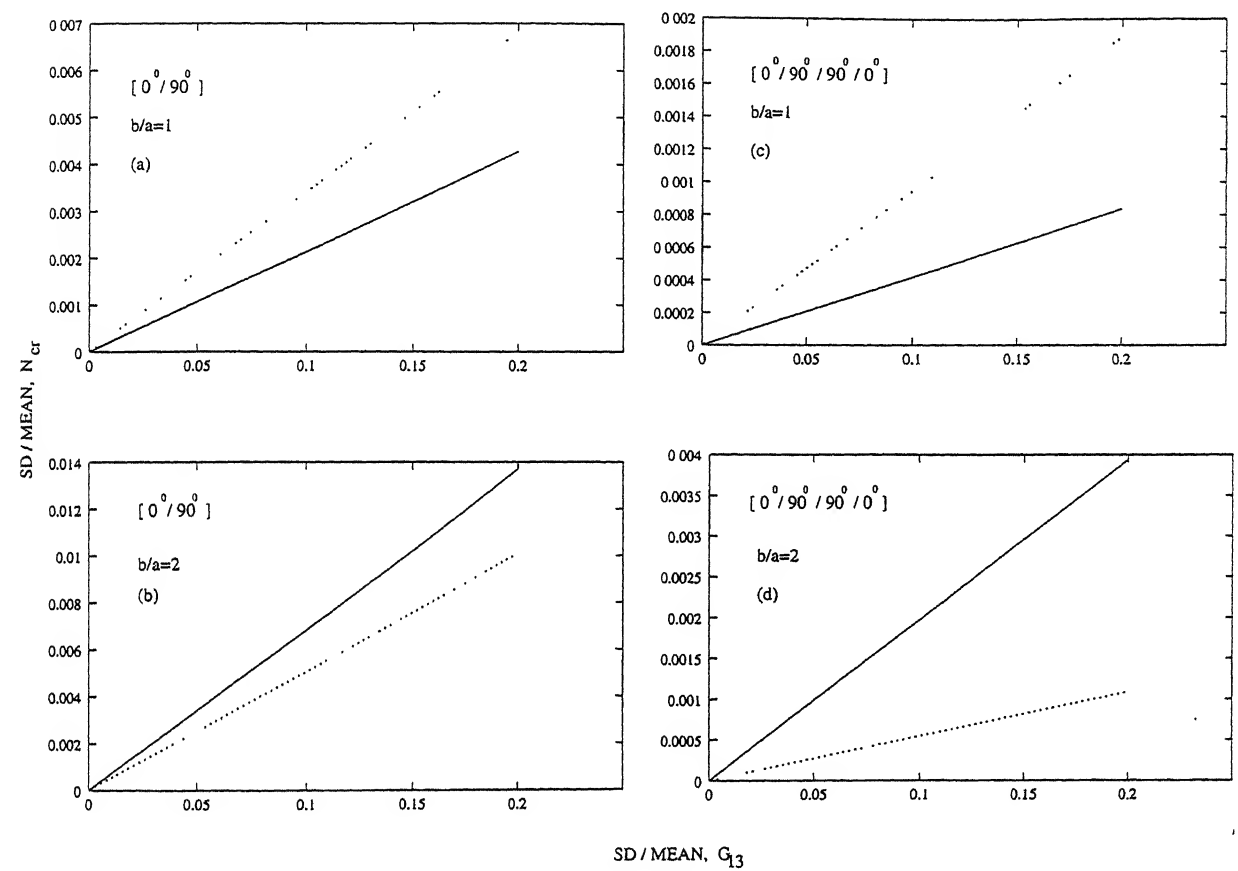


Figure 4.21: Sensitivity of SD of spherical panel buckling loads with SD of basic material property, G_{13} for $b/h=100$ and $R/b=5$.
Key: As in Figure 4.12.

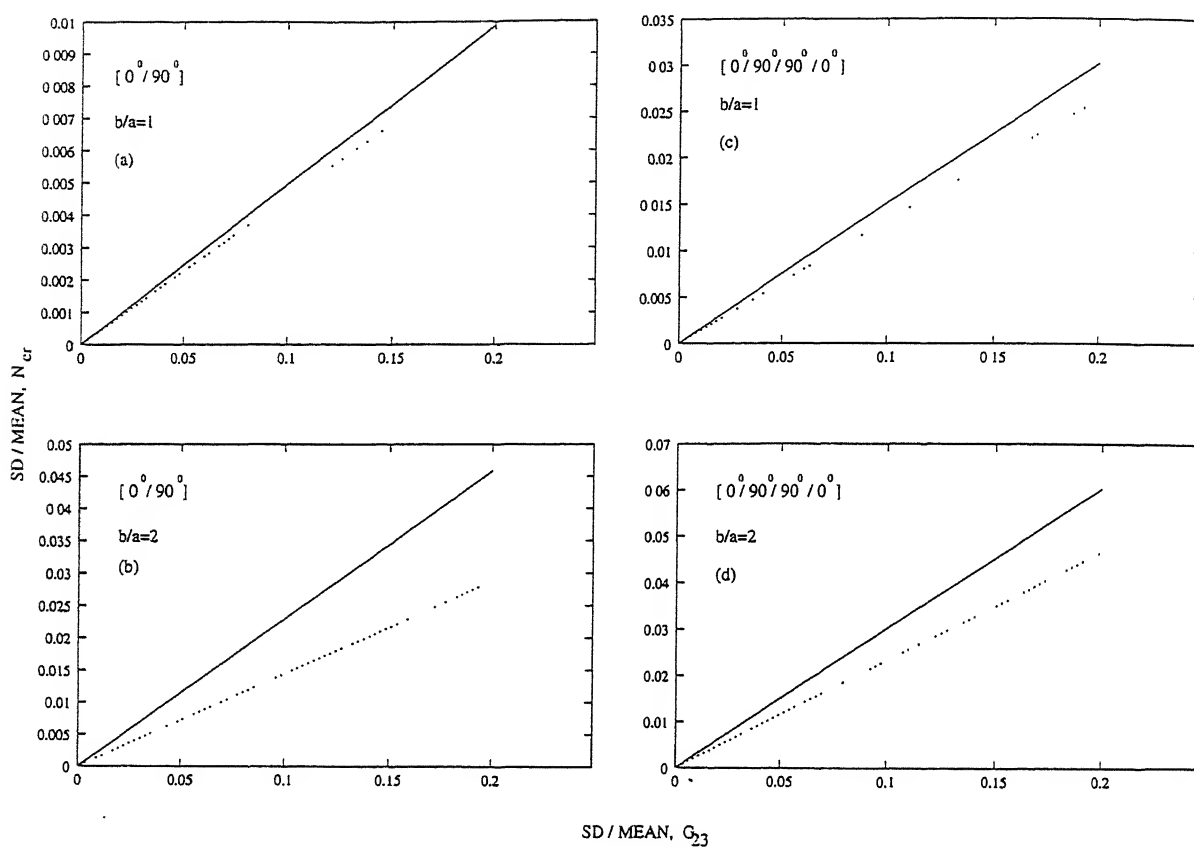


Figure 4.22: Sensitivity of SD of spherical panel buckling loads with SD of basic material property, G_{23} for $b/h=10$ and $R/b=5$.

Key: As in Figure 4.12.

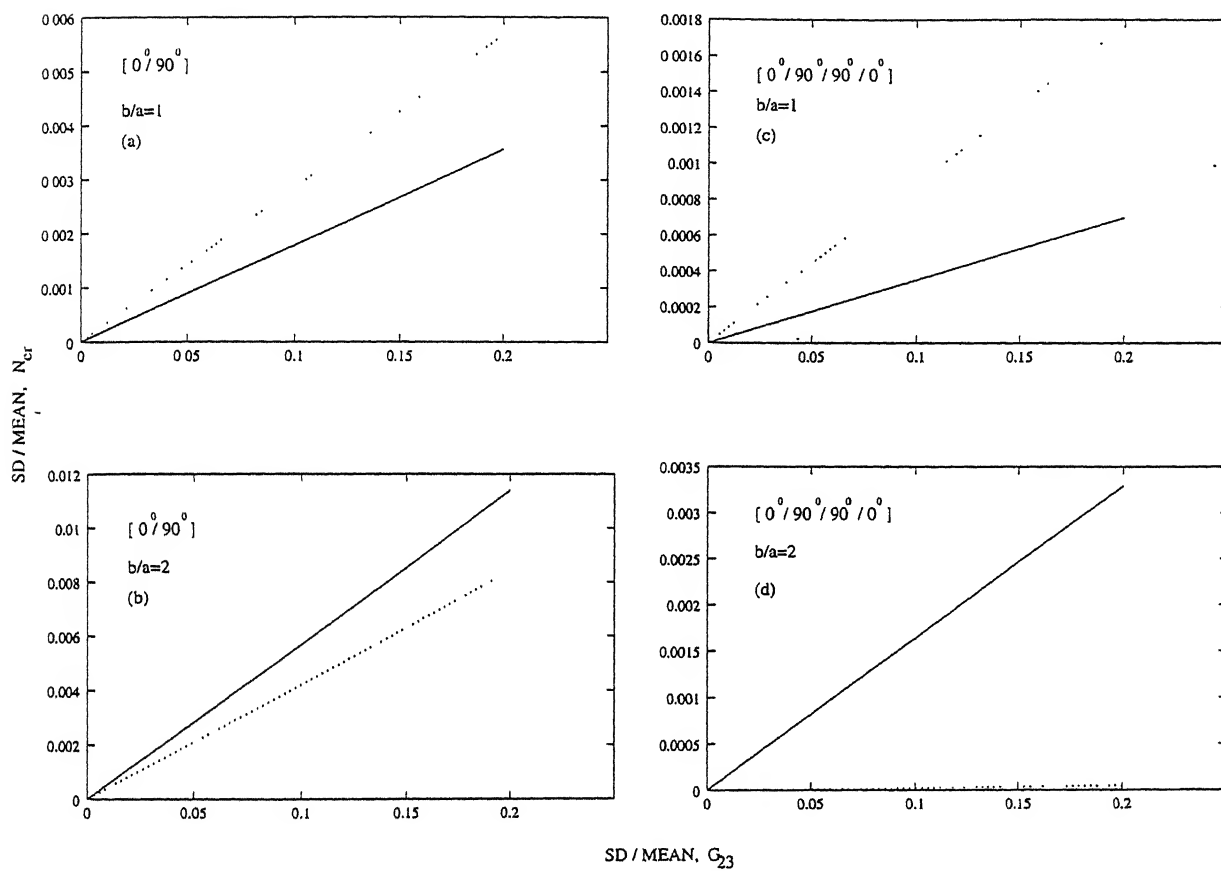


Figure 4.23: Sensitivity of SD of spherical panel buckling loads with SD basic material property, G_{23} for $b/h=100$ and $R/b=5$.
Key: As in Figure 4.12.

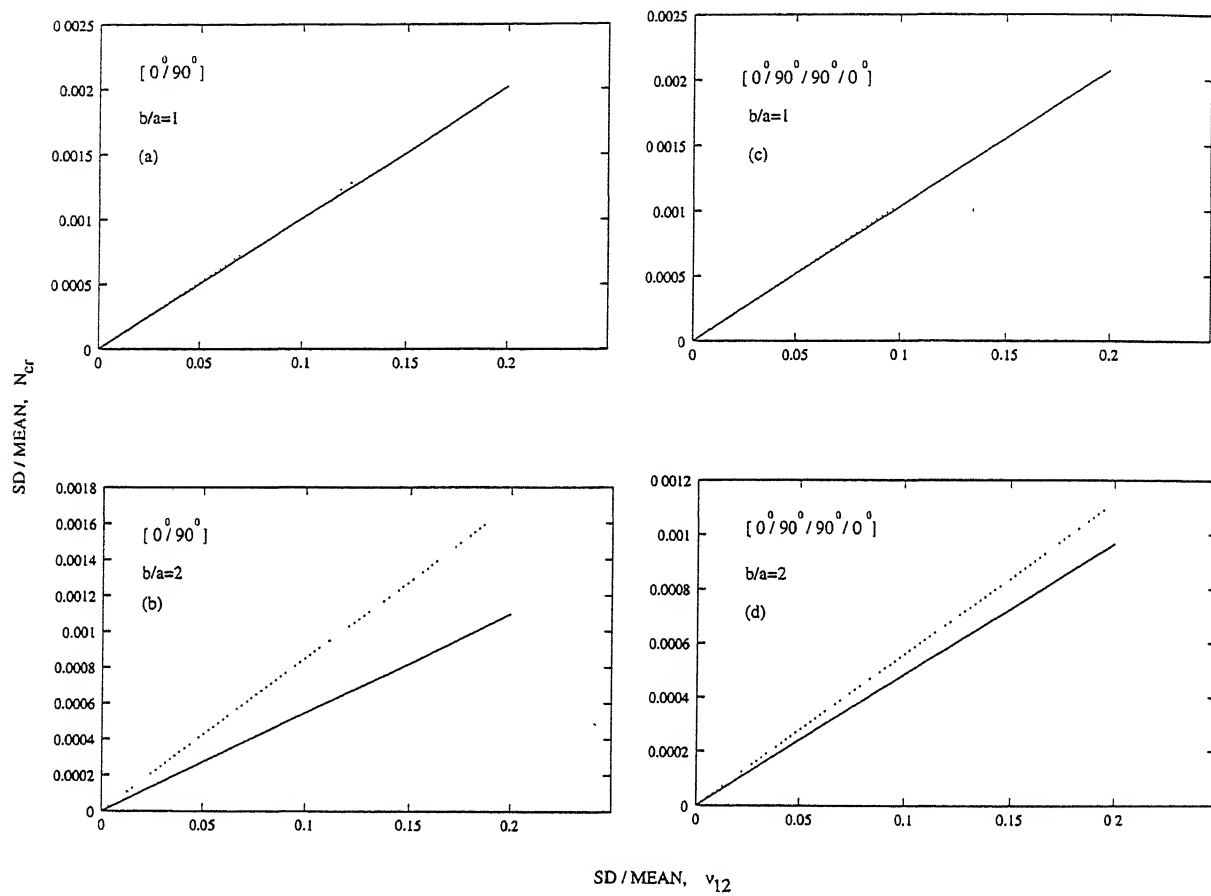


Figure 4.24: Sensitivity of SD of spherical panel buckling loads with SD basic material property, ν_{12} for $b/h=10$ and $R/b=5$.

Key: As in Figure 4.12.

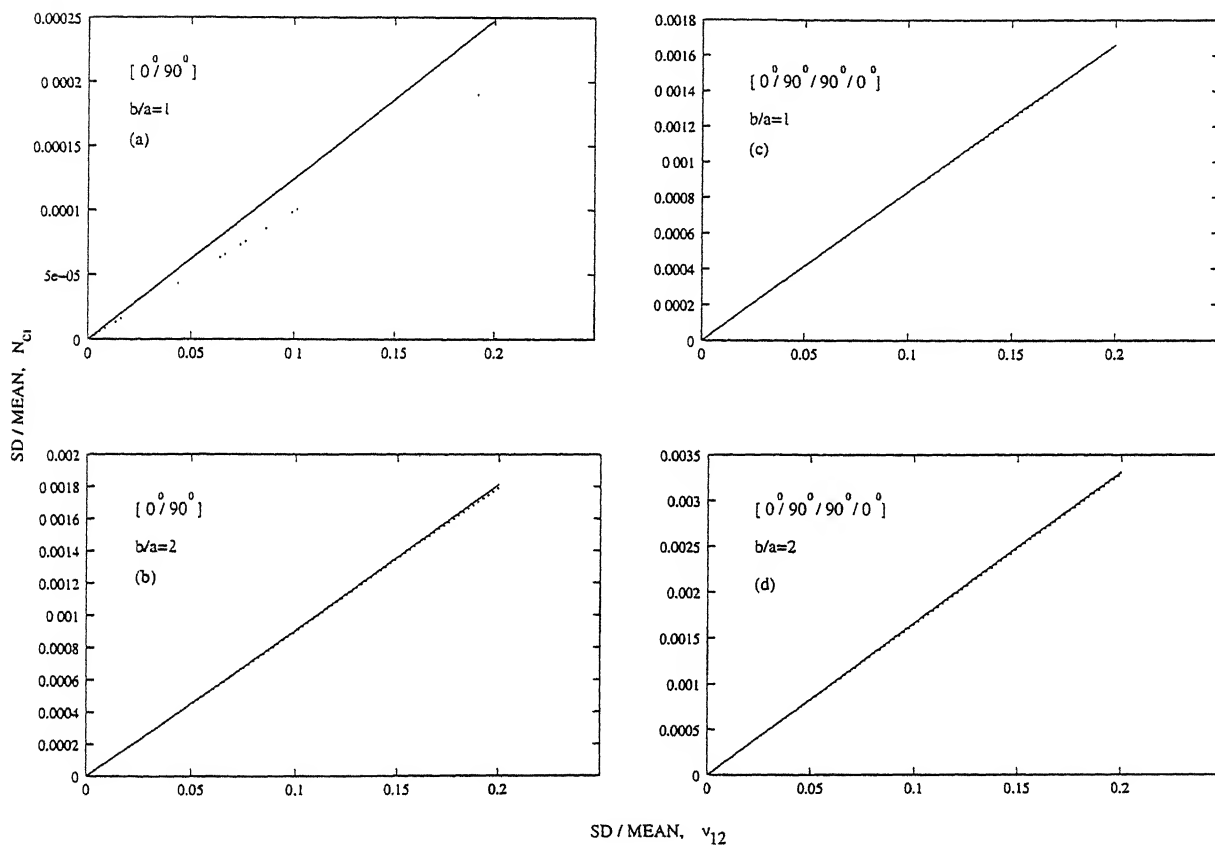


Figure 4.25: Sensitivity of SD of spherical panel buckling loads with SD basic material property, ν_{12} for $b/h=10$ and $R/b=5$.
Key: As in Figure 4.12.

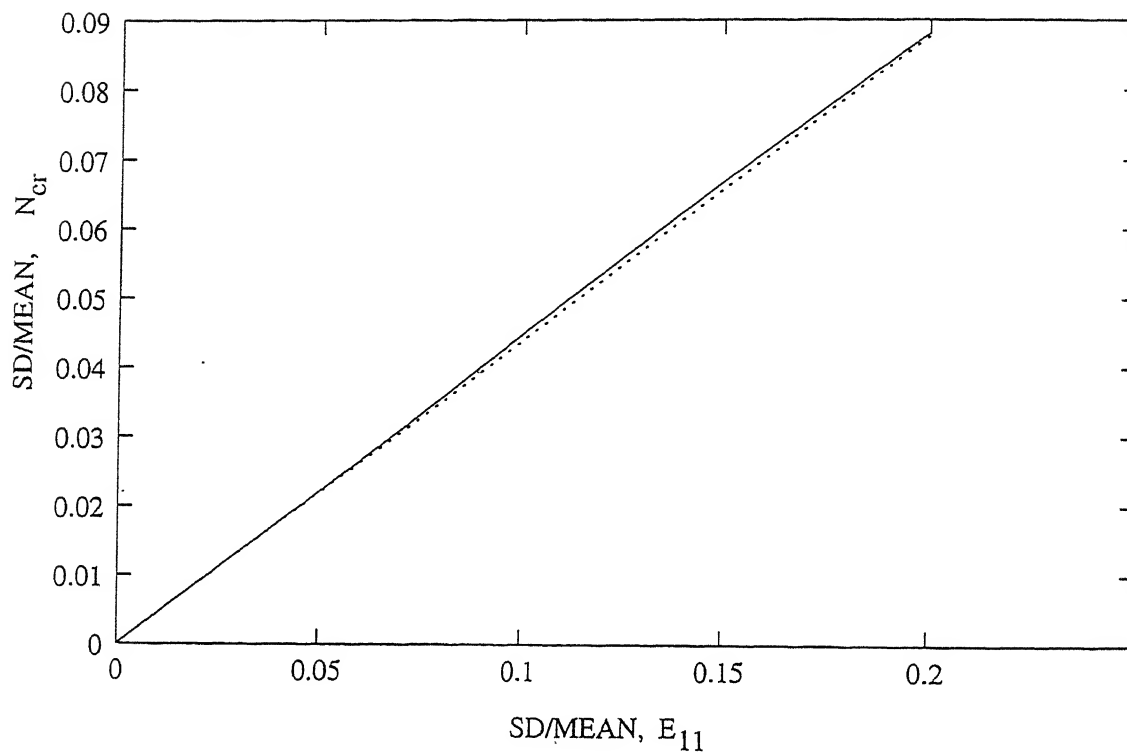


Figure 4.26: Validation of buckling load for a square plate by the present approach, with Monte Carlo simulation, $[0^\circ/90^\circ]$ laminate, with $b/h=5$.

Key:-: Present approach, —: MCS.

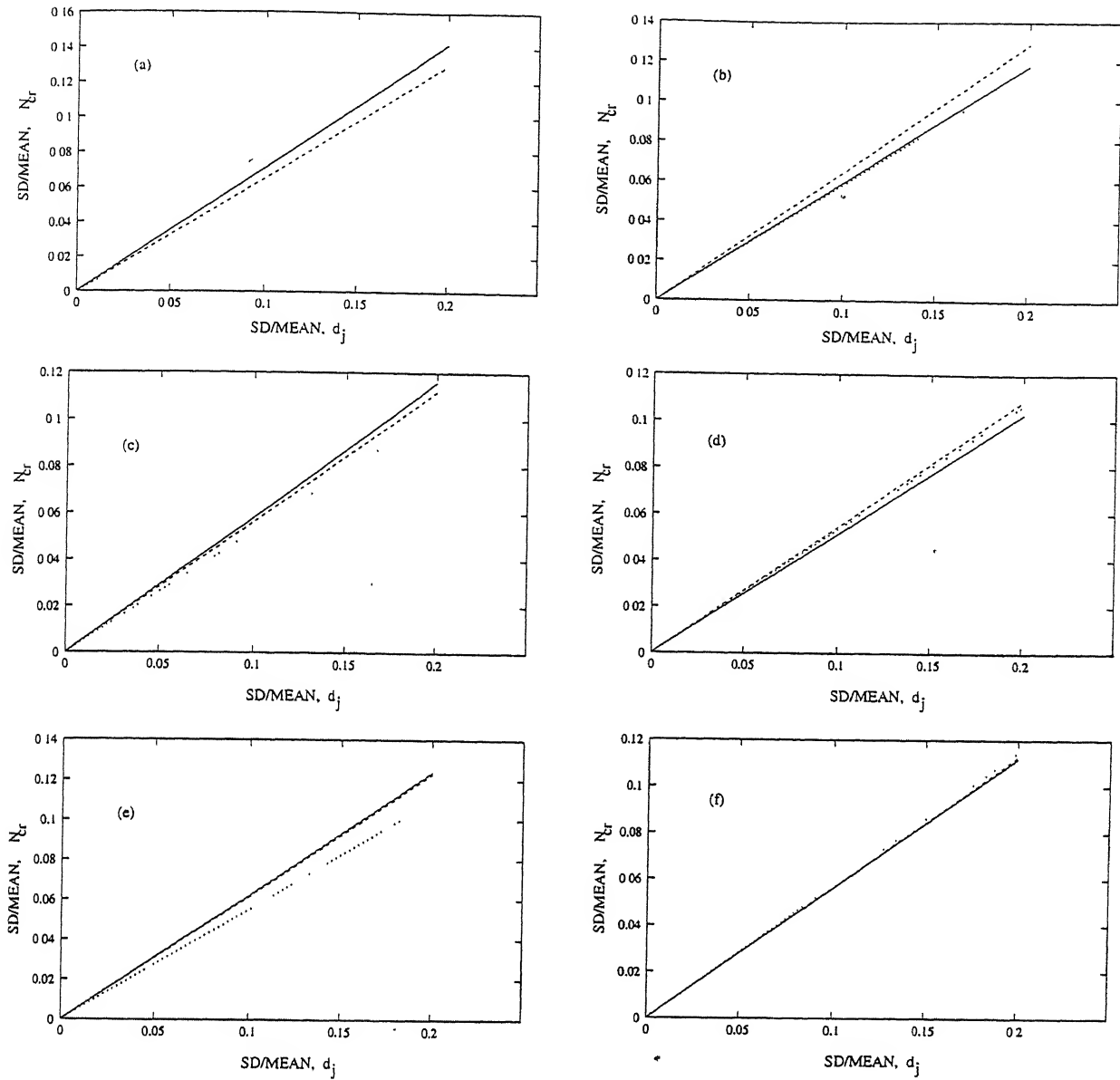


Figure 4.27: Variation of SD/mean of the nondimensionalised buckling loads with SD of basic material properties, square laminate with all basic material properties changing simultaneously.

- (a) $b/h=5$ and $[60^\circ / -60^\circ / 60^\circ / -60^\circ]$; (b) $b/h=10$ and $[60^\circ / -60^\circ / 60^\circ / -60^\circ]$;
 (c) $b/h=5$ and $[30^\circ / -30^\circ / 30^\circ / -30^\circ]$; (d) $b/h=10$ and $[30^\circ / -30^\circ / 30^\circ / -30^\circ]$;
 (e) $b/h=5$ and $[45^\circ / -45^\circ / 45^\circ / -45^\circ]$; (f) $b/h=10$ and $[45^\circ / -45^\circ / 45^\circ / -45^\circ]$.

Key:- — :CCCC, :CFCF, - - - :SSSS.

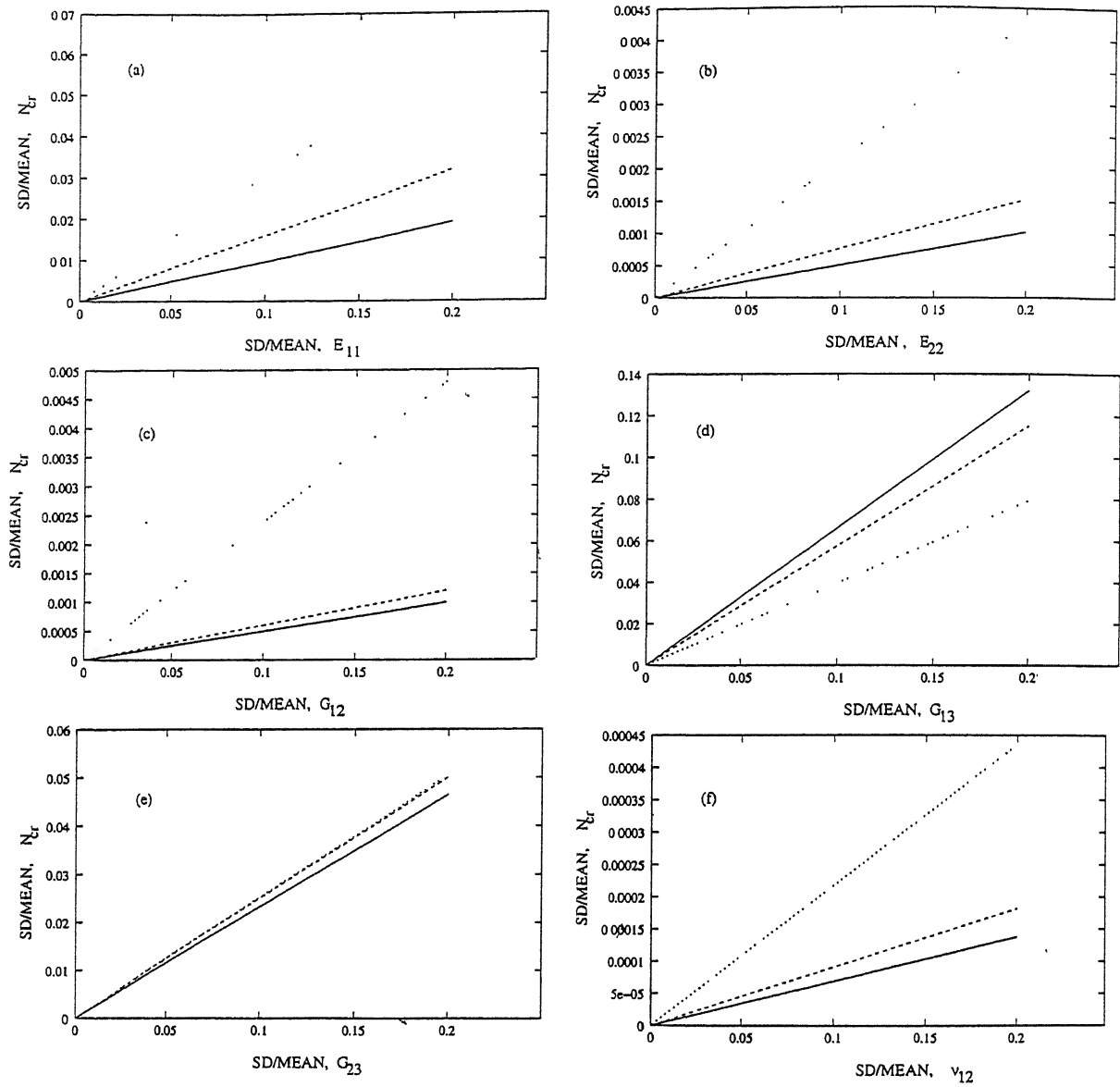


Figure 4.28: Variation of SD/mean of the nondimensionalised buckling loads with SD of basic material properties, $[60^\circ / -60^\circ / 60^\circ / -60^\circ]$ square laminate, with $b/h=5$.

(a) only E_{11} varying; (b) only E_{22} varying; (c) only G_{12} varying;
 (d) only G_{13} varying; (e) only G_{23} varying; (f) only ν_{12} varying.

Key: As in Figure 4.27.

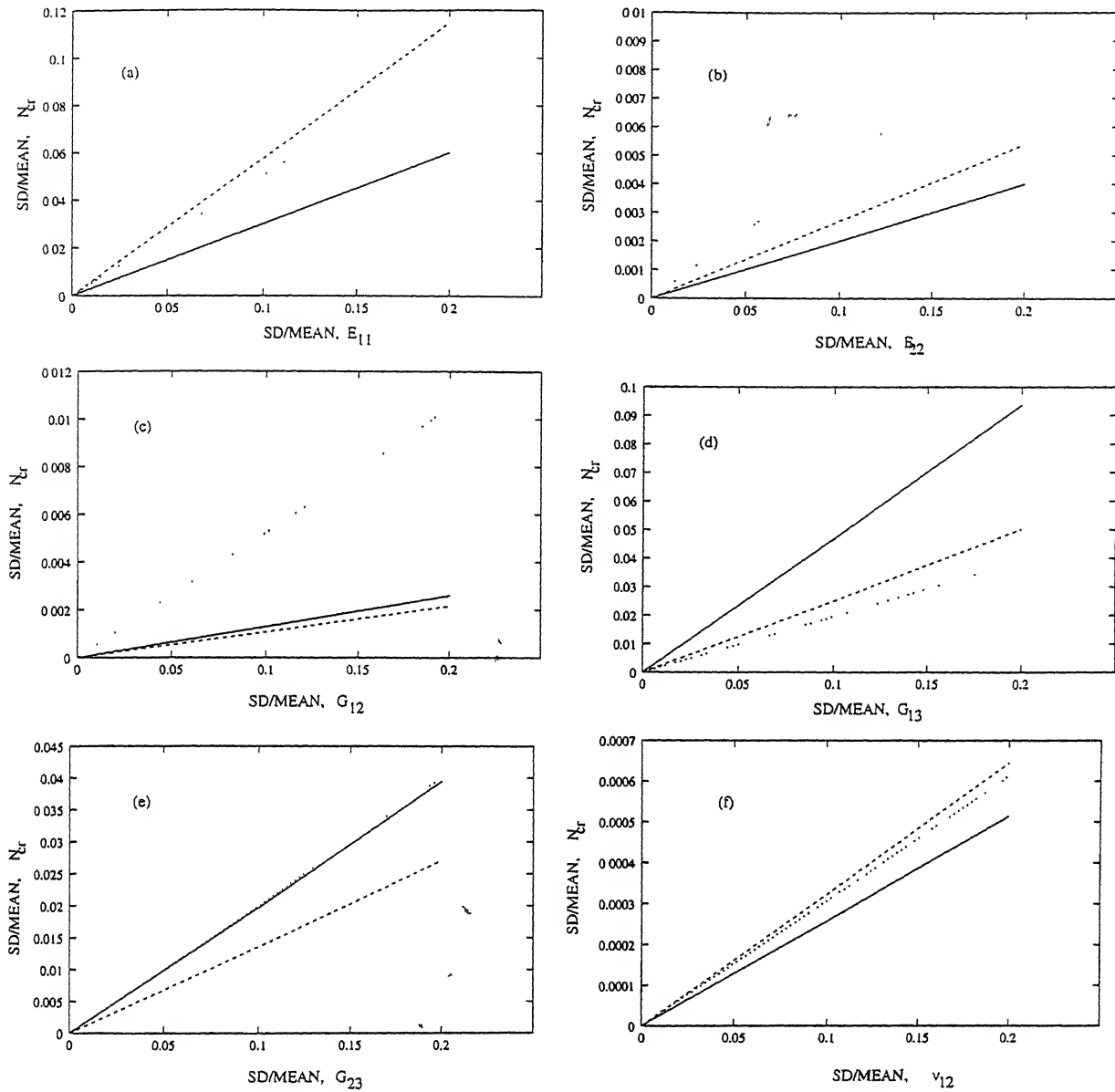


Figure 4.29: Variation of SD/mean of the nondimensionalised buckling loads with SD of basic material properties, $[60^\circ/-60^\circ/60^\circ/-60^\circ]$ square laminate, with $b/h=10$.

(a) only E_{11} varying; (b) only E_{22} varying; (c) only G_{12} varying;
 (d) only G_{13} varying; (e) only G_{23} varying; (f) only ν_{12} varying.

Key: As in Figure 4.27.

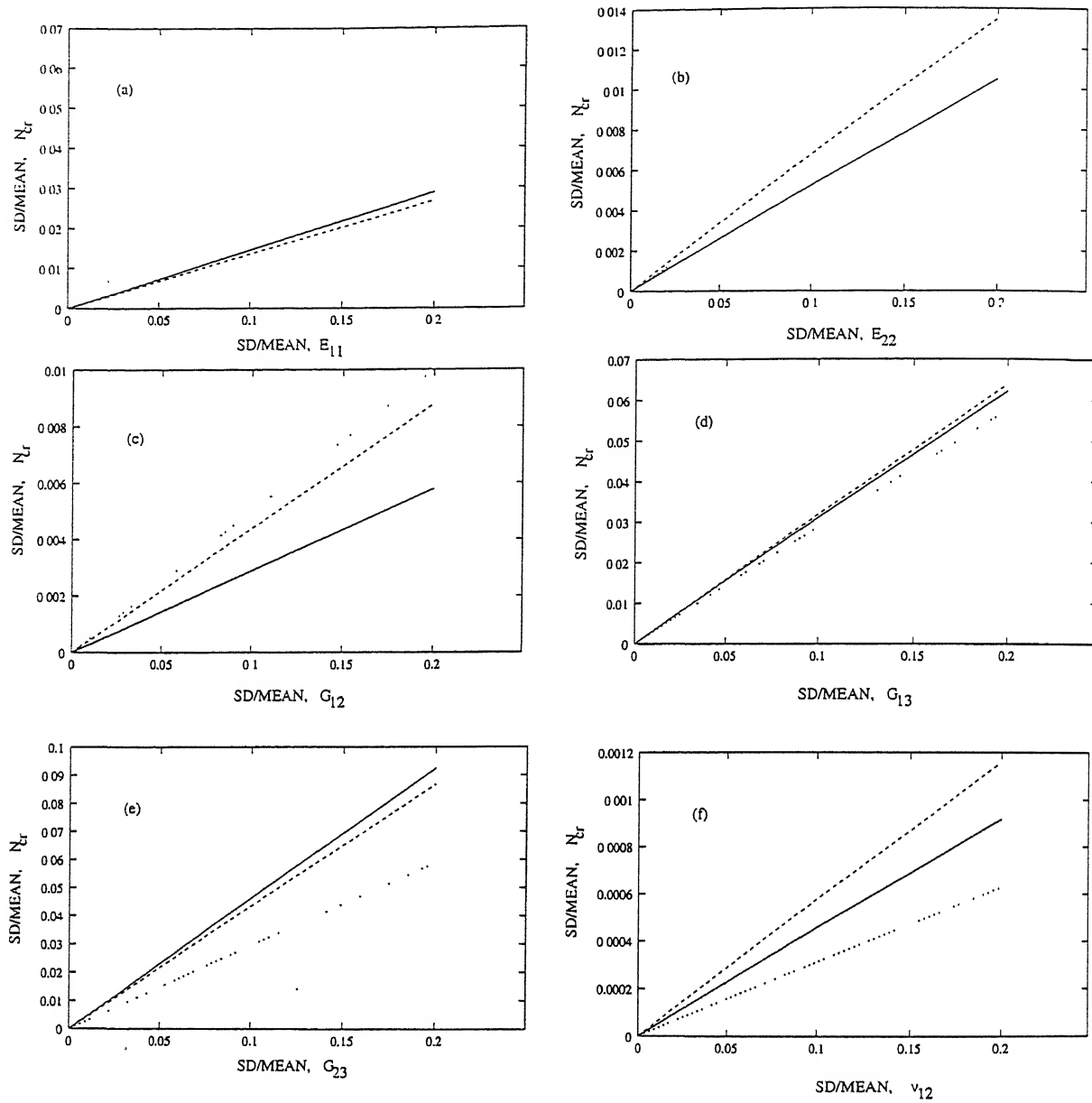


Figure 4.30: Variation of SD/mean of the nondimensionalised buckling loads with SD of basic material properties, $[30^\circ / -30^\circ / 30^\circ / -30^\circ]$ square laminate, with $b/h = 5$.

(a) only E_{11} varying; (b) only E_{22} varying; (c) only G_{12} varying;
 (d) only G_{13} varying; (e) only G_{23} varying; (f) only ν_{12} varying.

Key: As in Figure 4.27.

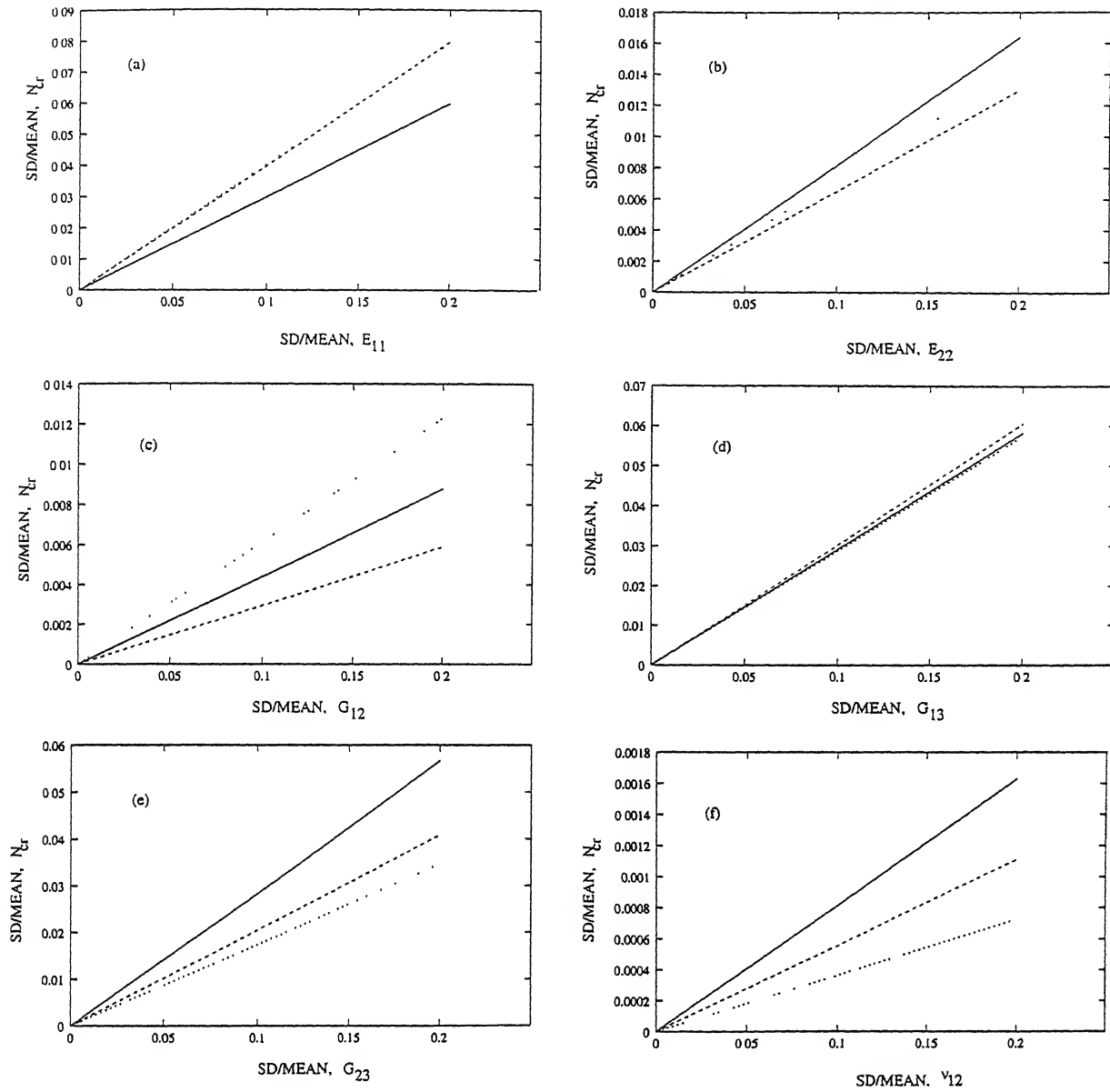


Figure 4.31: Variation of SD/mean of the nondimensionalised buckling loads with SD of basic material properties, $[30^\circ/-30^\circ/30^\circ/-30^\circ]$ square laminate, with $b/h=10$.

(a) only E_{11} varying; (b) only E_{22} varying; (c) only G_{12} varying;

(d) only G_{13} varying; (e) only G_{23} varying; (f) only ν_{12} varying

Key: As in Figure 4.27.

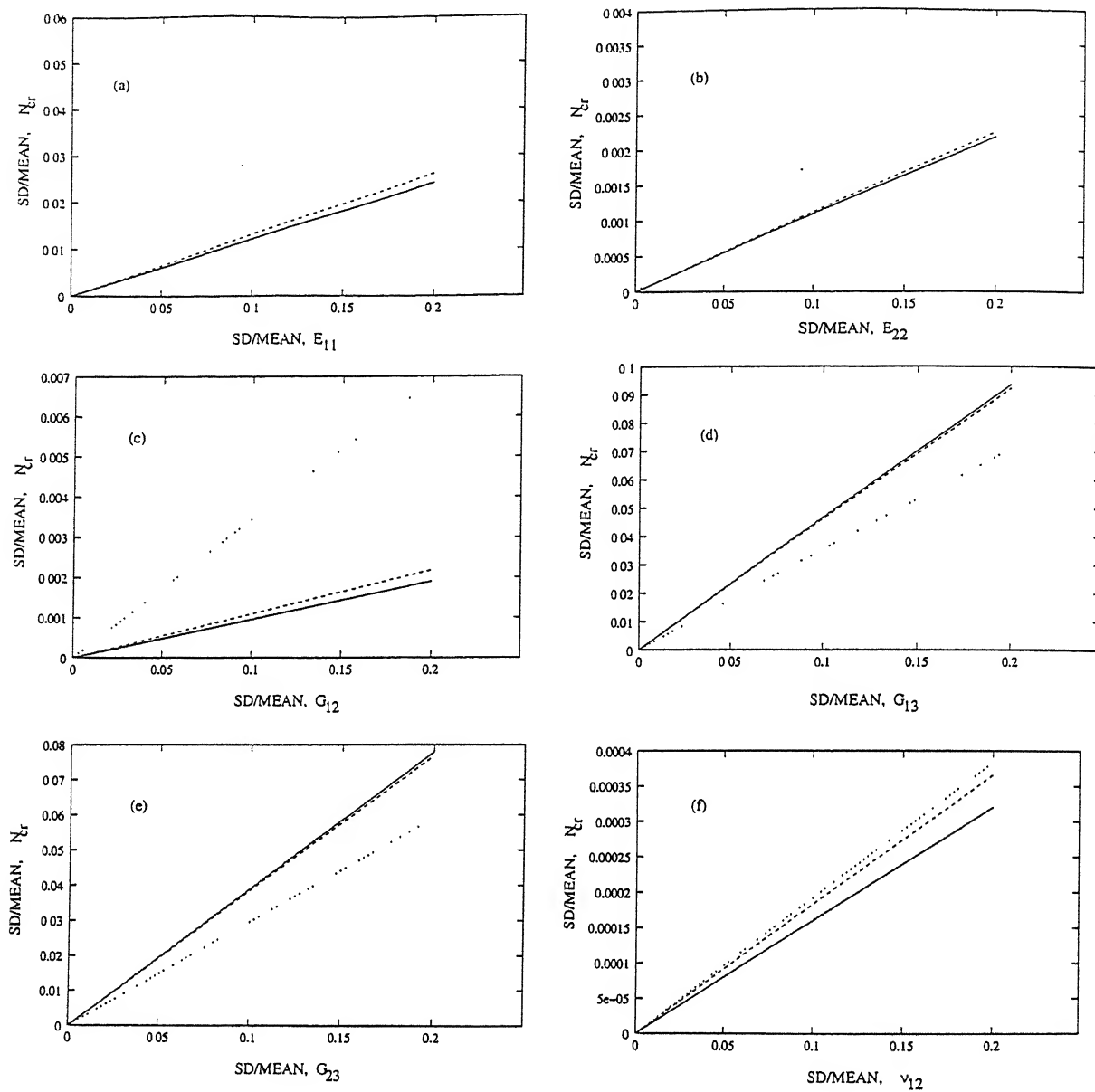


Figure 4.32: Variation of SD/mean of the nondimensionalised buckling loads with SD of basic material properties, $[45^\circ / -45^\circ / 45^\circ / -45^\circ]$ square laminate, with $b/h=5$.

(a) only E_{11} varying; (b) only E_{22} varying; (c) only G_{12} varying;
 (d) only G_{13} varying; (e) only G_{23} varying; (f) only ν_{12} varying.

Key: As in Figure 4.27.

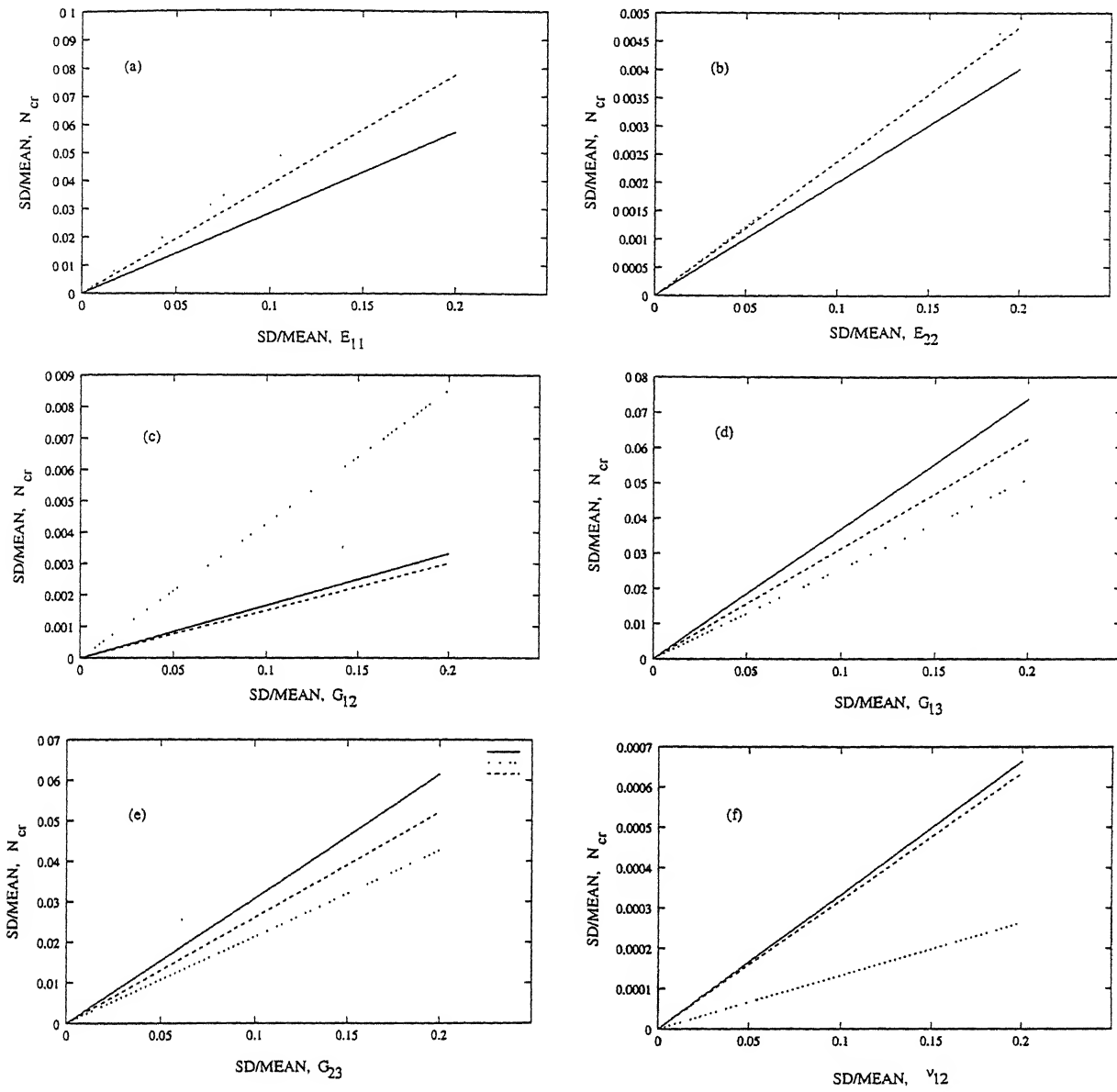


Figure 4.33: Variation of SD/mean of the nondimensionalised buckling loads with SD of basic material properties, $[45^\circ/-45^\circ/45^\circ/-45^\circ]$ square laminate, with $b/h=10$.

(a) only E_{11} varying; (b) only E_{22} varying; (c) only G_{12} varying;

(d) only G_{13} varying; (e) only G_{23} varying; (f) only ν_{12} varying.

Key: As in Figure 4.27.

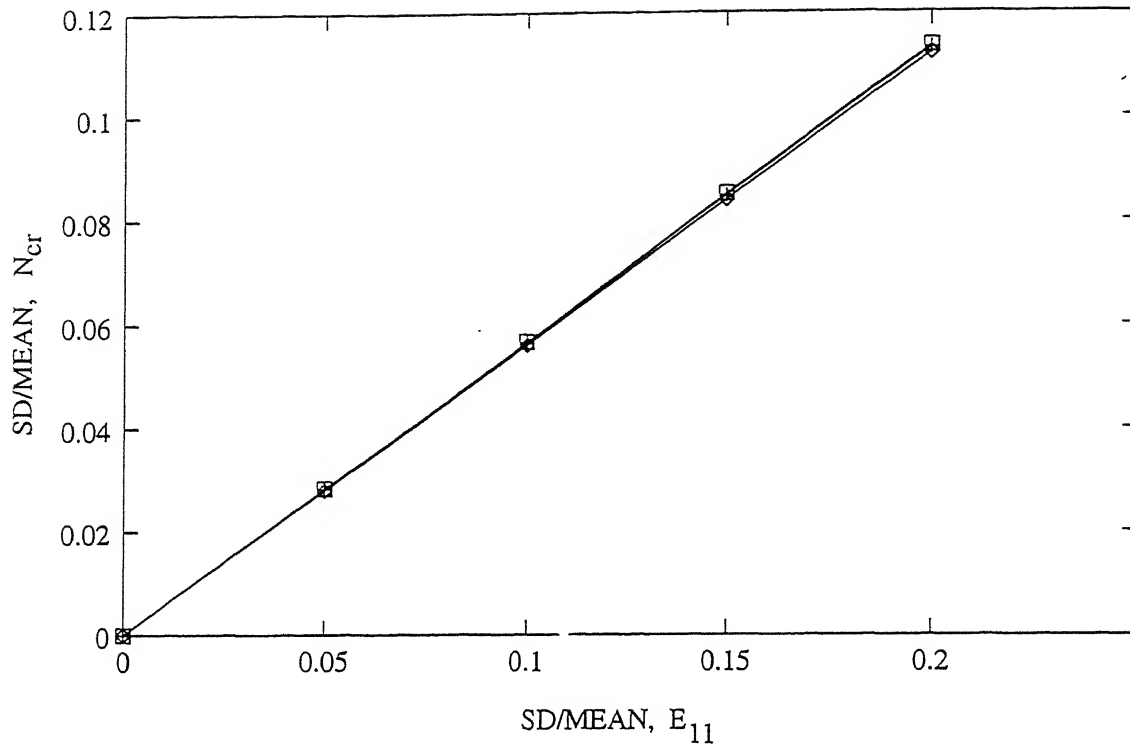


Figure 4.34: Validation of results by the present SFEM approach with Monte Carlo simulation and available results for $[0^\circ/90^\circ]$ square cylindrical laminate, with $R/b=5$, and $b/h=10$.

Key:- \diamond : Present approach, $+$: SCA, \square : MCS.

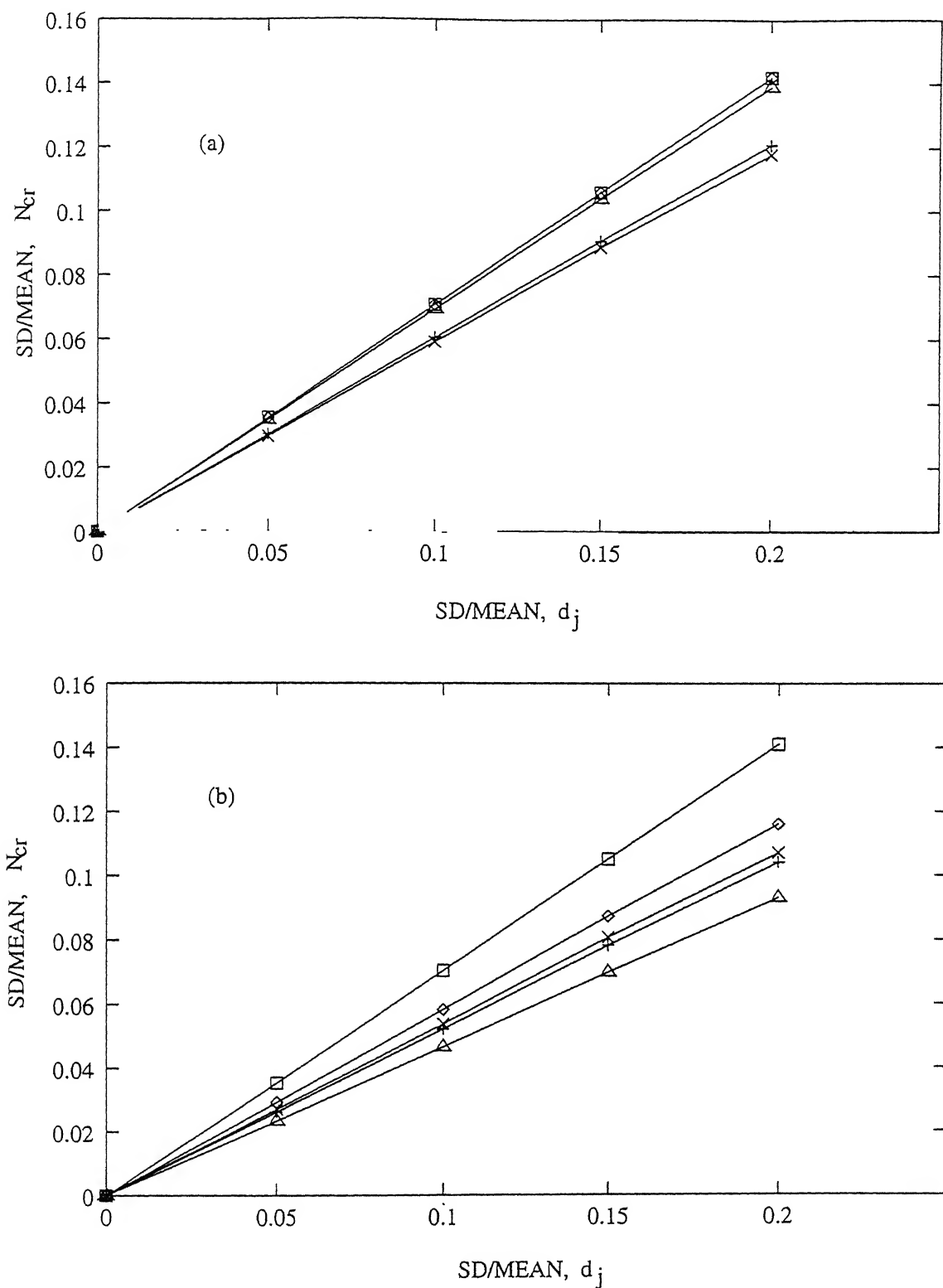


Figure 4.35: Variation of SD/mean of the nondimensionalised buckling loads with SD of basic material properties, $[0^\circ/45^\circ/-45^\circ/90^\circ]$ square cylindrical laminate and $R/b=5$, with all basic material properties changing simultaneously.

(a) $b/h=2$; (b) $b/h=5$.
Key:- \diamond : CCCC, $+$: CCCF, \square : CCCS, \times : CFCF, \triangle : SSSS.

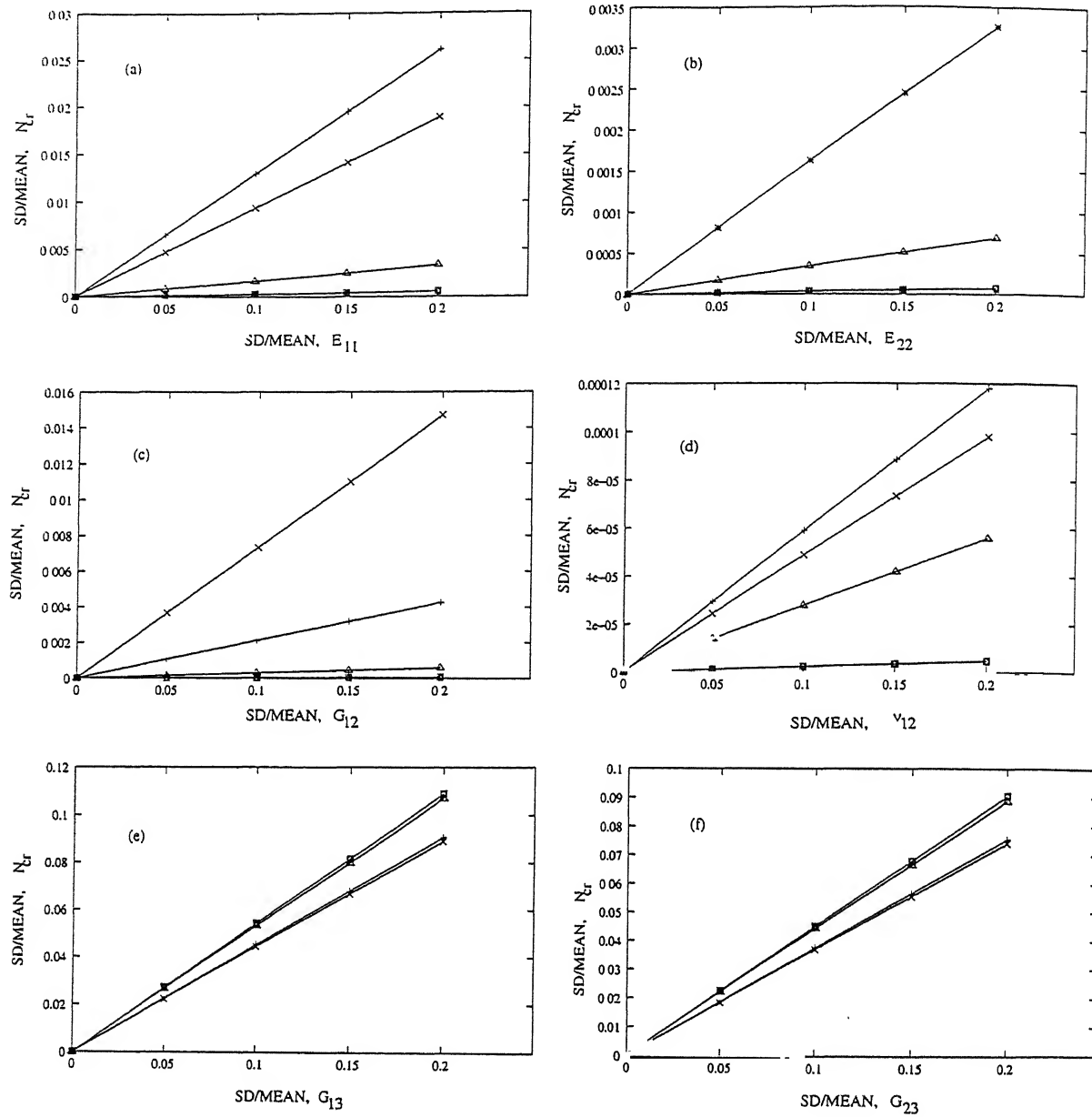


Figure 4.36: Variation of SD/mean of the nondimensionalised buckling loads with SD of basic material properties, $[0^\circ/45^\circ/-45^\circ/90^\circ]$ square cylindrical laminate, with $R/b=5$ and $b/h=2$.

(a) only E_{11} varying; (b) only E_{22} varying; (c) only G_{12} varying;
 (d) only G_{13} varying; (e) only G_{23} varying; (f) only ν_{12} varying.

Key: As in Figure 4.35.

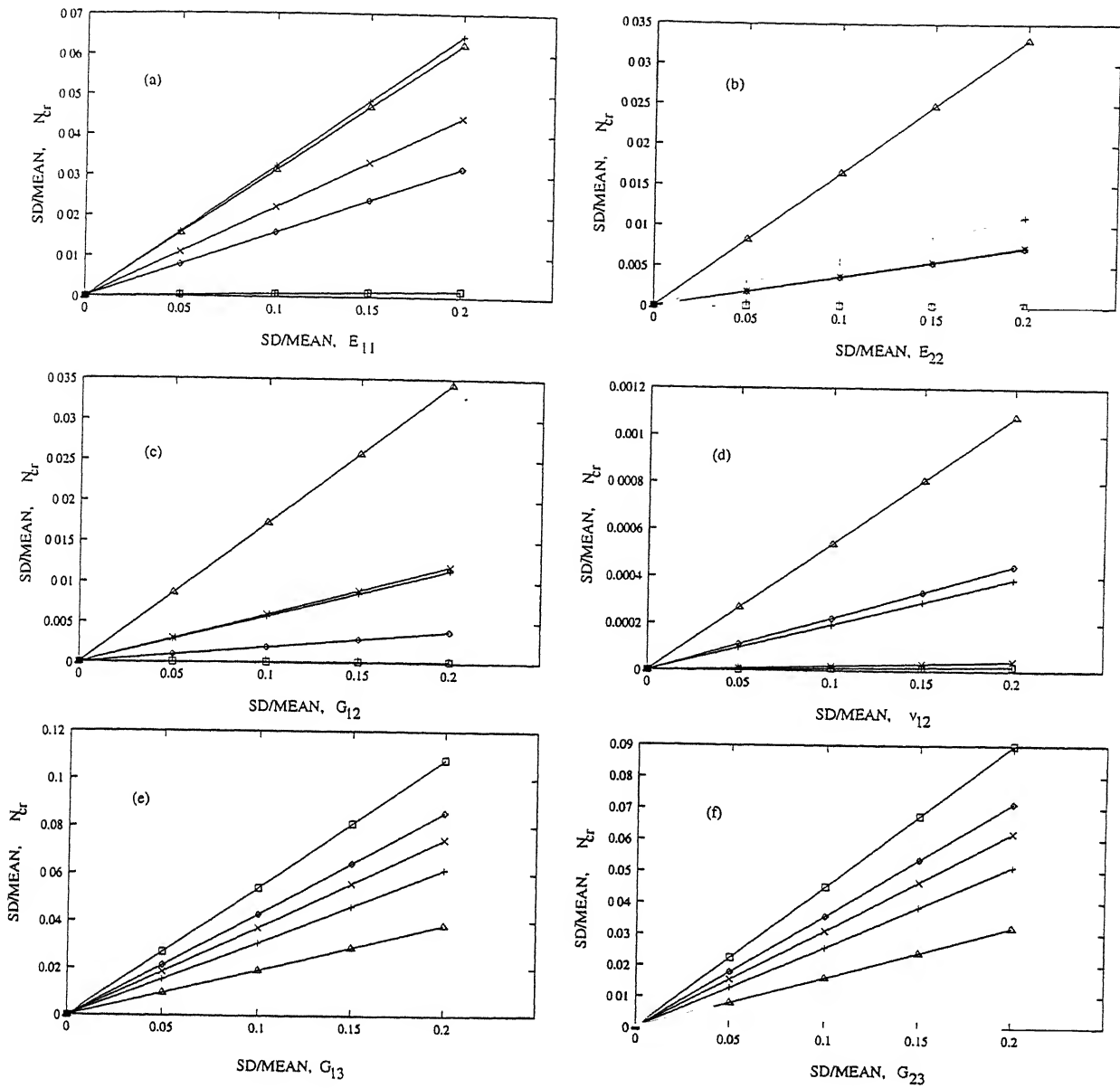


Figure 4.37: Variation of SD/mean of the nondimensionalised buckling loads with SD of basic material properties, $[0^\circ/45^\circ/-45^\circ/90^\circ]$ square cylindrical laminate, with $R/b=5$ and $b/h=5$.

(a) only E_{11} varying; (b) only E_{22} varying; (c) only G_{12} varying;
 (d) only G_{13} varying; (e) only G_{23} varying; (f) only ν_{12} varying.

Key: As in Figure 4.35.

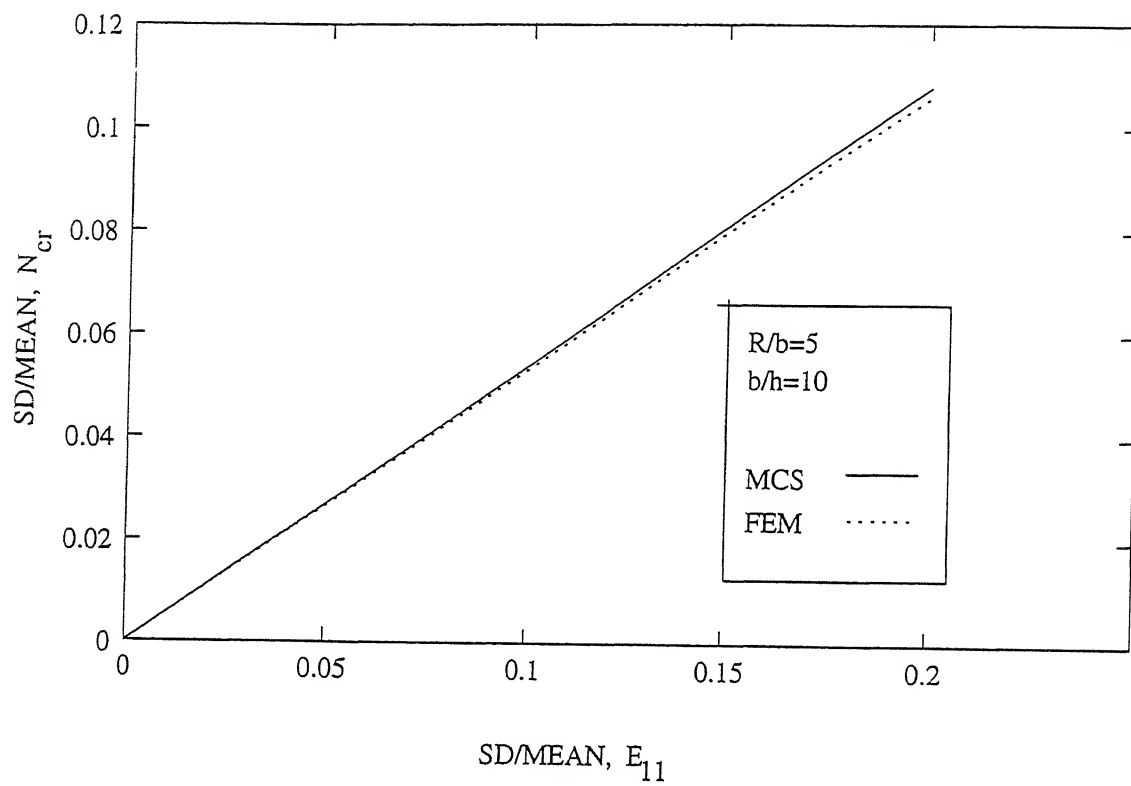


Figure 4.38: Validation of results for a $[0^\circ/90^\circ]$ spherical panel variance of nondimensionalised buckling load.

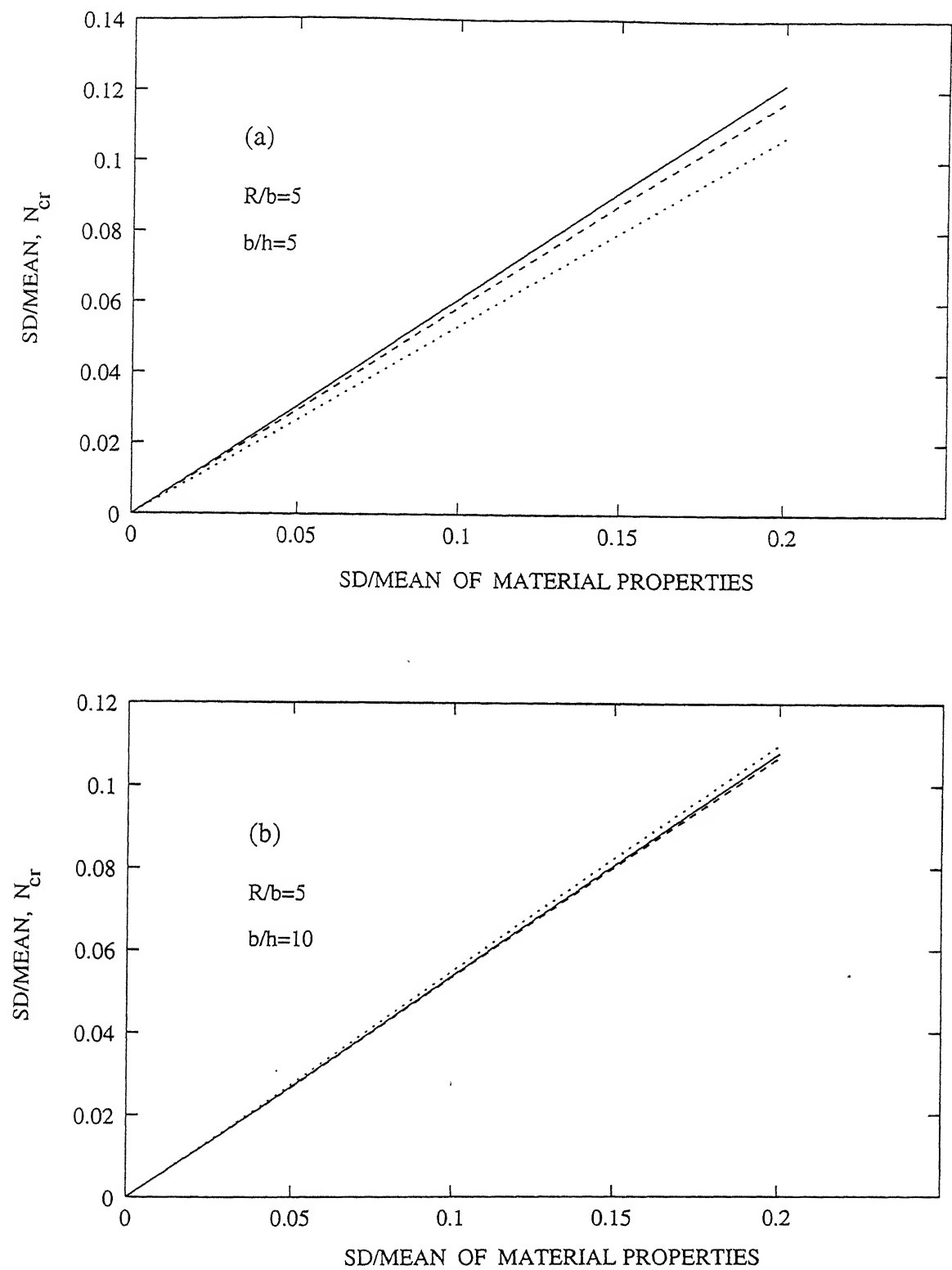


Figure 4.39: Variation of standard deviation (SD) of the nondimensionalised buckling load of a $[45^\circ / -45^\circ / 45^\circ / -45^\circ]$ laminated spherical square panel with all basic material properties changing simultaneously.

Key:- — :CCCC, :CFCF, - - - :SSSS.

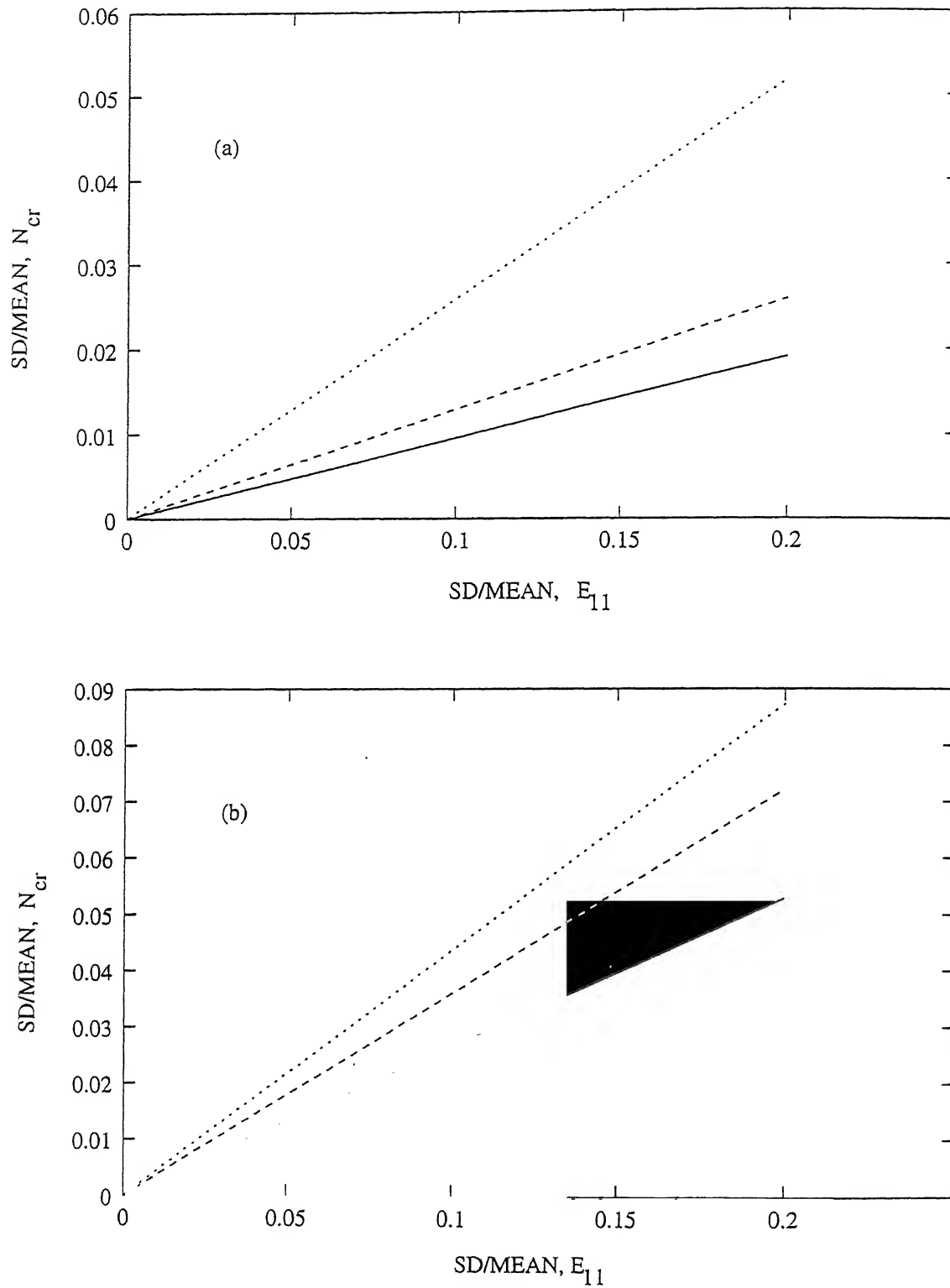


Figure 4.40: Variation of SD/mean of the nondimensionalised buckling load of a $[45^\circ / -45^\circ / 45^\circ / -45^\circ]$ square spherical laminate with SD of E_{11} .

Key: As in Figure 4.39.

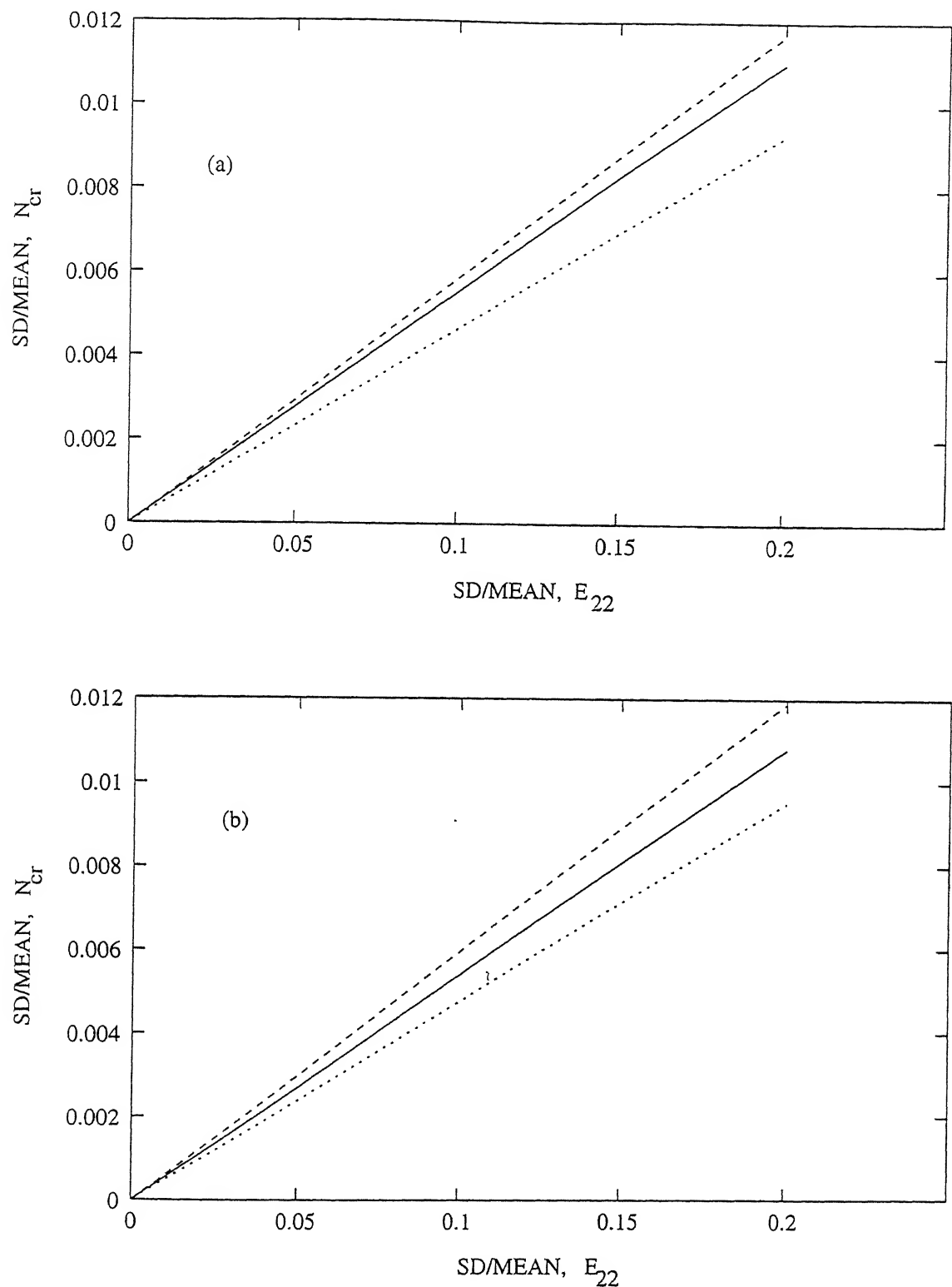


Figure 4.41: Variation of SD/mean of the nondimensionalised buckling load of a $[45^\circ/-45^\circ/45^\circ/-45^\circ]$ square spherical laminate with SD of E_{22} .
Key: As in Figure 4.39.

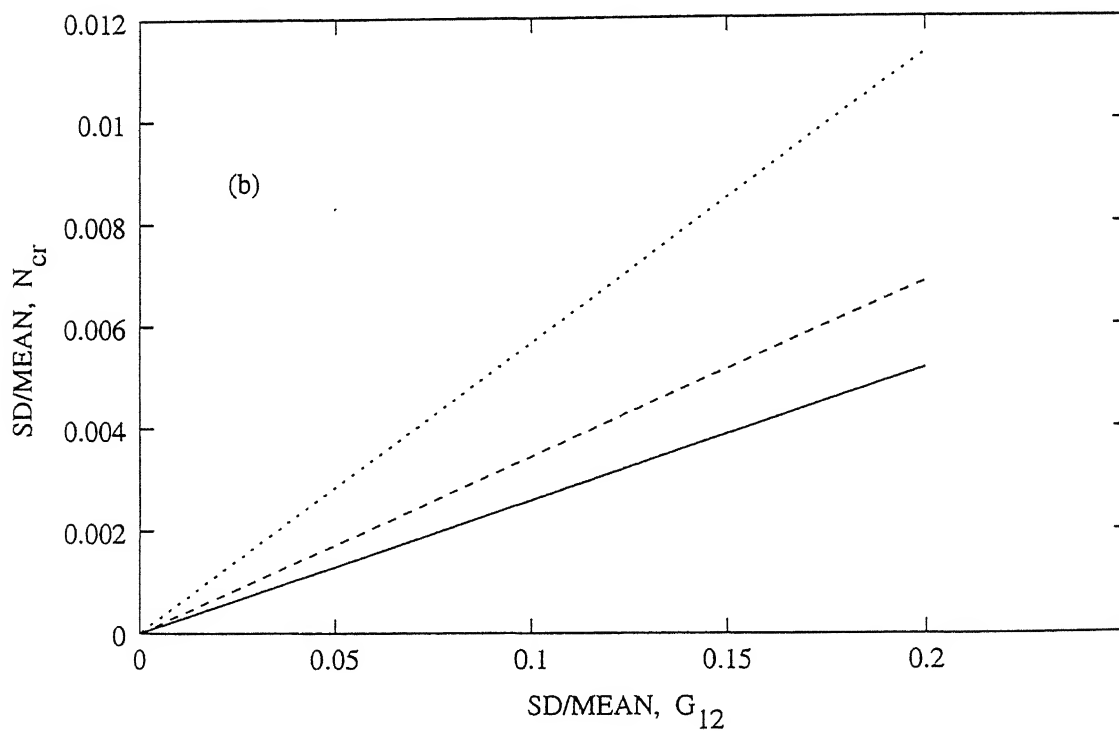
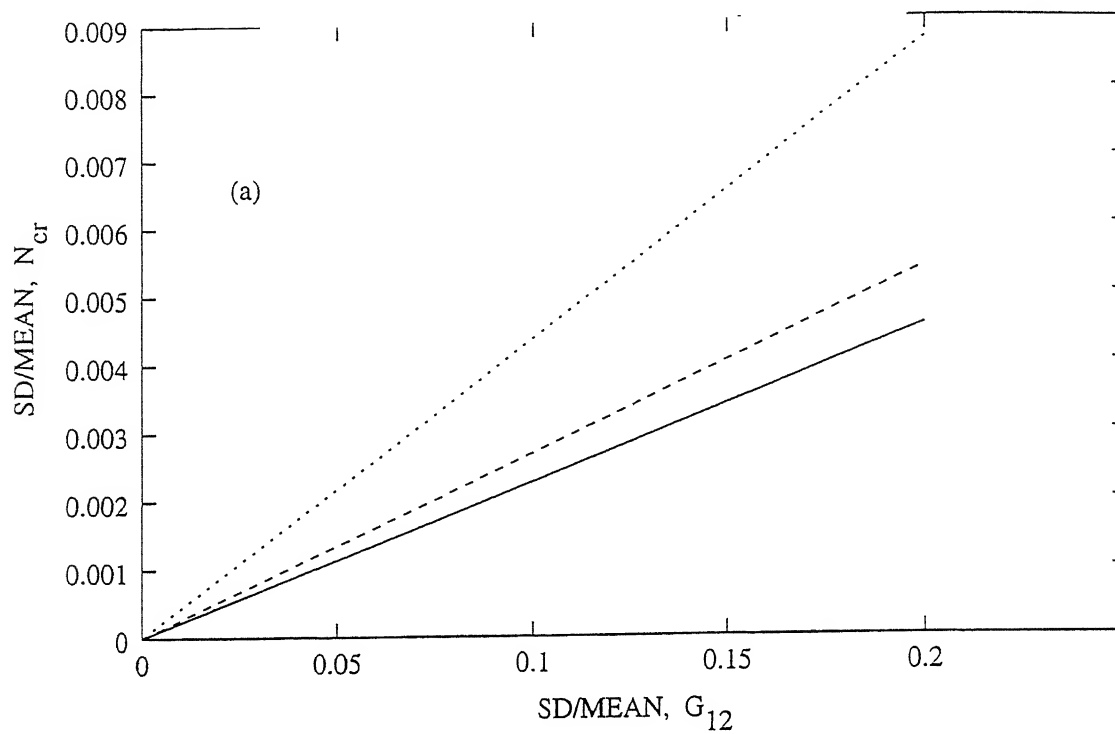


Figure 4.42: Variation of SD/mean of the nondimensionalised buckling load of a $[45^\circ / -45^\circ / 45^\circ / -45^\circ]$ square spherical laminate with SD of G_{12} .

Key: As in Figure 4.39.

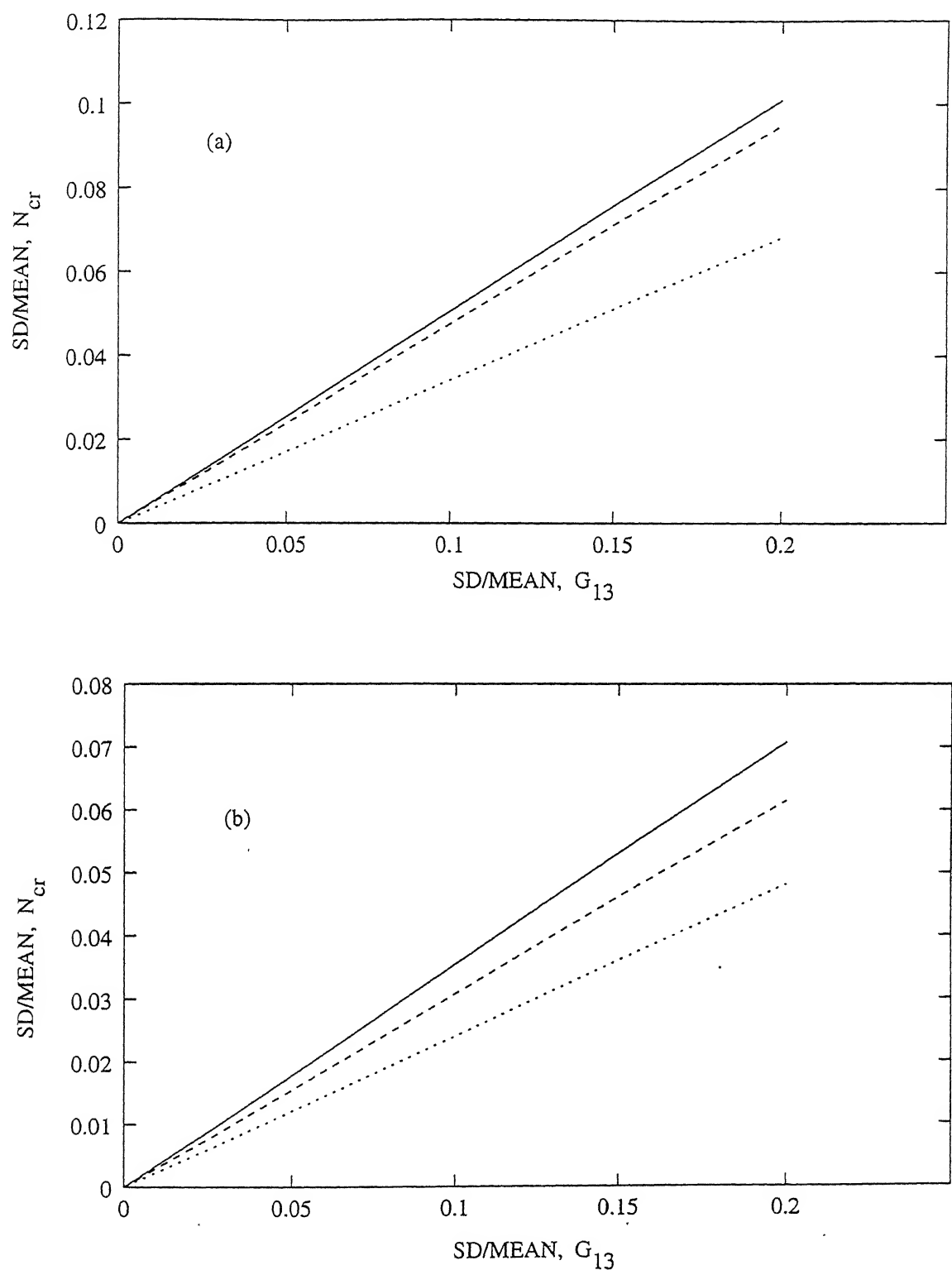


Figure 4.43: Variation of SD/mean of the nondimensionalised buckling load of a $[45^\circ / -45^\circ / 45^\circ / -45^\circ]$ square spherical laminate with SD of G_{13} .
Key: As in Figure 4.39.

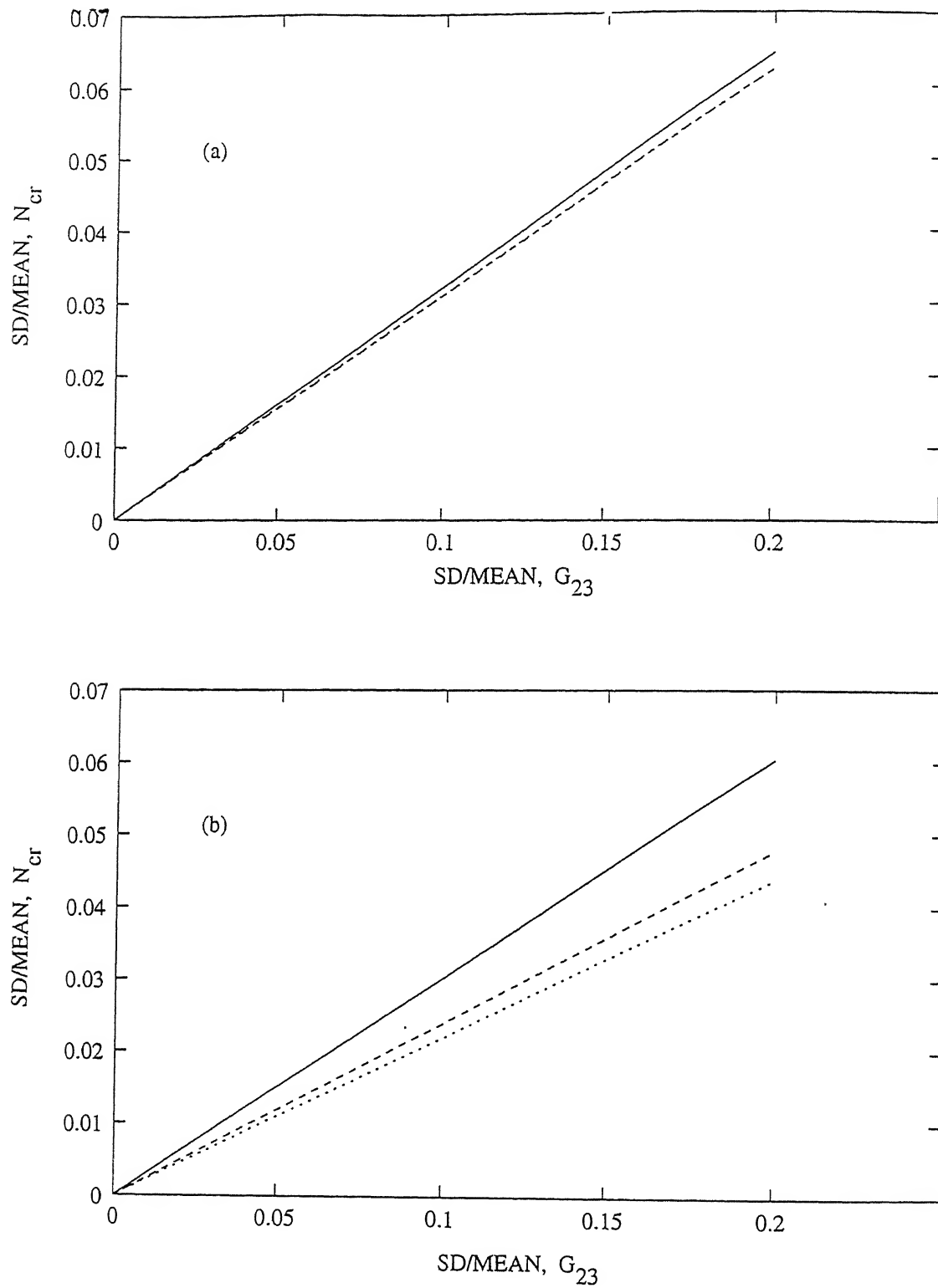


Figure 4.44: Variation of SD/mean of the nondimensionalised buckling load of a $[45^\circ / -45^\circ / 45^\circ / -45^\circ]$ square spherical laminate with SD of G_{23} .

Key: As in Figure 4.39.

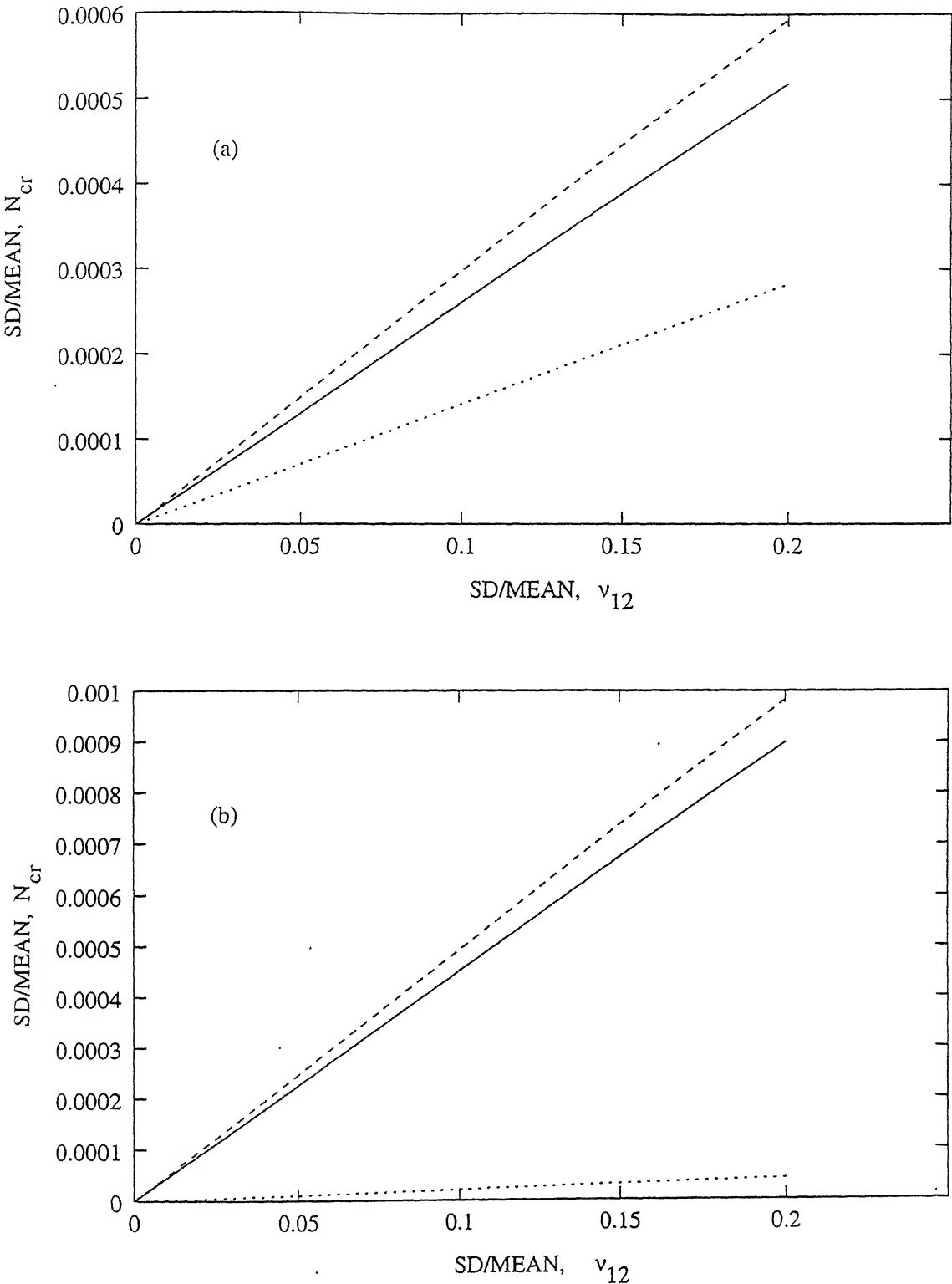


Figure 4.45: Variation of SD/mean of the nondimensionalised buckling load of a $[45^\circ / -45^\circ / 45^\circ / -45^\circ]$ square spherical laminate with SD of ν_{12} .
Key: As in Figure 4.39.

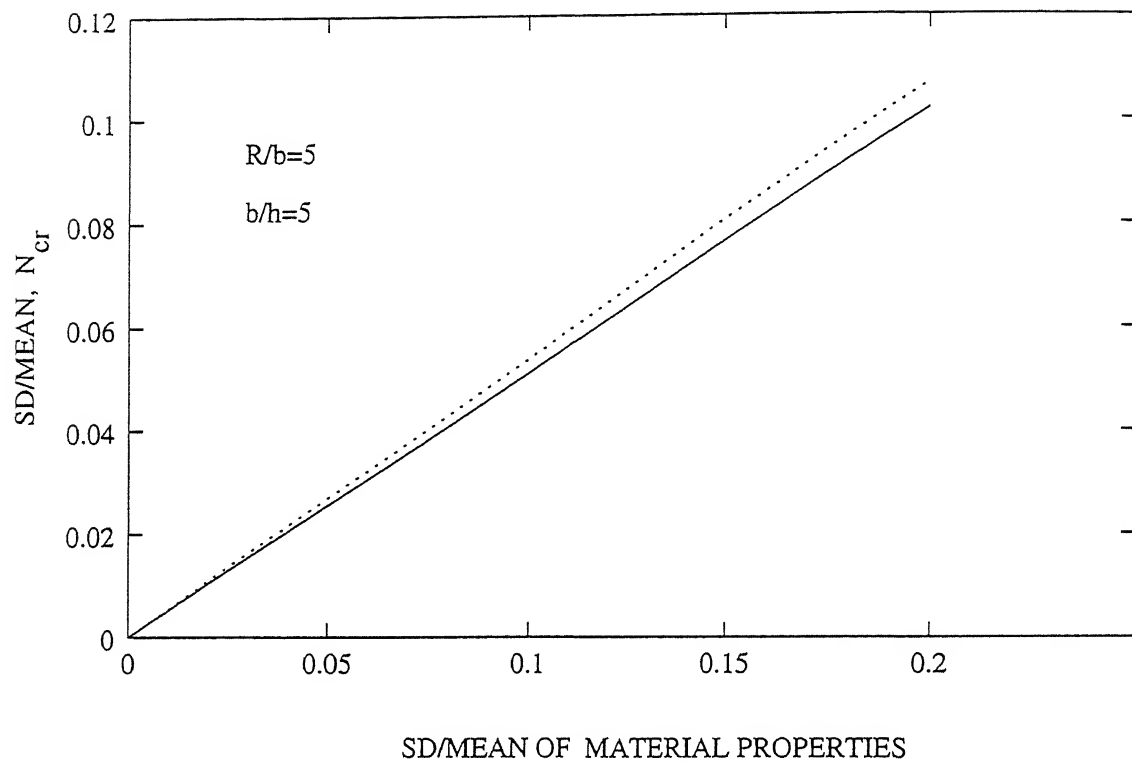


Figure 4.46: Comparison of a $[0^\circ/45^\circ/-45^\circ/90^\circ]$ spherical laminated panel buckling load scattering with a $[0^\circ/45^\circ/-45^\circ/90^\circ]$ cylindrical laminated panel with all basic properties changing simultaneously.

Key:- — :Spherical Panel, :Cylindrical Panel.

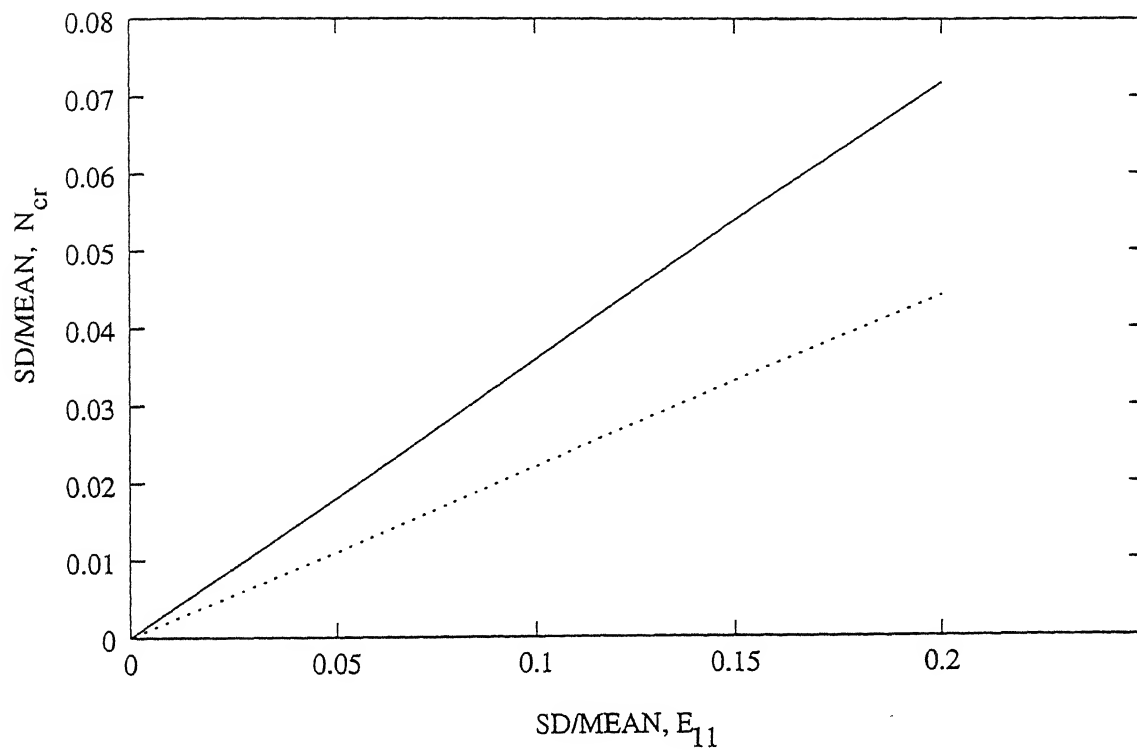


Figure 4.47: Comparison of a $[0^\circ/45^\circ/-45^\circ/90^\circ]$ spherical laminated panel buckling load scattering with a $[0^\circ/45^\circ/-45^\circ/90^\circ]$ cylindrical laminated panel with SD of E_{11} .

Key: As in Figure 4.46.

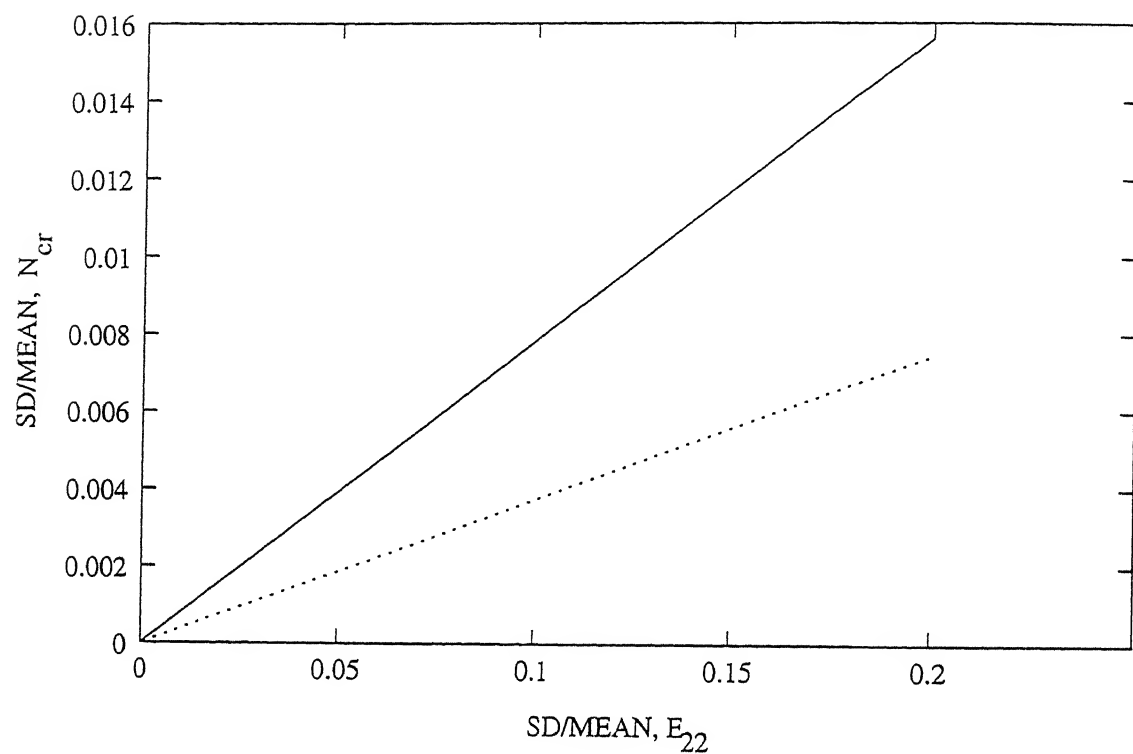


Figure 4.48: Comparison of a $[0^\circ/45^\circ/-45^\circ/90^\circ]$ spherical laminated panel buckling load scattering with a $[0^\circ/45^\circ/-45^\circ/90^\circ]$ cylindrical laminated panel with SD of E_{22} .

Key: As in Figure 4.46.

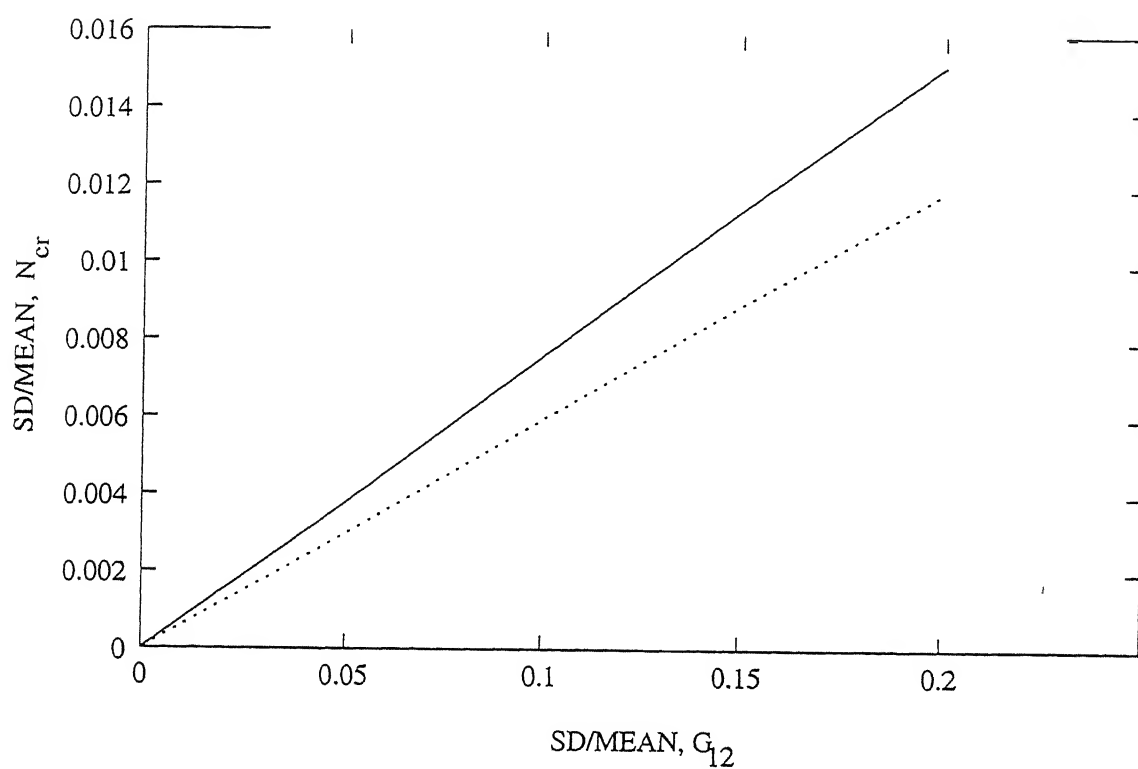


Figure 4.49: Comparison of a $[0^\circ/45^\circ/-45^\circ/90^\circ]$ spherical laminated panel buckling load scattering with a $[0^\circ/45^\circ/-45^\circ/90^\circ]$ cylindrical laminated panel with SD of G_{12} .
Key: As in Figure 4.46.

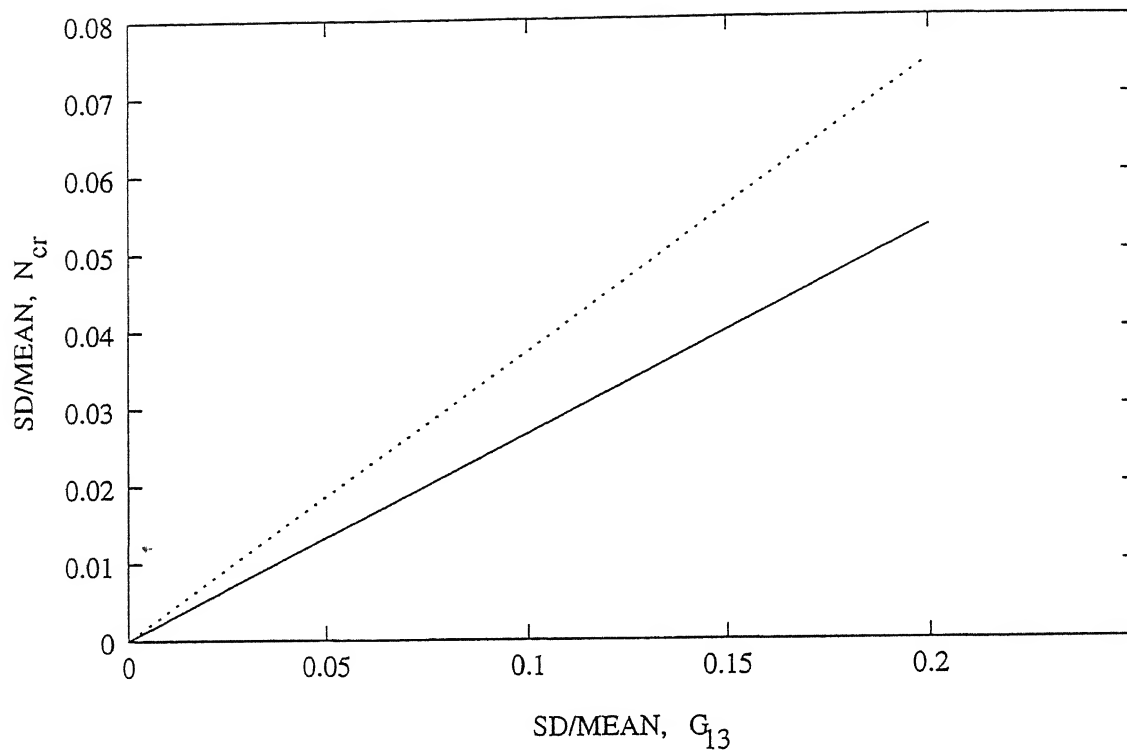


Figure 4.50: Comparison of a $[0^\circ/45^\circ/-45^\circ/90^\circ]$ spherical laminated panel buckling load scattering with a $[0^\circ/45^\circ/-45^\circ/90^\circ]$ cylindrical laminated panel with SD of G_{13} .

Key: As in Figure 4.46.

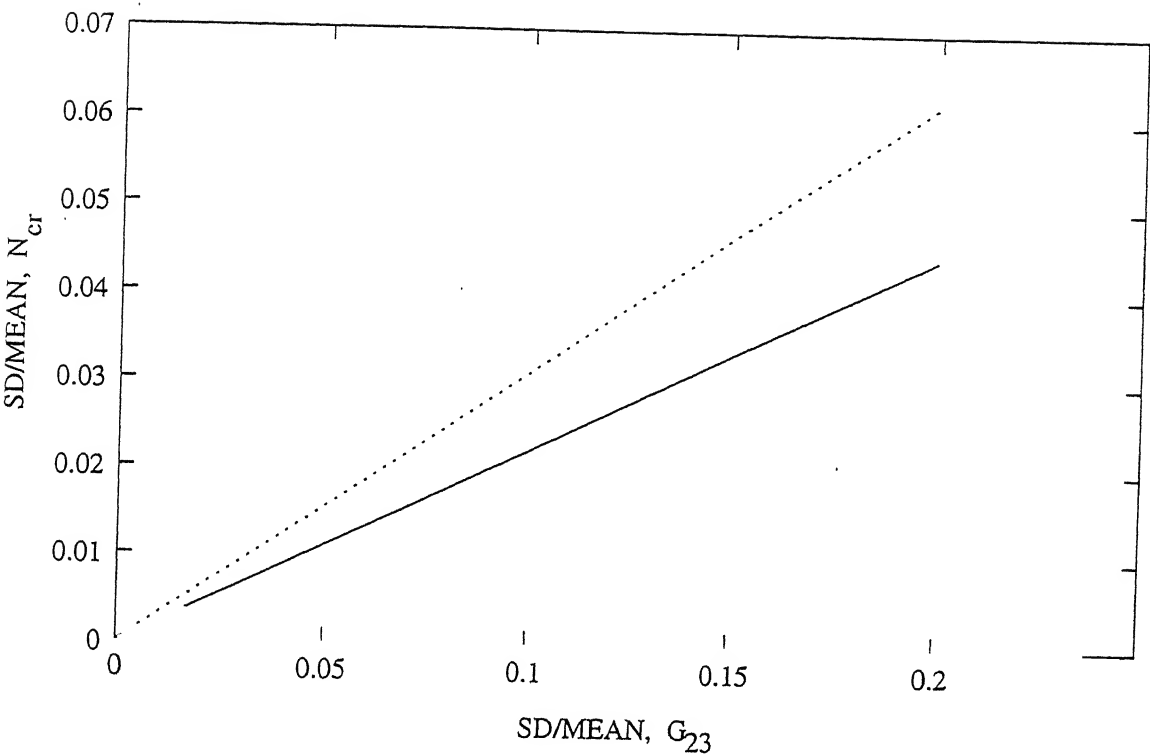


Figure 4.51: Comparison of a $[0^\circ/45^\circ/-45^\circ/90^\circ]$ spherical laminated panel buckling load scattering with a $[0^\circ/45^\circ/-45^\circ/90^\circ]$ cylindrical laminated panel with SD of G_{23} .
Key: As in Figure 4.46.

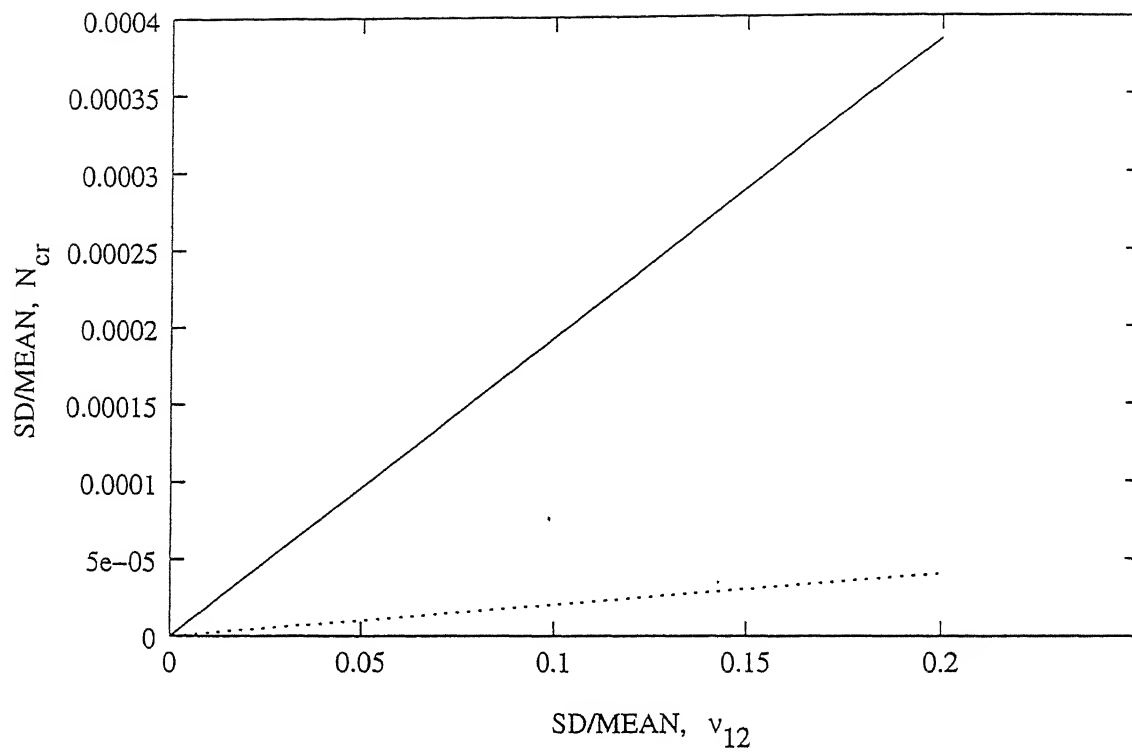


Figure 4.52: Comparison of a $[0^\circ/45^\circ/-45^\circ/90^\circ]$ spherical laminated panel buckling load scattering with a $[0^\circ/45^\circ/-45^\circ/90^\circ]$ cylindrical laminated panel with SD of ν_{12} .

Key: As in Figure 4.46.

CHAPTER V

FREE VIBRATION OF COMPOSITE PANELS

5.1 Introduction

Most structures, irrespective of their place of use, are subjected to dynamic loads during their operational life. The aim of the designer is to control undesirable vibrations, otherwise it may eventually lead to the failure of the structures due to fatigue. To achieve this, it is necessary to have a thorough understanding of the dynamic response of the structures.

Composite materials are finding extensive applications in primary and secondary structures in aeronautical and space projects, like advanced aircrafts, helicopters, launch vehicles, satellite, space stations etc. As stated earlier in *Chapter I*, the composite laminates do exhibit random material properties. It is important to point out that computer simulation of some of the proposed configurations of aeronautical and large outer-space installations often show closely packed/overlapping natural frequencies of some of the components. In such cases, even a slightest shift in characteristics of the components can have pronounced effects on the response of the structures and it becomes imperative to model the material properties as random.

In this chapter, a probabilistic solution procedure based on the classical approach and finite element method in conjunction with first order perturbation technique is presented for free vibration analysis of composite laminates, cylindrical and spherical panels with random material properties. The shear deformation and rotatory inertia effects have been incorporated for deriving the equation governing the random eigen value problem. Second order statistics for natural frequencies of the panel with known second order statistics of material properties have been obtained for different panel curvature to side ratios (R/a) and side to thickness ratios (a/h) for different boundary conditions.

5.2 Stochastic Classical Approach (SCA)

The Navier and Levy type solutions are possible for cross-ply composite panels with certain boundary conditions. When these solutions are combined with the probabilistic method, it is possible to analyze the random generalized eigen value problem associated with free vibration of composite laminated panels with random material properties. A detailed study is presented in this section to obtain the second moments of the natural frequencies of laminated composite plates, cylindrical and spherical panels using SCA.

5.2.1 Formulation

The free vibration equation is obtained by setting the in-plane loads and excitation terms to zero in the governing Equation (3.34).

The solution technique changes with the edge support conditions of the panel. For all edges simply supported, Navier type exact solution is possible for cross-ply panels. When two opposite edges are simply supported while the other two side edges have a combination of free, fixed and simple support, a Levy type closed form solution is possible in conjunction

with state-space approach. Detailed sequence of steps is outlined below for such problems to obtain the second order statistics of the natural frequencies and mode shapes.

For combinations of edge support conditions that are not amenable to exact solution, the generalized eigen value solution can be obtained by using series representation, approximate energy and variational methods, finite element method and other numerical techniques. It may be noted that the steps required for computing the statistics of the natural frequencies and mode shapes remain the same as presented below for the exact solutions.

5.2.1.1 Navier Type Solution

The displacements are expressed in the following form for all edges simply supported cross-ply panels vibrating in its principal mode

$$\begin{aligned}
 u &= \sum_{m,n=1}^{\infty} U_{mn} f_1(x_1, x_2) \exp(i\omega^* t); & v &= \sum_{m,n=1}^{\infty} V_{mn} f_2(x_1, x_2) \exp(i\omega^* t); \\
 w &= \sum_{m,n=1}^{\infty} W_{mn} f_3(x_1, x_2) \exp(i\omega^* t); & \phi_1 &= \sum_{m,n=1}^{\infty} \phi_{mn}^{(1)} f_1(x_1, x_2) \exp(i\omega^* t); \\
 \phi_2 &= \sum_{m,n=1}^{\infty} \phi_{mn}^{(2)} f_2(x_1, x_2) \exp(i\omega^* t),
 \end{aligned} \tag{5.1}$$

where $i = \sqrt{-1}$ and

$$\begin{aligned}
 f_1(x_1, x_2) &= \cos \alpha x_1 \sin \beta x_2; & f_2(x_1, x_2) &= \sin \alpha x_1 \cos \beta x_2; \\
 f_3(x_1, x_2) &= \sin \alpha x_1 \sin \beta x_2; & \alpha &= m\pi / a; \quad \beta = n\pi / b.
 \end{aligned} \tag{5.2}$$

Substitution of Equation (5.1) into Equation (3.34) results in an exact solution, which can be arranged as a generalized eigen value problem form as

$$\mathbf{K}\Delta = \lambda \mathbf{M}\Delta \quad m, n = 1, 2, \dots, \infty \tag{5.3}$$

where $\Delta = [U_{mn} \ V_{mn} \ W_{mn} \ \phi_{mn}^{(1)} \ \phi_{mn}^{(2)}]^T$, \mathbf{K} and \mathbf{M} are real symmetric stiffness and inertia matrices, and $\lambda = \omega^{*2}$, ω^* is the frequency of natural vibration in radians.

5.2.1.2 Levy Type Solution

The state-space concept [102, 103] is used to analyze the free vibration problem of cross-ply panels. The edges $x_2=0$ and $x_2 = b$ are assumed to be simply supported, while the remaining ones $x_1=0$ and $x_1 = a$ may have any arbitrary combination of free, clamped, and simply supported edge conditions. The generalized displacements are expressed as products of undetermined functions and known trigonometric functions which satisfy identically the simply supported boundary conditions at $x_2=0$ and $x_2 = b$: given by

$$u = w = \phi_1 = N_2 = M_2 = P_2 = 0.$$

The system is assumed to vibrate in its principal mode. The displacement quantities may be expressed as

$$\begin{aligned} u &= U_m(x_1) f_1(x_2) \exp(i\omega^* t); & v &= V_m(x_1) f_2(x_2) \exp(i\omega^* t); \\ w &= W_m(x_1) f_3(x_2) \exp(i\omega^* t); & \phi_1 &= X_m(x_1) f_1(x_2) \exp(i\omega^* t); \\ \phi_2 &= Y_m(x_1) f_2(x_2) \exp(i\omega^* t), \end{aligned} \quad (5.4)$$

where

$$f_1(x_2) = \sin \beta x_2; \quad f_2(x_2) = \cos \beta x_2; \quad f_3(x_2) = \sin \beta x_2; \quad \beta = n\pi/b, \quad (5.5)$$

Substitution of Equations (5.4) in Equations (3.34) results in equations dependent on only spatial coordinates. These are put in the state-space form by introducing the following variables.

$$\begin{aligned} Z_1 &= U_m; \quad Z_2 = U'_m; \quad Z_3 = V_m; \quad Z_4 = V'_m; \quad Z_5 = W_m; \quad Z_6 = W'_m; \quad Z_7 = W''_m; \\ Z_8 &= W'''_m; \quad Z_9 = X_m; \quad Z_{10} = X'_m; \quad Z_{11} = Y_m; \quad Z_{12} = Y'_m, \end{aligned} \quad (5.6)$$

where primes over the variables indicate differentiation with respect to x_1 . The system equation takes the form

$$\mathbf{Z}' = \mathbf{A} \mathbf{Z}; \quad (5.7)$$

in which matrix \mathbf{A} depends on the system stiffness, rotatory inertia and wavelength parameters. Since the stiffness coefficients are random, the elements are also random.

Solution to Equation (5.7) can be written as [102, 103]

$$\mathbf{Z}(x_1) = e^{\mathbf{A}x_1} \Delta \quad (5.8)$$

where Δ is a constant column vector associated with the boundary conditions and $e^{\mathbf{A}x_1}$ is given by

$$e^{\mathbf{A}x_1} = \mathbf{S} \begin{bmatrix} e^{\lambda_1 x_1} & & 0 \\ & \ddots & \\ 0 & & e^{\lambda_n x_1} \end{bmatrix} \mathbf{S}^{-1} \quad (5.9)$$

The value of n is 12 for the present formulation. Here λ_i denote the eigenvalues of \mathbf{A} and \mathbf{S} the modal column matrix of eigen vectors of \mathbf{A} .

Boundary Conditions

The boundary conditions for simply supported (S), clamped (C), and free (F) along the edges $x_1=0$ and $x_1=a$ are

$$\begin{aligned} \text{S:} \quad & v = w = \phi_2 = N_1 = M_1 = P_1 = 0; \\ \text{C:} \quad & u = v = w = \frac{\partial w}{\partial x_1} = \phi_1 = \phi_2 = 0; \\ \text{F:} \quad & N_1 = N_6 = M_1 = P_1 = (M_6 - \frac{4}{3h^2} P_6) = [Q_1 - \frac{4}{h^2} R_1 + \frac{4}{3h^2} (\frac{\partial P_1}{\partial x_1} + \frac{\partial P_6}{\partial x_2})] = 0. \end{aligned} \quad (5.10)$$

Eigen Value Problem

Substitution of Equation (5.8) into the boundary conditions associated with the remaining two opposite edges $x_1=0$ and $x_1=a$, results in a homogeneous system of equations which can be rearranged into a generalized eigen value problem form as

$$\mathbf{K}\Delta = \lambda\mathbf{M}\Delta; \quad (5.11)$$

where \mathbf{K} and \mathbf{M} are the stiffness and inertia matrices, and Δ is the mode shape and $\lambda = \omega^{*2}$ with ω^* as the frequency of natural vibration.

The stiffness matrix \mathbf{K} is random in nature, being dependent on the system material properties. Therefore, the eigen values λ and natural frequency ω^* are also random. Consequently eigen vectors and the associated displacement shape functions are also random. The solution approach being outlined below attempts to obtain the statistics of these characteristics.

5.2.2 Probabilistic Analysis: A Perturbation Technique

Without any loss of generality, as stated in Section 4.2.2, the random variables may be written as the sum of a mean and a zero mean random part (refer Equation 4.44).

$$\lambda_i = \bar{\lambda}_i + \lambda_i^r; \quad \Delta_i = \bar{\Delta}_i + \Delta_i^r \quad \mathbf{K} = \bar{\mathbf{K}} + \mathbf{K}^r \quad (5.12)$$

$$\text{where } \bar{\lambda}_i = \bar{\omega}^{*2}; \quad \lambda_i^r = 2\bar{\omega}^* \omega_i^{*r} + \omega_i^{*r2}, \quad i=1, 2, \dots, n. \quad (5.13)$$

The study is restricted to a class of problems where the random variation is small as compared with the mean of the material properties. This is true of the materials used in engineering applications including composites. Further, it is quite logical to assume that the dispersion in derived quantities like λ , ω^* , Δ and \mathbf{K} are also small as compared to their mean values.

Substituting Equation (5.12) into Equation (5.11), expanding and collecting same order of magnitude terms for i th eigenvalue, one obtains for zero and first order terms:

$$\bar{\mathbf{K}}\bar{\Delta}_i = \bar{\lambda}_i\bar{\mathbf{M}}\bar{\Delta}_i; \quad (5.14)$$

$$(\bar{\mathbf{K}} - \bar{\lambda}_i\bar{\mathbf{M}})\Delta_i^r = -(\mathbf{K}^r - \lambda_i^r\bar{\mathbf{M}})\bar{\Delta}_i. \quad (5.15)$$

Equation (5.14) is a deterministic equation relating the mean quantities and is the same as obtained for the deterministic analysis. The mean eigen values and corresponding mean eigen vectors can be determined by any standard conventional eigen solution procedures [102].

For the all-distinct eigen values, the normalized eigen vectors satisfy the orthogonality conditions [120]

$$\begin{aligned}\bar{\Delta}_i^T \mathbf{M} \bar{\Delta}_j &= \delta_{ij}; \\ \bar{\Delta}_i^T \mathbf{K} \bar{\Delta}_j &= \delta_{ij} \bar{\lambda}_i, \quad i, j = 1, 2, \dots, n\end{aligned}\tag{5.16}$$

where δ_{ij} is the Kronecker delta.

The mean eigenvectors form a complete orthonormal set and any vector in the space can be expressed as their linear combinations. Hence, the i th random part of the eigenvectors can be written as [102, 119]

$$\Delta_i^r = \sum_{j=1}^n C_{ij}^r \bar{\Delta}_j, \quad j \neq i; \quad C_{ii}^r = 0, \tag{5.17}$$

where, C_{ij}^r 's are small random coefficients yet to be determined.

Substituting Equation (5.17) in Equation (5.15), pre-multiplying by $\bar{\Delta}_i^T$ and $\bar{\Delta}_k^T$ ($k \neq i$), respectively and invoking the orthogonality conditions given in Equation (5.16), one gets [119]

$$\lambda_i^r = \bar{\Delta}_i^T \mathbf{K}^r \bar{\Delta}_i; \tag{5.18}$$

$$\Delta_i^r = \sum_{j=1}^n \bar{\Delta}_j \frac{\bar{\Delta}_j^T \mathbf{K}^r \bar{\Delta}_i}{\bar{\lambda}_i - \bar{\lambda}_j}, \quad j \neq i. \tag{5.19}$$

In the case of repeated eigenvalues obtain from Equation (5.14), the eigenvectors are not unique and to obtain the orthogonality conditions in Equation (5.16) the following modification is required.

For the l multiple eigen values $\bar{\lambda}_i$, λ_i^r is determined by [48]

$$\mathbf{D}\eta - \lambda_i^r \mathbf{C}\eta = 0, \quad (5.20)$$

where \mathbf{D} and \mathbf{C} are the matrices with elements

$$d_{kj} = \bar{g}_k^T K^r \bar{g}_j, \quad c_{kk} = \bar{g}_k^T M \bar{g}_k, \quad c_{kj} = 0, \quad k \neq j, \quad (5.21)$$

where \bar{g}_k , $k = 1, 2, \dots, l$ are eigenvectors corresponding to $\bar{\lambda}_i$. From the expression

$$\bar{\Delta}_i = \sum_{j=1}^m \eta_i^j \bar{g}_j, \quad i = 1, 2, \dots, l \quad (5.22)$$

one gets the l eigenvectors $\bar{\Delta}_i$, $i = 1, 2, \dots, l$ that are orthogonal to each other as well as the other eigenvectors and Δ_k^r can be expressed by

$$\begin{aligned} \Delta_k^r &= \sum_{j=1}^n \bar{\Delta}_j \frac{\bar{\Delta}_j^T \mathbf{K}^r \bar{\Delta}_k}{\bar{\lambda}_k - \bar{\lambda}_j}, \quad k = i, i+1, \dots, i+l-1, \quad j = 1, \dots, i+1, \dots, n \\ &= 0, \quad k, j = i, i+1, \dots, i+l-1, \quad k \neq j \end{aligned} \quad (5.23)$$

For the present case λ , ω^* , Δ and K are random because of the material properties, as stated earlier, are random. Let b_1, b_2, \dots, b_m denote the random material properties. The b_j 's can be expressed as (refer Equation 4.52)

$$b_j = \bar{b}_j + b_j^r \quad (5.24)$$

According to first order Taylor's rule, when b_j^r are small compared with their mean values, we can expand the dependent quantities λ , Δ and K about their mean values, giving their random parts as (refer Equation 4.53)

$$\lambda_i^r = \sum_{j=1}^m \bar{\lambda}_{i,j} b_j^r; \quad \Delta_i^r = \sum_{j=1}^m \bar{\Delta}_{i,j} b_j^r; \quad \mathbf{K}_i^r = \sum_{j=1}^m \bar{\mathbf{K}}_{i,j} b_j^r, \quad (5.25)$$

For the distinct eigen value systems, we have [119]

$$\bar{\lambda}_{i,j} = \bar{\Delta}_i^T \bar{\mathbf{K}}_{i,j} \bar{\Delta}_i \quad (5.26)$$

$$\bar{\Delta}_{i,j} = \sum_{s=1}^n \bar{\Delta}_s \frac{\bar{\Delta}_s^T \bar{\mathbf{K}}_{i,j} \bar{\Delta}_i}{\bar{\lambda}_i - \bar{\lambda}_s} \quad (5.27)$$

For the multiple eigen values, $\bar{\lambda}_{i,j}$ satisfies the following relation

$$\mathbf{A}\eta - \bar{\lambda}_{i,j} \mathbf{C}\eta = 0, \quad (5.28)$$

where \mathbf{C} is the same matrix as in Equation (5.20). The elements of \mathbf{A} are

$$A_{rs} = \bar{g}_r^T \bar{K}_j \bar{g}_s, \quad r, s = 1, 2, \dots, l. \quad (5.29)$$

and

$$\bar{\Delta}_{i,j} = \sum_{s=1}^n \bar{\Delta}_s \frac{\bar{\Delta}_s^T \bar{K}_j \bar{\Delta}_i}{\bar{\lambda}_i - \bar{\lambda}_s}, \quad s \neq i, i+1, \dots, i+l-1. \quad (5.30)$$

Using above first and second parts of Equation (5.25), the eigen value and mode shape covariance are obtained as (refer Equation 4.55)

$$Var(\lambda_i) = \sum_{j=1}^m \sum_{k=1}^m \bar{\lambda}_{i,j} \bar{\lambda}_{i,k} Cov(b_j, b_k); \quad Var(\Delta_i \Delta_i^{*T}) = \sum_{j=1}^m \sum_{k=1}^m \bar{\Delta}_{i,j} \bar{\Delta}_{i,k} Cov(b_j, b_k); \quad (5.31)$$

The variances of λ_i and Δ_i can be evaluated from Equation (5.31) with the help of Equations (5.26), (5.27), (5.29) and (5.30).

5.2.3 Results and Discussion

The second order statistics of the first five natural frequencies for composite panels have been obtained using HSDT. The lamina material properties E_{11} , E_{22} , G_{12} , G_{13} , G_{23} and ν_{12} are modeled as basic RVs. E_{11} and E_{22} are the longitudinal and transverse elastic moduli, respectively. G_{12} is the inplane shear modulus, G_{13} and G_{23} are the out of plane shear moduli and ν_{12} is the Poisson ratio. The lamina stacking sequences of $[0^0/90^0]$ and $[0^0/90^0/90^0/0^0]$ have been used for numerical computations.

The following two sets of numerical values and relationships between the mean values of the material properties for graphite/epoxy composite have been used for the computation:

Material -1: $E_{11} = 25E_{22}, G_{12} = G_{13} = 0.5E_{22}, G_{23} = 0.2E_{22}, \nu_{12} = 0.25, \rho = 1$

Material-2: $E_{11} = 40E_{22}, G_{12} = G_{13} = 0.6E_{22}, G_{23} = 0.5E_{22}, \nu_{12} = 0.25, \rho = 1$

The shear correction factors are taken as $5/6$.

The influence of the scattering in the material properties on natural frequency has been obtained by allowing the ratio of the SD (σ) to mean (μ) to vary from 0% to 20% [51] for laminated cross-ply panels. The transverse shear and rotatory inertia effects have been accounted for in the study as detailed in the formulation. The mean natural frequencies have been nondimensionalized as $\bar{\omega} = (\bar{\omega}^* a^2 \sqrt{\rho/E_{22}})/h$. While, the variances of the square of the nondimensionalised natural frequency have been normalized with the corresponding mean values. The proposed approach has been validated by comparison with an independent Monte Carlo simulation results.

5.2.3.1 Composite Plates

Validation

Figure 5.1 shows the results obtained from the perturbation approach and Monte Carlo simulation for $[0^0/90^0/90^0/0^0]$ laminated square plate with all edges simply supported with $a/h=10$ for Material -1. The number of samples used for the simulation is 15000. This number has been arrived at on the basis of satisfactory convergence of the second moments. It is observed that the perturbation results are in good agreement with the MCS. The variation in the natural frequencies scatter is almost linear with the scatter in the material property. The variances of the natural frequencies obtained using both the approaches vary linearly with SD of the material property. Therefore, it can be concluded that the first order perturbation technique is capable of capturing the complete behavior of the variation of the fundamental frequency. This is important as terms up to first order only has been considered in Taylor's

series expansion making the response dispersion a linear function of SD of material property. However, no such restriction regarding linearity was put in case of MCS approach. The difference in the nature of the two approaches is indicated by the deviations seen for the higher value of σ/μ for E_{11} particularly in the third natural frequency.

Second Order Statistics

Results have been obtained for a square plate with $a/h=10$ and 100 . All edges simply supported have been assumed for the panel. To examine the effect of orthotropy, the Material -2 is also used for computations. To check efficacies of various theories, a comparison of the results with CLT, FSDT and HSDT models have been made.

Tables 5.1(a) and 5.1(b) list the first five nondimensionalised mean natural frequencies for a square laminate with $a/h = 10$ and 100 and for Material -1 and Material -2 for the two stacking sequences. The higher value of fundamental frequencies, as expected, is observed for symmetric as compared to anti-symmetric cross-ply laminate. However, this observation is not always true for higher frequencies. It depends on the mode of vibration, a/h and modular ratios. The mean values of the mode shapes, also evaluated as a part of the computation, have not been presented here. It is seen that the transverse oscillations are dominant over any other oscillations.

Figures 5.2(a) and 5.2(c) for Material -1 and Figures 5.2(b) and 5.2(d) for Material -2 show the variation of frequencies with SD of basic RVs changing simultaneously for $[0^0/90^0]$ laminate, with $a/h=10$ and 100 , respectively. It is observed that the scattering in fundamental frequency is maximum for $a/h=10$ and Material -2. In general, higher deviations are observed for Material -2 as compared to Material -1.

Sensitivity of frequency to changes in only one basic variable at a time for anti-symmetric laminate with $a/h=10$ is presented in Figures 5.3(a) to 5.3(f) for Material -1 and in

Figures 5.4(a) to 5.4(f) for Material -2. The individual variation of E_{11} , E_{22} , G_{12} and ν_{12} has dominant effect on the scattering of the fundamental frequency as compared to any other frequencies. E_{11} has the maximum effect on the lower natural frequencies. The two materials exhibit different sensitivities to the individual material properties.

Figures 5.5(a) to 5.5(f) and 5.6(a) to 5.6(f) show the plots for the Material-1 & 2 for $a/h=100$. Here also, it is observed that the fundamental natural frequency is most sensitive to E_{11} . The two materials show different effect to the change in thickness ratio. For the dominant material property E_{11} , the thinner plate shows larger variations in the normalized frequency.

Figures 5.7(a) and 5.7(c) for Material -1 and Figures 5.7(b) and 5.7(d) for Material -2 plot the sensitivity of frequencies with SD of all basic material properties changing simultaneously for $[0^0/90^0/90^0/0^0]$ laminate with $a/h=10$ and 100. These graphs show that the most sensitive natural frequencies to change in basic RVs for the two materials are different for the two thickness ratios. Most sensitive frequencies for $a/h=10$ is the fundamental frequency for the two materials while for $a/h=100$, Material -1, it is the third while for Material -2, the fourth frequency is most sensitive.

Figures 5.8(a) to 5.8(f) for Material -1 and Figures 5.9(a) to 5.9(f) for Material -2 show the sensitivity of frequencies to individual variation of basic material properties for symmetric laminate with $a/h=10$: It is observed that the fundamental frequency is more sensitive to Changes in E_{11} , G_{12} and ν_{12} for both the materials with E_{11} being the dominant material property. Material -1 indicates slightly greater sensitivity to material property changes except for E_{11} and G_{23} .

The corresponding behavior of the frequencies for the two materials are plotted in Figures 5.10(a) to 5.10(f) and 5.11(a) to 5.11(f) for $a/h=100$. Here also, it may be noted that the variation of E_{11} has dominant effect on all the frequencies.

Comparison of Plate Theories

The effect of classical laminate theory (CLT), first-order shear deformation theory (FSDT) and higher order shear deformation theory (HSDT) on the scatter in the natural frequencies has been brought out by computing the variation of the fundamental frequency with material property SD for each of these models. The results have been computed for $[0^0/90^0/90^0/0^0]$ square laminate with $a/h=10$ for Material-1.

Figure 5.12 shows the results for a case when SD of all the material properties are changing simultaneously. From these results, it is clear that the CLT over predicts the fundamental frequency as compared to HSDT and FSDT. The FSDT also over predicts the fundamental frequency as compared to HSDT. However, the deviations are less as compared with the case of CLT.

Figures 5.13(a) to 5.13(f) show the sensitivity of the fundamental frequency predicted by the three theories with variation of only one material property SD at a time, others being held deterministic. It is noted that the fundamental frequency computed using CLT over predicts as compared to FSDT and HSDT for individual variation of E_{11} , G_{12} and ν_{12} while, it gives values comparable to HSDT for E_{22} , G_{13} , and G_{23} . Further, it is also noted that the FSDT over predicts the fundamental frequency for individual variation of E_{11} and G_{13} and under predicts for G_{23} . It gives values close to HSDT for variation in E_{22} , G_{12} and ν_{12} . It can be concluded that the results obtained using HSDT are always better than that of FSDT and CLT.

Conclusions

The second order statistics of the first five natural frequencies have been obtained for the two stacking sequences of cross-ply laminates. The following conclusions are drawn from the results for graphite – epoxy laminated plates with all edges simply supported:

- The fundamental mean frequency for anti-symmetric cross-ply is always lower than symmetric cross-ply laminate. However, the relative values of the other natural frequencies depend on the a/h ratio, mode of vibration and modular ratio.
- The dispersions in the square of nondimensionalised natural frequency (ω^2) show linear variation with SD of the material properties.
- The influence of SD of natural frequencies shows different sensitivity to different material properties. The sensitivity changes with the laminate construction, mode of vibration, a/h ratios and the material. However, any pattern in the variation in the sensitivity is not apparent in the cases studied.
- Increase in thickness ratio of the plate results in reduction in the frequency scatter.
- The classical laminate theory over predicts the scatter in the fundamental frequency. Even for thin plates, the use of classical laminate theory may not be appropriate for study of scatter in the fundamental frequency.

5.2.3.2 Composite Cylindrical Panels

Validation

The results obtained for Material-1 by the perturbation approach have been compared with those obtained by MCS. Figure 5.14 shows the comparison of results for a $[0^0/90^0/90^0/0^0]$ square laminate with $R/a=5$ and $a/h=10$. Normal distribution of the properties has been assumed for MCS. The random numbers are generated with specified means and standard deviations for the material properties. The total number of samples used for simulation based on convergence, is 15000. For Figure 5.14 only E_{11} is taken as random while the other parameters are left as deterministic. The plot shows the linear variation of the normalized square of frequency (ω^2) for both the approaches studied. It is observed that with

increase in SD/mean of E_{11} , more deviation is seen between the third natural frequency given by two approaches as compared to other frequencies. It is further observed that the present approximation underestimates the frequencies for all the cases. In general, for the range of SD of input RVs considered, the results are close to MCS results particularly the fundamental frequency.

Mean and Variance

Stacking Sequence: $[0^0/90^0]$

The first five-nondimensionalised mean natural frequencies for Material-1 have been obtained from Equation (5.14). The corresponding normalized mode shapes have also been obtained. Results are presented in Table 5.2(a). It is observed that there is large difference in natural frequencies between first and second modes as against any other consecutive modes. It is also observed that there is considerable change in mean natural frequencies as a/h increases. The fundamental frequencies are lower for $R/a=10$ than for $R/a=5$ for $a/h=10$. From the examination of mode shapes, it is seen that the radial oscillations are dominant. The mode shapes also reveal that the circumferential displacements are significant.

The normalized SD of the square of the natural frequencies has been obtained for different SD of the basic material properties for Material-1. Figures 5.15(a) to 5.15(d) show the variation of the normalized SD of the first five natural frequencies to normalized SD of the material properties changing simultaneously. The ratio of SD/mean is assumed to be same for all RVs. Figures 5.16 (a) to 5.16(f), 5.17(a) to 5.17(f), 5.18(a) to 5.18(f) and 5.19(a) to 5.19(f) show the plots for the two ratios of side to thickness and curvature of the panel to side with SD of only one material property changing at a time, others being held constant. These graphs show a linear behavior. There is significant change in frequencies as a/h increases.

The effect of scattering in material properties is found to be sensitive to panel thickness ratio. It is observed that the fundamental and fifth natural frequencies are most affected by simultaneous change in the basic RVs for both the ratios of R/a considered for $a/h=10$ and 100 , respectively. For $a/h=10$, the effects of scattering in material properties are found to be insensitive to the R/a ratio. However, for $a/h=100$, the impact of variation in material properties except G_{12} is seen to be insensitive to R/a ratios considered. The effect of E_{11} on fundamental frequency is found to be strongest for $a/h=10$ while, the effect of G_{12} is found to be strongest for $a/h=100$ for the R/a ratios considered.

Stacking Sequence: $[0^0/90^0/90^0/0^0]$

The deterministic Equation (5.14) has been solved for different combinations of m and n and the first five mean natural frequencies and their mode shapes for Material-1 have been evaluated. The natural frequencies have been nondimensionalized and mode shapes have been normalized. Table 5.2(b) lists nondimensionalized natural frequencies and normalized mode shapes against a/h , R/a and axial and circumferential numbers m and n . It is seen that the fundamental frequency decrease as R/a increases for a given value of a/h . Like case 1 with stacking sequence $[0^0/90^0]$, there is significant change in the mean frequencies as a/h increases. The mode shapes reveal that the displacements other than radial and circumferential are insignificant. It also reveals that the radial displacements are dominant over other modes.

The normalized SD of the square of the first five natural frequencies is plotted in Figures 5.20 to 5.24 for the two ratios of a/h and R/a against normalized SD of the basic variables. Figures 5.20(a) to 5.20(d) represent the variations in the natural frequencies due to simultaneous change in all the basic variables. Figures 5.21(a) to 5.21(f), 5.22(a) to 5.22(f),

5.23(a) to 5.23(f) and 5.24(a) to 5.24(f) present the sensitivities of frequencies to change in only one basic variable at a time.

The panel natural frequencies are least affected with changes in R/a ratio for $a/h=10$ and 100. However, for $a/h=100$, results show some variation with scattering in G_{12} . The panel natural frequencies are very sensitive to the a/h ratios considered.

The fundamental frequency is most and fourth natural frequency is least affected by changes in all basic RVs at a time for $a/h=10$ for the two R/a ratios considered. However, for $a/h=100$ the fifth and the fourth natural frequencies are most affected for $R/a=5$ and 10, respectively and the fundamental frequency is least affected for all the R/a values considered.

The effects of E_{11} on fundamental and G_{13} on the fourth natural frequency are found to be the strongest for $a/h=10$. However, for $a/h=100$, the effects of E_{11} on the fifth and fourth frequencies are dominant for $R/a=5$ and 10, respectively and G_{12} on fundamental frequency for both the R/a considered.

Conclusions

An approach has been presented to evaluate the second order statistics of the first five natural frequencies for the two stacking sequences and Material-1 of composite panel. The following conclusions are drawn from the studies carried out for laminated graphite-epoxy cross-ply cylindrical panels with all edges simply supported:

- The mean fundamental frequency is higher for symmetric than for anti-symmetric cross-ply panels. However, for other modes, the relative values of the frequencies depend on the stacking sequence, R/a and a/h . The radial oscillations are dominant in the first five modes.

- The normalized SD of the square of the natural frequency changes linearly with SD of the material properties.
- The natural frequencies show different sensitivity to randomness in different basic material properties. The dominant material property depends on the laminate construction, mode of vibration, R/a and a/h .
- The natural frequencies show different sensitivity to a/h for a fixed ratio of curvature of panels to side (R/a). It is observed that there is significant change in frequencies as a/h ratio increases from 10 for a given value of R/a for the two stacking sequences considered.
- The natural frequencies also have different sensitivities to symmetric and anti-symmetric cross-ply stacking sequences.
- The natural frequencies are found to be insensitive to R/a for $a/h=10$ for the two stacking sequences considered.
- The frequencies are also found to be less affected by R/a for scattering in material properties except G_{12} for $a/h=100$ for the stacking sequences taken.
- The natural frequencies are more sensitive to symmetric as compared to anti-symmetric cross-ply laminates for simultaneous change in the basic RVs with the sensitivity being dependent on mode of vibration, a/h and R/a .
- The thin panels are more sensitive as compared to thick panels for variation in material properties.

5.2.3.3 Composite Spherical Panels

Validation

Validation of the present approach has been done on similar lines as in the case of laminates. The results for Material -1 obtained by the technique presented have been

compared with MCS. Figure 5.25 shows the comparison for a $[0^0/90^0/90^0/0^0]$ laminate with $R/a=5$, $a/b=1$, $a/h=10$ and only E_{11} is assumed as random, while other material properties being treated as deterministic for all edges simply supported (SSSS). The number of samples considered for simulation based on convergence is 15000. For the range of SD considered in the variable E_{11} the results from the present approach comes very close to MCS results. One can conclude that the FOPT adopted for the present analysis is sufficient to give accurate results for the level of variations considered in the basic random variables.

Second Order Moments: Anti-Symmetric Cross-Ply Laminate $[0^0/90^0]$

The outlined approach is validated by comparison with MCS results and then used to evaluate the second order statistics for the natural frequencies of two layers anti-symmetric cross-ply $[0^0/90^0]$ graphite-epoxy spherical panels for Material-1. The Levy type stochastic classical approach has been used for obtaining second moments of natural frequencies

The panel geometry used is $R/a=5$, $a/b=1$ and $a/h=10$. Results have been obtained for the mean and the variances of the natural frequencies and mode shapes for SSSS, SCSC, SSSC, SFSS, and SFSC boundary conditions..

Mean frequency

The mean values of the natural frequencies and mode shapes have been obtained as the solution of the deterministic eigen value problem expressed by Equation (5.14). Table 5.3 shows the first five nondimensionalised mean natural frequencies for the laminate with all edges simply supported (SSSS). The difference in mean natural frequencies between first and second modes is more as compared to any other consecutive modes.

To examine the effects of different support conditions on natural frequency, the mean values of the non –dimensionalised fundamental frequency for the laminate with SCSC,

SSSC, SFSS, and SFSC boundary conditions are presented in Table 5.4. The results show that the fundamental frequency for SCSC and SSSC are higher as compared to any other support conditions. It also shows that the fundamental frequency for SFSS and SFSC are small as compared to any other support conditions.

Frequency variance

The variances of the square of the non-dimensionalised natural frequencies have been obtained for different SD of the basic material properties. Figure 5.26 represents the variation of the normalized SD of the first five natural frequencies of the laminate to normalized SD of the material properties for all edges simply supported (SSSS) while Figures 5.27(a) to 5.27(f) show the plots with only one material property SD changing at a time, others being held constant at zero level. These graphs show that the change in the normalized SD of the square of natural frequency is linear with the change in the material property SD. The dispersion in first five natural frequencies shows close growth rates with simultaneous variations in the material properties. The effect of simultaneous changes in all basic RVs on the fundamental frequency is found to be more as compared to any other natural frequencies for the thickness ratio considered. The fundamental frequency shows higher sensitivity compared to the others with regard to the individual variation of E_{11} , G_{12} , E_{22} and ν_{12} . Amongst all the material properties the effect of E_{11} on natural frequencies is found to be the strongest.

Figure 5.28 shows the variation of the normalized SD of the non-dimensionalised fundamental frequency of the laminate to SD of the material properties changing simultaneously for SSSS, SCSC, SSSC, SFSS, and SFSC for Material-1. It is observed that the effect of simultaneous changes in the material properties on the fundamental frequency is maximum for SFSS and lowest for SSSS. SFSC lies in between SSSC and SCSC. However, these differences in dispersion are very small. It is further observed that almost equal

sensitivity is shown by the pairs SFSS with SFSC and SSSC with SCSC. Figures 5.29(a) to 5.29(f) show the variation of the fundamental frequency of the laminate with the change in only one material property at a time for SSSS, SCSC, SSSC, SFSS, and SFSC. From examination of the results, it is observed that the effect of E_{11} on dispersion in the fundamental frequency for SFSS and SFSC is the highest while, the dispersions for SSSS is lowest. It is also observed that the influence of G_{12} for SSSS is more as compared to any other support conditions considered in this study. The supports with free boundary condition are also more sensitive towards changes in E_{22} as compared to other boundary conditions. In general, the fundamental frequency is most affected with scatter in E_{11} and shows significant sensitivity with scatter in G_{12} , E_{22} and G_{13} for all support conditions considered. The fundamental frequency is least affected with the changes in ν_{12} . The SCSC and SSSC are more sensitive towards changes in G_{23} as compared to any other boundary conditions.

Conclusions

The second order statistics of the natural frequencies for spherical laminates with rectangular plan form and different edge support conditions has been obtained. The following conclusions can be drawn from the results for graphite-epoxy laminated cross-ply spherical panels-

- The SD of the square of the natural frequency changes linearly with SD of the material properties.
- The fundamental frequency is most affected with simultaneous changes in SD of the material properties as compared to subsequent four natural frequencies.
- For the SSSS laminate the effect of E_{11} is most dominant on dispersion in the natural frequencies and effect of ν_{12} is least dominant. Out of all the natural frequencies, the fundamental frequency is most sensitive to changes in E_{11} .

- The SFSS and SFSC are most sensitive while the SSSS are least sensitive against simultaneous changes in the material properties.
- The effect of dispersion in longitudinal elastic modulus, E_{11} on the scatter in the fundamental frequency is most important for all support conditions considered while, the effect of ν_{12} is least important.

5.3 Stochastic Finite Element Method (SFEM)

For combinations of edge supports that are not amenable to closed form solution, the solution of the problem can be attempted by using approaches like- series solutions, approximate energy and variational methods, finite element method and other numerical techniques. In this section, a stochastic finite element method is presented for free vibration studies of composite plates, cylindrical and spherical panels with random material properties. The lamina material properties are modeled as random variables. These are incorporated into finite element formulation, which results in a random eigenvalue problem. A mean centered first order perturbation technique is then used to find the probabilistic free vibration response. Second order moments of the fundamental frequency of composite panels have been evaluated for various combinations of geometrical parameters, stacking sequences and boundary conditions.

5.3.1 System Equations formulation

The free vibration problem of laminated composite panels has been formulated by employing the Hamilton's principle and solving the random eigen value problem arising due to randomness in material properties.

5.3.1.1 Strain Energy

The strain energy due to bending of a laminated composite panel is given by (refer Equation 3.35)

$$U = \frac{1}{2} \int_A \bar{\epsilon}^T \mathbf{D} \bar{\epsilon} dA; \quad (5.32)$$

For finite element analysis, this equation can be written as (Section 3.6 refer Equations 3.50, 3.52 and 3.53)

$$\begin{aligned} U &= \sum_{e=1}^{NE} U^{(e)} \\ &= \sum_{e=1}^{NE} \frac{1}{2} \int_{A^{(e)}} \bar{\epsilon}^T \mathbf{D} \bar{\epsilon} dA \end{aligned} \quad (5.33)$$

$$U^{(e)} = \frac{1}{2} \int_{A^{(e)}} \Lambda^{T(e)} \mathbf{B}^T \mathbf{D} \mathbf{B} \Lambda^{(e)} dA; \quad (5.34)$$

$$= \Lambda^{T(e)} \mathbf{K}^{(e)} \Lambda^{(e)}, \quad (5.35)$$

where $\Lambda^{(e)}$ and $\mathbf{K}^{(e)}$ are the element displacement vector and stiffness matrices respectively.

5.3.1.2 Kinetic Energy

The kinetic energy of a vibrating panel in bending is

$$T = \frac{1}{2} \int_A \left(\sum_{k=1}^{NL} \int_{\zeta_{k-1}}^{\zeta_k} \rho^{(k)} \dot{\mathbf{u}}^T \dot{\mathbf{u}} d\zeta \right) dA; \quad (5.36)$$

where \mathbf{u} is the global displacement vector and is given by (refer Equation 3.42)

$$\mathbf{u} = \{\bar{u} \ \bar{v} \ \bar{w}\} = \bar{\mathbf{N}} \Lambda \quad (5.37)$$

where $\bar{\mathbf{N}}$ and Λ are as defined in Equations (3.44) and (3.8), respectively.

Equation (5.36) can be rewritten as (refer Equation 3.45)

$$T = \frac{1}{2} \int_A \left(\sum_{k=1}^{NL} \int_{\zeta_{k-1}}^{\zeta_k} \rho^{(k)} \dot{\Lambda}^T \bar{\mathbf{N}}^T \bar{\mathbf{N}} \dot{\Lambda} d\zeta \right) dA = \frac{1}{2} \int_A \dot{\Lambda}^T \mathbf{m} \dot{\Lambda} dA; \quad (5.38)$$

where \mathbf{m} is the inertia matrix as defined in Equation (3.46)

$$\mathbf{m} = \sum_{k=1}^{NL} \int_{\zeta_{k-1}}^{\zeta_k} \rho^{(k)} \bar{\mathbf{N}}^T \bar{\mathbf{N}} d\zeta. \quad (5.39)$$

Simplifying this equation we get

$$\mathbf{m} = \begin{bmatrix} p & 0 & 0 & 0 & q_2 & 0 & q_1 \\ & p & 0 & q_2 & & q_1 & \\ & & p & 0 & 0 & 0 & 0 \\ & & & I_2 & 0 & I_3 & 0 \\ & & & & I_2 & 0 & I_3 \\ & & & & & I_1 & 0 \\ & & & & & & I_1 \end{bmatrix} \quad (5.40)$$

The inertia terms in Equation (5.40) are given by

$$(p, q_1, q_2, I_1, I_2, I_3) = \sum_{k=1}^{NL} \int_{\zeta_{k-1}}^{\zeta_k} \rho^{(k)} [1, f_1(\zeta), f_2(\zeta), f_1^2(\zeta), f_2^2(\zeta), f_1(\zeta) f_2(\zeta)] d\zeta \quad (5.41)$$

In terms of elemental values, the above equation may be written as

$$\mathbf{T} = \sum_{e=1}^{NE} \mathbf{T}^{(e)} \quad (5.42)$$

where,

$$\mathbf{T}^{(e)} = \frac{1}{2} \int_{A^{(e)}} \dot{\mathbf{\Lambda}}^{T(e)} \mathbf{m} \dot{\mathbf{\Lambda}}^{(e)} dA \quad (5.43)$$

Further, we have from Equation (3.47)

$$\mathbf{\Lambda} = \sum_{i=1}^{NN} \varphi_i \mathbf{\Lambda}_i \quad (5.44)$$

Substituting this in Equation (5.43), we get

$$\mathbf{T}^{(e)} = \frac{1}{2} \int_{A^{(e)}} \dot{\mathbf{\Lambda}}_i^{T(e)} \varphi^{T(e)} \mathbf{m} \varphi^{(e)} \dot{\mathbf{\Lambda}}_i^{(e)} dA \quad (5.45)$$

Equation (5.45) may be rewritten as

$$\mathbf{T}^{(e)} = \dot{\mathbf{q}}^{*T(e)} \mathbf{M}^{(e)} \dot{\mathbf{q}}^{*(e)} \quad (5.46)$$

where $\mathbf{M}^{(e)}$ is the element mass matrix.

$$\mathbf{M}^{(e)} = \frac{1}{2} \int_{A^{(e)}} \boldsymbol{\varphi}^{T(e)} \mathbf{m} \boldsymbol{\varphi}^{(e)} dA \quad (5.47)$$

5.3.1.3 Governing Equations

Using Variational principles, the governing equations for free vibration can be derived.. The Lagrange's equation for a conservative system can be written as [97, 120]

$$\frac{d}{dt}(\partial T / \partial \dot{q}_i^*) + \frac{\partial U}{\partial q_i^*} = 0; \quad \text{for } i=1, 2, \dots \quad (5.48)$$

Here q_i^* represent the generalized coordinates and \dot{q}_i^* denote the generalized velocities.

Substituting Equations (5.35) and (5.46) in Equation (5.48) yields

$$\mathbf{K} \mathbf{q}^* + \mathbf{M} \ddot{\mathbf{q}}^* = 0 \quad (5.49)$$

Assuming that the system vibrates in its principal mode, Equation (5.49) can be written as

$$(\mathbf{K} - \lambda \mathbf{M}) \mathbf{q}^* = 0 \quad (5.50)$$

where $\lambda = \omega^{*2}$ with ω^* as natural frequency of vibration and

$\mathbf{q}^* = \sum_{e=1}^{NE} \mathbf{q}^{*(e)}$ - Global displacement vector

$\mathbf{K} = \sum_{e=1}^{NE} \mathbf{K}^{(e)}$ - Global stiffness matrix

$\mathbf{M} = \sum_{e=1}^{NE} \mathbf{M}^{(e)}$ - Global inertia matrix

It is often desirable to solve a standard eigenvalue problem as opposed to a generalized eigenvalue problem because the behavior of a standard eigenvalue problem is much better understood. If \mathbf{M} is positive definite, it is always possible to transform Equation (5.50) into a standard eigenvalue problem [119].

$$\mathbf{A} \mathbf{q}^* = \lambda \mathbf{q}^*; \quad (5.51)$$

where

$$\mathbf{A} = \mathbf{M}^{-1} \mathbf{K} \quad (5.52)$$

Equation (5.51) is the characteristic equation for free vibration of the laminated composite panels.

In Equation (5.51) the elements of \mathbf{A} matrix are random because the material properties are random. Consequently, the natural frequencies and its mode shapes are also random.

Therefore, a straightforward solution, as in a deterministic case would not be possible. The method of solution of this random equation is presented in the next section.

5.3.2. Method of solution

The sequence of steps as given in *Chapter IV*, Sub section 4.3.2 for probabilistic analysis of random standard eigenvalue problem in case of initial buckling of composite panels would basically remain the same for the free vibration response of random standard eigenvalue problem. In this section, an approach based on left and right eigenvectors are suggested which is suitable for handling large size of stiffness matrix arising from the finite element analysis [119].

The random variables may be split up without any loss of generality (refer Equations 5.12 and 5.13)

$$b_i = \bar{b}_i + b_i^r; \quad \mathbf{A} = \bar{\mathbf{A}} + \mathbf{A}^r; \quad \lambda_j = \bar{\lambda}_j + \lambda_j^r; \quad \mathbf{q}_j^* = \bar{\mathbf{q}}_j^* + \mathbf{q}_j^{*r}; \quad \omega_j^* = \bar{\omega}_j^* + \omega_j^{*r} \quad (5.53)$$

Substituting Equation (5.53) into Equation (5.51) and keeping only terms up to first order, one obtain (refer Equations 4.47 and 4.48)

$$\text{Zeroth order: } \bar{\mathbf{A}} \bar{\mathbf{q}}_j^* = \bar{\lambda}_j \bar{\mathbf{q}}_j^*; \quad (5.54)$$

$$\text{First order: } \bar{\mathbf{A}} \mathbf{q}_j^{*r} + \mathbf{A}^r \bar{\mathbf{q}}_j^* = \bar{\lambda}_j \mathbf{q}_j^{*r} + \lambda_j^r \bar{\mathbf{q}}_j^* \quad (5.55)$$

In Equation (5.55) \mathbf{A}^r can be obtained from Equation (5.52) making use of Equation (5.53). Following the same procedure of separation of the first two equations, the expression for \mathbf{A}^r is given as

$$\mathbf{A}^r = \mathbf{M}^{-1} \mathbf{K}^r \quad (5.56)$$

The j th first order random vector can be written as (refer Equation 4.49)

$$\mathbf{q}_j^{*r} = \sum_{l=1}^N C_{lj}^r \bar{\mathbf{q}}_l^*, l \neq j; \quad C_{jj}^r = 0, \quad (5.57)$$

Substituting Equation (5.57) in the first order Equation (5.55), pre-multiplying the resultant expression by $\bar{\mathbf{q}}_j^T$ and making use of the orthogonality conditions [119], one gets

$$\lambda_j^r = \bar{\mathbf{q}}_j^T \mathbf{A}^r \bar{\mathbf{q}}_j^*; \quad (5.58)$$

where, the eigenvectors $\bar{\mathbf{q}}_j$ and $\bar{\mathbf{q}}_j^*$ are also known as the left and right eigenvectors of $\bar{\mathbf{A}}$, respectively.

The random variation is assumed to be very small as compared with the mean part of the material properties, which is the situation in most sensitive engineering applications, where composites are being used. It is, therefore, reasonable to assume that the dispersion in derived quantities like λ , ω , \mathbf{q}^* and \mathbf{A} are also small as compared to their mean values.

The random variables, λ , \mathbf{q}_j^* , \mathbf{q}_j and \mathbf{A} can be represented by Taylor's series expansion about \bar{b}_i , $i=1, 2, \dots, m$. Keeping only first order terms, the relation are (refer Equation 4.53)

$$\lambda_j^r = \sum_{i=1}^m \bar{\lambda}_{j,i} b_i^r; \quad \mathbf{q}_j^r = \sum_{i=1}^m \bar{\mathbf{q}}_{j,i} b_i^r; \quad \mathbf{q}_j^{*r} = \sum_{i=1}^m \bar{\mathbf{q}}_{j,i}^* b_i^r \quad \mathbf{A} = \sum_{i=1}^m \mathbf{A}_{,i} b_i^r, \quad (5.59)$$

where, $,i$ is the partial differentiation with respect to b_i evaluated at \bar{b}_i .

On substitution of Equation (5.59) into Equation (5.58) and comparing the coefficients of a basic random variable b_i^r , we get

$$\bar{\lambda}_{j,i} = \bar{\mathbf{q}}_j \mathbf{A}_{,i} \bar{\mathbf{q}}_j^* \quad (5.60)$$

The variance of the eigenvalue can now be written as (refer Equation 5.31) [111]

$$Var(\lambda_j) = \sum_{i=1}^m \sum_{k=1}^m \bar{\lambda}_{j,i} \bar{\lambda}_{j,k} Cov(b_i, b_k) \quad (5.61)$$

where $Cov(b_i, b_k)$ is the covariance between b_i and b_k .

5.3.3 Results and Discussion

Using the technique presented in the previous sections, second order statistics of the fundamental frequency of graphite-epoxy panels have been evaluated with different support conditions using HSDT. The material properties of the composite lamina have been modeled as basic random variables. A nine noded Langrangian isoparametric element, with 63 DOFs per element for the HSDT model has been used for discretizing laminated shallow panels of rectangular plan form. These elements are found to be quite stable. Results have been computed by employing the full (3×3) integration rule for thick panels and reduced (2×2) integration rule for thin panels. Based on convergence study conducted for the second order statistics of the fundamental frequency, a (5×5) mesh has been used throughout the study. The following non-dimensional mean fundamental frequency has been defined:

$$\bar{\omega} = (\bar{\omega}^* a^2 \sqrt{\rho / \bar{E}_{22}}) / h;$$

in which $\bar{\omega}^*$ is the dimensional mean fundamental frequency.

Various combinations of edge support conditions of clamped (C), free (F) and simple-supports (S) have been used for the investigation. The boundary conditions for the panel are, therefore,

Clamped edge: $u = v = w = \phi_1 = \phi_2 = \theta_1 = \theta_2 = 0;$

Free edge: $u \neq v \neq w \neq \phi_1 \neq \phi_2 \neq \theta_1 \neq \theta_2 \neq 0;$

Simply supported edge: $v = w = \theta_2 = \phi_2 = 0$ or $u = w = \theta_1 = \phi_1 = 0.$

The following mean material properties have been used in the present investigation:

$$\bar{E}_{11} = 25 \bar{E}_{22}, \bar{G}_{12} = \bar{G}_{13} = 0.5 \bar{E}_{22}, \bar{G}_{23} = 0.2 \bar{E}_{22}, \bar{\nu}_{12} = 0.25, \text{ and } \rho = 1.$$

This is the same as Material-1 of Section 5.2.3.

5.3.3.1 Composite Plates

Validation

Figure 5.30 shows the comparison of the probabilistic finite element results with MCS and that obtained from SCA for $[0^0/90^0/90^0/0^0]$ laminated square plate with all edges simply supported with $a/h=10$. Here also, the number of samples used for the MCS study is 15000. It is observed that the results are in overall good agreement with the MCS and SCA. However, the SFEM results show more difference with MCS in comparison to SCA. This may be due to the large numerical round off errors involved with SFEM. For the range of scatter in the materials considered, the square of the fundamental frequency varies linearly with material properties.

Table 5.5 shows the comparison of the nondimensionalised mean fundamental frequency obtained using SFEM and SCA for a square laminate with $a/h = 10$ and 100 for the two stacking sequences $[0^0/90^0]$ and $[0^0/90^0/90^0/0^0]$. The results are in good agreement.

Second Order Statistics

Second order statistics of fundamental frequency have been evaluated for a graphite-epoxy square plate with $a/h=5$ and 10 with CCCC, SSSS and CFCF boundary conditions. The stacking sequence considered for the study is $[0^0/45^0/-45^0/90^0]$.

Frequency expectation

Table 5.6 list the non-dimensional mean fundamental frequency ($\bar{\omega}$), for the laminated composite square plates for $a/h=5$ and 10 with CCCC, CFCF and SSSS boundary conditions. As expected, the CCCC panels give higher values as compared to others support conditions. The fundamental frequency increases as a/h ratio increases.

Frequency Variance

Figures 5.31 (a) and 5.31 (b) show the variation of square of the fundamental frequency of the square plate with SD of material properties varying simultaneously for $a/h=5$ and 10, respectively. From the examination of results, it is observed that for $a/h=5$, CCCC panel shows larger scatter in frequency as compared to SSSS and CFCF panels. The difference between CCCC and CFCF are small, while the difference is large between CCCC and SSSS panels. For $a/h=10$, the CCCC and CFCF panels show almost the same sensitivity. Other observations are similar to the panel of $a/h=5$. The sensitivity of panels changes as the a/h ratio changes. These changes are appreciable in the cases of CCCC and CFCF panels as compared to SSSS panel.

Figures 5.32(a) - 5.32(f) present the variation of normalized SD of square of the fundamental frequency (ω^2) for the square plate with SD of material property changing one at a time, other deterministic for $a/h=5$, while Figures 5.33(a)-5.33(f) plot for $a/h=10$ for different edge conditions.

For $a/h=5$, it may be noted that the CCCC panel is least affected with scatter in E_{11} , E_{22} , G_{12} and ν_{12} , while it is most affected with scatter in out of plane shear moduli. Further, it is also important to note that the CCCC and CFCF panels show closeness in scatter in frequency against variation in material properties. However, it is not so in the case of Poisson's ratio scatter. The CCCC and CFCF panels are most sensitive to G_{13} , while SSSS

panel is most sensitive to E_{11} . The panels are least affected with changes in the Poisson's ratio.

For $a/h=10$, the panels are most affected with SD of the E_{11} , while least affected with the SD of Poisson's ratio. The effects of G_{13} on scatter of the fundamental frequency of CCCC and CFCF panels are considerable. The CFCF panel is most sensitive as compared to other edge conditions against individual variation of material properties. The results reveal that the sensitivity of CCCC and CFCF panels are close to each other for the case of all material property variations except in the case of Poisson ratio. The results also reveal that SSSS panels do not show that much sensitivity against variation of the out of plane shear moduli compared with other end conditions panels.

Conclusions

The second moments of the square of the fundamental frequency of a laminated composite plate have been obtained using SFEM. The main conclusions are:

- The scatter in the fundamental frequency increases with the individual variations of E_{11} , E_{22} , G_{12} and ν_{12} as the side to thickness ratio increases, while the scatter decreases with G_{13} and G_{23} .
- CCCC panel with $a/h=5$ is most sensitive against simultaneous change in the material properties, while SSSS panel with $a/h=5$ is least sensitive.
- The dominance on scatter in the fundamental frequency changes from E_{11} to G_{13} as a/h ratio changes from 10 to 5.
- The panels are least affected with changes in the Poisson's ratio.

5.3.3.2 Composite Cylindrical Panels

Validation

Validation study of the proposed technique for cylindrical panels has been done on similar lines as in the case of plates. Figure 5.34 shows the results obtained by the SFEM along with the exact independent MCS for a $[0^0/90^0/0^0]$ laminated cylindrical panel with all edges simply supported for Material-1. The panel parameters are $R/a=5$, $a/b=1$ and $a/h=10$. Only longitudinal elastic modulus E_{11} has been taken as random variable. In this study, the exact MCS implies that the variance has been obtained using the Navier type solution approach, which is possible for all edges simply supported cylindrical panel [95]. A reasonably good agreement is seen. It is observed that with increase in SD/mean of E_{11} , there is some deviation between the two results. The present approximation underestimates the fundamental frequency compared with those of MCS. This may be due to the numerical round off in the computations.

Statistical moments of the fundamental frequency

Using the approach presented in the previous section, second order statistics of fundamental frequency of graphite-epoxy cylindrical panels have been evaluated for $R/a=5$, $a/b=1$ and $a/h=5$ and 10 with different support conditions using HSDT.

Frequency expectation

Table 5.7 list the non-dimensional mean fundamental frequency (ω), $R/a=5$ and $a/b=1$, of $[0^0/45^0/-45^0/90^0]$ CCCC, CFCF and SSSS laminated composite cylindrical panels for $a/h=5$ and 10. As expected, the CCCC panels give higher frequency as compared to others support conditions. The fundamental frequency (ω) increases as the a/h ratio increases.

Frequency variance

Figures 5.35(a) and 5.35(b) represent the scatter of the square of non-dimensional fundamental frequency (ω^2) with $R/a=5$ and $a/b=1$ with normalized standard deviation (SD/mean) of all material properties changing at a time for $[0^\circ/45^\circ/-45^\circ/90^\circ]$, CCCC, CFCF and SSSS laminated composite cylindrical panels for $a/h=5$ and 10, respectively, while Figures 5.36 - 5.41 present the dispersion of the non-dimensional fundamental frequency (ω^2), $R/a=5$, $a/b=1$ and $a/h=5$ and 10 with SD of the individual variation of the material property, keeping others deterministic for CCCC, CFCF and SSSS composite cylindrical panels. Results have been computed for different SD of material constants.

(i) *All material properties varying simultaneously – Figures. 5.35(a) and 5.35 (b)*

It is observed that CCCC panel with $a/h=10$ are most sensitive, while SSSS panel with $a/h=5$ is least sensitive compared to other support conditions and thickness ratio considered. The sensitivity of the fundamental frequency increases as a/h ratio increases for CCCC and SSSS panels. However, the trend is reverse in case of CFCF panel. For $a/h=5$, the difference in scatter between CCCC and SSSS panels are significant, while for $a/h=10$ these are insignificant.

(ii) *Only longitudinal elastic modulus E_{11} varying - Figures. 5.36(a) and 5.36(b)*

The dispersion of the fundamental frequency increases as a/h ratio increases. The CCCC panels with $a/h=10$ are most affected with SD of the material property, while CFCF panels with $a/h=5$ is least affected as compared to other parameters and support conditions considered in the study. The difference in scatter is insignificant between CCCC and SSSS panels for $a/h=5$, while for others, it is significant.

(iii) *Only transverse elastic modulus E_{22} varying - Figures 5.37(a) and 5.37(b)*

The SSSS panels are most sensitive to change in the material property as compared to other support conditions for both the thickness ratios considered, while CCCC panels are least sensitive. The sensitivity also increases, like E_{11} , as a/h ratio increases.

(iv) *Only in-plane shear modulus G_{12} varying - Figures 5.38(a) and 5.38(b)*

The behavior of dispersion is almost similar to E_{22} . However, the level of dispersion is low as compared to dispersion due to E_{22} .

(v) *Only out-of-plane shear modulus (G_{13}) varying - Figures 5.39(a) and 5.39(b)*

The sensitivity of the fundamental frequency decreases as a/h ratio increases. This indicates reversed trend in comparison with inplane elastic moduli. The dominance in scatter of CCCC panels with $a/h=5$ is observed, while least sensitivity in scatter for SSSS panels with $a/h=10$ is seen.

(vi) *Only out-of-plane shear modulus G_{23} varying - Figures 5.40(a) and 5.40(b)*

The trend is similar to G_{13} . However, the level of dispersion is small compared to G_{23} .

(vii) *Only Poisson ratio ν_{12} varying- Figures 5.41(a) and 5.41(b)*

The dispersion is least affected with changes in ν_{12} returning very low values compared to the other materials. SSSS panel shows highest sensitivity out of the three support conditions considered for both the thickness ratios considered.

Conclusions

A C^0 finite element technique in conjunction with first order perturbation technique has been developed for solving random standard eigenvalue problem associated with free vibration of laminated composite cylindrical panels. Using this approach, second order statistics of the fundamental frequency has been obtained for different panel boundary conditions. Following conclusions can be drawn from this study:

- CCCC panel with $a/h=10$ is most sensitive, while SSSS panel with $a/h=5$ is least sensitive against simultaneous changes of material properties.
- Sensitivity of panels increases as a/h ratio increases with variation of SD of in-plane elastic and shear moduli and Poisson's ratio. The trend is reversed in case of out-of-plane shear moduli.
- The dominant effect of G_{13} on scatter in fundamental frequency changes to E_{11} when a/h ratio changes from 5 to 10. However, SSSS panel maintains E_{11} dominant for both the thickness ratios. The panels are least sensitive for changes in Poisson's ratio.

5.3.3.3 Composite Spherical Panels

Validation

Validation study of the present technique has been done on similar lines as in the case of plates. The results obtained by SFEM have been compared with MCS and SCA. Figure 5.42 presents the comparison for SD of square of the fundamental frequency a $[0^0/90^0/90^0/0^0]$ square laminate, Material-1 with $R/a=5$, $a/h=10$ with only E_{11} assumed as random, other material properties being deterministic for all edges simply supported (SSSS). The results are in good agreement with MCS and SCA. However, the SFEM results are not so close to MCS as the SCA. This may be due to numerical round off error in the finite element computations.

Table 5.8 shows the comparison of the nondimensionalized fundamental frequency obtained using SFEM and SCA for SSSS for a $[0^0/90^0]$ composite spherical panel. The panel geometry used is $R/a=5$, $a/b=1$ and $a/h=10$. Results are in good agreements.

Second Order Moments of the fundamental frequency

Second order statistics of fundamental frequency of $[45^0/-45^0/45^0/-45^0]$ graphite-epoxy spherical panels Material-1 have been evaluated for $R/a=5$, $a/b=1$ and $a/h=5$ and 10 with CCCC, CFCF and SSSS. A comparison of SD of square of the fundamental frequency for composite plates, cylindrical and spherical panels is also presented for all edges simply supported.

Frequency expectation

Table 5.9 lists the nondimensionalized mean fundamental frequency with CCCC, CFCF and SSSS panels. The results are on the expected lines.

Frequency variance

Figures 5.43 (a) and 5.43(b) show the dispersion in the fundamental frequency for composite spherical panels with CCCC, CFCF and SSSS against the material properties varying simultaneously for $a/h=5$ and 10, respectively. It is observed that the effect of a/h ratio on scatter of the frequency is insignificant for CCCC and CFCF panels, while it is significant for SSSS panel. The SSSS panel with $a/h=10$ is most sensitive, while CFCF with $a/h=5$ is least sensitive. However, the difference is small.

Figures 5.44(a)-5.44(f) show sensitivity of the fundamental frequency for $a/h=5$ with CCCC, CFCF and SSSS against individual variation of material property SD. The dominant effect of G_{13} on dispersion of fundamental frequency of composite panels is observed. However, the effect of E_{11} and G_{23} on scatter is also significant. The panels are least affected with scatter in the Poisson's ratio.

Figures 5.45(a) –5.45(b) plot dispersion of the fundamental frequency for $a/h=10$ with SD of the individual material property for CCCC, CFCF and SSSS boundary panel. It is seen

that the effect of E_{11} is dominant. However, the effect of G_{13} and G_{23} is also appreciable. SSSS panel is most sensitive, while CCCC panel for changes in E_{11} is least sensitive. The sensitivity of CCCC and CFCF panels is close to each other for this case. The fundamental frequency is least affected with changes in Poisson's ratio. The effect of G_{12} in case of CFCF panel is also appreciable.

Comparison with plate and cylindrical panel

A comparison of the scatter in the fundamental frequency for $[0^0/45^0/-45^0/90^0]$ composite plates ($a/b=1$ and $a/h=10$), cylindrical ($a/b=1$, $R/a=5$ and $a/h=10$) and spherical ($a/b=1$, $R/a=5$ and $a/h=10$) panels is presented in Figure 5.46 for SSSS boundary condition with simultaneous change in the material properties. The comparison aims at bringing out the relative sensitivities of the three geometry to changes in the material properties. The results show that the spherical panel is more sensitive as compared to plate and cylindrical panel. The difference in scatter in the fundamental frequency of spherical with cylindrical panels is smaller than its difference with plates.

Similar comparison is presented in Figures 5.47(a) – 5.47(f) for SSSS boundary condition against individual variation of the material property. No definite pattern is observed as in the case of simultaneous variation of the material properties. Curved panels are less sensitive as compared to plates against variation of the material property except E_{11} .

Conclusions

The second moments of the fundamental frequency have been obtained using SFEM with different support conditions. A comparison among plate, cylindrical and spherical panels have been also presented for all edges simply supported. The following are the main conclusions:

- The sensitivity trend of panel changes with change in a/h ratio against simultaneous variation of the material properties. The SSSS and CCCC panels sensitivity are very close for $a/h=5$, while it is not so for $a/h=10$. For $a/h=10$, the CCCC and CFCF panels sensitivity are close.
- The SSSS moderately thick panel is most sensitive to simultaneous variation of the material properties as compared to other type of panels in terms of support conditions studied.
- The dominant effect of E_{11} is changed to G_{13} as the thickness ratio changes from 10 to 5. The panels are least sensitive to the Poisson's ratio.

5.4 Summary

The SCA and SFEM developed in this Chapter are applied to the study of free vibration of laminated composite plates, cylindrical and spherical panels with random material properties. Comparison with the results obtained from Monte Carlo simulation shows the usefulness of these techniques for the study of composite panels. Sensitivity of natural frequencies of plates, cylindrical and spherical panels to changes in stacking sequence, aspect ratio and boundary condition are presented. Efficacies of various theories are also examined. A comparison among dispersion in the three panels for all edges simply supported is also presented.

Table 5.1: Mean Natural Frequencies, $\bar{\omega} = (\bar{\omega}^* a^2 \sqrt{\rho/E_{22}})/h$, for all edges simply supported composite square plates

(a) Stacking Sequence: $[0^0/90^0]$

Mode (1)	Material-1		Material -2	
	a/h=10 (2)	a/h=100 (3)	a/h=10 (4)	a/h=100 (5)
1	8.98083	10.47657	10.56565	11.90491
2	21.9336	27.48786	26.30276	31.69695
3	30.34590	38.27912	36.34791	45.23941
4	39.98180	57.00877	48.70060	67.09281
5	45.59216	64.64992	55.14367	76.19473

(b) Stacking Sequence: $[0^0/90^0/90^0/0^0]$

Mode (1)	Material-1		Material -2	
	a/h=10 (2)	a/h=100 (3)	a/h=10 (4)	a/h=100 (5)
1	11.77252	15.17055	15.10799	19.13029
2	21.83344	28.27569	26.43976	32.86094
3	27.37726	53.83362	37.06150	64.79179
4	33.23205	54.08102	43.15083	67.81584
5	37.43603	60.05661	44.22175	74.66206

Table 5.2: Nondimensionalised mean natural frequencies of laminated cylindrical panels with $a/b=1$, $\bar{\omega} = (\bar{\omega}^* a^2 \sqrt{\rho/E_{22}})/h$

(a) Stacking sequence: $[0^0/90^0]$

R/a (1)	Mode (2)	Nondimensional Mean Frequency, $\bar{\omega}$	
		a/h=10 (3)	a/h=100 (4)
5	1	9.0213	17.4809
5	2	21.8501	28.1466
5	3	22.0437	37.9768
5	4	30.2819	40.5736
5	5	39.8693	56.9662
10	1	8.9768	11.7674
10	2	21.8793	27.5738
10	3	21.9623	29.6930
10	4	30.3099	39.5438
10	5	39.9256	57.2848

(b) Stacking sequence: $[0^0/90^0/90^0/0^0]$

R/a (1)	Mode (2)	Nondimensional Mean Frequency, $\bar{\omega}$	
		a/h=10 (3)	a/h=100 (4)
5	1	11.8322	20.5152
5	2	21.8279	28.7186
5	3	27.4614	53.2215
5	4	33.2467	59.6511
5	5	37.4490	61.6323
10	1	11.7906	16.4195
10	2	21.8279	27.4193
10	3	27.3972	53.5511
10	4	33.2229	55.0981
10	5	37.4474	60.9492

Table 5.3: Nondimensionalised mean natural frequencies of laminated spherical panels with $R_1=R_2=R$, $a/b=1$, $a/h=10$ and $R/a=5$, $\bar{\omega} = (\bar{\omega}^* a^2 \sqrt{\rho/\bar{E}_{22}})/h$: Stacking sequence: $[0^0/90^0]$ for all edges simply supported (SSSS)

Nondimensional Mean Natural Frequency, $\bar{\omega}$					
Mode	1	2	3	4	5
(1)	(2)	(3)	(4)	(5)	(6)
$\bar{\omega}$	9.3412	22.0381	22.02027	30.4377	39.9879

Table 5.4: Nondimensionalised mean fundamental frequency of $[0^0/90^0]$ spherical panels with $R_1=R_2=R$ and $R/a=5$, $a/b=1$, $a/h=10$, $\bar{\omega} = (\bar{\omega}^* a^2 \sqrt{\rho/\bar{E}_{22}})/h$ with various boundary conditions

Nondimensional Mean Fundamental Frequency, $\bar{\omega}$				
SCSC	SSSC	SFSS	SFSC	SSSS
(1)	(2)	(3)	(4)	(5)
4.5235	14.4838	6.4025	6.4245	9.3412

Table 5.5: Comparisons of nondimensionalised mean fundamental frequency for a square plate, $\bar{\omega} = (\bar{\omega}^* a^2 \sqrt{\rho/\bar{E}_{22}})/h$, for all edges simply supported (SSSS)

Methods	Nondimensionalised Mean Fundamental Frequency, $\bar{\omega}$			
	$[0^0/90^0]$		$[0^0/90^0/90^0/0^0]$	
	a/h=10 (2)	a/h=100 (3)	a/h=10 (4)	a/h=100 (5)
(1) SCA (refer Table 5.1)	8.98083	10.47657	11.77252	15.28034
SFEM	8.93477	11.40352	11.67937	11.28034

Table 5.6: Nondimensionalised mean fundamental frequency, $\bar{\omega} = (\bar{\omega}^* a^2 \sqrt{\rho/\bar{E}_{22}})/h$, for a $[0^0/45^0/-45^0/90^0]$ square plate with different boundary conditions

Support conditions	Nondimensionalised Mean Fundamental Frequency, $\bar{\omega}$	
	a/h=5 (2)	a/h=10 (3)
(1) CCCC	10.74303	16.39915
CFCF	7.38198	11.05700
SSSS	7.17246	8.889832

Table 5.7: Non-dimensional mean fundamental frequency, $\bar{\omega} = (\bar{\omega}^* a^2 \sqrt{\rho/E_{22}})/h$, of a $[0^0/45^0/-45^0/90^0]$ composite cylindrical panel with different panel edge conditions ($a/b=1$, $R/a=5$).

Support Conditions	Nondimensionalised Mean Fundamental Frequency, $\bar{\omega}$	
	$a/h=5$	$a/h=10$
(1)	(2)	(3)
CCCC	11.25068	17.70168
CFCF	7.47890	11.34840
SSSS	7.24656	9.27205

Table 5.8: Comparison of the nondimensionalised mean fundamental frequency for a square $[0^0/90^0]$ laminated spherical panel, $\bar{\omega} = (\bar{\omega}^* a^2 \sqrt{\rho/E_{22}})/h$, for all edges simply supported (SSSS)

Methods	Nondimensionalised Mean Fundamental Frequency, $\bar{\omega}$
	$a/h=10$
(1)	(2)
SCA (refer Table 5.3)	9.3412
SFEM	9.3667

Table 5.7: Non-dimensional mean fundamental frequency, $\bar{\omega} = (\bar{\omega}^* a^2 \sqrt{\rho/E_{22}})/h$, of a $[0^0/45^0/-45^0/90^0]$ composite cylindrical panel with different panel edge conditions ($a/b=1$, $R/a=5$).

Support Conditions	Nondimensionalised Mean Fundamental Frequency, $\bar{\omega}$	
	$a/h=5$	$a/h=10$
(1)	(2)	(3)
CCCC	11.25068	17.70168
CFCF	7.47890	11.34840
SSSS	7.24656	9.27205

Table 5.8: Comparison of the nondimensionalised mean fundamental frequency for a square $[0^0/90^0]$ laminated spherical panel, $\bar{\omega} = (\bar{\omega}^* a^2 \sqrt{\rho/E_{22}})/h$, for all edges simply supported (SSSS)

Methods	Nondimensionalised Mean Fundamental Frequency, $\bar{\omega}$
	$a/h=10$
(1)	(2)
SCA (refer Table 5.3)	9.3412
SFEM	9.3667

Table 5.9: Nondimensionalised mean fundamental frequency, $\bar{\omega} = (\bar{\omega}^* a^2 \sqrt{\rho/E_{22}})/h$, for a $[0^\circ/45^\circ/-45^\circ/90^\circ]$ spherical panel with different boundary conditions

Support conditions (1)	Nondimensionalised Mean Fundamental Frequency, ϖ	
	$a/h=5$ (2)	$a/h=10$ (3)
CCCC	11.90323	20.16317
CFCF	7.61402	11.83930
SSSS	10.68355	16.58312

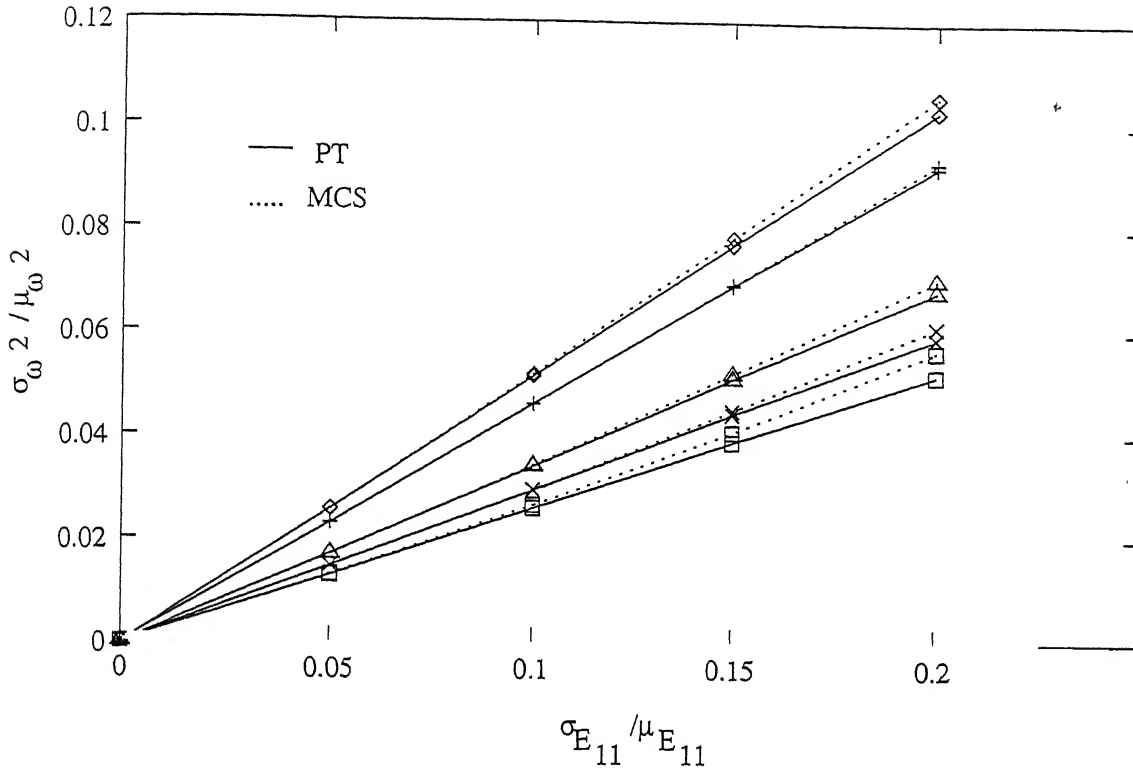


Figure 5.1: Comparison of result from MCS with the present approach, $[0^\circ/90^\circ/90^\circ/0^\circ]$ plate, with $a/b=1$, Material-1 and $a/h=10$.

Key:- ◇: first mode, + : second mode, □ : third mode, ×: fourth mode, △: fifth mode.

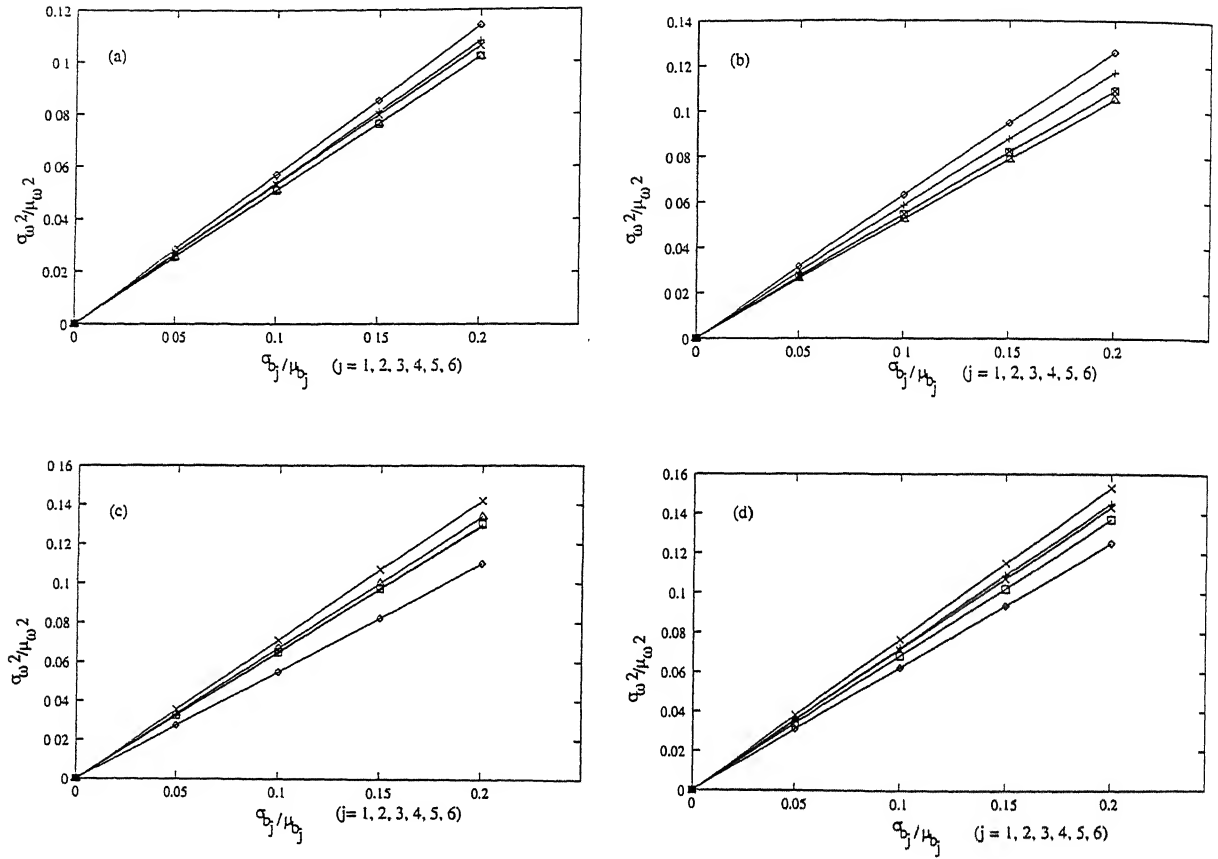


Figure 5.2: Influence of SD of basic material properties on SD of square of the first five natural frequencies, $[0^\circ/90^\circ]$ plate, $a/b=1$, with all basic material properties changing at a time.

- (a) $a/h=10$ and Material -1; (b) $a/h=10$ and Material -2; (c) $a/h=100$ and Material -1;
 (d) $a/h=100$ and Material -2.

Key: As in Figure 5.1.

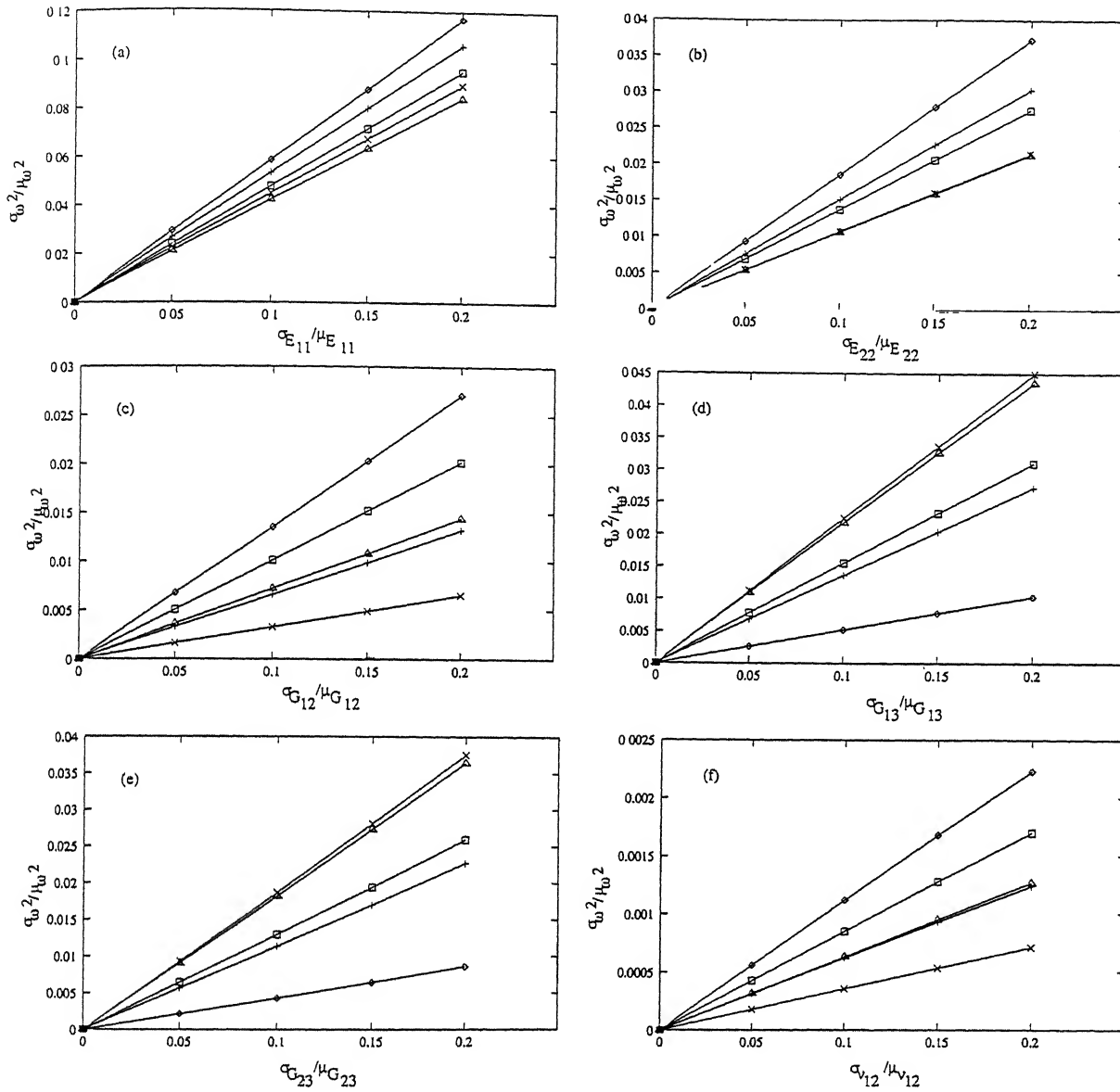


Figure 5.3: Influence of SD of basic material properties on SD of square of the first five natural frequencies, $[0^\circ/90^\circ]$ plate, with $a/b=1$, Material -2 and $a/h=10$.

(a) only E_{11} varying; (b) only E_{22} varying; (c) only G_{12} varying; (d) only G_{13} varying; (e) only G_{23} varying; (f) only ν_{12} varying.

Key: As in Figure 5.1.

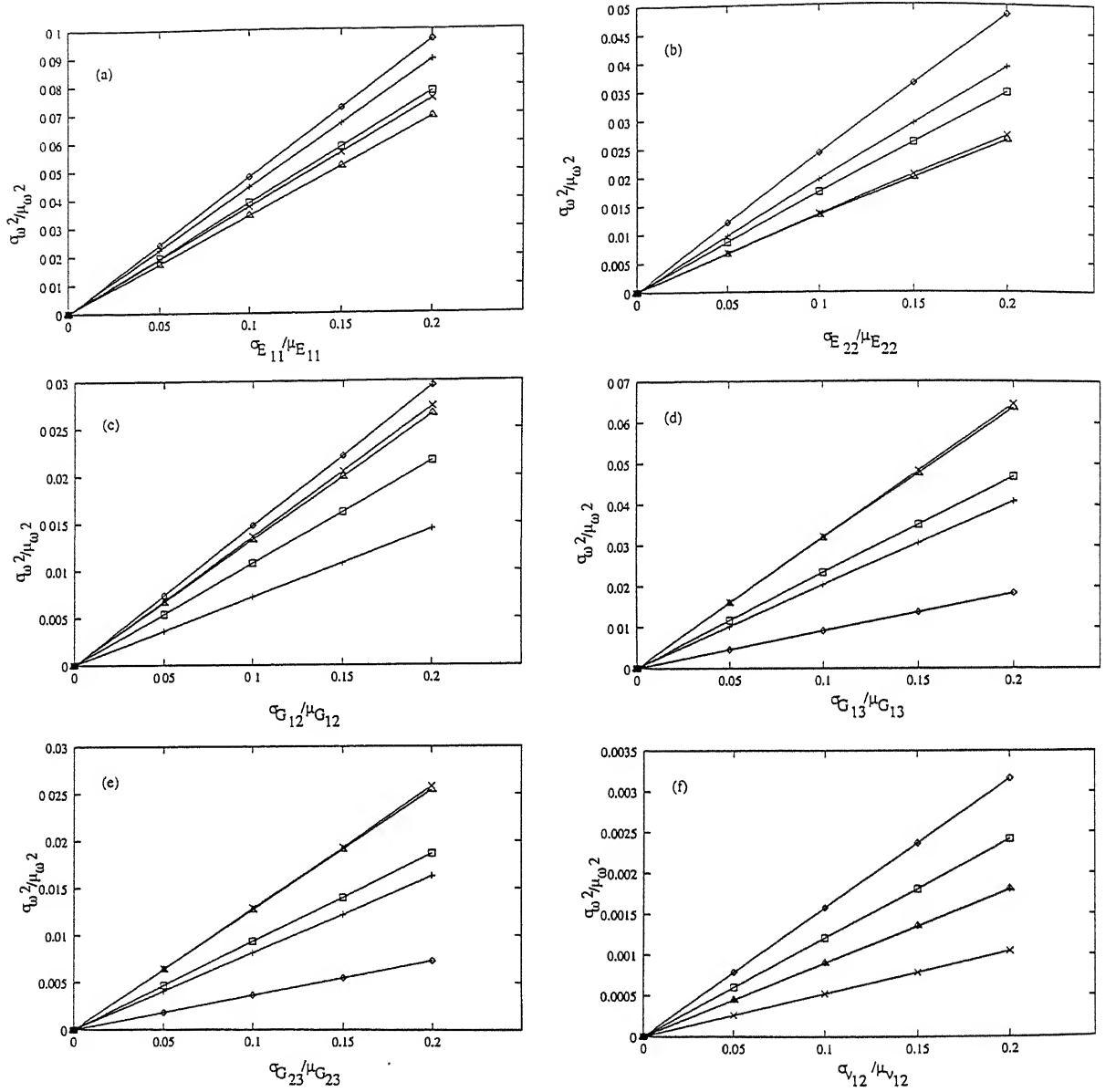


Figure 5.4: Influence of SD of basic material properties on SD of square of the first five natural frequencies, $[0^\circ/90^\circ]$ plate, with $a/b=1$, Material -1 and $a/h=10$.
 (a) only E_{11} varying; (b) only E_{22} varying; (c) only G_{12} varying; (d) only G_{13} varying; (e) only G_{23} varying; (f) only ν_{12} varying.

Key: As in Figure 5.1.

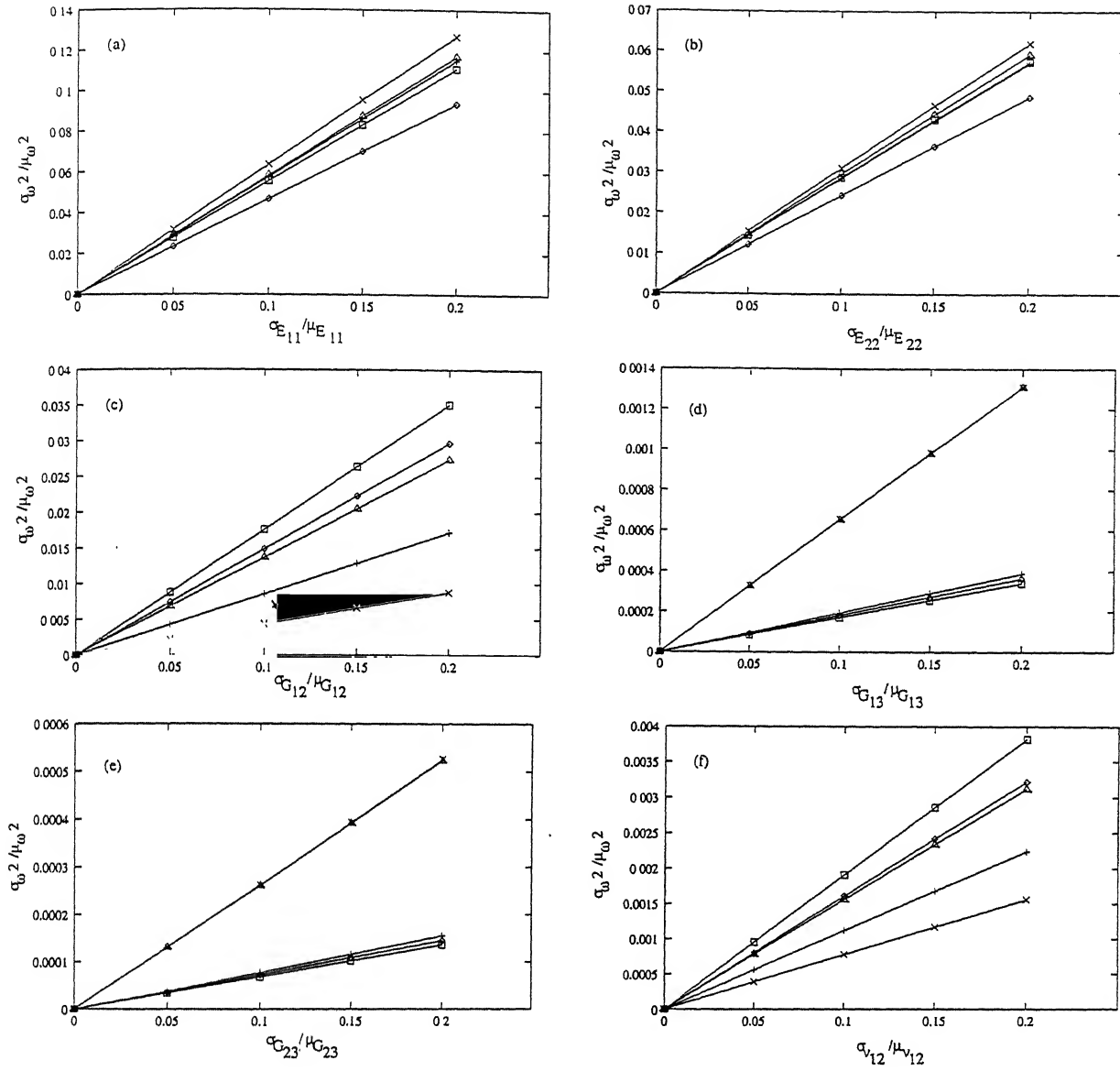


Figure 5.5: Influence of SD of basic material properties on SD of square of the first five natural frequencies, $[0^\circ/90^\circ]$ plate, with $a/b=1$, Material -1 and $a/h=100$.
 (a) only E_{11} varying; (b) only E_{22} varying; (c) only G_{12} varying; (d) only G_{13} varying; (e) only G_{23} varying; (f) only ν_{12} varying.

Key: As in Figure 5.1

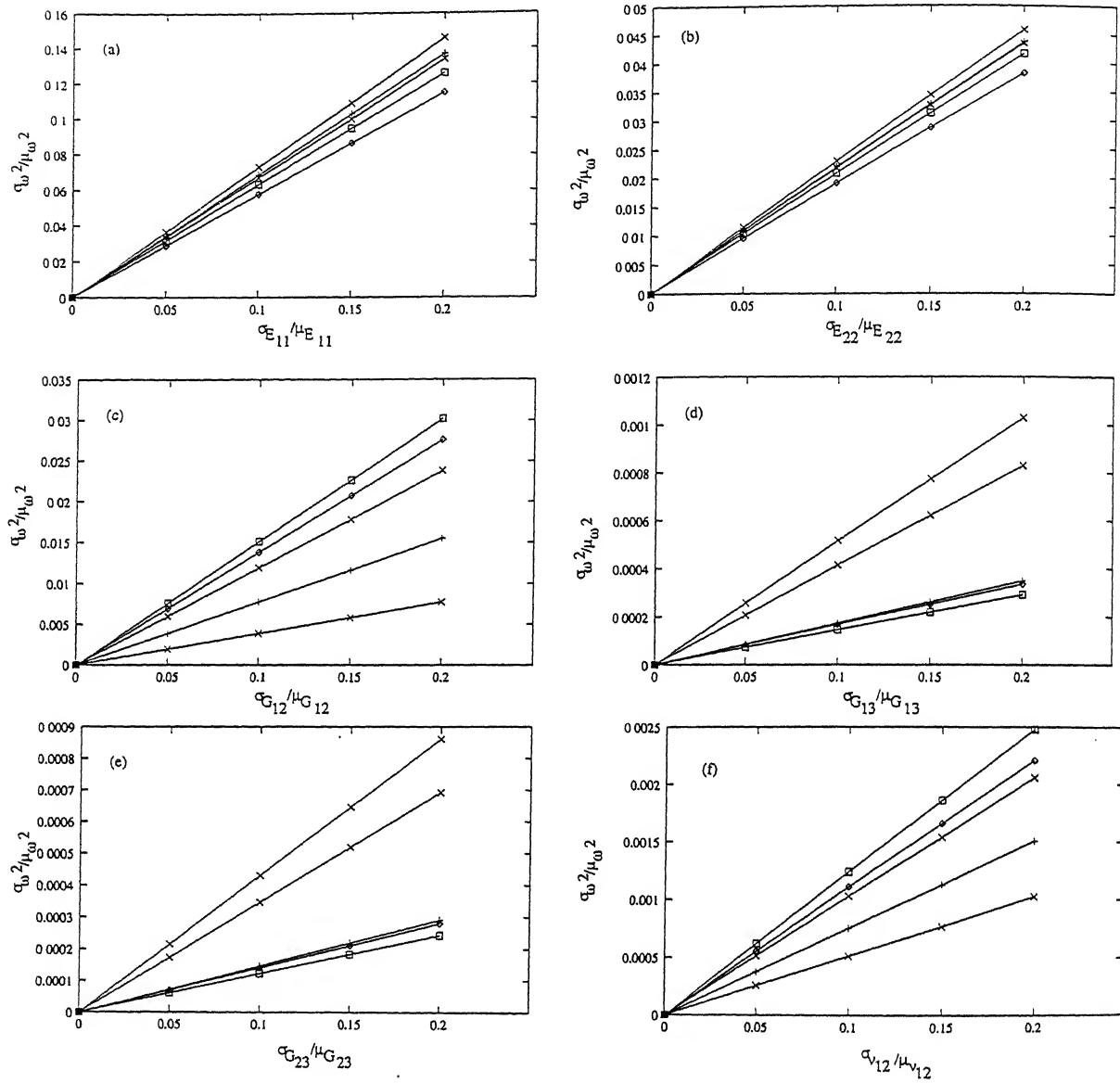


Figure 5.6: Influence of SD of basic material properties on SD of square of the first five natural frequencies, $[0^\circ/90^\circ]$ plate, with $a/b=1$, Material -2 and $a/h=100$.
 (a) only E_{11} varying; (b) only E_{22} varying; (c) only G_{12} varying; (d) only G_{13} varying; (e) only G_{23} varying; (f) only ν_{12} varying.

Key: As in Figure 5.1.

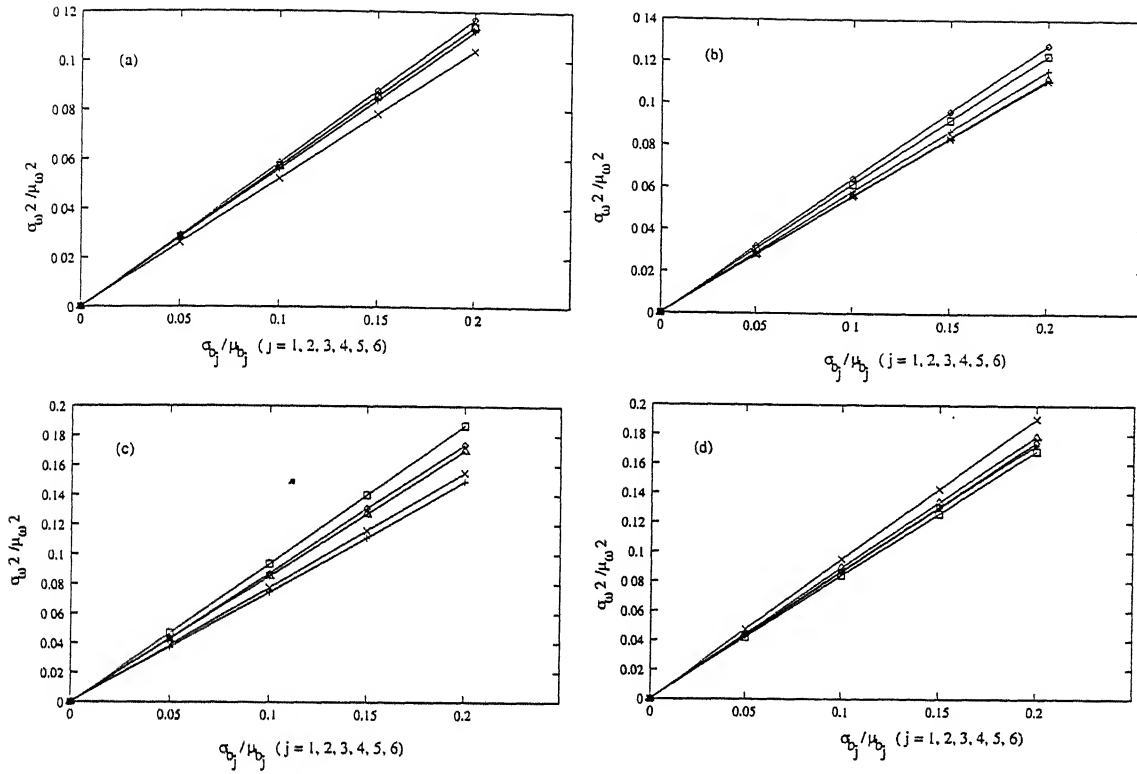


Figure 5.7: Influence of SD of basic material properties on SD of square of the first five natural frequencies, $[0^\circ/90^\circ/90^\circ/0^\circ]$ plate, with $a/b=1$, with all basic material properties changing at a time.

- (a) $a/h=10$ and Material -1; (b) $a/h=10$ and Material -2 (c) $a/h=100$ and Material -1;
(d) $a/h=100$ and Material -2.

Key: As in Figure 5.1

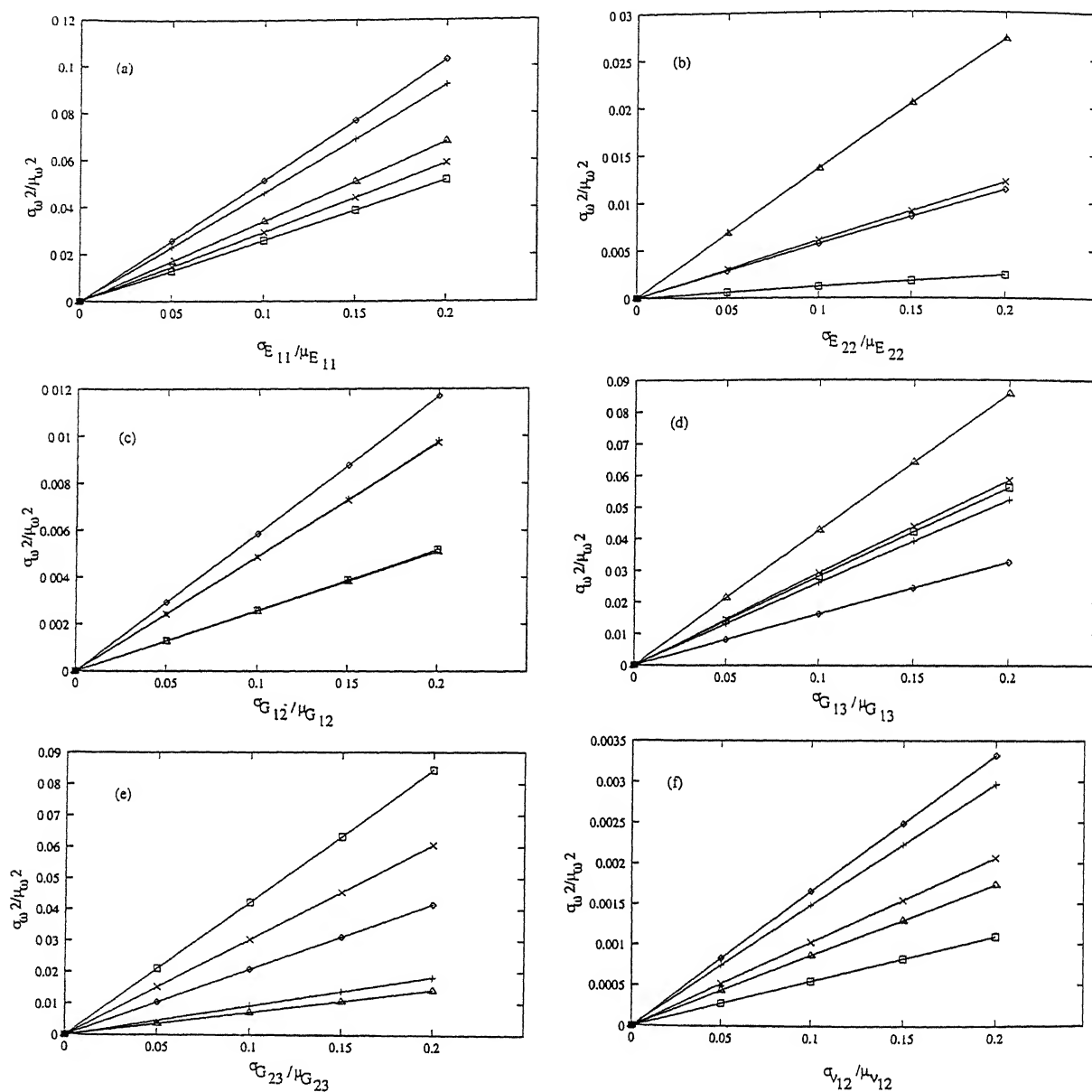


Figure 5.8: Influence of SD of basic material properties on SD of square of the first five natural frequencies, $[0^\circ/90^\circ/90^\circ/0^\circ]$ plate, with $a/b=1$, Material -1 and $a/h=10$.
 (a) only E_{11} varying; (b) only E_{22} varying; (c) only G_{12} varying; (d) only G_{13} varying; (e) only G_{23} varying; (f) only ν_{12} varying.

Key: As in Figure 5.1.

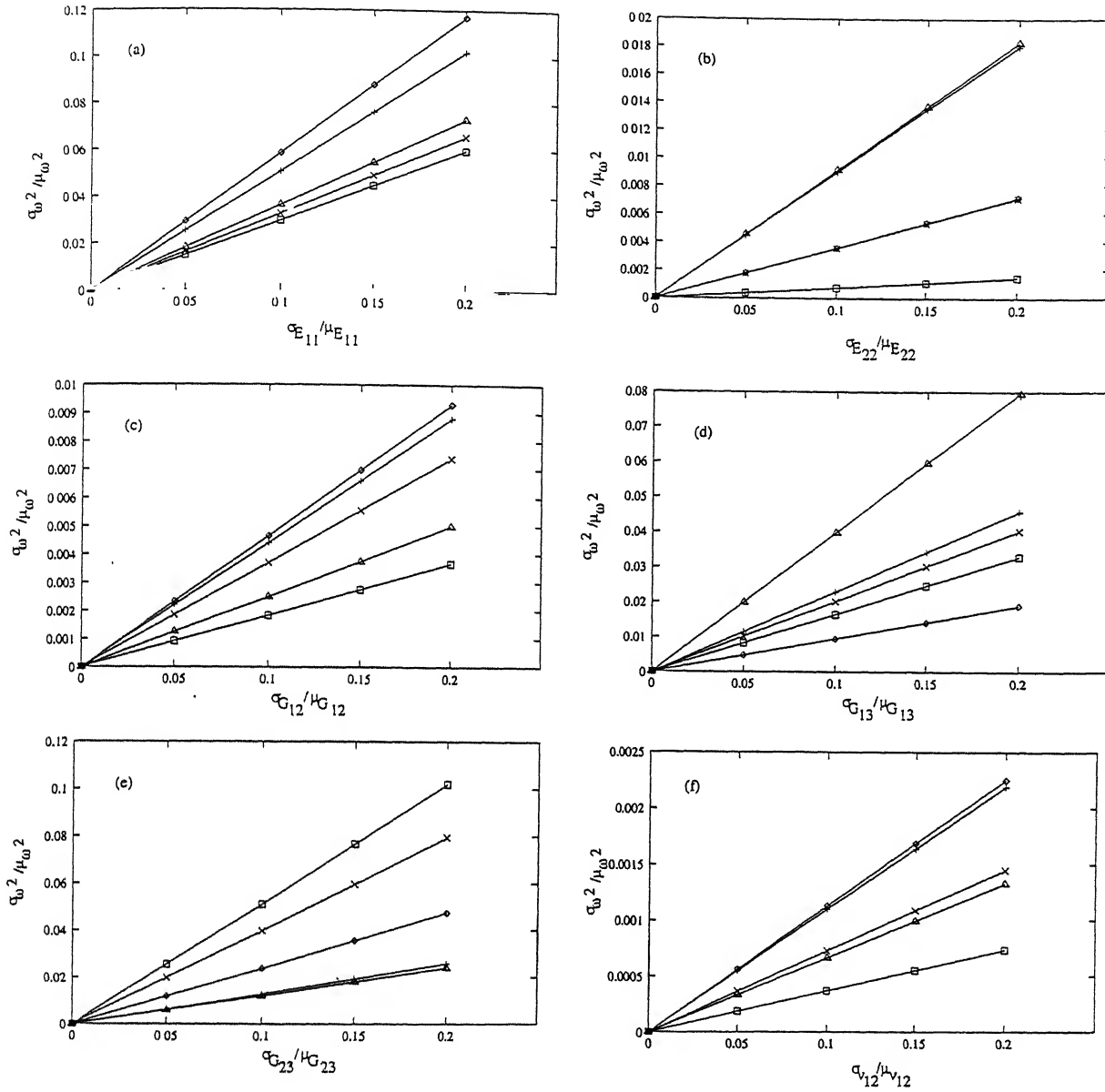


Figure 5.9: Influence of SD of basic material properties on SD of square of the first five natural frequencies, $[0^\circ/90^\circ/90^\circ/0^\circ]$ plate, with $a/b=1$, Material -2 and $a/h=10$.
 (a) only E_{11} varying; (b) only E_{22} varying; (c) only G_{12} varying; (d) only G_{13} varying; (e) only G_{23} varying; (f) only ν_{12} varying.

Key: As in Figure 5.1.

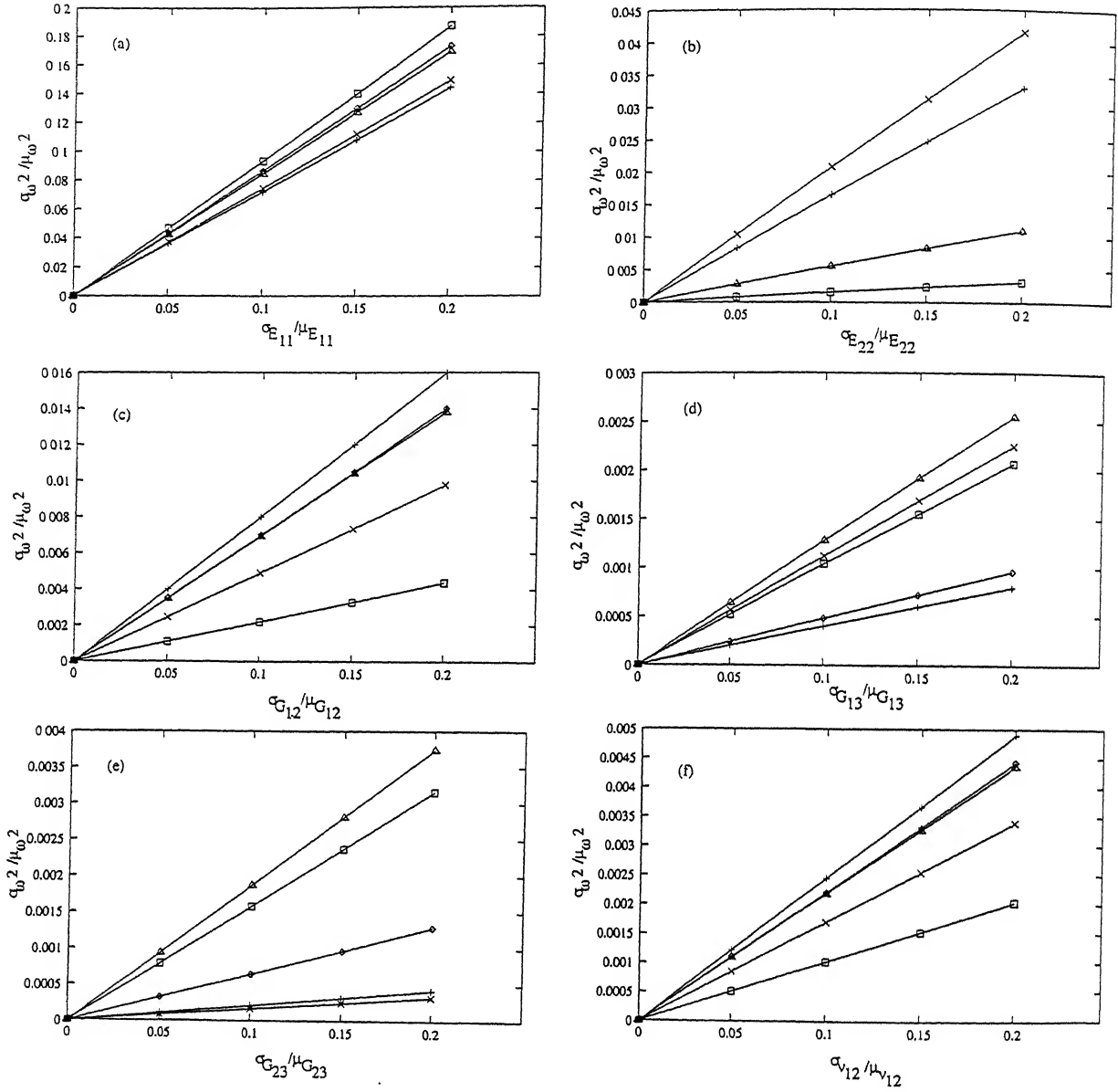


Figure 5.10: Influence of SD of basic material properties on SD of square of the first five natural frequencies, $[0^\circ/90^\circ/90^\circ/0^\circ]$ plate, with $a/b=1$, Material -1 and $a/h=100$. (a) only E_{11} varying; (b) only E_{22} varying; (c) only G_{12} varying; (d) only G_{13} varying; (e) only G_{23} varying; (f) only ν_{12} varying.

Key: As in Figure 5.1.

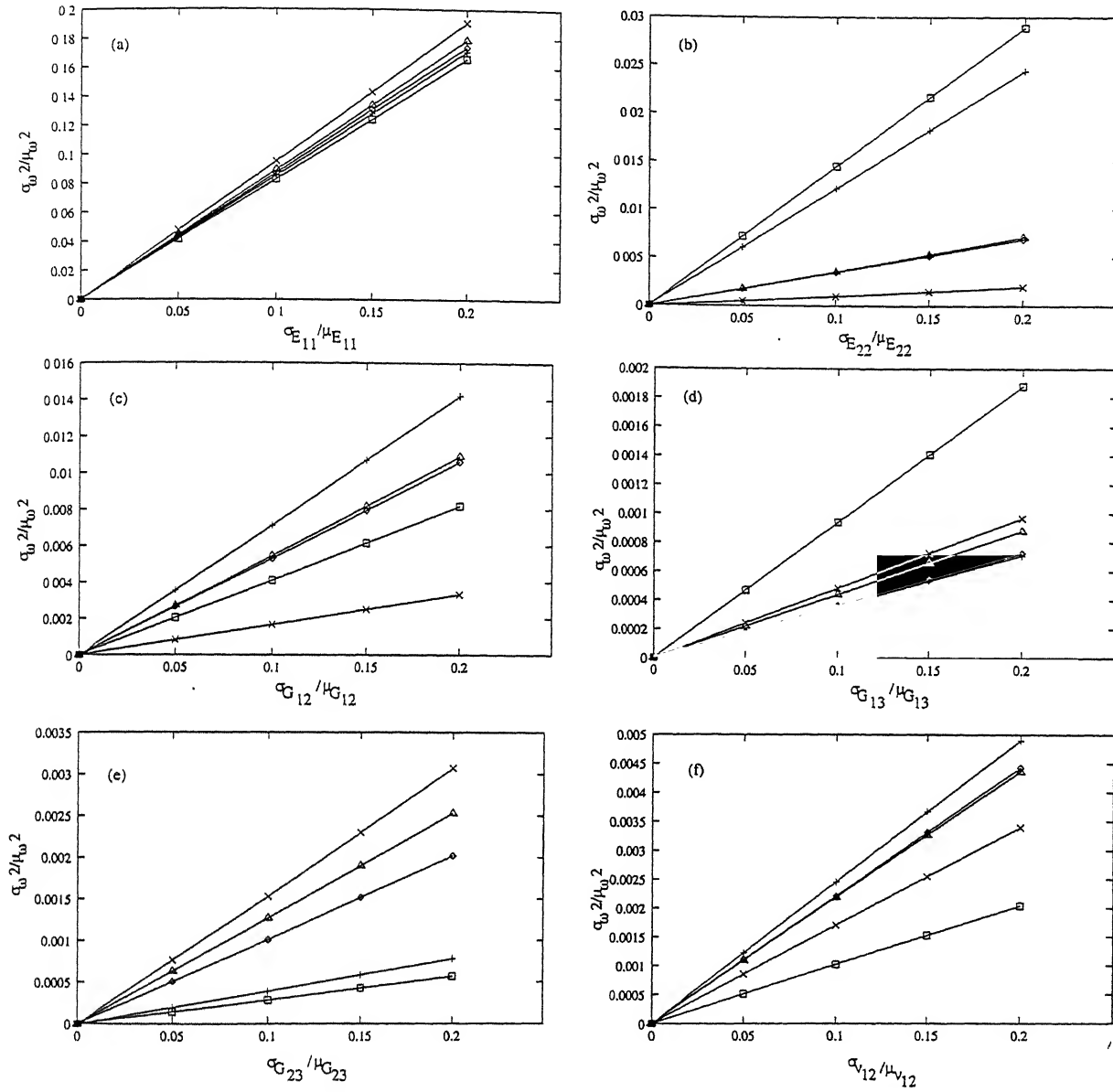


Figure 5.11: Influence of SD of basic material properties on SD of square of the first five natural frequencies, $[0^\circ/90^\circ/90^\circ/0^\circ]$ plate, with $a/b=1$, Material -2 and $a/h=100$.

(a) only E_{11} varying; (b) only E_{22} varying; (c) only G_{12} varying; (d) only G_{13} varying; (e) only G_{23} varying; (f) only ν_{12} varying.

Key: As in Figure 5.1.

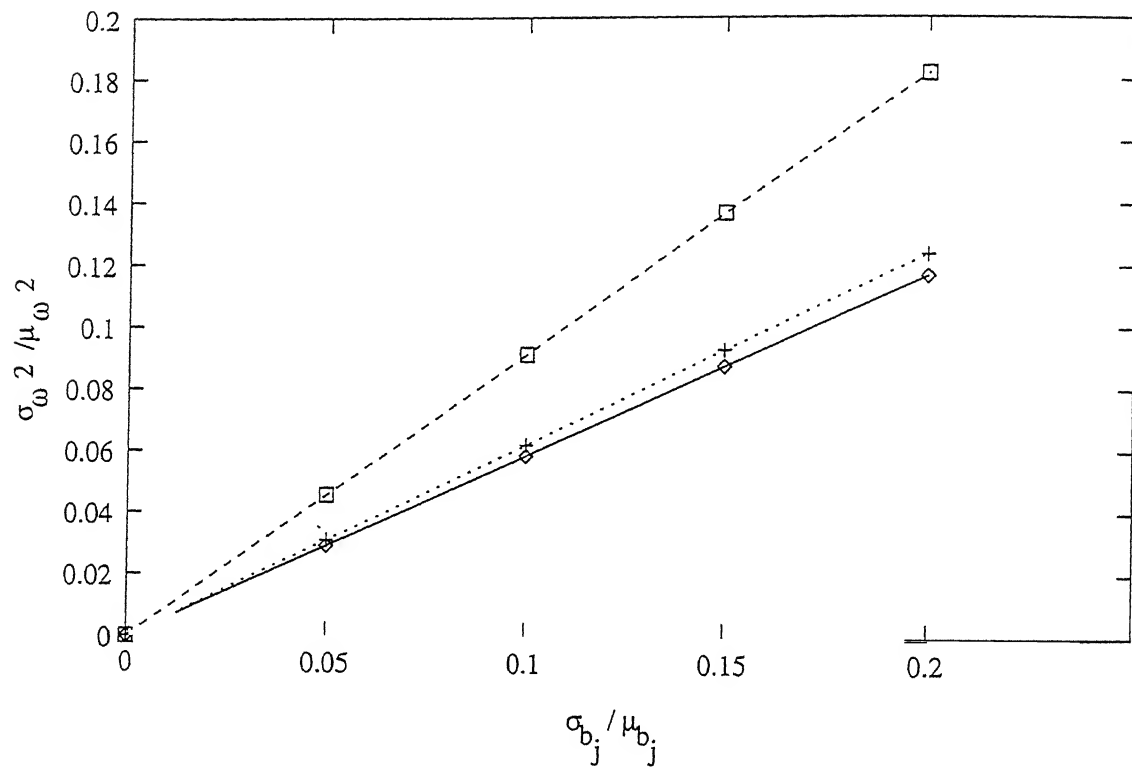


Figure 5.12: Influence of SD of basic material properties on SD of square of the first five natural frequencies, $[0^\circ/90^\circ/90^\circ/0^\circ]$ plate, $a/b=1$, Material -1 and $a/h=10$, with all basic material properties changing at a time.

Key:— HSDT, FSDT, - - - CLT.

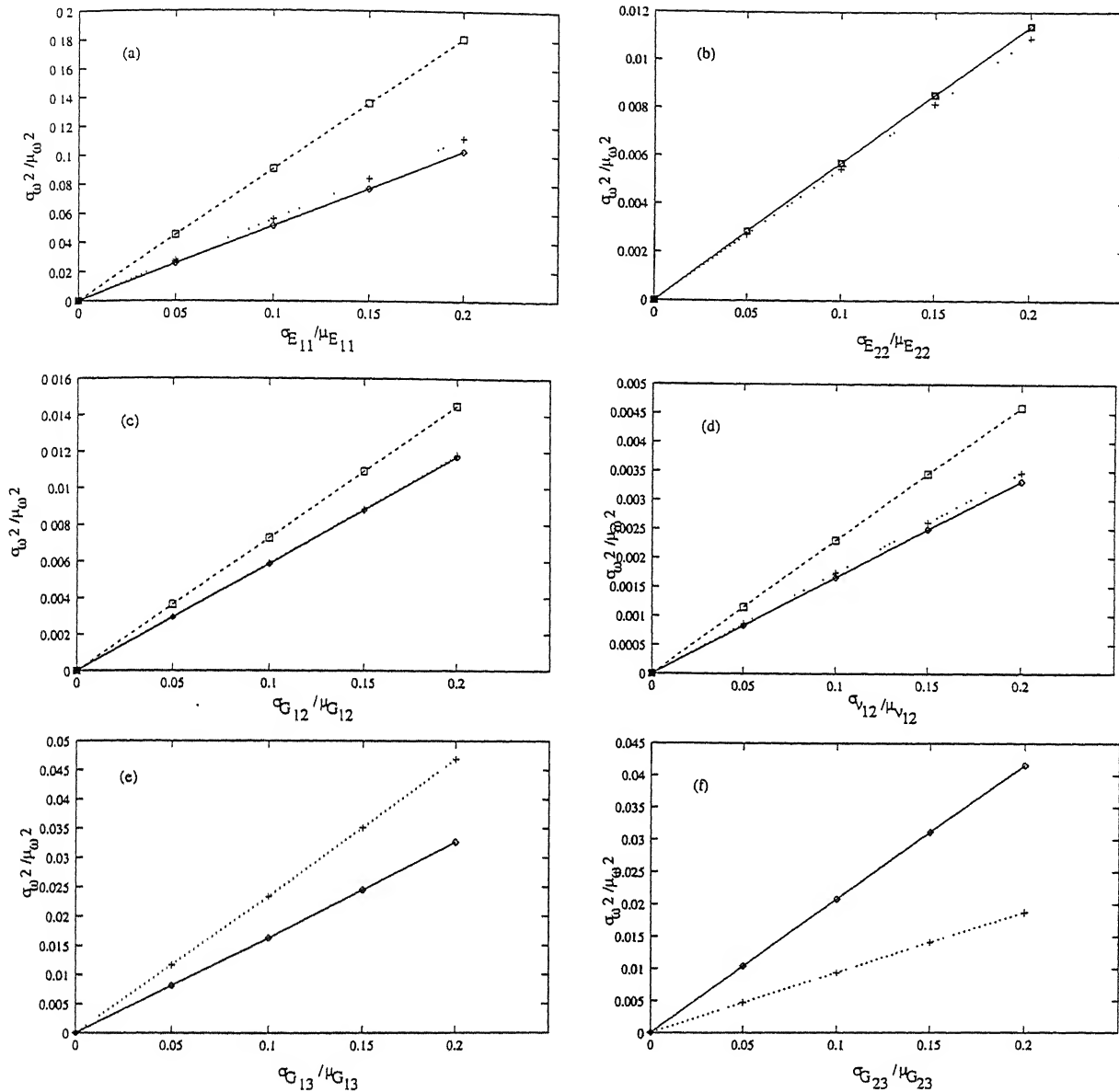


Figure 5.13: Comparison of influence of SD of basic material properties on SD of square of the fundamental frequency by three theories, $[0^\circ/90^\circ/90^\circ/0^\circ]$ plate, with $a/b=1$, Material -1 and $a/h=10$.

(a) only E_{11} varying; (b) only E_{22} varying; (c) only G_{12} varying; (d) only G_{13} varying; (e) only G_{23} varying; (f) only ν_{12} varying.

Key: As in Figure 5.12.

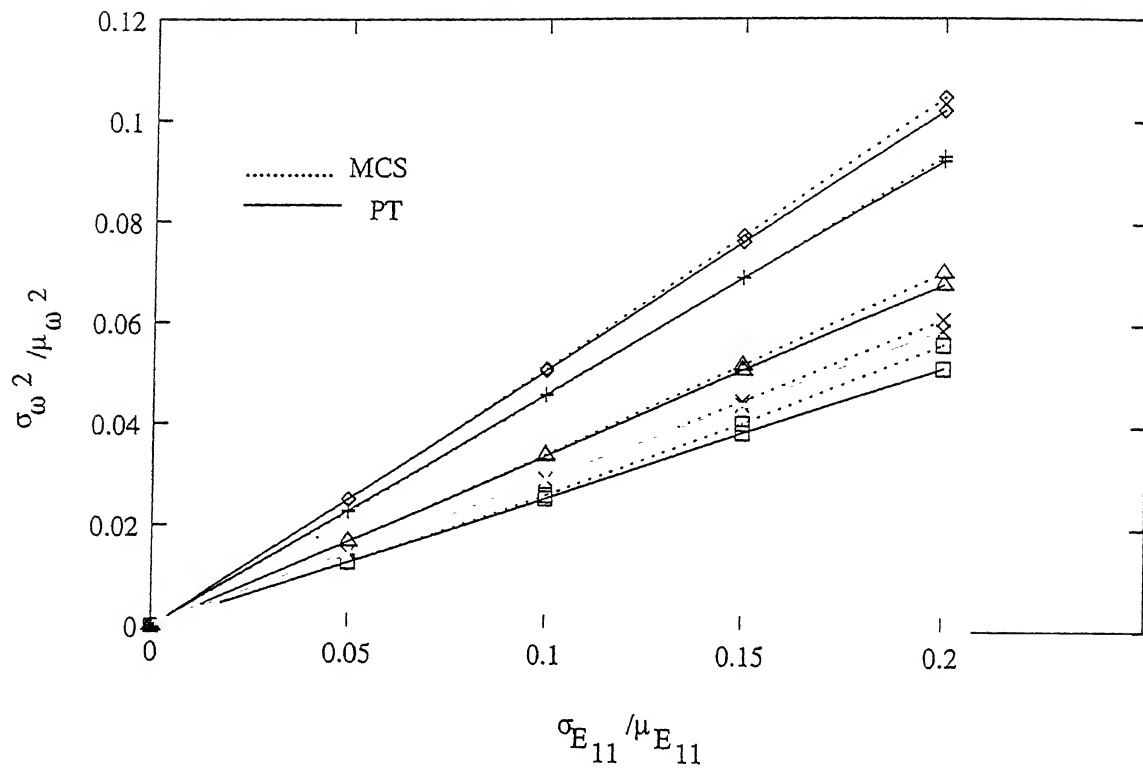


Figure 5.14: Comparison of the present approach results to Monte Carlo simulation $[0^\circ/90^\circ/90^\circ/0^\circ]$ cylindrical panel, with $R/a=5$, $a/b=1$ and $a/h=10$.

Key:- \diamond : first mode, $+$: second mode, \square : third mode, \times : fourth mode, \triangle : fifth mode.

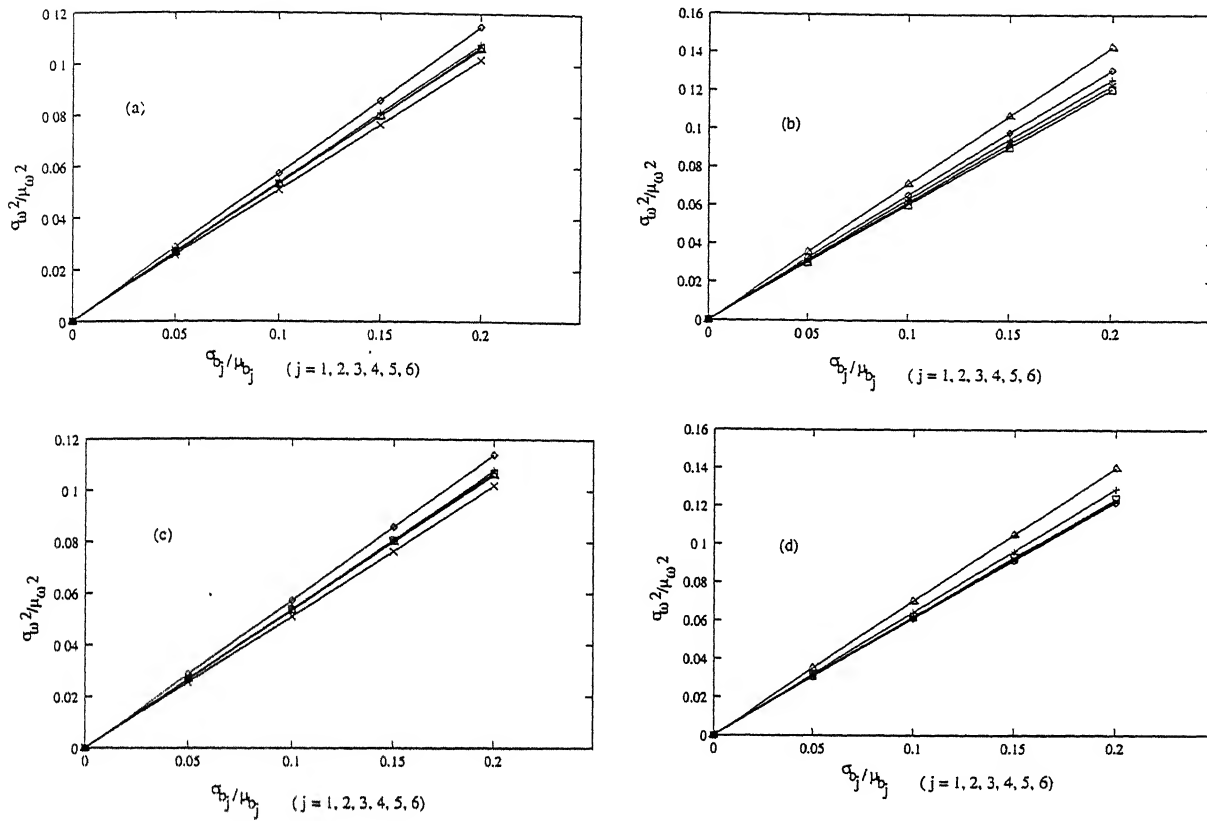


Figure 5.15: Sensitivity of SD of square of the first five natural frequencies with SD of basic material properties, $[0^\circ/90^\circ]$ cylindrical panel, $a/b=1$, with all basic material properties changing simultaneously.

(a) $R/a=5$ and $a/h=10$; (b) $R/a=5$ and $a/h=100$; (c) $R/a=10$ and $a/h=10$; (d) $R/a=10$ and $a/h=100$.

Key: As in Figure 5.14

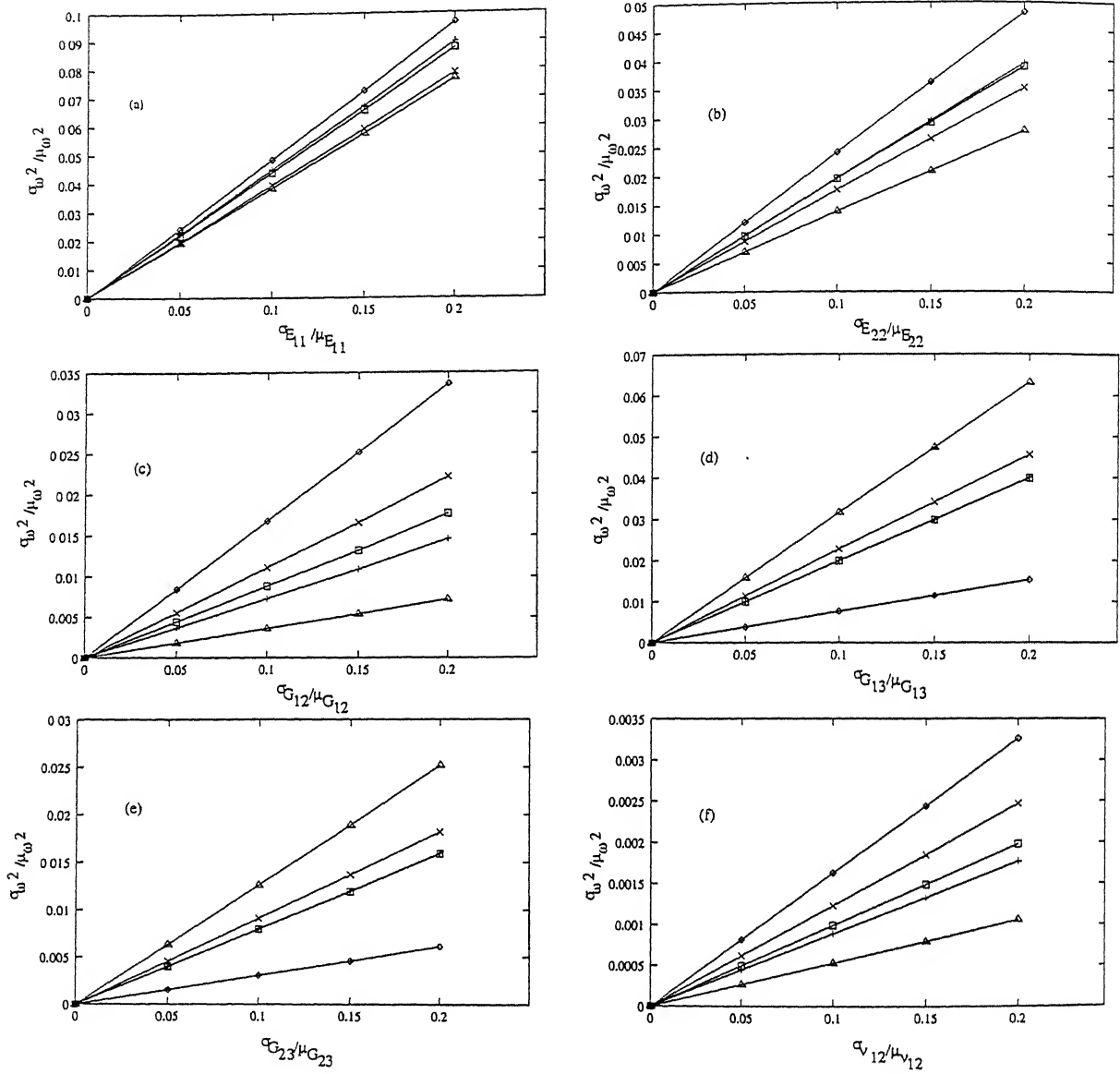


Figure 5.16: Sensitivity of SD of square of the first five natural frequencies with SD of basic material properties, $[0^\circ/90^\circ]$ cylindrical panel, with $R/a=5$, $a/b=1$ and $a/h=10$. (a) only E_{11} varying; (b) only E_{22} varying; (c) only G_{12} varying; (d) only G_{13} varying; (e) only G_{23} varying; (f) only ν_{12} varying.

Key: As in Figure 5.14.

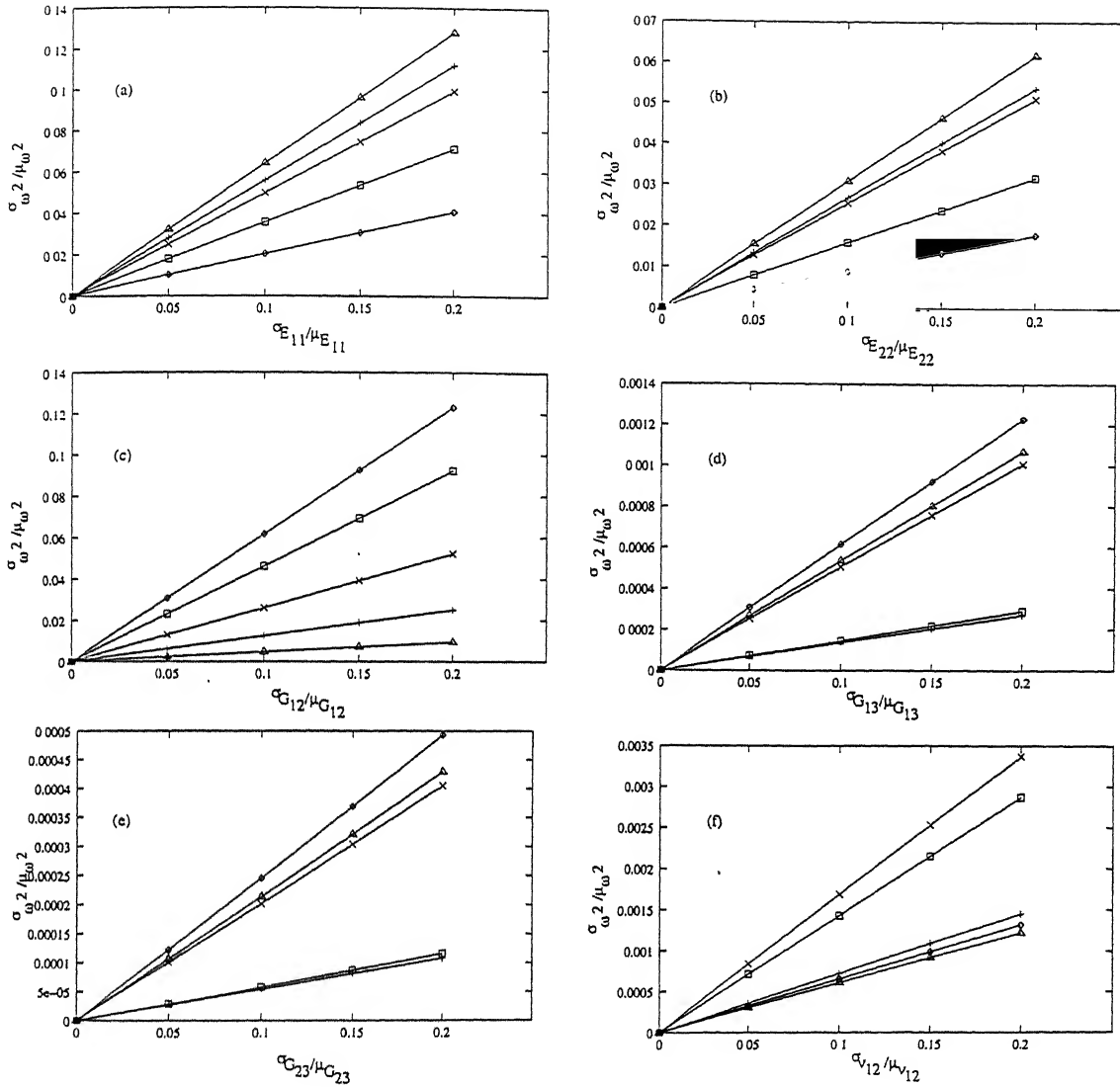


Figure 5.17: Sensitivity of SD of square of the first five natural frequencies with SD of basic material properties, $[0^\circ/90^\circ]$ cylindrical panel, with $R/a=5$, $a/b=1$ and $a/h=100$. (a) only E_{11} varying; (b) only E_{22} varying; (c) only G_{12} varying; (d) only G_{13} varying; (e) only G_{23} varying; (f) only ν_{12} varying. Key: As in Figure 5.14.

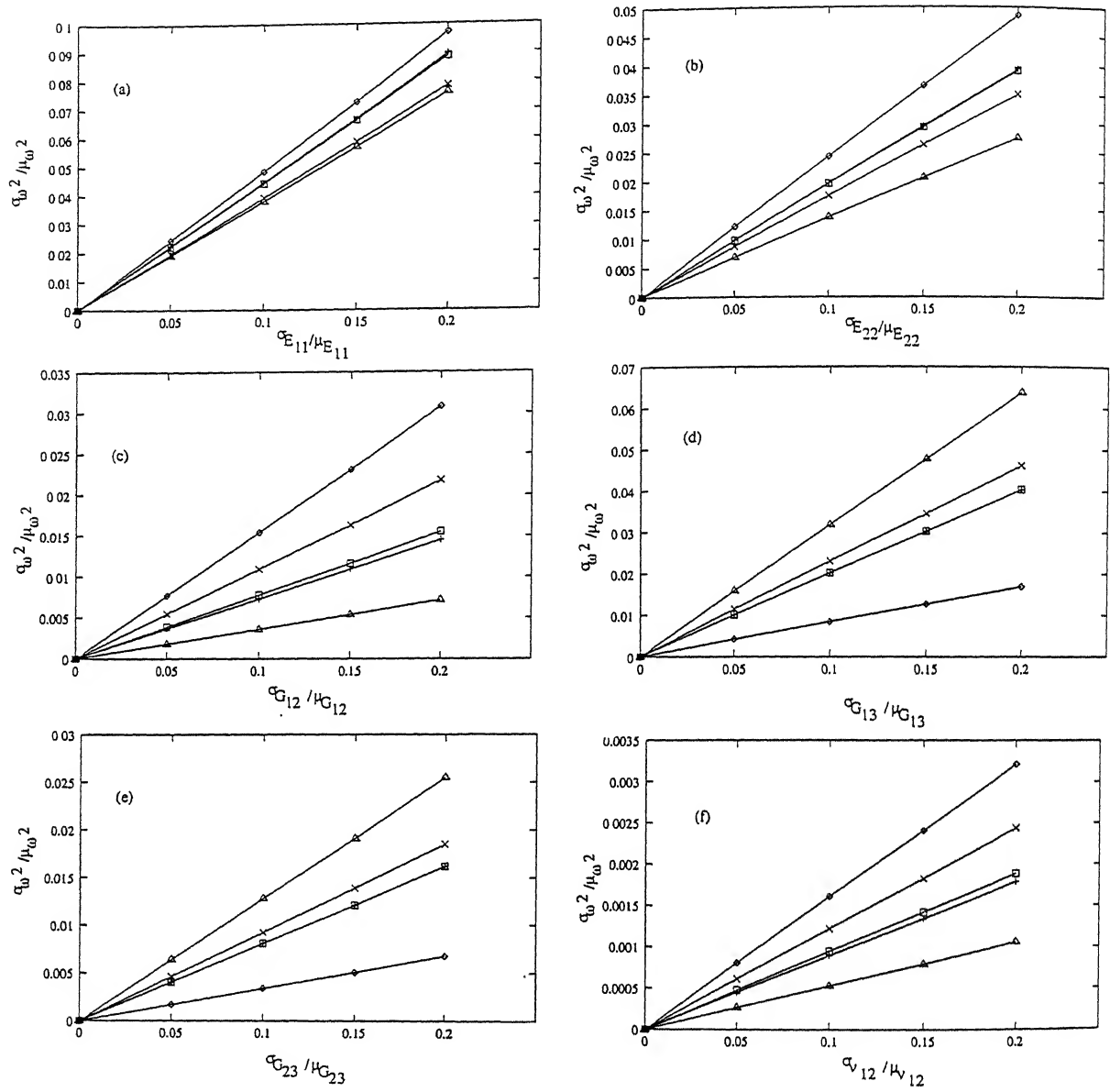


Figure 5.18: Sensitivity of SD of square of the first five natural frequencies with SD of basic material properties, $[0^\circ/90^\circ]$ cylindrical panel, with $R/a=10$, $a/b=1$ and $a/h=10$. (a) only E_{11} varying; (b) only E_{22} varying; (c) only G_{12} varying; (d) only G_{13} varying; (e) only G_{23} varying; (f) only ν_{12} varying.

Key: As in Figure 5.14.

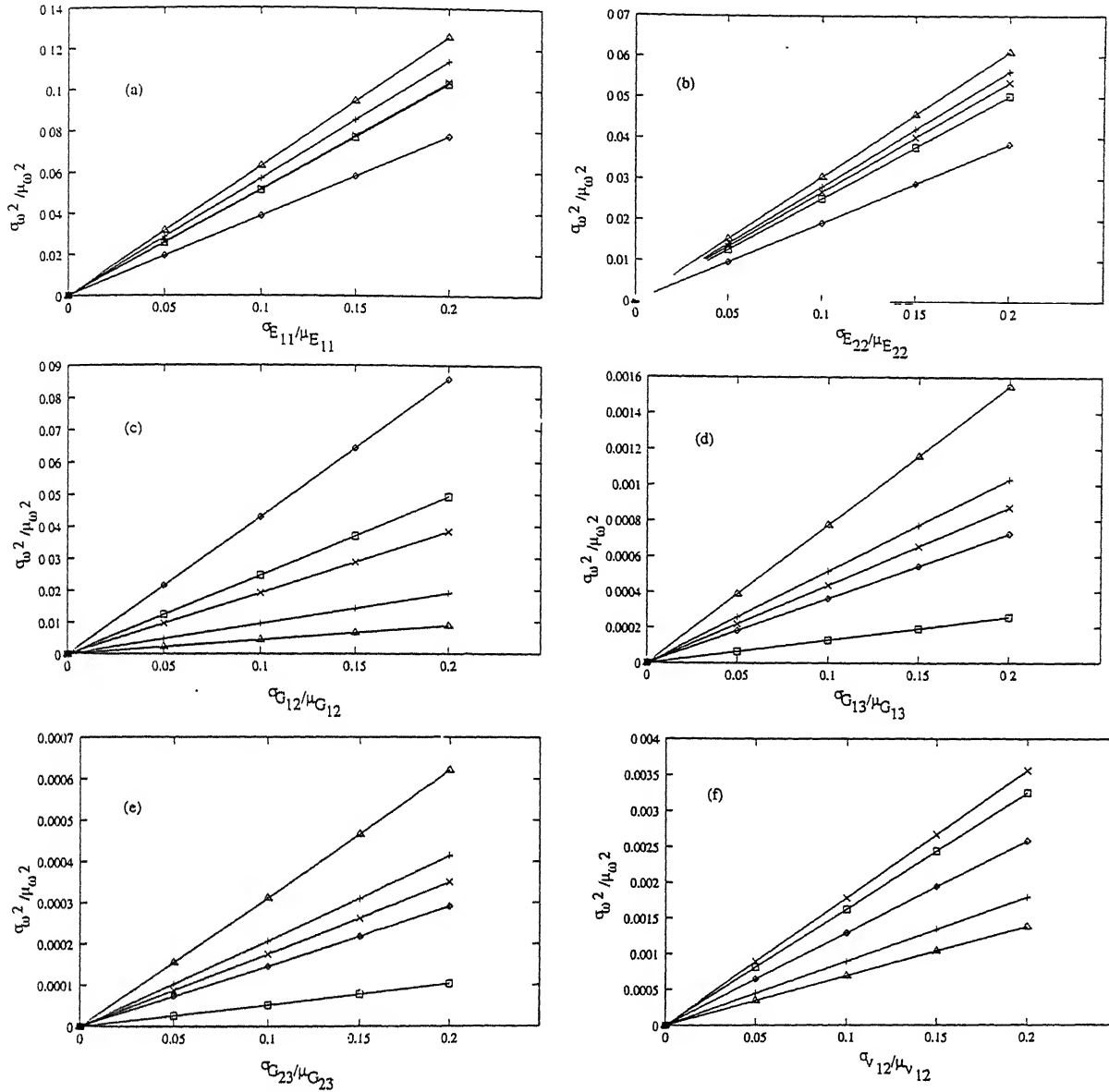


Figure 5.19: Sensitivity of SD of square of the first five natural frequencies with SD of basic material properties, $[0^\circ/90^\circ]$ cylindrical panel, with $R/a=10$, $a/b = 1$ and $a/h=100$. (a) only E_{11} varying; (b) only E_{22} varying; (c) only G_{12} varying; (d) only G_{13} varying; (e) only G_{23} varying; (f) only ν_{12} varying.

Key: As in Figure 5.14.

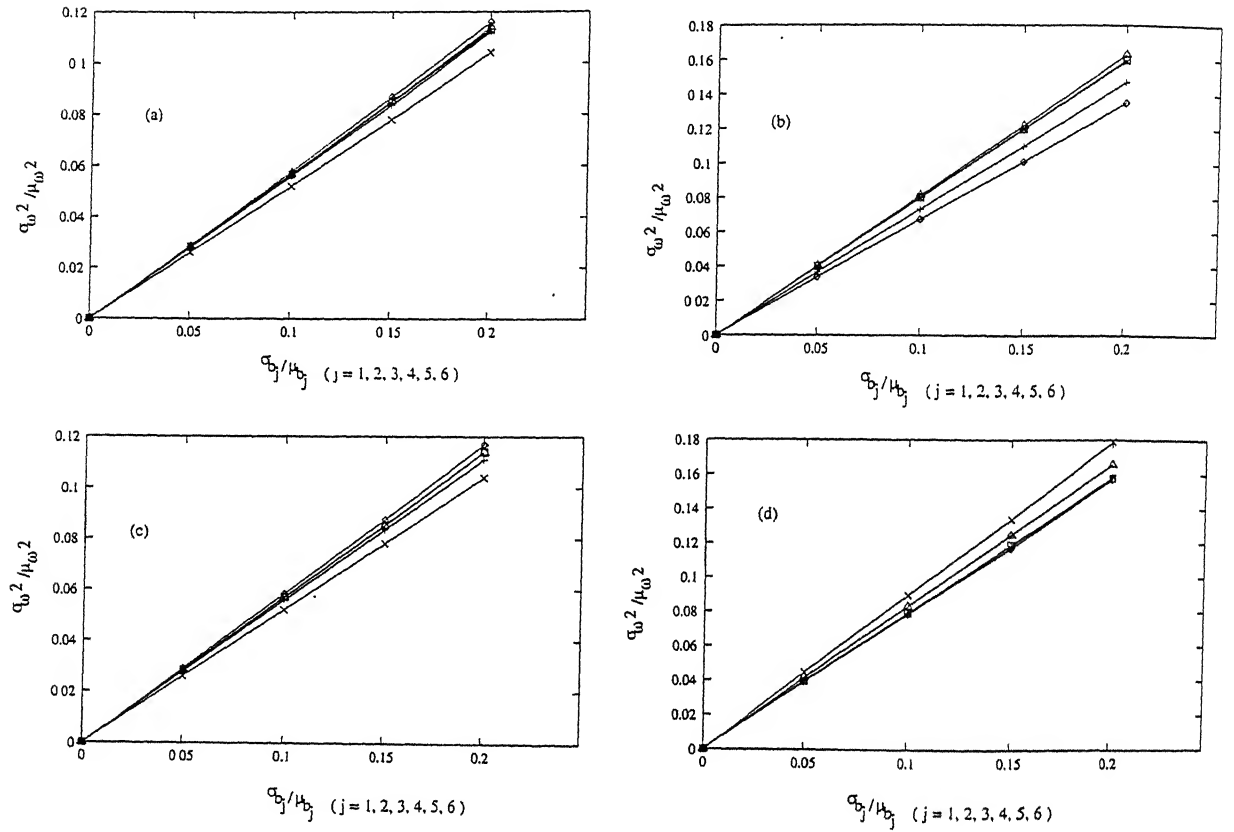


Figure 5.20: Sensitivity of SD of square of the first five natural frequencies with SD of basic material properties, $[0^\circ/90^\circ/90^\circ/0^\circ]$ cylindrical panel, $a/b=1$, with all basic material properties changing simultaneously.
 (a) $R/a=5$ and $a/h=10$; (b) $R/a=5$ and $a/h=100$; (c) $R/a=10$ and $a/h=10$; (d) $R/a=10$ and $a/h=100$.

Key: As in Figure 5.14.

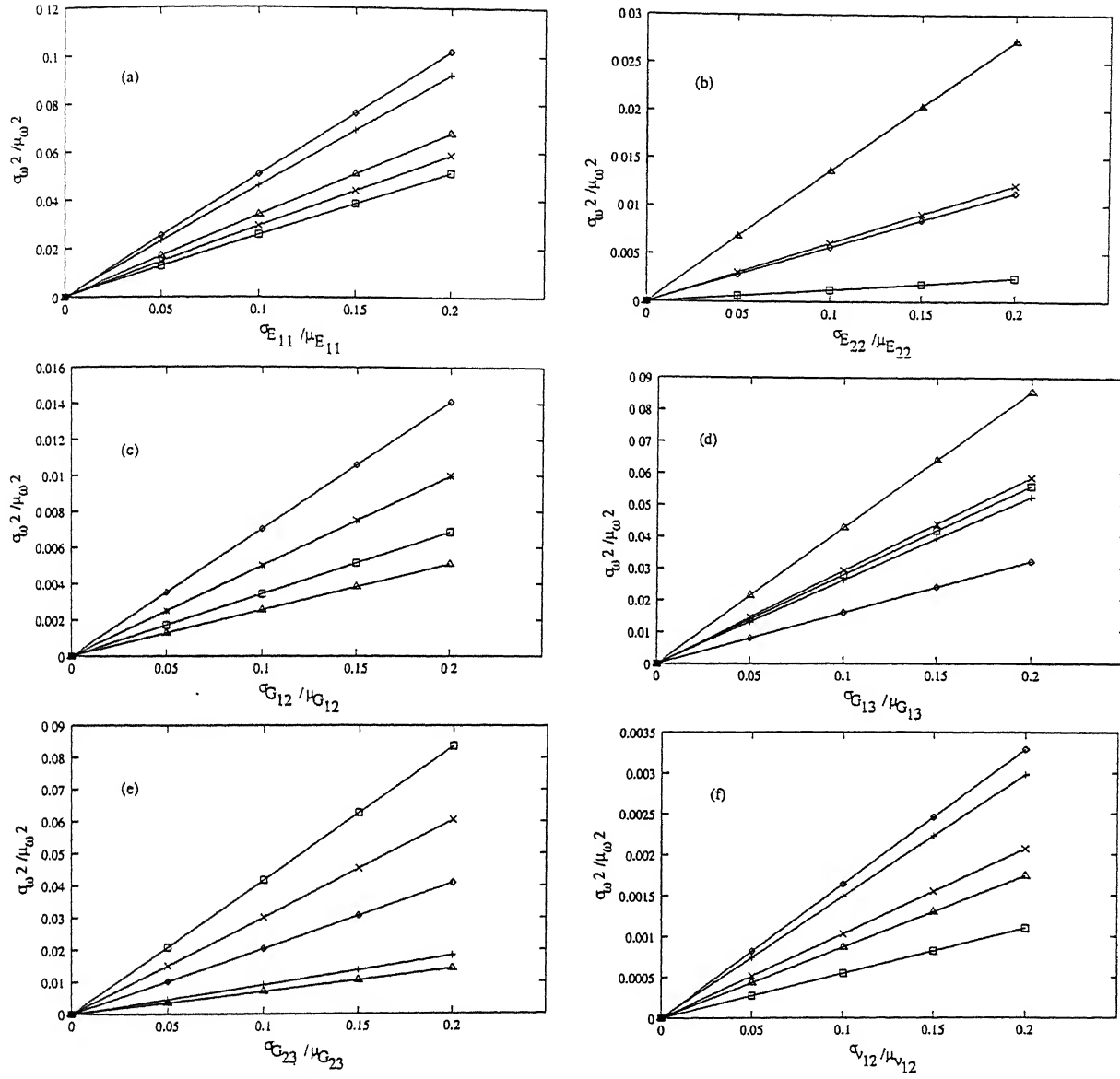


Figure 5.21: Sensitivity of SD of square of the first five natural frequencies with SD of basic material properties, $[0^\circ/90^\circ/90^\circ]$ cylindrical panel, with $R/a=5$, $a/b=1$ and $a/h=10$. (a) only E_{11} varying; (b) only E_{22} varying; (c) only G_{12} varying; (d) only G_{13} varying; (e) only G_{23} varying; (f) only ν_{12} varying.

Key: As in Figure 5.14.

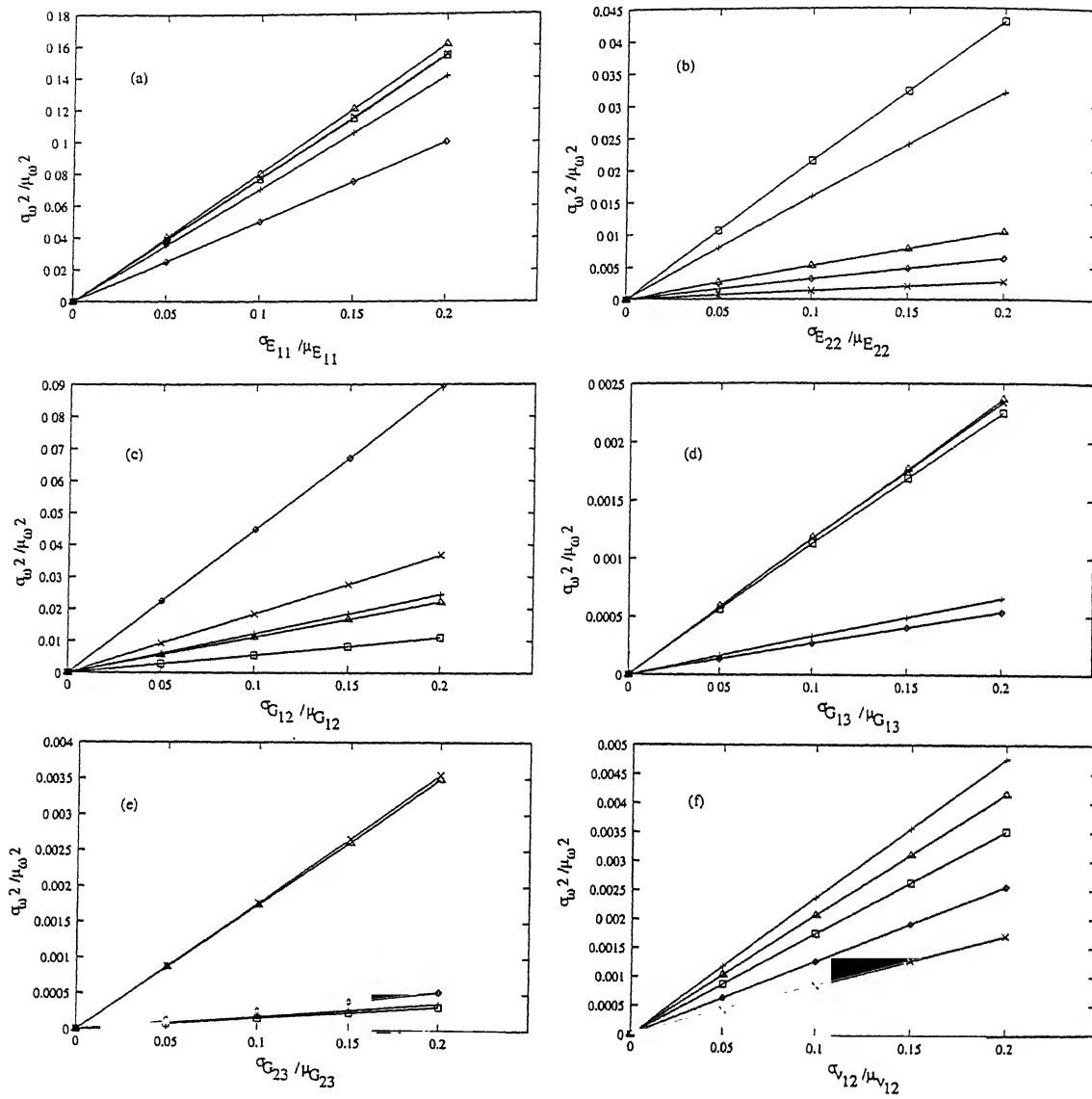


Figure 5.22: Sensitivity of SD of square of the first five natural frequencies with SD of basic material properties, $[0^\circ/90^\circ/90^\circ/0^\circ]$ cylindrical panel, with $R/a=10$, $a/b = 1$ and $a/h=100$.

(a) only E_{11} varying; (b) only E_{22} varying; (c) only G_{12} varying; (d) only G_{13} varying; (e) only G_{23} varying; (f) only ν_{12} varying.

Key: As in Figure 5.14.

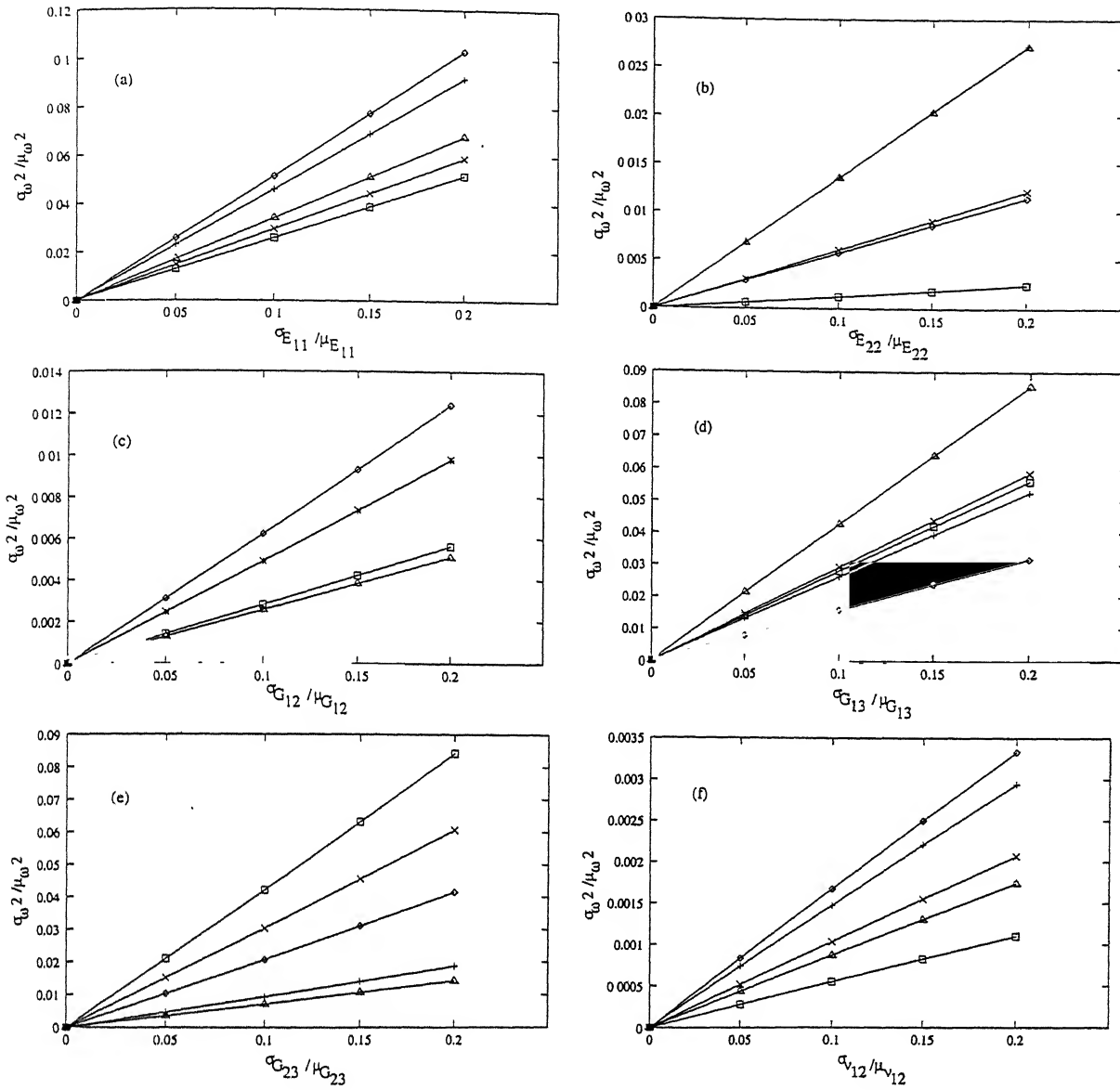


Figure 5.23: Sensitivity of SD of square of the first five natural frequencies with SD of basic material properties, $[0^\circ/90^\circ/90^\circ/0^\circ]$ cylindrical panel, with $R/a=10$, $a/b = 1$ and $a/h=10$.

(a) only E_{11} varying; (b) only E_{22} varying; (c) only G_{12} varying; (d) only G_{13} varying; (e) only G_{23} varying; (f) only ν_{12} varying.

Key: As in Figure 5.14.

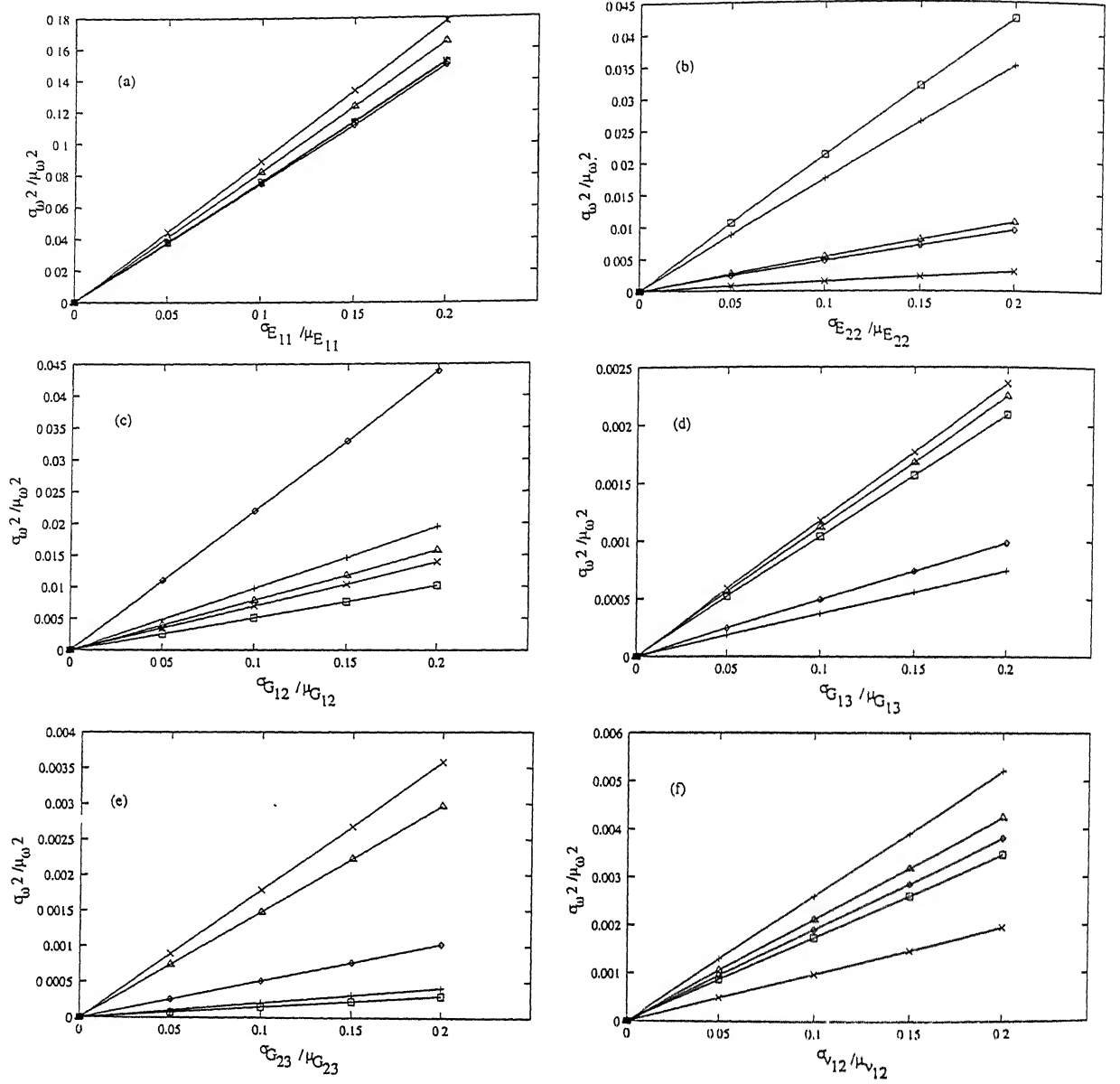


Figure 5.24: Sensitivity of SD of square of the first five natural frequencies with SD of basic material properties, $[0^\circ/90^\circ/90^\circ/0^\circ]$ cylindrical panel, with $R/a=10$, $a/b=1$ and $a/h=100$.

(a) only E_{11} varying; (b) only E_{22} varying; (c) only G_{12} varying; (d) only G_{13} varying; (e) only G_{23} varying; (f) only ν_{12} varying.

Key: As in Figure 5.14.

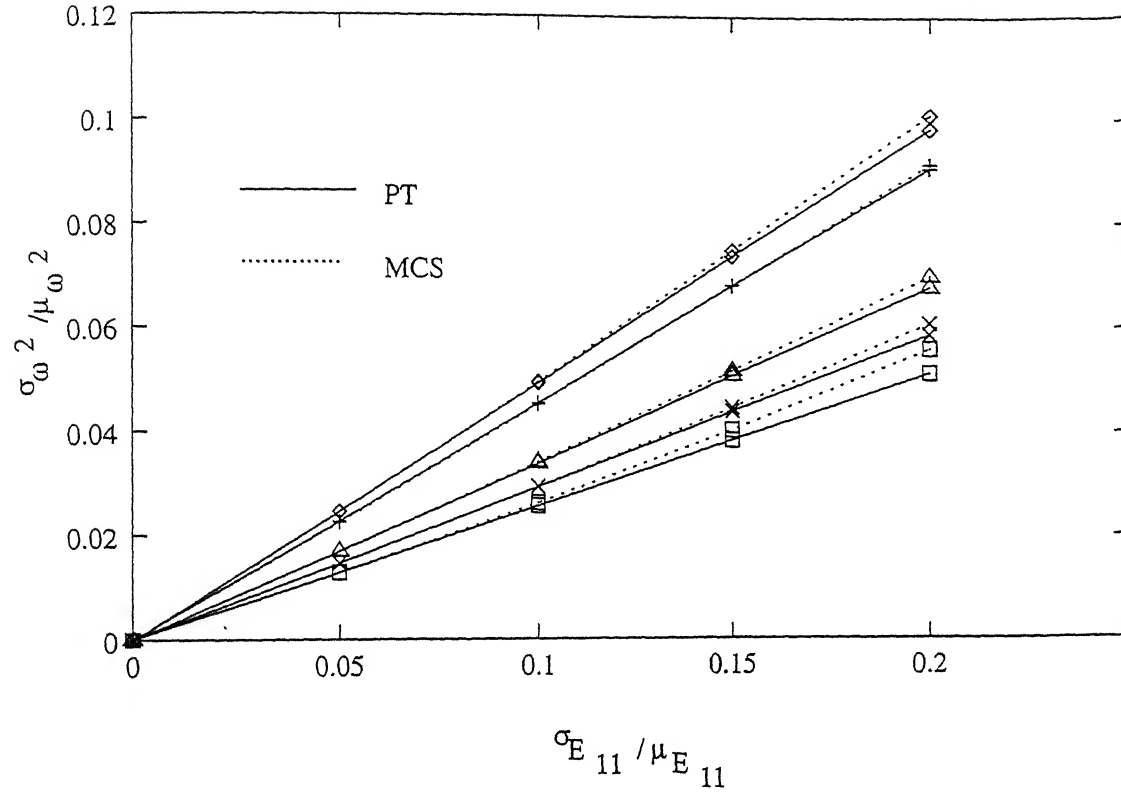


Figure 5.25: Comparison of result from Monte Carlo simulation with the present approach, $[0^\circ/90^\circ/90^\circ/0^\circ]$ spherical panel, with $R/a=5$, $a/b=1$ and $a/h=10$ for SSSS. Key:- \diamond : first mode, $+$: second mode, \square : third mode, \times : fourth mode, \triangle : fifth mode.

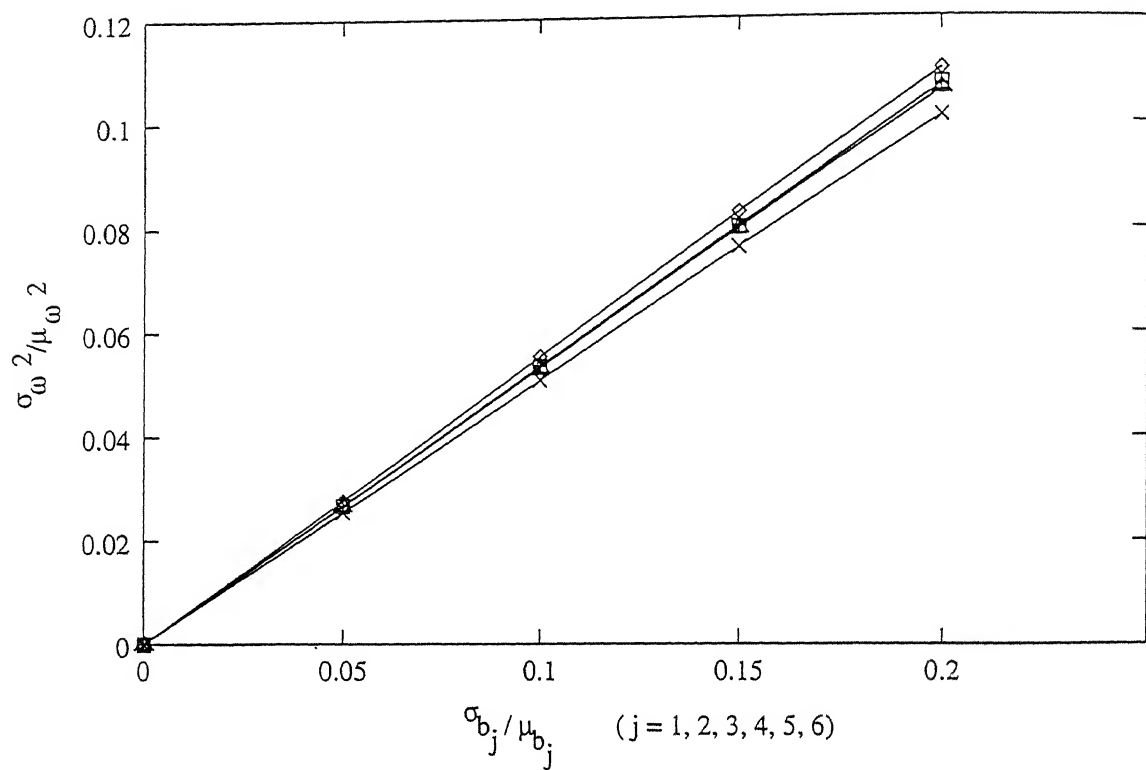


Figure 5.26: Variation of SD of square of the first five natural frequencies with SD of basic material properties, $[0^\circ/90^\circ]$ spherical panel, $R/a=5$, $a/h=10$ and $a/b=1$, with all basic material properties changing simultaneously for SSSS.

Key: As in Figure 5.25.

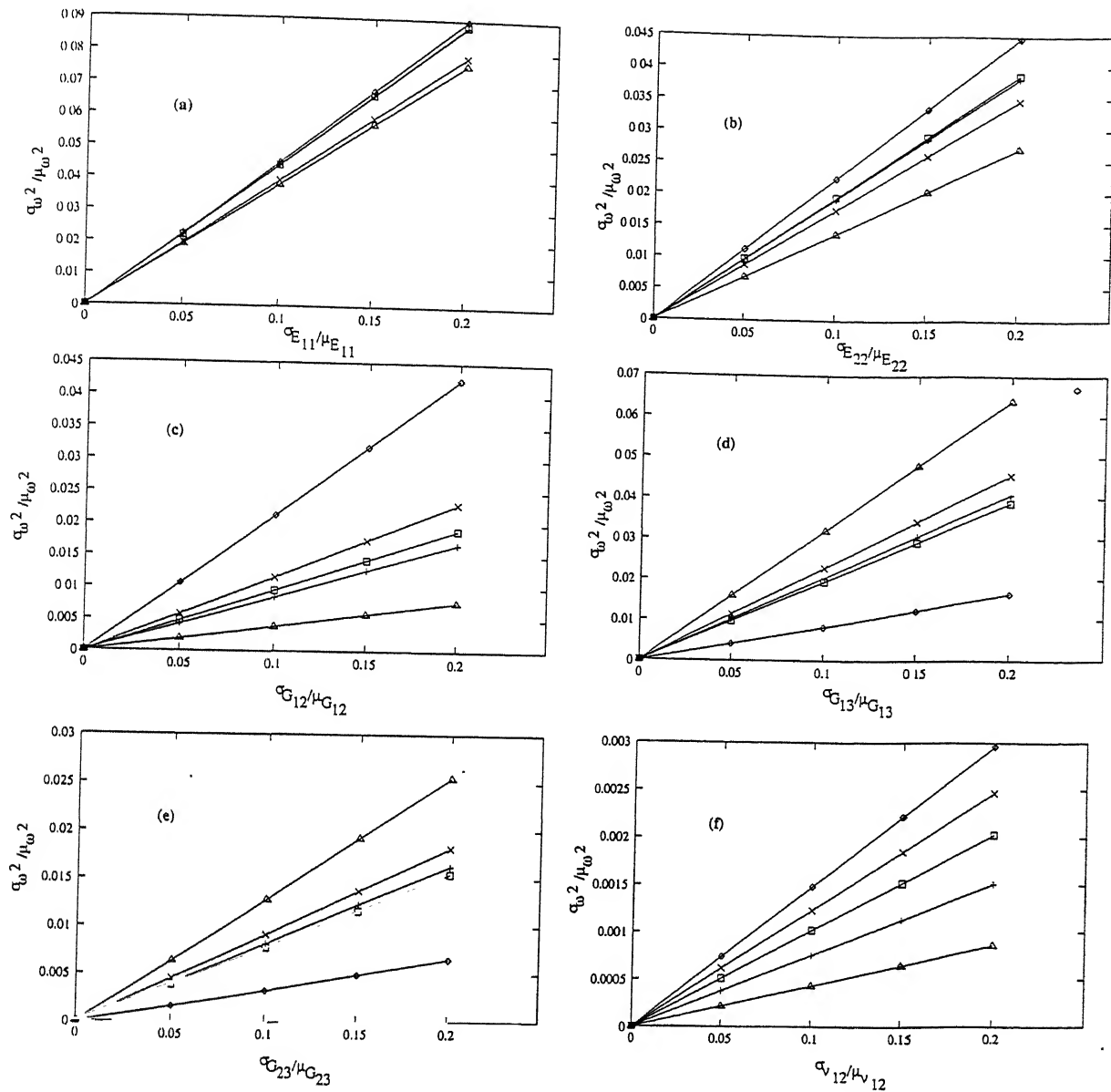


Figure 5.27: Variation of SD of square of the first five natural frequencies with SD of basic material properties, $[0^\circ/90^\circ]$ spherical panel, with $R/a=5$, $a/b=1$ and $a/h=10$ for SSSS. (a) only E_{11} varying; (b) only E_{22} varying; (c) only G_{12} varying; (d) only G_{13} varying; (e) only G_{23} varying; (f) only ν_{12} varying.

Key: As in Figure 5.25.

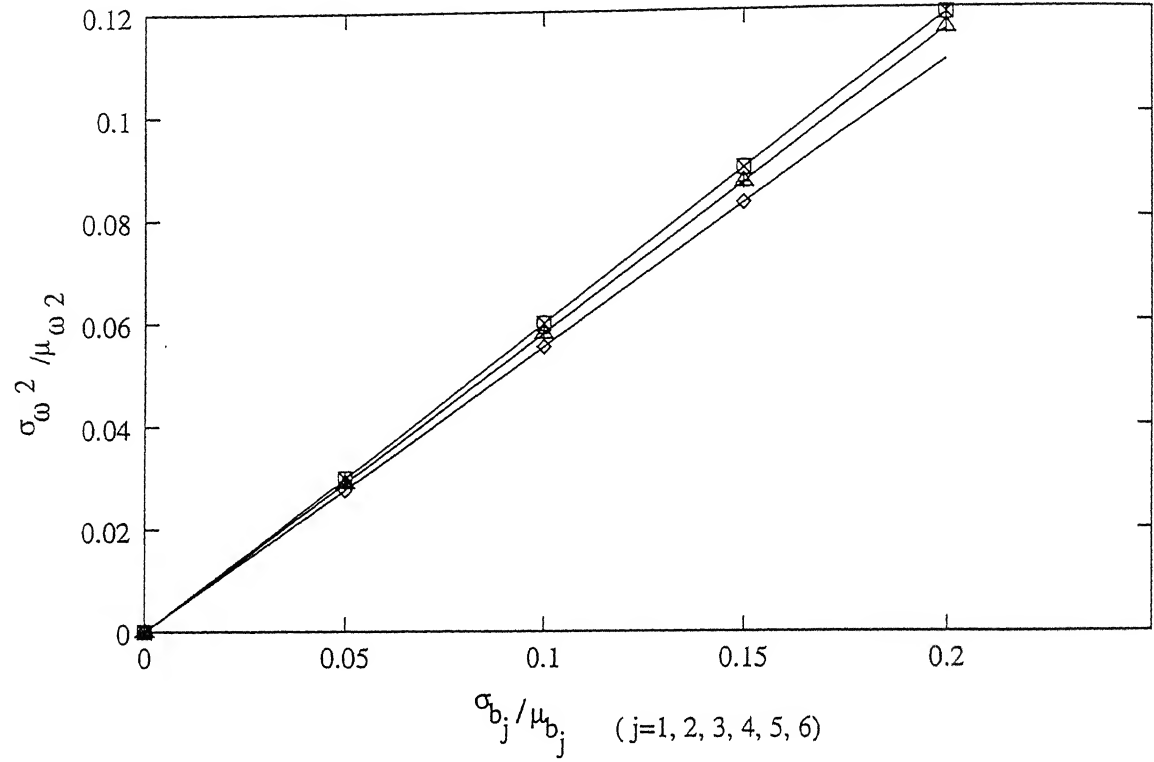


Figure 5.28: Variation of SD of square of the fundamental frequency with SD of basic material properties $[0^\circ/90^\circ]$ spherical panel, $R/a=5$, $a/h=10$ and $a/b=1$, with all basic material properties changing simultaneously.

Key:- \diamond : SSSS +: SCSC, \square : SFSC, \times : SFSS, \triangle : SSSC.

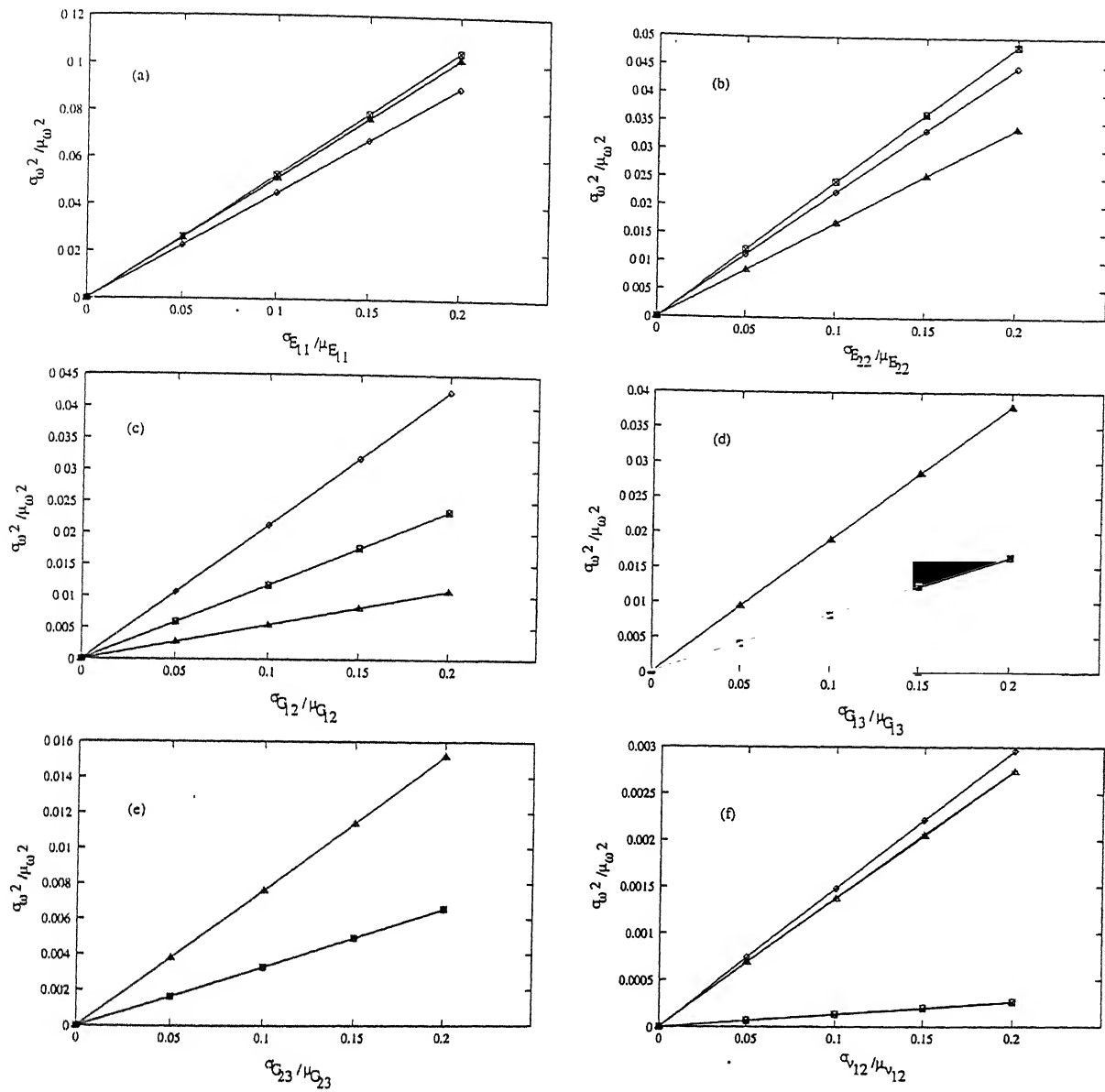


Figure 5.29: Variation of SD of square of the first five natural frequencies with SD of basic material properties, $[0^\circ/90^\circ]$ spherical panel, with $R/a=5$, $a/b=1$ and $a/h=10$.
 (a) only E_{11} varying; (b) only E_{22} varying; (c) only G_{12} varying; (d) only G_{13} varying; (e) only G_{23} varying; (f) only ν_{12} varying.

Key: As in Figure 5.28.

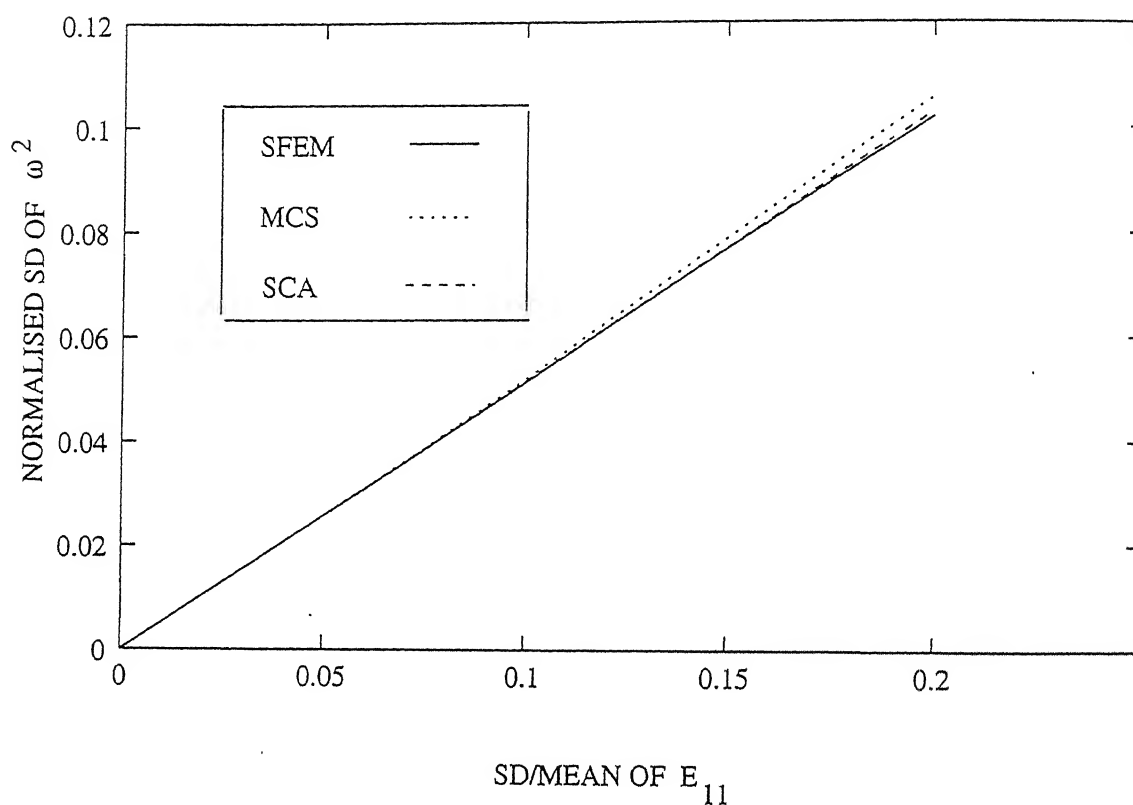


Figure 5.30: Comparison of the probabilistic finite element results with MCS and SCA for $[0^\circ/90^\circ/90^\circ/0^\circ]$ laminated SSSS square plate, with $a/h=10$.

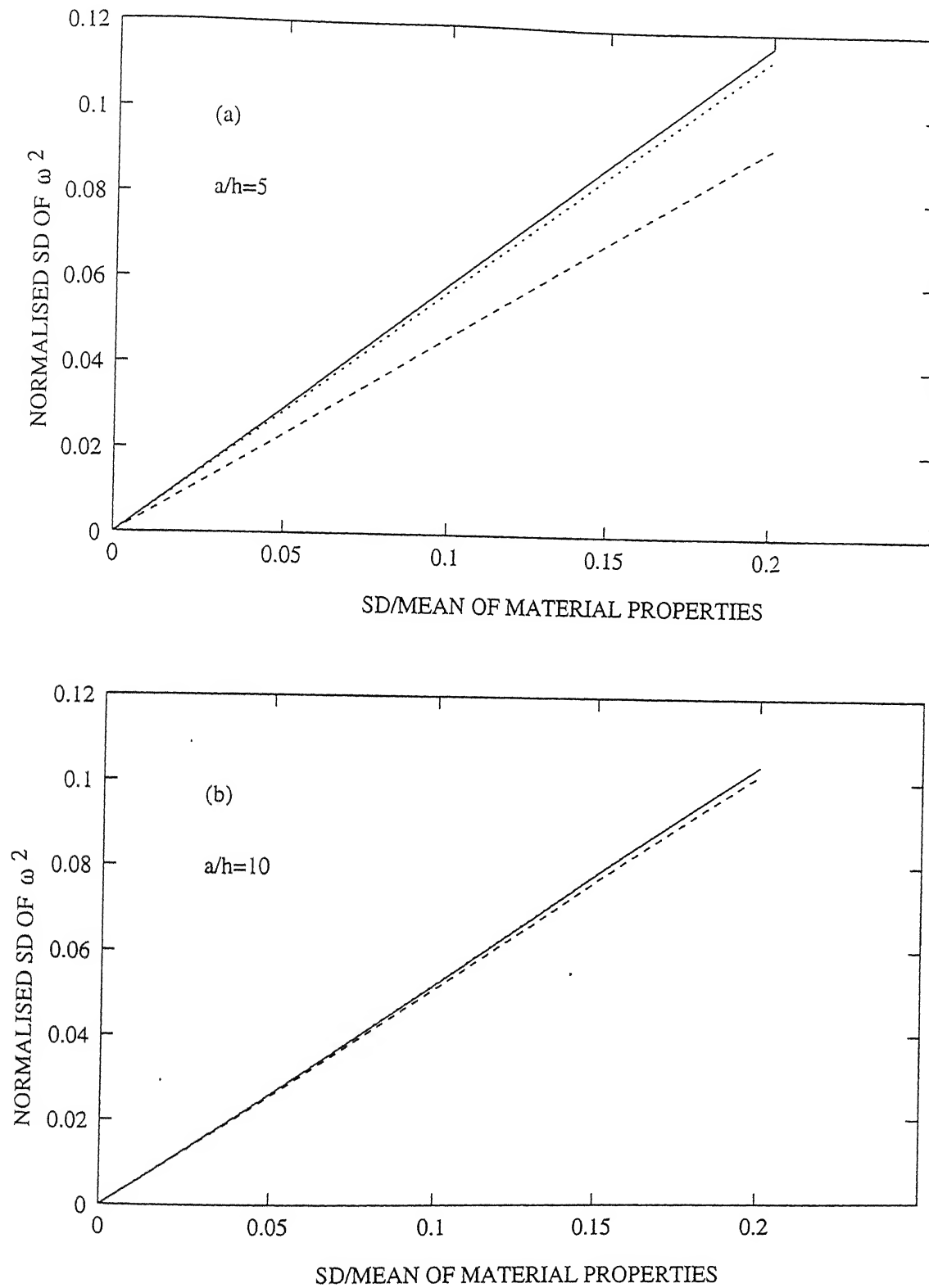


Figure 5.31: Variation of square of the fundamental frequency of a $[0^\circ/45^\circ/-45^\circ/90^\circ]$ laminated composite square plate with SD of material properties varying simultaneously for $a/h=5$ and 10.

Key:- — SSSS, CFCF, - - - CCCC.

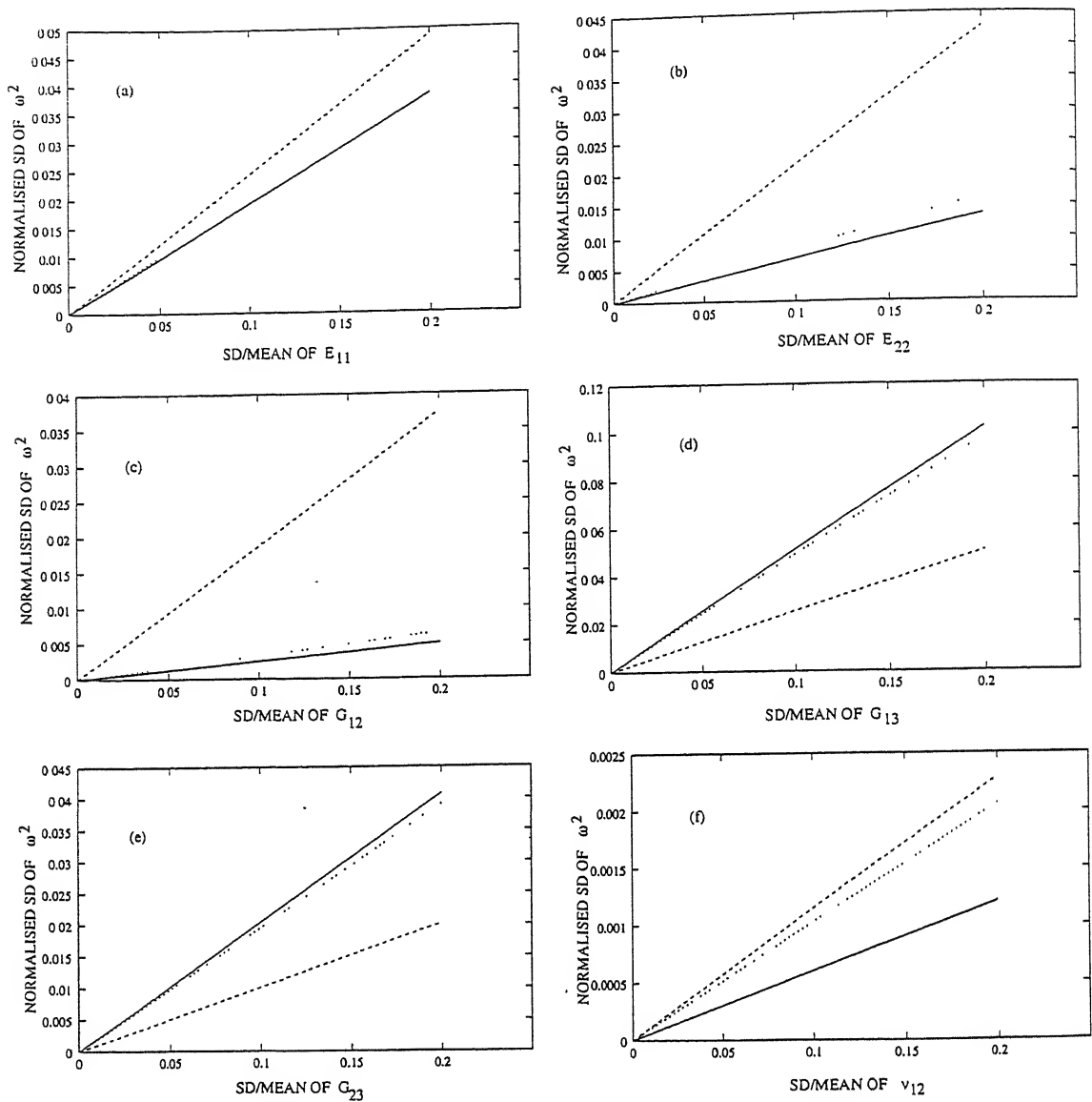


Figure 5.32: Variation of normalized SD of square of the fundamental frequency of a $[0^\circ/45^\circ/-45^\circ/90^\circ]$ laminated square plate with SD of material properties changing at a time for $a/h=5$.
Key: As in Figure 5.31.

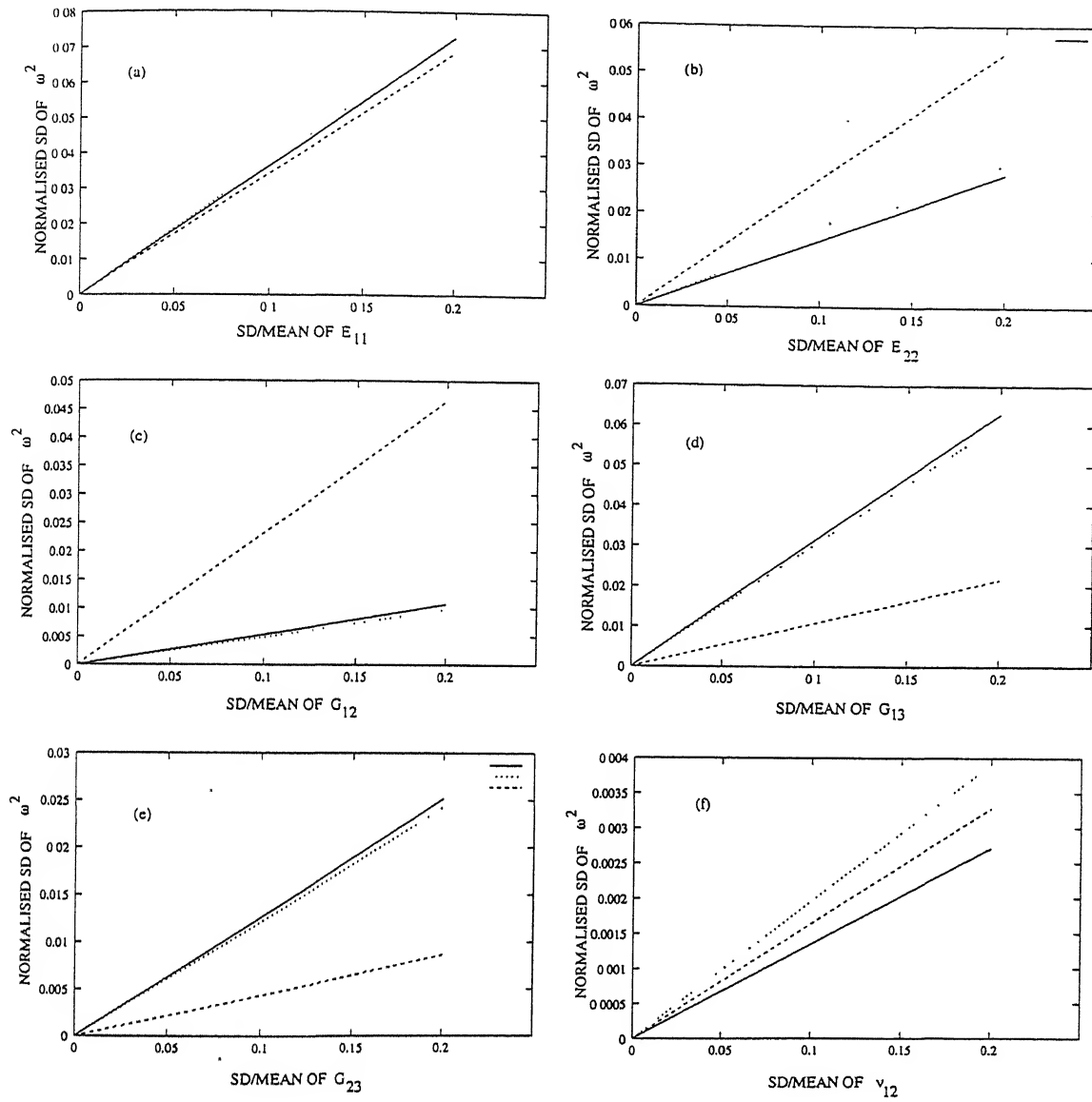


Figure 5.33: Variation of normalized SD of square of the fundamental frequency of a $[0^\circ/45^\circ/-45^\circ/90^\circ]$ laminated square plate with SD of material properties changing at a time for $a/h = 10$.

Key: As in Figure 5.31.

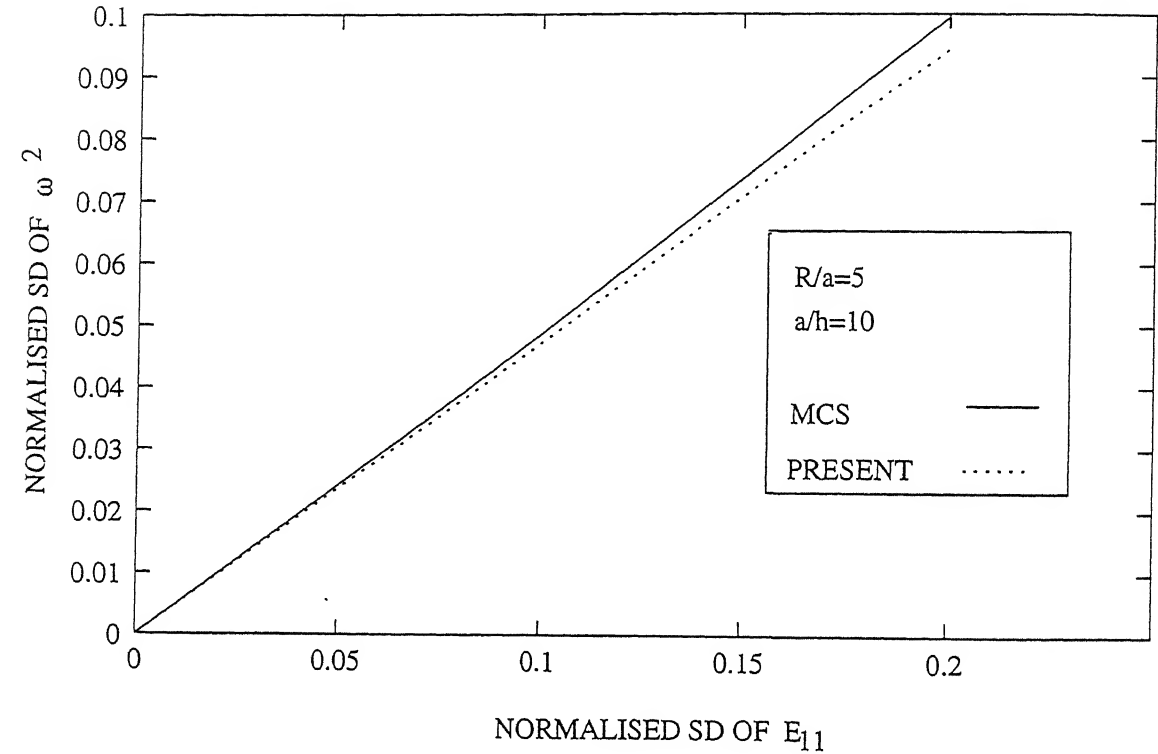


Figure 5.34: Comparison of the probabilistic finite element results with MCS for a $[0^\circ/90^\circ/0^\circ]$ cylindrical square panel.

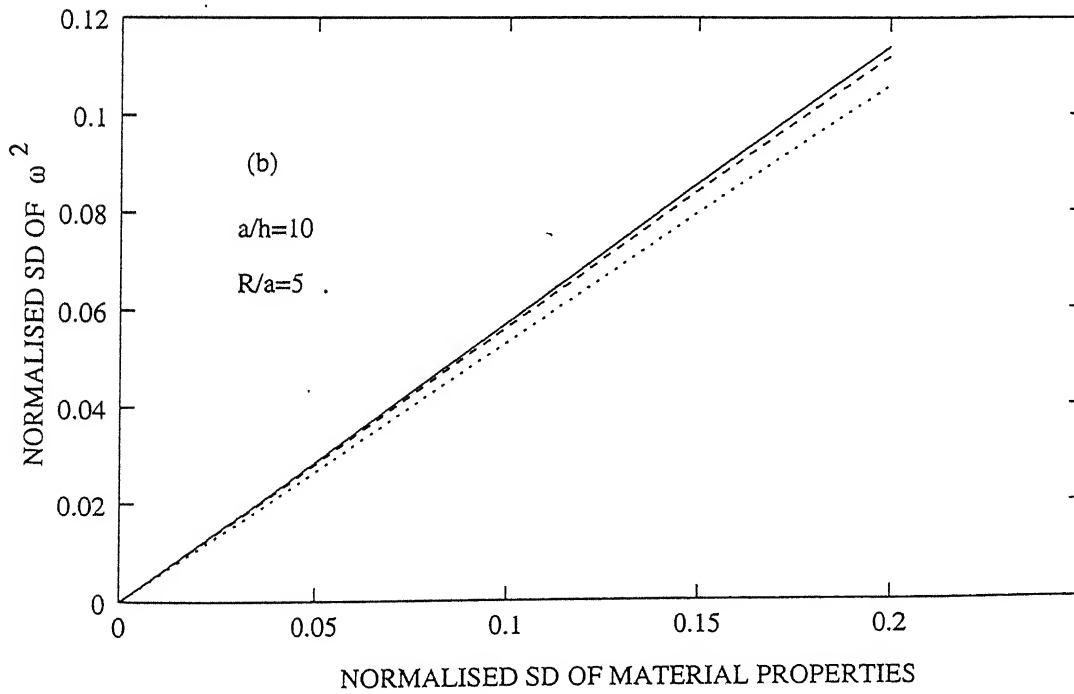
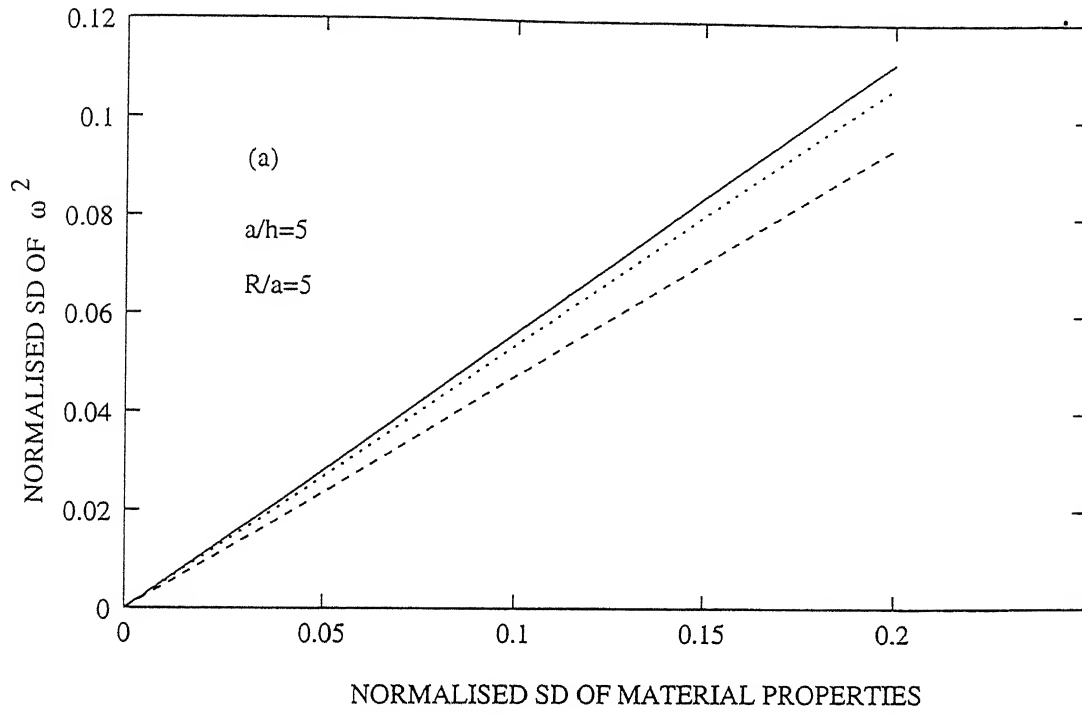


Figure 5.35: Variation of SD of square of the fundamental frequency of a $[0^\circ/45^\circ/-45^\circ/90^\circ]$ cylindrical square panel with SD of basic material properties changing simultaneously.

Key:- — :CCCC, :CFCF, - - - :SSSS.

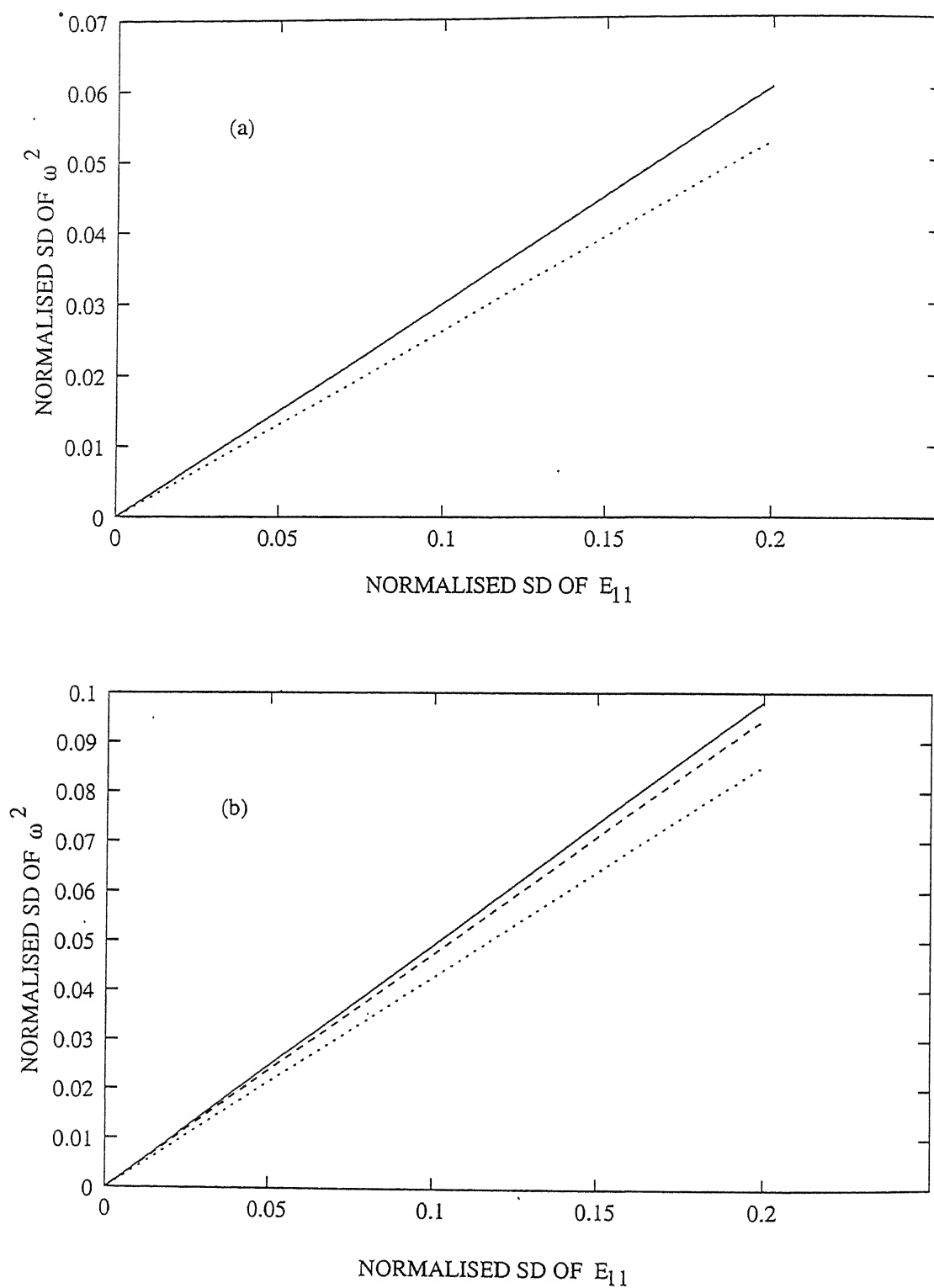


Figure 5.36: Variation of SD of square of the fundamental frequency of a $[0^\circ/45^\circ/-45^\circ/90^\circ]$ cylindrical square panel with SD of longitudinal elastic modulus E_{11} .

Key: As in Figure 5.35.

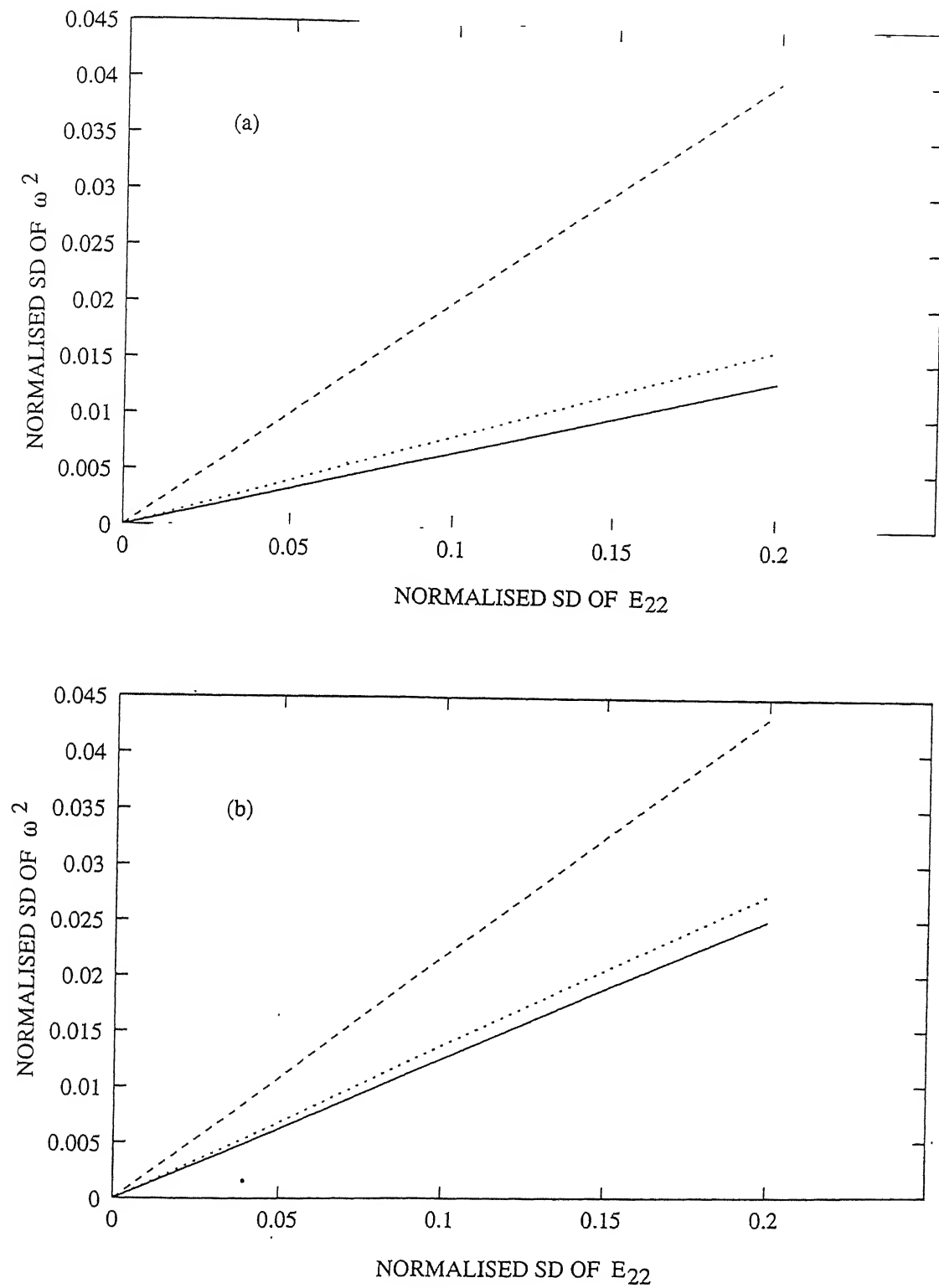


Figure 5.37: Variation of SD of square of the fundamental frequency of a $[0^\circ/45^\circ/-45^\circ/90^\circ]$ cylindrical square panel with SD of transverse elastic modulus E_{22} .
Key: As in Figure 5.35.

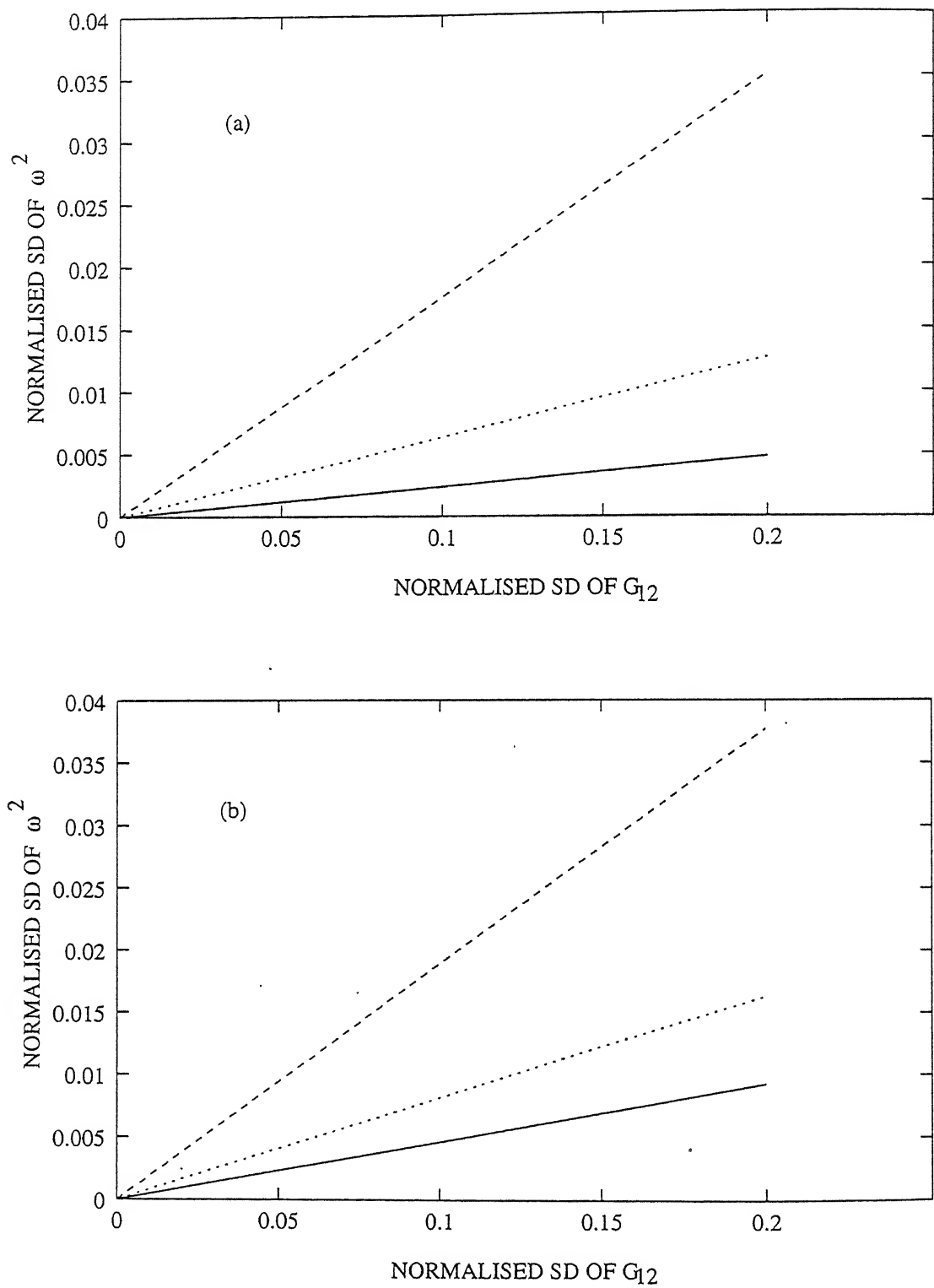


Figure 5.38: Variation of SD of square of the fundamental frequency of a $[0^\circ/45^\circ/-45^\circ/90^\circ]$ cylindrical square panel with SD of in plane shear modulus G_{12} .
Key: As in Figure 5.35.

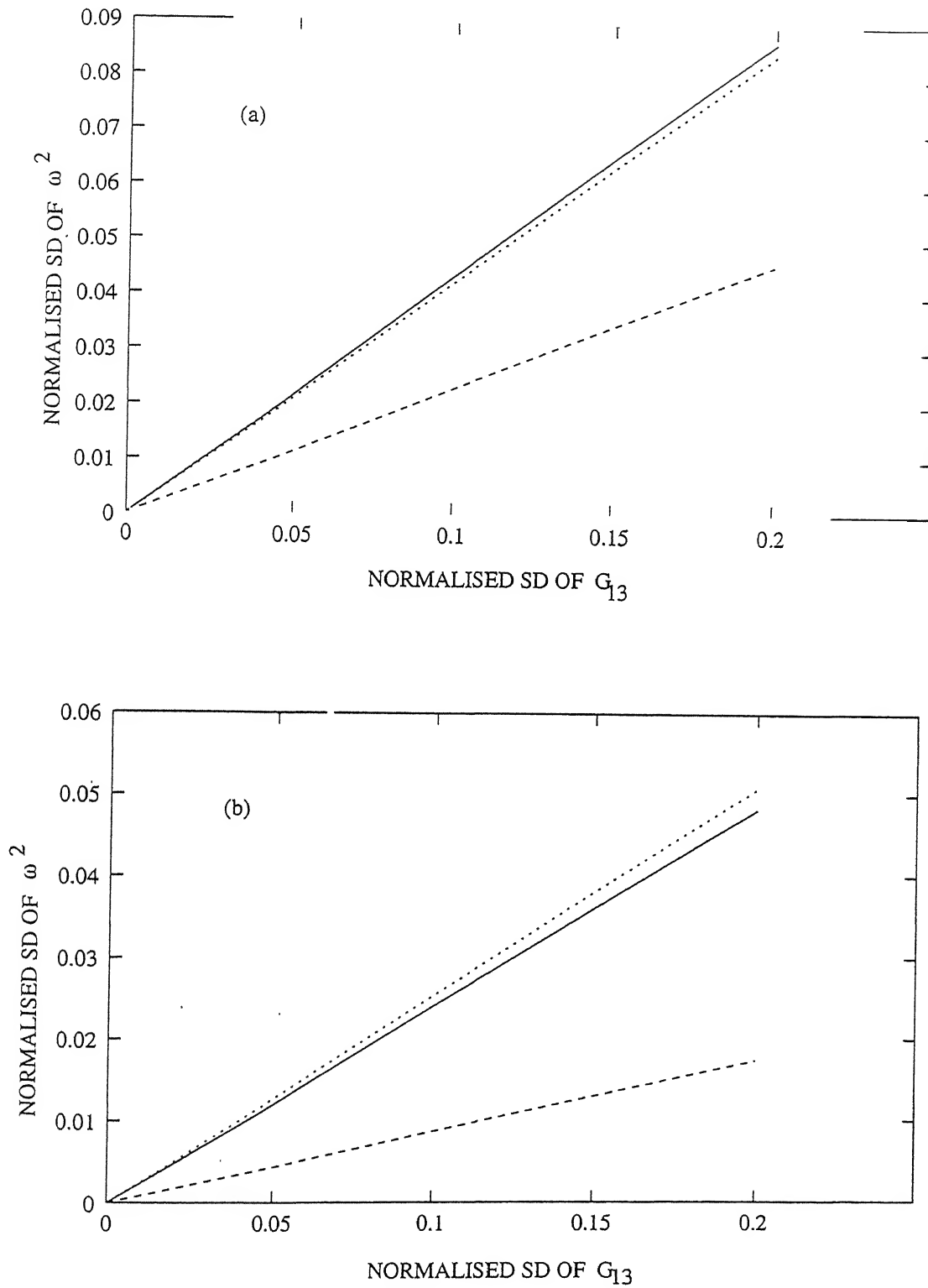


Figure 5.39: Variation of SD of square of the fundamental frequency of a $[0^\circ/45^\circ/-45^\circ/90^\circ]$ cylindrical square panel with SD of out-of-plane shear modulus G_{13} .
Key: As in Figure 5.35.

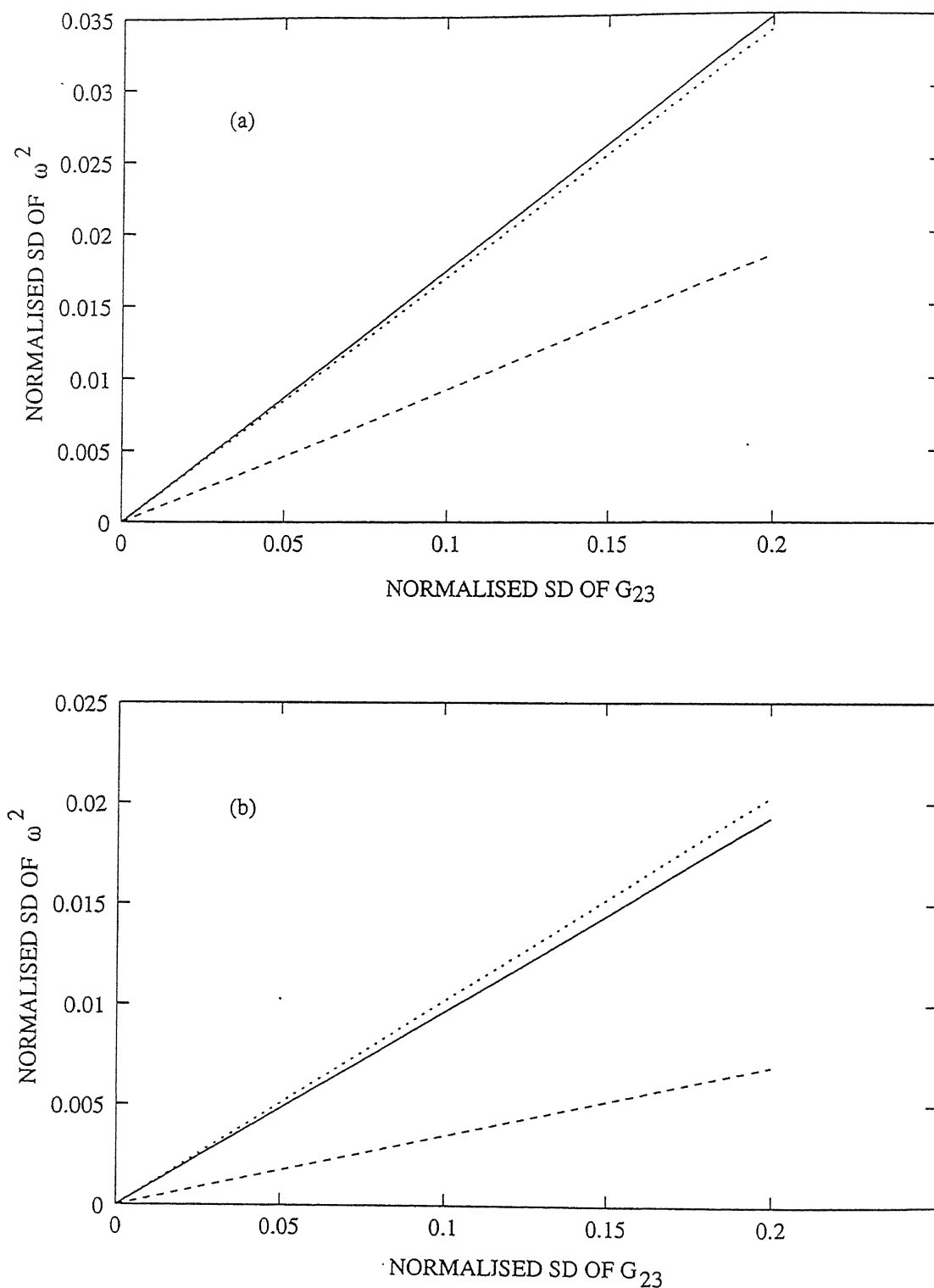


Figure 5.40: Variation of SD of square of the fundamental frequency of a $[0^\circ/45^\circ/-45^\circ/90^\circ]$ cylindrical square panel with SD of out-of-plane shear modulus G_{23} .
Key: As in Figure 5.35.

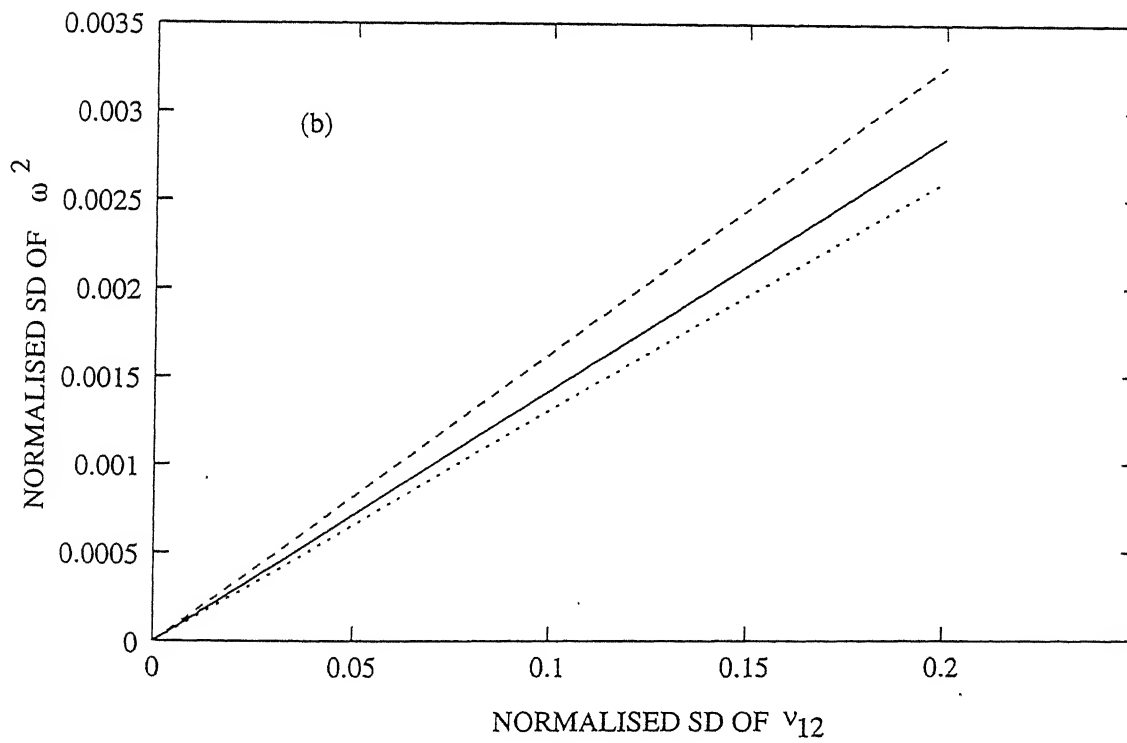
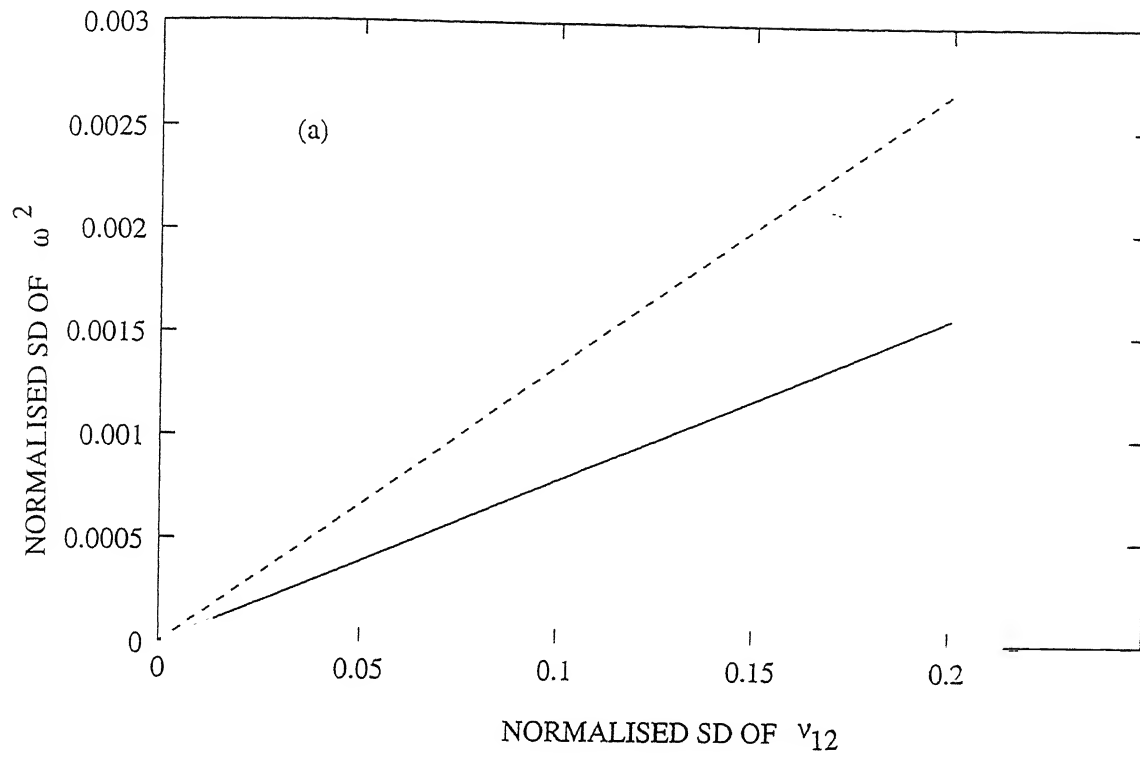


Figure 5.41: Variation of SD of square of the fundamental frequency of a $[0^\circ/45^\circ/-45^\circ/90^\circ]$ cylindrical square panel with SD of Poisson's ratio ν_{12} .

Key: As in Figure 5.35.

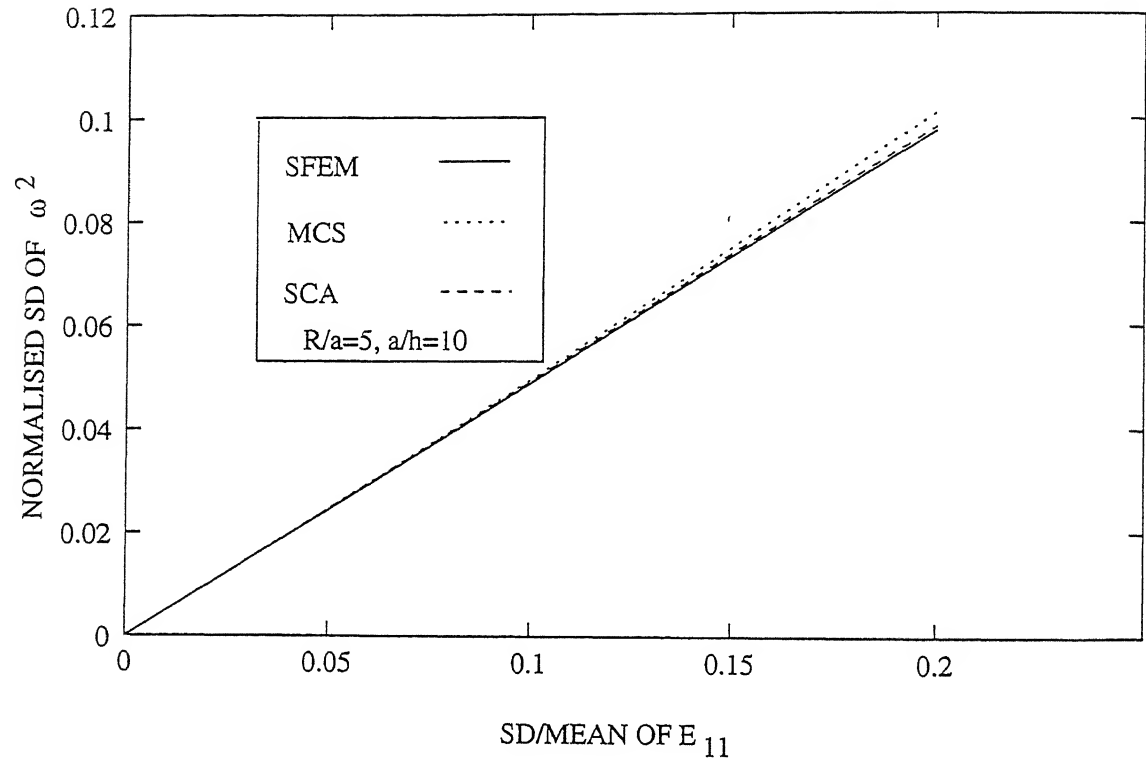


Figure 5.42: Comparison of probabilistic finite element results with MCS and SCA for a $[0^\circ/90^\circ/90^\circ/0^\circ]$ spherical laminate with $a/b=1$.

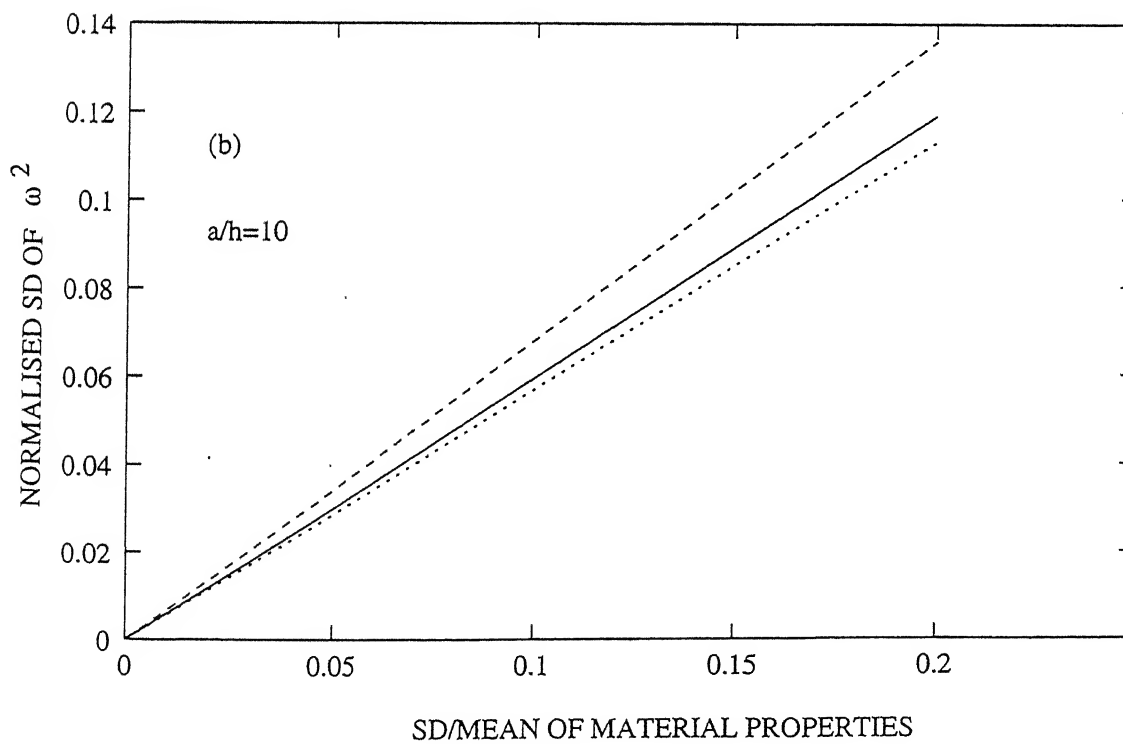
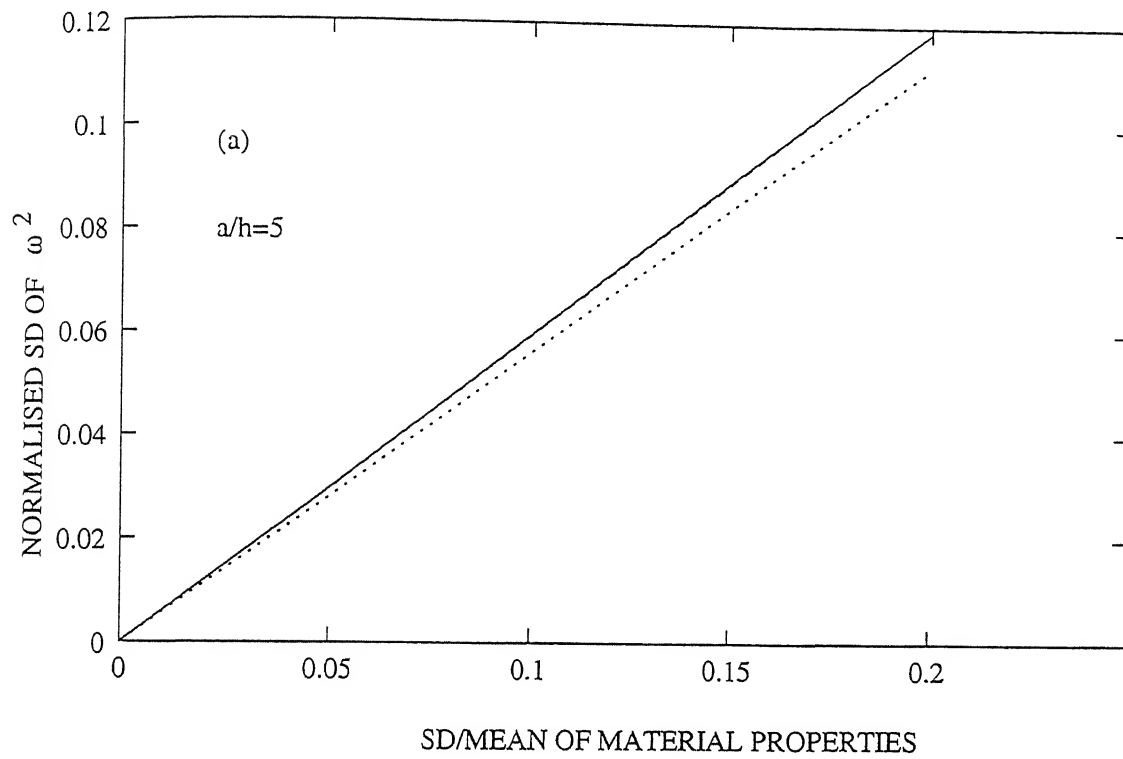


Figure 5.43: Variation of dispersion of square of the fundamental frequency of a $[45^\circ/-45^\circ/45^\circ/-45^\circ]$ spherical square panel against simultaneous variation of material properties.

Key: As in Figure 5.35.

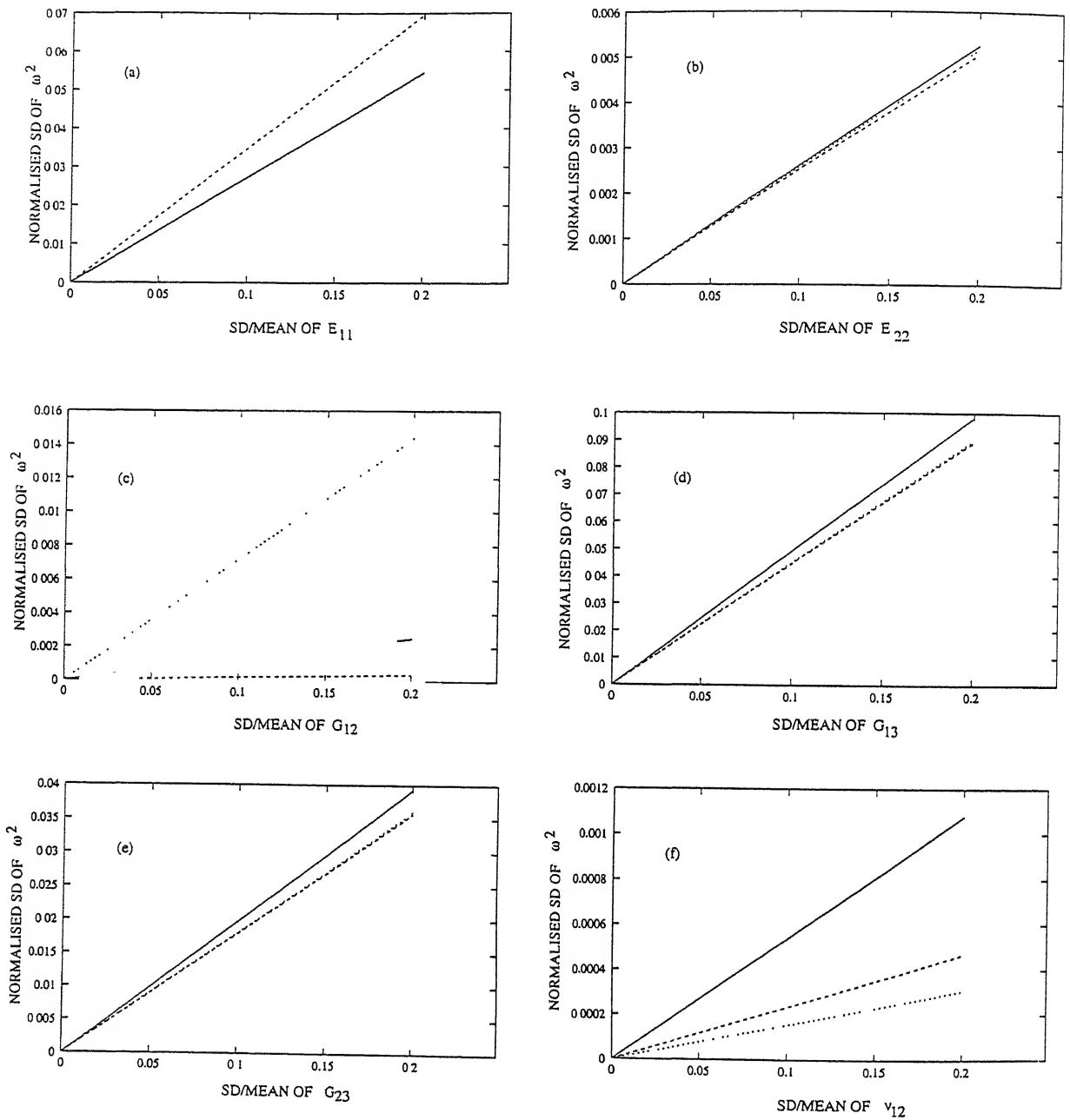


Figure 5.44: Sensitivity of the square of the fundamental frequency of a $[45^\circ/-45^\circ/45^\circ/-45^\circ]$ spherical square panel against individual variation of material property SD for $a/h=5$.
Key: As in Figure 5.35.

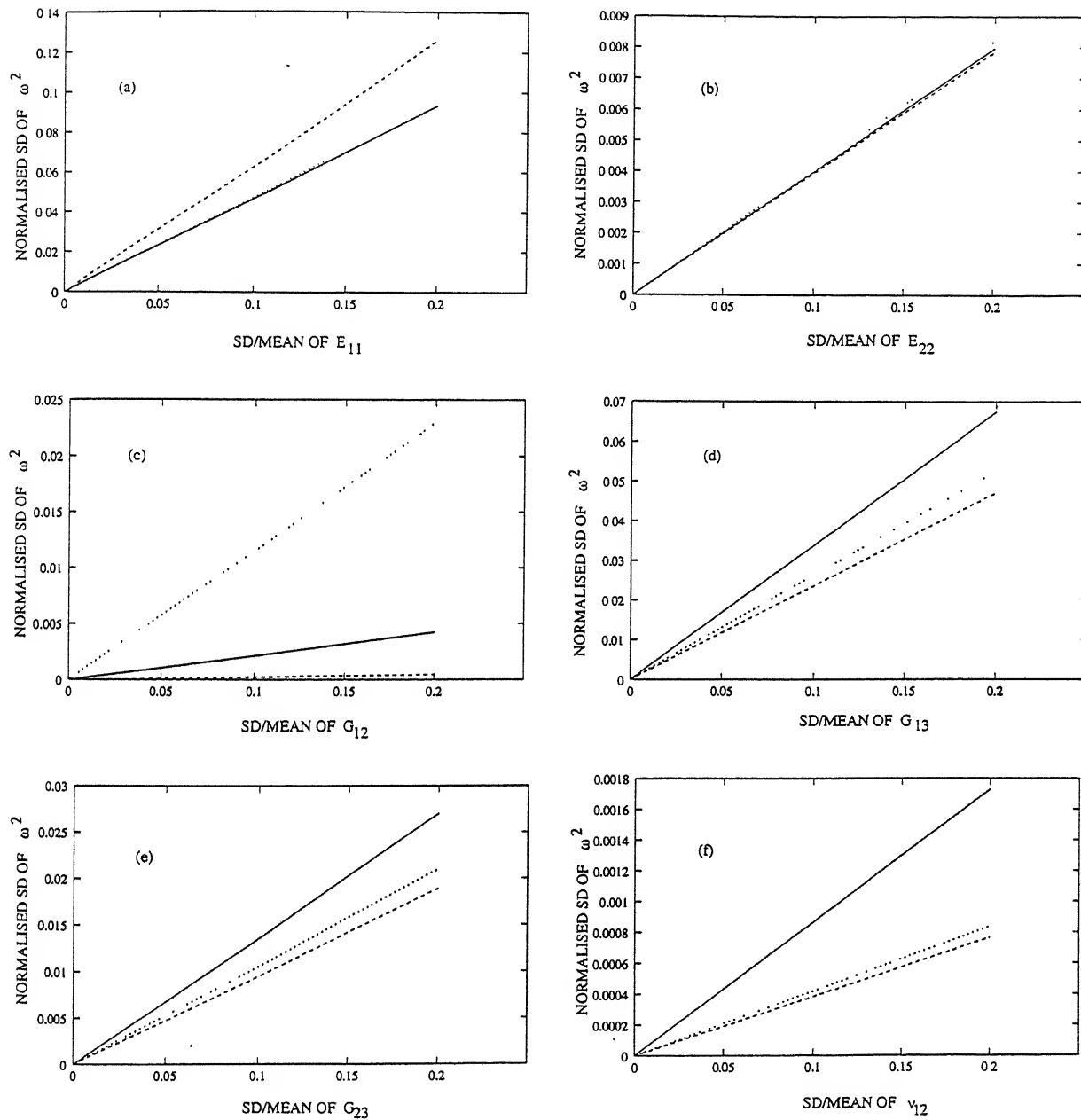


Figure 5.45: Sensitivity of the square of the fundamental frequency of a $[45^\circ / -45^\circ / 45^\circ / -45^\circ]$ spherical square panel against individual variation of material property SD for $a/h=10$.

Key: As in figure 5.35.

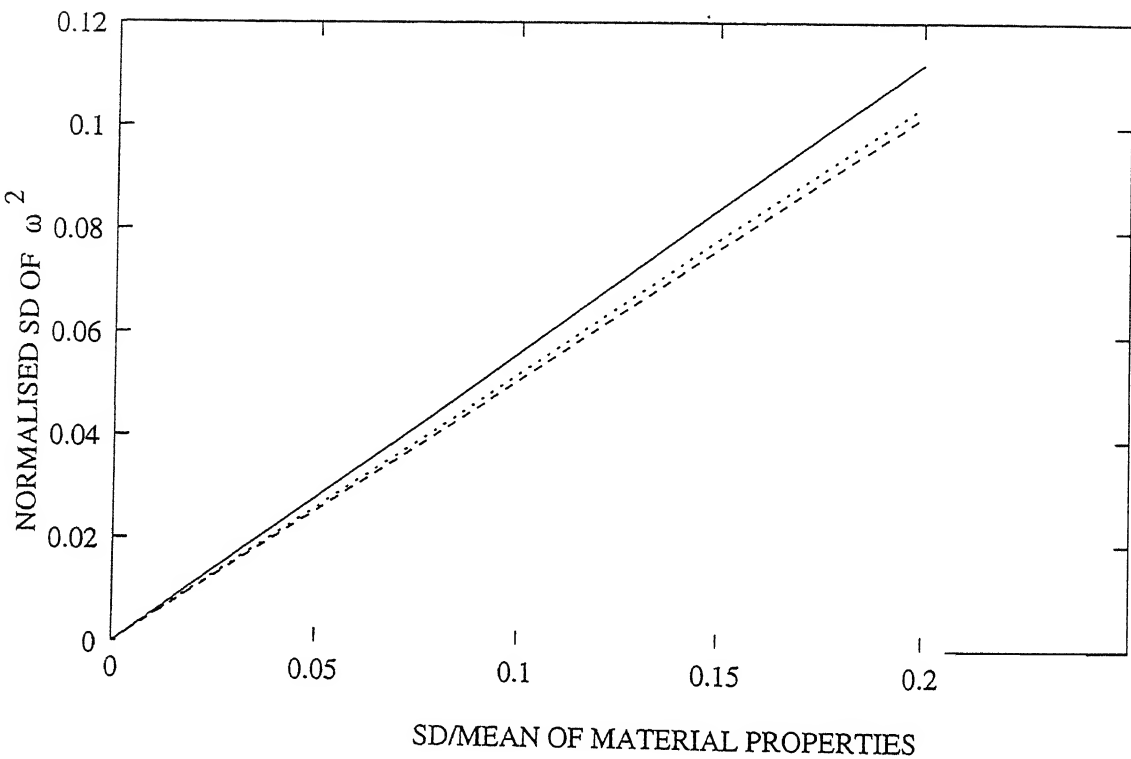


Figure 5.46: Comparison of the scatter of square of the fundamental frequency in $[0^\circ/-45^\circ/45^\circ/90^\circ]$ plate, cylindrical and spherical panels against simultaneous change in material properties.

Key: — :Spherical, :cylindrical, - - - :plate.

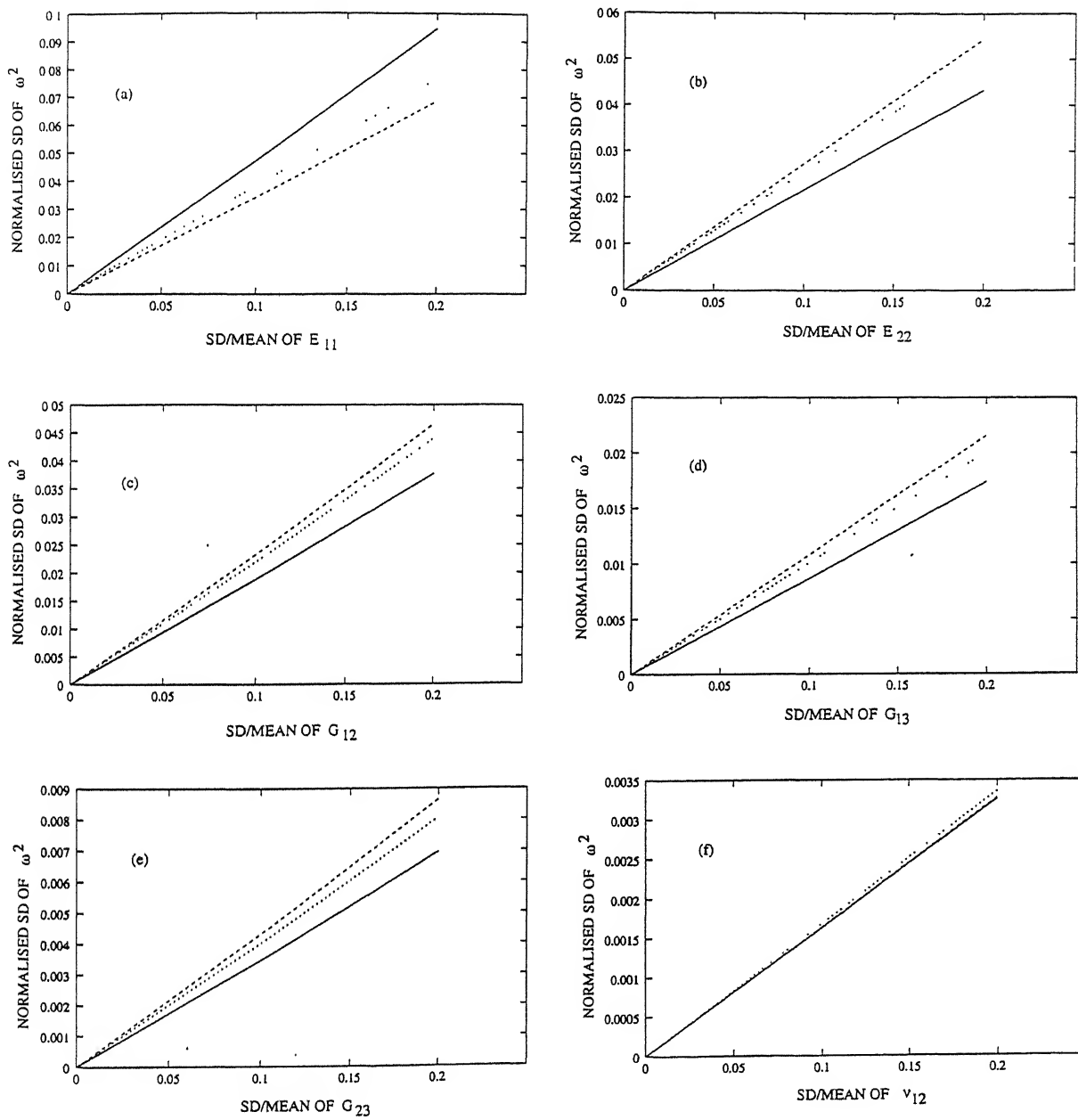


Figure 5.47: Comparison of the scatter of square of the fundamental frequency of a $[0^\circ/-45^\circ/45^\circ/90^\circ]$ spherical panel with plate and cylindrical panel against individual change in material property.

Key: As in figure 5.46.

CHAPTER VI

FORCED VIBRATION OF COMPOSITE PANELS

6.1 Introduction

In most engineering applications, vibration is generally undesirable. The detrimental effects of vibrations on a structure are well known. An excessive vibration of the structures may even lead to its complete failure. Often, apparently harmless vibrations, if allowed to continue over a long period, may eventually cause fatigue failure of the structures. Such drastic failures have been observed in all kinds of structures. Hence, accurate prediction of the dynamic response of the structures is an important field of investigation, especially in the case of composites as the response depends on large number of parameters.

In determining the dynamic response of system made of composites, it is customary to assume that the given system has precisely defined properties. It is further assumed that the applied excitation is deterministic as mentioned earlier. However, the system properties can at best be determined only within a certain range due to the large number of parameters associated with its manufacturing and fabrication processes and our inability to control them precisely. Similar is the case with loading also, which cannot be determined exactly. The uncertainties inherent in system response induced by uncertainties in system parameters and randomness in applied excitation need to be incorporated in the system modeling for a rigorous analysis. For reliability of the design, it is essential that the response should be

predicted exactly. This consideration results in the need for modeling of the system properties and excitation as random. In the present work the material properties have been modeled as random variables and the excitation as a random process in time.

Considerable research has been carried out to characterize the dynamic response of structures made of FRPs. Much of the work is based on classical random vibration theory, which focuses on the uncertainty in the response resulting from a prescribed excitation but the structural properties are assumed to be deterministic. This has been observed on the basis of the literature review (refer Chapter II). One prominent feature frequently observed in many engineering problems is the uncertainty in structural properties. Also as reported in *Chapter II*, the literature on the analysis of structures with random system parameters to deterministic as well as random excitations is very limited. Some published material is available dealing with the forced vibration analysis of metallic structures with random parameters to deterministic as well as random excitations. Very little information is available on the forced vibration response of composite structures with random system parameters to deterministic as well as random loading. At this stage, it is to be pointed out that the assumption regarding no correlation between the material properties and random loading in Chapter I can be used to divide the problem into two groups- structural response with uncertain material properties to deterministic loading and structural response with deterministic material properties to random loading. The second problem has been dealt with in detail in the available literature. In the technique presented in this chapter, expressions for response statistics for both the problems have been obtained from a single unified analysis.

In this Chapter, a general probabilistic analysis procedure based on the state space form of the system equations has been presented. These are derived using the classical and the finite element approaches for forced vibration response of composite laminates, cylindrical and spherical panels with random material properties subjected to deterministic as

well as random excitation. Like the previous chapters, first order perturbation technique has been chosen to handle the randomness in material properties. As discussed earlier, the formulation is based on the HSDT including rotatory inertia effects. Second order statistics of the transverse displacement of the panel with known second order statistics of material properties and external excitation have been obtained.

6.2 Stochastic Classical Approach (SCA)

Navier type exact solutions for the dynamic response of the governing equations exist for some typical boundary conditions for shallow panels as discussed at Section 5.2. The lamination scheme could be either anti-symmetric or symmetric cross-ply. Substitution of appropriate deflection forms satisfying the required boundary conditions in the system Equation (3.34) yields nonhomogeneous linear ordinary governing differential equation in time with random coefficients and inputs. It also requires the external excitation to be expressed in the Fourier expansion form. These equations are then expressed in state space form. When these are combined with probabilistic method, it is possible to develop the response expressions for the random equations. A detailed study is presented in this chapter to obtain the second moments of response of laminated composite plates, cylindrical and spherical panels using SCA.

6.2.1 Formulation: State Space Approach

Following the state space technique [102, 103], we assume the solution form that satisfies the boundary conditions (refer Sub-section 5.2.1.2):

$$u(x_1, x_2, t) = \sum_{m,n=1}^{\infty} U_{mn}(t) f_1(x_1, x_2); \quad v(x_1, x_2, t) = \sum_{m,n=1}^{\infty} V_{mn}(t) f_2(x_1, x_2);$$

$$w(x_1, x_2, t) = \sum_{m,n=1}^{\infty} W_{mn}(t) f_3(x_1, x_2); \quad \phi_1(x_1, x_2, t) = \sum_{m,n=1}^{\infty} X_{mn}(t) f_1(x_1, x_2); \quad (6.1)$$

$$\phi_2(x_1, x_2, t) = \sum_{m,n=1}^{\infty} Y_{mn}(t) f_1(x_1, x_2);$$

where,

$$\begin{aligned} f_1(x_1, x_2) &= \cos(\alpha x_1) \sin(\beta x_2); & f_2(x_1, x_2) &= \sin(\alpha x_1) \cos(\beta x_2); \\ f_3(x_1, x_2) &= \sin(\alpha x_1) \sin(\beta x_2); & \alpha &= m\pi/a; & \beta &= n\pi/b \end{aligned} \quad (6.2)$$

The transverse dynamic load in general can also be written in a double Fourier expansion form as

$$q(x_1, x_2, t) = \sum_{m,n=1}^{\infty} Q_{mn}(t) f_3(x_1, x_2), \quad (6.3)$$

where, Q_{mn} denotes the undetermined coefficient in the double Fourier expansion.

Substituting Equations (6.1) and (6.3) into the system Equations (3.34), results in the following set of equations

$$[M] \begin{Bmatrix} \ddot{U}_{mn} \\ \ddot{V}_{mn} \\ \ddot{W}_{mn} \\ \ddot{X}_{mn} \\ \ddot{Y}_{mn} \end{Bmatrix} + [K] \begin{Bmatrix} U_{mn} \\ V_{mn} \\ W_{mn} \\ X_{mn} \\ Y_{mn} \end{Bmatrix} = \begin{Bmatrix} 0 \\ 0 \\ Q_{mn} \\ 0 \\ 0 \end{Bmatrix} \quad m, n=1, 2, \dots, \infty \quad (6.4)$$

The linear system of ordinary differential equations as given by Equation (6.4) can be solved using the State Variable Technique. In this approach the state vector $Z(t)$ is defined by

$$\begin{aligned} Z_1 &= U_{mn}; & Z_2 &= V_{mn}; & Z_3 &= W_{mn}; & Z_4 &= X_{mn}; & Z_5 &= Y_{mn}; \\ Z_6 &= \dot{U}_{mn}; & Z_7 &= \dot{V}_{mn}; & Z_8 &= \dot{W}_{mn}; & Z_9 &= \dot{X}_{mn}; & Z_{10} &= \dot{Y}_{mn}. \end{aligned} \quad (6.5)$$

Making use of Equation (6.5), Equation (6.4) can be rewritten in the form:

$$\dot{Z} = A Z + B U; \quad (6.6)$$

where

$$A = \begin{bmatrix} 0 & 0 & 0 & 0 & 0 & 1 & 0 & 0 & 0 & 0 \\ 0 & 0 & 0 & 0 & 0 & 0 & 1 & 0 & 0 & 0 \\ 0 & 0 & 0 & 0 & 0 & 0 & 0 & 1 & 0 & 0 \\ 0 & 0 & 0 & 0 & 0 & 0 & 0 & 0 & 1 & 0 \\ 0 & 0 & 0 & 0 & 0 & 0 & 0 & 0 & 0 & 1 \\ R_{11} & R_{12} & R_{13} & R_{14} & R_{15} & 0 & 0 & 0 & 0 & 0 \\ R_{21} & R_{22} & R_{23} & R_{24} & R_{25} & 0 & 0 & 0 & 0 & 0 \\ R_{31} & R_{32} & R_{33} & R_{34} & R_{35} & 0 & 0 & 0 & 0 & 0 \\ R_{41} & R_{42} & R_{43} & R_{44} & R_{45} & 0 & 0 & 0 & 0 & 0 \\ R_{51} & R_{52} & R_{53} & R_{54} & R_{55} & 0 & 0 & 0 & 0 & 0 \end{bmatrix} \quad (6.7)$$

$$B = \begin{bmatrix} 0 & 0 \\ 0 & M^{-1} \end{bmatrix}, \quad U = (0 \ 0 \ 0 \ 0 \ 0 \ 0 \ 0 \ 0 \ Q_{mn}(t) \ 0 \ 0) \quad (6.8)$$

$$B U = (0 \ 0 \ 0 \ 0 \ 0 \ b_{11} \ b_{21} \ b_{31} \ b_{41} \ b_{51})^T \quad (6.9)$$

with

$$R = -M^{-1}K \quad (6.10)$$

and

$$b = M^{-1} \begin{Bmatrix} 0 \\ 0 \\ Q_{mn} \\ 0 \\ 0 \end{Bmatrix} \quad (6.11)$$

The solution of Equations (6.6) is given by

$$Z(t) = e^{A(t-t_0)} Z(t_0) + \int_{t_0}^t e^{A(t-\tau)} B U(\tau) d\tau \quad (6.12)$$

where t_0 is the initial time and $Z(t_0)$ is the initial input vector. The operator $e^{A(t-\tau)}$ can be expressed in terms of the matrix of eigenvectors S and distinct eigen values λ_i associated with matrix A as

$$e^{A(t-\tau)} = S \begin{bmatrix} e^{\lambda_1(t-\tau)} & & 0 \\ & \ddots & \\ 0 & & e^{\lambda_n(t-\tau)} \end{bmatrix} S^{-1} \quad (6.13)$$

The solution of Equation (6.6) as given by Equation (6.12) would be possible only when the system parameters are deterministic even if the excitation is random. In the present study, as mentioned earlier, the material properties are random. Therefore, the elements of matrix A are random. A straightforward solution of Equation (6.6), therefore, is not possible. Further processing is required to arrive at the appropriate solution.

6.2.2 Method of Solution

Without any loss of generality the random variable may be split up as the sum of the mean variable and a zero mean random part (refer Section 5.2.2, Equation 5.12).

Consider a class of problems where the random vibrations is very small compared with the mean part, as the case is in most engineering applications, One can therefore write

$$\mathbf{Z} = \bar{\mathbf{Z}} + \varepsilon \mathbf{Z}^r; \quad \mathbf{A} = \bar{\mathbf{A}} + \varepsilon \mathbf{A}^r; \quad \mathbf{U} = \bar{\mathbf{U}} + \varepsilon \mathbf{U}^r; \quad (6.14)$$

where ε is a small parameter, over bar denotes 'mean' and superscript 'r' denotes the zero mean random part of the variables.

On substitution of Equation (6.14) in Equation (6.6) and collecting terms up to first order results in

$$\text{Zeroth order: } \dot{\bar{\mathbf{Z}}} = \bar{\mathbf{A}} \bar{\mathbf{Z}} + \mathbf{B} \bar{\mathbf{U}} \quad (6.15)$$

$$\text{First-order: } \dot{\mathbf{Z}}^r = \bar{\mathbf{A}} \mathbf{Z}^r + \mathbf{A}^r \bar{\mathbf{Z}} + \mathbf{B} \mathbf{U}^r \quad (6.16)$$

Equation (6.15) is the zeroth order equation giving the mean value of the response \mathbf{Z} . This equation is the same as obtained in deterministic analysis of the problem. Following Equation (6.12), its solution is given as [102, 103]

$$\bar{\mathbf{Z}}(t) = e^{\bar{\mathbf{A}}(t-t_0)} \bar{\mathbf{Z}}(t_0) + \int_{t_0}^t e^{\bar{\mathbf{A}}(t-\tau)} \mathbf{B} \bar{\mathbf{U}}(\tau) d\tau \quad (6.17)$$

where

$$e^{\bar{A}(t-\tau)} = \bar{S} \begin{bmatrix} e^{\bar{\lambda}_1(t-\tau)} & & \mathbf{0} \\ & \ddots & \\ \mathbf{0} & & e^{\bar{\lambda}_n(t-\tau)} \end{bmatrix} \bar{S}^{-1} \quad (6.18)$$

Equation (6.16) can also be solved for the random part \mathbf{Z}^r in terms of mean and random parts of system stiffness and forcing function.

It can be seen that the random deviations from the mean value for the derived variables are due to the presence of scatter about the mean in basic random variables. Further, the contributions of the random parts are small compared to the mean values. A Taylor series expansion, therefore, is admissible for the variations in the dependent variables. Thus, one can write

$$A_{ij}^r = \sum_{l=1}^n \left(\frac{\partial A_{ij}}{\partial b_l} \right)_{b_l=\bar{b}_l} b_l^r + \frac{1}{2!} \sum_{k=1}^n \sum_{l=1}^n \left(\frac{\partial^2 A_{ij}}{\partial b_l \partial b_k} \right)_{\bar{b}_l \bar{b}_k} b_l^r b_k^r + \dots \quad (6.19)$$

Retaining only the first terms in the series, Equation (6.19) is approximated as

$$A_{ij}^r = \sum_{l=1}^n \left(\frac{\partial A_{ij}}{\partial b_l} \right)_{b_l=\bar{b}_l} b_l^r \quad (6.20)$$

Similar representations are obtained for the other random quantities also.

Following Equation (6.20), Equation (6.16) can be rewritten as

$$\dot{\mathbf{Z}}^r = \bar{\mathbf{A}} \mathbf{Z}^r + \sum_{l=1}^m \left(\partial \mathbf{A} / \partial b_l \right)_{b_l=\bar{b}_l} b_l^r \bar{\mathbf{Z}} + \mathbf{B} \mathbf{U}^r \quad (6.21)$$

Simplifying Equation (6.21), it can be written as

$$\dot{\mathbf{Z}}^r = \bar{\mathbf{A}} \mathbf{Z}^r + \mathbf{C}^r; \quad (6.22)$$

with

$$\mathbf{C}^r = \sum_{l=1}^m \left(\partial \mathbf{A} / \partial b_l \right)_{b_l=\bar{b}_l} b_l^r \bar{\mathbf{Z}} + \mathbf{B} \mathbf{U}^r \quad (6.23)$$

where b_l^r 's ($l=1, 2, \dots, m$.) are the basic material properties which are modeled as random variable.

The solution of Equation (6.22) can be written as

$$\mathbf{Z}^r(t) = e^{\bar{\mathbf{A}}(t-t_0)} \mathbf{Z}^r(t_0) + \int_{t_0}^t e^{\bar{\mathbf{A}}(t-\tau)} \mathbf{C}^r(\tau) d\tau. \quad (6.24)$$

The system to be at rest at $t=t_0$, assuming $e^{\bar{\mathbf{A}}(t-t_0)} \mathbf{Z}^r(t_0) = \mathbf{0}$, Equation (6.24) can be written as

$$\mathbf{Z}^r(t) = \int_{t_0}^t e^{\bar{\mathbf{A}}(t-\tau)} \mathbf{C}^r(\tau) d\tau \quad (6.25)$$

The following relation is obtained for correlation function of $\mathbf{Z}(t)$, with $\epsilon=1$ [19, 111].

$$\mathbf{K}_{zz}(t_1, t_2) = E[\mathbf{Z}^r(t_1) \mathbf{Z}^r(t_2)^{*T}] = \int_{t_0}^{t_1} \int_{t_0}^{t_2} e^{\bar{\mathbf{A}}(t_1-\tau_1)} \mathbf{K}_{cc}(\tau_1, \tau_2) e^{\bar{\mathbf{A}}(t_2-\tau_2)} d\tau_1 d\tau_2 \quad (6.26)$$

with

$$\mathbf{K}_{cc}(t_1, t_2) = E[\mathbf{C}^r(\tau_1) \mathbf{C}^r(\tau_2)^{*T}] ; \quad (6.27)$$

where $E[\]$ stands for expectation.

The equation (6.26) can be further expressed as

$$\mathbf{K}_{zz}(t_1, t_2) = \int_{t_0}^{t_1} \int_{t_0}^{t_2} \mathbf{S} \Lambda_1 \mathbf{P} \mathbf{K}_{cc}(\tau_1, \tau_2) \mathbf{P} \mathbf{P} \Lambda_2 \mathbf{S} \mathbf{S} d\tau_1 d\tau_2 \quad (6.28)$$

where \mathbf{S} is the modal matrix of \mathbf{A} and

$$\Lambda_1 = \begin{bmatrix} e^{\bar{\lambda}_1(t_1-\tau_1)} & \mathbf{0} \\ \mathbf{0} & \ddots & e^{\bar{\lambda}_n(t_1-\tau_1)} \end{bmatrix};$$

$$\Lambda_2 = \begin{bmatrix} e^{\bar{\lambda}_1(t_2-\tau_2)} & [0] \\ [0] & \ddots & e^{\bar{\lambda}_n(t_2-\tau_2)} \end{bmatrix}; \quad (6.29)$$

$$\mathbf{P} = \mathbf{S}^{-1}; \quad \mathbf{S} \mathbf{S} = \mathbf{S}^{*T}; \quad \mathbf{P} \mathbf{P} = \mathbf{P}^{*T}.$$

Thus Equations (6.17) and (6.28) give the expression for mean and covariance of the dynamic response, respectively.

6.3 Stochastic Finite Element Method (SFEM)

As pointed out in *Chapter V*, Section 5.3, the finite element method is combined with first order perturbation technique to obtain the second moments of the dynamic response of

composite plates, cylindrical and spherical panels with random material properties subjected to deterministic or random loading. The lamina material properties are modeled as RVs. The nonhomogeneous ordinary differential equations in time with random coefficient and input are obtained from the system equation by using the finite element modeling. These equations are transformed into first order differential equations with state–space technique. The solution of these equations is obtained by FOPT. The detailed sequences of steps are presented below.

6.3.1 Formulation

The governing equation for the dynamic response analysis of composite laminates, cylindrical and spherical panels is obtained by using the Hamilton's principle in a manner similar to the free vibration problem presented in Section 5.3.

6.3.1.1 Strain Energy

The strain energy due to bending of a laminated composite panel was shown in *Chapter III* to be (refer Equation 3.35)

$$U = \frac{1}{2} \int_A \bar{\boldsymbol{\epsilon}}^T \mathbf{D} \bar{\boldsymbol{\epsilon}} dA ; \quad (6.30)$$

It was further shown by employing finite element modeling, these equations reduce (Section 3.6 refer Equations 3.50, 3.52 and 3.53) to

$$\begin{aligned} U &= \sum_{e=1}^{NE} U^{(e)} \\ &= \sum_{e=1}^{NE} \frac{1}{2} \int_{A^{(e)}} \bar{\boldsymbol{\epsilon}}^T \mathbf{D} \bar{\boldsymbol{\epsilon}} dA \end{aligned} \quad (6.31)$$

$$U^{(e)} = \frac{1}{2} \int_{A^{(e)}} \boldsymbol{\Lambda}^{T(e)} \mathbf{B}^T \mathbf{D} \mathbf{B} \boldsymbol{\Lambda}^{(e)} dA ; \quad (6.32)$$

$$= \boldsymbol{\Lambda}^{T(e)} \mathbf{K}^{(e)} \boldsymbol{\Lambda}^{(e)} , \quad (6.33)$$

where $\boldsymbol{\Lambda}^{(e)}$ and $\mathbf{K}^{(e)}$ are the element displacement vector and stiffness matrices respectively.

6.3.1.2 Potential Energy

The work done by external mechanical load $q(x_1, x_2, t)$ is given by (Refer Equation 3.40)

$$V = -W = \int_A q(x_1, x_2, t) w dA \quad (6.34)$$

In finite element notation this equation reduces to

$$V = \sum_{e=1}^{NE} V^{(e)} \quad (6.35)$$

where

$$V^{(e)} = - \int_A \Lambda^{(e)T} \bar{q} dA \quad (6.36)$$

with,

$$\bar{q} = \{0 \ 0 \ q(x_1, x_2, t) \ 0 \ 0 \ 0 \ 0\}^T. \quad (6.37)$$

The excitation $q(x_1, x_2, t)$ is the transverse, time dependent, distributed load acting on the panels. It can have any arbitrary distribution. It can be expressed in a Fourier series if it has periodic components. In the present analysis, the lateral, distributed load is assumed to be a sinusoidal function as a generic term..

$$q(x_1, x_2, t) = q_0 \sin(\pi x_1 / a) \sin(\pi x_2 / b) Q(t) \quad (6.38)$$

Substituting Equation (3.47) in Equation (6.36),

$$V^{(e)} = -\Lambda^{(e)T} F^{(e)}, \quad (6.39)$$

where,

$$F^{(e)} = \int_{A^{(e)}} \varphi^{(e)} \bar{q}^{(e)} dA, \quad (6.40)$$

Here,

$$\varphi = \begin{bmatrix} \varphi_1 & 0 & 0 & \dots & 0 \\ 0 & \varphi_2 & 0 & \dots & 0 \\ 0 & 0 & \varphi_3 & \dots & 0 \\ \vdots & \vdots & \vdots & \ddots & \vdots \\ \vdots & \vdots & 0 & \vdots & 0 \\ \dots & 0 & 0 & \varphi_{NN-1} & 0 \\ \dots & \dots & 0 & 0 & \varphi_{NN} \end{bmatrix} \quad (6.41)$$

$$\bar{q}^{(e)} = \sum_{i=1}^{NN} \bar{q}_i \quad (6.42)$$

$$\varphi_i = \begin{bmatrix} \varphi_i & 0 & 0 & \dots & 0 \\ 0 & \varphi_i & 0 & \dots & 0 \\ \vdots & \vdots & \vdots & \ddots & \vdots \\ \dots & 0 & 0 & \varphi_i & 0 \\ \dots & \dots & 0 & 0 & \varphi_i \end{bmatrix}_{(7 \times 7)} \quad (6.43)$$

$$\bar{q}^T = \{0 \quad 0 \quad q_i \quad 0 \quad 0 \quad 0 \quad 0\}. \quad (6.44)$$

q_i is the transverse load acting at the i^{th} node.

6.3.1.3 Kinetic Energy

The kinetic energy of a panel subjected to a mechanical load is given by (Refer Equation 5.46)

$$T^{(e)} = \dot{\mathbf{q}}^{*T(e)} \mathbf{M}^{(e)} \dot{\mathbf{q}}^{*(e)} \quad (6.45)$$

where $\mathbf{M}^{(e)}$ is the element mass matrix and is as defined as in Equation (5.47).

6.3.1.4 Governing Equation

Using Variational principles, the governing equation for forced vibration can be derived. The Lagrange's equation for a conservative system can be written as (Refer Equation 5.48)

$$\frac{d}{dt} \left(\frac{\partial T}{\partial \dot{q}_i^*} \right) + \frac{\partial U}{\partial q_i^*} = 0; \quad \text{for } i=1, 2, \dots \quad (6.46)$$

Substituting of Equations (6.33), (6.39) and (6.45) in Equation (6.46) yields

$$\mathbf{K} \mathbf{q}^* + \mathbf{M} \ddot{\mathbf{q}}^* = \mathbf{F} \quad (6.47)$$

where

$$\mathbf{q}^* = \sum_{e=1}^{NE} \mathbf{q}^{*(e)} - \text{Global displacement vector}$$

$$\mathbf{K} = \sum_{e=1}^{NE} \mathbf{K}^{(e)} - \text{Global stiffness matrix}$$

$$\mathbf{M} = \sum_{e=1}^{NE} \mathbf{M}^{(e)} - \text{Global inertia matrix}$$

and

$$\mathbf{F} = - \sum_{e=1}^{NE} \mathbf{F}^{(e)} \quad (6.48)$$

Equation (6.47) represents the governing equation of motion for forced response of composite panels. Following the procedure given in Sub-section 6.2.1, the governing Equation (6.47) can also be transformed into nonhomogeneous ordinary differential equations in time using the State Variables technique. The state vectors are defined on similar lines as given in Equation (6.5). The Equation (6.47) can then be written in the form:

$$\dot{\mathbf{Z}} = \mathbf{A} \mathbf{Z} + \mathbf{B} \mathbf{U} \quad (6.49)$$

Equation (6.49) is the governing equation for the dynamic response problem. Due to uncertainty in material properties and loading, the equation has random coefficients and inputs. The solution of Equation (6.49) can be obtained by the probabilistic solution procedure discussed in Sub-section 6.2.2. However, due to large size of the matrices and vectors involved in Equation (6.49), the computational difficulties are many. A suitable numerical procedure based on perturbation approach is presented in the next subsection.

6.3.2 Method of Solutions: Perturbation Technique

The random variables may be split up as the sum of the mean variable and a zero mean random part (Refer Sub-section 6.2.2 and Equation 6.14).

$$\mathbf{Z} = \bar{\mathbf{Z}} + \varepsilon \mathbf{Z}'; \quad \mathbf{A} = \bar{\mathbf{A}} + \varepsilon \mathbf{A}'; \quad \mathbf{U} = \bar{\mathbf{U}} + \varepsilon \mathbf{U}'; \quad (6.50)$$

On substitution of Equation (6.50) in Equation (6.49) and collecting up to first order terms, we obtain (Refer Equations 6.15 and 6.16)

$$\text{Zeroth order: } \dot{\bar{\mathbf{Z}}} = \bar{\mathbf{A}} \bar{\mathbf{Z}} + \mathbf{B} \bar{\mathbf{U}}; \quad (6.51)$$

$$\text{First-order: } \dot{\mathbf{Z}}' = \bar{\mathbf{A}} \mathbf{Z}' + \mathbf{A}' \bar{\mathbf{Z}} + \mathbf{B} \mathbf{U}'. \quad (6.52)$$

Solution of Equation (6.51) gives the mean value of the response \mathbf{Z} as the only unknown (Refer Equation 6.17). The solution for Equation (6.52) can be written as

$$\mathbf{Z}' = \mathbf{Z}'_1 + \mathbf{Z}'_2; \quad (6.53)$$

where

$$\dot{\mathbf{Z}}'_2 = \bar{\mathbf{A}} \mathbf{Z}'_2 + \mathbf{B} \mathbf{U}' \quad (6.54)$$

$$\dot{\mathbf{Z}}'_1 = \bar{\mathbf{A}} \mathbf{Z}'_1 + \mathbf{A}' \bar{\mathbf{Z}} \quad (6.55)$$

Equation (6.54) is an example of classical random vibration theory. Its solution can be obtained by the standard procedure [17, 111]. To solve Equation (6.55), we adopt a different approach. Following the procedure of Taylor's series expansion for $\dot{\mathbf{Z}}'_1$ and \mathbf{Z}'_1 (Refer Equation 6.20), Equation (6.55) can be written as

$$\sum_{i=1}^m (\partial \dot{\mathbf{Z}}_1 / \partial b_i)_{b_i=\bar{b}_i} b_i' = \bar{\mathbf{A}} \sum_{i=1}^m (\partial \mathbf{Z}_1 / \partial b_i)_{b_i=\bar{b}_i} b_i' + \sum_{i=1}^m (\partial \mathbf{A} / \partial b_i)_{b_i=\bar{b}_i} b_i' \bar{\mathbf{Z}}. \quad (6.56)$$

The above equation can be rewritten as

$$\sum_{i=1}^m \dot{\bar{\mathbf{Z}}}_{1,i} b_i' = \bar{\mathbf{A}} \sum_{i=1}^m \bar{\mathbf{Z}}_{1,i} b_i' + \sum_{i=1}^m \bar{\mathbf{A}}_{,i} b_i' \bar{\mathbf{Z}}. \quad (6.57)$$

where

$$\dot{\bar{Z}}_{1,i} = (\partial \dot{Z}_1 / \partial b_i^r)_{b_i = \bar{b}_i} \text{ and } \bar{Z}_{1,i} = (\partial Z_1 / \partial b_i^r)_{b_i = \bar{b}_i}. \quad (6.58)$$

Comparing the coefficients of the b_i^r in Equation 6.57, we obtain

$$\dot{\bar{Z}}_{1,i} = \bar{A} \bar{Z}_{1,i} + \bar{A}_{,i} \bar{Z}; \quad i = 1, 2, \dots, m. \quad (6.59)$$

We can see that obtaining the solution of Equation (6.59) is equivalent to obtaining the solution of Equation (6.55). Since there is no random variable in Equation (6.59), this method is very convenient. We can use various numerical methods of time integration to solve both Equations (6.51) and (6.59). Each of them has their own advantages and limitations. In the present study Adams method for numerical integration has been employed [121]. For this purpose, Numerical Algorithms Groups (NAG) subroutine D02CJF has been used for computations. The time step has been selected based on the convergence study.

The full value of the zero mean random part is obtained by combining Z_1^r and Z_2^r . The mean and the variance of the dynamic response can be obtained from first part of Equation (6.50).

The first part of Equation (6.50) indicates the mean value of the displacement response to be

$$E[Z] = \bar{Z}. \quad (6.60)$$

Taking the second moment of Equation (6.50) one gets the expression for the variance

$$\text{Var}(Z_i) = \varepsilon^2 \sum_{j=1}^m \sum_{k=1}^m \bar{Z}_{,j}^i \bar{Z}_{,k}^i \text{Cov}(b_j, b_k); \quad (6.61)$$

The above two equations are used to obtain the second order statistics of flat, cylindrical and spherical panels.

6.4 Results and Discussion

The applicability, accuracy and efficiency of the proposed techniques within the framework of first order perturbation technique are demonstrated for composite laminates, cylindrical and spherical shallow panels with random material properties and deterministic

loading. The second moments of transverse mid-point displacement are computed as a function of time. The excitation has been modeled as random process in time and assumed to be a white noise for computations. The results have been validated with MCS. To get idea insight the effects of material property randomness and loading on response of composite structures, the results have also been computed for structural response with deterministic material properties to random loading.

The panel is subjected to distributed transverse loading, given by

$$Q_{mn}(t) = \begin{cases} q_0 \sin(\pi t / t_1), & 0 \leq t \leq t_1 \\ 0, & \text{otherwise} \end{cases}.$$

The following material properties in lamina principal material coordinates have been used in generating the results:

$E_{11}=132.864$ GPa, $E_{22}=10.79$ GPa, $G_{12}=G_{13}=5.67$ GPa, $G_{23}=3.6192$ GPa and $\nu_{12}=0.24$. Other system values are taken as: $q_0=13.84$ N/mm², psd (white noise)=0.01s, $\rho=3.27 \times 10^{-9}$ kg/mm³, $a=b=508$ mm, $a/h=10$, $R=2540$ mm and $t_1=0.003$ s and 0.005 s.

The mean and SD of transverse center displacement as a function of time have been computed for graphite-epoxy laminates, cylindrical and spherical panels having stacking sequences $[0^0/90^0]$, $[0^0/90^0/90^0/0^0]$ and $[0^0/45^0/-45^0/90^0]$ with the following set of boundary condition: SSSS and CCCC

6.4.1 Validation

Second order statistics of transverse mid-point displacement as a function of time, for a $[0^0/90^0/90^0/0^0]$ spherical panel with $R/a=5$, $a/h=10$ and $t_1=0.005$ s have been obtained using the proposed approaches SCA and SFEM. Results have also been obtained with MCS for the purpose of comparison. E_{11} has been taken as random and loading is assumed to be deterministic for these evaluations. The number of samples used for the study for MCS is

15000. The mean and SD of the transverse mid-point displacement with time are presented for SD of E_{11} as 10% of its mean value in Figures 6.1 and 6.2, respectively along with the MCS results. The mean responses obtained using SCA and SFEM are in very good agreement with that of MCS. The SD of the response by the two approaches also shows agreement with that of MCS in the forced vibration zone, while it does not agree so well at the peaks and the valleys in the free vibration zone. The reason may be due to non-removal of secular terms. However, these deviations are small in magnitudes. The SD obtained by SCA and SFEM indicates good agreement between them.

6.4.2 Composite Plates: Second order statistics

The results presented in Figures 6-3-6.8 have been obtained using SCA for SSSS laminates, while the results for Figures 6.9 and 6.10 have been obtained using SFEM for CCCC laminates.

Figure 6.3 shows mean transverse mid-point displacement of a $[0^0/90^0/90^0/0^0]$ laminate as a function of time with $t_1=0.003s$. From the examination of results, it is observed that the mean response initially increases and reaches a maximum value and then decreases with increase in time in forced vibration zone. In the free vibration zone, the behavior of the mean response is sinusoidal with constant amplitude. This indicates achievement of the steady state response.

Figure 6.4 shows mean transverse mid-point displacement of a $[0^0/90^0]$ laminate as a function of time with $t_1=0.003s$. It is observed that in the forced vibration region the maximum displacement occurs at one point only. In the free vibration zone, the nature of the response is sinusoidal with constant amplitude, as we have also seen in symmetric laminate. Here also, beyond time t_1 the response attains the steady state value.

Figures 6.5(a)-(f) shows the SD of the transverse mid-point displacement of a $[0^0/90^0/90^0/0^0]$ laminate as a function of time for the individual material property SD of 10% of its mean value, keeping others as fixed. The SD of displacement increases initially and after reaching a peak value it decreases. Further, the peak value of each increasing - decreasing part increases continuously in the time range studied. This appears to be dangerous from reliability point of view. The dispersion in response is most affected with scatter in E_{11} and least affected with scatter in the Poisson 's ratio. The sensitivity of response to scatter in E_{22} , G_{12} , G_{13} and G_{23} is of the same order of magnitude.

Figures 6.6(a)-(f) presents the SD of the transverse mid-point displacement of a $[0^0/90^0]$ laminate as a function of time with changes in the six individual material property normalized SD only one at a time being random. The SD of the material properties selected for the study is 5, 10, 15 and 20 percent of its mean value. The curves appear to be in the same phase. The conclusions in general remain similar to Figures 6.5(a)-(f). However, the magnitude of sensitivity of displacement towards scatter in the material properties is different.

Figure 6.7 represent the SD of the transverse mid-point displacement of a $[0^0/90^0]$ laminate with normalized SD of material property G_{12} alone changing at $t=0.002s$ and $0.004s$. The two times selected for the study falls in the forced and free vibration zones, respectively. It is observed that the dispersions in displacement vary almost linearly with normalized SD of material property. This observation is somewhat similar to the cases of buckling and natural frequency SD variation as reported in *Chapters IV and V* respectively. It is also observed that the scatter in displacement at $t=0.002s$ is more than that at $t=0.004s$. This may be due to the mean at $t=0.002s$ being larger than $t=0.004s$. This behavior can also be attributed to the fact that the scatter in displacement for different SD of material properties is in the same phase.

Figure 6.8 shows the scatter in the transverse mid-point displacement of a $[0^0/90^0/90^0/0^0]$ laminate as a function of time with deterministic material properties and random excitation. It is observed that the scatter in displacement is more compared to the scatter due to material properties.

Figure 6.9 plots the mean response for a $[0^0/45^0/-45^0/90^0]$ laminate obtained by SFEM as a function of time with $t_1=0.005s$ for CCCC laminates. The behavior of displacement response in forced vibration shows two peaks and then quick attainment of steady state condition. Figures 6.10(a)-(f) show the plot of the SD of the mid-point displacement for the above laminates as a function of time with $t_1=0.005s$ for SD of 5% of its mean values for CCCC support. The fluctuating amplitude has a tendency to grow with time in the free vibration range for the duration of the plot. It is observed that the displacement SD is most affected with changes in G_{13} and least affected with changes in Poisson's ratio. The effects of E_{11} and G_{23} are also significant. The response sensitivity displacement due to G_{12} and E_{22} is of comparable order of magnitude.

6.4.3 Composite Cylindrical Panels: Second order statistics

The discussion presented below are based on the Figures 6.11 to 6.15 using SCA and Figures 6.16 and 6.17 using SFEM.

Variation of the mean displacement response of $[0^0/90^0/90^0/0^0]$ and $[0^0/90^0]$ SSSS cylindrical panel with time is presented in Figure 6.11 for $t_1=0.003s$. The general behavior of the mean response is similar to the plate. The peak value in forced vibration zone is more in the case of antisymmetric laminate as compared to symmetric laminate. The magnitude of the constant amplitude in free vibration zone is also more in the case of antisymmetric panel when compared to symmetric panel.

Variation of SD of the displacement for a $[0^0/90^0/90^0/0^0]$ SSSS cylindrical panel is presented in Figures 6.12(a)-(f) with time for $t_1=0.003s$. The general nature of the behavior is same as in the case of rectangular laminate. However, the magnitudes of sensitivity with respect to material property SD are different. The scatter in E_{11} has maximum influence on the dispersion of the displacement. The sensitivity of G_{12} and G_{23} are of the same order of magnitude.

Sensitivity of displacement of a $[0^0/90^0]$ SSSS panel with time for $t_1=0.003s$ against SD of material properties is presented in Figures 6.13(a)-(f). It is observed that the peak value of SD of displacement increases as SD of the material property increases. Further as observed in the case of laminate, they are in the same phase. The effects of E_{11} and E_{22} on response are of the same order of magnitude. The effect of G_{12} is dominant. It can be seen that the effect of Poisson's ratio is also significant.

The results have also been plotted for SD of the transverse mid-point displacement at a particular time against different SD of the material property. For this purpose, $t=0.002s$ and $0.004s$ have been selected with the material property E_{11} having SD of 5, 10, 15 and 20 percent of its mean value. The results are presented in Figure 6.14 for a $[0^0/90^0]$ SSSS panel. It has been observed that SD of response varies almost linearly with SD of the material property.

The SD of displacement of a $[0^0/90^0/90^0/0^0]$ SSSS panel with deterministic material properties subjected to random excitation is also presented in Figure 6.15. The pattern of the curve is similar as in the case of laminate. However, the magnitudes are different.

Variation of the mean response obtained by SFEM is presented in Figure 6.16 with time for a $[0^0/45^0/-45^0/90^0]$ CCCC panel for $t_1=0.005s$. The nature of the curve is similar to that of the laminate. Variation of SD of the displacement for $[0^0/45^0/-45^0/90^0]$ CCCC cylindrical panel is presented in Figures 6.17(a)-(f) with material property SD of 5 percent of

their mean values for $t_1=0.003s$. The pattern of sensitivity of displacement is similar to that of the laminate.

6.4.4 Composite Spherical Panels: Second order statistics

Figure 6.18 shows the variation of the mean displacement for a $[0^0/90^0/90^0/0^0]$ SSSS spherical panel for $t_1=0.003s$ using SCA. The behavior is similar to the cylindrical panel. However, transverse response magnitude is different.

Figures 6.19(a)-(f) show the time plot of the transverse mid-point displacement of a $[0^0/90^0/90^0/0^0]$ SSSS spherical panel with individual material property SD of 10 percent of its mean value for $t_1=0.003s$ using SCA. Similar patterns with different magnitudes are observed as seen in the case of laminate and cylindrical panels.

Figure 6.20 shows variation of SD of the displacement of a $[0^0/90^0/90^0/0^0]$ SSSS spherical panel as a function of time with deterministic material properties subjected to random excitation for $t_1=0.003s$ using SCA. Similar behavior but with different magnitude is observed as compared to laminate and cylindrical panel.

Figure 6.21 presents the variation of the mean displacement with time for a $[0^0/45^0/-45^0/90^0]$ CCCC spherical panel for $t_1=0.005s$ obtained by SFEM. The nature of the curve is similar to the laminate and cylindrical panel. Sensitivity of the displacement for a $[0^0/45^0/-45^0/90^0]$ CCCC spherical panel is presented in Figures 6.22(a)-(f) with material property SD of 5 percent of their mean values for $t_1=0.005s$. The pattern of variation of SD of the displacement is similar to the laminate and cylindrical panel.

6.4.5 Conclusions

The following conclusion can be drawn from this limited study:

- In the forced vibration region, the mean transverse mid-point displacement of plate is more as compared to cylindrical and spherical panels. However, in the free vibration zone spherical panel shows larger displacement.
- Symmetric cross-ply SSSS laminated panel is more sensitive to scatter in longitudinal elastic modulus E_{11} while in the case of antisymmetric laminated panel, the in plane shear modulus has more impact on dispersion of the displacement. The displacement is least affected with scatter in Poisson's ratio.
- The SD of the displacement varies almost linearly with individual variation of material property.
- The peak values of SD increase with time increases in the free vibration region. However, this is not true in the case of forced vibration response. Therefore very little confidence can be placed on the response for free vibration if material properties cannot be calculated precisely. This is not the case with classical random vibration.
- In general, the dispersion in displacement is more in the case of random vibration as compared to stochastic structural analysis.

6.5 Summary

A unified probabilistic approach dealing with the classical random vibration and stochastic structural analysis based on the state-space form has been presented. A solution procedure based on stochastic classical and finite element approaches has been detailed. The lamina material properties have been modeled as random variable. The higher order shear

deformation theory including rotatory inertia effects has been employed for basic formulation. Second order statistics of transverse mid-point displacement of composite laminates, cylindrical and spherical panels as a function of time with different boundary conditions has been obtained.

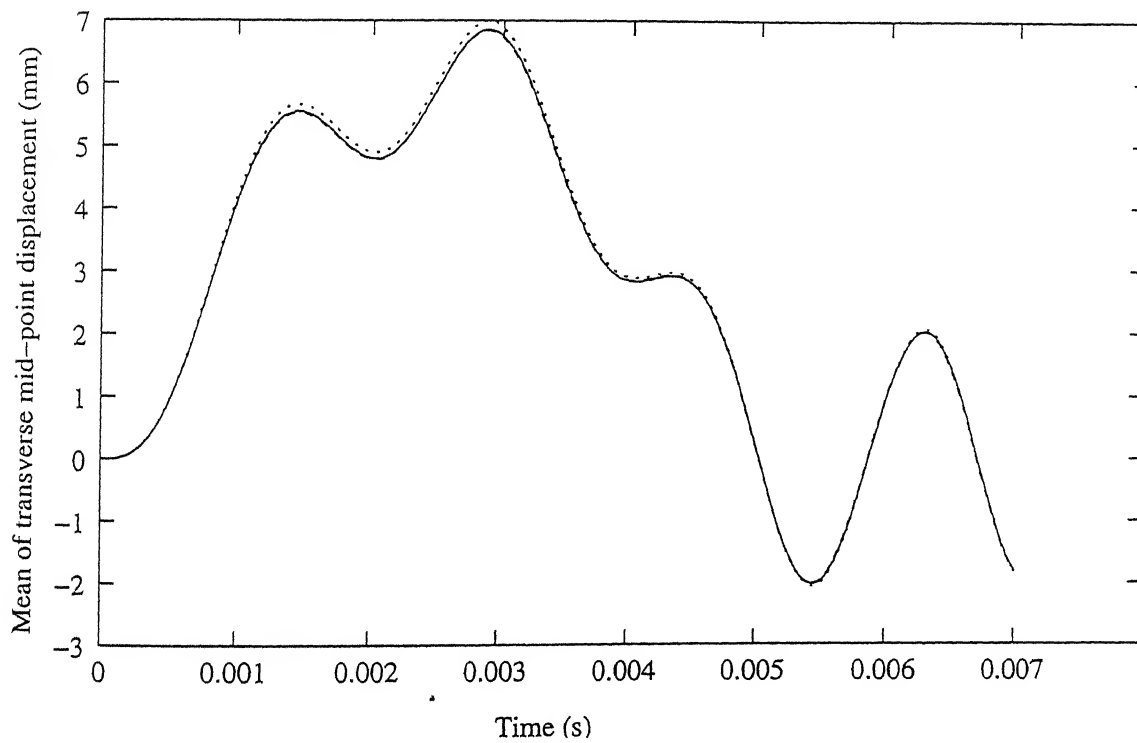


Figure 6.1: Validation of mean transverse mid-point displacement of a $[0^\circ/90^\circ/90^\circ/0^\circ]$ SSSS spherical panel obtained by the present SFEM and SCA approaches with MCS.
Key:- — :SCA, :SFEM, - - - :MCS.

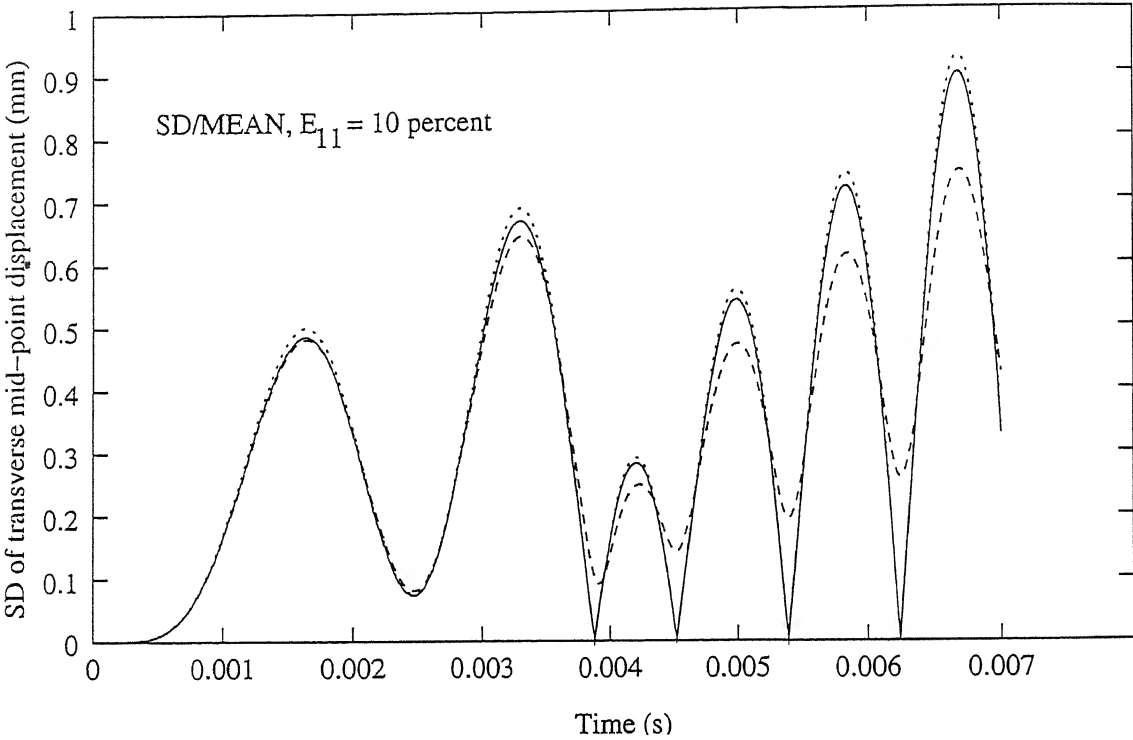


Figure 6.2: Validation of SD the transverse mid-point displacement for a $[0^\circ/90^\circ/90^\circ/0^\circ]$ SSSS spherical panel obtained from the present SCA and SFEM approaches with MCS.
Key: As in Figure 6.1.

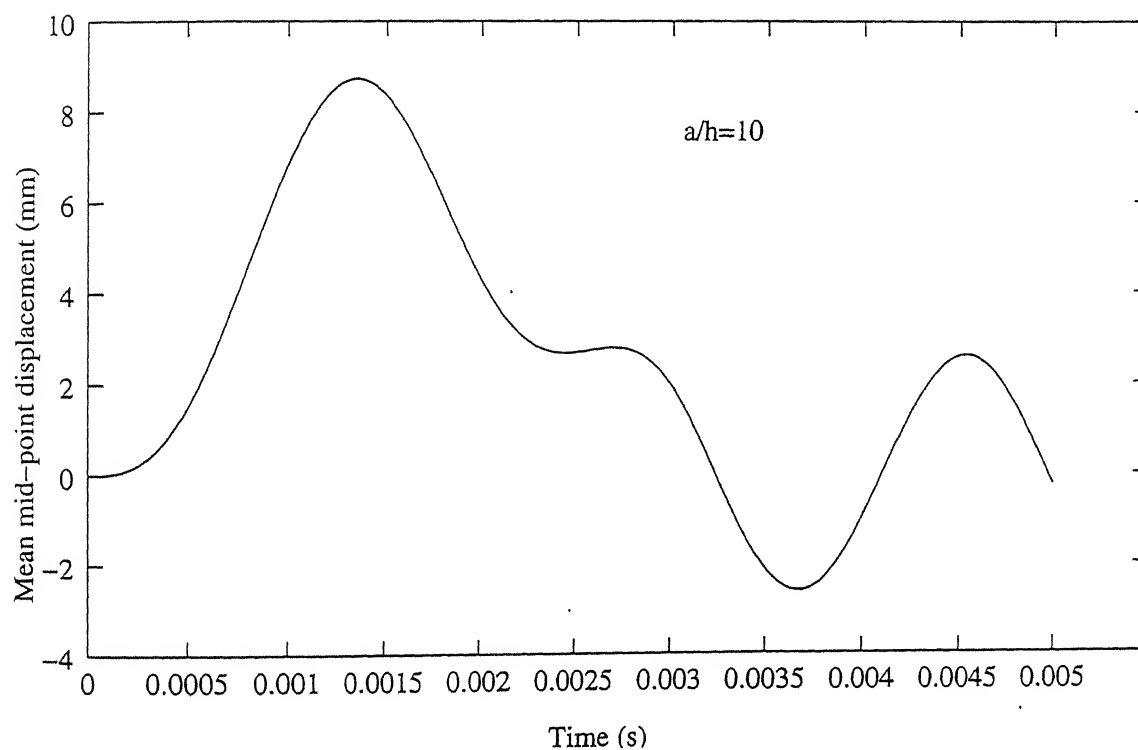


Figure 6.3: Variation of mean value of the transverse mid-point displacement of a $[0^\circ/90^\circ/90^\circ/0^\circ]$ SSSS laminate by SCA

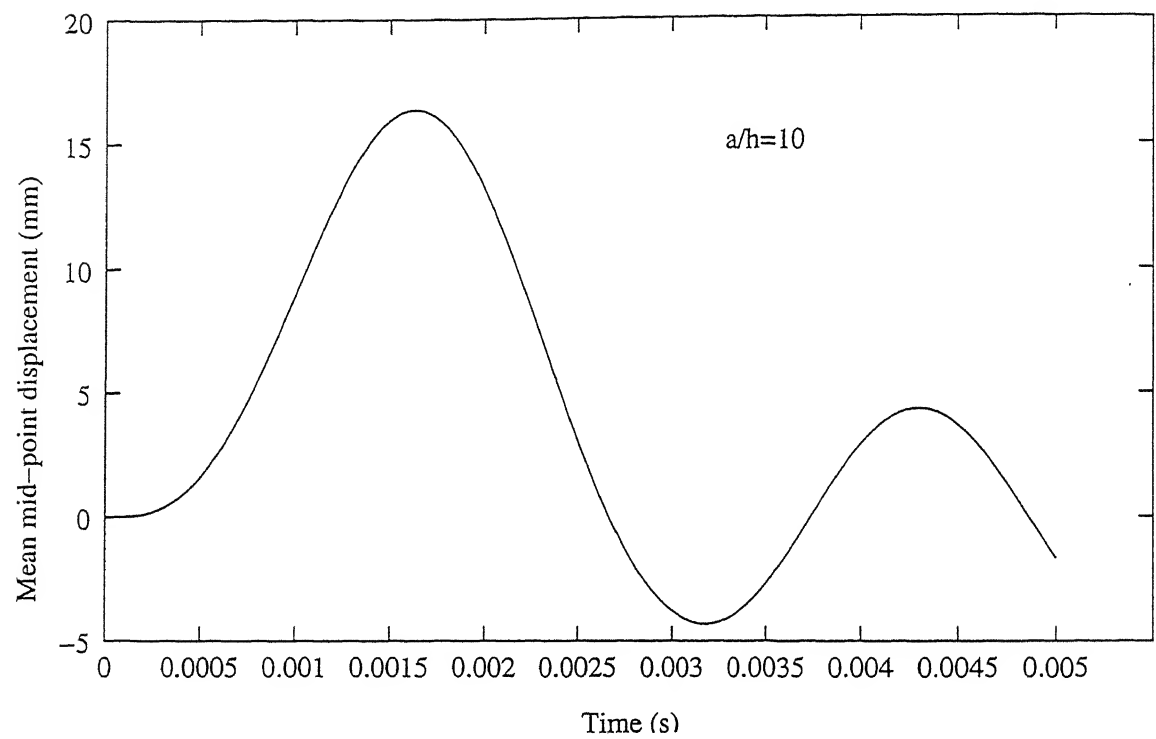


Figure 6.4: Variation of mean value of the transverse mid-point displacement of a $[0^\circ/90^\circ]$ SSSS laminate by SCA.

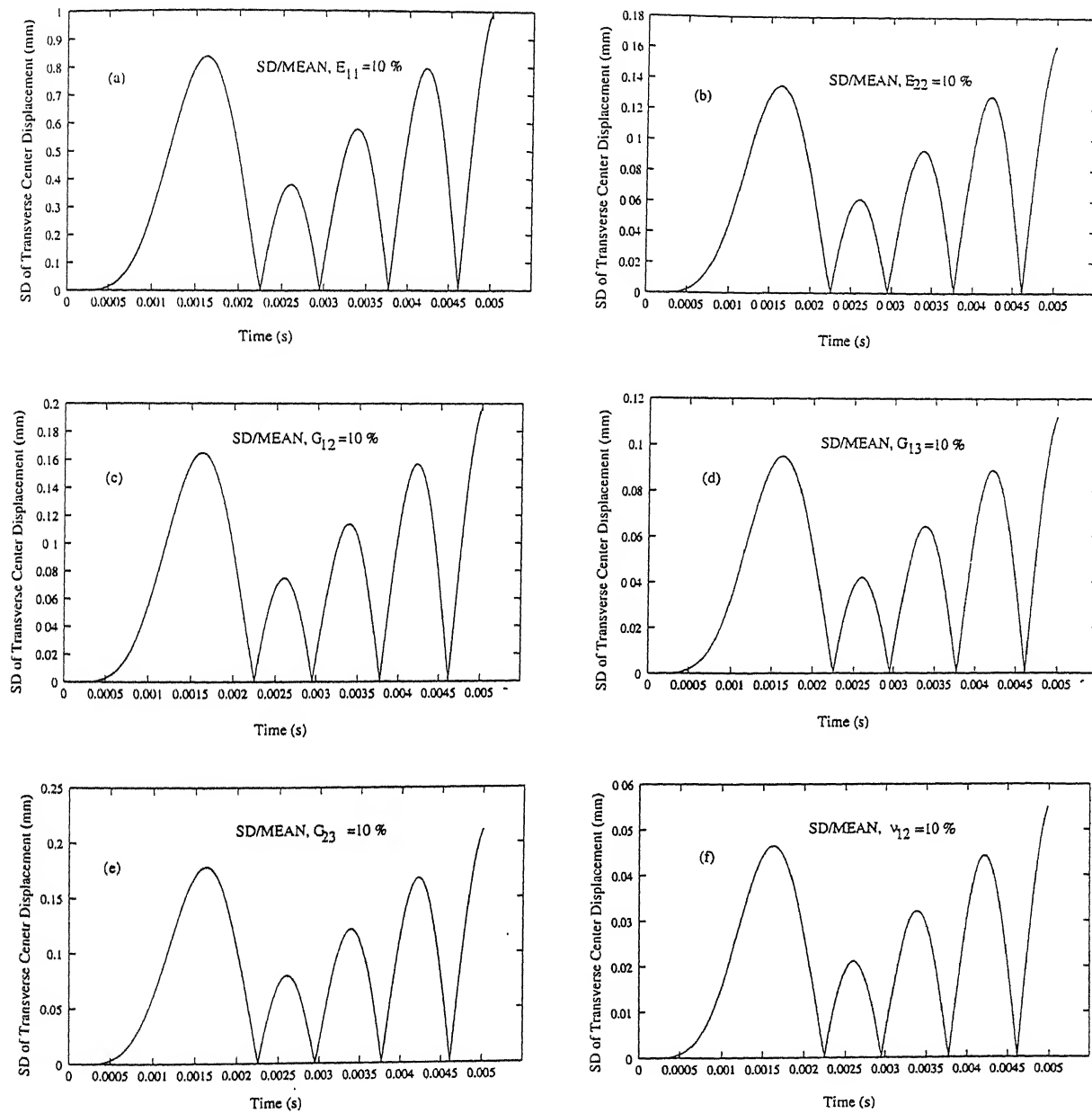


Figure 6.5: Variation of SD of the transverse mid-point displacement of a $[0^\circ/90^\circ/90^\circ/0^\circ]$ SSSS laminate by SCA with individual material properties as random.

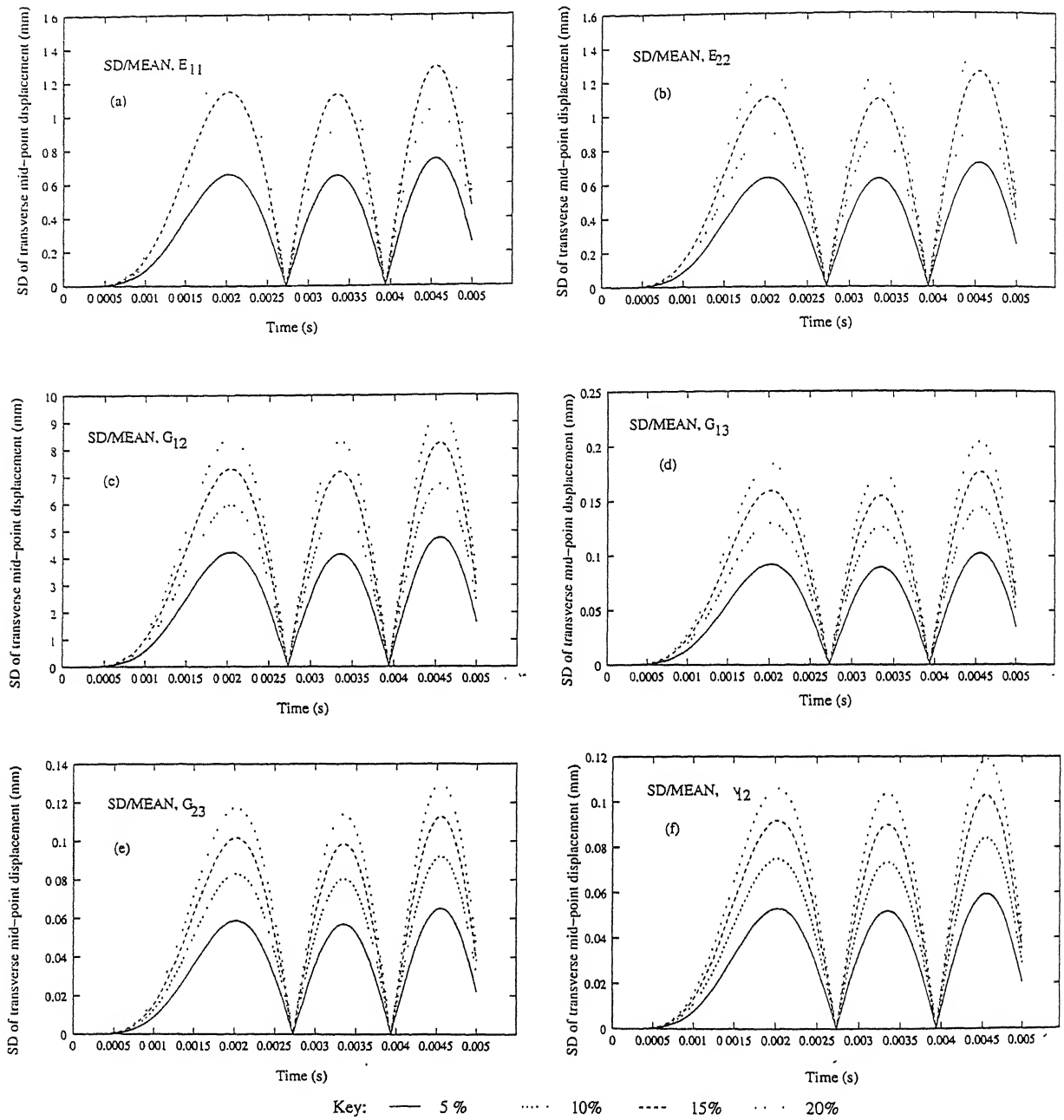


Figure 6.6: Variation of SD of the transverse mid-point displacement of a $[0^\circ/90^\circ]$ SSSS laminate by SCA.

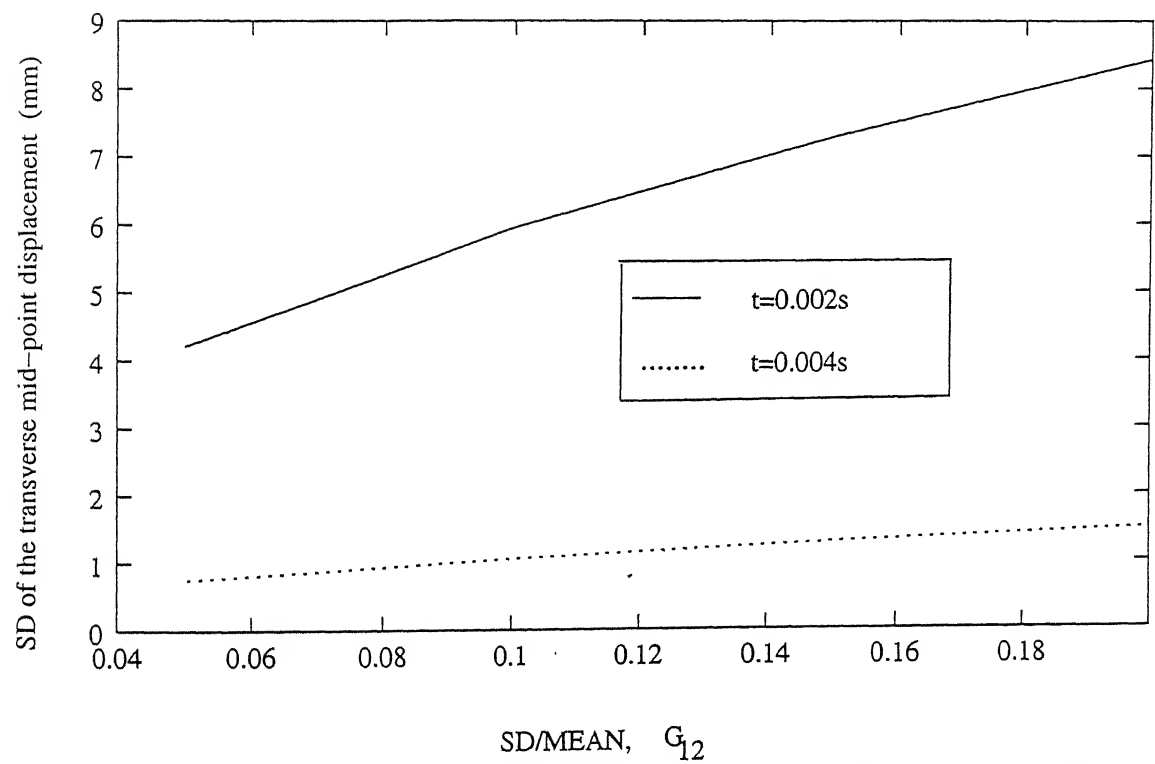


Figure 6.7: Variation of SD of the transverse mid-point displacement by SCA of a $[0^\circ/90^\circ]$ SSSS laminate with SD of material property G_{12} at $t=0.002s$ and $0.004s$.

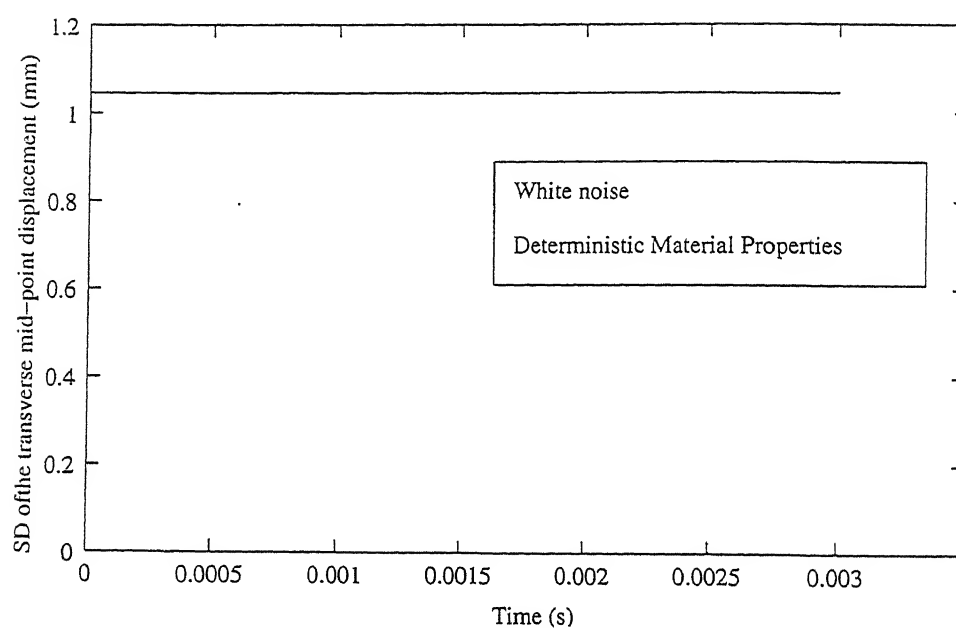


Figure 6.8: Variation of SD of the transverse mid-point displacement of a $[0^\circ/90^\circ/90^\circ/0^\circ]$ SSSS laminate with deterministic material properties and random excitation by SCA.

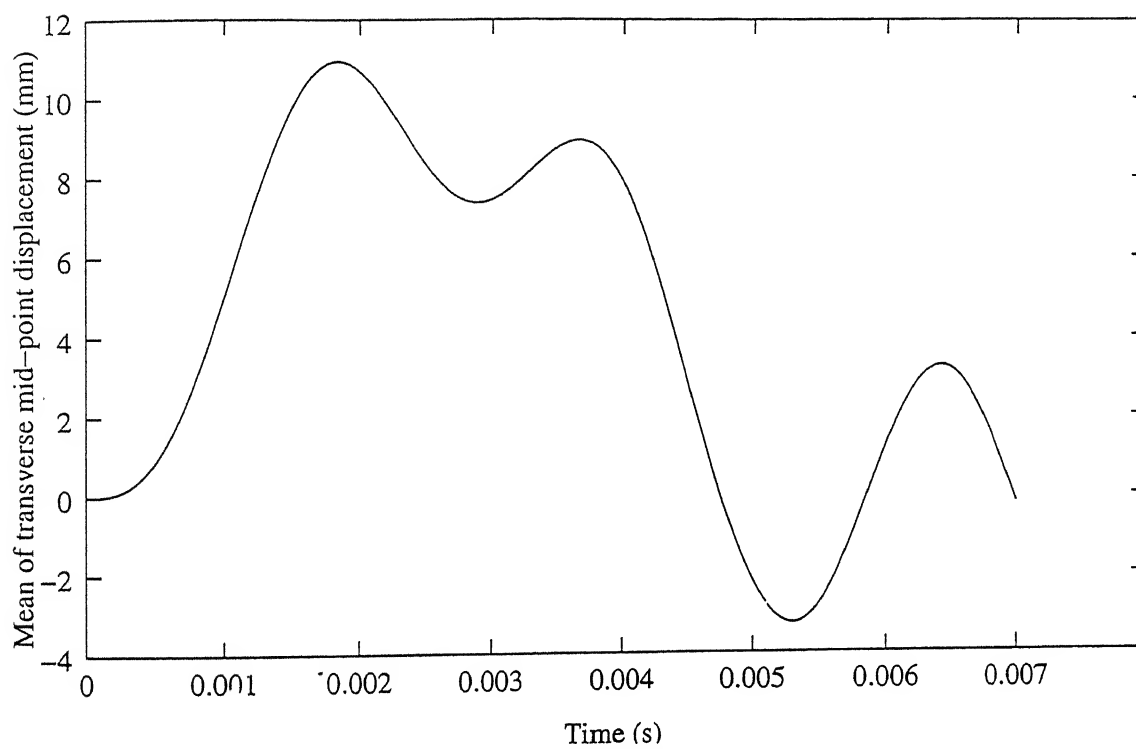


Figure 6.9: Mean Transverse mid-point displacement of a $[0^\circ/45^\circ/-45^\circ/90^\circ]$ CCCC laminate by SFEM.

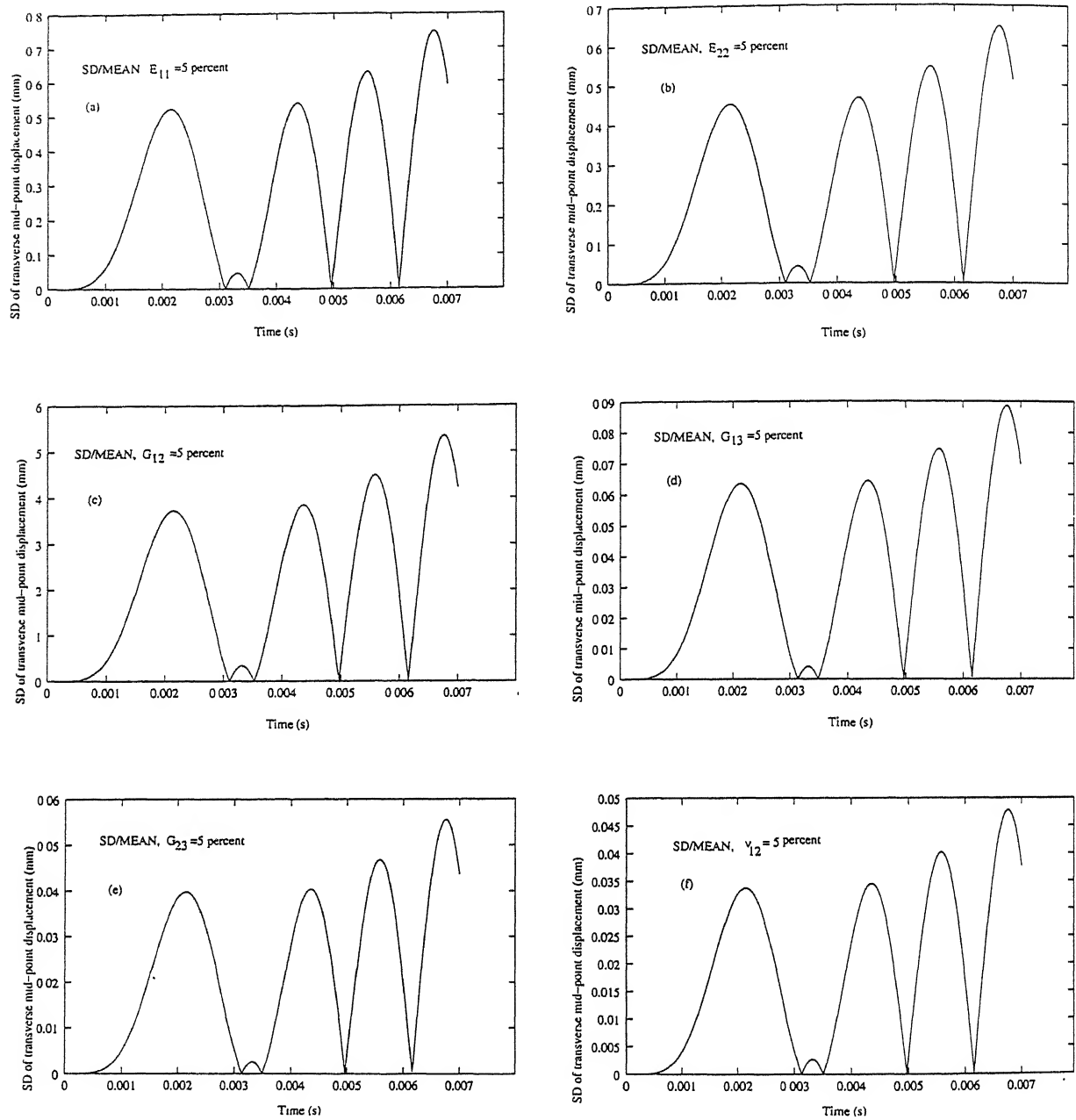


Figure 6.10 : Variation of SD of transverse mid-point displacement of a $[0^\circ/45^\circ/-45^\circ/90^\circ]$ laminate by SFEM.

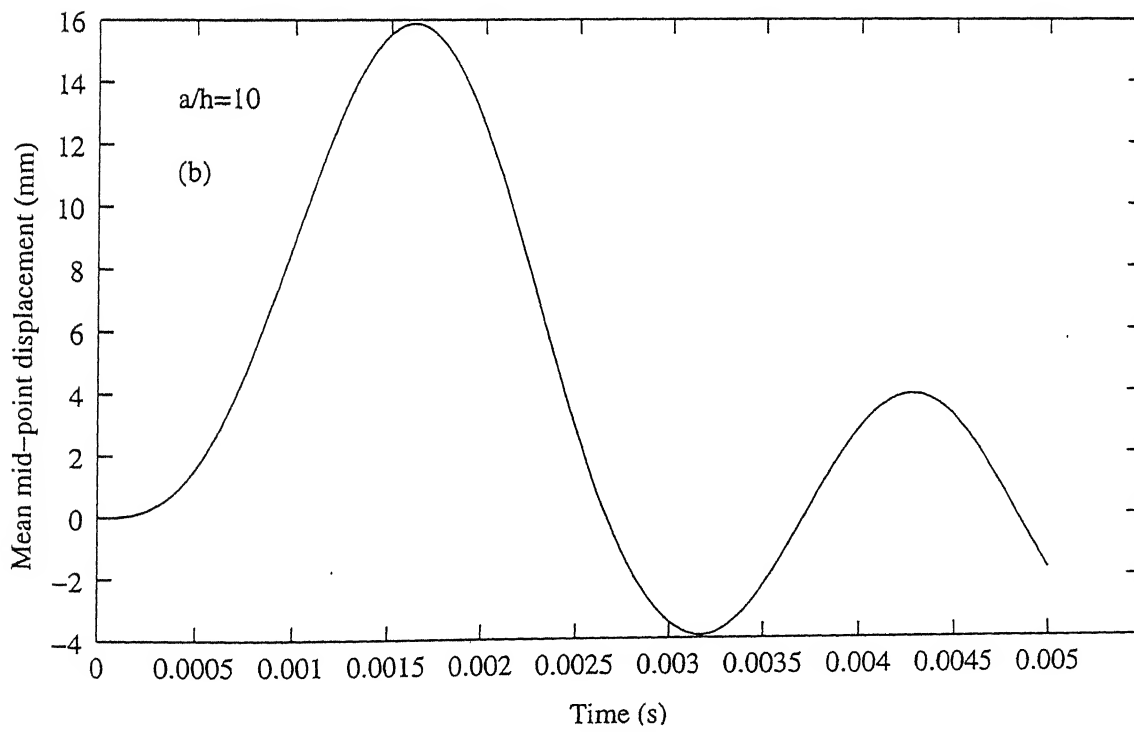
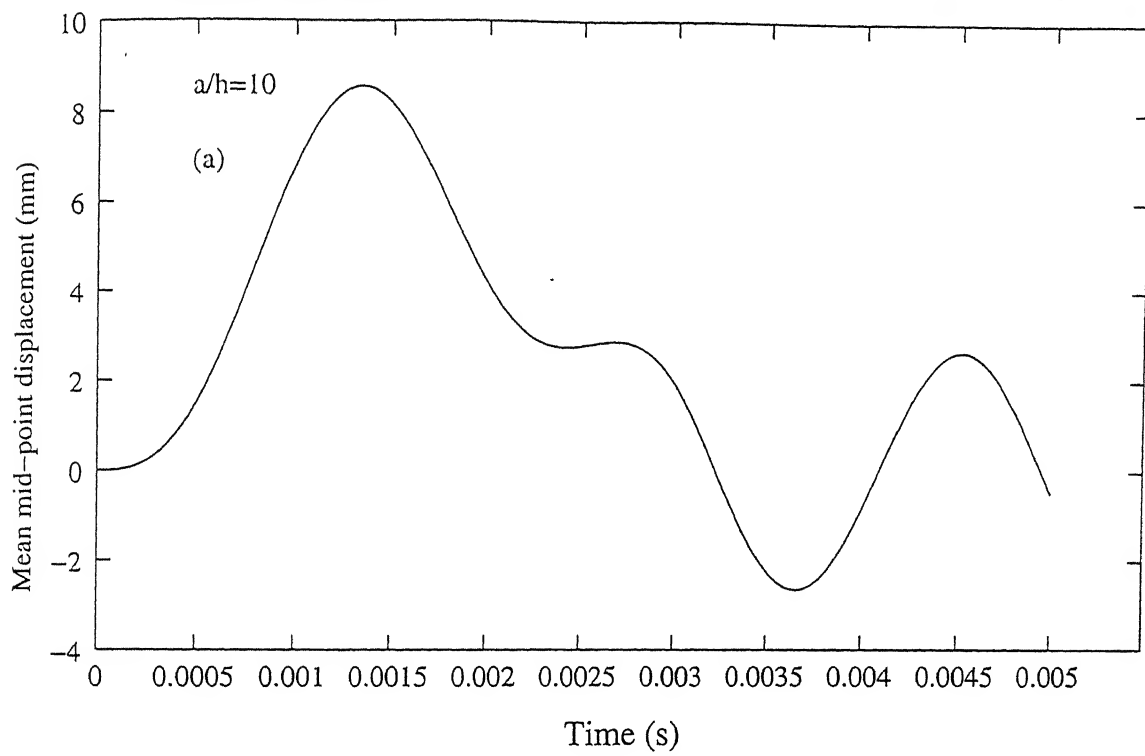


Figure 6.11 : Variation of the mean transverse mid-point displacement of (a) $[0^\circ/90^\circ/90^\circ/0^\circ]$ and (b) $[0^\circ/90^\circ]$ SSSS cylindrical panels by SCA.

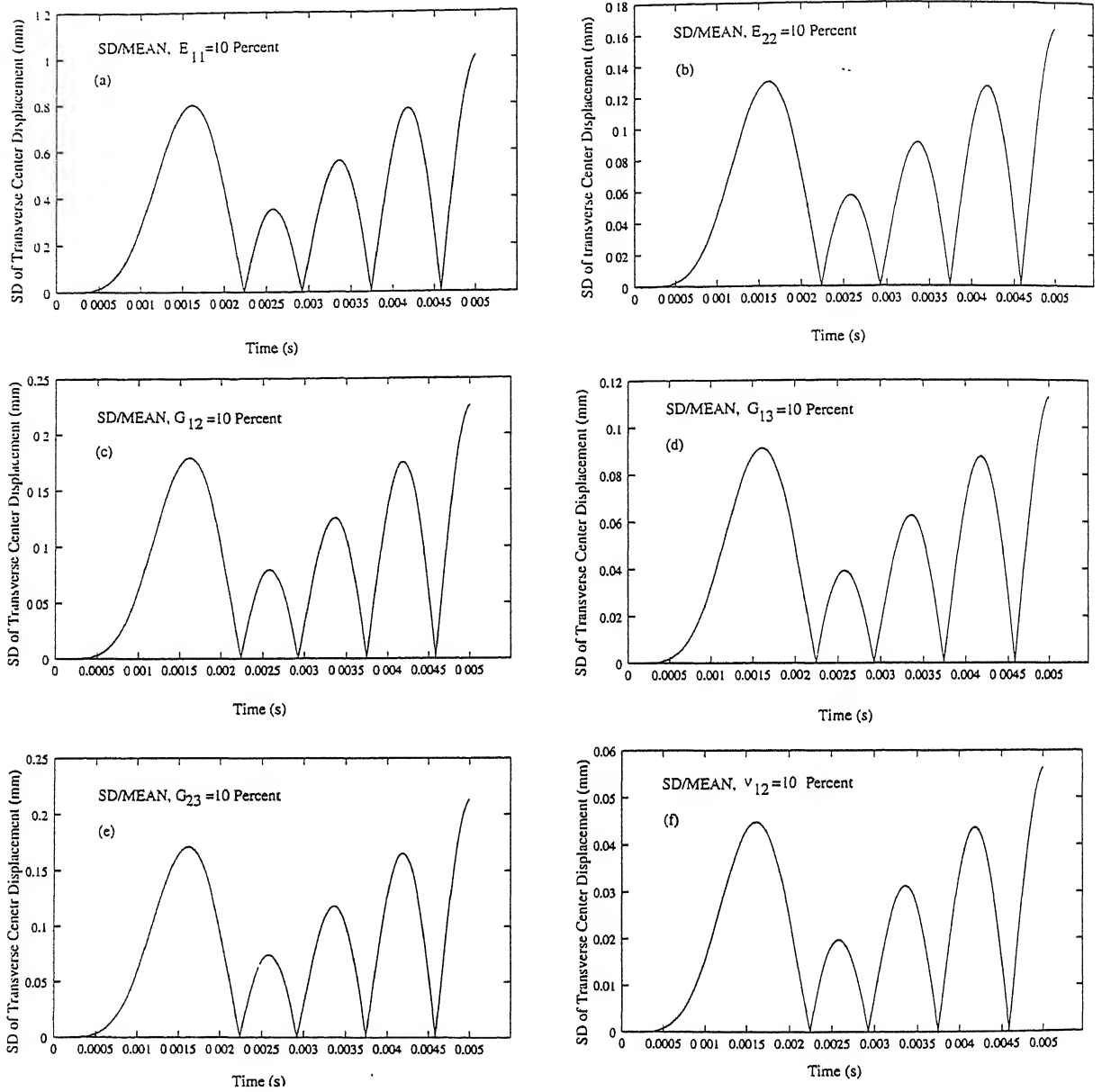


Figure 6.12 : Variation of SD of transverse mid-point displacement for a $[0^\circ/90^\circ/90^\circ/0^\circ]$ SSSS cylindrical panel by SCA.

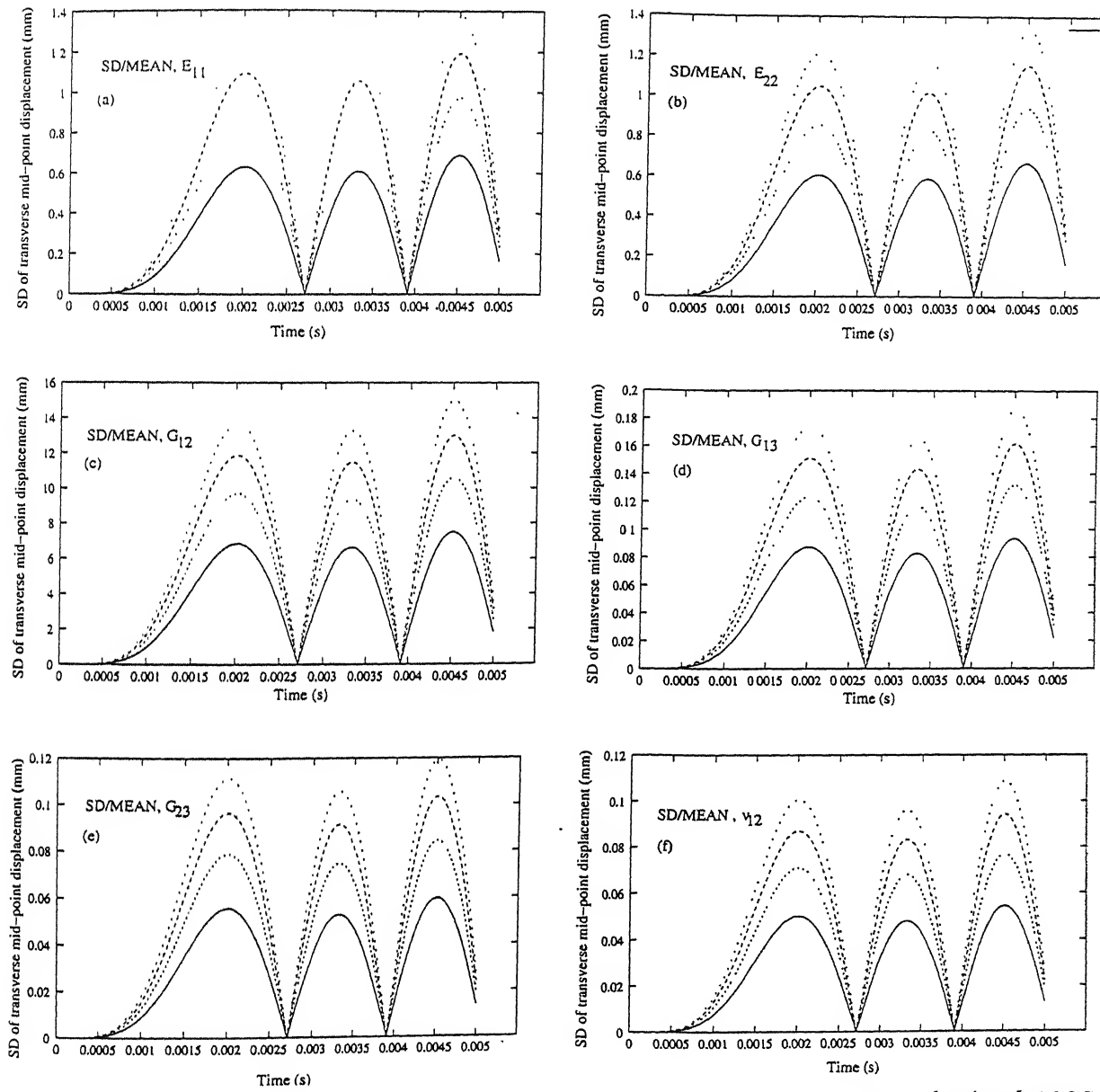


Figure 6.13 : Variation of SD of transverse mid-point displacement for a $[0^\circ/90^\circ]$ SSSS cylindrical panel by SCA.

Key: As in figure 6.6.

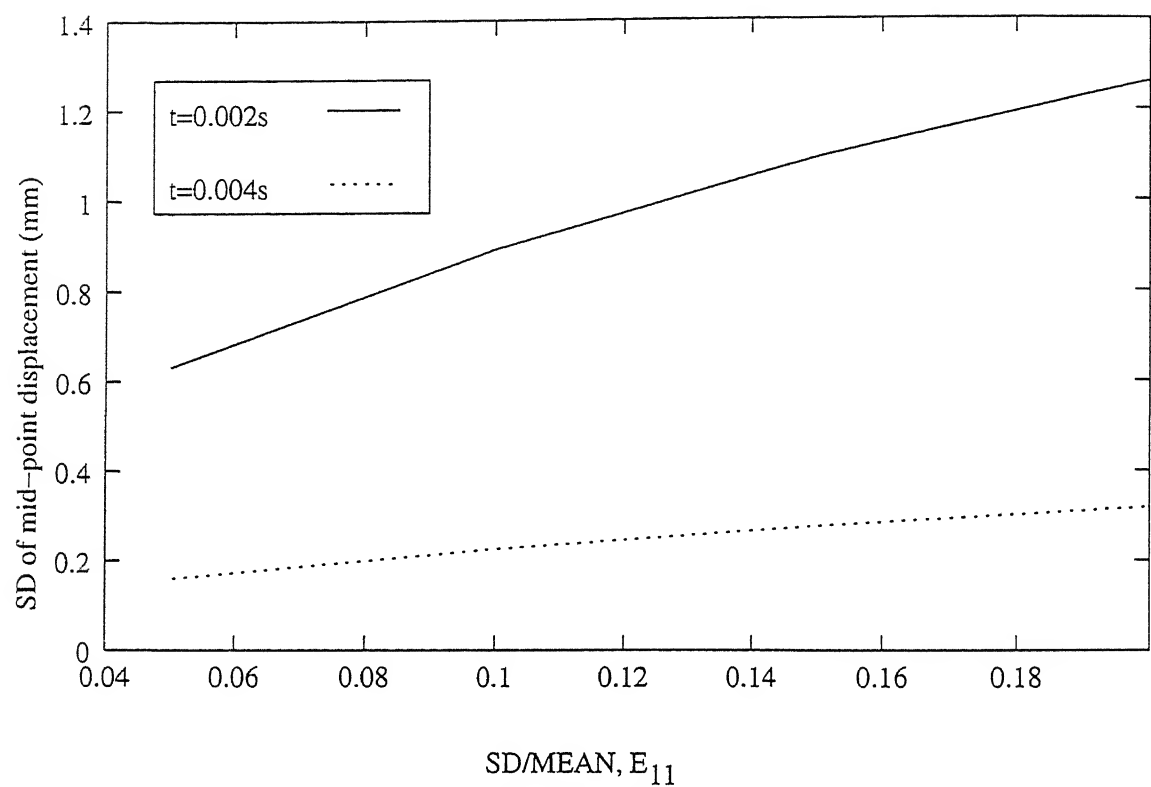


Figure 6.14: Variation of normalized SD of the transverse mid-point displacement of a $[0^{\circ}/90^{\circ}]$ SSSS cylindrical panel with SD of material property E_{11} at $t=0.002s$ and $0.004s$ by SCA.

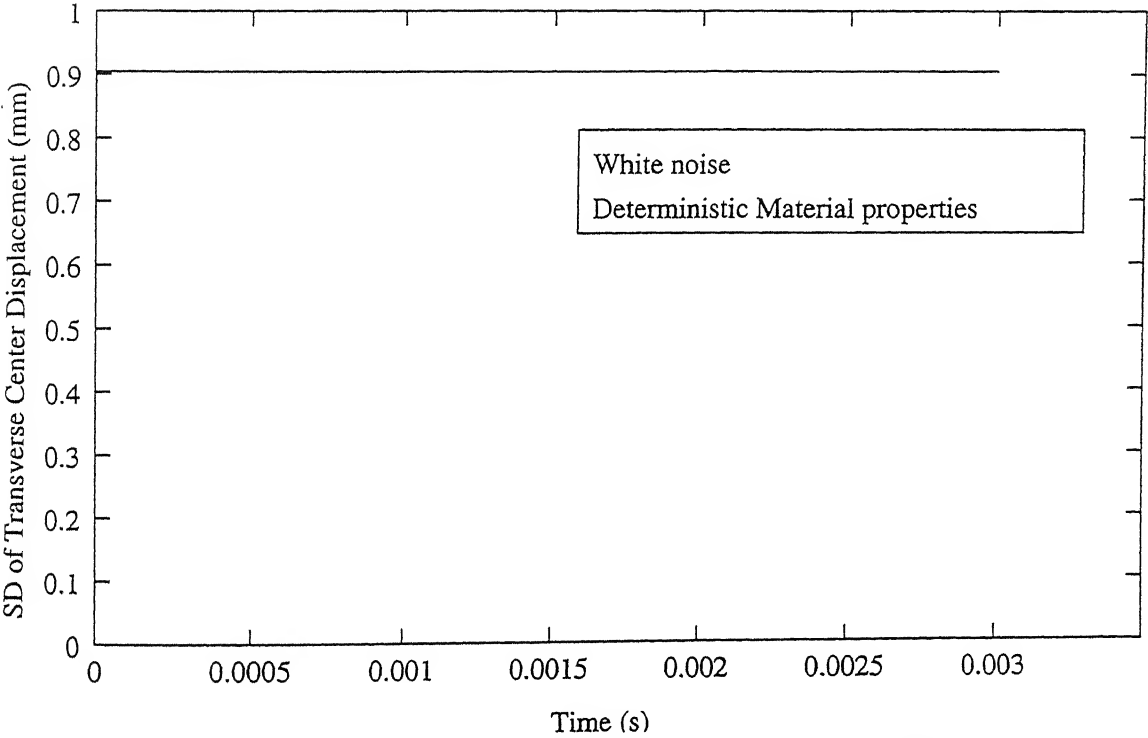


Figure 6.15: Variation of SD of the transverse mid-point displacement of a $[0^\circ/90^\circ/90^\circ/0^\circ]$ SSSS cylindrical panel with deterministic material properties and random excitation by SCA.

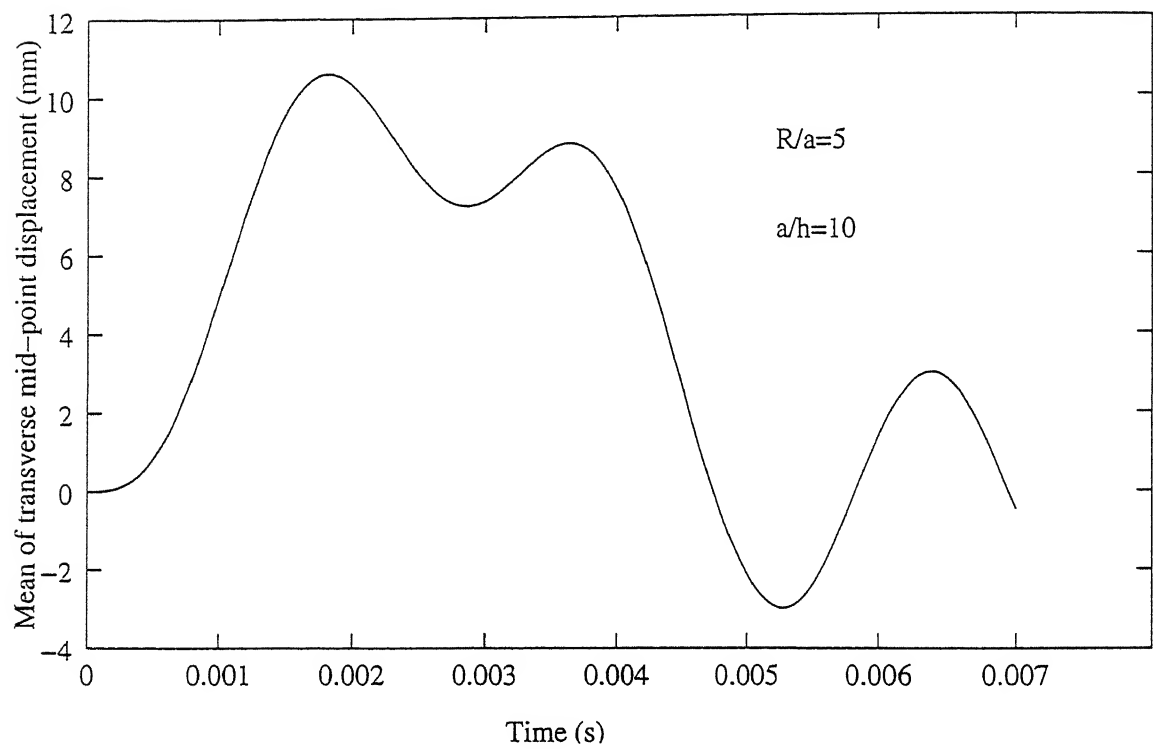


Figure 6.16: Mean Transverse mid-point displacement of a $[0^\circ/45^\circ/-45^\circ/90^\circ]$ CCCC cylindrical panel by SFEM.

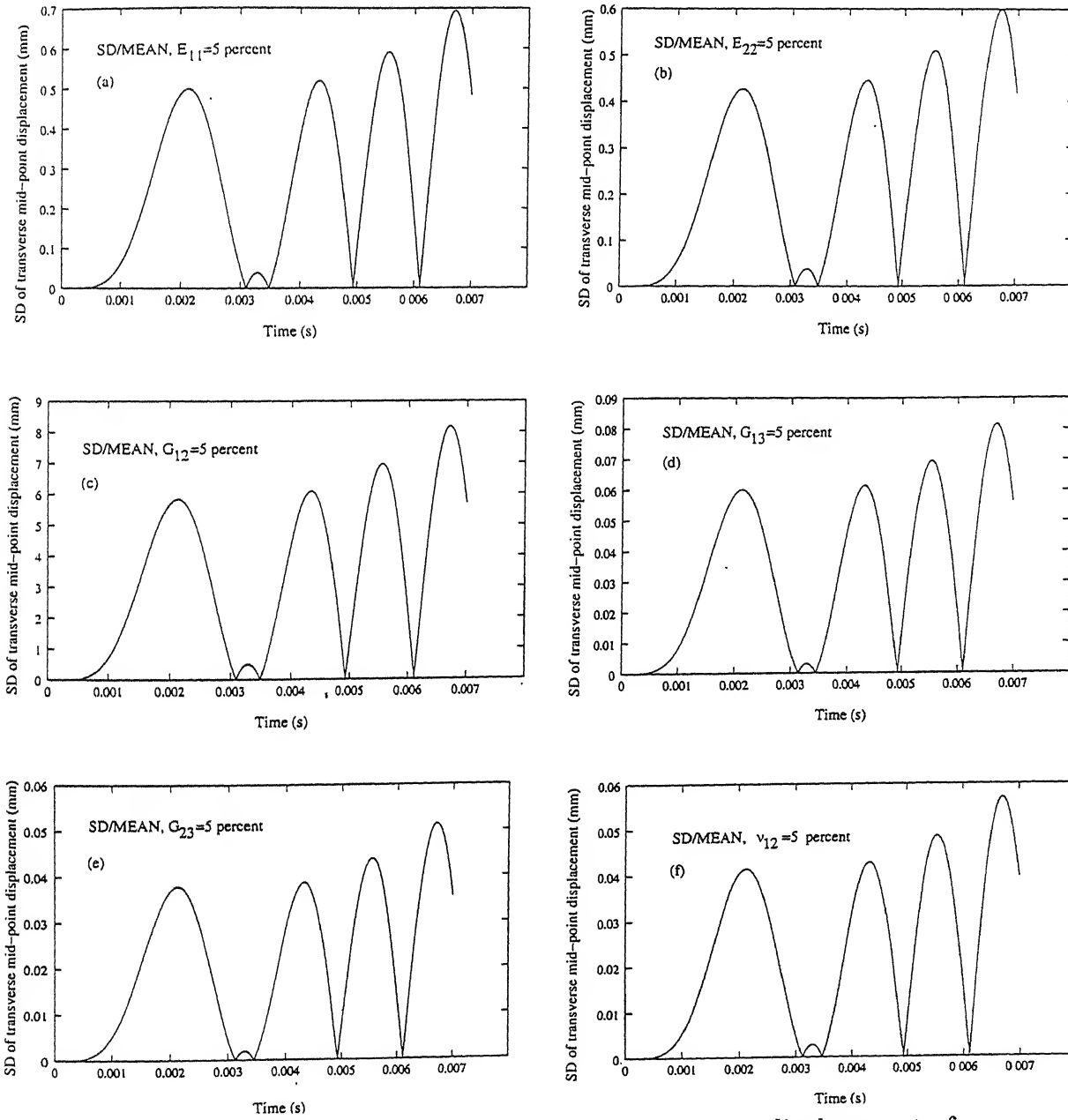


Figure 6.17: Variation of SD of transverse mid-point displacement of a $[0^\circ/45^\circ/-45^\circ/90^\circ]$ CCCC cylindrical panel by SFEM.

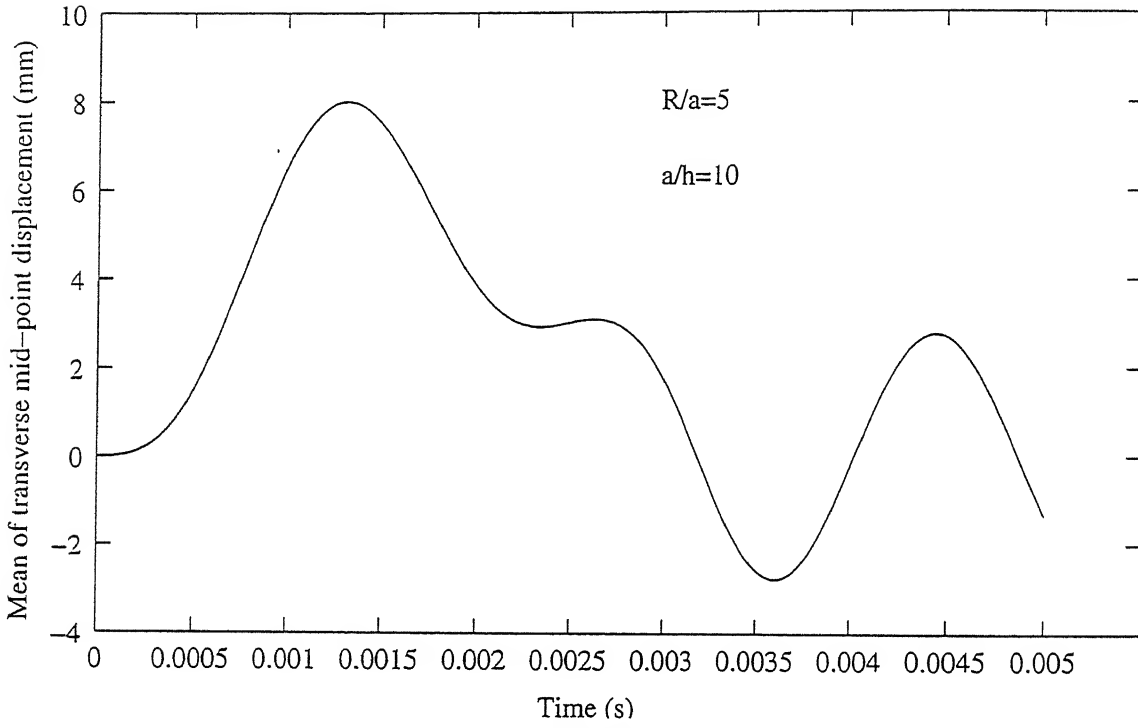


Figure 6.18: Mean transverse mid-point displacement of a $[0^\circ/90^\circ/90^\circ/0^\circ]$ SSSS spherical panel by SCA.

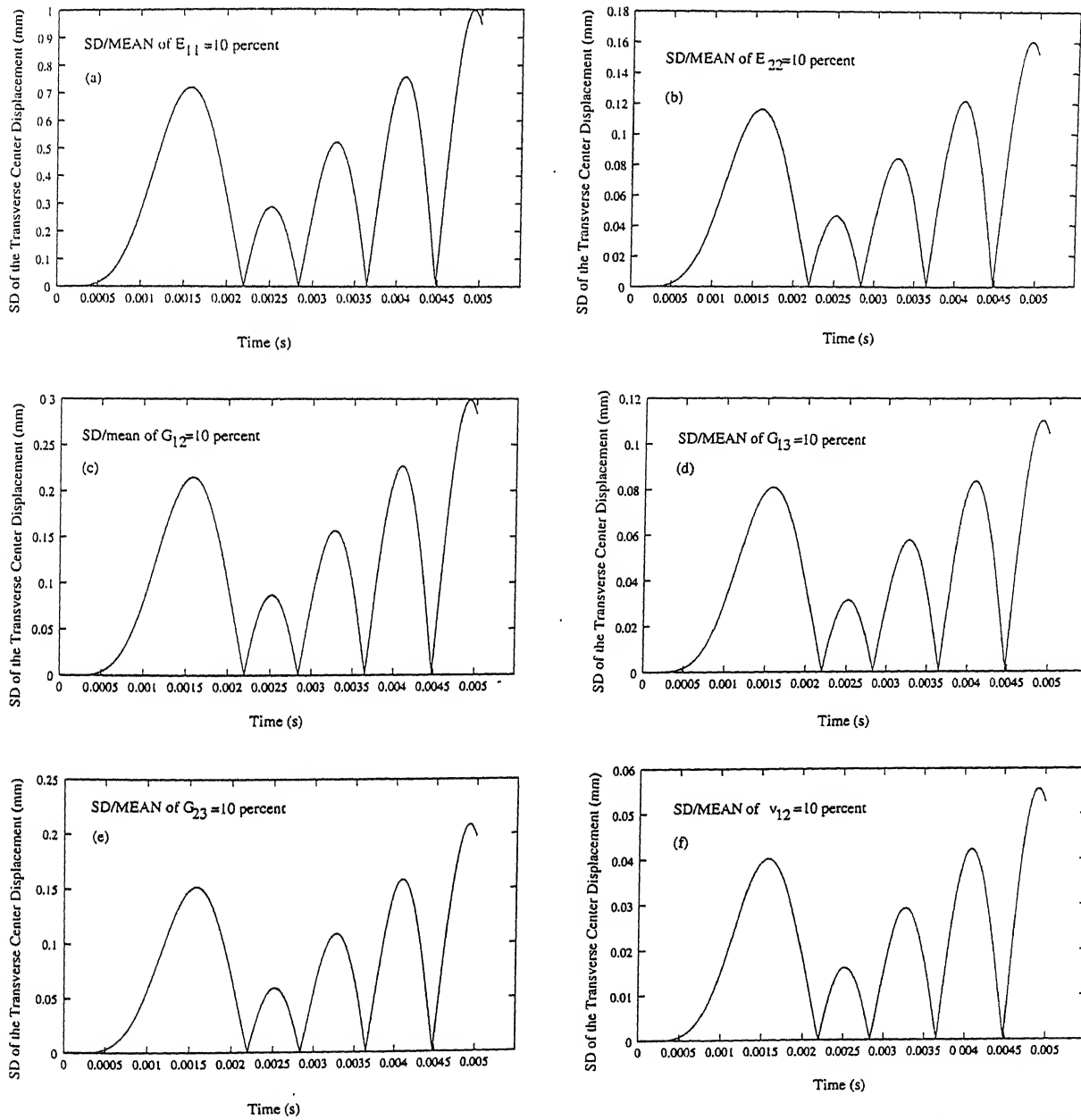


Figure 6.19: Sensitivity of transverse mid-point displacement of a $[0^\circ/90^\circ/90^\circ/0^\circ]$ SSSS spherical panel by SCA.

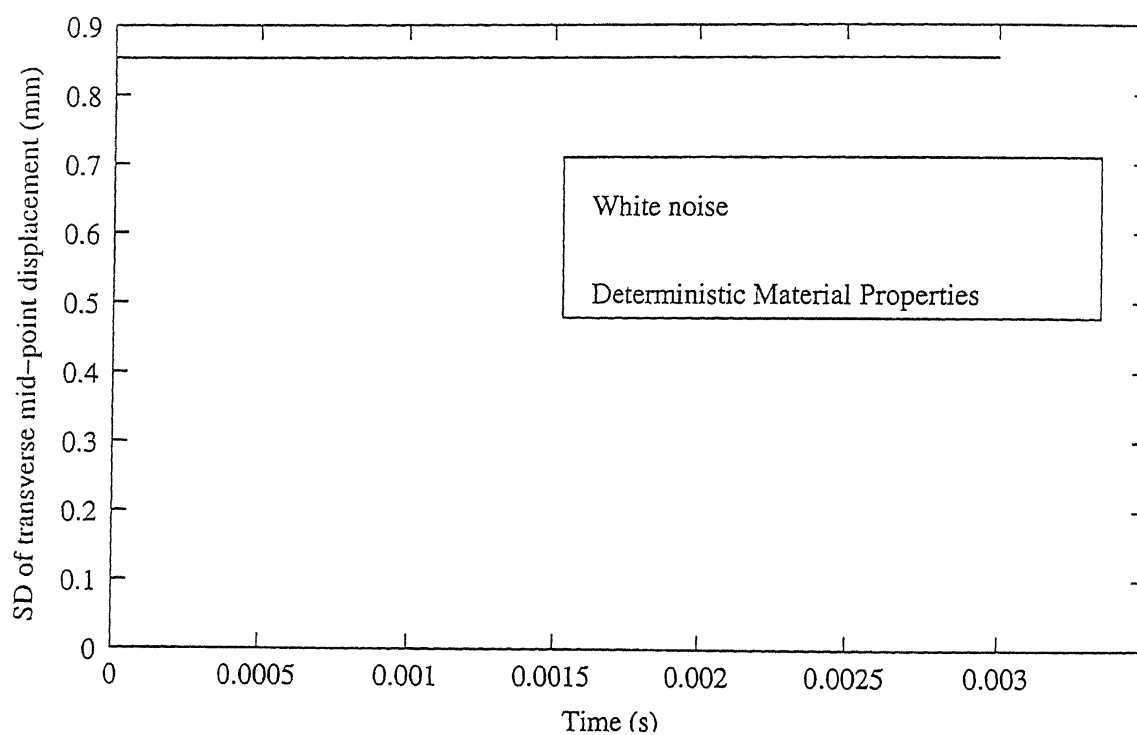


Figure 6.20: Sensitivity of transverse mid-point displacement of a $[0^\circ/90^\circ/90^\circ/0^\circ]$ SSSS spherical panel with deterministic material properties and random loading by SCA.

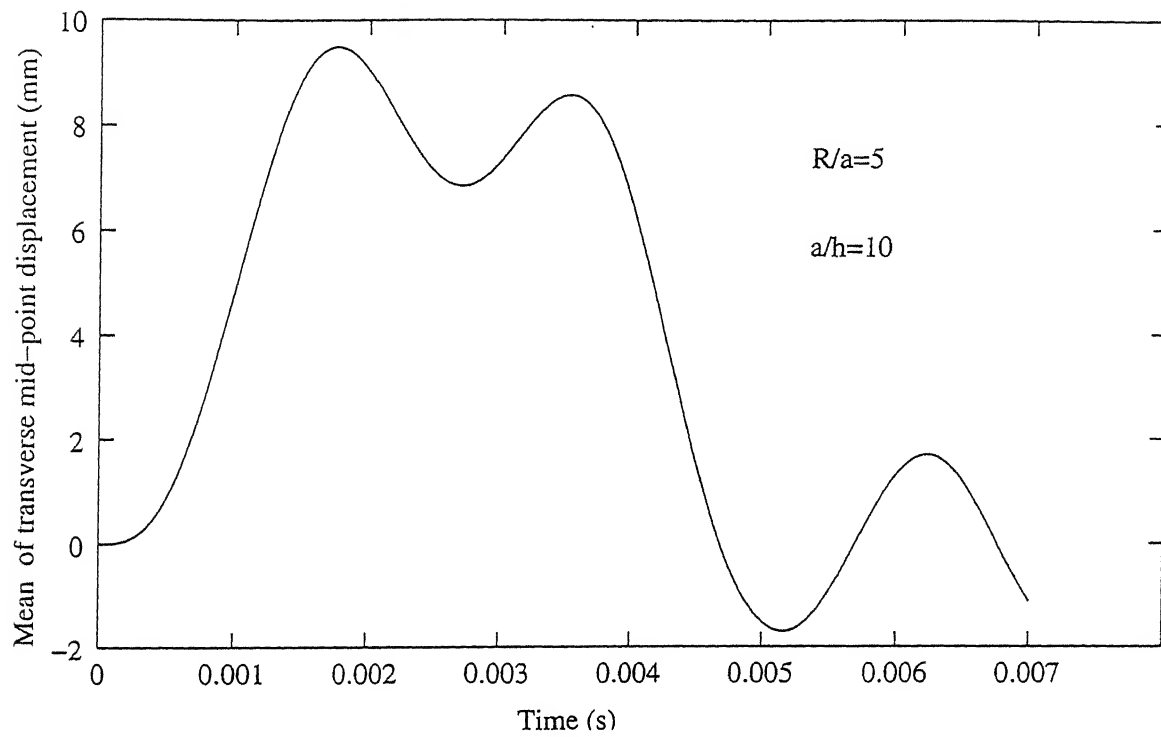


Figure 6.21 : Mean response of transverse mid-point displacement for a $[0^\circ/45^\circ/-45^\circ/90^\circ]$ CCCC spherical panel by SFEM.

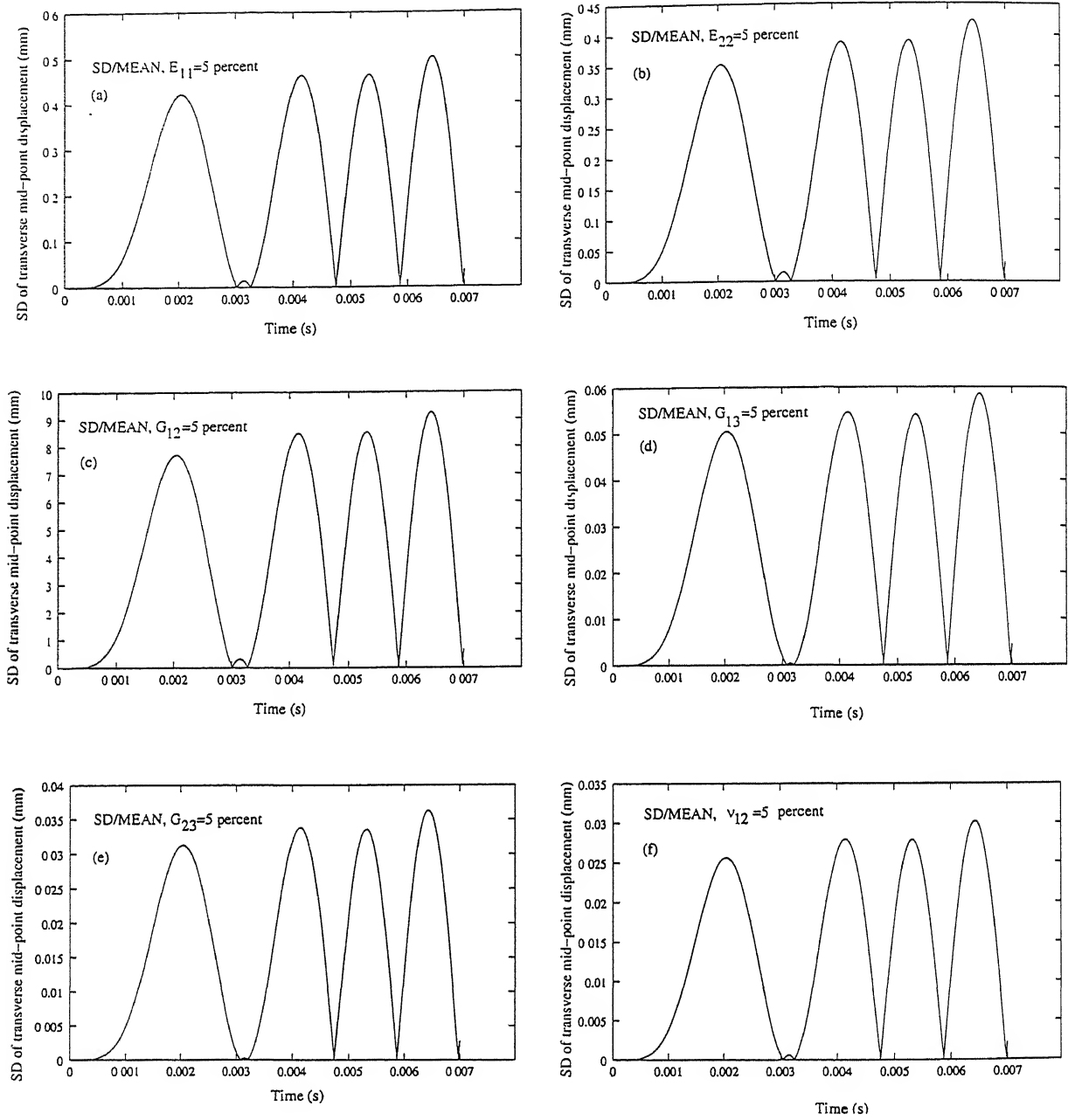


Figure 6.22: Sensitivity of the transverse mid point displacement for a $[0^\circ/45^\circ/-45^\circ/90^\circ]$ CCCC spherical panel by SFEM.

CHAPTER VII

CONCLUDING REMARKS AND SUGGESTIONS FOR FUTURE STUDIES

7.1 Introduction

The relevance of the present study, background and general formulation has been discussed in *Chapters* I, II and III. Specific formulation, probabilistic analysis, results and discussion related to buckling, free and forced vibrations of composite laminates, cylindrical and spherical panels using stochastic classical approach and stochastic finite element method have been discussed in *Chapters* IV, V and VI. Conclusions particular to the specific problems have also been presented in these chapters. In this chapter, we present the main concluding remarks based on the results obtained along with suggestions for future studies.

7.2 Concluding Remarks

From the critical examination of the conclusions presented in the previous chapters it is observed that the effect of randomness in the material properties and excitation on the response of composite panels is a complex phenomena. It is not possible to predict the effect in an exact

sense as a large number of parameters are involved in the evaluation of the response statistics.

Some of the main observations from the present study are:

- The first order perturbation approximation is quite capable to capture complete system behavior for the class of problems investigated and for the range of variation in the input SD considered.
- The study provides information regarding the need of the relative level of control required for the material properties during fabrication of laminated composite panels.
- The dispersions in structural responses vary linearly with scatter in the material properties.
- Classical laminate theory is not able to predict the response with sufficient accuracy even for thin laminates in the evaluation of probabilistic characteristics.
- The behavior of scatter in responses using shear deformation theories is different for all edges simply supported, anti-symmetric and symmetric cross-ply laminates.
- The longitudinal elastic modulus has been found to be the dominant material property for probabilistic analysis. However, in some of the cases, the shear moduli have also been found to be dominant.
- The dispersion in responses is least affected with scatter in Poisson's ratio.
- The sensitivity of response dispersion to variation in material properties is different for different edge conditions, curvature to side ratio and side to thickness ratio.
- In terms of buckling load scatter, cylindrical panel is more sensitive compared to spherical panel against dispersion in material properties, while, the trend is reversed for inplane modulus.

- For SSSS cross-ply laminate, the fundamental mean frequency for anti-symmetric laminate is always lower than symmetric laminate. However, the relative values of the other natural frequencies depend on the thickness ratio, mode of vibration and modular ratio.
- The natural frequencies show different sensitivity to randomness in different basic material properties. The dominant material property depends on the laminate construction, mode of vibration and geometrical parameters.
- For SSSS panel, the fundamental frequency of spherical panel is more sensitive as compared to other panels considered.
- At the start of motion in free vibration, the peak value of transverse displacement SD increases as time increases. The scatter in transverse displacement due to random excitation is large as compared to scatter due to randomness in material properties. Hence, very little confidence can be placed on the transverse displacement for free vibration, if material properties can not be obtained precisely.
- Sensitivity of displacement statistics depends on the support conditions and the stacking sequence.

7.3 Suggestions For Future Studies

The present study is only a step towards understanding the structural response of laminated composite plates, cylindrical and spherical panels with random material properties subjected to deterministic as well as random loading. Therefore, there is enough scope to extend the present work. Some of the possible extensions are:

- The system properties need to be modeled at the micro-mechanics level. With the help of this information, the material property statistics at the macro-level can be derived.
- The analysis should be extended to problems where geometric parameters and boundary conditions are uncertain. More realistic boundary conditions can be adopted for the study.
- A comprehensive study is needed to examine suitability of modeling of material properties as random field and random variable.
- The present study can be extended to include the effect of large deformations.
- Effect of hygrothermal behavior on the response.
- Effect of nonstationary excitation.

REFERENCES

- [1] C. Zweben, H.T. Hahn and T. W. Chou, *Mechanical behavior and properties of composite materials, Delaware composite design encyclopedia*, Vol. 1, Technomic Lancaster, (1989).
- [2] Z. Maekawa, H. Hamada, A. Yokoyama, S. Ishibashi and T. Tanimoto, Reliability evaluation of unidirectional CFRP, Proceedings of the 4th US-Japan Conference on Composite Materials, Washington D.C., (1988), pp. 1025-1034.
- [3] R. A. Ibrahim, Structural dynamics with parameter uncertainties, Trans. ASME, Applied Mechanics Review, 40(3), (1987), pp. 309-328.
- [4] L.F. Tenn, *Statistical analysis of fibrous composite strength data, test methods and design allowable for fibrous composites*, ASTM STP 734, American Society for Testing and Materials, (1981), pp. 229-244.
- [5] H. Fukuda, T.W. Chou and K. Kawata, Probabilistic approach on the strength of fibrous composites, Composite Materials, Proceedings Japan-US Conference, Tokyo, (1981), pp. 181-193.
- [6] Z. Maekawa, H. Hamada, K. Lee and T. Kitagawa, Reliability evaluation of mechanical properties of AS4/PEEK composites, Composites, 25(1), (1994), pp. 37-45.
- [7] S. C. Lin and T.Y. Kam, Probabilistic failure analysis of transversely loaded laminated composite plates using first order second moment method, ASCE J. Engineering Mechanics, 126(8), (2000), pp. 812-820.
- [8] M. Shinozuka and C.M. Jan, Digital simulation of random process and its applications, J. Sound and Vibration, 25(1), (1972), pp.111-128.
- [9] M. Shinozuka, Digital simulation of random process in engineering mechanics with the aid of FFT techniques, *Stochastic Problems in Mechanics*, Edited by S. T. Ariaratnam and H.H.E. Leipholtz, University of Waterloo Press, Waterloo, (1974).
- [10] A.H. Nayfeh, *Perturbation Methods*, John Wiley and Sons, New York, (1973).

- [11] D.W. Jordan and P. Smith, *Nonlinear Ordinary Differential Equations*, Oxford University Press, Oxford, (1977).
- [12] S. Nakagiri and T. Hisada, Stochastic finite element method applied to structural analysis with uncertain parameters, *Proceedings Int. Conference on FEM*, (1982), pp. 206-211.
- [13] T. Hisada and S. Nakagiri, Role of the stochastic finite element method in structural safety and reliability, *ICOSSAR'85, Proceedings Int. Conference on Structural Safety and Reliability*, (1985), pp. I-385.
- [14] W.K. Liu, T. Belytschko and A. Mani, Probabilistic finite elements for transient analysis in nonlinear continua, *Advances in Aerospace Structural Analysis*, *Proceedings ASME WAM*, Miami Beach, Fl., edited by O. H. Burnside and C.H. Pharr, Vol. AD-09, (1985), pp. 9-24.
- [15] W.K. Liu, G. Besterfield and A. Mani, Probabilistic finite element methods in nonlinear structural dynamics, *Computer Methods in Applied Mechanics and Engineering*, 57, (1986), pp. 61-81.
- [16] W.K. Liu, G. Besterfield and T. Belytschko, Transient probabilistic systems, *Computer Methods in Applied Mechanics and Engineering*, 67, (1988), pp. 27-54.
- [17] N.C. Nigam and S. Narayanan, *Applications of random vibrations*, Narosa Publishing House, New Delhi, (1994).
- [18] C. A. Shankara and N. G. R. Iyengar, A C^0 element for the free vibration analysis of laminated composite plates, *J. Sound and Vibration*, 191(5), (1996), pp. 721-738.
- [19] Y.K. Lin, *Probabilistic theory of structural dynamics*, McGraw-Hill, New York, (1967).
- [20] Y.K. Lin, F. Kozin, Y.K. Wen, F. Casciati, G.I. Schueller, A. Der Kiureghian, O. Ditlevsen and E.H. Vanmarke, Methods of stochastic dynamics, *Structural Safety*, 3, (1986), pp. 167-194.
- [21] T. Y. Yang and R.K. Kapania, Finite element random response analysis of cooling tower, *ASCE J. Engineering Mechanics*, 110(4), (1984), pp. 589-609.
- [22] V.V. Bolotin, *Statistical Methods in Structural mechanics*, Holden-Day, Inc., San Francisco, London, Amsterdam.
- [23] I. Elishakoff, *Probabilistic methods in theory of structures*, John Wiley & Sons, New York, (1983).
- [24] C. S. Manohar and R. A. Ibrahim, Progress in structural dynamics with stochastic parameter variations: 1987-1998, *Trans. ASME, Applied Mechanic Review*, 52(5), (1999), pp. 177-196.

- [25] R. Vaicaitis, Free vibrations of beams with random characteristics, *J. Sound and Vibration*, 35(1), (1974), pp. 13-21.
- [26] C. S. Manohar and R. N. Iyengar, Natural frequencies of simple stochastic structural systems, *Advances in structural testing, analysis & design*, Vol. I, ICSTAD Proceedings, Bangalore, August (1990), pp. 302-307.
- [27] M. Shinozuka and C. J. Astill, Random eigenvalue problems in structural analysis, *AIAA J.*, 10(4), (1972), pp. 656-662.
- [28] C. J. Astill, S.B. Nosseir and M. Shinozuka, Impact loading on structures with random properties, *J. Structural Mechanics*, 1(1), (1972), pp. 63-77.
- [29] I. Elishakoff, Y. J. Ren and M. Shinozuka, Variational principles developed for and applied to analysis of stochastic beam, *ASCE J. Engineering Mechanics*, 122(6), (1996), pp. 559-565.
- [30] Y.J. Ren, I. Elishakoff and M. Shinozuka, FEM for stochastic beams based on variational principles, *Trans. of the ASME J. Applied Mechanics*, 64, (1997), pp. 664-669.
- [31] T. D. Hien and M. Kleiber, Finite element analysis on stochastic Hamilton variational principle, *Computers & Structures*, 37(6), (1990), pp. 893-902.
- [32] R. Singh and C. Lee, Frequency response of linear systems with parameter uncertainties, *J. Sound and Vibration*, 168(1), (1993), pp. 71-92.
- [33] C. Lee and R. Singh, Analysis of discrete vibratory system with parameter uncertainties, Part I: eigen solution, *J. Sound and Vibration*, 174(3), (1994), pp. 379-394.
- [34] C. Lee and R. Singh, Analysis of discrete vibratory system with parameter uncertainties, Part II: Impulse response, *J. Sound and Vibration*, 174(3), (1994), pp. 395-412.
- [35] J. D. Collins and W. T. Thomson, The eigenvalue problem for structural systems with statistical properties, *AIAA J.*, 7(4), (1969), pp. 642-648.
- [36] P. Caravani and W. T. Thomson, Frequency response of a dynamic system with statistical damping, *AIAA J.*, 11(2), (1973), pp. 170-173.
- [37] P. C. Chen and W. W. Soroka, Multi-degree dynamic response of a system with statistical properties, *J. Sound and Vibration*, 37(4), (1974), pp. 547-556.
- [38] P. C. Chen and W.W. Soroka, Impulse response of a dynamic system with statistical properties, *J. Sound and Vibration*, 31(3), (1973), pp. 309-314.
- [39] C. Mok and E. A. Murray, Free vibrations of a slender bar with non-uniform characteristics, *J. The Acoustical Society of America*, 40(2), (1965), pp. 385-389.

- [40] M. Grigoriu, Eigenvalue problem for uncertain systems, *Trans. of the ASME, Applied Mechanics Review*, 44(11), part2, (1991), pp. S89-S95.
- [41] G. Deodatis, Weighted integral method. I: Stochastic stiffness matrix, *ASCE J Engineering. Mechanics*, 117(8), (1991), pp. 1851-1864.
- [42] G. Deodatis and M. Shinozuka, Weighted integral method. II: Response variability and reliability, *ASCE J. Engineering Mechanics*, 117(8), (1991), pp. 1865-1877.
- [43] C. G. Bucher and C. E. Brenner, Stochastic response of uncertain systems, *Archive of Applied Mechanics*, 62, (1992), pp. 507-516.
- [44] H. R. Millwater, S. V. harren and B. H. Thacker, Probabilistic analysis of structures involving random stress-strain behavior, *Proceedings of AIAA 32nd Structures, Structural Dynamics and Materials Conference*, Baltimore, April (1991), pp. 1236-1242.
- [45] S. Chen and Z. Zhang, The response sensitivity analysis for the complex stochastic structures to arbitrary deterministic excitation, *Advances in Structural Testing Analysis and Design, ICSTAD Proceedings*, Bangalore, India, July (1990), pp. 251-258.
- [46] P. H. Prasthofer and C. W. Beadle, Dynamic response of structures with statistical uncertainties in their stiffness, *J. Sound and Vibration*, 42(4), 1975, pp. 477-493.
- [47] D.O. Bliven and T. T. Soong, On frequencies of elastic beams with random imperfections, *J. of the Franklin Institute*, 287(4), (1969), pp. 297-304.
- [48] A. Zhang and S. Chen, The standard deviations of the eigensolutions for random MDOF systems, *Computers and Structures*, 39(6), (1991), pp. 603-07.
- [49] K. H. Low, A comprehensive approach for the eigenproblem of beams with arbitrary conditions, *Computers and Structures*, 39(6), (1991), pp. 671-678.
- [50] E. Vanmarcke and M. Grigoriu, Stochastic finite element analysis of simple beams, *ASCE J. Engineering Mechanics*, 109(5), (1983), pp. 1203-1214.
- [51] W.K.Liu, T. Belytschko and A. Mani, Random field finite elements, *International J. Numerical Methods in Engineering*, 23, (1986), pp. 1831-1845.
- [52] D. J. Gorman, Free vibration analysis of rectangular plates with non-uniform lateral elastic edge support, *Trans. ASME J. Applied mechanics*, 60, (1993), pp. 998-1003.
- [53] W. D. Iwan and H. Jenson, On the dynamic response of continuos systems including model uncertainty, *Trans. ASME J. Applied mechanics*, 60, (1993), pp. 484-490.
- [54] H. Jenson and W.D. Iwan, Response of system with uncertain parameters to stochastic excitation, *ASCE J. Engineering Mechanics*, 118(5), (1992), pp. 1012-1025.

- [55] S. Chen, Z. Liu and Z. Zhang, Random vibration analysis for large-scale structures with random parameters, *Computers & Structures*, 43(4), (1992), pp. 681-685.
- [56] J. Zhang and B. Ellingwood, Effects of uncertain material properties on structural stability, *ASCE J. Structural Engineering*, 121(4), (1995), pp. 705-716.
- [57] M. Shinozuka, Structural response variability, *ASCE J. Engineering Mechanics*, 113(6), (1987), pp. 825-842.
- [58] C. G. Bucher and M. Shinozuka, Structural response variability II, *ASCE J. Engineering Mechanics*, 114(12), (1988), pp. 2035-2053.
- [59] A. Kardara and C.G. Bucher and M. Shinozuka, Structural response variability III, *ASCE J. Engineering Mechanics*, 115(8), (1989), pp. 1726-1747.
- [60] G. Deodatis and M. Shinozuka, Bounds on response variability of stochastic systems, *ASCE J. Engineering Mechanics*, 115(11), (1989), pp. 2543-2563.
- [61] J. Wall and G. Deodatis, Variability response functions of stochastic plane stress/strain problems, *ASCE J. Engineering Mechanics*, 120(9), (1994), pp. 1963-1981.
- [62] M. A. Lawrence, Basic random variables in finite element analysis, *International J. for Numerical Methods in Engineering*, 24, (1987), pp. 1849-1863.
- [63] F. Yamazaki, M. Shinozuka and G. Dasgupta, Neumann expansion for stochastic finite element analysis, *ASCE J. Engineering Mechanics*, 114(8), (1988), pp. 1335-1354.
- [64] R. Ghanem and P. D. Spanos, Polynomial chaos in stochastic finite elements, *Trans. ASME, J. Applied Mechanics*, 57, (1990), pp. 197-202.
- [65] P.D. Spanos and R. Ghanem, Stochastic finite element expansions for random media, *ASCE J. Engineering Mechanics*, 115(5), (1989), pp. 1035-1053.
- [66] Q.S. Li, J.Q. Fang and D.K. Liu, Evaluation of structural dynamic responses by stochastic finite element method, *Structural Engineering and Mechanics*, 8(5), (1999), pp. 477-490.
- [67] I.D.Gupta and R. G. Joshi, Response spectrum superposition for structures with uncertain parameters, *ASCE J. Engineering Mechanics*, 127(3), (2001), pp. 233-241.
- [68] L.L Graham and E.F. Siragy, Stochastic finite element analysis for elastic buckling of stiffened panels, *ASCE J. Engineering Mechanics*, 127(1), (2001), pp. 91-97.
- [69] K. Handa and K. Andersson, Application of finite element methods in the statistical analysis of structures, *Proceedings of 3rd International Conference on Structural Safety and Reliability*, (1981), pp. 409-417.

- [70] W.Q. Zhu, Y.J. Ren and W.Q. Wu, Stochastic FEM based on local averages of random vector fields, *ASCE J. Engineering Mechanics*, 118(3), (1992), pp. 496-511.
- [71] S. Chakraborty and S. S. Dey, A stochastic finite element dynamic analysis of structures with uncertain parameters, *International Journal of Mechanical Sciences*, 40(11), (1998), pp. 1071-1087.
- [72] Z. Lei and C. Qiu, Nuemann dynamic stochastic finite element method of vibration for structures with stochastic parameters to random excitation, *Computers & Structures*, 77, (2000), pp. 651-657.
- [73] S. Nakagiri, H. Takabatake and S. Tani, Uncertain eigenvalue analysis of composite laminated plates by the stochastic finite element method, *Trans. Of The ASME J. of Engineering for Industry*, 109, (1987), pp. 9-12.
- [74] S. P. Engelstad and J.N. Reddy, Probabilistic methods for the analysis of metal matrix composites, *Composite Science and Technology*, 50, (1994), pp. 91-107.
- [75] A. F. Martin and A.W. Leissa, Application of the Ritz method to plane elasticity problems for composite sheets with variable fibre spacing, *Int. J. Numerical Methods in Engineering*, 28(1989), pp. 1813-1825.
- [76] A.W. Leissa and A. F. Martin, Vibration and buckling of rectangular composite plates with variable fibre spacing, *Composite Structures*, 14, (1990), pp. 339-357.
- [77] S. Adali, I. Elishakoff, A. Richter and V.E. Verijenko, Optimal design of symmetric angle-ply laminates for maximum buckling load with scatter in material properties, *Proceedings of AIAA Conference*, (1994), pp. 1041-1045.
- [78] G. Van Vinckenroy and W. P. de Wilde, The use of Monte Carlo techniques in statistical finite element methods for the determination of the structural behavior of composite materials structural components, *Composite Structures*, 32, (1995), pp. 247-253.
- [79] S. Salim, D. Yadav and N. G. R. Iyengar, Analysis of composite plates with random material characteristics, *Mechanics Research Communications*, 20(5), (1993), pp. 405-414.
- [80] S. Salim, N. G. R. Iyengar and D. Yadav, Buckling of laminated plates with random material characteristics, *Applied Composite Materials*, 5, (1998), pp. 1-9.
- [81] S. Salim, N.G.R. Iyengar and D. Yadav, Natural frequency characteristics of composite plate with random properties, *Structural Engineering Mechanics, An International Journal*, 6(6), (1998), pp. 659-671.
- [82] B. N. Raj, N. G. R. Iyengar and D. Yadav, Response of composite plates with random material properties using FEM and Monte Carlo simulation, *Advanced Composite Materials*, 7(3), (1998), pp. 219-237.

- [83] D. Yadav and N. Verma, Free vibration of composite circular cylindrical shells with random material properties Part I: general theory, *Composite Structures*, 41, (1997), pp. 331-338.
- [84] D. Yadav and N. Verma, Free vibration of composite circular cylindrical shells with random material properties Part II: applications, *Composite Structures*, 51(4), (2001), pp. 371-380.
- [85] D. Yadav and N. Verma, Buckling of composite circular cylindrical shells with random material properties, *Composite Structures*, 37(3/4), (1997), pp. 385-391.
- [86] V. S. Jagdish, Static response of composite laminates with randomness in material properties and external loading, M.Tech thesis, Dept. of Aerospace Engineering, IIT Kanpur, India, May 1998.
- [87] K. S. Raju, Buckling of composite laminates with random material properties using Monte Carlo simulation, M. Tech. Thesis, Dept. of Aerospace Engineering, IIT Kanpur, India, December 1998.
- [88] C. B. Smith, Some new types of orthotropic plates laminated of orthotropic material, *Trans. Of The ASME J. Applied Mechanics*, 20, (1953), pp. 286-288.
- [89] E. Reissner and Y. Stavsky, Bending and stretching of certain types of heterogeneous anisotropic elastic plates, *Trans. of the ASME J. Applied Mechanics*, 28, (1961), pp. 402-408.
- [90] S.G. Lekhnitskii, *Anisotropic plates*, translated from Russian, second edition by S. W. Tsai and T. Cheron, Gordon and Breach, (1968).
- [91] J.M. Whitney and A. W. Leissa, Analysis of heterogeneous anisotropic plates, *Trans. Of The ASME J. Applied Mechanics*, 36, (1969), pp. 261-266.
- [92] E. Reissner, Effects of transverse shear deformation on the bending of elastic plates, *Trans. Of The ASME J. Applied Mechanics*, 12, (1945), pp. A68-A77.
- [93] J.M. Whitney and C. T. Sun, A higher order theory for extensional motion of laminated composites, *J. Sound and Vibration*, 30, (1973), pp. 85-97.
- [94] P.M. Naghdi, On the theory of thin elastic shells, *Quart. App. Math.*, 14, (1957), pp. 369-380.
- [95] J. N. Reddy and C. F. Liu, A higher-order shear deformation theory of laminated elastic shells, *Int. J. Engineering Sciences*, 23(3), (1985), pp. 319-330.
- [96] J.N. Reddy, A simple higher order theory for laminated composite plates, *Trans. Of The ASME J. Applied Mechanics*, 51, (1984), pp. 745-752.
- [97] J.N. Reddy, *Energy and variational methods in applied mechanics*, John Wiley & Sons, New York, (1981).

- [98] K. P. Soldatos, On certain refined theories for plate bending, *Trans. of the ASME J. Applied Mechanics*, 55, (1988), pp. 994-995.
- [99] K. P. Soldatos, Vectorial approach for formulation of variationally consistent higher-order plate theories, *Composite Engineering*, 3(1), (1993), pp. 3-17.
- [100] J. R. Vinson and R. L. Seirakowski, *The behavior of structures composed of composite materials*, Martinus Nijhoff Publishers, Dordrecht, (1986).
- [101] R.M. Jones, *Mechanics of composite materials*, Script, Washington DC, (1975).
- [102] J. N. Franklin, *Matrix theory*, NJ, Prentice- Hall, Englewood Cliffs, (1968).
- [103] W. L. Brogan, *Modern control theory*. NJ, Prentice -Hall, Englewood Cliffs, (1985).
- [104] J.N. Reddy, *An introduction to the finite element method*, McGraw-Hill International Editions, (1985).
- [105] E. Hinton and D. R.J.Owen, *Finite element software for Plates and Shells*. Swansea, Pnmeridge Press, (1984).
- [106] L.C. Bank, Modification to beam theory for bending and twisting of open section composite beams, *Composite Structures*, 15, (1990), pp. 93-114.
- [107] J. F. Devalos, Y-C. Kim, and E.J. Barbero, Analysis of laminated beams with a layer-wise constant shear theory, *Composite Structures*, 28, (1994), pp. 241-253.
- [108] I. Raftoyiannis, L. A. Godoy, and E. J. Barbero, Buckling mode interaction of composite plate assemblies *Trans. of the ASME, Applied Mechanics Review*, 48(11, Part2), (1995), pp. 52-60.
- [109] J. L. Teply, J. N. Reddy, and E. J. Barbero, Bending, vibration and stability of ARALL laminates using a generalized laminated plate theory." *Int. J. Solids & Structures*, 27(5), (1991), 585-599.
- [110] G. J. Turvey and I.H. Marshall, *Buckling and post buckling of composite plates*, Chapman & Hall, London, (1995).
- [111] N. C. Nigam, *Introduction of Random Vibrations*. Cambridge, London: MIT Press, (1983).
- [112] A. A. Khdeir and J.N. Reddy, On the forced motions of antisymmetric cross-ply laminated plates, *Int. J. Mechanical Sciences*, 27(12), (1988), pp. 1808-1817.
- [113] A. A. Khdeir, J. N. Reddy and D. Frederick, A study of bending, vibration and buckling of cross-ply circular cylindrical shells with various shell theories, *Int. J. Engineering Sciences*, 27, (1989), pp. 1337-1351.

-
- [114] M. Kleiber and T.D.Hien, The stochastic finite element method, John & Wiley & Sons Ltd., Chichester, England, (1992).
 - [115] A. Kareem, W. J. Sun, Dynamic response of structures with uncertain damping, Engineering Structures, 12, (1990), pp. 1-8.
 - [116] A. K. Noor, Stability of multi-layered composite plates, Fibre Science & Technology, 8(2), (1975), pp. 81-89.
 - [117] N. S. Putcha and J. N. Reddy, Stability and natural vibration analysis of laminated plates by using a mixed element based on a refined plate theory, J. Sound & Vibration, 104(8), (1986), pp. 285-300.
 - [118] J. N. Reddy and A. A. Khdeir, Buckling and vibration of laminated composite plates using various plate theories, AIAA J., 27(12), (1989), pp. 1808-1817.
 - [119] P. D. Cha, W. Gu, Comparing the perturbed eigensolutions of a generalized and a standard eigen value problem, J. Sound & Vibration, 227(5), (1999), pp. 1122-1132.
 - [120] L. Meirovitch, *Elements of vibration analysis*, McGraw-Hill, International edition, Singapore, (1986).
 - [121] C. F. Gerald and P. O. Wheatley, *Applied numerical analysis*, Addison-Wesley Publishing Co., Fourth edition, California, USA, (1989).

APPENDIX A

DIFFERENTIAL OPERATORS

A.1 Plate

$$L_{11} = A_{11}d_1^2 + A_{66}d_2^2 - \bar{I}_1 d_t^2; \quad L_{12} = (A_{12} + A_{66})d_1 d_2;$$

$$L_{13} = -c_2[E_{11}d_1^3 + (E_{12} + 2E_{66})d_1 d_2^2] + \bar{I}_3 d_1 d_t^2;$$

$$L_{14} = (B_{11} - c_2 E_{11})d_1^2 + (B_{66} - c_2 E_{66})d_2^2 - \bar{I}_2 d_t^2;$$

$$L_{15} = [B_{12} + B_{66} - c_2(E_{12} + E_{66})]d_1 d_2; \quad L_{22} = A_{66}d_1^2 + A_{22}d_2^2 - \bar{I}_1' d_t^2;$$

$$L_{23} = -c_2[E_{22}d_2^3 + (E_{12} + 2E_{66})d_1^2 d_2] + \bar{I}_3' d_2 d_t^2;$$

$$L_{24} = L_{15}; \quad L_{25} = (B_{22} - c_2 E_{22})d_2^2 + (B_{66} - c_2 E_{66})d_1^2 - \bar{I}_2' d_t^2;$$

$$L_{33} = [c_1(D_{55} - c_1 F_{55}) - (A_{55} - c_1 D_{55})]d_1^2 + [c_1(D_{44} - c_1 F_{44}) - (A_{44} - c_1 D_{44})]d_2^2 + c_2^2[H_{11}d_1^4 + (2H_{12} + 4H_{66})d_1^2 d_2^2 + H_{22}d_2^4] + I_1 d_t^2 - c_2^2 I_7 (d_1^2 d_t^2 + d_2^2 d_t^2);$$

$$L_{34} = [c_1(D_{55} - c_1 F_{55}) - (A_{55} - c_1 D_{55})]d_1 - c_2[(F_{11} - c_2 H_{11})d_1^3 + [2F_{66} + F_{12} - c_2(2H_{66} + H_{12})]d_1 d_2^2 + \bar{I}_5 d_1 d_t^2];$$

$$L_{35} = [c_1(D_{44} - c_1 F_{44}) - (A_{44} - c_1 D_{44})]d_2 - c_2[(F_{22} - c_2 H_{22})d_2^3 + [2F_{66} + F_{12} - c_2(2H_{66} + H_{12})]d_1^2 d_2] + \bar{I}_5' d_2 d_t^2;$$

$$L_{44} = c_1(D_{55} - c_1 F_{55}) - (A_{55} - c_1 D_{55}) + [D_{11} - 2c_2 F_{11} + c_2^2 H_{11}]d_1^2 + [D_{66} - 2c_2 F_{66} + c_2^2 H_{66}]d_2^2 - \bar{I}_4 d_t^2;$$

$$\begin{aligned}
L_{45} &= [D_{12} + D_{66} - 2c_2(F_{12} + F_{66}) + c_2^2(H_{12} + H_{66})]d_1d_2; \\
L_{55} &= c_1(D_{44} - c_1F_{44}) - (A_{44} - c_1D_{44}) + [D_{22} - 2c_2F_{22} + c_2^2H_{22}]d_2^2 + [D_{66} - 2c_2F_{66} \\
&\quad + c_2^2H_{66}]d_1^2 - \bar{I}'_4d_t^2;
\end{aligned} \tag{A-1}$$

where $c_1 = 4/h^2$, $c_2 = c_1/3$, $d'_j = \partial^j / \partial x'_j$, $d_t^i = \partial^i / \partial t^i$.

A.2 Cylindrical Panel:

$$\begin{aligned}
L_{11} &= A_{11}d_1^2 + A_{66}d_2^2 - \bar{I}_1d_t^2; & L_{12} &= (A_{12} + A_{66})d_1d_2; \\
L_{13} &= -c_2[E_{11}d_1^3 + (E_{12} + 2E_{66})d_1d_2^2] + A_{12}d_1/R + \bar{I}_3d_1d_t^2; \\
L_{14} &= (B_{11} - c_2E_{11})d_1^2 + (B_{66} - c_2E_{66})d_2^2 - \bar{I}_2d_t^2; \\
L_{15} &= [B_{12} + B_{66} - c_2(E_{12} + E_{66})]d_1d_2; & L_{22} &= A_{66}d_1^2 + A_{22}d_2^2 - \bar{I}'_1d_t^2; \\
L_{23} &= -c_2[E_{22}d_2^3 + (E_{12} + 2E_{66})d_1^2d_2] + A_{22}d_2/R + \bar{I}'_3d_2d_t^2; \\
L_{24} &= L_{15}; & L_{25} &= (B_{22} - c_2E_{22})d_2^2 + (B_{66} - c_2E_{66})d_1^2 - \bar{I}'_2d_t^2; \\
L_{33} &= [c_1(D_{55} - c_1F_{55}) - (A_{55} - c_1D_{55})]d_1^2 + [c_1(D_{44} - c_1F_{44}) - (A_{44} - c_1D_{44})]d_2^2 \\
&\quad + c_2^2[H_{11}d_1^4 + (2H_{12} + 4H_{66})d_1^2d_2^2 + H_{22}d_2^4] - 2c_2(E_{12}d_1^2 + E_{22}d_2^2)/R - A_{22}/R^2 + I_1d_t^2 \\
&\quad - c_2^2I_7(d_1^2d_t^2 + d_2^2d_t^2); \\
L_{34} &= [c_1(D_{55} - c_1F_{55}) - (A_{55} - c_1D_{55})]d_1 - c_2[(F_{11} - c_2H_{11})d_1^3 + [2F_{66} + F_{12} \\
&\quad - c_2(2H_{66} + H_{12})]d_1d_2^2 + [B_{12}/R - c_2E_{12}/R]d_1 + \bar{I}_5d_1d_t^2; \\
L_{35} &= [c_1(D_{44} - c_1F_{44}) - (A_{44} - c_1D_{44})]d_2 - c_2[(F_{22} - c_2H_{22})d_2^3 + [2F_{66} + F_{12} \\
&\quad - c_2(2H_{66} + H_{12})]d_1^2d_2 + [B_{22}/R - c_2E_{22}/R]d_2 + \bar{I}'_5d_2d_t^2; \\
L_{44} &= c_1(D_{55} - c_1F_{55}) - (A_{55} - c_1D_{55}) + [D_{11} - 2c_2F_{11} + c_2^2H_{11}]d_1^2 + [D_{66} \\
&\quad - 2c_2F_{66} + c_2^2H_{66}]d_2^2 - \bar{I}_4d_t^2; \\
L_{45} &= [D_{12} + D_{66} - 2c_2(F_{12} + F_{66}) + c_2^2(H_{12} + H_{66})]d_1d_2; \\
L_{55} &= c_1(D_{44} - c_1F_{44}) - (A_{44} - c_1D_{44}) + [D_{22} - 2c_2F_{22} + c_2^2H_{22}]d_2^2 \\
&\quad + [D_{66} - 2c_2F_{66} + c_2^2H_{66}]d_1^2 - \bar{I}'_4d_t^2;
\end{aligned} \tag{A-2}$$

where $c_1 = 4/h^2$, $c_2 = c_1/3$, $d_j^i = \partial^i / \partial x_j^i$, $d_t^i = \partial^i / \partial t^i$.

A.3 Spherical Panel:

$$\begin{aligned}
L_{11} &= A_{11}d_1^2 + A_{66}d_2^2 - \bar{I}_1d_t^2; & L_{12} &= (A_{12} + A_{66})d_1d_2; \\
L_{13} &= -c_2[E_{11}d_1^3 + (E_{12} + 2E_{66})d_1d_2^2] + A_{11}d_1/R + A_{12}d_1/R + \bar{I}_3d_1d_t^2; \\
L_{14} &= (B_{11} - c_2E_{11})d_1^2 + (B_{66} - c_2E_{66})d_2^2 - \bar{I}_2d_t^2; \\
L_{15} &= [B_{12} + B_{66} - c_2(E_{12} + E_{66})]d_1d_2; & L_{22} &= A_{66}d_1^2 + A_{22}d_2^2 - \bar{I}_1'd_t^2; \\
L_{23} &= -c_2[E_{22}d_2^3 + (E_{12} + 2E_{66})d_1^2d_2] + A_{12}d_2/R + A_{22}d_2/R + \bar{I}_3'd_2d_t^2; \\
L_{24} &= L_{15}; & L_{25} &= (B_{22} - c_2E_{22})d_2^2 + (B_{66} - c_2E_{66})d_1^2 - \bar{I}_2'd_t^2; \\
L_{33} &= [c_1(D_{55} - c_1F_{55}) - (A_{55} - c_1D_{55})]d_1^2 + [c_1(D_{44} - c_1F_{44}) - (A_{44} - c_1D_{44})]d_2^2 + c_2^2[H_{11}d_1^4 \\
&+ (2H_{12} + 4H_{66})d_1^2d_2^2 + H_{22}d_2^4] - 2c_2(E_{12}d_1^2 + E_{22}d_2^2)/R - 2c_2(E_{11}d_1^2 + E_{12}d_2^2)/R \\
&- (A_{11}/R_1^2 + 2A_{12}/R_1R + A_{22}/R_2^2) + I_1d_t^2 - c_2^2I_7(d_1^2d_t^2 + d_2^2d_t^2); \\
L_{34} &= [c_1(D_{55} - c_1F_{55}) - (A_{55} - c_1D_{55})]d_1 - c_2[(F_{11} - c_2H_{11})d_1^3 + [2F_{66} + F_{12} \\
&- c_2(2H_{66} + H_{12})]d_1d_2^2 + [B_{11}/R + B_{12}/R - c_2(E_{11}/R + E_{12}/R)]d_1 + \bar{I}_5d_1d_t^2; \\
L_{35} &= [c_1(D_{44} - c_1F_{44}) - (A_{44} - c_1D_{44})]d_2 - c_2[(F_{22} - c_2H_{22})d_2^3 + [2F_{66} + F_{12} \\
&- c_2(2H_{66} + H_{12})]d_1^2d_2] + [B_{12}/R + B_{22}/R - c_2(E_{12}/R + E_{22}/R)]d_2 + \bar{I}_5'd_2d_t^2; \\
L_{44} &= c_1(D_{55} - c_1F_{55}) - (A_{55} - c_1D_{55}) + [D_{11} - 2c_2F_{11} + c_2^2H_{11}]d_1^2 + [D_{66} - 2c_2F_{66} + c_2^2H_{66}]d_2^2 \\
&- \bar{I}_4d_t^2; \\
L_{45} &= [D_{12} + D_{66} - 2c_2(F_{12} + F_{66}) + c_2^2(H_{12} + H_{66})]d_1d_2; \\
L_{55} &= c_1(D_{44} - c_1F_{44}) - (A_{44} - c_1D_{44}) + [D_{22} - 2c_2F_{22} + c_2^2H_{22}]d_2^2 \\
&+ [D_{66} - 2c_2F_{66} + c_2^2H_{66}]d_1^2 - \bar{I}_4'd_t^2;
\end{aligned} \tag{A-3}$$

where $c_1 = 4/h^2$, $c_2 = c_1/3$, $d_j^i = \partial^i / \partial x_j^i$, $d_t^i = \partial^i / \partial t^i$.

APPENDIX B

STRAIN-DISPLACEMENT MATRIX

B.1 Plate

$$\mathbf{B}_i = \begin{bmatrix} \varphi_{i,x_1} & 0 & 0 & 0 & 0 & 0 & 0 \\ 0 & \varphi_{i,x_2} & 0 & 0 & 0 & 0 & 0 \\ \varphi_{i,x_2} & \varphi_{i,x_1} & 0 & 0 & 0 & 0 & 0 \\ 0 & 0 & 0 & 0 & 0 & 0 & C_1 \varphi_{i,x_1} \\ 0 & 0 & 0 & 0 & 0 & C_1 \varphi_{i,x_2} & 0 \\ 0 & 0 & 0 & 0 & 0 & C_1 \varphi_{i,x_1} & C_1 \varphi_{i,x_2} \\ 0 & 0 & 0 & 0 & -C_4 \varphi_{i,x_1} & 0 & -C_2 \varphi_{i,x_1} \\ 0 & 0 & 0 & -C_4 \varphi_{i,x_2} & 0 & -C_2 \varphi_{i,x_2} & 0 \\ 0 & 0 & 0 & -C_4 \varphi_{i,x_1} & -C_4 \varphi_{i,x_2} & -C_2 \varphi_{i,x_1} & -C_2 \varphi_{i,x_2} \\ 0 & 0 & \varphi_{i,x_2} & 0 & 0 & C_1 \varphi_i & 0 \\ 0 & 0 & \varphi_{i,x_1} & 0 & 0 & 0 & C_1 \varphi_i \\ 0 & 0 & 0 & -3C_4 \varphi_i & 0 & -3C_2 \varphi_i & 0 \\ 0 & 0 & 0 & 0 & -3C_4 \varphi_i & 0 & -3C_2 \varphi_i \end{bmatrix}; \quad (\text{B-1})$$

B-2 Cylindrical Panel

$$\mathbf{B}_i = \begin{bmatrix} \varphi_{i,x_1} & 0 & 0 & 0 & 0 & 0 & 0 \\ 0 & \varphi_{i,x_2} & \varphi_i / R & 0 & 0 & 0 & 0 \\ \varphi_{i,x_2} & \varphi_{i,x_1} & 0 & 0 & 0 & 0 & 0 \\ 0 & 0 & 0 & 0 & 0 & 0 & C_1 \varphi_{i,x_1} \\ 0 & 0 & 0 & 0 & 0 & C_1 \varphi_{i,x_2} & 0 \\ 0 & 0 & 0 & 0 & 0 & C_1 \varphi_{i,x_1} & C_1 \varphi_{i,x_2} \\ 0 & 0 & 0 & 0 & -C_4 \varphi_{i,x_1} & 0 & -C_2 \varphi_{i,x_1} \\ 0 & 0 & 0 & -C_4 \varphi_{i,x_2} & 0 & -C_2 \varphi_{i,x_2} & 0 \\ 0 & 0 & 0 & -C_4 \varphi_{i,x_1} & -C_4 \varphi_{i,x_2} & -C_2 \varphi_{i,x_1} & -C_2 \varphi_{i,x_2} \\ 0 & 0 & \varphi_{i,x_2} & 0 & 0 & C_1 \varphi_i & 0 \\ 0 & 0 & \varphi_{i,x_1} & 0 & 0 & 0 & C_1 \varphi_i \\ 0 & 0 & 0 & -3C_4 \varphi_i & 0 & -3C_2 \varphi_i & 0 \\ 0 & 0 & 0 & 0 & -3C_4 \varphi_i & 0 & -3C_2 \varphi_i \end{bmatrix}; \quad (\text{B-2})$$

B.3 Spherical Panel

$$\mathbf{B}_i = \begin{bmatrix} \varphi_{i,x_1} & 0 & \varphi_i / R & 0 & 0 & 0 & 0 \\ 0 & \varphi_{i,x_2} & \varphi_i / R & 0 & 0 & 0 & 0 \\ \varphi_{i,x_2} & \varphi_{i,x_1} & 0 & 0 & 0 & 0 & 0 \\ 0 & 0 & 0 & 0 & 0 & 0 & C_1 \varphi_{i,x_1} \\ 0 & 0 & 0 & 0 & 0 & C_1 \varphi_{i,x_2} & 0 \\ 0 & 0 & 0 & 0 & 0 & C_1 \varphi_{i,x_1} & C_1 \varphi_{i,x_2} \\ 0 & 0 & 0 & 0 & -C_4 \varphi_{i,x_1} & 0 & -C_2 \varphi_{i,x_1} \\ 0 & 0 & 0 & -C_4 \varphi_{i,x_2} & 0 & -C_2 \varphi_{i,x_2} & 0 \\ 0 & 0 & 0 & -C_4 \varphi_{i,x_1} & -C_4 \varphi_{i,x_2} & -C_2 \varphi_{i,x_1} & -C_2 \varphi_{i,x_2} \\ 0 & 0 & \varphi_{i,x_2} & 0 & 0 & C_1 \varphi_i & 0 \\ 0 & 0 & \varphi_{i,x_1} & 0 & 0 & 0 & C_1 \varphi_i \\ 0 & 0 & 0 & -3C_4 \varphi_i & 0 & -3C_2 \varphi_i & 0 \\ 0 & 0 & 0 & 0 & -3C_4 \varphi_i & 0 & -3C_2 \varphi_i \end{bmatrix}; \quad (\text{B-3})$$

where $\varphi_{i,x_j} = \partial \varphi_i / \partial x_j$; $j=1, 2$.

APPENDIX C

DETAILS OF EQUATIONS (4.11) AND (4.12)

C.1: Equation (4.11)

$$\begin{aligned} \text{Norm1} = & (a15^{**2}) * (a24^{**2}) * a33 - 2. * a14 * a15 * a24 * a25 * a33 \\ & + a14^{**2} * a25^{**2} * a33 - \\ & 2. * a15^{**2} * a23 * a24 * a34 + 2. * a14 * a15 * a23 * a25 * a34 + \\ & 2. * a13 * a15 * a24 * a25 * a34 - \\ & 2. * a13 * a14 * a25^{**2} * a34 + a15^{**2} * a22 * a34^{**2} - \\ & 2. * a12 * a15 * a25 * a34^{**2} + \\ & a11 * a25^{**2} * a34^{**2} + 2. * a14 * a15 * a23 * a24 * a35 - \\ & 2. * a13 * a15 * a24^{**2} * a35 - \\ & 2. * a14^{**2} * a23 * a25 * a35 + 2. * a13 * a14 * a24 * a25 * a35 - \\ & 2. * a14 * a15 * a22 * a34 * a35 \end{aligned}$$

$$\begin{aligned} \text{Norm2} = & 2. * a12 * a15 * a24 * a34 * a35 + 2. * a12 * a14 * a25 * a34 * a35 - \\ & 2. * a11 * a24 * a25 * a34 * a35 + \\ & a14^{**2} * a22 * a35^{**2} - 2. * a12 * a14 * a24 * a35^{**2} + \\ & a11 * a24^{**2} * a35^{**2} + \\ & a15^{**2} * a23^{**2} * a44 - \\ & 2. * a13 * a15 * a23 * a25 * a44 + a13^{**2} * a25^{**2} * a44 - \\ & a15^{**2} * a22 * a33 * a44 + \\ & 2. * a12 * a15 * a25 * a33 * a44 - a11 * a25^{**2} * a33 * a44 + \\ & 2. * a13 * a15 * a22 * a35 * a44 - \\ & 2. * a12 * a15 * a23 * a35 * a44 - 2. * a12 * a13 * a25 * a35 * a44 + \\ & 2. * a11 * a23 * a25 * a35 * a44 \end{aligned}$$

$$\begin{aligned} \text{Norm3} = & a12^{**2} * a35^{**2} * a44 - a11 * a22 * a35^{**2} * a44 - \\ & 2. * a14 * a15 * a23^{**2} * a45 + \\ & 2. * a13 * a15 * a23 * a24 * a45 + 2. * a13 * a14 * a23 * a25 * a45 - \\ & 2. * a13^{**2} * a24 * a25 * a45 + \\ & 2. * a14 * a15 * a22 * a33 * a45 - 2. * a12 * a15 * a24 * a33 * a45 - \\ & 2. * a12 * a14 * a25 * a33 * a45 + \\ & 2. * a11 * a24 * a25 * a33 * a45 - 2. * a13 * a15 * a22 * a34 * a45 + \end{aligned}$$

$$\begin{aligned}
& 2.*a12*a15*a23*a34*a45 + \\
& 2.*a12*a13*a25*a34*a45 - 2.*a11*a23*a25*a34*a45 - \\
& 2.*a13*a14*a22*a35*a45
\end{aligned}$$

$$\begin{aligned}
\text{Norm4} = & 2.*a12*a14*a23*a35*a45 + \\
& 2.*a12*a13*a24*a35*a45 - \\
& 2.*a11*a23*a24*a35*a45 - \\
& 2.*a12**2*a34*a35*a45 + 2.*a11*a22*a34*a35*a45 + \\
& a13**2*a22*a45**2 - \\
& 2.*a12*a13*a23*a45**2 + a11*a23**2*a45**2 + \\
& a12**2*a33*a45**2 - \\
& a11*a22*a33*a45**2 + a14**2*a23**2*a55 - \\
& 2.*a13*a14*a23*a24*a55 + a13**2*a24**2*a55 - \\
& a14**2*a22*a33*a55 + 2.*a12*a14*a24*a33*a55
\end{aligned}$$

$$\begin{aligned}
\text{Norm5} = & -a11*a24**2*a33*a55 + 2*a13*a14*a22*a34*a55 \\
& -2.*a12*a14*a23*a34*a55 - \\
& -2*a12*a13*a24*a34*a55 + 2.*a11*a23*a24*a34*a55 + \\
& a12**2*a34**2*a55 - \\
& a11*a22*a34**2*a55 - a13**2*a22*a44*a55 + \\
& 2.*a12*a13*a23*a44*a55 - \\
& a11*a23**2*a44*a55 - a12**2*a33*a44*a55 + \\
& a11*a22*a33*a44*a55
\end{aligned}$$

$$\begin{aligned}
z = & -(-a15**2*a24**2 + 2*a14*a15*a24*a25 - \\
& a14**2*a25**2 + \\
& a15**2*a22*a44 - 2*a12*a15*a25*a44 + \\
& a11*a25**2*a44 - \\
& 2*a14*a15*a22*a45 + 2*a12*a15*a24*a45 + \\
& 2*a12*a14*a25*a45 - \\
& 2*a11*a24*a25*a45 - a12**2*a45**2 + \\
& a11*a22*a45**2 \\
& + a14**2*a22*a55 - 2*a12*a14*a24*a55 + \\
& a11*a24**2*a55 + a12**2*a44*a55 - \\
& a11*a22*a44*a55)
\end{aligned}$$

$$s = (\text{Norm1} + \text{Norm2} + \text{Norm3} + \text{Norm4} + \text{norm5}) / z$$

If $N_{x_1} = N_{cr}$ and $N_{x_2} = N_{x_1 x_2} = 0$, then

$$\begin{aligned}
s &= s / \alpha^2 \\
\overline{N}_{cr} &= s
\end{aligned}$$

If $N_{x_2} = N_{cr}$ and $N_{x_1} = N_{x_1 x_2} = 0$, then

$$\begin{aligned}
s &= s / \beta^2 \\
\overline{N}_{cr} &= s
\end{aligned}$$

where $a_{ij} = \overline{a}_{ij}$ and α and β are wavelength parameters defined in Equation (4.2).

C.2: Equation (4.12)

$$\begin{aligned}
Y1 = & a25^{**2} * a34^{**2} * b11 - 2 * a24 * a25 * a34 * a35 * b11 + a24^{**2} * a35^{**2} * b11 \\
& - a25^{**2} * a33 * a44 * b11 + 2 * a23 * a25 * a35 * a44 * b11 - a22 * a35^{**2} * a44 * b11 \\
& 2 * a24 * a25 * a33 * a45 * b11 - 2 * a23 * a25 * a34 * a45 * b11 - \\
& 2 * a23 * a24 * a35 * a45 * b11 + \\
& 2 * a22 * a34 * a35 * a45 * b11 + a23^{**2} * a45^{**2} * b11 - \\
& a22 * a33 * a45^{**2} * b11 - \\
& a24^{**2} * a33 * a55 * b11 + 2 * a23 * a24 * a34 * a55 * b11
\end{aligned}$$

$$\begin{aligned}
Y2 = & -a22 * a34^{**2} * a55 * b11 - \\
& a23^{**2} * a44 * a55 * b11 + a22 * a33 * a44 * a55 * b11 - \\
& 2 * a15 * a25 * a34^{**2} * b12 + \\
& 2 * a15 * a24 * a34 * a35 * b12 + 2 * a14 * a25 * a34 * a35 * b12 - \\
& 2 * a14 * a24 * a35^{**2} * b12 + 2 * a15 * a25 * a33 * a44 * b12 \\
& - 2 * a15 * a23 * a35 * a44 * b12 - 2 * a13 * a25 * a35 * a44 * b12 + \\
& 2 * a12 * a35^{**2} * a44 * b12 - 2 * a15 * a24 * a33 * a45 * b12 - \\
& 2 * a14 * a25 * a33 * a45 * b12 + \\
& 2 * a15 * a23 * a34 * a45 * b12 + 2 * a13 * a25 * a34 * a45 * b12
\end{aligned}$$

$$\begin{aligned}
Y3 = & 2 * a14 * a23 * a35 * a45 * b12 + \\
& 2 * a13 * a24 * a35 * a45 * b12 - 4 * a12 * a34 * a35 * a45 * b12 - \\
& 2 * a13 * a23 * a45^{**2} * b12 + \\
& 2 * a12 * a33 * a45^{**2} * b12 + 2 * a14 * a24 * a33 * a55 * b12 - \\
& 2 * a14 * a23 * a34 * a55 * b12 - \\
& 2 * a13 * a24 * a34 * a55 * b12 + 2 * a12 * a34^{**2} * a55 * b12 + \\
& 2 * a13 * a23 * a44 * a55 * b12 - 2 * a12 * a33 * a44 * a55 * b12 + \\
& 2 * a15 * a24 * a25 * a34 * b13 - 2 * a14 * a25^{**2} * a34 * b13 \\
& - 2 * a15 * a24^{**2} * a35 * b13 + 2 * a14 * a24 * a25 * a35 * b13
\end{aligned}$$

$$\begin{aligned}
Y4 = & - 2 * a15 * a23 * a25 * a44 * b13 + 2 * a13 * a25^{**2} * a44 * b13 + \\
& 2 * a15 * a22 * a35 * a44 * b13 - 2 * a12 * a25 * a35 * a44 * b13 + \\
& 2 * a15 * a23 * a24 * a45 * b13 + \\
& 2 * a14 * a23 * a25 * a45 * b13 - 4 * a13 * a24 * a25 * a45 * b13 - \\
& 2 * a15 * a22 * a34 * a45 * b13 + \\
& 2 * a12 * a25 * a34 * a45 * b13 - 2 * a14 * a22 * a35 * a45 * b13 + \\
& 2 * a12 * a24 * a35 * a45 * b13 + \\
& 2 * a13 * a22 * a45^{**2} * b13 - 2 * a12 * a23 * a45^{**2} * b13 \\
& - 2 * a14 * a23 * a24 * a55 * b13 + 2 * a13 * a24^{**2} * a55 * b13
\end{aligned}$$

$$\begin{aligned}
Y5 = & 2 * a14 * a22 * a34 * a55 * b13 - 2 * a12 * a24 * a34 * a55 * b13 - \\
& 2 * a13 * a22 * a44 * a55 * b13 + 2 * a12 * a23 * a44 * a55 * b13 \\
& - 2 * a15 * a24 * a25 * a33 * b14 + \\
& + 2 * a14 * a25^{**2} * a33 * b14 + \\
& 2 * a15 * a23 * a25 * a34 * b14 - 2 * a13 * a25^{**2} * a34 * b14 + \\
& 2 * a15 * a23 * a24 * a35 * b14 - \\
& 4 * a14 * a23 * a25 * a35 * b14 + 2 * a13 * a24 * a25 * a35 * b14 - \\
& 2 * a15 * a22 * a34 * a35 * b14 + \\
& 2 * a12 * a25 * a34 * a35 * b14 + 2 * a14 * a22 * a35^{**2} * b14
\end{aligned}$$

$$\begin{aligned}
Y6 = & -2*a12*a24*a35**2*b14 - 2*a15*a23**2*a45*b14 \\
& + 2*a13*a23*a25*a45*b14 + 2*a15*a22*a33*a45*b14 - \\
& 2*a12*a25*a33*a45*b14 - 2*a13*a22*a35*a45*b14 + \\
& 2*a12*a23*a35*a45*b14 + \\
& 2*a14*a23**2*a55*b14 - 2*a13*a23*a24*a55*b14 - \\
& 2*a14*a22*a33*a55*b14 + \\
& 2*a12*a24*a33*a55*b14 + 2*a13*a22*a34*a55*b14 - \\
& 2*a12*a23*a34*a55*b14 + \\
& 2*a15*a24**2*a33*b15 - 2*a14*a24*a25*a33*b15
\end{aligned}$$

$$\begin{aligned}
Y7 = & -4*a15*a23*a24*a34*b15 + 2*a14*a23*a25*a34*b15 + \\
& 2*a13*a24*a25*a34*b15 + \\
& 2*a15*a22*a34**2*b15 - 2*a12*a25*a34**2*b15 \\
& + 2*a14*a23*a24*a35*b15 - \\
& 2*a13*a24**2*a35*b15 - 2*a14*a22*a34*a35*b15 + \\
& 2*a12*a24*a34*a35*b15 + \\
& 2*a15*a23**2*a44*b15 - 2*a13*a23*a25*a44*b15 - \\
& 2*a15*a22*a33*a44*b15
\end{aligned}$$

$$\begin{aligned}
Y8 = & 2*a12*a25*a33*a44*b15 + 2*a13*a22*a35*a44*b15 - \\
& 2*a12*a23*a35*a44*b15 - \\
& 2*a14*a23**2*a45*b15 + 2*a13*a23*a24*a45*b15 + \\
& 2*a14*a22*a33*a45*b15 - \\
& 2*a12*a24*a33*a45*b15 - 2*a13*a22*a34*a45*b15 + \\
& 2*a12*a23*a34*a45*b15 \\
& + a15**2*a34**2*b22 - 2*a14*a15*a34*a35*b22 + \\
& a14**2*a35**2*b22 - a15**2*a33*a44*b22
\end{aligned}$$

$$\begin{aligned}
Y9 = & 2*a13*a15*a35*a44*b22 - \\
& a11*a35**2*a44*b22 + 2*a14*a15*a33*a45*b22 \\
& - 2*a13*a15*a34*a45*b22 - \\
& 2*a13*a14*a35*a45*b22 + 2*a11*a34*a35*a45*b22 + \\
& a13**2*a45**2*b22 - \\
& a11*a33*a45**2*b22 - a14**2*a33*a55*b22 + \\
& 2*a13*a14*a34*a55*b22 - \\
& a11*a34**2*a55*b22 - a13**2*a44*a55*b22 + \\
& a11*a33*a44*a55*b22
\end{aligned}$$

$$\begin{aligned}
Y10 = & -2*a15**2*a24*a34*b23 + \\
& 2*a14*a15*a25*a34*b23 + 2*a14*a15*a24*a35*b23 - \\
& 2*a14**2*a25*a35*b23 + \\
& 2*a15**2*a23*a44*b23 - 2*a13*a15*a25*a44*b23 - \\
& 2*a12*a15*a35*a44*b23 + \\
& 2*a11*a25*a35*a44*b23 - 4*a14*a15*a23*a45*b23 + \\
& 2*a13*a15*a24*a45*b23 + \\
& 2*a13*a14*a25*a45*b23 + 2*a12*a15*a34*a45*b23 - \\
& 2*a11*a25*a34*a45*b23
\end{aligned}$$

$$Y11 = 2*a12*a14*a35*a45*b23 - 2*a11*a24*a35*a45*b23 -$$

$$\begin{aligned}
& 2*a_{12}*a_{13}*a_{45}**2*b_{23} + \\
& + 2*a_{11}*a_{23}*a_{45}**2*b_{23} + 2*a_{14}**2*a_{23}*a_{55}*b_{23} \\
& - 2*a_{13}*a_{14}*a_{24}*a_{55}*b_{23} - \\
& 2*a_{12}*a_{14}*a_{34}*a_{55}*b_{23} + 2*a_{11}*a_{24}*a_{34}*a_{55}*b_{23} + \\
& 2*a_{12}*a_{13}*a_{44}*a_{55}*b_{23} - \\
& 2*a_{11}*a_{23}*a_{44}*a_{55}*b_{23}
\end{aligned}$$

$$\begin{aligned}
Y_{12} = & + 2*a_{15}**2*a_{24}*a_{33}*b_{24} - 2*a_{14}*a_{15}*a_{25}*a_{33}*b_{24} - \\
& 2*a_{15}**2*a_{23}*a_{34}*b_{24} + 2*a_{13}*a_{15}*a_{25}*a_{34}*b_{24} + \\
& 2*a_{14}*a_{15}*a_{23}*a_{35}*b_{24} - \\
& 4*a_{13}*a_{15}*a_{24}*a_{35}*b_{24} + 2*a_{13}*a_{14}*a_{25}*a_{35}*b_{24} + \\
& 2*a_{12}*a_{15}*a_{34}*a_{35}*b_{24}
\end{aligned}$$

$$\begin{aligned}
Y_{13} = & -2*a_{11}*a_{25}*a_{34}*a_{35}*b_{24} \\
& - 2*a_{12}*a_{14}*a_{35}**2*b_{24} + \\
& 2*a_{11}*a_{24}*a_{35}**2*b_{24} + \\
& 2*a_{13}*a_{15}*a_{23}*a_{45}*b_{24} - 2*a_{13}**2*a_{25}*a_{45}*b_{24} - \\
& 2*a_{12}*a_{15}*a_{33}*a_{45}*b_{24} + \\
& 2*a_{11}*a_{25}*a_{33}*a_{45}*b_{24} + 2*a_{12}*a_{13}*a_{35}*a_{45}*b_{24} - \\
& 2*a_{11}*a_{23}*a_{35}*a_{45}*b_{24} - \\
& 2*a_{13}*a_{14}*a_{23}*a_{55}*b_{24} + 2*a_{13}**2*a_{24}*a_{55}*b_{24}
\end{aligned}$$

$$\begin{aligned}
Y_{14} = & 2*a_{12}*a_{14}*a_{33}*a_{55}*b_{24} - \\
& 2*a_{11}*a_{24}*a_{33}*a_{55}*b_{24} - 2*a_{12}*a_{13}*a_{34}*a_{55}*b_{24} + \\
& 2*a_{11}*a_{23}*a_{34}*a_{55}*b_{24} \\
& - 2*a_{14}*a_{15}*a_{24}*a_{33}*b_{25} + 2*a_{14}**2*a_{25}*a_{33}*b_{25} + \\
& 2*a_{14}*a_{15}*a_{23}*a_{34}*b_{25} + 2*a_{13}*a_{15}*a_{24}*a_{34}*b_{25} - \\
& 4*a_{13}*a_{14}*a_{25}*a_{34}*b_{25} - \\
& 2*a_{12}*a_{15}*a_{34}**2*b_{25} + 2*a_{11}*a_{25}*a_{34}**2*b_{25} \\
& - 2*a_{14}**2*a_{23}*a_{35}*b_{25} + \\
& 2*a_{13}*a_{14}*a_{24}*a_{35}*b_{25} + 2*a_{12}*a_{14}*a_{34}*a_{35}*b_{25}
\end{aligned}$$

$$\begin{aligned}
Y_{15} = & -2*a_{11}*a_{24}*a_{34}*a_{35}*b_{25} - \\
& 2*a_{13}*a_{15}*a_{23}*a_{44}*b_{25} + 2*a_{13}**2*a_{25}*a_{44}*b_{25} + \\
& 2*a_{12}*a_{15}*a_{33}*a_{44}*b_{25} - \\
& 2*a_{11}*a_{25}*a_{33}*a_{44}*b_{25} - 2*a_{12}*a_{13}*a_{35}*a_{44}*b_{25} + \\
& 2*a_{11}*a_{23}*a_{35}*a_{44}*b_{25} + \\
& 2*a_{13}*a_{14}*a_{23}*a_{45}*b_{25} - 2*a_{13}**2*a_{24}*a_{45}*b_{25} - \\
& 2*a_{12}*a_{14}*a_{33}*a_{45}*b_{25} + \\
& 2*a_{11}*a_{24}*a_{33}*a_{45}*b_{25} + 2*a_{12}*a_{13}*a_{34}*a_{45}*b_{25}
\end{aligned}$$

$$\begin{aligned}
Y_{16} = & -2*a_{11}*a_{23}*a_{34}*a_{45}*b_{25} \\
& + a_{15}**2*a_{24}**2*b_{33} - \\
& 2*a_{14}*a_{15}*a_{24}*a_{25}*b_{33} + a_{14}**2*a_{25}**2*b_{33} - \\
& a_{15}**2*a_{22}*a_{44}*b_{33} + \\
& 2*a_{12}*a_{15}*a_{25}*a_{44}*b_{33} - a_{11}*a_{25}**2*a_{44}*b_{33} \\
& + 2*a_{14}*a_{15}*a_{22}*a_{45}*b_{33} - \\
& 2*a_{12}*a_{15}*a_{24}*a_{45}*b_{33} - 2*a_{12}*a_{14}*a_{25}*a_{45}*b_{33} + \\
& 2*a_{11}*a_{24}*a_{25}*a_{45}*b_{33} +
\end{aligned}$$

$$a_{12}^2 a_{45}^2 b_{33} - a_{11} a_{22} a_{45}^2 b_{33} - a_{14}^2 a_{22} a_{55} b_{33}$$

$$\begin{aligned} Y_{17} = & 2 a_{12} a_{14} a_{24} a_{55} b_{33} - a_{11} a_{24}^2 a_{55} b_{33} - \\ & a_{12}^2 a_{44} a_{55} b_{33} + a_{11} a_{22} a_{44} a_{55} b_{33} \\ & - 2 a_{15}^2 a_{23} a_{24} b_{34} + 2 a_{14} a_{15} a_{23} a_{25} b_{34} + 2 a_{13} a_{15} a_{24} a_{25} b_{34} - \\ & 2 a_{13} a_{14} a_{25}^2 b_{34} + 2 a_{15}^2 a_{22} a_{34} b_{34} - 4 a_{12} a_{15} a_{25} a_{34} b_{34} \\ & + 2 a_{11} a_{25}^2 a_{34} b_{34} - 2 a_{14} a_{15} a_{22} a_{35} b_{34} + 2 a_{12} a_{15} a_{24} a_{35} b_{34} + \\ & 2 a_{12} a_{14} a_{25} a_{35} b_{34} \end{aligned}$$

$$\begin{aligned} Y_{18} = & -2 a_{11} a_{24} a_{25} a_{35} b_{34} - 2 a_{13} a_{15} a_{22} a_{45} b_{34} + \\ & 2 a_{12} a_{15} a_{23} a_{45} b_{34} + 2 a_{12} a_{13} a_{25} a_{45} b_{34} - 2 a_{11} a_{23} a_{25} a_{45} b_{34} - \\ & 2 a_{12}^2 a_{35} a_{45} b_{34} + 2 a_{11} a_{22} a_{35} a_{45} b_{34} + 2 a_{13} a_{14} a_{22} a_{55} b_{34} - \\ & 2 a_{12} a_{14} a_{23} a_{55} b_{34} - 2 a_{12} a_{13} a_{24} a_{55} b_{34} + 2 a_{11} a_{23} a_{24} a_{55} b_{34} + \\ & 2 a_{12}^2 a_{34} a_{55} b_{34} - 2 a_{11} a_{22} a_{34} a_{55} b_{34} \end{aligned}$$

$$\begin{aligned} Y_{19} = & 2 a_{14} a_{15} a_{23} a_{24} b_{35} - 2 a_{13} a_{15} a_{24}^2 b_{35} - \\ & 2 a_{14}^2 a_{23} a_{25} b_{35} + 2 a_{13} a_{14} a_{24} a_{25} b_{35} - \\ & 2 a_{14} a_{15} a_{22} a_{34} b_{35} + 2 a_{12} a_{15} a_{24} a_{34} b_{35} + 2 a_{12} a_{14} a_{25} a_{34} b_{35} - \\ & 2 a_{11} a_{24} a_{25} a_{34} b_{35} + 2 a_{14}^2 a_{22} a_{35} b_{35} - 4 a_{12} a_{14} a_{24} a_{35} b_{35} + \\ & 2 a_{11} a_{24}^2 a_{35} b_{35} + 2 a_{13} a_{15} a_{22} a_{44} b_{35} - 2 a_{12} a_{15} a_{23} a_{44} b_{35} \end{aligned}$$

$$\begin{aligned} Y_{20} = & -2 a_{12} a_{13} a_{25} a_{44} b_{35} + 2 a_{11} a_{23} a_{25} a_{44} b_{35} + 2 a_{12}^2 a_{35} a_{44} b_{35} - \\ & 2 a_{11} a_{22} a_{35} a_{44} b_{35} - 2 a_{13} a_{14} a_{22} a_{45} b_{35} + 2 a_{12} a_{14} a_{23} a_{45} b_{35} + \\ & 2 a_{12} a_{13} a_{24} a_{45} b_{35} - 2 a_{11} a_{23} a_{24} a_{45} b_{35} - 2 a_{12}^2 a_{34} a_{45} b_{35} + \\ & 2 a_{11} a_{22} a_{34} a_{45} b_{35} + a_{15}^2 a_{23}^2 b_{44} \end{aligned}$$

$$\begin{aligned} Y_{21} = & -2 a_{13} a_{15} a_{23} a_{25} b_{44} + a_{13}^2 a_{25}^2 b_{44} - \\ & a_{15}^2 a_{22} a_{33} b_{44} + 2 a_{12} a_{15} a_{25} a_{33} b_{44} - a_{11} a_{25}^2 a_{33} b_{44} + \\ & 2 a_{13} a_{15} a_{22} a_{35} b_{44} - 2 a_{12} a_{15} a_{23} a_{35} b_{44} - 2 a_{12} a_{13} a_{25} a_{35} b_{44} + \\ & 2 a_{11} a_{23} a_{25} a_{35} b_{44} + a_{12}^2 a_{35}^2 b_{44} - a_{11} a_{22} a_{35}^2 b_{44} - \\ & a_{13}^2 a_{22} a_{55} b_{44} + \end{aligned}$$

$$2*a_{12}*a_{13}*a_{23}*a_{55}*b_{44} - a_{11}*a_{23}^2*a_{55}*b_{44}$$

$$\begin{aligned} Y_{22} = & -a_{12}^2*a_{33}*a_{55}*b_{44} + \\ & a_{11}*a_{22}*a_{33}*a_{55}*b_{44} - \\ & 2*a_{14}*a_{15}*a_{23}^2*b_{45} + 2*a_{13}*a_{15}*a_{23}*a_{24}*b_{45} + \\ & 2*a_{13}*a_{14}*a_{23}*a_{25}*b_{45} - \\ & 2*a_{13}^2*a_{24}*a_{25}*b_{45} + 2*a_{14}*a_{15}*a_{22}*a_{33}*b_{45} - \\ & 2*a_{12}*a_{15}*a_{24}*a_{33}*b_{45} - \\ & 2*a_{12}*a_{14}*a_{25}*a_{33}*b_{45} + 2*a_{11}*a_{24}*a_{25}*a_{33}*b_{45} - \\ & 2*a_{13}*a_{15}*a_{22}*a_{34}*b_{45} \end{aligned}$$

$$\begin{aligned} Y_{23} = & 2*a_{12}*a_{15}*a_{23}*a_{34}*b_{45} + 2*a_{12}*a_{13}*a_{25}*a_{34}*b_{45} - \\ & 2*a_{11}*a_{23}*a_{25}*a_{34}*b_{45} - \\ & 2*a_{13}*a_{14}*a_{22}*a_{35}*b_{45} + 2*a_{12}*a_{14}*a_{23}*a_{35}*b_{45} + \\ & 2*a_{12}*a_{13}*a_{24}*a_{35}*b_{45} - \\ & 2*a_{11}*a_{23}*a_{24}*a_{35}*b_{45} - 2*a_{12}^2*a_{34}*a_{35}*b_{45} + \\ & 2*a_{11}*a_{22}*a_{34}*a_{35}*b_{45} + \\ & 2*a_{13}^2*a_{22}*a_{45}*b_{45} - 4*a_{12}*a_{13}*a_{23}*a_{45}*b_{45} + \\ & 2*a_{11}*a_{23}^2*a_{45}*b_{45} \end{aligned}$$

$$\begin{aligned} Y_{24} = & 2*a_{12}^2*a_{33}*a_{45}*b_{45} - 2*a_{11}*a_{22}*a_{33}*a_{45}*b_{45} \\ & + a_{14}^2*a_{23}^2*b_{55} - \\ & 2*a_{13}*a_{14}*a_{23}*a_{24}*b_{55} + a_{13}^2*a_{24}^2*b_{55} \\ & - a_{14}^2*a_{22}*a_{33}*b_{55} + \\ & 2*a_{12}*a_{14}*a_{24}*a_{33}*b_{55} - a_{11}*a_{24}^2*a_{33}*b_{55} + \\ & 2*a_{13}*a_{14}*a_{22}*a_{34}*b_{55} - \\ & 2*a_{12}*a_{14}*a_{23}*a_{34}*b_{55} - 2*a_{12}*a_{13}*a_{24}*a_{34}*b_{55} + \\ & 2*a_{11}*a_{23}*a_{24}*a_{34}*b_{55} + \\ & a_{12}^2*a_{34}^2*b_{55} - a_{11}*a_{22}*a_{34}^2*b_{55} \end{aligned}$$

$$\begin{aligned} Y_{25} = & -a_{13}^2*a_{22}*a_{44}*b_{55} + \\ & 2*a_{12}*a_{13}*a_{23}*a_{44}*b_{55} - a_{11}*a_{23}^2*a_{44}*b_{55} - \\ & a_{12}^2*a_{33}*a_{44}*b_{55} + \\ & a_{11}*a_{22}*a_{33}*a_{44}*b_{55} \end{aligned}$$

$$\begin{aligned} Z = & -(-a_{15}^2*a_{24}^2 + 2*a_{14}*a_{15}*a_{24}*a_{25} - \\ & a_{14}^2*a_{25}^2 + \\ & a_{15}^2*a_{22}*a_{44} - 2*a_{12}*a_{15}*a_{25}*a_{44} + \\ & a_{11}*a_{25}^2*a_{44} - \\ & 2*a_{14}*a_{15}*a_{22}*a_{45} + 2*a_{12}*a_{15}*a_{24}*a_{45} + \\ & 2*a_{12}*a_{14}*a_{25}*a_{45} - 2*a_{11}*a_{24}*a_{25}*a_{45} - \\ & + a_{12}^2*a_{45}^2 + \\ & a_{11}*a_{22}*a_{45}^2 + a_{14}^2*a_{22}*a_{55} - \\ & 2*a_{12}*a_{14}*a_{24}*a_{55} + a_{11}*a_{24}^2*a_{55} + \\ & a_{12}^2*a_{44}*a_{55} - a_{11}*a_{22}*a_{44}*a_{55}) \end{aligned}$$

$$\begin{aligned} Y_{26} = & a_{25}^2*a_{44}*b_{11}*s - 2*a_{24}*a_{25}*a_{45}*b_{11}*s + \\ & a_{22}*a_{45}^2*b_{11}*s + a_{24}^2*a_{55}*b_{11}*s - \\ & a_{22}*a_{44}*a_{55}*b_{11}*s - \end{aligned}$$

$$\begin{aligned}
& 2*a_{15}*a_{25}*a_{44}*b_{12}*s + 2*a_{15}*a_{24}*a_{45}*b_{12}*s + \\
& 2*a_{14}*a_{25}*a_{45}*b_{12}*s - \\
& 2*a_{12}*a_{45}**2*b_{12}*s - 2*a_{14}*a_{24}*a_{55}*b_{12}*s + \\
& 2*a_{12}*a_{44}*a_{55}*b_{12}*s \\
& + 2*a_{15}*a_{24}*a_{25}*b_{14}*s - 2*a_{14}*a_{25}**2*b_{14}*s - \\
& 2*a_{15}*a_{22}*a_{45}*b_{14}*s + 2*a_{12}*a_{25}*a_{45}*b_{14}*s
\end{aligned}$$

$$\begin{aligned}
Y_{27} = & 2*a_{14}*a_{22}*a_{55}*b_{14}*s - \\
& 2*a_{12}*a_{24}*a_{55}*b_{14}*s - 2*a_{15}*a_{24}**2*b_{15}*s + \\
& 2*a_{14}*a_{24}*a_{25}*b_{15}*s + \\
& 2*a_{15}*a_{22}*a_{44}*b_{15}*s - 2*a_{12}*a_{25}*a_{44}*b_{15}*s - \\
& 2*a_{14}*a_{22}*a_{45}*b_{15}*s + \\
& 2*a_{12}*a_{24}*a_{45}*b_{15}*s + a_{15}**2*a_{44}*b_{22}*s - \\
& 2*a_{14}*a_{15}*a_{45}*b_{22}*s + \\
& a_{11}*a_{45}**2*b_{22}*s
\end{aligned}$$

$$\begin{aligned}
Y_{28} = & a_{14}**2*a_{55}*b_{22}*s - a_{11}*a_{44}*a_{55}*b_{22}*s - \\
& 2*a_{15}**2*a_{24}*b_{24}*s + \\
& 2*a_{14}*a_{15}*a_{25}*b_{24}*s + \\
& 2*a_{12}*a_{15}*a_{45}*b_{24}*s - 2*a_{11}*a_{25}*a_{45}*b_{24}*s - \\
& 2*a_{12}*a_{14}*a_{55}*b_{24}*s + \\
& 2*a_{11}*a_{24}*a_{55}*b_{24}*s + 2*a_{14}*a_{15}*a_{24}*b_{25}*s - \\
& 2*a_{14}**2*a_{25}*b_{25}*s - 2*a_{12}*a_{15}*a_{44}*b_{25}*s + \\
& 2*a_{11}*a_{25}*a_{44}*b_{25}*s
\end{aligned}$$

$$\begin{aligned}
Y_{29} = & 2*a_{12}*a_{14}*a_{45}*b_{25}*s - 2*a_{11}*a_{24}*a_{45}*b_{25}*s + \\
& a_{15}**2*a_{22}*b_{44}*s - \\
& 2*a_{12}*a_{15}*a_{25}*b_{44}*s + \\
& a_{11}*a_{25}**2*b_{44}*s + \\
& a_{12}**2*a_{55}*b_{44}*s - a_{11}*a_{22}*a_{55}*b_{44}*s - \\
& 2*a_{14}*a_{15}*a_{22}*b_{45}*s \\
& + 2*a_{12}*a_{15}*a_{24}*b_{45}*s + \\
& 2*a_{12}*a_{14}*a_{25}*b_{45}*s - 2*a_{11}*a_{24}*a_{25}*b_{45}*s
\end{aligned}$$

$$\begin{aligned}
Y_{30} = & - 2*a_{12}**2*a_{45}*b_{45}*s + 2*a_{11}*a_{22}*a_{45}*b_{45}*s + a_{14}**2*a_{22}*b_{55}*s \\
& - 2*a_{12}*a_{14}*a_{24}*b_{55}*s + a_{11}*a_{24}**2*b_{55}*s + a_{12}**2*a_{44}*b_{55}*s \\
& - a_{11}*a_{22}*a_{44}*b_{55}*s
\end{aligned}$$

$$\begin{aligned}
r_1 &= Y_1 + Y_2 + Y_3 + Y_4 + Y_5 + Y_6 + Y_7 + Y_8 + Y_9 + Y_{10} \\
r_2 &= Y_{11} + Y_{12} + Y_{13} + Y_{14} + Y_{15} + Y_{16} + Y_{17} + Y_{18} \\
r_3 &= Y_{19} + Y_{20} + Y_{21} + Y_{22} + Y_{23} + Y_{24} + Y_{25} + Y_{26} \\
r_4 &= Y_{27} + Y_{28} + Y_{29} + Y_{30} \\
r &= (r_1 + r_2 + r_3 + r_4) / Z
\end{aligned}$$

$$\text{If } N_{x_1} = N_{cr} \text{ and } N_{x_2} = N_{x_1 x_2} = 0, \text{ then } N'_{cr} = r / \alpha^2$$

$$\text{If } N_{x_2} = N_{cr} \text{ and } N_{x_1} = N_{x_1 x_2} = 0, \text{ then } N'_{cr} = r / \beta^2$$

$$\text{where } a_{ij} = \bar{a}_{ij} \text{ and } b_{ij} = a'_{ij} \text{ and } s \text{ as defined in C.1.}$$